frontiers | Research Topics

Challenges and current research status of vertigo/vestibular diseases,
2nd Edition

Edited by
Sulin Zhang, Hubertus Axer, Tino Prell, Lisheng Yu, Pei Liang and Jian-hua Zhuang

Published in
Frontiers in Neurology
Frontiers in Neuroscience

FRONTIERS EBOOK COPYRIGHT STATEMENT

The copyright in the text of individual articles in this ebook is the property of their respective authors or their respective institutions or funders. The copyright in graphics and images within each article may be subject to copyright of other parties. In both cases this is subject to a license granted to Frontiers.

The compilation of articles constituting this ebook is the property of Frontiers.

Each article within this ebook, and the ebook itself, are published under the most recent version of the Creative Commons CC-BY licence. The version current at the date of publication of this ebook is CC-BY 4.0. If the CC-BY licence is updated, the licence granted by Frontiers is automatically updated to the new version.

When exercising any right under the CC-BY licence, Frontiers must be attributed as the original publisher of the article or ebook, as applicable.

Authors have the responsibility of ensuring that any graphics or other materials which are the property of others may be included in the CC-BY licence, but this should be checked before relying on the CC-BY licence to reproduce those materials. Any copyright notices relating to those materials must be complied with.

Copyright and source acknowledgement notices may not be removed and must be displayed in any copy, derivative work or partial copy which includes the elements in question.

All copyright, and all rights therein, are protected by national and international copyright laws. The above represents a summary only. For further information please read Frontiers' Conditions for Website Use and Copyright Statement, and the applicable CC-BY licence.

ISSN 1664-8714
ISBN 978-2-8325-4267-5
DOI 10.3389/978-2-8325-4267-5

About Frontiers

Frontiers is more than just an open access publisher of scholarly articles: it is a pioneering approach to the world of academia, radically improving the way scholarly research is managed. The grand vision of Frontiers is a world where all people have an equal opportunity to seek, share and generate knowledge. Frontiers provides immediate and permanent online open access to all its publications, but this alone is not enough to realize our grand goals.

Frontiers journal series

The Frontiers journal series is a multi-tier and interdisciplinary set of open-access, online journals, promising a paradigm shift from the current review, selection and dissemination processes in academic publishing. All Frontiers journals are driven by researchers for researchers; therefore, they constitute a service to the scholarly community. At the same time, the *Frontiers journal series* operates on a revolutionary invention, the tiered publishing system, initially addressing specific communities of scholars, and gradually climbing up to broader public understanding, thus serving the interests of the lay society, too.

Dedication to quality

Each Frontiers article is a landmark of the highest quality, thanks to genuinely collaborative interactions between authors and review editors, who include some of the world's best academicians. Research must be certified by peers before entering a stream of knowledge that may eventually reach the public - and shape society; therefore, Frontiers only applies the most rigorous and unbiased reviews. Frontiers revolutionizes research publishing by freely delivering the most outstanding research, evaluated with no bias from both the academic and social point of view. By applying the most advanced information technologies, Frontiers is catapulting scholarly publishing into a new generation.

What are Frontiers Research Topics?

Frontiers Research Topics are very popular trademarks of the *Frontiers journals series*: they are collections of at least ten articles, all centered on a particular subject. With their unique mix of varied contributions from Original Research to Review Articles, Frontiers Research Topics unify the most influential researchers, the latest key findings and historical advances in a hot research area.

Find out more on how to host your own Frontiers Research Topic or contribute to one as an author by contacting the Frontiers editorial office: frontiersin.org/about/contact

Challenges and current research status of vertigo/vestibular diseases, 2nd Edition

Topic editors

Sulin Zhang — Huazhong University of Science and Technology, China
Hubertus Axer — Jena University Hospital, Germany
Tino Prell — University Hospital in Halle, Germany
Lisheng Yu — Peking University People's Hospital, China
Pei Liang — Hubei University, China
Jian-hua Zhuang — Department of Neurology, Shanghai Changzheng Hospital, China

Citation

Zhang, S., Axer, H., Prell, T., Yu, L., Liang, P., Zhuang, J.-h., eds. (2024). *Challenges and current research status of vertigo/vestibular diseases, 2nd Edition*. Lausanne: Frontiers Media SA. doi: 10.3389/978-2-8325-4267-5

Publisher's note: This is a 2nd edition due to an article retraction.

Table of contents

frontiers | Frontiers in Neurology

ORIGINAL RESEARCH
published: 03 June 2022
doi: 10.3389/fneur.2022.927853

Positive Relationship Between Paroxysmal Vertigo and Right-to-Left Shunt: A Large Observational Study

Kaiming Liu[1†], Xiulin Tian[1†], Wenwu Hong[2†], Yujin Xiao[3†], Juanyan Chen[4†], Haidi Jin[5], Faming Wang[2], Xiaopei Xu[1], Tao Zang[6], Liang Zhang[1], Mengxiong Pan[7] and Xiaodong Zou[8]*

[1] Department of Neurology, School of Medicine, Second Affiliated Hospital, Zhejiang University, Hangzhou, China, [2] Department of Neurology, Tiantai People's Hospital of Zhejiang Province, Taizhou, China, [3] Department of Neurology, Jiaxing Hospital of Traditional Chinese Medicine, Jiaxing, China, [4] Department of Neurology, Dongyang People's Hospital, Dongyang, China, [5] Department of Neurology, Wanna Medical College, Wuhu, China, [6] Department of Neurology, Tongxiang Second People's Hospital, Tongxiang, China, [7] Department of Neurology, First People's Hospital of Huzhou, Huzhou, China, [8] Department of Neurology, Tongde Hospital of Zhejiang Province, Hangzhou, China

OPEN ACCESS

Edited by:
Su-Lin Zhang,
Huazhong University of Science and Technology, China

Reviewed by:
Rui Li,
Shaanxi Provincial People's Hospital, China
Tjasse Bruintjes,
Gelre Hospitals, Netherlands

***Correspondence:**
Xiaodong Zou
zxd753268@sina.com

[†]These authors have contributed equally to this work

Specialty section:
This article was submitted to Neuro-Otology, a section of the journal Frontiers in Neurology

Received: 25 April 2022
Accepted: 11 May 2022
Published: 03 June 2022

Citation:
Liu K, Tian X, Hong W, Xiao Y, Chen J, Jin H, Wang F, Xu X, Zang T, Zhang L, Pan M and Zou X (2022) Positive Relationship Between Paroxysmal Vertigo and Right-to-Left Shunt: A Large Observational Study. Front. Neurol. 13:927853. doi: 10.3389/fneur.2022.927853

Background: The association between paroxysmal vertigo and right-to-left shunt (RLS) is rarely reported. This study investigates the prevalence and correlation of RLS in patients with different paroxysmal vertigo diseases.

Methods: Patients with paroxysmal vertigo from seven hospitals in China were included in this observational study between 2017 and 2021. Migraine patients within the same period were included for comparison. Demographic data and medical history were collected; contrast transthoracic echocardiography was performed; and the clinical features, Dizziness Handicap Inventory, and incidence of RLS in each group were recorded.

Results: A total of 2,751 patients were enrolled. This study's results demonstrated that the proportion of RLS in patients with benign recurrent vertigo (BRV) and vestibular migraine (VM) was significantly higher than that in patients with benign paroxysmal positional vertigo, Meniere's disease, and vestibular paroxysmia ($P < 0.05$). No statistical difference was shown between the frequency of RLS in patients with BRV and those with migraine and VM. A positive correlation was shown between the RLS grade and Dizziness Handicap Inventory scores of patients with VM and BRV ($P < 0.01$) after effectively controlleding the effect of confounding variables.

Conclusions: RLS was significantly associated with BRV and VM. RLS may be involved in the pathogeneses of BRV and VM and may serve as a differential reference index for the paroxysmal vertigo.

Trial Registration: CHRS, NCT04939922, registered 14 June 2021- retrospectively registered, https://register.clinicaltrials.gov.

Keywords: benign recurrent vertigo, contrast transthoracic echocardiography, paroxysmal vertigo, right-to-left shunt, vestibular migraine

INTRODUCTION

Paroxysmal vertigo resulting from different diseases has distinct clinical symptoms and signs. However, significant overlaps exist in the clinical symptoms of different vestibular diseases, such as vestibular migraine (VM), which may have manifestations similar to Meniere's disease or benign paroxysmal positional vertigo (BPPV) (1). Furthermore, some patients with VM may have no headache, while Meniere's disease may be accompanied by migraine, photophobia, phonophobia, and other symptoms. This increases the difficulty in distinguishing these diseases from one another (2, 3).

Benign recurrent vertigo (BRV) was first described by Slater as a group of clinical syndromes with recurrent vertigo without nervous system and cochlear symptoms (4). Currently, no recognized diagnostic criteria for paroxysmal vertigo exist; thus, diagnosis is often made by exclusion (5). Follow-up studies have shown that BRV is closely associated with migraine, as 51–87% of BRV cases are comorbid with migraine (6, 7). This proportion of BRV meets the description of a definite or possible VM.

BRV and VM differ in terms of their definition and diagnostic criteria. BRV can have no headache and migraine, while VM requires at least a history of migraine or migraine-like symptoms (8). Given that BRV and VM have no specific physical or auxiliary examination findings, clinical diagnosis is often challenging. Therefore, identifying anatomic features related to certain forms of paroxysmal vertigo that may aid in establishing a diagnosis could help clinicians make a correct diagnosis. Such identification could also help determine the pathogenesis of diseases with similar clinical symptoms.

Previous studies have found that patent foramen ovale (PFO) prevalence in patients with migraine is significantly higher than that in healthy individuals (9, 10). The relationship between PFO and migraine has been studied and is a major concern (11). However, there is no good quality evidence to support a link between migraine and PFO. VM is related to vestibular symptoms caused by migraine mechanisms, and its pathogenesis may be related to ion channel defects, enhanced cortical excitability, and central sensitization, which are caused by genetic susceptibility (12, 13).

PFO is the most common cause of right-to-left shunt (RLS), which refers to the potentially abnormal channels between the left and right atrium and ventricle or systemic and pulmonary circulations. RLS can be categorized as intracardiac shunt or extracardiac based on its location. Intracardiac shunt includes PFO, while extracardiac includes pulmonary arteriovenous malformation and patent ductus arteriosus.

To date, there is little published research on the relationship between RLS and paroxysmal vertigo. Diagnostic tests used for detecting RLS include contrast transcranial Doppler, contrast transthoracic echocardiography (cTTE), and contrast transoesophageal echocardiography. Given that cTTE is easy to perform and has high sensitivity and specificity (14), we chose this method to investigate the prevalence of paroxysmal vertigo (VM with headache, VM without headache, BRV, Meniere's disease, BPPV, and vestibular paroxysmia (VP)) in adults with RLS compared to patients with migraine. This helped evaluate the correlation between RLS and different types of paroxysmal vertigo diseases.

Abbreviations: BPPV, benign paroxysmal positional vertigo; BRV, benign recurrent vertigo; cTTE, contrast transthoracic echocardiography DHI, Dizziness Handicap Inventory; MA, migraine with aura; MD, Meniere's disease; MoA, migraine without aura; PAVM, pulmonary arteriovenous malformation; PFO, patent foramen ovale; RLS, right-to-left shunt; VM, vestibular migraine; VP, vestibular paroxysmia.

METHODS

Study Design and Patient Population

Patients from the headache and vertigo clinics of seven hospitals in China were included in the study between July 2017 and July 2021 (ClinicalTrial.gov ID: NCT04939922). The study used a consecutive sampling of patients ($n = 4{,}536$) with migraine or paroxysmal vertigo aged >18 years. Patients were screened for VM, pure BRV, definite Meniere's disease, BPPV, VP, migraine with aura, and migraine without aura and, if positive, were included in the study. Patients who were diagnosed with probable migraine, psychiatric vestibular disorder, probable Meniere's disease, probable VP, functional vestibular disorder, vertebral basilar transient ischemic attack, migraine with brainstem aura, episodic ataxia, cerebellopontine angle tumor, vestibular epilepsy, or superior canal dehiscence/perilymphatic fistula, and patients with other paroxysmal vertigo who did not meet the diagnostic criteria of all other vertigo diseases, were excluded. A flowchart of patient inclusion and exclusion is depicted in **Figure 1**.

The inclusion criteria for patients with VM met the definite and probable diagnostic criteria for VM established by the International Bárány Society and the International Headache Society (8). The inclusion criteria for BRV in this study were based on the exclusive diagnostic method proposed in the literature (15) and a personal history of no migraine headache, visual aura, photophobia, or phonophobia (to distinguish and exclude definite VM and probable VM), which we defined as pure BRV here (**Table 1**).

The selection criteria for patients with definite Meniere's disease, BPPV, and VP were in accordance with the diagnostic criteria established by the Bárány Association, and the selection criteria for migraine were consistent with the diagnostic criteria of the International Classification of Headache Disorders, 3rd edition (16–19). As RLS is strongly related to migraine with auras, migraine was further divided into migraine with aura and migraine without aura. VM was further divided into VM with and without migrainous headache. All patients with VP selected in this study were responsive to carbamazepine treatment. All patients were independently diagnosed by two experienced neurologists to reduce bias.

The patients included in this study underwent cTTE and were assigned to one of eight groups based on diagnosis: VM with migrainous headache, VM without migrainous headache, pure BRV, definite Meniere's disease, BPPV, VP, migraine with aura, and migraine without aura. This study was approved by the ethics committees of the participating centers, and all patients provided written informed consent.

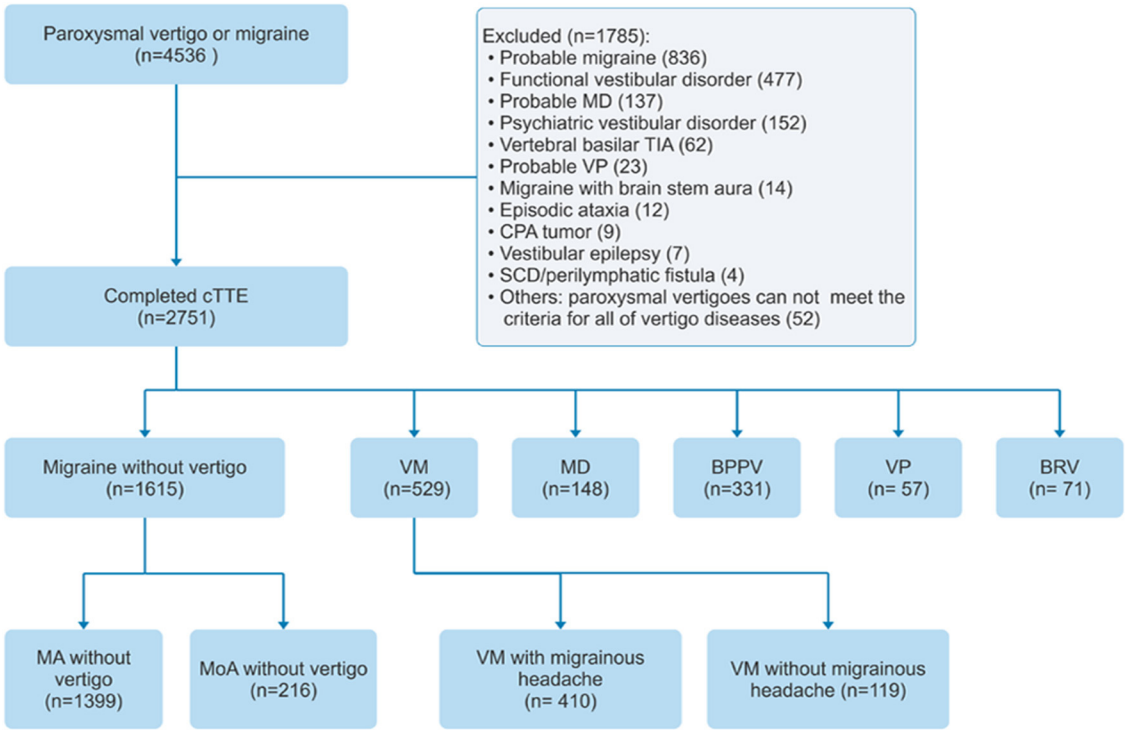

FIGURE 1 | Flowchart of the inclusion and exclusion of patients.

Contrast Transthoracic Echocardiography Inspection Method

While the patients were in the supine position, venous access was established by conventional elbow venipuncture, and a three-way tube was connected to the puncture site. The contrast medium was formulated after 8 mL saline, 1 mL venous blood, and 1 mL air were fully injected and concussed through the tee tube. The contrast was quickly injected while the patient was at rest and the Valsalva maneuver was performed. The apical four-chamber section was selected, and the number of microbubble signals in the left cardiac system was observed within 10 cardiac cycles after the right cardiac system was filled with microbubble signals. RLS of the heart was considered when there was more than one microbubble in the left cardiac cavity.

The RLS was graded quantitatively according to the number of microbubbles in the left ventricular cavity after the Valsalva maneuver. The grading standard is as follows: grade 0: no microbubbles in the left cardiac cavity and no RLS; grade I: 1–10 microbubbles/frame were seen in the left ventricular cavity and a small amount of RLS; grade II: 10–30 microbubbles/frame were seen in the left cardiac cavity and a medium amount of RLS; and grade III: more than 30 microbubbles/frame was seen in the left ventricular cavity, or the left ventricular cavity was almost full of microbubbles (20).

RLS from PFO was considered when microbubbles were found within 3–5 cardiac cycles, while RLS from pulmonary arteriovenous malformations was considered when microbubbles were found in more than five cardiac cycles during the cTTE examination (21).

Dizziness Handicap Inventory

The quality of life measure for vestibular disorders was assessed using the 25-item Dizziness Handicap Inventory (DHI), which has three response categories: the functional, emotional, and physical aspects of life (22). The total score ranges from 0 (not handicapped) to 100 (severely handicapped).

Statistical Analysis

Data measurements assumed a normal distribution and are expressed as $x \pm s$. We used the χ^2 test and *t*-test (or Mann–Whitney *U*-test) to compare categorical and continuous variables. Spearman's correlation coefficient was used to analyse the correlation between the DHI and RLS grades. The level of statistical significance was set at $P < 0.05$. All analyses were performed using SPSS software version 20 (IBM Corp., Armonk, NY, USA).

RESULTS

Patient Demographic and Clinical Characteristics at Baseline

Within the time frame, a total of 2,751 patients completed cTTE at the outpatient departments of the seven participating centers. The mean age was 43.16 ± 14.58 years, and 65.18% were women.

The demographics and clinical characteristics of the patients are summarized in **Table 2**.

Right-to-Left Shunt in Patients From Different Groups

The patients (61.98%) who were RLS-positive patients were detected by cTTE after the Valsalva maneuver. The proportion of RLS in patients with BRV and VM with and without migrainous headache was significantly higher than that in patients with Meniere's disease, BPPV, or VP ($P < 0.05$). There was no statistical difference between the frequency of RLS in patients with BRV and those with migraine without aura ($P = 0.931$), migraine with aura ($P = 0.997$), VM with migrainous headache ($P = 0.787$), and VM without migrainous headache ($P = 0.754$) (**Table 3** and **Figure 2**).

TABLE 1 | Inclusion criteria for pure benign recurrent vertigo.

More than two attacks of spontaneous rotational vertigo that does not occur during the head movements or positional changes
No associated migrainous headaches or auditory symptoms during or between the attacks
No associated photophobia and phonophobia
No associated visual aura
No associated focal neurologic symptom during the attack or afterward suggesting episodic ataxia, transient ischemic attack, or vestibular epilepsy
No evidence of peripheral vestibulopathy on head-impulse, caloric, and rotatory tests
No asymmetric hearing impairment documented in pure-tone audiometry
No lesions on brain magnetic resonance imaging responsible for the benign recurrent vertigo
No history of disorders that may explain the recurrent vertigo
Not better accounted for by another vestibular disorder, including compensated vestibular neuritis, vestibular migraine, Meniere's disease, benign paroxysmal positional vertigo, and vestibular paroxysmia

Right-to-Left Shunt in Patients With Benign Recurrent Vertigo

The proportion of RLS in seven patients with BRV lasting <1 min was similar to those lasting for more than 1 min (71.43 vs. 73.44%). This was significantly higher than in VP (26.31%) and BPPV (25.38%). The proportion of RLS in patients with BRV aged <50 years and those aged ≥50 years was similar (73.08 vs. 73.68%), and the difference was not statistically significant.

Association Between Right-to-Left Shunt Grade and Dizziness Handicap Inventory Scores

Based on the semi-quantitative classification of RLS, the DHI scores of grades 0, I, II, and III of patients from different groups are shown in **Table 3**. The RLS grade and DHI scores in patients with VM with migrainous headache ($r = 0.361$, 95% confidence interval [CI] 0.27–0.44), without migrainous headache ($r = 0.528$, 95% CI 0.38–0.65), and BRV ($r = 0.565$, 95% CI 0.38–0.71) are shown in **Figures 3A–C**, respectively. The DHI scores and RLS grades of all patients with VM or BRV ($r = 0.412$, 95% CI 0.34–0.48) are presented in **Figure 3D**. In patients with VM and BRV, the DHI scores increased with increasing RLS grades, and there was a positive correlation between them ($P < 0.01$).

DISCUSSION

Common paroxysmal vertigo can be categorized based on the following etiologies: central and peripheral. The most common central causes are VM and transient ischemic attack, and the most common peripheral causes are BPPV, Meniere's disease, and VP.

TABLE 2 | Demographic and clinical characteristics of patients at baseline.

	MoA without vertigo (*n* = 1,399)	MA without vertigo (*n* = 216)	VM with migrainous headache (*n* = 410)	VM without migrainous headache (*n* = 119)	MD (*n* = 148)	BPPV (*n* = 331)	VP (*n* = 57)	BRV (*n* = 71)
Sex (female, %)	73.27	75.46	76.83	72.27	57.43	64.65	59.65	71.83
Age (mean±SD)	39.85 ± 15.47	37.7 ± 15.41	42.67 ± 12.56	36.67 ± 14.99	52.35 ± 7.28	56.13 ± 10.48	53.74 ± 6.15	50.7 ± 18.93
Duration of attacks								
<1			45	17	0	331	47	7
<5	NA	NA	94	15	0	0	10	13
<1			128	29	85	0	0	26
<24			118	41	63	0	0	18
<24			25	17	0	0	0	7
Migrainous headache	1,399	216	410	0	0	0	0	0
Aura	0	216	53	16	0	0	0	0
Photophobia	992	156	386	107	0	2	1	3
Phonophobia	984	167	389	110	1	0	0	1
Photophobia and phonophobia	961	144	372	101	0	0	0	0

BPPV, benign paroxysmal positional vertigo; BRV, benign recurrent vertigo; h, hour; MA, migraine with aura; MD, Meniere's disease; min, minute; MoA, migraine without aura; NA, not available; VM, vestibular migraine; SD, standard deviation; VP, vestibular paroxysmia.

TABLE 3 | Right-to-left shunt and Dizziness Handicap Inventory in patients from different groups.

	MoA without vertigo (n = 1,399)	MA without vertigo (n = 216)	VM with migrainous headache (n = 410)	VM without migrainous headache (n = 119)	MD (n = 148)	BPPV (n = 331)	VP (n = 57)	BRV (n = 71)
RLS (%)	65.33	81.01	77.07	76.47	27.03	25.38	26.31	73.24
PFO	828	153	292	79	35	73	14	46
PAVM	57	12	19	9	2	8	1	4
PFO & PAVM	29	10	5	3	3	3	0	2
Grading of RLS								
0	485	41	94	28	108	247	42	19
I	263	33	68	17	17	40	7	12
II	257	54	106	34	14	30	3	18
III	394	88	142	40	9	14	5	22
DHI	NA	NA	46.33 ± 10.61	47.46 ± 9.40	51.26 ± 9.48	47.37 ± 13.42	50.69 ± 6.87	46.87 ± 10.37

BPPV, benign paroxysmal positional vertigo; BRV, benign recurrent vertigo; DHI, Dizziness Handicap Inventory; MA, migraine with aura; MD, Meniere's disease; MoA, migraine without aura; NA, not available; PAVM, pulmonary arteriovenous malformation; PFO, patent foramen ovale; RLS, right-to-left shunt; VM, vestibular migraine; VP, vestibular paroxysmia.

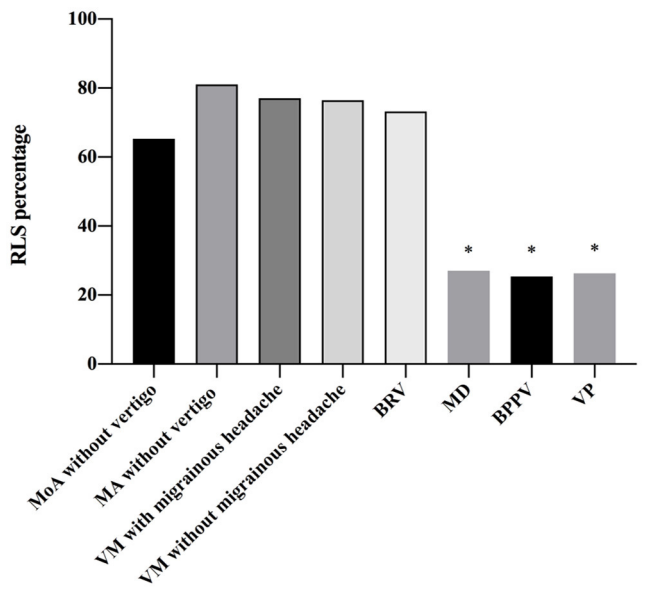

FIGURE 2 | Frequency of right-to-left shunt (RLS) in patients with different diseases. There is a statistical difference between the frequency of RLS in patients with benign recurrent vertigo (BRV) and that in patients with Meniere's disease (MD), benign paroxysmal positional vertigo (BPPV), and vestibular paroxysmia (VP). The proportion of RLS in patients with BRV is significantly higher than that in patients with MD, BPPV, and VP ($P < 0.05$). The proportion of RLS in patients vestibular migraine (VM) with and without migrainous headaches is also significantly higher than that in patients with MD, BPPV, and VP ($P < 0.05$). However, there is no statistical difference between the frequency of RLS in patients with BRV and that in migraine without aura ($P = 0.931$), MA ($P = 0.997$), VM with migrainous headache ($P = 0.787$), and VM without migrainous headache ($P = 0.754$). BPPV, benign paroxysmal positional vertigo; BRV, benign recurrent vertigo; MA, migraine with aura; MD, Meniere's disease; MoA, migraine without aura; RLS, right-to-left shunt; VM, vestibular migraine; VP, vestibular paroxysmia. *$P < 0.05$.

VM is a separate disease entity with a genetic predisposition to recurrent dizziness or vertigo, with or without headache (23, 24). The BRV selected in previous clinical studies did not rule out a history of migraine and migraine-related symptoms; therefore, a considerable number of BRV cases may have met the diagnostic criteria for VM (6, 7). To avoid confusion, the selected BRV cases in this study only showed paroxysmal vertigo, that is, pure BRV. The selected patients with VM without headache could be differentiated from pure BRV by its migraine characteristics, such as photophobia, phonophobia, or visual aura. This study's results demonstrated, for the first time, that patients with BRV had a significantly higher proportion of RLS than those with peripheral vertigo diseases such as Meniere's disease, BPPV, or VP. Moreover, there was no statistical difference between RLS frequency in patients with BRV and those with VM and migraine. It is unknown whether BRV is a peripheral or central disorder. There have been some efforts to further categorize patients with BRV according to their etiology. For instance, Lee et al. described a new type of BRV with headshaking nystagmus of central origin (15). Although there were no central symptoms of photophobia, phonophobia, or visual aura, we speculate whether the central mechanisms are involved in pure BRV, and this is worthy of further study to clarify this disease entity.

There is a dose-effect relationship between PFO and migraine. Larger PFO, permanent PFO, and anatomical variation of PFO can aggravate RLS, which is associated with migraine attacks (11, 24). Moreover, PFO is more associated with migraine with aura than migraine without aura. The correlation between RLS and migraine does not imply causality, and the mechanism between the two is not clear. The possible mechanism is that vasoactive substances and microemboli from the venous system directly enter systemic circulation without passing through the pulmonary circulation. Thereby causing transient hypoperfusion in the area supplied by the cerebral arteries or cortical spreading

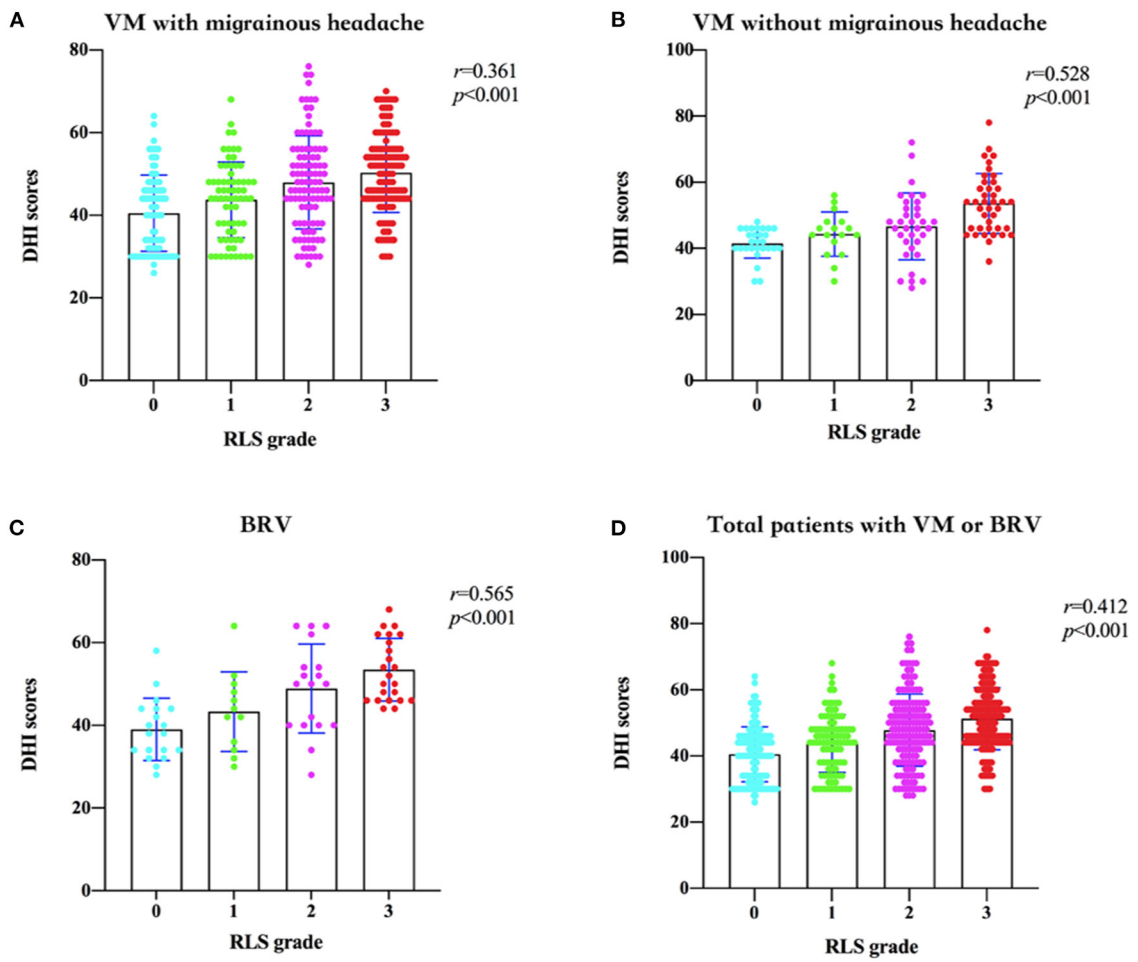

FIGURE 3 | Dizziness Handicap Inventory (DHI) scores and the right-to-left shunt (RLS) grades in patients with vestibular migraine (VM) and benign recurrent vertigo (BRV). **(A)** In patients with VM with migrainous headaches, the DHI scores increase with increasing RLS grades, and there is a positive correlation between them. **(B)** In patients with VM without migrainous headaches, the DHI scores increase with increasing RLS grades, and there is a positive correlation between them. **(C)** In patients with BRV, the DHI scores increase with increasing RLS grades, and there is a positive correlation between them. **(D)** In all patients with VM or BRV, the DHI scores increase with increasing RLS grades, and there is a positive correlation between them. DHI, Dizziness Handicap Inventory; RLS, right-to-left shunt; VM, vestibular migraine; BRV, benign recurrent vertigo.

depression, activating the trigeminal neurovascular system, and causing migraine attacks (25, 26). The initiating mechanism of VM is considered to be similar to that of migraine because RLS not only induces migraine but also causes vertigo by inducing plasma extravasation in the inner ear (27). In addition, microemboli or vasoactive substances may induce cortical spreading depression and activate the caudal parabrachial nucleus, which receives both trigeminal receptors and vestibular nerve afferents, resulting in simultaneous vestibular and migraine symptoms (1, 28). Therefore, we speculate that RLS may be involved in the pathogenesis of VM.

Many studies have found that BRV is highly correlated with migraine or VM and may have similar pathogenesis (6, 29, 30). However, some research has suggested otherwise (31). The question of whether BRV is a separate entity remains controversial, but a considerable number of BRVs are free from inner ear dysfunction and migraine and, therefore, do not develop into Meniere's disease and VM, suggesting that there may be different mechanisms in this aspect of BRV (7).

This study showed that the proportion of RLS in patients with BRV, VM, and migraine was significantly higher than in those with peripheral vertigo disease, suggesting that RLS might play an important role in the pathogenesis of BRV, VM, and migraine. The current literature remains discordant as to whether a link exists between RLS grade and the degree of vertigo. We found that the DHI score increased with RLS, suggesting that RLS plays an important role in the degree of vertigo and quality of life of vestibular disorders. The proportions of RLS in patients with BRV and VM were similar to those of migraine, suggesting that the above-mentioned mechanisms may share some features in the pathogenesis of migraine.

When the related mechanism of migraine involves only the vestibular system, it can manifest as pure BRV, whereas when the vestibular system and trigeminal neurovascular system are simultaneously involved, it can manifest as VM. When only the trigeminal neurovascular system is involved, the symptoms may include migraine, suggesting that BRV and VM may be subtypes or equivalents of migraine. VM and pure BRV can thus be unified in the migraine category. In this study, the RLS of patients with BPPV and VP was significantly lower than that of patients with migraine, suggesting that RLS was not involved in the pathogenesis of these peripheral vertigo diseases. RLS can play a role in the differential reference index of paroxysmal vertigo. In the future, for patients with refractory VM and BRV, the evaluation, intervention, and treatment of RLS would be worthy of further exploration.

Previous publications in the literature have predominantly defined the duration of BRV as more than 1 min or, in some studies, even more than 5 min; this extended duration primarily distinguishes BRV from BPPV and VP, which each have a duration of <1 min. There are few reports of a BRV of <1 min. A previous study found six cases of BRV with migraine that were <1 min, and only one case of BRV without migraine was <1 min (6). In clinical practice, there are truly spontaneous recurrent vertigo episodes lasting <1 min. These patients do not meet the diagnostic criteria for BPPV, VP, and VM. The duration of BRV was not specifically limited in this study. The proportion of RLS between the patients with BRV lasting less and more than 1 min was similar and significantly higher than that of VP and BPPV. Thus, strictly defining the duration as a criterion for diagnosing BRV may be debatable, and the evaluation of RLS may help provide a reference for BRV diagnosis.

Owing to the low probability of migraine onset after age 50 (32), patients with headache-free BRV after the age of 50 years have a low probability of developing VM, while patients with BRV before age 50 years have the possibility of progressing to VM. Therefore, we regarded age 50 as the threshold for the intragroup (subgroup) analysis of BRV. This study's results showed that the proportion of RLS in patients with BRV before and after age 50 was not significantly different and was similar to that of migraine. This may be related to the fact that BRV rarely evolves into VM (33).

With the insight into VM and the gradual clarification of its concept, there is an overlap between the classical concepts of BRV and VM, leading to ambiguity in the concept of BRV; thus, the effective use of the concept of BRV in clinics is difficult. In this study, pure BRV was proposed for the first time, and it can be effectively distinguished from VM in the absence of migraine-related characteristics. Pure BRV can also be effectively distinguished from peripheral vertigo, such as Meniere's disease. Therefore, the concept of pure BRV is helpful for clinicians to further study the mechanism, clinical characteristics, and prognosis of the disease. The concept and classification of VM and BRV in the future are worthy of further discussion.

There are some limitations to this study. First, vertebral basilar transient ischemic attack, persistent postural-perceptual dizziness, epileptic vertigo, and paroxysmal ataxia were excluded from the selection criteria of BRV in this study, therefore, these paroxysmal vertigo diseases were not compared with RLS. Second, there was a selection bias because the final selected patients were from both headache clinic and vertigo clinic. Additionally, BRV with headshaking nystagmus has been reported to originate from the central nervous system, and in this study, BRV was not subdivided according to whether it was associated with headshaking nystagmus.

CONCLUSIONS

This is a large multicentre study, and the findings show that RLS differs in different types of paroxysmal vertigo. The prevalence of RLS in pure BRV and VM was similar but significantly higher than that in Meniere's disease, BPPV, and VP. There was a positive correlation between the RLS grading and DHI among patients with BRV and VM. The existence of RLS is valuable in the etiological diagnosis of paroxysmal vertigo and may be used as a differential reference index for the paroxysmal vertigo.

DATA AVAILABILITY STATEMENT

The raw data supporting the conclusions of this article will be made available by the authors, without undue reservation.

ETHICS STATEMENT

The studies involving human participants were reviewed and approved by the Ethics Committee of the Second Affiliated Hospital, School of Medicine, Zhejiang University. The patients/participants provided their written informed consent to participate in this study.

AUTHOR CONTRIBUTIONS

KL conducted the design and conceptualization of the study, interpretation of the data, and revising the manuscript. XZ wrote and designed the manuscript. XT analyzed and interpreted the data. WH, YX, JC, HJ, XX, TZ, LZ, and MP collected and organized the data. All authors contributed to the article and approved the submitted version.

FUNDING

This study was funded by the Zhejiang Provincial Natural Science Foundation of China [Grant Nos. LY19H090025 and LQ15H090003] and the National Natural Science Foundation of China [Grant Nos. 82171561 and 82174132]. The funders had no role in the design of this study or in the interpretation or presentation of its results.

REFERENCES

1. Furman JM, Marcus DA, Balaban CD. Vestibular migraine: clinical aspects and pathophysiology. *Lancet Neurol.* (2013) 12:706–15. doi: 10.1016/S1474-4422(13)70107-8
2. Stolte B, Holle D, Naegel S, Diener HC, Obermann M. Vestibular migraine. *Cephalalgia.* (2015) 35:262–70. doi: 10.1177/0333102414535113
3. Radtke A, Lempert T, Gresty MA, Brookes GB, Bronstein AM, Neuhauser H. Migraine and Meniere's disease: is there a link? *Neurology.* (2002) 59:1700–4. doi: 10.1212/01.WNL.0000036903.22461.39
4. Slater R. Benign recurrent vertigo. *J Neurol Neurosurg Psychiatry.* (1979) 42:363–7. doi: 10.1136/jnnp.42.4.363
5. van Esch BF, van Wensen E, van der Zaag-Loonen HJ, Benthem PPGV, van Leeuwen RB. Clinical characteristics of benign recurrent vestibulopathy: clearly distinctive from vestibular migraine and Meniere's disease? *Otol Neurotol.* (2017) 38:e357–63. doi: 10.1097/MAO.0000000000001553
6. Cha YH, Lee H, Santell LS, Baloh RW. Association of benign recurrent vertigo and migraine in 208 patients. *Cephalalgia.* (2009) 29:550–5. doi: 10.1111/j.1468-2982.2008.01770.x
7. Brantberg K, Baloh RW. Similarity of vertigo attacks due to Meniere's disease and benign recurrent vertigo, both with and without migraine. *Acta Otolaryngol.* (2011) 131:722–7. doi: 10.3109/00016489.2011.556661
8. Lempert T, Olesen J, Furman J, Waterston J, Seemungal B, Carey J, et al. Vestibular migraine: diagnostic criteria. *J Vestib Res.* (2012) 22:167–72. doi: 10.3233/VES-2012-0453
9. Lip PZ, Lip GY. Patent foramen ovale and migraine attacks: a systematic review. *Am J Med.* (2014) 127:411–20. doi: 10.1016/j.amjmed.2013.12.006
10. Tariq N, Tepper SJ, Kriegler JS. Patent foramen ovale and migraine: closing the debate - a review. *Headache.* (2016) 56:462–78. doi: 10.1111/head.12779
11. Liu K, Wang BZ, Hao Y, Song S, Pan M. The correlation between migraine and patent foramen ovale. *Front Neurol.* (2020) 11:543485. doi: 10.3389/fneur.2020.543485
12. Baloh RW. Vestibular migraine I: mechanisms, diagnosis, and clinical features. *Semin Neurol.* (2020) 40:76–82. doi: 10.1055/s-0039-3402735
13. Dieterich M, Obermann M, Celebisoy N. Vestibular migraine: the most frequent entity of episodic vertigo. *J Neurol.* (2016) 263:S82–9. doi: 10.1007/s00415-015-7905-2
14. Mojadidi MK, Winoker JS, Roberts SC, Msaouel P, Gevorgyan R, Zolty R. Two-dimensional echocardiography using second harmonic imaging for the diagnosis of intracardiac right-to-left shunt: a meta-analysis of prospective studies. *Int J Cardiovasc Imaging.* (2014) 30:911–23. doi: 10.1007/s10554-014-0426-8
15. Lee SU, Choi JY, Kim HJ, Kim JS. Recurrent spontaneous vertigo with interictal headshaking nystagmus. *Neurology.* (2018) 90:e2135–45. doi: 10.1212/WNL.0000000000005689
16. Lopez-Escamez JA, Carey J, Chung WH, Goebel JA, Magnusson M, Mandalà M, et al. Diagnostic criteria for Menière's disease. *J Vestib Res.* (2015) 25:1–7. doi: 10.3233/VES-150549
17. von Brevern M, Bertholon P, Brandt T, Fife T, Imai T, Nuti D, et al. Benign paroxysmal positional vertigo: diagnostic criteria. *J Vestib Res.* (2015) 25:105–17. doi: 10.3233/VES-150553
18. Strupp M, Lopez-Escamez JA, Kim JS, Straumann D, Jen JC, Carey J, et al. Vestibular paroxysmia: diagnostic criteria. *J Vestib Res.* (2016) 26:409–15. doi: 10.3233/VES-160589
19. Headache Classification Committee of the international headache S. The International Classification of Headache Disorders. 3rd ed. (beta version). *Cephalalgia.* (2013) 33:629–808. doi: 10.1177/0333102413485658
20. Zhao E, Wei Y, Zhang Y, Zhai N, Zhao P, Liu B, et al. comparison of Transthroracic Echocardiograpy and transcranial Doppler with contrast agent for detection of patent foramen ovale with or without the valsalva maneuver. *Med (Baltim).* (2015) 94:e1937. doi: 10.1097/MD.0000000000001937
21. Freeman JA, Woods TD. Use of saline contrast echo timing to distinguish intracardiac and extracardiac shunts: failure of the 3- to 5-beat rule. *Echocardiography.* (2008) 25:1127–30. doi: 10.1111/j.1540-8175.2008.00741.x
22. Jacobson GP, Newman CW. The development of the Dizziness Handicap Inventory. *Arch Otolaryngol Head Neck Surg.* (1990) 116:424–7. doi: 10.1001/archotol.1990.01870040046011
23. Huang TC, Wang SJ, Kheradmand A. Vestibular migraine: an update on current understanding and future directions. *Cephalalgia.* (2020) 40:107–21. doi: 10.1177/0333102419869317
24. Kumar P, Kijima Y, West BH, Tobis JM. The connection between patent foramen ovale and migraine. *Neuroimaging Clin N Am.* (2019) 29:261–70. doi: 10.1016/j.nic.2019.01.006
25. Beda RD, Gill EA Jr. Patent foramen ovale: does it play a role in the pathophysiology of migraine headache? *Cardiol Clin.* (2005) 23:91–6. doi: 10.1016/j.ccl.2004.10.004
26. Morelli N, Rota E. Migraine and patent foramen ovale: barking up the wrong tree? *Front Neurol.* (2014) 5:99. doi: 10.3389/fneur.2014.00099
27. Koo JW, Balaban CD. Serotonin-induced plasma extravasation in the murine inner ear: possible mechanism of migraine-associated inner ear dysfunction. *Cephalalgia.* (2006) 26:1310–9. doi: 10.1111/j.1468-2982.2006.01208.x
28. Marano E, Marcelli V, Di Stasio E, Bonuso S, Vacca G, Manganelli F, et al. Trigeminal stimulation elicits a peripheral vestibular imbalance in migraine patients. *Headache.* (2005) 45:325–31. doi: 10.1111/j.1526-4610.2005.05069.x
29. Neuhauser H, Leopold M, von Brevern M, Arnold G, Lempert T. The interrelations of migraine, vertigo, and migrainous vertigo. *Neurology.* (2001) 56:436–41. doi: 10.1212/WNL.56.4.436
30. Oh AK, Lee H, Jen JC, Corona S, Jacobson KM, Baloh RW. Familial benign recurrent vertigo. *Am J Med Genet.* (2001) 100:287–91. doi: 10.1002/ajmg.1294
31. Lee HK, Ahn SK, Jeon SY, Kim JP, Park JJ, Hur DG, et al. Clinical characteristics and natural course of recurrent vestibulopathy: a long-term follow-up study. *Laryngoscope.* (2012) 122:883–6. doi: 10.1002/lary.23188
32. Charles A. Migraine. *N Engl J Med.* (2017) 377:553–61. doi: 10.1056/NEJMcp1605502
33. Pan Q, Zhang Y, Zhang S, Wang W, Jiang H, Fan Y, et al. Clinical features and outcomes of benign recurrent vertigo: a longitudinal study. *Acta Neurol Scand.* (2020) 141:374–9. doi: 10.1111/ane.13214

Conflict of Interest: The authors declare that the research was conducted in the absence of any commercial or financial relationships that could be construed as a potential conflict of interest.

Publisher's Note: All claims expressed in this article are solely those of the authors and do not necessarily represent those of their affiliated organizations, or those of the publisher, the editors and the reviewers. Any product that may be evaluated in this article, or claim that may be made by its manufacturer, is not guaranteed or endorsed by the publisher.

Copyright © 2022 Liu, Tian, Hong, Xiao, Chen, Jin, Wang, Xu, Zang, Zhang, Pan and Zou. This is an open-access article distributed under the terms of the Creative Commons Attribution License (CC BY). The use, distribution or reproduction in other forums is permitted, provided the original author(s) and the copyright owner(s) are credited and that the original publication in this journal is cited, in accordance with accepted academic practice. No use, distribution or reproduction is permitted which does not comply with these terms.

frontiers | Frontiers in Neurology

ORIGINAL RESEARCH
published: 15 June 2022
doi: 10.3389/fneur.2022.927235

Correlation Between the Prognosis of Sudden Total Deafness and the Peripheral Blood Inflammation Markers

Tongxiang Diao[1†], *Yujie Ke*[1†], *Junbo Zhang*[2†], *Yuanyuan Jing*[1†] *and Xin Ma*[1*]

[1] *Department of Otolaryngology, Head and Neck Surgery, People's Hospital, Peking University, Beijing, China,* [2] *Department of Otolaryngology, Head and Neck Surgery, Peking University First Hospital, Beijing, China*

Objective: To analyze the correlation between prognosis of sudden total deafness (STD) and peripheral blood inflammation markers including white blood cell count (WBC), monocytes, neutrophil/lymphocyte ratio (NLR), platelet/lymphocyte ratio (PLR), fibrinogen (FIB).

Methods: 125 patients with STD who were hospitalized in our department from 2014 to 2019 were enrolled. The general physical conditions, clinical manifestations, pure tone audiometry, imaging examination, and peripheral blood inflammation markers were collected, and all patients were divided into effective and ineffective two groups according to the degree of hearing recovery at the time of discharge. Then binary logistic regression was used to analyze the correlation between multiple factors and prognosis, meanwhile the receiver operating characteristic (ROC) curve was used to evaluate the predictive value of the above prognostic factors.

Results: Compared with the ineffective group, patients in the effective group were younger and have higher PLR level and lower FIB levels. Age and PLR are independent prognostic factors. Taking age ≤56 years old, PLR >142.6 as the standard to predict the prognosis of patients with STD has the largest AUC with the potential effective rate reaching 78.1%.

Conclusions: Age and PLR are independent prognostic factors for patients with STD. The younger the age and the higher the PLR, the better the prognosis. Clinically, the prognosis of patients with STD can be evaluated by the patient's age and PLR level, which is of great significance to predict the prognosis of patients with STD.

Keywords: peripheral blood inflammation markers, prognosis, sudden total deafness, PLR, inflammation

OPEN ACCESS

Edited by:
Jian-hua Zhuang,
Shanghai Changzheng Hospital, China

Reviewed by:
Dongzhen Yu,
Shanghai Jiao Tong University, China
Takwa Gabr,
Kafrelsheikh University, Egypt
Yuanchia Chu,
Taipei Veterans General Hospital, Taiwan

***Correspondence:**
Xin Ma
13581709195@163.com

[†] These authors have contributed equally to this work

Specialty section:
This article was submitted to Neuro-Otology, a section of the journal Frontiers in Neurology

Received: *24 April 2022*
Accepted: *20 May 2022*
Published: *15 June 2022*

Citation:
Diao T, Ke Y, Zhang J, Jing Y and Ma X (2022) Correlation Between the Prognosis of Sudden Total Deafness and the Peripheral Blood Inflammation Markers. Front. Neurol. 13:927235. doi: 10.3389/fneur.2022.927235

INTRODUCTION

Sudden sensorineural hearing loss (SSHL) refers to sensorineural hearing loss with no identifiable cause that occurs within 72 h. The Clinical Practice Guideline: Sudden Hearing Loss of American Academy of Otolaryngology (2019) defines it as a decrease in hearing of ≥30 dB affecting at least 3 consecutive frequencies, may be accompanied by tinnitus, ear fullness, numbness, dizziness and other discomforts. Clinically, it usually manifests as unilateral disease, and bilateral SSHL

is rare. According to previous studies, the incidence of SSHL is 5-160/100,000 (1, 2), and there is an increasing trend year by year. The etiology and pathophysiological mechanism of sudden deafness have not been fully elucidated. At present, the mechanisms that may be related include blood vessels, immunity, viruses, inner ear hydrops, etc. In recent years, with the hypothesis of pathological activation of cellular stress pathways, chronic inflammation has drawn more attention for its important role in the pathogenesis of SSHL.

Chronic inflammation has been proved to be an important risk factor for microvascular injury and atherosclerosis (3). Researchers believe that it can also damage the vascular endothelial function of the inner ear, leading to hearing loss (4). The correlation between peripheral blood inflammatory markers, such as white blood cell (WBC) count, WBC subtype count, neutrophil to lymphocyte ratio (NLR) and platelet to lymphocyte ratio (PLR) and SSHL has been widely recognized by clinical researchers. At present, it is considered that these inflammatory markers, especially NLR, are significantly correlated with the SSHL (5, 6), However, the correlation between NLR and PLR and the prognosis of SSHL is still controversial (6, 7). SSHL has great heterogeneity. The degree of hearing loss, audiogram shapes and different accompanying symptoms may suggest different pathologies. Previous studies have not classified SSHL, which may explain the inconsistent conclusions. According to Chinese guidelines for the diagnosis and treatment of sudden deafness (2015) (8), sudden total deafness (STD) refers to absent response at all tested frequencies, with an average hearing threshold ≥80 dB HL (2015) (8). Because of the severe hearing loss, patients with STD always be accompanied with many symptoms, including tinnitus (9), dizziness or vertigo (10), numbness around the ear (11), anxiety, depression, and insomnia, which would greatly reduce the quality of life. This study chose patients with STD as the research subjects to explore the relationship between the peripheral blood inflammatory markers and the prognosis of STD, trying to seek for markers that may indicate the prognosis of STD.

MATERIALS AND METHODS

Study Subjects

Between Jan 2014 and Jan 2019, eligible patients with STD who were hospitalized in our department for treatments were continuously enrolled. The detailed inclusion criteria were: (1) sudden sensorineural hearing loss occurred within 72 h; (2) the hearing thresholds of all frequencies were increased and were nearly consistent, with an average hearing threshold of 250–8,000Hz (250, 500, 1,000, 2,000, 3,000, 4,000, and 8,000 Hz) ≥80dBnHL; (3) the time from onset of hearing loss to treatments was <30 days. (4) receive no treatment before admission. (5) acoustic neuroma and other diseases are excluded from CT or MRI. Patients who could not cooperate due to severe mental factors and patients whose hearing loss had clear causes were excluded, such as excessive noise exposure, Meniere's disease, middle ear structure malformation, post-cochlear diseases, and histories of ototoxic drug use, head trauma, and ear surgery.

A total of 125 patients with STD were finally included. All pure-tone audiometry tests were performed by a same audiologist in a soundproof room using the Interacoustics Clinical Audiometer AC40. The following baseline information of these patients were collected for analysis, including sex, age, affected ear side, body mass index (BMI), disease course (the time from onset to therapy), accompanying symptoms such as tinnitus or dizziness, the average value of 250, 500-, 1,000-, 2,000-, 3,000, 4,000, and 8,000-Hz air conduction pure tone average hearing thresholds (PTA) of affected ear, chronic diseases history such as hypertension, diabetes, and hyperlipidemia. The blood routine data included white blood cell count (WBC), neutrophil count (NEU), monocyte count (MONO), platelet count (PLT), neutrophil/lymphocyte count ratio (NLR), platelet/lymphocyte count ratio (PLR), and fibrinogen level (FIB).

Treatments

The treatments of this group of patients were nearly the same according to Chinese guidelines for treating sudden deafness in 2015 (8), which included ginkgo biloba extract injection for improving microcirculation, batroxobin for decreasing plasma fibrinogen level, mecobalamin, glucocorticoid, etc.

Evaluation of Treatment Efficacy

The treatment efficacy was evaluated by comparing hearing thresholds of impaired frequencies (IF) before and 2–4 weeks after treatments. A patient was defined as effective if the IF of affected ear decreased by 15 or more than 15 dB. While when the IF of affected ear decreased by <15 dB a patient was defined as in-effective (2015).

Ethics Statement

The Peking University People's Hospital Ethical permission committee approved study (2021PHB149) and all subjects provided written informed consents.

Statistical Analysis

All the statistical analysis of this study were completed by SPSS 20.0 soft package (IBM, Armonk, NY, USA). All continuous data were displayed as mean±standard deviation. The unpaired student's *t*-test was used to compare the quantitative variables among different groups. Pearson's Chi-square test was used to compare the categorical variables among different groups. Multiple logistic regression analysis was used to evaluate the significance of independent variables of treatment efficacy. The Receiver Operating Characteristic (ROC) curve-test was used to determine the best cutoff value of independent variables. A $p < 0.05$ was considered to be statistically significant.

RESULTS

Baseline Information

Totally, among the 125 patients with STD 68 patients were effective and 57 patients were in-effective, with an overall effective rate of 54.4%. The comparisons of baseline information before treatments were shown in **Table 1**, suggested significantly smaller age, higher PLR value, and lower FIB value in effective group

TABLE 1 | The comparisons of baseline information between effective and in-effective group.

	All patients ($n = 125$)	Effective group ($n = 68$)	In-effective group ($n = 57$)	P
Age (years)	50.0 ± 17.4	46.6 ± 17.5	54.1 ± 16.5	0.015*
BMI (kg/m^2)	24.5 ± 3.2	24.4 ± 3.3	24.7 ± 3.0	0.632
Affected side (left)	62	34	28	1.000
Sex (female)	63	32	31	0.474
Onset-therapy (days)	10.38 ± 9.44	9.59 ± 8.81	11.32 ± 10.15	0.310
PTA (dB)	106.9 ± 14.1	107.3 ± 13.7	106.3 ± 14.5	0.694
WBC	8.5 ± 3.0	8.7 ± 3.2	8.3 ± 2.8	0.432
NEU	6.1 ± 2.9	6.4 ± 3.1	5.8 ± 2.6	0.330
NLR	3.9 ± 2.7	4.3 ± 2.9	3.5 ± 2.4	0.131
PIT	231.4 ± 60.1	240.9 ± 62.0	220.1 ± 56.2	0.051
PLR	146.2 ± 8.0	160.1 ± 94.3	129.8 ± 56.2	0.028*
MONO	0.4 ± 0.2	0.4 ± 0.2	0.4 ± 0.2	0.979
FIB	216.3 ± 105.0	197.6 ± 100.8	238.6 ± 106.4	0.030*
Dizziness (Yes)	68	34	34	0.367
Tinnitus (Yes)	105	61	47	0.298
Diabetes (Yes)	21	11	10	1.000
Hypertension (Yes)	35	21	14	0.549
Hyperlipemia (Yes)	15	7	8	0.585

BMI, body mass index; PTA, pure tone average hearing thresholds; WBC, white blood cell count; NEU, neutrophil count; NLR, neutrophil/lymphocyte count ratio; PIT, platelet count; PLR, platelet/lymphocyte count ratio; MONO, monocyte count; FIB, fibrinogen level.
$^*P < 0.05$.

TABLE 2 | Logistic predictors to prognosis of patients with STD.

	OR value	95%CI	*P*
Age (years)	1.024	1.002–1.048	0.036*
PLR (10^9/L)	0.993	0.988–0.999	0.022*
FIB	1.004	1.000–1.007	0.063

STD, sudden total deafness; PLR, platelet/lymphocyte count ratio; FIB, fibrinogen level.
$^*P < 0.05$.

than in in-effective group (all $P < 0.05$). No other factors differed significantly between these two groups of patients (all $P > 0.05$).

Independent Predictors for Prognosis of Patients With Sudden Total Deafness

In order to further explore independent predictors for prognosis of patients with STD, the pre-treatment factors which differed significantly between effective and in-effective group, including age, PLR value, and FIB value, were all incorporated into a logistic analysis for predicting treatment response. As shown in **Table 2**, only age and PLR value could be included, and the OR values were 1.024 for age (95%CI: 1.002–1.048) and 0.993 for PLR (95%CI: 0.988–0.999), respectively.

Predictive Efficacies of Age and PLR for Prognosis of Patients With Sudden Total Deafness

The predictive efficacies for prognosis of patients with STD were all analyzed by ROC curve-test. As shown in **Table 3**, the area under the curve (AUC) calculated was 0.660 for the combination of age and PLR value, which was higher than that of both age alone (0.628) and PLR alone (0.589), suggested a higher predictive efficacy of the combination of these two factors. According to Yorden Index, the best cut-off value for age was 56.5 years with sensitivity and specificity of 54.4 and 67.6%, respectively, and the best cut-off value for PLR was 142.6 with sensitivity and specificity of 51.5 and 68.4%, respectively. As shown in **Table 4** and **Figure 1**, the effective rates of different groups of STD patients according to such cut-off values were significantly different ($P < 0.05$). The effective rate of patients with age of $\leq$56 years and PLR value of $>$142.6 could reach to 78.1%, which was significantly higher than that of all the other three groups of patients ($P < 0.05$).

DISCUSSION

This study found that age was an independent prognostic factor of sudden total deafness. The younger the age, the better the prognosis, which is consistent with previous studies (12). Previous studies have shown that sudden deafness can occur at all ages, mainly in adults aged 18–59. Overwork and emotional fluctuation are the main inducing factors. This may be due to certain degenerative changes occurs in vascular wall compliance, microcirculation hemorheology and inner ear auditory function with age.

In recent years, with the draw of pathological activation of cell stress pathway hypothesis, people began to realize that inflammatory response may play an important role in the pathogenesis of sudden deafness. At present, the research on the etiology of SSHL mainly focuses on its relation with chronic

TABLE 3 | The predictive efficacies of age, PLR value, and the combination of age and PLR value for prognosis in patients with STD.

	AUC	95%CI	Best cut-off value	Sensitivity	Specificity	*P*
Age	0.628	0.530∼0.726	56.6	54.4%	67.6%	0.014
PLR	0.589	0.489∼0.688	142.6	51.5%	68.4%	0.088
Combination	0.660	0.565∼0.754	–	64.9%	60.3%	0.002

STD, sudden total deafness; PLR, platelet/lymphocyte count ratio.

TABLE 4 | The effective rates according to different age and PLR values.

	Effective rate	*P*
Age ≤ 56.5 years, PLR>142.6	78.1% (25/32)	0.010*
Age ≤ 56.5 years, PLR≤142.6	52.5% (21/40)	
Age > 56.5 years, PLR>142.6	47.6% (10/21)	
Age > 56.5 years, PLR≤142.6	37.5% (12/32)	

PLR, platelet/lymphocyte count ratio.
**P < 0.05.*

inflammation (13). It is believed that the inner ear is a "terminal organ" without collateral circulation, and its blood supply mainly depends on the labyrinth artery. The hair cells in the cochlea consume a lot of oxygen and are extremely sensitive to hypoxia. Therefore, the reduction of blood flow will lead to SSHL. In addition, due to the clinical characteristics of acute onset and unilateral multiple, SSHL is considered to be similar to the pathogenesis of ischemic diseases such as myocardial infarction, transient ischemic attack or transient amaurosis (14). So we deemed that in addition to the inner ear circulation disorder, chronic inflammation also plays an important role in the occurrence of SSHL. The inflammatory reaction could destroy the vascular endothelium and damage the blood flow of the inner ear, trigger the formation of atherosclerosis, then damage the vascular stria and increase the risk of ischemia (6). The wide application of anti-inflammatory steroids in the treatment of SSHL also confirms the important role of inflammation in the pathogenesis.

The peripheral blood inflammatory cells mainly include leukocytes, neutrophils, lymphocytes and platelets, which play important roles in the control of inflammation. These inflammatory markers and the ratios obtained from these markers, such as NLR and PLR, have been concerned by many researchers as markers of systemic inflammation (15, 16), for they are easy to collect, cheap, and has the same predictive effect with those expensive markers, such as interleukin (IL)-6, IL-8, IL-1β, and tumor necrosis factor- α (17). The correlation between inflammatory markers, especially NLR, PLR and sudden deafness has been widely recognized by clinical researchers. However, there is still controversy about their correlation with the prognosis of sudden deafness. Chen et al. (6) found that NLR and PLR, as comprehensive indicators of two complementary immune pathways, have a certain correlation with the occurrence and prognosis of SSHL, namely NLR and PLR can be used as biomarkers for the diagnosis and prognosis of SSHL. Cao et al. (16) also reported similar correlation between PLR, NLR and SSHL in their meta-analysis. Seo et al. found that the levels of NLR and PLR in patients with SSHL were significantly higher than those of control group, while the level of NLR in the recovered group was lower than the un-recovered group (18). Durmuş et al. in 2016 also reported that the NLR and PLR values of SSHL patients were higher than the control group, and un-recovered SSHL patients had higher NLR and PLR levels than the recovered-group (17). Therefore, it is considered that NLR and PLR are of certain value in predicting the prognosis of SSHL. Similarly, Kum et al. (19) also reported higher NLR levels in un-recovered SSHL patients, but the average platelet volume, a sensitive indicator of platelet activity, was not significantly correlated with the prognosis. Ikinciogullari et al. (20) also found that patients with SSHL had higher NLR and PLR values, but both of these two inflammation markers had no significant correlation with the prognosis of sudden deafness. He believed that patients with higher NLR values responded better to anti-inflammatory drugs (steroids). Similarly, in 2020 Mehmet Eser Sancaktar (7) found that NLR and PLR decreased with the increase of the severity of hearing loss, and the patients with completely recovered and ascending audiogram had the highest values of NLR and PLRt, suggesting that high NLR and PLR may be prognostic factors of SSHL patients (21, 22). The heterogeneity of current findings on inflammation and SSHL may be related to the lack of classification for SSHL, as it is believed that the pathology of SSHL vary across clinical subtypes. Therefore, this study only selected patients with STD as research subjects to explore the correlation between inflammatory response and STD.

In this study, NLR has no significant correlation with the prognosis of STD, while PLR has a significant correlation with the efficacy of patients withSTD. The higher the PLR, the better the prognosis, which is consistent with the results of Mehmet Eser Sancaktar. Therefore, we speculated that inflammatory response played an important role in the occurrence of STD. Patients with elevated PLR have better response to anti-inflammatory drugs (steroids), so their prognosis are better. As a new peripheral inflammatory marker, PLR is associated with thrombosis and inflammation, which are closely related to the pathogenesis and progression of SSHL (23). In addition to its definite hemostatic and thrombotic functions, platelets are also considered to be an essential pro-inflammatory factor in atherosclerosis, allergy and rheumatoid arthritis. The increase of platelet count may promote platelet activation and increase the release of inflammatory

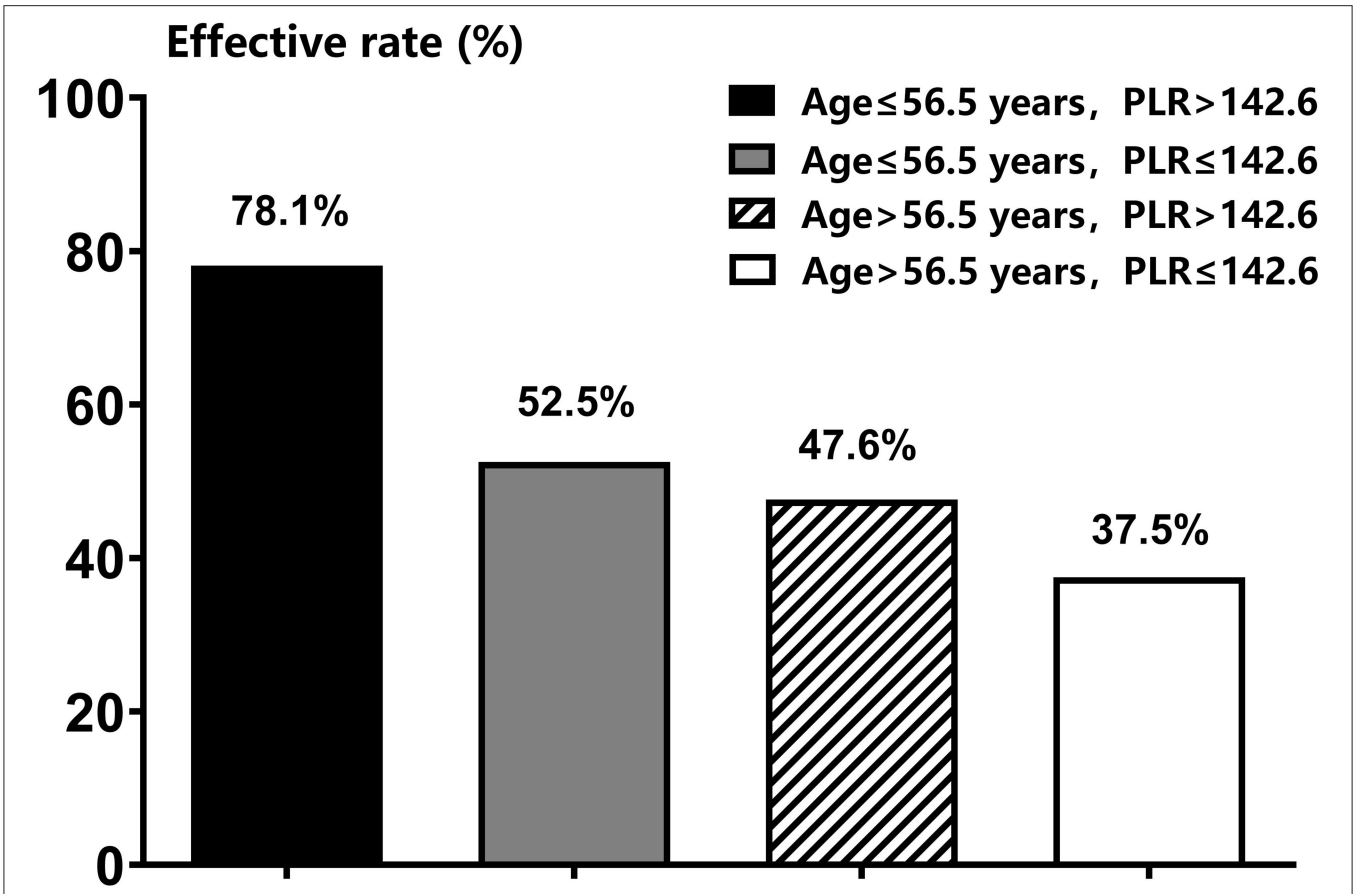

FIGURE 1 | The effective rates between sudden total deafness patients with different age and PLR values.

mediators, resulting in an harmful inflammatory process to the body (24). While lymphocyte is considered to play an important role as immune regulation during all the inflammatory reaction stages of atherosclerosis (25), namely has a certain anti-inflammatory effect. So, PLR, which comes from the ratio of peripheral platelet count and lymphocyte count, includes the changes of platelets and lymphocytes, is more valuable than using any one of these two indicators in reflecting the inflammatoion level of our body. Therefore, the relationship between PLR and SSHL has gradually been concerned by more and more researchers.

The ROC analysis was finally applied in this study, and the effective rate of patients with age of ≤56 years and PLR value of >142.6 could reach to 78.1%, which was significantly higher than that of all the other three groups of patients. It has important clinical significance for guiding the prognosis of patients with STD in clinical practice.

LIMITATION

This study did not monitor the peripheral inflammatory indexes at discharge, which is a defect of the study design. Therefore, it is impossible to indirectly show the correlation between various peripheral inflammatory markers and prognosis of SSHL. The role of inflammatory markers in the occurrence and development of sudden deafness needs to be confirmed by further well-designed randomized controlled studies.

CONCLUSION

In summary, we found that Age and PLR are independent factors related to the prognosis of STD. The younger the onset age, the higher the PLR, the better the prognosis. The increase of PLR in patients with STD indicates that micro blood structure inflammation plays an important role in the occurrence of STD, suggesting that we need to re-explore the pathogenesis of STD and adjust the treatment to obtain better prognosis. In addition, PLR, which can be detected conveniently, combined with age, can predict the prognosis of patients with STD to a certain extent, the effective rate of patients with age of ≤56 years and PLR value of >142.6 could reach to 78.1%, which can help carry out personalized treatment reliably and economically.

DATA AVAILABILITY STATEMENT

The raw data supporting the conclusions of this article will be made available by the authors, without undue reservation.

ETHICS STATEMENT

The studies involving human participants were reviewed and approved by the Peking University People's Hospital Ethical Permission Committee approved study (2021PHB149). The patients/participants provided their written informed consent to participate in this study. Written informed consent was obtained from the individual(s) for the publication of any potentially identifiable images or data included in this article.

AUTHOR CONTRIBUTIONS

XM contributed to the study conception and design and made critical revision for important intellectual content. TD supervised this research. TD, YK, JZ, and YJ contributed to the material preparation and data collection. TD, YK, and JZ contributed to the analysis and interpretation of data. TD and JZ wrote the first draft of the manuscript. All authors read and approved the final manuscript.

FUNDING

This study was supported by Peking University People's Hospital Scientific Research Development Funds (RDL2021–14 and RDY2021–25), and National Key research and development program of China (2020YFC2005200).

REFERENCES

1. Alexander TH, Harris JP. Incidence of sudden sensorineural hearing loss. *Otol Neurotol.* (2013) 34:1586–9. doi: 10.1097/MAO.0000000000000222
2. Chandrasekhar SS, Tsai Do BS, Schwartz SR, Bontempo LJ, Faucett EA, Finestone SA, et al. Clinical Practice Guideline: Sudden Hearing Loss (Update). *Otolaryngol Head Neck Surg 161(1_suppl).* (2019) S1–45. doi: 10.1177/0194599819859883
3. Hoffman M, Blum A, Baruch R, Kaplan E, Benjamin M. Leukocytes and coronary heart disease. *Atherosclerosis.* (2004) 172:1–6. doi: 10.1016/S0021-9150(03)00164-3
4. Ciccone MM, Cortese F, Pinto M, Di Teo C, Fornarelli F, Gesualdo M, et al. Endothelial function and cardiovascular risk in patients with idiopathic sudden sensorineural hearing loss. *Atherosclerosis.* (2012) 225:511–6. doi: 10.1016/j.atherosclerosis.2012.10.024
5. Fasano T, Pertinhez TA, Tribi L, Lasagni D, Pilia A, Vecchia L, et al. Laboratory assessment of sudden sensorineural hearing loss: a case-control study. *Laryngoscope.* (2017) 127:2375–81. doi: 10.1002/lary.26514
6. Chen L, Zhang G, Zhang Z, Wang Y, Hu L, Wu J. Neutrophil-to-lymphocyte ratio predicts diagnosis and prognosis of idiopathic sudden sensorineural hearing loss: a systematic review and meta-analysis. *Medicine (Baltimore).* (2018) 97:e12492. doi: 10.1097/MD.0000000000012492
7. Sancaktar ME, Agri I, Çeçen AB, Akgül G, Çelebi M. The Prognostic Value of Circulating Inflammatory Cell Counts in Sudden Sensorineural Hearing Loss and the Effect of Cardiovascular Risk Factors. *Ear Nose Throat J.* (2020) 99:464–9. doi: 10.1177/0145561320920968
8. [Guideline of diagnosis and treatment of sudden deafness (2015)]. *Zhonghua Er Bi Yan Hou Tou Jing Wai Ke Za Zhi.* (2015) 50:443–7.
9. Goto F, Sugaya N, Arai M, Masuda K. Psychiatric disorders in patients with intractable dizziness in the department of otolaryngology. *Acta Otolaryngol.* (2018) 138:646–7. doi: 10.1080/00016489.2018.1429652
10. Liang H, Zhong SX. [Analysis of the relevant factors for recurrent sudden sensorineural hearing loss]. *Zhonghua Er Bi Yan Hou Tou Jing Wai Ke Za Zhi.* (2016) 51:691–4.
11. Chen GH, Zhang R, Wang YG, Ye SN, Lin C, Cheng JM, et al. [Multi-center study of clinical treatment on the flat type of sudden hearing loss]. *Zhonghua Er Bi Yan Hou Tou Jing Wai Ke Za Zhi.* (2013) 48:374–8.
12. Kang WS, Yang CJ, Shim M, Song CI, Kim TS, Lim HW, et al. Prognostic Factors for Recovery from Sudden Sensorineural Hearing Loss: a Retrospective Study. *J Audiol Otol.* (2017) 21:9–15. doi: 10.7874/jao.2017.21.1.9
13. Hiramatsu M, Teranishi M, Uchida Y, Nishio N, Suzuki H, Kato K, et al. Polymorphisms in genes involved in inflammatory pathways in patients with sudden sensorineural hearing loss. *J Neurogenet 26(3-4).* (2012) 387–96. doi: 10.3109/01677063.2011.652266
14. Ballesteros F, Alobid I, Tassies D, Reverter JC, Scharf RE, Guilemany JM, et al. Is there an overlap between sudden neurosensorial hearing loss and cardiovascular risk factors? *Audiol Neurootol.* (2009) 14:139–45. doi: 10.1159/000171475
15. Hao X, Li D, Wu D, Zhang N. The Relationship between Hematological Indices and Autoimmune Rheumatic Diseases (ARDs), a Meta-Analysis. *Sci Rep.* (2017) 7:10833. doi: 10.1038/s41598-017-11398-4
16. Cao Z, Li Z, Xiang H, Huang S, Gao J, Zhan X, et al. Prognostic role of haematological indices in sudden sensorineural hearing loss: review and meta-analysis. *Clin Chim Acta.* (2018) 483:104–11. doi: 10.1016/j.cca.2018.04.025
17. Durmuş K, Terzi H, Karataş TD, Dogan M, Uysal I, Sencan M, et al. Assessment of hematological factors involved in development and prognosis of idiopathic sudden sensorineural hearing loss. *J Craniofac Surg.* (2016) 27:e85–91. doi: 10.1097/SCS.0000000000002241
18. Seo YJ, Jeong JH, Choi JY, Moon IS. Neutrophil-to-lymphocyte ratio and platelet-to-lymphocyte ratio: novel markers for diagnosis and prognosis in patients with idiopathic sudden sensorineural hearing loss. *Dis Markers.* (2014) 2014:702807. doi: 10.1155/2014/702807
19. Kum RO, Ozcan M, Baklaci D, Yurtsever Kum N, Yilmaz YF, Unal A, et al. Investigation of neutrophil-to-lymphocyte ratio and mean platelet volume in sudden hearing loss. *Braz J Otorhinolaryngol.* (2015) 81:636–41. doi: 10.1016/j.bjorl.2015.08.009
20. Ikinciogullari A, Köseoglu S, Kiliç M, Atan D, Özcan KM, Çetin MA, et al. (2014). New inflammation parameters in sudden sensorineural hearing loss: neutrophil-to-lymphocyte ratio and platelet-to-lymphocyte ratio. *J Int Adv Otol.* 10:197-200 doi: 10.5152/iao.2014.76
21. Salvago P, Rizzo S, Bianco A, Martines F. Sudden sensorineural hearing loss: is there a relationship between routine haematological parameters and audiogram shapes? *Int J Audiol.* (2017) 56:148–53. doi: 10.1080/14992027.2016.1236418
22. Sun Y, Xia L, Wang H, Chen Z, Wu Y, Chen B, et al. Is nucleate cell count and neutrophil to lymphocyte ratio related to patients with audiographically distinct sudden sensorineural hearing loss? *Medicine (Baltimore).* (2018) 97:e10586. doi: 10.1097/MD.0000000000010586
23. Taşoglu I, Sert D, Colak N, Uzun A, Songur M, Ecevit A. Neutrophil-lymphocyte ratio and the platelet-lymphocyte ratio predict the limb survival in critical limb ischemia. *Clin Appl Thromb Hemost.* (2014) 20:645–50. doi: 10.1177/1076029613475474
24. Nikolsky E, Grines CL, Cox DA, Garcia E, Tcheng JE, Sadeghi M, et al. Impact of baseline platelet count in patients undergoing primary percutaneous coronary intervention in acute myocardial infarction (from the CADILLAC trial). *Am J Cardiol.* (2007) 99:1055–61. doi: 10.1016/j.amjcard.2006.11.066

25. Aghdaii N, Ferasatkish R, Mohammadzadeh Jouryabi A, Hamidi SH. Significance of preoperative total lymphocyte count as a prognostic criterion in adult cardiac surgery. *Anesth Pain Med.* (2014) 4:e20331. doi: 10.5812/aapm.20331

Conflict of Interest: The authors declare that the research was conducted in the absence of any commercial or financial relationships that could be construed as a potential conflict of interest.

Publisher's Note: All claims expressed in this article are solely those of the authors and do not necessarily represent those of their affiliated organizations, or those of the publisher, the editors and the reviewers. Any product that may be evaluated in this article, or claim that may be made by its manufacturer, is not guaranteed or endorsed by the publisher.

Copyright © 2022 Diao, Ke, Zhang, Jing and Ma. This is an open-access article distributed under the terms of the Creative Commons Attribution License (CC BY). The use, distribution or reproduction in other forums is permitted, provided the original author(s) and the copyright owner(s) are credited and that the original publication in this journal is cited, in accordance with accepted academic practice. No use, distribution or reproduction is permitted which does not comply with these terms.

frontiers | Frontiers in Neuroscience

ORIGINAL RESEARCH
published: 30 June 2022
doi: 10.3389/fnins.2022.925095

Correlation Analysis of Vestibular Symptoms and Migraine and Non-migraine Headaches: An Epidemiological Survey of 708 Female Nurses

Tongxiang Diao†, Jinling Zhu†, Lisheng Yu and Xin Ma**

Department of Otolaryngology, Head and Neck Surgery, People's Hospital, Peking University, Beijing, China

Objective: This study is oriented to study the correlation between different vestibular symptoms and migraine and non-migraine headaches.

Materials and Methods: A questionnaire containing factors related to vestibular symptoms and migraine was designed to survey nurses in a tertiary hospital. Then, all study subjects were divided into three groups: no headache, migraine, and non-migraine headache, and the general physical condition and incidence of different vestibular symptoms were compared among the three groups.

Results: Among all the 708 subjects, 233 had headaches. The incidence of migraine was 13.3%. There were 235 cases had vestibular symptoms. Dizziness and vertigo are independent factors related to headaches, especially migraine. The risk of migraine and other types of headaches in the vertigo group is 2.808 and 2.526 times of those without vertigo, while in the dizziness group, the risk is 8.248 and 5.732 times of those without dizziness.

Conclusion: Different vestibular symptoms were all related to migraine. And different vestibular symptoms and non-migraine headaches also showed a clear correlation.

Keywords: vestibular symptoms, dizziness, vertigo, headache, migraine, nurses

OPEN ACCESS

Edited by:
Jian-hua Zhuang, Shanghai Changzheng Hospital, China

Reviewed by:
Yong You, The Second Affiliated Hospital of Hainan Medical University, China
Wei Fu, Fourth Military Medical University, China

****Correspondence:***
Lisheng Yu
yulish68@163.com
Xin Ma
13581709195@163.com

† These authors have contributed equally to this work and share first authorship

Specialty section:
This article was submitted to Perception Science, a section of the journal Frontiers in Neuroscience

Received: *21 April 2022*
Accepted: *06 June 2022*
Published: *30 June 2022*

Citation:
Diao T, Zhu J, Yu L and Ma X (2022) Correlation Analysis of Vestibular Symptoms and Migraine and Non-migraine Headaches: An Epidemiological Survey of 708 Female Nurses. Front. Neurosci. 16:925095. doi: 10.3389/fnins.2022.925095

INTRODUCTION

In 2012, the Bárány Society first proposed and formulated the definition and diagnostic criteria of vestibular migraine and probable vestibular migraine (VM) (Lempert et al., 2012), in which, the vestibular symptoms are defined as spontaneous vertigo including internal vertigo, external vertigo, positional vertigo, visually induced vertigo, head motion-induced vertigo, and head motion-induced dizziness with nausea (the dizziness here is only referred to a sense of spatial disorientation). Since then, the correlation between vestibular symptoms and headache has attracted much more attention from clinicians. At present, the vestibular symptoms included in the diagnostic criteria for VM are mainly vertigo and dizziness accompanied by spatial disorientation.

Meanwhile, the 2009 International Classification of Vestibular Diseases defines vestibular symptoms as vertigo, dizziness, vestibulo-visual, and postural symptoms (Bisdorff et al., 2009). A few studies have already proposed that dizziness and postural symptoms are also significantly related to migraine besides vertigo (Vuković et al., 2007). Moreover, although the relationship

between vestibular symptoms and migraine has gradually become clear, few studies have focused on the relationship between vestibular symptoms and non-migraine headaches. The nursing profession is subject to occupational stress, which can be a trigger for headaches. Durham et al. (1998) found that 17% of nurses have migraines according to the International Headache Society (IHS) criteria. Menon and Remadevi (2021) also found that a total of 20% of nursing students had headaches of which 85% had migraine in their study. In this study, nurses who have a high incidence of headaches were selected as the subjects (Wang et al., 2015), to further explore the correlation between different vestibular symptoms and migraine and non-migraine headaches, providing more clinical diagnostic evidence for VM.

MATERIALS AND METHODS

Study Design

This is a cross-sectional study conducted through a self-designed questionnaire among the nurses from a tertiary A hospital in Beijing. Researchers have undergone uniform training to be familiar with the contents of the questionnaire. The electronic questionnaire was distributed through the WeChat platform. Before distributing the questionnaire, researchers went to each department to conduct training for filling the questionnaire, clarifying the purpose, significance, and filling requirements of the survey to ensure its quality. The questionnaires are filled out voluntarily by the respondents. It takes about 20 min to complete each questionnaire. Complete and effective questionnaires are selected by researchers in the end.

Participants

The nurses were on-the-job from January to June 2019. Inclusion criteria were as follows: (1) Registered nurses in tertiary A hospitals; (2) Female; (3) Engaged in ward nursing work with working experience no less than 3 years; (4) Can answer questions independently; (5) Volunteer to participate in the survey; (6) Vestibular dysfunctions such as Meniere's disease and vestibular neuritis were excluded; (7) Organic lesions, such as acoustic neuroma, were excluded. Exclusion criteria were as follows: severe physical and mental illness and those who cannot complete the survey due to various reasons. A total of 1,052 questionnaires were distributed by the WeChat platform, 722 were recovered, and finally, 708 valid questionnaires were collected with 14 questionnaires deleted for missing Information (**Figure 1**).

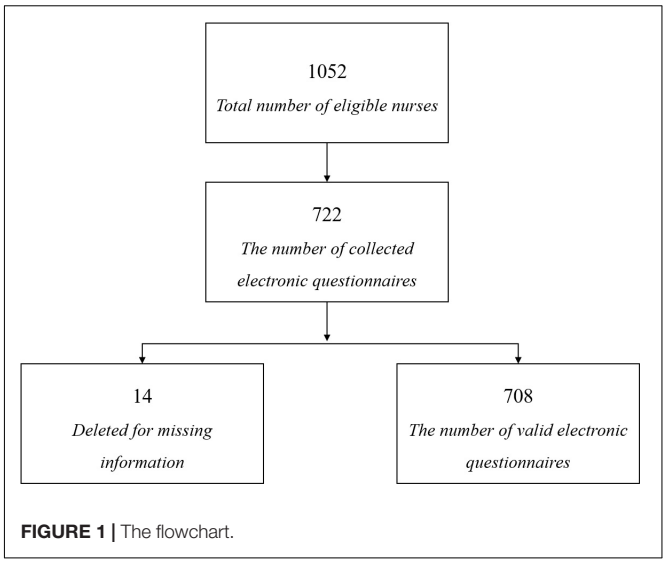

FIGURE 1 | The flowchart.

Data Collection

This study used a self-designed questionnaire, including the contents as following:

General Physical Condition

Age, department (internal medicine, surgery), professional title (junior, middle-level, senior), BMI, whether to work the night shift, addiction to tobacco or alcohol (yes or no), and exercise status. The exercise status includes the following: (1) Daily pedometer steps (<2,000, 2,000–5,000, 5,000–10,000, and >10,000); (2) Is it possible to guarantee moderate-intensity exercises more than 30 min at least twice a week? Chronic disease history includes the following: hypertension, hyperglycemia, hyperlipidemia, ototoxic drug, noise exposure which refers to an 8 h average exposure of greater than 83 dBA (Roberts and Neitzel, 2019), and long-term low-dose noise exposure (limited or similar to Walkman, more than 60 min, and/or more than 4 times a week).

The Clinical Characteristics of Headache

Include the following: (1) headache history and (2) the modified ID-migraine: ① Your headaches limited your ability to work, study, or do what you needed to do for at least one day (Yes or No). ② You felt nauseated or sick to your stomach (Yes or No). ③ Light bothered you a lot more than when you do not have headaches (Yes or No). When ID-migraine was initially proposed, it only required to record headaches during the last 3 months. Individuals who indicated that they had two or three of these features were said to screen positive for migraine (Rapoport and Bigal, 2004). However, this study considered that migraine is a paroxysmal disease, and the frequency of attacks is variable, so the 3-month time limit was canceled. Clinical characteristics also include (3) the location, nature, and duration of the headache.

The Clinical Characteristics of Vestibular Symptoms

Including (1) history of vestibular symptoms and (2) classification of vestibular symptoms, such as vertigo, dizziness, and postural symptoms. These three vestibular symptoms are defined as follows: vertigo is the sensation of self-motion when no self-motion is occurring or the sensation of distorted self-motion during an otherwise normal head movement; dizziness is the sensation of disturbed or impaired spatial orientation without a false or distorted sense of motion; postural symptoms are balance symptoms related to maintenance of postural stability, occurring only while upright (seated, standing, or walking) (Bisdorff et al., 2009); (3) if vertigo is combined, the frequency of vertigo attacks, duration, incentives, and mitigating factors are registered.

TABLE 1 | Epidemiological characteristics of 708 nurses.

Variables		$\bar{x} \pm \mu$	*n*
Age		32.39 ± 8.924	708/708
Department	Internal medicine		454/708 (63.0%)
	Surgery		254/708 (35.2%)
Professional title	Junior		342/708 (48.3%)
	Middle-level		225/708 (31.8%)
	Senior		141/708 (19.9%)
BMI		21.667 ± 3.080	422/708 (59.6%)
Night shift			469/708 (66.2%)
Pedometer steps (/day)	<2000		264/708 (37.3%)
	(2000, 5000)		33/708 (4.7%)
	(5000, 10000)		215/708 (30.4%)
	≥10000		196/708 (27.7%)
Moderate-intensity exercise over 30 min at least twice a week			182/708 (25.7%)
Hypertension*			53/708 (7.5%)
Diabetes*			26/708 (3.7%)
Hyperlipidemia*			45/708 (6.4%)
Ototoxic drug use history*			6/708 (0.8%)
Noise exposure*			29/708 (4.1%)
Long-term low-dose noise exposure			172/708 (24.3%)
Smoking history*			4/708 (0.6%)
Drinking history*			15/708 (2.1%)

*PS: (1) The data on BMI is incomplete, with an average of 21.67 (13.521∼30.819), which is not included in the follow-up statistics; (2) The positive response rate of history of hypertension, diabetes, hyperlipidemia, ototoxic drugs, noise exposure, and addiction to tobacco or alcohol are less than 10%, which are not included in the following statistics. *Indicates that the response rate is <10%.*

Ethics Statement

The Peking University People's Hospital Ethical permission committee approved the study (2019PHB099-01) and all subjects provided their informed consent.

Statistical Analysis

SPSS 23.0 statistical software was used for statistical analysis. Frequency and percentage are used to describe the distribution, while the means are used to describe the average level. The Chi-square test and ANOVA are used to compare categorical and continuous variables, respectively. According to whether migraine was combined, all participants were divided into no headache group, migraine group, and non-migraine headache group. First, univariate analysis was used to screen statistically significant influencing factors, then multivariate analysis was used to explore the independent correlation factors between migraine and other types of headaches. All p values are bidirectional, and $p < 0.05$ values are considered statistically significant.

RESULTS

Epidemiological Characteristics

A total of 708 women nurses were enrolled in this study, with an average age of 32.39 ± 8.924 years old (23–57 years old), and an average BMI of 21.667 ± 3.08 (13.521–30.819). Among the nurses, 454 were in internal medicine and 254 were in surgery. Junior, middle level, and senior professional titles are 342, 225, and 141, respectively. The general physical condition was well, subjects with high blood pressure, diabetes, and hyperlipidemia were 53, 26, and 45, respectively. Subjects with smoking and drinking history were 4 and 15, respectively. The specific description of its epidemiological characteristics is shown in **Table 1**.

Clinical Characteristics of Headaches

Among all the 708 subjects, 233 (28.7%) had headaches, with an average history of 7.91 ± 7.642 years, of which 94 cases were consistent with the diagnosis of migraine (individuals who indicated that they had two or three of these features were said to screen positive for migraine), accounting for about 13.3% of all subjects, and 40.3% of headache population. According to whether migraine was companied, headache patients were divided into migraine group (94 cases) and non-migraine headache group (139 cases) and included in the follow-up statistical analysis. The positive response rate of each question in ID-migraine is shown in **Figure 2**.

Characteristics of the Vestibular Symptoms

Among all the 708 subjects, 235 (33.2%) complained of multiple vestibular symptoms, with an average history of 5.91 ± 6.551 years. Among them, 155 cases had only

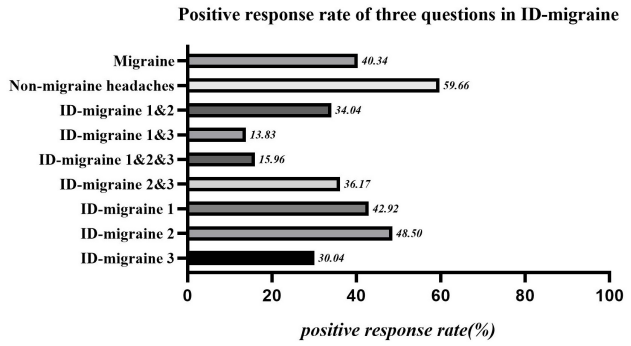

FIGURE 2 | Positive response rate of three questions in ID-migraine. ID-migraine 1: If there is one day or more you can't work, study, or do daily activities normally because of headache?; ID-migraine 2: Is there nausea or stomach upset during headache?; ID-migraine 3: Is there photophobia companied with headache?

one single vestibular symptom, and 80 cases had multiple vestibular symptoms. According to the 2019 Bárány Association's classification criteria for vestibular symptoms, this study divided vestibular symptoms into vertigo, dizziness, and postural symptoms, of which 96 cases were combined with vertigo, 173 cases were combined with dizziness, and 66 cases were combined with postural symptoms. The clinical characteristics of the vestibular symptoms are shown in **Figure 3**.

Correlation of Different Vestibular Symptoms and Headaches

According to whether migraine is accompanied, all the subjects were divided into three groups: no headache, migraine, and non-migraine headache group. Univariate analysis was used to screen out the statistically significant factors: age, professional title, whether to work night shifts, dizziness, vertigo, and postural symptoms, then all these factors were included in the following multiple logistic regression. The results showed that: different vestibular symptoms all showed a certain correlation with migraine, among which dizziness and vertigo were independent related factors of migraine and non-migraine headaches. The incidence of combining migraine and non-migraine headaches were 2.808 and 2.526 times that in the non-vertigo group, respectively. The incidence of combining migraine and non-migraine headaches was 8.248 and 5.732 times that in the non-dizziness group, respectively (**Table 2**).

DISCUSSION

Incidence of Headaches and Migraine

Among all the 708 subjects admitted in this study, the incidence of headache and migraine were 28.7 and 13.3%,

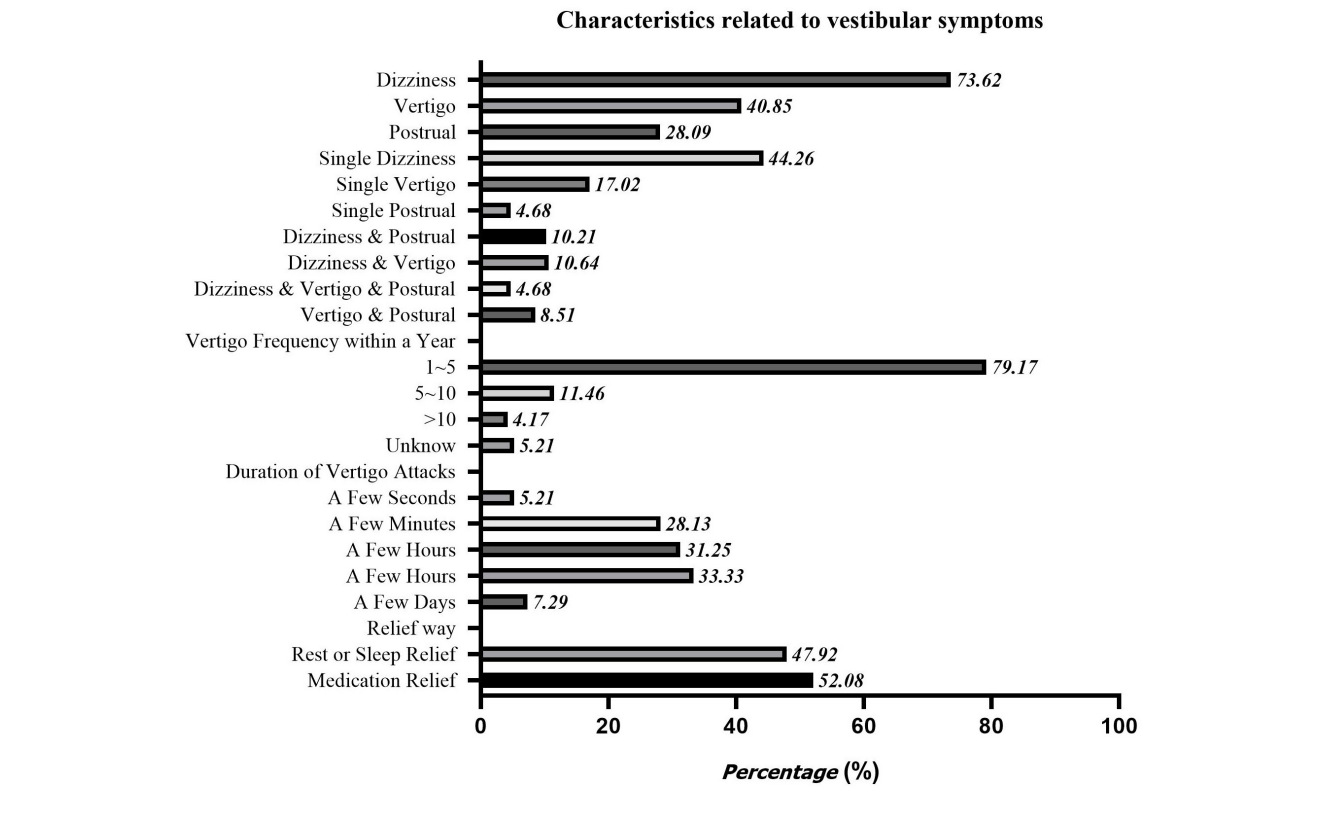

FIGURE 3 | Characteristics related to vestibular symptoms.

respectively. It has been reported that the incidence of idiopathic headaches in mainland China is about 23.8%, of which the incidence among women is around 36.8% (Yu et al., 2012). Research conducted by Shengyuan Yu found that the incidence of idiopathic headache, migraine, and tension-type headache among nursing staff with high pressure can be as high as 45.3, 14.8, and 26.2% (Wang et al., 2015). Compared with previous studies, the incidence of headaches in this study is lower, but the incidence of migraine is basically the same. We deem that the migraine is moderate to severe headache, which affects daily life and tends to be reported. While a mild headache, it tends to be thought of as a normal physiological phenomenon rather than a disease after a night shift. There is no undue fear of them, and people tend not to report it in the survey. This is also the reason for the gap between the electronic self-evaluation questionnaire and the face-to-face evaluation.

The Correlation Between Different Vestibular Symptoms and Migraine

In this study, the incidence of dizziness, vertigo, and postural symptoms were 24.44, 13.56, and 9.32%, respectively. About 1/3 of the subjects had complained about vestibular symptoms, which was close to the lifetime prevalence of dizziness and balance instability among American adults (Formeister et al., 2018). Among all the nurses with vestibular symptoms, about 65.96% complained of a single vestibular symptom, and 34.03% complained of two or more vestibular symptoms, which reminded us that although the Barany Association distinguished dizziness, vertigo, vestibulo-visual and postural

TABLE 2 | Factors related to migraine and non-migraine headache.

A. Univariate analysis

Variables		Non-headache *(n = 475)*	Migraine *(n = 94)*	Non-migraine headache *(n = 139)*	*p*
Age		31.31 ± 8.586	33.72 ± 8.907	34.79 ± 9.541	0.000*
Department	Internal	326/475	65/94	105/139	0.288
	Surgery	149/475	29/94	34/139	
Professional title	Junior	249/475	41/94	55/139	0.000*
	Middle-level	155/475	26/94	42/139	
	Senior	71/475	27/94	42/139	
Night shift	No	145/475	29/94	67/139	0.000*
	Yes	330/475	65/94	72/139	
Pedometer steps (/day)	<2000	173/475	38/94	53/139	0.959
	(2000, 5000)	21/475	5/94	7/139	
	(5000, 10000)	146/475	25/94	44/139	
	≥10000	135/475	26/94	35/139	
Moderate intensity exercise over 30 min at least twice a week	No	356/475	66/94	104/139	0.623
	Yes	119/475	28/94	35/139	
Long-term low-dose noise exposure	No	351/475	72/94	114/139	0.142
	Yes	124/475	22/94	25/139	
Dizziness		54/475	54/94	65/139	0.000*
Vertigo		38/475	26/94	32/139	0.000*
Postural symptom		24/475	21/94	21/139	0.000*

B. Multivariate analysis

Variables		Migraine		Non-migraine	
		Odds ratio (95% CI)	*p*	Odds ratio (95% CI)	*p*
Age		1.018 (0.975∼1.062)	0.420	1.015 (0.981∼1.050)	0.392
Professional title	Junior	1		1	
	Middle-level	0.880 (0.450∼1.720)	0.708	0.937 (0.536∼1.637)	0.818
	Senior	2.205 (0.864∼5.626)	0.098	1.421 (0.655∼3.080)	0.374
Night shift		1.875 (0.961∼3.658)	0.065	0.669 (0.406∼1.102)	0.114
Dizziness		8.248 (4.882∼13.933)	0.000*	5.732 (3.607∼9.110)	0.000*
Vertigo		2.808 (1.480∼5.328)	0.002*	2.526 (1.420∼4.492)	0.002*
Postural symptom		1.758 (0.834∼3.705)	0.138	1.200 (0.585∼2.463)	0.619

*$P < 0.05$.

symptom clearly in 2009, different vestibular symptoms may coexist or appear sequentially in one patient (Bisdorff et al., 2009). The previous literature also pointed out that about 60% of patients with vestibular symptoms complained of multiple vestibular symptoms consistent with the result of our research (Kerber et al., 2017). Although most clinical researchers believe that only the patients with spontaneous vertigo that meets the current diagnostic criteria for VM can be diagnosed (Cohen and Escasena, 2015), there is a wide range of vestibular symptoms associated with migraine in fact. One study aimed at VM found that the descriptions of vestibular symptoms were complex and diverse, including instability (91%), dizziness (77%), vertigo (57%), internal head rotation (45%), or the feeling of being on a rocking boat (41%) (Cohen and Escasena, 2015). Migraine is also associated with a slight but significant postural instability originating from the central vestibule, which is manifested as a greater swing speed, a shift in the eccentric center of gravity, and an increase in stride length during tandem walking (Calhoun et al., 2011). In this study, different vestibular symptoms and migraine all showed a significant correlation. The dizziness group was more likely to be accompanied by migraine than the vertigo group (8.248 vs. 2.808), suggesting that we should not ignore the correlation between other vestibular symptoms and VM, to avoid a missing diagnosis of VM that may not meet the current diagnostic criteria (Yu et al., 2016).

The Correlation Between Vestibular Symptoms and Non-migraine Headaches

We further found that different vestibular symptoms also correlated significantly with non-migraine headaches. Compared with vertigo group patients, the dizziness group patients were more likely to suffer from non-migraine headaches (5.732 vs. 2.526). These suggested that similar to migraine, non-migraine headaches could also be accompanied with vestibular symptoms. Migraine and tension-type headaches, the current most common primary headaches, were thought to be independent diseases according to the International Headache Classification [ICHD] (2018). However, there was a growing number of studies that had focused on the similarities between migraine and tension-type headache (TTH). In fact, Migraine patients often had typical TTH symptoms such as muscle tension and neck pain (Blaschek et al., 2012). Similarly, TTH patients often had symptoms of photophobia and phonophobia which could aggravate after activities (Spierings et al., 2001). In addition to the overlap of symptoms, patients with these two diseases could have similar pathogenic factors, such as age, sex, BMI, sleep disorders, negative emotions, sunshine exposure, anxiety, and depression (Wang et al., 2013; Tai et al., 2019). Migraine and TTH both had a significant familial predisposition, which could be reflected by the fact that the twins of affected individuals have obvious increased risks of migraine and TTH, confirming the importance of genetic factors in disease pathogenesis (Ligthart et al., 2018). Moreover, these two diseases are both thought to be related to central sensitization mechanisms (Yunus, 2007). The strict definitions of migraine and TTH in ICHD are artificial to some extent, and they may be one disease with different severities: TTH is mild, while migraine is severe (continuous severity theory; Waters, 1973) (Turner et al., 2015; Ligthart et al., 2018). The boundaries between them could become more blurred in young patients or in patients with chronic disease courses (Turner et al., 2015). In this study, the patients' overall age was relatively young, and the relationships between migraine, non-migraine headache, and vestibular symptoms then showed high consistency.

LIMITATION

Similar to several epidemiological studies, this study had some limitations that need to be addressed. The first was the self-misclassification of study subjects, including (1) patients were given certain options to describe their subjective symptoms, and had to choose from them; (2) patients were not provided with sufficient options which could cover all specific subcategories, leading to wrong classification of their symptoms. Second, the age distribution of study subjects is not regular, which may cause some bias in the results. Third, the view that vestibular dysfunction may induce visual impairment is not commonly accepted by patients, and we focused mainly on the correlations between vestibular symptoms and headache. Therefore, the vestibular visual symptoms were not included in this study. Finally, we did not provide relevant questions about the diagnostic criteria of tension headache. Although a great portion of non-migraine headaches might be tension headaches, without accurate diagnoses, we could not explore the relationship between dizziness and tension headaches, which will be further explored in our future studies.

CONCLUSION

Different vestibular symptoms were all closely related to migraine, among which dizziness and vertigo were both significantly related. Compared with patients with vertigo, patients with dizziness were more likely to be accompanied by migraine. This suggested that when diagnosing vestibular migraine according to current criteria, some patients with non-vertigo vestibular symptoms might be missed. On the other hand, different vestibular symptoms also showed a clear correlation with non-migraine headaches.

DATA AVAILABILITY STATEMENT

The raw data supporting the conclusions of this article will be made available by the authors, without undue reservation.

ETHICS STATEMENT

The studies involving human participants were reviewed and approved by The Peking University People's Hospital Ethical Permission Committee (2019PHB099-01). The

patients/participants provided their written informed consent to participate in this study.

AUTHOR CONTRIBUTIONS

XM, TD, and JZ supervised this research. XM and TD contributed to the analysis and interpretation of data and wrote the first draft of the manuscript. XM and LY made critical revision for important intellectual content. All authors contributed to the study conception and design, material preparation, and data collection, read, and approved the final manuscript.

FUNDING

This work was supported by the Peking University People's Hospital Scientific Research Development Funds (RDY2021–25 and RDL2021–14) and the National Key Research and Development Program of China (2020YFC2005200).

REFERENCES

Bisdorff, A., Von Brevern, M., Lempert, T., and Newman-Toker, D. E. (2009). Classification of vestibular symptoms: towards an international classification of vestibular disorders. *J. Vestib. Res.* 19, 1–13. doi: 10.3233/ves-2009-0343

Blaschek, A., Milde-Busch, A., Straube, A., Schankin, C., Langhagen, T., Jahn, K., et al. (2012). Self-reported muscle pain in adolescents with migraine and tension-type headache. *Cephalalgia* 32, 241–249. doi: 10.1177/0333102411434808

Calhoun, A. H., Ford, S., Pruitt, A. P., and Fisher, K. G. (2011). The point prevalence of dizziness or vertigo in migraine–and factors that influence presentation. *Headache* 51, 1388–1392. doi: 10.1111/j.1526-4610.2011.01970.x

Cohen, J. M., and Escasena, C. A. (2015). Headache and dizziness: how to differentiate vestibular migraine from other conditions. *Curr. Pain Headache Rep.* 19:31. doi: 10.1007/s11916-015-0502-3

Durham, C. F., Alden, K. R., Dalton, J. A., Carlson, J., Miller, D. W., Englebardt, S. P., et al. (1998). Quality of life and productivity in nurses reporting migraine. *Headache* 38, 427–435. doi: 10.1046/j.1526-4610.1998.3806427.x

Formeister, E. J., Rizk, H. G., Kohn, M. A., and Sharon, J. D. (2018). The epidemiology of vestibular migraine: a population-based survey study. *Otol. Neurotol.* 39, 1037–1044. doi: 10.1097/mao.0000000000001900

International Headache Classification [ICHD] (2018). Headache classification committee of the international headache society (IHS) the international classification of headache disorders, 3rd edition. *Cephalalgia* 38, 1–211. doi: 10.1177/0333102417738202

Kerber, K. A., Callaghan, B. C., Telian, S. A., Meurer, W. J., Skolarus, L. E., Carender, W., et al. (2017). Dizziness symptom type prevalence and overlap: a US nationally representative survey. *Am. J. Med.* 130, 1465.e1–1465.e9. doi: 10.1016/j.amjmed.2017.05.048

Lempert, T., Olesen, J., Furman, J., Waterston, J., Seemungal, B., Carey, J., et al. (2012). Vestibular migraine: diagnostic criteria. *J. Vestib. Res.* 22, 167–172. doi: 10.3233/ves-2012-0453

Ligthart, L., Huijgen, A., Willemsen, G., de Geus, E. J. C., and Boomsma, D. I. (2018). Are migraine and tension-type headache genetically related? An investigation of twin family data. *Twin Res. Hum. Genet.* 21, 112–118. doi: 10.1017/thg.2018.5

Menon, B., and Remadevi, N. (2021). Migraine in nursing students-a study from a tertiary care center in South India. *J. Neurosci. Rural Pract.* 12, 129–132. doi: 10.1055/s-0040-1721556

Rapoport, A. M., and Bigal, M. E. (2004). ID-migraine. *Neurol. Sci.* 25(Suppl. 3), S258–S260. doi: 10.1007/s10072-004-0301-9

Roberts, B., and Neitzel, R. L. (2019). Noise exposure limit for children in recreational settings: review of available evidence. *J. Acoust. Soc. Am.* 146:3922. doi: 10.1121/1.5132540

Spierings, E. L., Ranke, A. H., and Honkoop, P. C. (2001). Precipitating and aggravating factors of migraine versus tension-type headache. *Headache* 41, 554–558. doi: 10.1046/j.1526-4610.2001.041006554.x

Tai, M. S., Yet, S. X. E., Lim, T. C., Pow, Z. Y., and Goh, C. B. (2019). Geographical differences in trigger factors of tension-type headaches and migraines. *Curr. Pain Headache Rep.* 23:12. doi: 10.1007/s11916-019-0760-6

Turner, D. P., Smitherman, T. A., Black, A. K., Penzien, D. B., Porter, J. A., Lofland, K. R., et al. (2015). Are migraine and tension-type headache diagnostic types or points on a severity continuum? An exploration of the latent taxometric structure of headache. *Pain* 156, 1200–1207. doi: 10.1097/j.pain.0000000000000157

Vuković, V., Plavec, D., Galinović, I., Lovrencić-Huzjan, A., Budisić, M., and Demarin, V. (2007). Prevalence of vertigo, dizziness, and migrainous vertigo in patients with migraine. *Headache* 47, 1427–1435. doi: 10.1111/j.1526-4610.2007.00939.x

Wang, J., Huang, Q., Li, N., Tan, G., Chen, L., and Zhou, J. (2013). Triggers of migraine and tension-type headache in China: a clinic-based survey. *Eur. J. Neurol.* 20, 689–696. doi: 10.1111/ene.12039

Wang, Y., Xie, J., Yang, F., Wu, S., Wang, H., Zhang, X., et al. (2015). The prevalence of primary headache disorders and their associated factors among nursing staff in North China. *J. Headache Pain* 16:4. doi: 10.1186/1129-2377-16-4

Yu, L. S., Si, F. Z., Ma, X., Han, L., and Jing, Y. Y. (2016). [Meniere disease and vestibular migraine]. *Lin Chung Er Bi Yan Hou Tou Jing Wai Ke Za Zhi* 30, 925–927. doi: 10.13201/j.issn.1001-1781.2016.12.001

Yu, S., Liu, R., Zhao, G., Yang, X., Qiao, X., Feng, J., et al. (2012). The prevalence and burden of primary headaches in China: a population-based door-to-door survey. *Headache* 52, 582–591. doi: 10.1111/j.1526-4610.2011.02061.x

Yunus, M. B. (2007). Fibromyalgia and overlapping disorders: the unifying concept of central sensitivity syndromes. *Semin. Arthritis Rheum.* 36, 339–356. doi: 10.1016/j.semarthrit.2006.12.009

Conflict of Interest: The authors declare that the research was conducted in the absence of any commercial or financial relationships that could be construed as a potential conflict of interest.

Publisher's Note: All claims expressed in this article are solely those of the authors and do not necessarily represent those of their affiliated organizations, or those of the publisher, the editors and the reviewers. Any product that may be evaluated in this article, or claim that may be made by its manufacturer, is not guaranteed or endorsed by the publisher.

Copyright © 2022 Diao, Zhu, Yu and Ma. This is an open-access article distributed under the terms of the Creative Commons Attribution License (CC BY). The use, distribution or reproduction in other forums is permitted, provided the original author(s) and the copyright owner(s) are credited and that the original publication in this journal is cited, in accordance with accepted academic practice. No use, distribution or reproduction is permitted which does not comply with these terms.

frontiers | Frontiers in Neurology

ORIGINAL RESEARCH
published: 12 July 2022
doi: 10.3389/fneur.2022.930542

Clinical Application of Different Vertical Position Tests for Posterior Canal-Benign Paroxysmal Positional Vertigo-Cupulolithiasis

Wenting Wang[1], Shuangmei Yan[2], Sai Zhang[1], Rui Han[2], Dong Li[2], Yihan Liu[1], Ting Zhang[1], Shaona Liu[2], Yuexia Wu[1], Ya Li[1], Xu Yang[3] and Ping Gu[1,2,4]**

[1] Department of Neurology, The First Hospital of Hebei Medical University, Shijiazhuang, China, [2] Department of Vertigo Center, The First Hospital of Hebei Medical University, Shijiazhuang, China, [3] Department of Neurology, Aerospace Center Hospital, Peking University Aerospace School of Clinical Medicine, Beijing, China, [4] Brain Aging and Cognitive Neuroscience Laboratory of Hebei Province, Shijiazhuang, China

OPEN ACCESS

Edited by:
Su-Lin Zhang,
Huazhong University of Science and Technology, China

Reviewed by:
Chen Taisheng,
Key Laboratory of Auditory Speech and Balance Medicine, China
Pedro L. Mangabeira-Albernaz,
Hospital Israelita Albert Einstein, Brazil

***Correspondence:**
Xu Yang
yangxu2011@163.com
Ping Gu
gpwh2000@126.com

Specialty section:
This article was submitted to Neuro-Otology, a section of the journal Frontiers in Neurology

Received: 28 April 2022
Accepted: 23 May 2022
Published: 12 July 2022

Citation:
Wang W, Yan S, Zhang S, Han R, Li D, Liu Y, Zhang T, Liu S, Wu Y, Li Y, Yang X and Gu P (2022) Clinical Application of Different Vertical Position Tests for Posterior Canal-Benign Paroxysmal Positional Vertigo-Cupulolithiasis. Front. Neurol. 13:930542. doi: 10.3389/fneur.2022.930542

Background: Posterior canal-benign paroxysmal positional vertigo-cupulolithiasis (PC-BPPV-cu) is a new and controversial type of benign paroxysmal positional vertigo (BPPV). At present, there are few relevant clinical studies as to whether the Half Dix-Hallpike test (Half D-HT) induces more obvious nystagmus than the Dix Hallpike test (D-HT) and straight head hanging test (SHH) in patients with PC-BPPV-cu.

Objectives: To investigate the clinical characteristics of PC-BPPV-cu, and analyze the diagnostic significance of the Dix-Hallpike test (D-HT), Half D-HT, and straight head hanging (SHH) test in these patients.

Methods: A total of 46 patients with PC-BPPV-cu were enrolled, and divided into two groups ($N = 23$): a group A (induction order: D-HT, Half D-HT, SHH) and a group B (induction order: Half D-HT, D-HT, SHH).

Results: Among 46 patients with PC-BPPV-cu, the bilateral and unilateral abnormality rates of the disease side were 5 cases and 41 cases, respectively. There were significant differences in the proportion of torsional-upbeating nystagmus and upbeating nystagmus among the three headhanging positions in 46 patients with PC-BPPV-cu ($P < 0.001$). The slow phase velocity (SPV) of induced nystagmus at half D-HT supine position was slower than D-HT supine position ($P < 0.05$) and SHH supine position ($P < 0.05$). The nystagmus latency of D-HT supine position was significantly shorter than half D-HT ($P < 0.05$) and SHH ($P < 0.05$). PC-BPPV-cu patients were accompanied by 53.5% semicircular canal paresis, 69.6% audiological abnormalities, 76% cervical vestibular evoked myogenic potential (cVEMP), and 75% video head impulse test (vHIT) abnormalities, the concordance rates of the four detection methods were similar ($\chi^2 = 0.243$, $P = 0.970$).

Conclusions: The Half D-HT is simple and feasible, but might have a risk of false-negative diagnoses of the torsional-upbeating nystagmus and upbeating nystagmus. The D-HT is still a classic induction method for PC-BPPV-cu. The two complement each other and may aid in the diagnosis of PC-BPPV-cu patients. Future clinical applications of Half D-HT require extensive research to determine its diagnostic efficacy.

Keywords: posterior semicircular canal, nystagmus, cupulolithiasis, vertigo, Dix-Hallpike test, benign paroxysmal positional vertigo

INTRODUCTION

Benign paroxysmal positional vertigo (BPPV) is one of the most common episodic vestibular diseases, arising from a problem in the inner ear (1). Symptoms are repeated and brief periods of vertigo with movement, characterized by a spinning sensation upon changes in the position of the head (2). When the head moves to a certain position, it can induce transient vertigo, accompanied by nystagmus and autonomic nerve symptoms (3). Approximately, 2.4% of people are affected at some point in time (1). BPPV is always found in people between the ages of 50 and 70, affecting women twice as often as men (4). The most frequently involved semicircular canal was the posterior semicircular canal (80–90%), followed by the lateral semicircular canal (10%), while the least involved semicircular canal was the superior semicircular canal (2%). The lifetime prevalence rate was approximate 3–10%.

In 2015, the international Barany society put forward the latest diagnostic criteria for BPPV (5). Posterior canal benign paroxysmal positional vertigo (PC-BPPV) is the most common type of BPPV (6). According to the pathophysiological mechanisms, PC-BPPV is divided into posterior canal benign paroxysmal positional vertigo canalithiasis (PC-BPPV-ca) and posterior canal-benign paroxysmal positional vertigo-cupulolithiasis (PC-BPPV-cu). Its nystagmus is characterized by upbeating and torsional nystagmus in the position-induced test, and the duration is less or more than one min. The golden diagnostic standard of PC-BPPV-ca is the Dix-Hallpike test (D-HT). PC-BPPV was diagnosed if vertical upbeat nystagmus with or without torsional component was induced by the Dix-Hallpike test, and the reversal of the nystagmus often occurred when returning to an upright position; if vertical upbeat nystagmus with torsional component was induced, the torsional component involved the beating of the upper pole of the eyes toward the affected side (7). PC-BPPV-cu is one of the new and controversial BPPV in the BPPV diagnostic criteria proposed by the International Barany Society. It refers to the appearance of upbeating and torsional nystagmus lasing $\geq$1 min in the position-induced test. Epley (8) proposed that the Half Dix-Hallpike test (Half D-HT) can cause the affected crest cap of PC-BPPV-cu patients to produce a greater degree of deflection under the action of gravity, thereby inducing strong positional nystagmus with a short or no incubation period.

As PC-BPPV-cu is one of the new and controversial BPPVs in the BPPV diagnostic criteria, the clinical characteristics of PC-BPPV-cu are not well-investigated. Additionally, the diagnostic efficiency of Half D-HT in comparison with D-HT and straight head hanging test (SHH) is rarely reported. This study intends to explore the clinical characteristics of PC-BPPV-cu and evaluate its nystagmus characteristics by different vertical position tests, so as to help the treatment of PC-BPPV-cu.

PATIENTS AND METHODS

Patients

A total of 46 patients with PC-BPPV-cu were collected in the Neurology Department and Vertigo Center of the First Hospital of Hebei Medical University from February 2019 to February 2022. The study was approved by the Ethics Committee of the First Hospital of Hebei Medical University. Written informed consent was obtained from each patient.

Among the patients, there were 20 men and 26women. Detailed basic information and medical history including gender, age, and current medical history (including duration, onset of seizure, duration of onset, triggers, motivating factors, accompanying symptoms), smoking, drinking history, and past history (including high blood pressure, diabetes, hyperlipidemia, coronary heart disease, cerebral infarction, migraine, brain injury, etc., Meniere's disease, vestibular neuritis, otitis media, osteoporosis, mood, and sleep disorders was) recorded. All patients underwent routine neuro-otology examination. Dynamic position tests included D-HT, Half D-HT, and SHH. Auxiliary examinations include pure tone audiometry, eye movement tests, canal paresis (CP) of caloric test, vestibular evoked myogenic potential (VEMP) (Interacoustics, Middelfart, Denmark. Model: Eclipse), video head impulse test (vHIT) (Interacoustics, Middelfart, Denmark. Model: EyeSeeCam) and video-nystagnography (VNG) (Interacoustics, Middelfart, Denmark. Model: V0425). If necessary, head computed tomography (CT), magnetic resonance imaging (MRI), CT angiography (CTA), CT perfusion (CTP) examinations were performed.

Methods

The diagnosis of PC-BPPV-cu refers to the latest BPPV diagnostic criteria proposed by the International Barany Society in 2015 (5), and the diagnosis of PC-BPPV-cu is based on the patient's typical nystagmus and its clinical manifestations: (1) D-HT and/or Half D-HT induces vertical nystagmus with torsion component. Nystagmus was often reversed when sitting up. If the vertical nystagmus was accompanied by a torsion component, the twisting direction of the upper pole of the eyeball was toward the

TABLE 1 | General condition of patients.

Variables	Group A ($n = 23$)	Group B ($n = 23$)	*P*-value
Age, median (IQR)	59 (31)	53 (21)	0.889
Course of disease (day), median (IQR)	12 (8)	9 (11)	0.627
Gender (Male), *n* (%)	8 (34.8)	12 (52.2)	0.234
Atherosclerosis, *n* (%)	16 (69.6)	17 (73.9)	0.743
Smoking, *n* (%)	4 (17.4)	6 (26.1)	0.475
Drinking, *n* (%)	4 (17.4)	8 (34.8)	0.179
Osteoporosis, *n* (%)	12 (52.2)	15 (65.2)	0.369
Mood and sleep disorders, *n* (%)	9 (39.1)	11 (47.8)	0.552
Head trauma, *n* (%)	2 (8.7)	3 (13.0)	1.000
History of abduction vestibule and otology, *n* (%)	13 (56.5)	12 (52.2)	0.767
History of migraine, *n* (%)	4 (17.4)	8 (34.8)	0.179
Immune disease, *n* (%)	7 (30.4)	6 (26.1)	0.743

IQR, interquartile range.

affected side. (2) The duration of nystagmus was ≥1 min. The random number table method was used to divide 46 patients into two groups ($N = 23$): group A (induction order: D-HT, Half D-HT, SHH) and group B (induction order: Half D-HT, D-HT, SHH). A G-Force BPPV diagnosis and treatment instrument (Product model: GYZ-ZLY-I. China Medical (TianJin) Group Co., LTD., China) was used to simulate the position tests were conducted. A 5-min rest between each position induction test was set to eliminate the fatigue. Three vertical position induction test methods were set as follows: (1) D-HT: The patient sits upright on the G-Force BPPV diagnosis and treatment instrument, head turned 45° to one side, and at the same time the patient is made tolie down and the head hang back at 20° below the horizontal plane. Vertigo and nystagmus were recorded until the nystagmus disappeared. The patients were quickly returned to the sitting position, followed by the check of the opposite side in the same way. (2) Half D-HT: The patient sits upright on the G-Force BPPV diagnosis and treatment instrument, head turned to one side by 45°, and then lies back to the supine position (∼30° tilted from the horizontal front). The patient's vertigo and nystagmus from this position were recorded, until the nystagmus disappeared and quickly returned to the sitting position, and then checked the opposite side in the same way. (3) SHH: The patient sits on the G-Force BPPV diagnosis and treatment instrument, lies down quickly, and hangs their head vertically at least 30° below the horizontal plane. The patient's vertigo and nystagmus at this position were recorded until the nystagmus disappeared. After disappearing, the patients were quickly returned to the sitting position. The G-Force BPPV diagnosis and treatment instrument was used to determine and record nystagmus. The subject was fixed on a swivel chair, wearing a high-definition 1080P eye video mask, in which the chair can complete more than 360° rotating motion and the display screen can clearly show the direction of eye movement and nystagmus parameters. In the position test, the maximum slow phase angular velocity of the nystagmus in the horizontal or vertical direction of the induced nystagmus in the postural position is used as the slow phase velocity (SPV) value. Positional nystagmus diagnosis of PC-BPPV-cu was observed through a video-oculography (Product model: GYZ-ZLY-I. China Medical (TianJin) Group Co., LTD., China) according to the manufacturer's instructions.

Statistical Analyses

SAS 9.3 software was used to analyze the data. The test results of a caloric test, audiology, cVEMP, vHIT, and the disease side were described in a cross table. The Chi-Squared test was used for comparison of count data between groups, and the Yates continuity correction or Fisher's exact test was performed if necessary. When the measurement data confirmed the normal distribution, the Student's *t*-test test was used for comparison between the two groups, and the Wilcoxon two-sample test was used when the measurement data did not conform to the normal distribution. For the comparison of measurement data among the three groups, one-way ANOVA analysis was used when the data were in a normal distribution. Otherwise, the Kruskal-Wallis test was used, and Student–Newman–Keuls (SNK) test was used for the comparison afterward. A $P < 0.05$ was considered to be statistically significant.

RESULTS

Basic Information

A total of 46 patients with PC-BPPV-cu were enrolled, accounting for 6.36% (46/723) of the BPPV patients during the same period. The ages ranged from 27 to 87 years old, with an average age of 54.91 ± 14.58 years. The peak age of onset was between 50 and 70 years old, accounting for 54.3% (**Table 1**). The course of the disease was about 12 days. Among them, there were 20 men (43.5%) and 26 women (56.5%). The ratio of men to women was 1:1.3.

Among 46 patients with PC-BPPV-cu, 33 cases (71.7%) were associated with atherosclerosis-related diseases, including 24 cases (52.2%) with hypertension, 22 cases (47.7%) with smoking and/or drinking history, 27 cases with osteoporosis (58.7%), 20 cases (43.5%) with mood and sleep disorder, 5 cases (10.9%) with brain trauma, 25 cases (54.4%) with history of abduction vestibule and otology, 12 cases (26.1%) with migraine, and 13 cases (28.3%) with autoimmune diseases. The abnormality rates on the disease side were as follows: 5 cases with bilateral abnormality, 25 cases with right abnormality, and 16 cases with left abnormality (**Table 1**). Thereafter, the 46 patients were divided into group A and group B. There was no significant difference in the age, sex ratio, and course of disease between group A and group B.

Comparison of Characteristics of Nystagmus Induced by PC-BPPV-cu Patients in Different Vertical Positions

There were significant differences in the torsional-upbeating nystagmus and upbeating nystagmus among the three supine positions in 46 patients with PC-BPPV-cu ($P < 0.001$) (**Table 2**, **Figure 1**). The proportion of torsional-upbeating and upbeating

TABLE 2 | Results of three types of vertical position induction tests.

Variables	Variable level	D-HT	Half D-HT	SHH	Row total	Test method	Statistics	*P*-value
Torsional nystagmus	Upbeating	8 (17.39)	7 (15.22)	15 (32.61)	30 (21.74)	Chi-Squared test	20.646	<0.001
	Upbeating and torsional	37 (80.43)	24 (52.17)	24 (52.17)	85 (61.59)			
	Others	1 (2.17)	15 (32.61)	7 (15.22)	23 (16.67)			
Reverse phase nystagmus	Yes	26 (56.52)	25 (54.35)	23 (50.00)	74 (53.62)	Fisher's exact test	–	0.156
	No	20 (43.48)	16 (34.78)	18 (39.13)	54 (39.13)			
	Without nystagmus	0 (0.00)	5 (10.87)	5 (10.87)	10 (7.25)			
Latency (s)	Mean ± SD	1.53 ± 0.76	2.55 ± 0.83[a]	2.46 ± 0.86[a]	2.13 ± 0.94	One-way Anova analysis	19.075	<0.001
SPV (°/ s)	Median (IQR)	22.0 (17.0, 31.0)	17.0 (10.0, 23.0)[a]	21.0 (15.0, 28.0)[b]	20.0 (15.0, 29.0)	Kruskal-Wallis test	6.923	0.031

Compared with D-HT, [a]P < 0.05.
Compared with Half D-HT, [b]P < 0.05.

nystagmus in the Dix-Hallpike test is the highest, followed by SHH and least in Half D-HT. The SPV of nystagmus at half D-HT headhanging position was slower than D-HT supine position ($P < 0.05$) and SHH headhanging position ($P < 0.05$). The nystagmus latency of D-HT supine position was significantly shorter than half D-HT suspended head position ($P < 0.05$) and SHH supine position ($P < 0.05$). There was no significant difference in the proportion of PC-BPPV-cu patients with reverse-phase nystagmus direction upon sitting up in three supine positions ($P > 0.05$) (**Table 2**, **Figure 2**).

Evaluation of Vestibular Audiology in Patients With PC-BPPV-cu and Its Correlation With Disease Side

The concordance rates of the four detection methods (canal paresis of caloric test, audiology, cVEMP, vHIT) were similar ($\chi^2 = 0.243$, $P = 0.970$). Among 46 patients with PC-BPPV-cu, 43 had undergone canal paresis of the caloric test. Among the patients with unilateral semicircular canal paresis, 12 patients (27.9%) were on the right side of semicircular canal paresis, and 7 patients were on the left side (16.3%) (**Table 3**).

All 46 Pc-BPPV-cu patients underwent pure-tone audiometry, of which 14 patients (30.4%) had normal hearing; 20 patients (43.5%) had unilateral hearing loss, and 7 patients (15.2%) had hearing loss on the left side. Among them, there were 13 cases (28.3%) with hearing loss on theright side, and 12 cases (26.1%) with bilateral hearing loss. Among 20 cases with unilateral hearing loss, there were 17 cases (85.0%) which were consistent with the side of the semicircular canal involved in their BPPV, while 3 cases (15.0%) were inconsistent with the side of the involved semicircular canal (**Table 3**).

During the data collection, the amplitude and latency of the first positive–negative peaks (p13–n23) were calculated from the average of 2 responses to confirm the reproducibility. An asymmetry ratio (AR) for cVEMPs was calculated in order to evaluate the p13-n23 component of the response. We recorded whether cVEMP was abnormal, and the side of the abnormality. The specific evaluation criteria: cVEMP latency wasprolonged, the amplitude was reduced or disappeared, the amplitude AR was >29%, the waveform could not be elicited, and the threshold was raised or lowered as abnormal results (9). Among 46 patients with PC-BPPV-cu, 29 had cVEMP, of which 7 cases (24.1%) had normal cVEMP; 15 cases (51.9%) had unilateral cVEMP abnormality, 7 cases (24.1%) of bilateral cVEMP abnormalities; of 15 cases of unilateral cVEMP abnormalities, 11 cases (73.3%) were consistent with the side of the BPPV involved semicircular canal, and 4 cases (26.7%) were the same as the side of the involved semicircular canal (**Table 3**).

During the data collection, we recorded whether vHIT was abnormal, and the side of the abnormality. The average gain value of the slow phase of vestibular-ocular reflex (VOR) (the ratio of eye movement velocity and head movement angular velocity at 60 s) can be recorded using vHIT software (10). The specific evaluation criteria were as follows: the normal vestibular eye movement reflex gain range of the horizontal semicircular canal was 0.79–1.20, and the normal range of the vertical semicircular canal was 0.7–1.2. In this study, any one of the following three points was regarded as abnormal vHIT: firstly, the instantaneous vHIT gain value of 60 ms was used as the evaluation index for the horizontal semicircular canal (<0.8 was determined to be abnormal) and the regression gain value was used as the evaluation index for the vertical semicircular canal (<0.7 was determined to be abnormal). Secondly, in 20 vHIT tests, 10 or more compensatory saccade waves (overt saccade or invisible saccade) were judged to be positive. Thirdly, a Bilateral asymmetry ratio >13% was judged to be abnormal. Among 46 patients with PC-BPPV-cu, 24 patients underwent vHIT, of which 6 patients had normal vHIT (25.0%); 11 patients had unilateral vHIT abnormality (45.8%); 7 patients had bilateral vHIT abnormality (29.2%). Among the 11 cases with unilateral vHIT abnormality, 8 cases (72.7%) were consistent with the side of BPPV involved semicircular canal, and 3 cases (27.3%) were

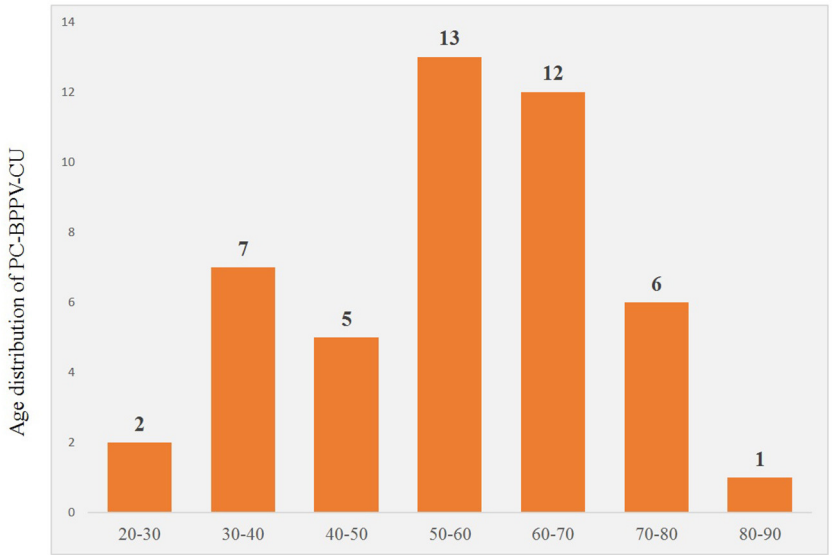

FIGURE 1 | Distribution of torsional nystagmus in three suspension positions in patients with PC-BPPV-cu. UBN, upbeating nystagmus; T-UBN, torsional-upbeating nystagmus.

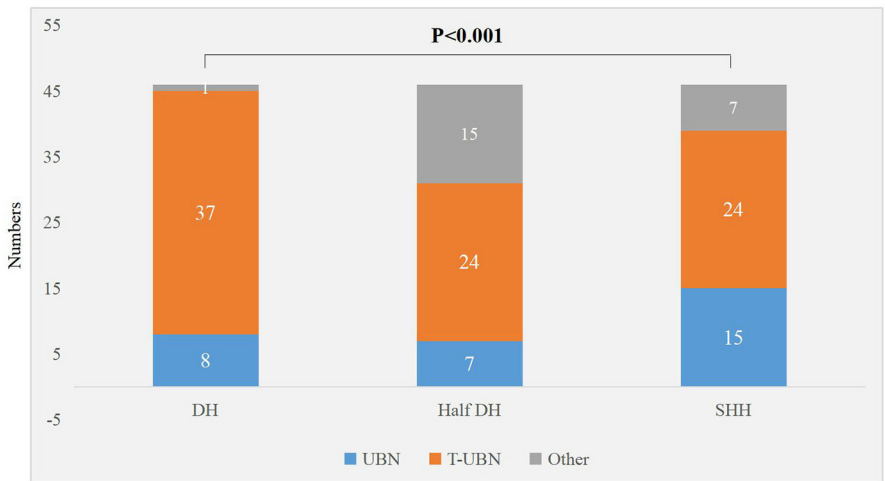

FIGURE 2 | Distribution of sit up and reverse nystagmus in three suspension positions in patients with PC-BPPV-cu.

inconsistent with the side of the involved semicircular canal (**Table 3**).

DISCUSSION

PC-BPPV-cu has received more and more attention in clinical practice. A previous study has found that PC-BPPV-cu accounts for about 6.3% of BPPV patients (11). In this study, we found that PC-BPPV-cu patients accounted for 6.36% (46/723) of the BPPV patients who visited during the same period, which is similar to the results of previous studies and our previous study (6). The male to female ratio of PC-BPPV-cu patients in this study was 1:1.3. There were mostly middle-aged and elderly people. Among patients with unilateral involvement of PC-BPPV-cu, the right-side involvement accounted for 64.3%. The reason is analyzed and the key factors of bone maintenance, bone formation, and bone resorption in middle-aged and elderly women decreasing year by year (12), leading to osteoporosis and abnormal calcium metabolism, affecting endolymph metabolism and inner ear microcirculation (13). Otoliths are deposited on the ampullary crest of the semicircular canal, making it more sensitive to changes in gravity. When the head position was changed, the ampulla cap otoliths of PC-BPPV-cu patients were displaced, resulting in clinical manifestations such as dizziness

TABLE 3 | Cross table of the test results of caloric test, audiology, cVEMP, vHIT, and the condition of the affected side.

Test methods	Results	Affected side, *n* (%)			Row total	Consistency rate of affected side (%)
		Bilateral abnormality	Right abnormality	Left abnormality		
Caloric test	Bilateral abnormality	2 (50.00)	1 (4.17)	1 (6.67)	4 (9.30)	46.51
	Right abnormality	1 (25.00)	11 (45.83)	0 (0.00)	12 (27.91)	
	Left abnormality	0 (0.00)	0 (0.00)	7 (46.67)	7 (16.28)	
	Normal	1 (25.00)	12 (50.00)	7 (46.67)	20 (46.51)	
Audiology	Bilateral abnormality	3 (60.00)	5 (20.00)	4 (25.00)	12 (26.09)	43.48
	Right abnormality	0 (0.00)	12 (48.00)	1 (6.25)	13 (28.26)	
	Left abnormality	1 (20.00)	1 (4.00)	5 (31.25)	7 (15.22)	
	Normal	1 (20.00)	7 (28.00)	6 (37.50)	14 (30.43)	
cVEMP	Bilateral abnormality	1 (25.00)	4 (26.67)	2 (20.00)	7 (24.14)	41.38
	Right abnormality	1 (25.00)	8 (53.33)	1 (10.00)	10 (34.48)	
	Left abnormality	0 (0.00)	2 (13.33)	3 (30.00)	5 (17.24)	
	Normal	2 (50.00)	1 (6.67)	4 (40.00)	7 (24.14)	
vHIT	Bilateral abnormality	2 (50.00)	4 (44.44)	1 (9.09)	7 (29.17)	41.67
	Right abnormality	1 (25.00)	4 (44.44)	1 (9.09)	6 (25.00)	
	Left abnormality	1 (25.00)	0 (0.00)	4 (36.36)	5 (20.83)	
	Normal	0 (0.00)	1 (11.11)	5 (45.45)	6 (25.00)	

cVEMP, cervical vestibular evoked myogenic potential; vHIT, video head impulse test.

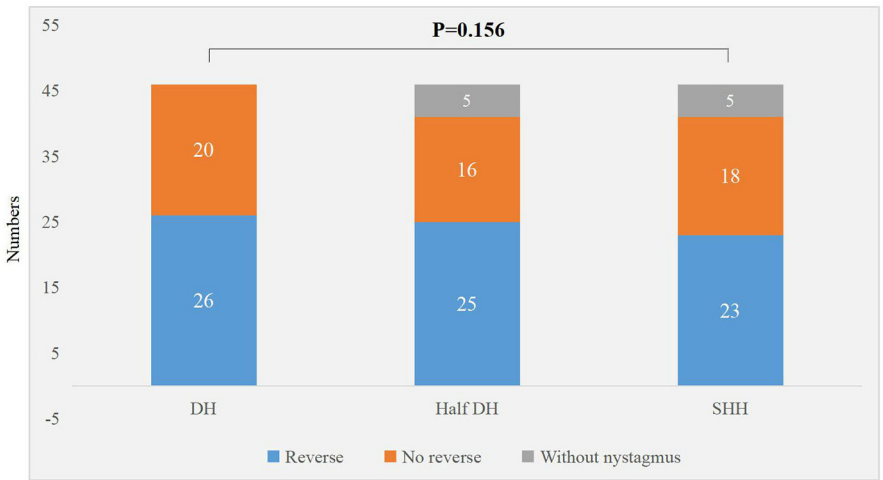

FIGURE 3 | Distribution of sit up and reverse nystagmus in three suspension positions in patients with PC-BPPV-cu.

and nystagmus. Therefore, PC-BPPV-cu is more common in elderly women and is often accompanied by a history of osteoporosis. The high morbidity on the right side is considered to be related to the fact that most patients are used to sleeping on the right side.

The typical nystagmus of PC-BPPV-cu is a nystagmus with a vertical component toward the upper pole of the eyeball and a twist component toward the ground (14). Theoretically, the D-HT test can make the affected crest cap be in a horizontal position, and produce a greater degree of deflection under the action of gravity (8). Our research found that the D-HT test and SHH test had a higher SPV of upbeating nystagmus in patients with PC-BPPV-cu than the Half D-HT test. Compared with the Half D-HT and SHH, D-HT has shorter latency of nystagmus. Carlos et al. (15) pointed out that the latency was an important factor for D-HT in patients with PC-BPPV. It is consistent with our above-mentioned PC-BPPV-cu research. The large-scale changes in spatial position have more obvious physical stimulation to the crest cap otoliths. The crest cap otoliths drive the ampullary crest to deviate to the tube side

(producing movement away from the ampullae), resulting in an imbalance of the vestibular tension on both sides. According to Flourens law, the semicircular canal is stimulated to cause the flow of endolymph, and the plane of nystagmus is consistent with the spatial plane of the semicircular canal. In addition, the crest cap is a peripheral sensor that is sensitive to angular acceleration. When the information of the gravity change received by the crest cap reaches a certain threshold and shifts to a certain level, the hair cells are excited to generate action potentials, and further pass through the VOR pathway to cause nystagmus. Cui et al. (16) found that the direction of the torsional component of PC-BPPV is uncertain. If a rotational nystagmus with a vertical upbeating component is induced in the Roll test, it is highly suggested that PC-BPPV may be possible; Hiroaki et al. (17) quantitatively analyzed the horizontal, vertical, and torsional components of nystagmus during the SHH test in patients with PC-BPPV-cu, and found that the SPV of nystagmus torsion in SHH suspension head position was significantly greater than that of nystagmus torsion after sitting up. In our study, although it was impossible to quantitatively compare the torsion component during the vertical position induction test in patients with PC-BPPV-cu, we found that there were significant statistical differences in the proportions of upbeating nystagmus, upbeating and rotational nystagmusin in the three head suspension positions. The proportion of upbeating and rotational nystagmus induced by the D-HT in PC-BPPV-cu patients was higher than that in the Half D-HT, followed by SHH, and least in Half D-HT. Dix Hallpike test is still a classic induction method for PC-BPPV-cu. Half D-HT is simple and easy, especially for patients with neck diseases who cannot look upwards by much. The straight head hanging (SHH) test has obvious significance for the diagnosis of anterior canal benign paroxysmal positional vertigo (18); for patients with PC-BPPV-cu, a roll test can be performed when necessary to help lateral diagnosis. Therefore, Half D-HT and SHH test are powerful supplements to D-HT in the diagnosis of patients with PC-BPPV-cu. The typical nystagmus of PC-BPPV-cu is a nystagmus with a vertical component toward the upper pole of the eye and a torsional component toward the ground (14). The nystagmus of patients with PC-BPPV-cu can usually be induced by vertical position test with vertigo symptoms. The direction of positional nystagmus induced by position test is consistent with the direction of the rotation axis of the stimulated semicircular canal (5). Most of the patients with PC-BPPV-cu in this study were complicated with peripheral vestibular lesions. After imaging examination, the patients in this study have excluded the correlation between positional nystagmus and central vestibular lesions. Patients with central vestibular lesions near the dorsolateral part of the fourth ventricle, dorsal vermis of the cerebellum, nucleus prepositus hypoglossi, cerebellar nodulus, and uvula can show paroxysmal central positional nystagmus in position tests (19, 20). The duration of paroxysmal central positional nystagmus is longer, so the nystagmus of PC-BPPV-cu and paroxysmal central vestibular disorders are often difficult to distinguish. Patients with central vestibular disorders are often accompanied by spontaneous and positional down-beating nystagmus, the direction of positional nystagmus induced by position test was not consistent with the axis of semicircular canal, vertigo may not be associated, and nystagmus cannot be suppressed by fixation. Paroxysmal central positional nystagmus may be ascribed to erroneous neural processing within the velocity-storage circuit that functions in estimating angular head velocity, gravity direction, and inertia (21).

It is speculated that the generation of reverse phase nystagmus may be related to the semicircular canal inertial rebound of the crest at the abdominal crest (22), there was no significant difference in the proportion of PC-BPPV-cu patients with reverse-phase nystagmus direction upon sitting up in three supine positions ($P > 0.05$) (**Table 2**, **Figure 3**), but among the three inducing methods, the proportion of reverse phase nystagmus in D-HT is the highest, D-HT is the most classical and reliable method to diagnose PC-BPPV-cu.

Baloh et al. (17) proposed that the hypofunction of the BPPV semicircular canal was not caused by ectopic otoliths, but by extensive vestibular peripheral organ diseases. Different patients with BPPV have different degrees of damage to the semicircular canal function. The combined application of the cold and heat test and vHIT test could objectively and comprehensively evaluate the semicircular canal function of patients with idiopathic BPPV. Bi et al. (23) found that the semicircular canal paresis rate of BPPV patients was 57%. Nakahara et al. (24) found that the abnormal rate of oVEMP in BPPV patients was higher than that of the normal population. We previously reported that unilateral vestibular dysfunction and audiological abnormalities assisted the positioning of multitubular BPPV (7). In this present study, most patients with PC-BPPV-cu had semicircular canal paresis and abnormalities in audiology, cVEMP, and vHIT. The hearing test is used as a routine examination and observation index for BPPV patients. There are many influencing factors, such as age, disease histories, and the patient's own subjective perception of hearing, etc. Therefore, for patients with PC-BPPV-cu, a combined application of semicircular canals and otolith function evaluation is helpful for the diagnosis and etiological treatment of patients with PC-BPPV-cu.

The sample size of this study is relatively small. Future work should expand the sample size and analyze the clinical characteristics of PC-BPPV-cu patients, such as a comparison of the correlation between the subtypes of different sleep disorders and the incidence of PC-BPPV-cu.

In summary, the Half D-HT is simple and feasible but might bring a risk of false-negatives to diagnosis of torsional-upbeating nystagmus and upbeating nystagmus. The D-HT is still a classic induction method for PC-BPPV-cu. The two complement each other and may aid in the diagnosis of PC-BPPV-cu patients. Future clinical applications of Half D-HT require extensive research to determine its diagnostic efficacy.

In addition, for patients with PC-BPPV-cu, we can combine audiology, semicircular canal and otolitic device function evaluation technology to assist patients' diagnoses. The diagnosis

of PC-BPPV-cu could guide the medication and rehabilitation of patients with PC-BPPV-cu, and correctly assess the prognosis.

DATA AVAILABILITY STATEMENT

The original contributions presented in the study are included in the article/supplementary material, further inquiries can be directed to the corresponding author/s.

ETHICS STATEMENT

The studies involving human participants were reviewed and approved by the First Hospital of Hebei Medical University. The patients/participants provided their written informed consent to participate in this study.

AUTHOR CONTRIBUTIONS

WW, PG, and SY have made substantial contributions to the conception, design of the study, and have been involved in drafting the manuscript. S and RH were involved in the acquisition of data, data entry, and data cleaning. DL, YLiu, and TZ were involved in the analysis and interpretation of data. SL, YW, and YLi were involved in revising the manuscript critically for important intellectual content. YW made contributions to data collection and analysis. All authors contributed substantially to its revision. All authors read and approved the final manuscript.

FUNDING

This study was funded by Hebei Provincial Health Commission (No. 20220174).

REFERENCES

1. You P, Instrum R, Parnes L. Benign paroxysmal positional vertigo. *Laryngosc Invest Otolaryngol.* (2019) 4:116–23. doi: 10.1002/lio2.230
2. Lee SH, Kim JS. Benign paroxysmal positional vertigo. *J Clin Neurol.* (2010) 6:51–63. doi: 10.3988/jcn.2010.6.2.51
3. Nuti D, Masini M, Mandala M. Benign paroxysmal positional vertigo and its variants. *Handb Clin Neurol.* (2016) 137:241–56. doi: 10.1016/B978-0-444-63437-5.00018-2
4. Balatsouras DG, Koukoutsis G, Fassolis A, Moukos A, Apris A. Benign paroxysmal positional vertigo in the elderly: current insights. *Clin Interv Aging.* (2018) 13:2251–66. doi: 10.2147/CIA.S144134
5. von Brevern M, Bertholon P, Brandt T, Fife T, Imai T, Nuti D, Newman-Toker D. Benign paroxysmal positional vertigo: diagnostic criteria. *J Vestib Res.* (2015) 25:105–17. doi: 10.3233/VES-150553
6. Ling X, Zhao DH, Shen B, Si LH, Li KZ, Hong Y, et al. Clinical characteristics of patients with benign paroxysmal positional vertigo diagnosed based on the diagnostic criteria of the barany society. *Front Neurol.* (2020) 11:602. doi: 10.3389/fneur.2020.00602
7. Si L, Ling X, Li Z, Li K, Shen B, Yang X. Clinical characteristics of patients with multi-canal benign paroxysmal positional vertigo. *Braz J Otorhinolaryngol.* (2022) 88:89–100. doi: 10.1016/j.bjorl.2020.05.012
8. Epley JM. Human experience with canalith repositioning maneuvers. *Ann N Y Acad Sci.* (2001) 942: 179–91. doi: 10.1111/j.1749-6632.2001.tb03744.x
9. Jacobson GP, McCaslin DL, Piker EG, Gruenwald J, Grantham SL, Tegel L. Patterns of abnormality in cVEMP, oVEMP, and caloric tests may provide topological information about vestibular impairment. *J Am Acad Audiol.* (2011) 22:601–11. doi: 10.3766/jaaa.22.9.5
10. Halmagyi GM, Chen L, MacDougall HG, Weber KP, McGarvie LA, Curthoys IS. The video head impulse test. *Front Neurol.* (2017) 8:258. doi: 10.3389/fneur.2017.00258
11. Schuknecht HF, Ruby RR. Cupulolithiasis. *Adv Oto Rhino Laryngol.* (1973) 20:434–43. doi: 10.1159/000393114
12. Ogun OA, Buki B, Cohn ES, Janky KL, Lundberg YW. Menopause and benign paroxysmal positional vertigo. *Menopause.* (2014) 21:886–9. doi: 10.1097/GME.0000000000000190
13. Jeong SH, Kim JS. Impaired calcium metabolism in benign paroxysmal positional vertigo: a topical review. *J Neurol Phys Ther.* (2019) 43(Suppl. 2):S37–41. doi: 10.1097/NPT.0000000000000273
14. Hornibrook J. Benign paroxysmal positional vertigo (BPPV): history, pathophysiology, office treatment and future directions. *Int J Otolaryngol.* (2011) 2011:835671. doi: 10.1155/2011/835671
15. Zuma e Maia FC, Albernaz PL, Cal RV. Behavior of the posterior semicircular canal after Dix-Hallpike Maneuver. *Audiol Res.* (2016) 6:140. doi: 10.4081/audiores.2016.140
16. Cui X, Feng Y, Mei L, He C, Lu X, Zhang H, et al. The analysis of nystagmus in patients with posterior canal benign paroxysmal positional vertigoin positioning test. *J Clin Otorhinolaryngl Head Neck Surg.* (2015) 29:27–30.
17. Ichijo H. Cupulolithiasis of the posterior semicircular canal. *Am J Otolaryngol.* (2013) 34:458–63. doi: 10.1016/j.amjoto.2013.04.001
18. Yang X, Ling X, Shen B, Hong Y, Li K, Si L, et al. Diagnosis strategy and Yacovino maneuver for anterior canal-benign paroxysmal positional vertigo. *J Neurol.* (2019) 266:1674–84. doi: 10.1007/s00415-019-09312-1
19. Leigh RJ, Zee DS. *Neurology of the Eye Movements*. 5th ed. New York, NY: Oxford University Press (2015). doi: 10.1093/med/9780199969289.001.0001
20. Richards MD, Wong A. Infantile nystagmus syndrome: clinicalcharacteristics, current theories of pathogenesis, diagnosis, and management. *Can J Ophthalmol.* (2015) 50:400-408 doi: 10.1016/j.jcjo.2015.07.010
21. Choi JY, Kim JS. Central positional nystagmus: characteristics and model-based explanations. *Prog Brain Res.* (2019) 249:211–25. doi: 10.1016/bs.pbr.2019.04.012
22. Wen C, Chen T, Chen F, Liu Q, Li S, Cheng Y, et al. [Investigation of the reverse phase nystagmus in positioning test for benign paroxysmal positional vertigo]. *Zhonghua Er Bi Yan Hou Tou Jing Wai Ke Za Zhi.* (2014) 49: 384–9.
23. Bi J, Liu B, Zhang Y, Duan J, Zhou Q. Caloric tests in clinical practice in benign paroxysmal positional vertigo. *Acta Oto Laryngol.* (2019) 139:671–6. doi: 10.1080/00016489.2019.1614220
24. Nakahara H, Yoshimura E, Tsuda Y, Murofushi T. Damaged utricular function clarified by oVEMP in patients with benign paroxysmal positional vertigo. *Acta Oto Laryngol.* (2013) 133:144–9. doi: 10.3109/00016489.2012.720030

Conflict of Interest: The authors declare that the research was conducted in the absence of any commercial or financial relationships that could be construed as a potential conflict of interest.

Publisher's Note: All claims expressed in this article are solely those of the authors and do not necessarily represent those of their affiliated organizations, or those of the publisher, the editors and the reviewers. Any product that may be evaluated in this article, or claim that may be made by its manufacturer, is not guaranteed or endorsed by the publisher.

Copyright © 2022 Wang, Yan, Zhang, Han, Li, Liu, Zhang, Liu, Wu, Li, Yang and Gu. This is an open-access article distributed under the terms of the Creative Commons Attribution License (CC BY). The use, distribution or reproduction in other forums is permitted, provided the original author(s) and the copyright owner(s) are credited and that the original publication in this journal is cited, in accordance with accepted academic practice. No use, distribution or reproduction is permitted which does not comply with these terms.

frontiers | Frontiers in Neuroscience

ORIGINAL RESEARCH
published: 13 July 2022
doi: 10.3389/fnins.2022.933520

The Spectrum of Vestibular Disorders Presenting With Acute Continuous Vertigo

Qingxiu Yao[1,2,3,4†], Zhuangzhuang Li[1,2,3†], Maoxiang Xu[1,2,3†], Yumeng Jiang[1,2,3], Jingjing Wang[1,2,3], Hui Wang[5], Dongzhen Yu[1,2,3] and Shankai Yin[1,2,3]*

[1] Department of Otolaryngology-Head and Neck Surgery, Shanghai Jiao Tong University Affiliated Sixth People's Hospital, Shanghai, China, [2] Otolaryngology Institute of Shanghai Jiao Tong University, Shanghai, China, [3] Shanghai Key Laboratory of Sleep Disordered Breathing, Shanghai, China, [4] Department of Otolaryngology, The First Affiliated Hospital, College of Medicine, Zhejiang University, Hangzhou, China, [5] Department of Otorhinolaryngology, ENT Institute, Affiliated Eye and ENT Hospital, Fudan University, Shanghai, China

Objective: To explore the composition of vestibular disorders presenting with the acute vestibular syndrome (AVS).

Methods: We performed a case analysis of 209 AVS patients between January 2016 and December 2020. These patients were grouped into different disorder categories according to the relevant diagnostic criteria.

Results: We classified the 209 patients into 14 disorder categories, including 110 cases of vestibular neuritis, 30 of idiopathic sudden sensorineural hearing loss with vertigo, 17 of the first attack of continuous vertigo with migraine, 15 of Ramsay Hunt syndrome, 11 of acute labyrinthitis secondary to chronic otitis media, 8 of vestibular schwannoma, 6 of posterior circulation infarction and/or ischemia, 3 of cerebellar abscess secondary to chronic otitis media, 3 of AVS caused by trauma or surgery, 2 of AVS with down-beating nystagmus, 1 of multiple sclerosis of the medulla oblongata, 1 of epidermoid cyst of the posterior cranial fossa, 1 of a probable acute otolithic lesion, and 1 of AVS without measurable vestibular dysfunction.

Conclusion: When a group of disorders present with AVS, characteristic clinical manifestations and imaging help with an accurate diagnosis.

Keywords: acute vestibular syndrome, vertigo, diagnosis, peripheral, central

OPEN ACCESS

Edited by:
Su-Lin Zhang,
Huazhong University of Science and Technology, China

Reviewed by:
Tzu-Pu Chang,
Taichung Tzu Chi General Hospital, Taiwan
Ganggang Chen,
Shanxi Medical University, China

***Correspondence:**
Dongzhen Yu
drdzyu@126.com

† These authors have contributed equally to this work

Specialty section:
This article was submitted to Perception Science, a section of the journal Frontiers in Neuroscience

Received: *01 May 2022*
Accepted: *15 June 2022*
Published: *13 July 2022*

Citation:
Yao Q, Li Z, Xu M, Jiang Y, Wang J, Wang H, Yu D and Yin S (2022) The Spectrum of Vestibular Disorders Presenting With Acute Continuous Vertigo. Front. Neurosci. 16:933520. doi: 10.3389/fnins.2022.933520

INTRODUCTION

Acute vestibular syndrome (AVS) is defined as the sudden onset of acute continuous vertigo associated with nausea, vomiting, motion intolerance, gait instability, and nystagmus lasting for days to weeks (Hotson and Baloh, 1998; Kattah et al., 2009; Chen et al., 2011; Newman-Toker et al., 2013a,b; Saber Tehrani et al., 2014; Mantokoudis et al., 2015b). A population-based descriptive study reported that 19.2% of dizzy patients have AVS, with an incidence of 92/100,000 population (Ljunggre et al., 2018). Although our understanding of AVS has improved recently, it is still not clear how many kinds of vestibular disorders present with AVS. Vestibular neuritis (VN) and stroke, which are both vestibular disorders that can provoke AVS, affect peripheral and central vestibular structures, respectively. However, other vestibular conditions, such as complications of chronic otitis media and demyelinating diseases (e.g., multiple sclerosis) are not well recognized, which can lead to delayed diagnosis, misdiagnosis, or improper treatment. Although progress has been made in basic and clinical vestibular studies, no histopathological, radiological, or physiological markers

or other confirmatory diagnostic tests are available for diagnosing many disorders presenting as AVS; thus, such disorders are still diagnosed based only on clinical experience. Many conditions manifesting as AVS have not been well studied, such as "first attack of continuous vertigo with migraine." In addition, due to the harm that AVS causes patients and the low efficiency of current diagnostic and treatment modalities, it is essential to improve our understanding of AVS.

Our previous study, with a relatively small sample size of 77 patients, classified AVS into various specific disorders (Yao et al., 2018a). The purpose of this study was to explore vestibular disorders that can be attributed to AVS. Therefore, we performed a case analysis of a relatively large number of AVS patients to explore the composition of vestibular disorders presenting with AVS. A definite or probable diagnosis was obtained for most patients based on the relevant diagnostic criteria.

MATERIALS AND METHODS

Subjects

We retrospectively enrolled 209 patients with AVS who visited our outpatient clinic for vertigo and balance disorders at the Shanghai Jiao Tong University Affiliated Sixth People's Hospital from June 2016 to December 2020. The study was performed in accordance with the recommendations of the Ethics Committee of the Shanghai Jiao Tong University Affiliated Sixth People's Hospital [2020-KY-004 (K)].

Inclusion and Exclusion Criteria

The inclusion criteria were acute-onset, persistent vertigo, dizziness, or instability lasting days to weeks (Venhovens et al., 2016). Exclusion criteria were a first attack duration of < 24 h, an episodic vestibular syndrome (EVS), such as Meniere's disease or benign paroxysmal positional vertigo, and chronic vertigo or dizziness lasting longer than 3 months, such as bilateral vestibulopathy.

Neuro-Otological Evaluation

In addition to symptom evaluation, the patients underwent examinations of the external auditory canal, tympanic membrane, and mastoid, as well as bedside examinations, and auxiliary examinations including pure tone audiometry (PTA), vestibular function testing [video head impulse test (vHIT), cervical vestibular-evoked myogenic potentials (cVEMPs) and ocular vestibular-evoked myogenic potentials (oVEMPs), and videonystagmography (VNG) test]. All patients took a horizontal head impulse test (h−HIT), 96.17% of patients took vHIT, 10.53% took cVEMPs and oVEMPs, and 33.01% took the VNG test. These tests were all performed in the acute stage.

Temporal bone computed tomography (CT) and craniocerebral magnetic resonance imaging (MRI) were performed where necessary. In our study, 21.53% of patients were screened using MRI, and all patients with abnormal ocular movements underwent MRI in the acute stage. Some patients with tinnitus and hearing loss, and whose symptoms did not improve after 3–7 days of treatment had MRI in remission stage.

Disease Diagnosis

Most disorders were diagnosed according to the diagnostic criteria (Hunt, 1907; Vazquez et al., 2003; Zhang et al., 2007; Stachler et al., 2012; Jeong et al., 2013; Förster et al., 2016; Thompson et al., 2018; Greene and Al-Dhahir, 2020; Spinato et al., 2021). Idiopathic sudden sensorineural hearing loss (ISSNHL) with vertigo was defined as a subtype of sudden sensorineural hearing loss accompanied by acute continuous vertigo or imbalance, with an unknown etiology and cannot be attributable to another disorder. The probable acute isolated otolithic lesion was defined as those patients who presented with symptoms of AVS and had normal results of all the vestibular function tests except the VEMPs. AVS without measurable vestibular dysfunction referred to patients who had symptoms of vertigo or nausea, vomiting, motion intolerance, and gait instability, had normal results of vestibular function tests, and were not attributable to another disorder. Other disorders were diagnosed according to the specific clinical manifestations and auxiliary examinations, such as CT and MRI.

Classification

Central and Peripheral Acute Vestibular Syndrome

Patients were grouped into different disorder categories according to the relevant diagnostic criteria. Vertigo caused by an impairment of the inner ear or vestibular nerve was classified as peripheral AVS. And the patients who had unilateral vestibular loss confirmed by vHIT and had normal MRI were classified into the group of peripheral AVS. If the lesion involved the vestibular nuclei, the vestibular connections of the brainstem, and/or the cerebellar circuits on CT or MRI, it was classified as central AVS (Bertholon et al., 2020).

Statistical Analysis

All statistical analyses were performed with SPSS software (ver. 22.0; IBM Corp., Armonk, NY, United States). The positive rates of h-HIT and spontaneous nystagmus (SN) were compared between ISSNHL with vertigo and VN patients using the Chi-square test. $p < 0.05$ was considered to indicate statistical significance.

RESULTS

We enrolled 209 patients presenting with AVS. Based on the diagnostic criteria, 14 disorders were classified as peripheral or central AVS (**Table 1**).

Peripheral Acute Vestibular Syndrome

In total, 175 patients presented with peripheral AVS, including 110 cases of VN, 30 of ISSNHL with vertigo, 15 of Ramsay Hunt syndrome, 11 of acute labyrinthitis secondary to chronic otitis media, 8 of vestibular schwannoma, and 1 of AVS caused by trauma.

Of these patients, 145 patients had SN. The vHIT results showed that all the patients had unilateral vestibular dysfunction.

Vestibular neuritis is one of the most common peripheral causes of AVS, of which the diagnosis is generally based on a

TABLE 1 | Comprehensive AVS classification system.

Classification	Case number	Male sex	Age (years)	Cardinal features (except vertigo)	Auxiliary examination	Peripheral/ Central AVS
Vestibular neuritis	110	56 (50.91)	46.35 ± 14.59	No hearing loss, no neurological symptoms or signs, no migraine	vHIT, VNG	Peripheral
Idiopathic sudden sensorineural hearing loss with vertigo	30	13 (43.33)	58.86 ± 11.13	Sudden hearing loss, no neurological symptoms or signs	PTA, vHIT, VEMP	Peripheral
First attack of continuous vertigo with migraine	17	3 (17.65)	42.29 ± 17.09	Migraine	vHIT, VNG, MRI	Peripheral/central
Ramsay Hunt syndrome	15	5 (33.33)	58.08 ± 15.45	Otalgia and auricular herpes, with or without facial nerve paralysis/hearing loss	vHIT	Peripheral
Acute labyrinthitis secondary to otitis media	11	2 (18.18)	61.91 ± 8.02	Otorrhea, hearing loss	vHIT, VNG, PTA, CT, MRI	Peripheral
Vestibular schwannoma	8	5 (62.50)	51.13 ± 12.10	Rapid hearing loss and/or tinnitus	vHIT, VNG, PTA, MRI	Peripheral
Posterior circulation infarction and/or ischemia	6	5 (83.33)	58.17 ± 10.02	Unstable gait, ataxia, motor and/or sensory aphasia, dysarthria, abnormal eye movements, gaze-evoked nystagmus	vHIT, VNG, MRI	Central
Cerebellar abscess or inflammation secondary to otitis media	3	2 (66.67)	61.33 ± 5.56	High fever, headache	vHIT, CT, MRI, VNG	Central
AVS caused by trauma or surgery	3	2 (66.67)	54.33 ± 4.19	Medical history of trauma or surgery	vHIT, CT, MRI, VNG	Peripheral/central
AVS with DBN	2	1 (50.00)	75.50 ± 1.50	DBN	vHIT, MRI, VNG	Peripheral/central
Multiple sclerosis of the medulla oblongata	1	0 (0.00)	19.00 ± 0.00	Instability, up-beating nystagmus	vHIT, MRI, VNG	Central
Epidermoid cyst of the posterior cranial fossa	1	0 (0.00)	43.00 ± 0.00	Instability, up-beating nystagmus	vHIT, MRI, VNG	Central
Probable acute otolithic lesion	1	0 (0.00)	52.00 ± 0.00	Only the VEMP is abnormal	vHIT, MRI, VNG, VEMP	Peripheral/central
AVS without measurable vestibular dysfunction	1	0 (0.00)	38.00 ± 0.00	Normal vestibular function	vHIT, MRI, VNG, VEMP	Peripheral/central

AVS, acute vestibular syndrome; VEMP, vestibular-evoked myogenic potential; DBN, down-beating nystagmus; v-HIT, video head impulse test; VNG, videonystagmography.
Values of male sex represent numbers (percentages), and values of age represent mean ± SD.

comprehensive interpretation of clinical and laboratory findings following reasonable exclusion of other disorders. Our study enrolled 110 patients with VN which accounted for 62.86% of peripheral AVS. No patient had hearing loss, and there were few patients with tinnitus and ear fullness, which were essential in differential diagnosis from ISSNHL with vertigo.

In our study, 30 patients were diagnosed with ISSNHL with vertigo. Thirty percent of patients were accompanied by tinnitus and 3.33% of patients were accompanied by ear fullness. Approximately 23.33% of patients were accompanied by nausea, vomiting, and gait instability. The positive rates of h-HIT (16.67% vs. 82.73%, $p < 0.001$) and SN (56.67% vs. 98.18%, $p < 0.001$) in ISSNHL with vertigo patients were significantly lower than those in VN patients.

Patients with Ramsay Hunt syndrome had unique symptoms and signs, including herpetic blisters on the skin of the external canal and auricle and severe otalgia (ear pain). In our study, 1 patient was accompanied with SN, and 1 patient with nausea and vomiting.

In total, 11 patients were diagnosed as acute labyrinthitis secondary to chronic otitis media. Patients performed history of chronic suppurative otitis media, ear pain, or discharge of pus from the external auditory canal. CT examination of the temporal bone was performed in all patients, 10 cases were accompanied by labyrinthine destruction, and there was no imaging manifestation of labyrinthitis in the other case, but only had symptoms of acute labyrinthitis.

Among the 8 patients with vestibular schwannoma, all patients had abnormal vHIT results, and most of them were subjected to lateral and superior semicircular canals.

Central Acute Vestibular Syndrome

In total, 13 patients presented with central AVS, including one case of multiple sclerosis of the medulla oblongata, one of an epidermoid cyst of the posterior cranial fossa, three of cerebellar abscess or inflammation secondary to otitis media, six of posterior circulation infarction and/or ischemia, and two of AVS after intracranial surgery.

In these patients, two patients had up-beating nystagmus (UBN), two had down-beating nystagmus (DBN), two had gaze-evoked nystagmus, two had positional nystagmus, and four had horizontal SN.

In two patients who presented with UBN, one patient was diagnosed with multiple sclerosis of the medulla oblongata. MRI was performed on suspicion of a central origin and revealed a demyelinating lesion in the medulla oblongata. The other patient was diagnosed with an epidermoid cyst of the posterior cranial fossa, this patient had a sudden onset of persistent vertigo with nausea and vomiting and perceived uneven ground while walking, perceived-up rotation of the surroundings when standing, and spontaneous UBN when the head was upright (**Supplementary Video 1A**) for the past month. The roll test revealed apogeotropic nystagmus on changes of direction (**Supplementary Video 1B**). MRI revealed abnormal signal intensities in the right cerebellopontine angle, manifesting as low signal intensity on T1-weighted images, and high signal intensity on T2-weighted and diffusion-weighted images (**Figure 1**).

Three patients developed cerebellar abscesses or inflammation secondary to otitis media. One patient developed dizziness, headache, nausea, vomiting, and gait instability 5 days after a modified radical mastoidectomy. One patient developed severe vertigo, headache, and high fever while waiting for sinusitis surgery in the hospital. All patients were confirmed to have a cerebellar abscess or inflammation on MRI (**Figure 2A**) and were transferred to the Department of Neurosurgery for surgical treatment (**Figure 2B**).

Six patients were diagnosed with posterior circulation infarction and/or ischemia, including 1 case of focal infarction of the medulla oblongata, 1 of infarction of the cochlear, and vestibular nuclei, 2 of cerebellar infarction, and 1 of extensive infarction of the brainstem and cerebellum. One patient with a focal infarction of the medulla oblongata had SN (III°), obvious oculomotor abnormalities (including gaze-evoked nystagmus; **Supplementary Video 2**), and abnormal saccade and pursuit. The vHIT results showed reduced VOR gains of three semicircular canals on the right side, and magnetic resonance angiography (MRA) revealed vertebrobasilar artery stenosis (**Figure 3A**). MRI revealed acute infarction of the right medulla oblongata, which involved the ipsilateral vestibular nucleus (**Figures 3B,C**). The patient with infarction of the cochlear and vestibular nuclei presented with persistent dizziness, right facial discomfort, and decreased muscle strength in the right limbs. Backward tilting was seen during the Romberg test and the Fukuda test was unstable. PTA indicated total deafness on the right side (**Figure 4A**). MRI showed that the infarcted focus of the right medulla oblongata near the pons involved the cochlear nucleus and vestibular nucleus (**Figure 4B**).

Two patients were diagnosed with cerebellar lesions. One patient presented with vertigo, accompanied by gait instability, nausea, and vomiting. A physical examination and vestibular function test revealed SN to the right (II°); and positive Romberg and Fukuda tests. The caloric test and cVEMP indicated decreased vestibular function on the right side, whereas the vHIT was normal and accompanied by negative Babinski and Kernig's signs. Cranial CT and MRI revealed a right cerebellar infarction (**Figure 4C**). The other patient presented with dizziness and sudden hearing loss on the right side, followed by the cerebellar herniation. Surgical treatment was applied in the Department of Neurosurgery.

Another patient presented with continuous dizziness and sudden bilateral hearing loss; MRI revealed extensive infarction of the brainstem and cerebellum. PTA showed bilateral sensorineural hearing loss (**Figure 5A**), and brain MRI revealed lacunar foci in the bilateral basal ganglia (**Figure 5B**). The symptoms of both patients with cerebral infarction included vertigo with nausea and vomiting for 1 day, accompanied by DBN (**Supplementary Video 3A**). Brain MRI revealed bilateral basal ganglia and paraventricular infarcts. The other two patients had brainstem and basal ganglia ischemia and presented with DBN (**Supplementary Video 3B**).

Two patients were diagnosed with AVS after surgery. One patient underwent microvascular decompression of the trigeminal nerve. The other patient presented with persistent oculomotor dysfunction after craniocerebral surgery, mainly characterized by horizontal–torsional nystagmus during the supine head-roll test (**Supplementary Video 4**). MRI revealed foci of malacia in the brainstem and left parietal lobe cortex after craniotomy (**Figure 6**).

Indeterminate Diagnosis

In total, 17 patients presented with continuous vertigo, accompanied by migraine attacks during, before, or after the onset of acute vertigo. Among them, 16 patients with migraine presented SN and 1 patient had gazing-evoked nystagmus. In addition, 1 patient of AVS without measurable vestibular dysfunction, 2 patients with DBN and a normal MRI, and 1 patient with probable acute otolithic lesion who had abnormal cVEMPs and oVEMPs were also placed in this category.

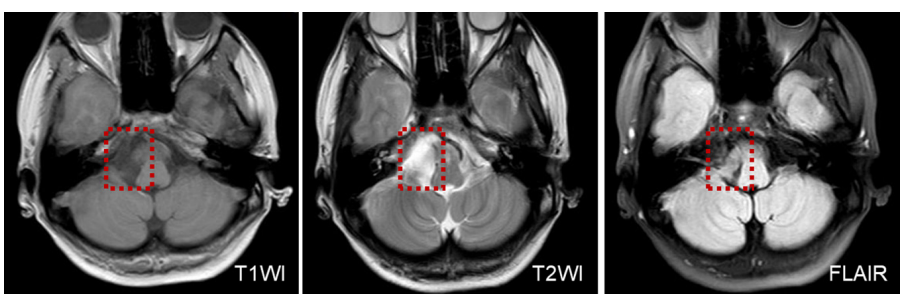

FIGURE 1 | MRI shows low T1WI signal intensity and an inhomogeneous texture, in a patient with an epidermoid cyst of the posterior cranial fossa.

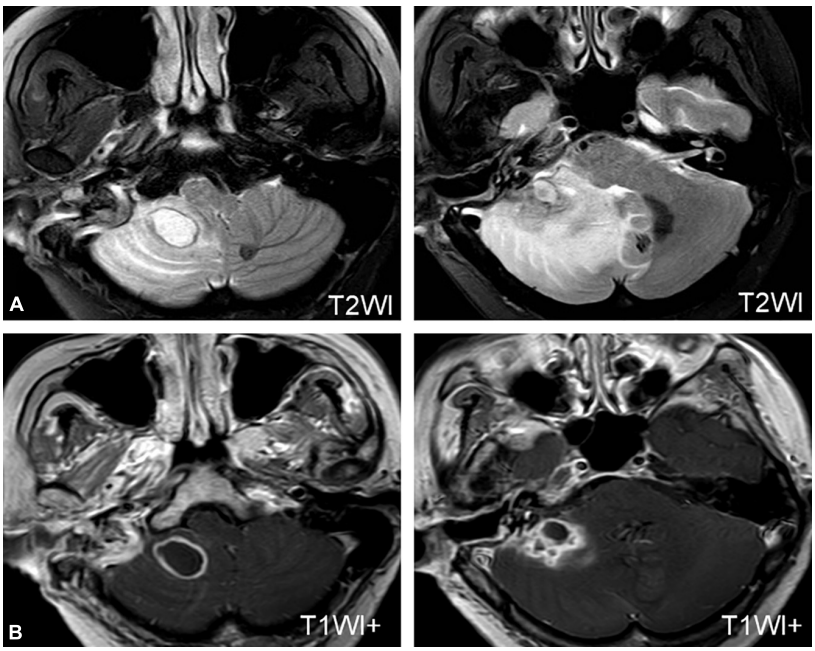

FIGURE 2 | MRI of a patient with a cerebellar abscess. **(A)** MRI shows an abscess in the right cerebellum. **(B)** MRI of the patient after neurosurgery.

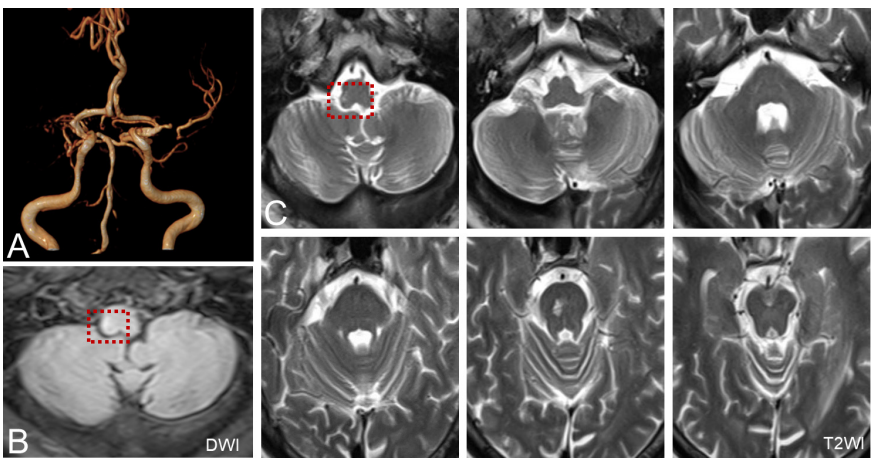

FIGURE 3 | MRA and MRI of a patient with posterior circulation infarction. **(A)** MRA shows vertebrobasilar artery stenosis. **(B,C)** MRI shows acute infarction of the right medulla oblongata, which involved the ipsilateral vestibular nucleus (red dotted line frame).

DISCUSSION

Acute vestibular syndrome is characterized by sudden-onset acute continuous vertigo and has a variety of etiologies and manifestations. Both the peripheral and central vestibular systems may be involved. Accurate diagnosis is important for patients presenting with AVS, as it can manifest as a variety of conditions. In this study, we found that 209 patients can be classified as having 14 vestibular disorders, including both peripheral and central disorders.

Among these vestibular disorder categories, some of them are easy to diagnose, such as Ramsay Hunt syndrome. Ramsay Hunt syndrome is characterized by a vesicular rash on the outer ear with or without acute peripheral facial nerve paralysis (caused by reactivation of the varicella–zoster virus at the geniculate ganglion) (Haginomori et al., 2016). Ear pain and herpes zoster are characteristic symptoms and signs of Ramsay Hunt syndrome, which make it easy to differentiate this disorder from other types of AVS.

In our study, 17 patients had migraine attacks during, before, or after the onset of acute vertigo. This category included patients who had symptoms of migraine and vertigo at the first medical visit, therefore, they were diagnosed with the first attack of AVS with migraine. Vestibular migraine (VM) usually presents as

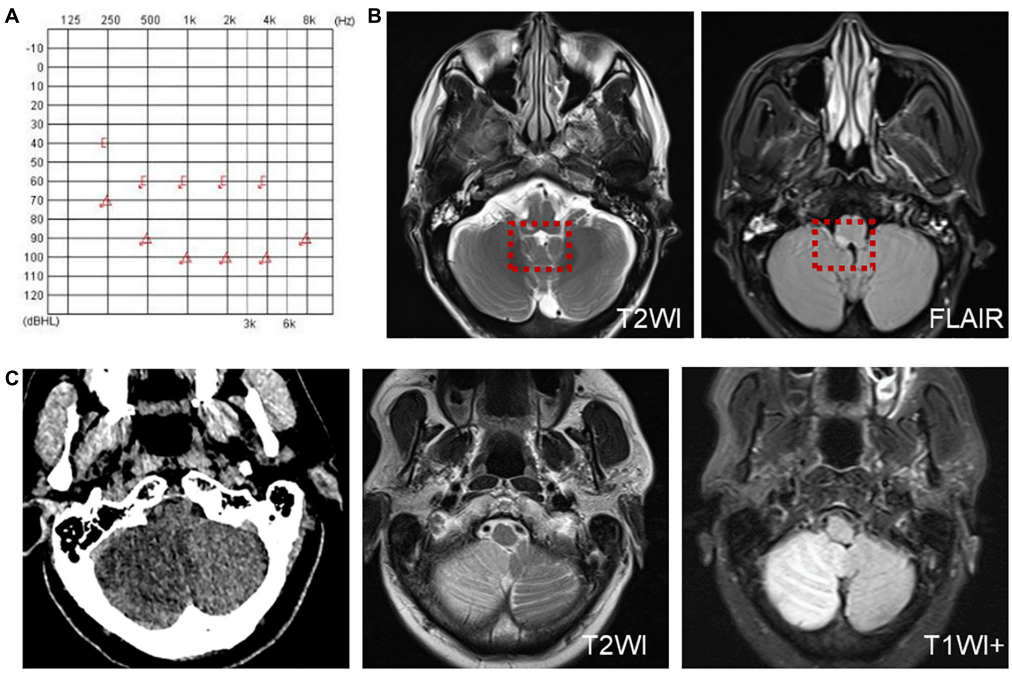

FIGURE 4 | Examination results of patients with infarction of the cochlear and vestibular nuclei **(A,B)** and right cerebellar infarction **(C)**. **(A)** PTA shows total deafness on the right side in a patient with infarction of the cochlear and vestibular nuclei. **(B)** MRI shows that the infarcted focus of the right medulla oblongata near the pons involved the cochlear nucleus and vestibular nucleus (red dotted line frame). **(C)** Cranial CT and MRI of the patient with right cerebellar infarction.

EVS; however, it should be considered as migraine-related AVS when migraine is accompanied. Therefore, we classified patients who presented with their first attack of vertigo simultaneous with migraine into a separate category, which should be treated as migraine, not VN.

In most cases, ocular movements (gaze-evoked nystagmus, abnormal saccades and/or pursuit, UBN, and DBN) help differentiate central and peripheral vestibular lesions (Strupp et al., 2011), vHIT helps identify most peripheral AVS (Halmagyi et al., 2017; Yao et al., 2018b; Li et al., 2020), and MRI is a method to confirm central AVS. A recent study demonstrated that examining ocular movements could be better than MRI for diagnosing AVS with a central or peripheral etiology (Kattah et al., 2009). Oculomotor dysfunction and central forms of nystagmus are signs of central vestibular disorders. UBN is nearly always caused by central disorders; two of our patients presenting with UBN had lesions in or next to the medulla oblongata. However, patients with a repaired superior semicircular canal fissure may also have UBN (Sharon et al., 2017). DBN is also nearly always a clinical sign of a central nervous system abnormality, including structural lesions in the vestibulocerebellum, and of diseases such as multiple system atrophy, multiple sclerosis, cerebellar degeneration, and hydrocephalus (Yabe et al., 2003; Kattah and Gujrati, 2005; Lee et al., 2009). In our study, one patient with cerebral infarction and one patient with posterior circulation ischemia had DBN. Moreover, patients with central vestibular disorders may also exhibit abnormal pursuit and saccades, and gaze-evoked nystagmus. In our study, the patient with posterior circulation infarction had abnormal gaze-evoked nystagmus. Previous studies reported that nine in 30% patients with posterior circulation infarction showed abnormalities in the gazing test. Abnormalities in eye movement, especially gaze-evoked nystagmus and saccades, can help to screen posterior circulation infarction patients (Ling et al., 2019). In addition, one patient had persistent oculomotor dysfunction after craniocerebral surgery in our study. A previous study also reported that a patient showed new-onset UBN after microsurgical excision of the cavernoma (Meling et al., 2020), and two cases of purely UBN after bilateral superior canal plugging (Sharon et al., 2017). Therefore, abnormal ocular movements have a certain significance for the differential diagnosis of peripheral and central vestibular disorders.

Some of these disorders require a detailed differential diagnosis, including AVS with hearing loss and AVS with otitis media. AVS with hearing loss can include ISSNHL with vertigo, extensive infarction of brainstem and cerebellum, infarction of the cochlear and vestibular nuclei, and vestibular schwannoma. The patient developed a brainstem and cerebellar infarction with a fatal outcome. The diagnosis of ISSNHL with vertigo is based on symptoms, a physical examination, and auditory–vestibular function tests, rather than an etiological diagnosis. MRI is the modality of choice for diagnosing vestibular schwannoma, given its high sensitivity and specificity. Although vestibular schwannoma is a slow-growing tumor, some patients may also show acute vertigo attacks. Previous studies have shown that sharp changes in tumor size, such as tumor growth or intratumoral bleeding or cystic changes, can oppress the

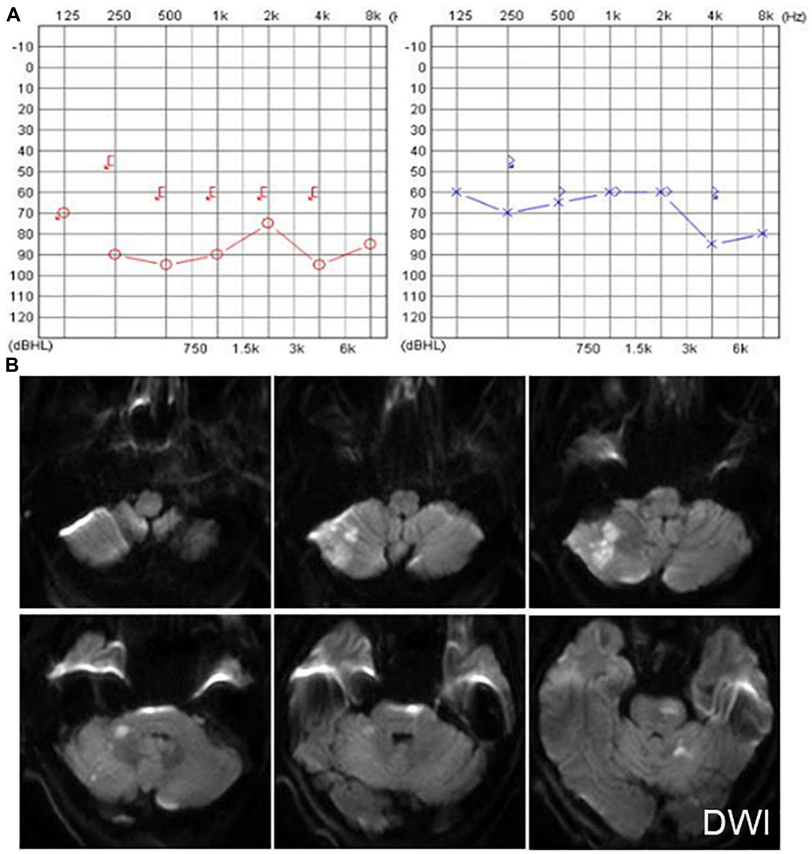

FIGURE 5 | The PTA and MRI of the patient with extensive infarction of the brainstem and cerebellum. **(A)** PTA shows a bilateral sensorineural hearing loss in a patient with extensive infarction of the brainstem and cerebellum. **(B)** Brain MRI shows lacunar foci in the bilateral basal ganglia.

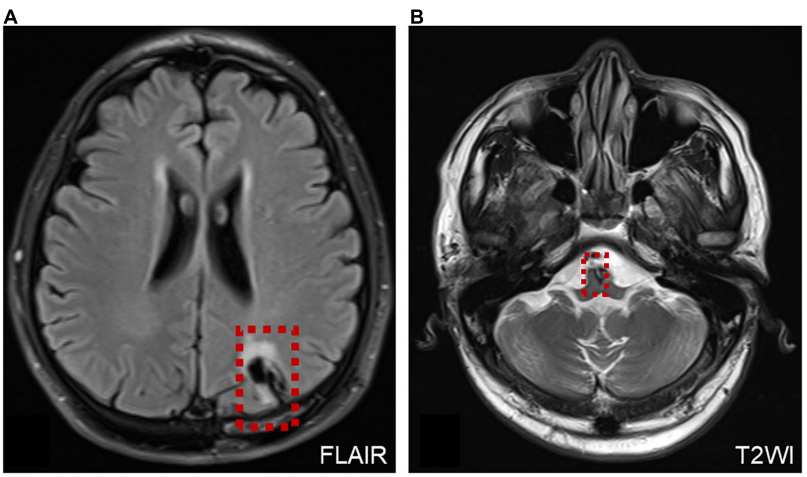

FIGURE 6 | MRI of a patient with AVS after surgery. **(A)** MRI shows the operation site on the left side of the brain (red dotted line frame). **(B)** Malacia foci were detected in the left parietal lobe cortex and brainstem after craniotomy, and a few ischemic foci were scattered within the bilateral frontal–parietal lobe (red dotted line frame).

vestibular nerve or cerebellum, leading to acute vestibular symptoms. In addition, metabolic changes caused by tumor secretions may lead to sudden loss of vestibular function (Dilwali et al., 2015). Posterior circulation infarction can involve cochlear and vestibular nuclei, and/or the peripheral labyrinth, and presents as neurological symptoms and signs. MRI reveals

the affected location. Notably, among posterior circulation infarctions, anterior inferior cerebellar artery territory infarction is most similar to ISSNHL with vertigo, as this artery mainly supplies peripheral vestibular and auditory structures (Lee, 2012; Kim and Lee, 2017). In addition, accumulating evidence indicates that vestibular symptoms could be secondary to otitis media, although AVS with otitis media has not been investigated (Monsanto et al., 2018). In total, 14 patients were diagnosed with AVS with otitis media. Patients in this category present not only with acute vertigo but also with typical symptoms of active otitis media, such as otalgia and otorrhea. Similar to sudden hearing loss, the complications of chronic otitis media can involve peripheral or central vestibular structures. In our study, 11 patients were diagnosed with acute suppurative labyrinthitis and three patients had intracranial complications. Foul-smelling purulent otorrhea, headache or severe pain in the deep ear, and fever are early signs and symptoms of intracranial complications caused by otitis media, neurological symptoms such as neck stiffness, and changes in mental status and gait ataxia are late manifestations (Schwaber et al., 1989). In addition, central signs such as oculomotor disturbances, directional-altering nystagmus, DBN, or UBN may be present. In patients with suppurative labyrinthitis, vHIT results showed abnormal gain and saccades. CT and MRI are of the highest importance to detect pathologies in suppurative labyrinthitis and intracranial complications (Kempf et al., 1998). Therefore, more attention should be paid to differentiating between peripheral and central involvement in AVS patients with hearing loss or otitis media.

In this study, patients attacked by acute vertigo after trauma or surgery were classified into a separate category. The vestibular system can be affected by trauma and surgery (Ibrahim et al., 2017; Marcus et al., 2019; Calzolari et al., 2021). Marcus et al. (2019) reported that, in 20% of cases, traumatic brain injury results in acute unilateral peripheral vestibular loss, typically due to petrous temporal bone fracture. Patients presenting with AVS after acute trauma should be monitored closely as their condition may deteriorate due to simultaneous injury of peripheral and central vestibular structures. The probable acute isolated otolithic lesion was also classified into a category, these patients who suffered from otolithic diseases occasionally perceive the visual world as tilted, or have an erroneous sensation of linear motion, postural unsteadiness, and neurovegetative symptoms such as nausea and vomiting (Denise et al., 1996).

Some disorders associated with AVS, such as labyrinthine hemorrhage, cerebral hemorrhage, and certain immune-mediated disorders, have not been included in our study. Other AVS disorders include Creutzfeldt–Jakob disease (Mantokoudis et al., 2015a), immune-mediated disorders such as cerebellitis and thiamine deficiency (Choi et al., 2007), medullary cavernous (Lee and Kim, 2017), primary central nervous system lymphoma involving the dorsal medulla (Lee et al., 2018), and functional and "psychiatric AVS"(Brandt and Dieterich, 2017).

Pseudo-vestibular neuritis (PVN) and acute ischemic stroke with audiovestibular loss (AISwAVL) are two types of malignant AVS. The clinical manifestations of PVN and VN are relatively similar. To differentiate PVN and VN, the results of nystagmus examination, head-shaking test, Fukuda and Romberg tests, and HINTS are useful. In addition, attention should be paid to whether the patient has disturbance of consciousness, headache, diplopia, and facial nerve palsy, dysphagia, and other central pathological signs, combined with the characteristics of central nystagmus, positive signs of ataxia, ocular movement disorders, and abnormal gravity perception (Ganggang et al., 2019). The clinical presentations of AISwAVL are similar to ISSNHL with vertigo. A previous study suggested that the HINTS "plus" hearing battery can help differentiate these two diseases (Saber Tehrani et al., 2014). Another study proposed that a combination of the HINTS and head-shaking nystagmus (HSN) can be useful. When the HINTS test is negative, HSN in the direction opposite to the SN and perverted HSN suggest the possibility of AISwAVL (Huh et al., 2013).

The HINTS examination can identify central AVS from peripheral AVS, relatively benign, and more common diagnostic alternatives (Kattah et al., 2009). vHIT provides an objective measurement of the VOR and can improve the diagnostic accuracy of AVS. vHIT combined with HINTS is a reliable tool to exclude posterior circulation stroke (Thomas et al., 2022). STANDING algorithm (spontaneous nystagmus, direction, head-impulse test, and standing) can be used by emergency physicians to independently identify central vertigo in AVS (Nakatsuka and Molloy, 2022).

Previous studies have identified various disorders presenting with AVS, including VN, brainstem lesions, and cerebellar infarction (Venhovens et al., 2016; Yao et al., 2018a; Kerber, 2020). However, those studies mainly focused on distinguishing central lesions involving the brainstem or cerebellum from VN; little attention was paid to other causes of AVS, such as otitis media and vestibular schwannoma (Venhovens et al., 2016; Yao et al., 2018a; Kerber, 2020). In this study, we enrolled a large number of patients to understand the composition of AVS, which can help deepen our understanding of AVS, and quickly distinguish peripheral from central AVS. A better understanding of the composition of acute vestibular disorders is helpful to make the correct diagnosis and differential diagnosis quickly. For example, some patients who initially show otitis media and vertigo need to be considered that they may be accompanied by labyrinthitis and even intracranial complications, which need to be diagnosed in time and avoid missed diagnosis. Furthermore, a variety of otological and neurological diseases, including some fatal diseases, manifest as AVS before a clear diagnosis, which requires the attention of clinicians. Therefore, classifying multiple types of AVS may help fast diagnosis and improve treatment outcomes, particularly for patients who need early and continuous vestibular rehabilitation.

This study had several limitations. As it was a retrospective study, the number of patients in some categories was small, and not all disorders with AVS were included. Patients in the retrospective study were enrolled from an ENT clinic which may introduce the selection bias, so the composition of the vestibular disorders in this study was different from those enrolled from an emergency room or neurology, which could not be generalized to other clinical settings. However, this study also shows that central AVS can also be seen in ENT practices, and otolaryngologists should also be vigilant to avoid missed diagnoses. In addition,

we could not confirm whether the first attack of continuous vertigo with migraine developed into VM due to a lack of long-term follow-up data. It is necessary to continue to collect patient follow-up data to expand the spectrum of vestibular disorders presenting with AVS.

CONCLUSION

This study enrolled a large case series and discussed the composition of vestibular disorders presenting with AVS and classified them into 14 categories according to the relevant diagnostic criteria, which can help deepen the understanding of AVS. Different from the previous AVS studies focusing on the differential diagnosis of vestibular neuritis and stroke, this study has an important significance for clinicians to broaden their list of differential diagnoses and consider other possibilities except for VN and stroke.

DATA AVAILABILITY STATEMENT

The original contributions presented in this study are included in the article/**Supplementary Material**, further inquiries can be directed to the corresponding author.

ETHICS STATEMENT

The study involving human participants was reviewed and approved by the Shanghai Jiao Tong University Affiliated Sixth People's Hospital. Written informed consent from the participants' legal guardian/next of kin was not required to participate in this study in accordance with the national legislation and the institutional requirements.

AUTHOR CONTRIBUTIONS

DY and SY designed and coordinated the study. QY, ZL, and MX analyzed the data and wrote the manuscript. QY, ZL, MX, YJ, JW, and HW performed the data collection. DY attested that all listed authors meet authorship criteria and that no others meeting the criteria have been omitted. All authors contributed to the article and approved the submitted version.

FUNDING

This study was supported by the National Key Research and Development Project of China (grant no. 2019YFC0119900) and the Shanghai Municipal Education Commission-Gaofeng Clinical Medicine (grant no. 20191921).

SUPPLEMENTARY MATERIAL

The Supplementary Material for this article can be found online at: https://www.frontiersin.org/articles/10.3389/fnins.2022.933520/full#supplementary-material

Supplementary Video 1 | Abnormal nystagmus in a patient with an epidermoid cyst in the posterior cranial fossa. **(A)** Spontaneous up-beating nystagmus. **(B)** Roll test examination shows apogeotropic nystagmus on changes of direction. Right beating nystagmus occurred when the patient was in the left supine position and left beating nystagmus occurred in the right supine position.

Supplementary Video 2 | Abnormal gaze-evoked nystagmus in a patient with posterior circulation infarction.

Supplementary Video 3 | Down-beating nystagmus. **(A)** Down-beating nystagmus in a patient with cerebral infarction. **(B)** Down-beating nystagmus in a patient with posterior circulation ischemia.

Supplementary Video 4 | Persistent oculomotor dysfunction in a patient with AVS after craniocerebral surgery, mainly characterized by horizontal–torsional nystagmus during the supine head-roll test.

REFERENCES

Bertholon, P., Thai-Van, H., Bouccara, D., Esteve-Fraysse, M., Wiener-Vacher, S., and Ionescu, E. (2020). Guidelines of the French Society of Otorhinolaryngology (SFORL) for teleconsultation in patients with vertigo during the COVID-19 pandemic. *Eur. Ann. Otorhinolaryngol. Head Neck Dis.* 138, 459–465. doi: 10.1016/j.anorl.2020.11.011

Brandt, T., and Dieterich, M. (2017). The dizzy patient: don't forget disorders of the central vestibular system. *Nat. Rev. Neurol.* 13, 352–362. doi: 10.1038/nrneurol.2017.58

Calzolari, E., Chepisheva, M., Smith, R. M., Mahmud, M., Hellyer, P. J., Tahtis, V., et al. (2021). Vestibular agnosia in traumatic brain injury and its link to imbalance. *Brain* 144, 128–143. doi: 10.1093/brain/awaa386

Chen, L., Lee, W., Chambers, B. R., and Dewey, H. M. (2011). Diagnostic accuracy of acute vestibular syndrome at the bedside in a stroke unit. *J. Neurol.* 258, 855–861. doi: 10.1007/s00415-010-5853-4

Choi, K. D., Oh, S. Y., Kim, H. J., and Kim, J. S. (2007). The vestibulo-ocular reflexes during head impulse in Wernicke's encephalopathy. *J. Neurol. Neurosurg. Psychiatry* 78, 1161–1162. doi: 10.1136/jnnp.2007.121061

Denise, P., Darlot, C., Ignatiew-Charles, P., and Toupet, M. (1996). Unilateral peripheral semicircular canal lesion and off-vertical axis rotation. *Acta Otolaryngol.* 116, 361–367. doi: 10.3109/00016489609137858

Dilwali, S., Landegger, L. D., Soares, V. Y., Deschler, D. G., and Stankovic, K. M. (2015). Secreted Factors from Human Vestibular Schwannomas Can Cause Cochlear Damage. *Sci. Rep.* 5:18599. doi: 10.1038/srep18599

Förster, A., Wenz, H., Böhme, J., Al-Zghloul, M., and Groden, C. (2016). Hyperintense Acute Reperfusion Marker on FLAIR in Posterior Circulation Infarction. *PLoS One* 11:e0157738. doi: 10.1371/journal.pone.0157738

Ganggang, C., Chunming, Z., Wei, G., Huiru, F., Hui, H., and Binquan, W. (2019). How to initially screen common central "malignant vertigo" at the bedside? *Chin J Otorhinolaryngol Head Neck Surg.* 54:7. doi: 10.3760/cma.j.issn.1673-0860.2019.08.017

Greene, J., and Al-Dhahir, M. A. (2020). *Acoustic Neuroma (Vestibular Schwannoma)*. Treasure Island (FL): StatPearls Publishing.

Haginomori, S., Ichihara, T., Mori, A., Kanazawa, A., Kawata, R., Tang, H., et al. (2016). Varicella-zoster virus-specific cell-mediated immunity in Ramsay Hunt syndrome. *Laryngoscope* 126:E35–E39. doi: 10.1002/lary.25441

Halmagyi, G. M., Chen, L., MacDougall, H. G., Weber, K. P., McGarvie, L. A., and Curthoys, I. S. (2017). The Video Head Impulse Test. *Front. Neurol.* 8:258. doi: 10.3389/fneur.2017.00258

Hotson, J. R., and Baloh, R. W. (1998). Acute vestibular syndrome. *N. Engl. J. Med.* 339, 680–685. doi: 10.1056/nejm199809033391007

Huh, Y. E., Koo, J. W., Lee, H., and Kim, J. S. (2013). Head-shaking aids in the diagnosis of acute audiovestibular loss due to anterior inferior cerebellar artery infarction. *Audiol. Neurootol.* 18, 114–124. doi: 10.1159/000345643

Hunt, J. R. (1907). On Herpetic Inflammation of the Geniculate Gangolion: A New Syndrome and Its Complications. *J. Nerv. Ment. Dis.* 34, 73–96.

Ibrahim, I., da Silva, S. D., Segal, B., and Zeitouni, A. (2017). Effect of cochlear implant surgery on vestibular function: meta-analysis study. *J. Otolaryngol Head Neck Surg.* 46:44. doi: 10.1186/s40463-017-0224-0

Jeong, S., Kim, H., and Kim, J. (2013). Vestibular neuritis. *Semin. Neurol.* 33, 185–194. doi: 10.1055/s-0033-1354598

Kattah, J., and Gujrati, M. (2005). Familial positional downbeat nystagmus and cerebellar ataxia: clinical and pathologic findings. *Ann. N. Y. Acad. Sci.* 1039, 540–543. doi: 10.1196/annals.1325.063

Kattah, J. C., Talkad, A. V., Wang, D. Z., Hsieh, Y. H., and Newman-Toker, D. E. (2009). HINTS to diagnose stroke in the acute vestibular syndrome: three-step bedside oculomotor examination more sensitive than early MRI diffusion-weighted imaging. *Stroke* 40, 3504–3510. doi: 10.1161/strokeaha.109.551234

Kempf, H. G., Wiel, J., Issing, P. R., and Lenarz, T. (1998). [Otogenic brain abscess]. *Laryngorhinootologie* 77, 462–466. doi: 10.1055/s-2007-997007

Kerber, K. A. (2020). Acute Vestibular Syndrome. *Semin. Neurol.* 40, 59–66. doi: 10.1055/s-0039-3402739

Kim, H. A., and Lee, H. (2017). Recent Advances in Understanding Audiovestibular Loss of a Vascular Cause. *J. Stroke* 19, 61–66. doi: 10.5853/jos.2016.00857

Lee, H. (2012). Audiovestibular loss in anterior inferior cerebellar artery territory infarction: a window to early detection? *J. Neurol. Sci.* 313, 153–159. doi: 10.1016/j.jns.2011.08.039

Lee, H., and Kim, H. (2017). Medullary cavernous malformation as a cause of isolated acute vestibular syndrome. *Neurol. Sci.* 38, 919–921. doi: 10.1007/s10072-017-2834-8

Lee, J., Lee, W., Kim, J., Kim, H., Kim, J., and Jeon, B. (2009). Perverted head-shaking and positional downbeat nystagmus in patients with multiple system atrophy. *Mov. Disord.* 24, 1290–1295. doi: 10.1002/mds.22559

Lee, S., Kim, H., Choi, J., Yang, X., and Kim, J. (2018). Isolated acute vestibular syndrome due to presumed primary central nervous system lymphoma involving the dorsal medulla. *J. Neurol.* 265, 1937–1939. doi: 10.1007/s00415-018-8947-z

Li, Z., Wang, H., Wang, H., and Yu, D. (2020). Quantitative Analysis of Saccade Gain in Video Head Impulse Testing. *Otolaryngol. Head Neck Surg.* 163, 799–805. doi: 10.1177/0194599820930669

Ling, X., Sang, W., Shen, B., Li, K., Si, L., and Yang, X. (2019). Diagnostic value of eye movement and vestibular function tests in patients with posterior circulation infarction. *Acta Otolaryngol.* 139, 135–145. doi: 10.1080/00016489.2018.1552367

Ljunggre, M., Persson, J., and Salzer, J. (2018). Dizziness and the Acute Vestibular Syndrome at the Emergency Department: A Population-Based Descriptive Study. *Eur. Neurol.* 79, 5–12. doi: 10.1159/000481982

Mantokoudis, G., Tehrani, A., Wozniak, A., Eibenberger, K., Kattah, J., Guede, C., et al. (2015b). VOR gain by head impulse video-oculography differentiates acute vestibular neuritis from stroke. *Otol. Neurotol.* 36, 457–465.

Mantokoudis, G., Saber Tehrani, A. S., and Newman-Toker, D. E. (2015a). An unusual stroke-like clinical presentation of Creutzfeldt-Jakob disease: acute vestibular syndrome. *Neurologist* 19, 96–98. doi: 10.1097/NRL.0000000000000019

Marcus, H. J., Paine, H., Sargeant, M., Wolstenholme, S., Collins, K., Marroney, N., et al. (2019). Vestibular dysfunction in acute traumatic brain injury. *J. Neurol.* 266, 2430–2433. doi: 10.1007/s00415-019-09403-z

Meling, T., Nouri, A., May, A., Guinand, N., Vargas, M., and Destrieux, C. (2020). Upbeat vertical nystagmus after brain stem cavernoma resection: a rare case of nucleus intercalatus/nucleus of roller injury. *J. Neurol.* 267, 2865–2870. doi: 10.1007/s00415-020-09891-4

Monsanto, R. D. C., Kasemodel, A. L. P., Tomaz, A., Paparella, M. M., and Penido, N. O. (2018). Current evidence of peripheral vestibular symptoms secondary to otitis media. *Ann. Med.* 50, 391–401. doi: 10.1080/07853890.2018.1470665

Nakatsuka, M., and Molloy, E. E. (2022). The HINTS examination and STANDING algorithm in acute vestibular syndrome: a systematic review and meta-analysis involving frontline point-of-care emergency physicians. *PLoS One* 17:e0266252. doi: 10.1371/journal.pone.0266252

Newman-Toker, D., Kerber, K., Hsieh, Y., Pula, J., Omron, R., Saber Tehrani, A., et al. (2013a). HINTS outperforms ABCD2 to screen for stroke in acute continuous vertigo and dizziness. *Acad. Emerg. Med.* 20, 986–996. doi: 10.1111/acem.12223

Newman-Toker, D., Saber Tehrani, A., Mantokoudis, G., Pula, J., Guede, C., Kerber, K., et al. (2013b). Quantitative video-oculography to help diagnose stroke in acute vertigo and dizziness: toward an ECG for the eyes. *Stroke* 44, 1158–1161. doi: 10.1161/STROKEAHA.111.000033

Saber Tehrani, A. S., Kattah, J. C., Mantokoudis, G., Pula, J. H., Nair, D., Blitz, A., et al. (2014). Small strokes causing severe vertigo: frequency of false-negative MRIs and nonlacunar mechanisms. *Neurology* 83, 169–173. doi: 10.1212/wnl.0000000000000573

Schwaber, M. K., Pensak, M. L., and Bartels, L. J. (1989). The early signs and symptoms of neurotologic complications of chronic suppurative otitis media. *Laryngoscope* 99, 373–375. doi: 10.1288/00005537-198904000-00002

Sharon, J., Carey, J., and Schubert, M. (2017). Upbeat nystagmus after bilateral superior canal plugging: a peripheral cause of vertical nystagmus. *Laryngoscope* 127, 1698–1700. doi: 10.1002/lary.26314

Spinato, G., Gaudioso, P., Falcioni, M., Mosto, M., Cocuzza, S., Maniaci, A., et al. (2021). Giant Epidermoid Cyst of Posterior Fossa-Our Experience and Literature Review. *Dose Response* 19:15593258211002061. doi: 10.1177/15593258211002061

Stachler, R., Chandrasekhar, S., Archer, S., Rosenfeld, R., Schwartz, S., Barrs, D., et al. (2012). Clinical practice guideline: sudden hearing loss. *Otolaryngol. Head Neck Surg.* 146:S1–S35. doi: 10.1177/0194599812436449

Strupp, M., Hüfner, K., Sandmann, R., Zwergal, A., Dieterich, M., Jahn, K., et al. (2011). Central oculomotor disturbances and nystagmus: a window into the brainstem and cerebellum. *Dtsch. Ärztebl. Int.* 108, 197–204. doi: 10.3238/arztebl.2011.0197

Thomas, J. O., Sharobeam, A., Venkat, A., Blair, C., Ozalp, N., Calic, Z., et al. (2022). Video head impulse testing to differentiate vestibular neuritis from posterior circulation stroke in the emergency department: a prospective observational study. *BMJ Neurol. Open* 4:e000284. doi: 10.1136/bmjno-2022-000284

Thompson, A., Banwell, B., Barkhof, F., Carroll, W., Coetzee, T., Comi, G., et al. (2018). Diagnosis of multiple sclerosis: 2017 revisions of the McDonald criteria. *Lancet Neurol.* 17, 162–173. doi: 10.1016/s1474-4422(17)30470-2

Vazquez, E., Castellote, A., Piqueras, J., Mauleon, S., Creixell, S., Pumarola, F., et al. (2003). Imaging of complications of acute mastoiditis in children. *Radiographics* 23, 359–372. doi: 10.1148/rg.232025076

Venhovens, J., Meulstee, J., and Verhagen, W. I. (2016). Acute vestibular syndrome: a critical review and diagnostic algorithm concerning the clinical differentiation of peripheral versus central aetiologies in the emergency department. *J. Neurol.* 263, 2151–2157. doi: 10.1007/s00415-016-8081-8

Yabe, I., Sasaki, H., Takeichi, N., Takei, A., Hamada, T., Fukushima, K., et al. (2003). Positional vertigo and macroscopic downbeat positioning nystagmus in spinocerebellar ataxia type 6 (SCA6). *J. Neurol.* 250, 440–443. doi: 10.1007/s00415-003-1020-5

Yao, Q., Wang, H., Luo, Q., Yu, Z., Shi, H., and Yin, S. (2018a). Classification of acute vestibular syndrome. *J. Clin. Otorhinolaryngol. Head Neck Surg.* 32, 827–830. doi: 10.13201/j.issn.1001-1781.2018.11.007

Yao, Q., Xu, C., Wang, H., Shi, H., and Yu, D. (2018b). Video head impulse test results suggest that different pathomechanisms underlie sudden sensorineural hearing loss with vertigo and vestibular neuritis: our experience in fifty-two patients. *Clin. Otolaryngol.* 43, 1621–1624. doi: 10.1111/coa.13196

Zhang, Z., Wang, Z., Xian, J., Fu, L., He, L., and Guo, J., (2007). MRI Diagnosis of Labyrinthitis. *J. Pract. Radiol.* 23, 25–27.

Conflict of Interest: The authors declare that the research was conducted in the absence of any commercial or financial relationships that could be construed as a potential conflict of interest.

Publisher's Note: All claims expressed in this article are solely those of the authors and do not necessarily represent those of their affiliated organizations, or those of the publisher, the editors and the reviewers. Any product that may be evaluated in this article, or claim that may be made by its manufacturer, is not guaranteed or endorsed by the publisher.

Copyright © 2022 Yao, Li, Xu, Jiang, Wang, Wang, Yu and Yin. This is an open-access article distributed under the terms of the Creative Commons Attribution License (CC BY). The use, distribution or reproduction in other forums is permitted, provided the original author(s) and the copyright owner(s) are credited and that the original publication in this journal is cited, in accordance with accepted academic practice. No use, distribution or reproduction is permitted which does not comply with these terms.

frontiers | Frontiers in Neurology

ORIGINAL RESEARCH
published: 14 July 2022
doi: 10.3389/fneur.2022.934627

Tolerance to Dizziness Intensity Increases With Age in People With Chronic Dizziness

Tino Prell[1]*, *Sarah Mendorf*[2] *and Hubertus Axer*[2,3]

[1] Department of Geriatrics, Halle University Hospital, Halle, Germany, [2] Department of Neurology, Jena University Hospital, Jena, Germany, [3] Center for Vertigo and Dizziness, Jena University Hospital, Jena, Germany

Background: Dizziness is a common complaint in older adults. To know which factors are instrumental in enabling patients with chronic dizziness to tolerate their symptoms to a certain degree in everyday life can help to develop tailored therapies.

Methods: Data from 358 patients with chronic dizziness and vertigo who had attended a multimodal daycare treatment program were recorded. Data included sociodemographic parameters, dizziness-related characteristics, the Vertigo Symptom Scale (VSS), and the Hospital Anxiety and Depression Scale (HADS). Descriptive statistics, elastic net regression, and mediation analysis were used.

Results: A higher tolerance of dizziness was associated with higher age, higher intensity of dizziness, lower burden of dizziness, higher HADS depression, structural reason for dizziness (type), permanent dizziness, absence of attacks, and longer disease duration. In contrast, younger persons with attack-like dizziness reported to tolerate less dizziness. Age had a significant direct effect on tolerance (72% of the total effect) and a significant indirect effect *via* intensity on tolerance (28% of the total effect) in the mediation analysis.

Conclusion: It can only be speculated that negative stereotypes about age-related complaints may play a role in this. Why older people tolerate more dizziness and to what extent this may contribute to lower healthcare utilization need to be investigated in further studies.

Keywords: dizziness, vertigo, older age, depression, mediation

OPEN ACCESS

Edited by:
Leonardo Manzari,
MSA ENT Academy Center, Italy

Reviewed by:
Erin Gillikin Piker,
James Madison University, United States
David Herdman,
King's College London, United Kingdom

***Correspondence:**
Tino Prell
tino.prell@uk-halle.de
orcid.org/0000-0002-6423-3108

Specialty section:
This article was submitted to Neuro-Otology, a section of the journal Frontiers in Neurology

Received: *02 May 2022*
Accepted: *21 June 2022*
Published: *14 July 2022*

Citation:
Prell T, Mendorf S and Axer H (2022) Tolerance to Dizziness Intensity Increases With Age in People With Chronic Dizziness. Front. Neurol. 13:934627. doi: 10.3389/fneur.2022.934627

INTRODUCTION

Vertigo and dizziness have a high lifetime prevalence and affect about 15% to over 20% of adults yearly in large population-based studies (1). They are caused by a variety of conditions and strongly influence activities of daily living and quality of life. Chronic or permanent dizziness often requires a multidisciplinary approach in specialized centers (2, 3) and goes along with high personal and healthcare burden (4). Especially, for chronic dizziness, it is essential that patients cope with the dizziness symptoms in daily living. In many chronic forms of dizziness, this means that patients have to tolerate dizziness to various degrees. The subjective perception of chronic dizziness is influenced by personality traits, psychosocial factors (e.g., anxiety with regard to unforeseeable

recurrence), associated symptoms, and the course of disease (unpredictable attacks or permanent problems) (5). With regard to therapeutic approaches, it is crucial to know what factors influence the patient's ability to deal with chronic dizziness.

Every person has different desires and expectations that are usually different from their current state of living. In the context of quality of life, this difference or gap between the hopes/expectations and actual experiences of an individual is called the Calman gap (6). This gap mainly influences the quality of life and individual satisfaction. If the individual's current condition worsens in the context of a disease (e.g., chronic vertigo), then the gap between the current and desired state may increase, thereby lowering the satisfaction of the individual. On the other hand, individuals can adapt their expectations and desires (e.g., tolerate dizziness under some circumstances). Patients can have different understandings of their illness and other reference points, which can change over time or with regard to treatment options. In the case of chronic diseases, patients do not necessarily expect the complaints/symptoms to disappear completely as a result of treatment (6). Rather, patients are willing to tolerate some of the discomfort. In the context of this study, we were interested in understanding which factors are instrumental in enabling patients with chronic dizziness to tolerate their symptoms to a certain degree in everyday life. This should serve as the basis for future studies that aim to adapt therapy programs more individually (e.g., focus on personal resources and resilience). Therefore, our question was how much dizziness intensity can be tolerated by affected persons and what factors modulate this tolerance to dizziness?

Based on theoretical considerations and the existing literature, we considered the following parameters as relevant for our research question. First, we considered the individual intensity of dizziness and the burden due to dizziness as relevant cofactors. These are linked to the type of dizziness (attack vs. permanent) and the dizziness-associated handicap (7–9). Two patient-reported scales have been widely used to evaluate dizziness-associated handicap and severity in patients with vertigo: the Dizziness Handicap Inventory (DHI) and the Vertigo Symptom Scale (VSS) (10, 11). In contrast to the DHI, the VSS assesses the frequency of vestibular-balance symptoms and the severity of autonomic-anxiety symptoms, which have a great impact on quality of life. We therefore used the VSS to comprehensively describe dizziness. We also assumed that the vertigo diagnosis plays a role, in particular, with regard to the distinction between somatic vs. psychic reasons for chronic dizziness (7, 9). Dizziness symptoms are often accompanied and interact with psycho-physiological symptoms, especially depression and anxiety (11–14). Besides anxiety and depression, autonomic symptoms are also known to affect dizziness handicap (15). In addition, age and gender might influence how much dizziness a person is willing to tolerate. It is known from other studies that coping with distinct or multiple diseases is influenced by age and sex (16).

To answer our research question, we analyzed data from patients with chronic dizziness attending our multimodal treatment program in the Center for Vertigo and Dizziness, Jena, Germany (3).

METHODS

Participants

This was a subgroup analysis of a larger longitudinal observational study in people with chronic dizziness attending a specialized vertigo center (17). The study was approved by the local ethics committee (Ethics Committee of the Friedrich-Schiller-University Jena, Number 5426-02/18), and written informed consent for study participation was obtained from all patients. The Center for Vertigo and Dizziness is a tertiary care outpatient project consisting of neurology, ear, nose, and throat and physiotherapy departments. The center provides interdisciplinary diagnoses of patients with chronic vertigo and dizziness and a day care multimodal therapy (2). Requirements for participation in this outpatient treatment program were chronic dizziness and vertigo (i.e., symptoms have persisted for at least 3 months or attacks have recurred at least 5 days per month), physical independence (i.e., walking independently), and no cognitive limitations that may affect the activities of daily living (3). During the study period (June 2013 to September 2017), 754 patients were treated in this therapy program. Six months after attendance of the therapy week, the patients were contacted *via* mail and asked to fill out questionnaires for follow-up assessment. Here, 444 (58.9%) of the patients completed the questionnaire and sent it back. Comparison between people with and without follow-up is given in **Supplement Table S1**. From these 444 datasets, 358 provided information about the dependent variable.

Dependent Variable

The item "Now indicate what intensity of dizziness would be tolerable for you with successful treatment?" (German "Geben Sie jetzt an, welche Schwindelintensität für Sie bei erfolgreicher Behandlung erträglich wäre.") was rated on a visual analog scale from 0 (no dizziness tolerable) to 10 (the strongest dizziness). This variable is termed "tolerance" (metric).

Independent Variables

We assessed the following sociodemographic and vertigo- and dizziness-related data:

- Age (metric; years), gender (binominal; male/female).
- Vertigo diagnosis as defined at our center; advanced neurologists and vertigo specialists medically diagnosed and psychologically evaluated every patient. Diagnoses are generally based on the International Classification of Vestibular Disorders (ICVD) of the Bárány Society.
- Description of symptoms (binominal; the presence or absence of attacks, permanent dizziness/vertigo).
- Duration of symptoms (binominal, 3–6 months, >6 months).
- The intensity of vertigo/dizziness in the last 6 months was quantified using a visual analog scale from 0 (no intensity) to 10 (maximal intensity).
- Burden due to vertigo/dizziness in the last 6 months was quantified using a visual analog scale from 0 (no burden) to 10 (maximal burden; German: "Wie belastet waren Sie durch den Schwindel durchschnittlich in den letzten 6 Monaten?").

- Hospital Anxiety and Depression Scale (HADS) to estimate depression (18).
- Vertigo Symptom Scale to quantify the symptoms of vertigo and dizziness (19) by vertigo-balance (VSS-V) and autonomic-anxiety (VSS-A) subscale.

Statistics

All analyses were conducted using IBM SPSS Statistics (version 25), R (version 4.1.1), and Jamovi (Version 1.8.2). Values are the mean and standard deviation (SD) or numbers and percentages. Normal distribution was determined using the Shapiro–Wilk test. Missing data were treated according to the pairwise deletion process. Spearman correlations were used for correlation analyses between different variables. Correlation between subgroups was compared using Fisher's z (20). Elastic net regularization was performed to determine the predictors of the dependent variable (tolerance). Elastic net regularization leads to parsimonious models, which are easier to interpret. Variable selection is performed by shrinking the parameters toward zero and attenuating overfitting, a well-known problem when applying regression models with a large number of predictors. A 10-fold cross-validation was performed to choose the best model with the lowest mean cross-validated error. Within the elastic net algorithm, variables remain in the model if the prediction error averaged over the 10-fold cross-validation samples is reduced. Regression coefficients of the model with confidence intervals (CIs) were reported. Elastic net regularization was performed using the package *glmnet* in R (version 3.6.2). Finally, a simple mediation model as implemented in Jamovi was used to study the mediating effect of age on tolerance *via* intensity by using a 1.000 bootstrapping procedure. All statistical tests were applied two-sided at a significance level of 0.05.

RESULTS

Sociodemographic parameters, diagnoses, and vertigo characteristics of the entire cohort are given in **Table 1**. The distributions of intensity, burden, and tolerance are displayed in **Figure 1**. The mean difference between the actual intensity of dizziness and the hypothetically tolerated dizziness (tolerance) was 2.0 (SD = 1.93) points on the visual analog scale. This means that patients wished that dizziness is reduced by ∼20%.

Spearman correlation between tolerance and independent variables is displayed in **Figure 2**. Here, tolerance correlated with age, the intensity of dizziness, the burden of dizziness, and HADS depression. In the non-parametric tests, significant group differences for tolerance were found in dizziness type (higher tolerance for organic reasons in comparison to psychic or unspecific vertigo), the permanence of vertigo (higher tolerance in permanent dizziness), attack-like dizziness (lower tolerance for attacks), and duration of dizziness (higher tolerance for longer disease duration), but not for sex ($p = 0.63$; **Figure 3**).

The significant parameters from univariate analyses were then entered into an elastic-net model. A higher tolerance of dizziness was associated with higher age, higher intensity of dizziness, lower burden of dizziness, higher HADS depression, organic reason for dizziness (type), permanent dizziness, absence of attacks, and longer disease duration (**Table 2**).

The flexplot in **Figure 4** shows that the correlation between tolerance and intensity differed between younger ($r = 0.28$, $p = 0.003$), middle-aged ($r = 0.226$, $p = 0.012$), and older persons ($r = 0.50$, $p < 0.001$). This means that higher intensity of dizziness is related to higher tolerance and this relationship is strongest in older adults (Fisher's $z = -1.9780$, $p = 0.048$ for young vs. older; Fisher's $z = -2.3824$, $p = 0.017$ for middle-aged vs. older). Given that age is also weakly correlated with intensity (**Figure 2**), we finally tested if the effect of age on tolerance could be mediated by intensity. Mediation analysis with 1.000 bootstrapping revealed that age had a significant direct effect on tolerance (72% of the total effect) and a significant indirect effect *via* intensity

TABLE 1 | Overview of descriptive data.

		M	SD
Age		57.58	14.60
VSS vertigo/balance subscale		8.89	8.81
VSS autonomic/anxiety subscale		11.94	9.42
VSS total		20.82	16.16
HADS depression		5.53	3.86
Tolerance (0–10)		2.65	1.42
Average intensity of dizziness (0–10)		4.64	1.85
Average burden of dizziness (0–10)		5.04	2.21
		n	**%**
Age group	Younger (20–50)	113	31.6
	Middle (51–64)	124	34.6
	Older (>65)	121	33.8
Sex	Female	215	60.1
	Male	143	39.9
Type	Organic	199	56.9
	Psychic	126	36.0
	Unspecific	25	7.1
Diagnosis	BPPV	12	3.4
	BV	16	4.5
	CV	20	5.6
	MD	27	7.5
	MultD	64	17.9
	PPPD	156	43.6
	VM	13	3.6
	VN	36	10.1
	VP	6	1.7
	VS	8	2.2
Permanent vertigo	Yes	188	55.8
	No	149	44.2
Attacks	Yes	194	62.0
	No	119	38.0
Duration of vertigo	3–6 months	37	10.9
	>6 months	304	89.1

HADS, Hospital Anxiety and Depression Scale; VSS, Vertigo Symptom Scale; BPPV, benign paroxysmal positional vertigo; BV, bilateral vestibulopathy; CV, central vertigo; MD, Meniere's disease; MultD, multisensory deficit; VM, vestibular migraine; VN, vestibular neuritis; VP, vestibular paroxysmia; VS, vestibular schwannoma.

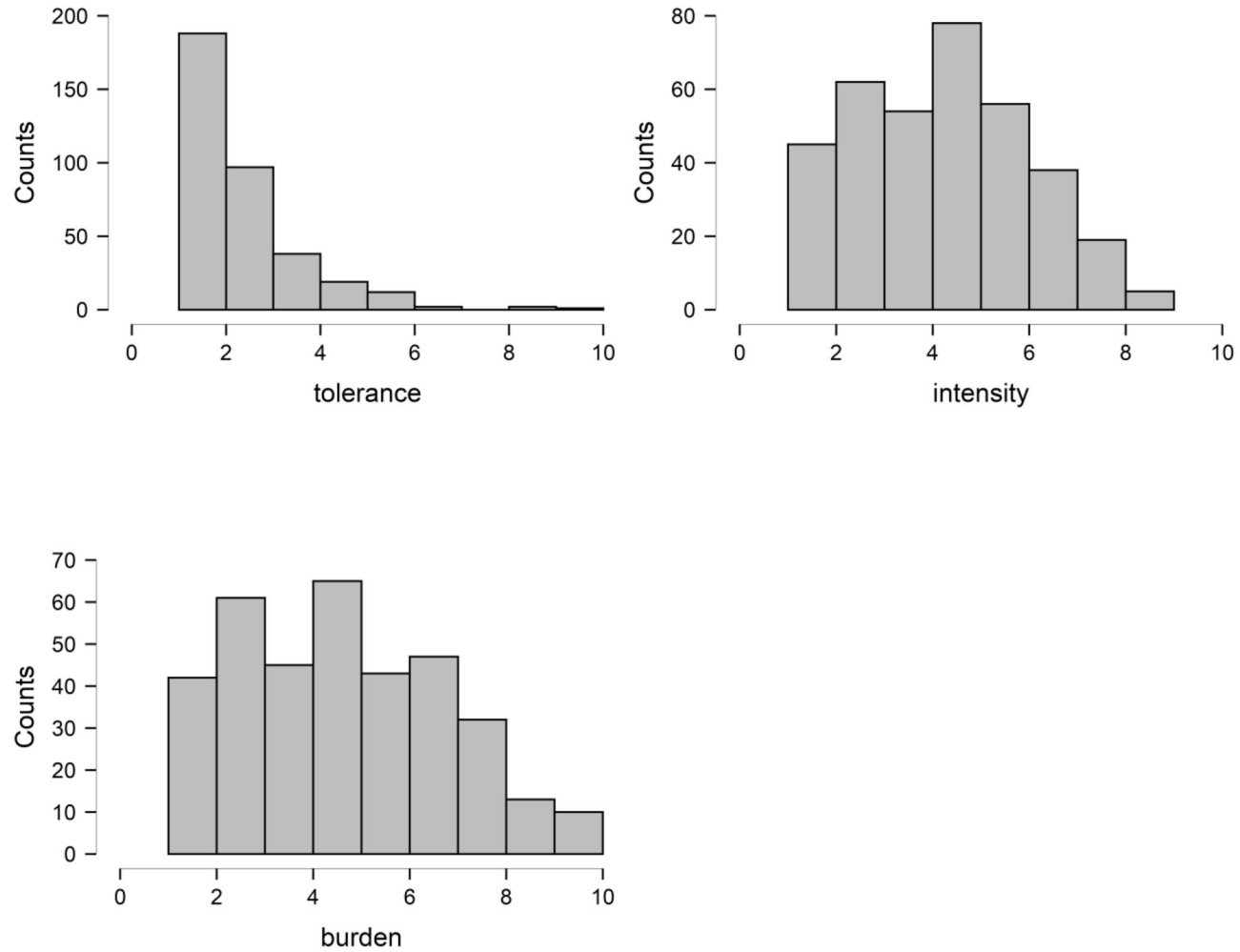

FIGURE 1 | The distributions of intensity, burden, and tolerable dizziness intensity.

on tolerance (28% of the total effect; **Table 3**). Therefore, the effect of age on tolerance occurs mainly independent of the perceived influence.

DISCUSSION

Dizziness and vertigo are common complaints associated with a substantial individual burden (4, 21–23). It is important to understand the impact of dizziness on individual wellbeing (24). In this study, we investigated which factors influence the ability of patients with chronic dizziness to tolerate their dizziness symptoms in everyday life. Our independent variables included age, sex, common dizziness-related measures, and psychological parameters. In terms of dizziness-related measures, we found that dizziness can be better tolerated when a higher baseline intensity of dizziness is present, when the burden is low, when there is a structural reason for dizziness (type), and when the disease duration is longer. In addition, permanent dizziness is better tolerated than attack-like dizziness. Moreover, we found that dizziness is better tolerated in higher age and people with depressive symptoms. The strongest influence on tolerance has the intensity and burden of dizziness.

When patients were asked how much dizziness was tolerable for them, they indicated on average that 20% less dizziness would be desirable. Only a small proportion stated that dizziness was not tolerable at all (i.e., rated 0 on the visual analog scale). This difference is comparable to the Calman gap, i.e., the difference between the current quality of life and desired quality of life in people with chronic diseases (6). We acknowledge that there are different methods (e.g., Pictorial Representation of Illness and Self Measure) to measure the burden of dizziness (24). However, here we used simple visual analog scales to measure intensity, burden, and tolerance to dizziness in order to get comparable outcome parameters.

The intensity of dizziness/vertigo, age, depression, type of vertigo (somatic vs. non-somatic), and persistence of symptoms (permanent or attack-like) play a role in

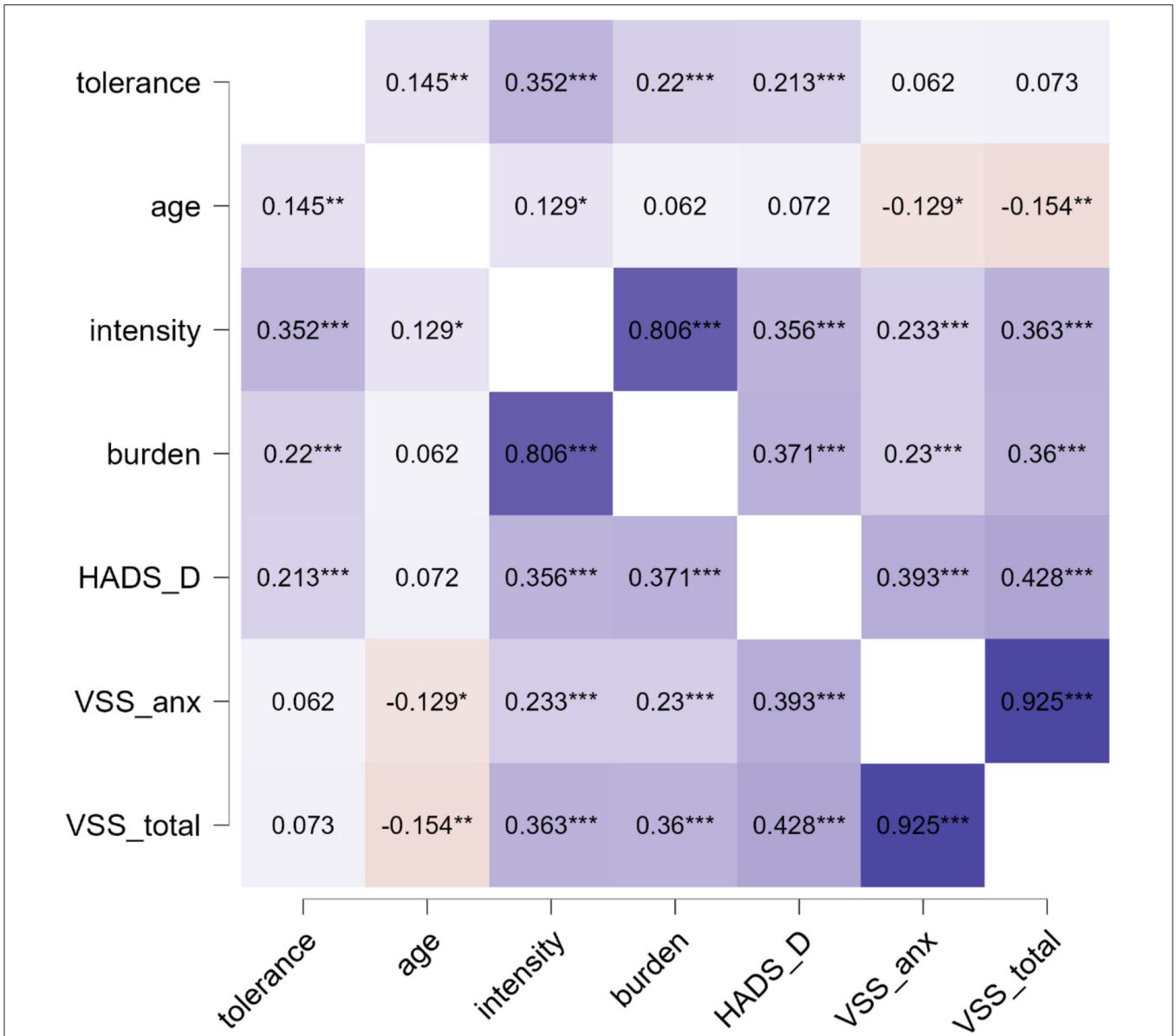

FIGURE 2 | Spearman's rho heatmap. *$p < 0.05$, **$p < 0.01$, ***$p < 0.001$. Blue indicates positive and red indicated negative correlation. HADS, hospital anxiety and depression scale; VSS_anx, vertigo severity scale autonomic-anxiety; VSS_total, total vertigo severity scale.

how much dizziness/vertigo is tolerable. Patients tolerate more dizziness/vertigo with increasing age. This could be demonstrated in the elastic net model after correction for cofactors and in the flexplot (**Figure 4**). This effect occurred independent from the intensity of dizziness/vertigo, although it is known that dizziness-associated handicap increases with age (25) and older patients with dizziness have less anxiety than younger patients (26).

In an earlier study, we found that younger people were more frequently hospitalized due to dizziness than older adults, and the number of consultations of healthcare providers was considerably higher in younger patients (26). Now, we can hypothesize that a higher tolerance of dizziness increases the threshold to initiate specialized vertigo therapy and could partly explain lower healthcare utilization in older patients. However, why older people tolerate more dizziness and to what extent this may contribute to lower healthcare utilization need to be investigated in further studies. At this point, it can only be speculated that also negative stereotypes about age-related complaints may play a role in this. Many studies provided evidence that ageism affects health outcomes (27–29). For example, when older adults are randomly assigned to a negative-age-stereotype condition, it impairs performance in cognitive tasks (30, 31). However, also age stereotypes that are directed at oneself in old age (self-perceptions of aging) affect functional health (29, 32, 33). Moreover, age

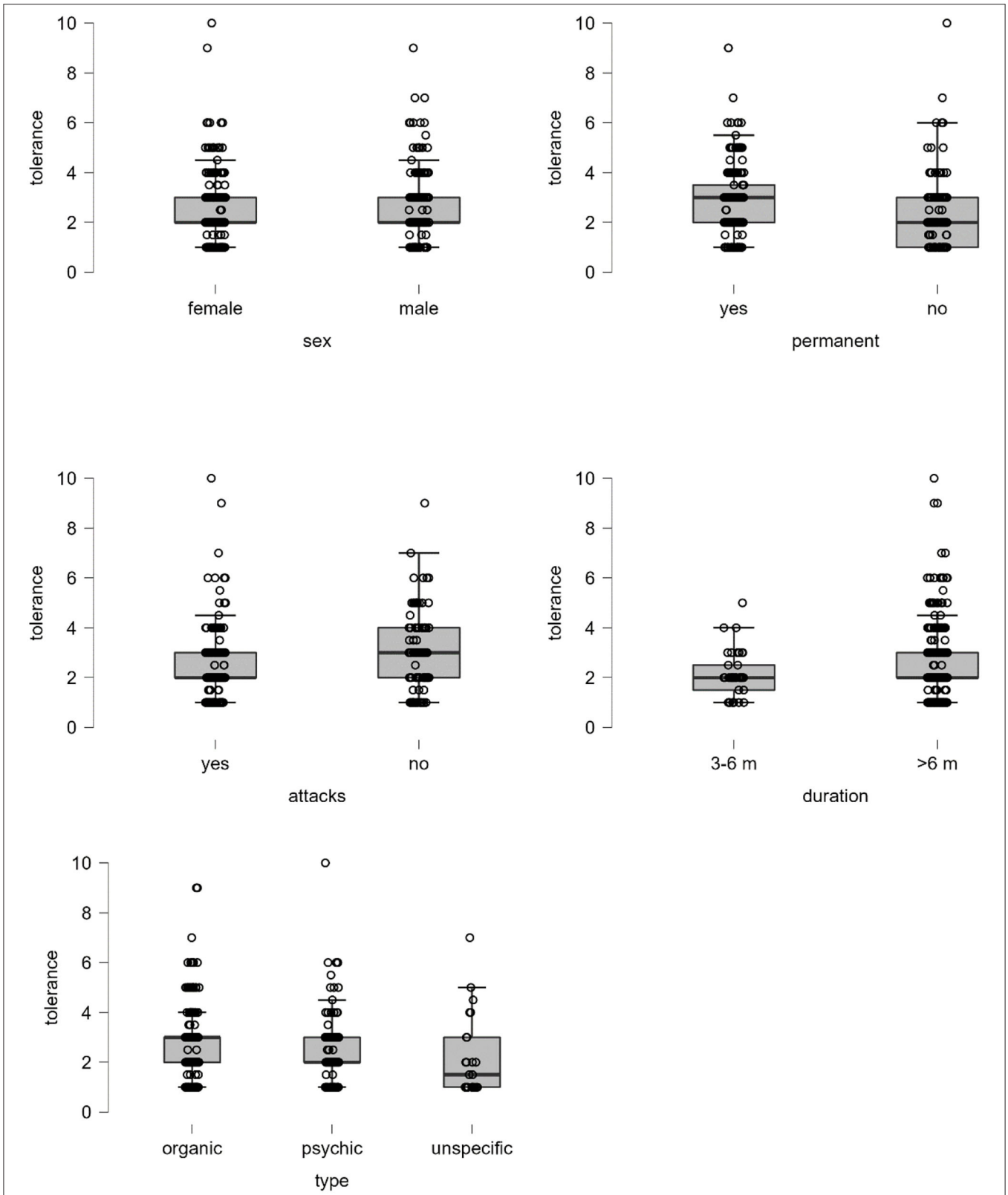

FIGURE 3 | Boxplots for tolerance. Test statistics for Mann–Whitney *U*-test: sex $p = 0.632$, permanent $p < 0.001$, attack $p < 0.001$, and duration $p = 0.026$. Test statistic for Kruskal–Wallis test: type $p = 0.001$, unspecific – psychic $p = 0.075$, unspecific – organic $p = 0.002$, psychic – organic $p = 0.016$.

stereotypes tend to be resistant to even extremely stressful events (34).

TABLE 2 | Elastic net regularization with tolerance as a dependent variable.

	Coefficient	2.5% CI	97.5% CI	*p*-value
Constant	1.327	0.527	2.128	0.001
Age	0.002	−0.011	0.014	0.805
Intensity	0.325	0.186	0.465	0.000
Burden	−0.160	−0.275	−0.044	0.007
HADS-D	0.042	−0.003	0.086	0.069
Type (organic/structural)	0.182	−0.207	0.572	0.360
Type (unspecific)	−0.226	−0.903	0.451	0.514
Permanent (no)	−0.132	−0.509	0.246	0.495
Attacks (no)	0.296	−0.078	0.670	0.122
Duration (>6 months)	0.136	−0.394	0.666	0.616

Model fit: $\chi^2(9) = 91.118$, $p < 0.001$, Pseudo-R^2 (Cragg-Uhler) = 0.164, AIC (Akaike Information Criterion) = 979.879, BIC (Bayesian information criterion) = 1,020.057. Hospital Anxiety and Depression Scale (HADS).

Another influencing factor for higher tolerance may be the finding that anxiety (measured with the VSS) does not play such a prominent role in the older patients with dizziness than in younger patients (3). Instead, we found that depressive symptoms (higher HADS-D) correlate with tolerance. To understand this finding, one has to keep in mind that depressive symptoms also correlate with the current intensity of dizziness. This means that people with depressive symptoms in general rate their current and tolerable dizziness higher in comparison to people with a lower HADS-D (while the gap between both remains stable). Given that older people with chronic dizziness report lower levels of depression and anxiety (26), we assume that the higher tolerance with increasing age occurs independently of these psychological cofactors. Our findings are in line with earlier studies, showing that depression is frequent and clinically relevant in people with dizziness and that depression influences the severity and outcome of dizziness (12, 35–37).

Our study has several limitations. Patients in our sample attended a highly specialized treatment program for chronic dizziness. Thus, there is a selection bias regarding their underlying diagnoses and the findings should be generalized

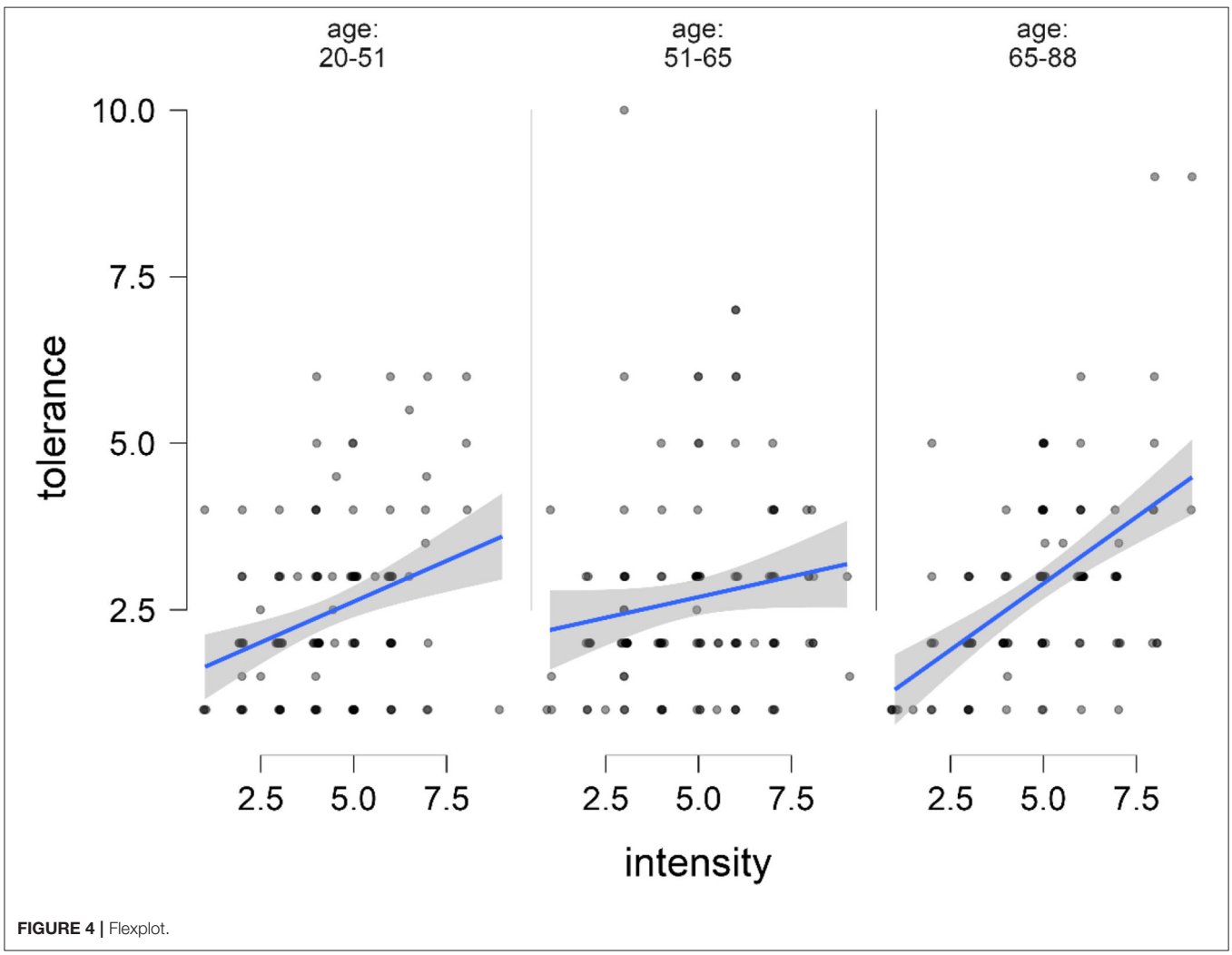

FIGURE 4 | Flexplot.

TABLE 3 | Mediation model.

Effect	Estimate	SE	95% C.I. (a)		β	z	p-value	% Mediation
			Lower	Upper				
Indirect effect								
Age⇒intensity⇒tolerance	0.003819	0.001863	2.272e-4	0.007529	0.03891	2.050	0.040	28.12
Component								
Age ⇒intensity	0.015462	0.006882	0.002280	0.029258	0.12151	2.247	0.025	
Intensity⇒tolerance	0.246988	0.042355	0.162887	0.328915	0.32021	5.831	<0.001	
Direct effect								
Age ⇒ tolerance	0.009761	0.004457	0.001065	0.018536	0.09946	2.190	0.029	71.88
Total effect								
Age ⇒ tolerance	0.013580	0.005152	0.003483	0.023677	0.13837	2.636	0.008	100.00

Confidence intervals (CIs) computed with method: parametric bootstrap. Betas are completely standardized effect sizes.

with caution. For example, only a few people had benign paroxysmal positional vertigo (BPPV) in our cohort, a common cause of dizziness among older adults (38). This is because many patients with BPPV were already treated by their general physicians, which makes an appointment in our center not necessary. Patients are referred to our tertiary care center only if symptoms become chronic. Although the response rate to our survey was relatively good for a postal/mail survey, this also limits the generalizability of the results. Our dependent variable was so far not validated. Nevertheless, we assume that a visual analog scale is suitable to track differences in the individual perceptions of illness. It is worth to note that other methods also exist to determine the burden of dizziness (i.e., Pictorial Representation of Illness and Self-Measure) (24) and that the kind of assessment may influence the results. Finally, our analysis is driven by a theoretical selection of independent variables. Further studies are therefore needed to gain a deeper understanding of the relationship between, for example, age and tolerance of dizziness.

The ability to cope and tolerate dizziness depends on the type and presentation of vertigo, age, and psychological comorbidities. Looking at how much dizziness patients can tolerate in order to cope with everyday life could be an interesting approach to develop new therapies. At least this view enriches the mere consideration of the handicap caused by the dizziness. In further studies, our approach could be used to focus more on the resources and resilience of patients in order to strengthen them and thus to cope better with dizziness in everyday life.

DATA AVAILABILITY STATEMENT

The raw data supporting the conclusions of this article will be made available by the authors, without undue reservation.

ETHICS STATEMENT

The studies involving human participants were reviewed and approved by Ethics Committee of the Friedrich-Schiller-University Jena, Number 5426-02/18. The patients/participants provided their written informed consent to participate in this study.

AUTHOR CONTRIBUTIONS

TP: design of the study and writing of the paper and analysis. HA: collection of data. HA and SM: revision of the paper. All authors contributed to the article and approved the submitted version.

SUPPLEMENTARY MATERIAL

The Supplementary Material for this article can be found online at: https://www.frontiersin.org/articles/10.3389/fneur.2022.934627/full#supplementary-material

REFERENCES

1. Neuhauser HK. The epidemiology of dizziness and vertigo. *Handb Clin Neurol.* (2016) 137:67–82. doi: 10.1016/B978-0-444-63437-5.00005-4
2. Axer H, Finn S, Wassermann A, Guntinas-Lichius O, Klingner CM, Witte OW, et al. Multimodal treatment of persistent postural-perceptual dizziness. *Brain Behav.* (2020) 10:e01864. doi: 10.1002/brb3.1864
3. Dietzek M, Finn S, Karvouniari P, Zeller MA, Klingner CM, Guntinas-Lichius O, et al. In older patients treated for dizziness and vertigo in multimodal rehabilitation somatic deficits prevail while anxiety plays a minor role compared to young and middle aged patients. *Front Aging Neurosci.* (2018) 10:345. doi: 10.3389/fnagi.2018.00345
4. Neuhauser HK, Radtke A, von Brevern M, Lezius F, Feldmann M, Lempert T, et al. Burden of dizziness and vertigo in the community. *Arch Intern Med.* (2008) 168:2118–24. doi: 10.1001/archinte.168.19.2118
5. Duracinsky M, Mosnier I, Bouccara D, Sterkers O, Chassany O, Working Group of the Société Française d'Oto-Rhino-Laryngologie (ORL). Literature review of questionnaires assessing vertigo and dizziness, and their impact on patients' quality of life. *Value Health.* (2007) 10:273–84. doi: 10.1111/j.1524-4733.2007.00182.x

6. Prell T, Teschner U, Witte OW, Kunze A. Current and desired quality of life in people with Parkinson's disease: the calman gap increases with depression. *J Clin Med.* (2020) 9:E1496. doi: 10.3390/jcm9051496
7. Best C, Tschan R, Eckhardt-Henn A, Dieterich M. Who is at risk for ongoing dizziness and psychological strain after a vestibular disorder? *Neuroscience.* (2009) 164:1579–87. doi: 10.1016/j.neuroscience.2009.09.034
8. Porter M, Boothroyd RA. Symptom severity, social supports, coping styles, and quality of life among individuals' diagnosed with Ménière's disease. *Chronic Illn.* (2015) 11:256–66. doi: 10.1177/1742395314567926
9. Tschan R, Best C, Beutel ME, Knebel A, Wiltink J, Dieterich M, et al. Patients' psychological well-being and resilient coping protect from secondary somatoform vertigo and dizziness (SVD) 1 year after vestibular disease. *J Neurol.* (2011) 258:104–12. doi: 10.1007/s00415-010-5697-y
10. Jacobson GP, Newman CW. The development of the Dizziness Handicap Inventory. *Arch Otolaryngol Head Neck Surg.* (1990) 116:424–7. doi: 10.1001/archotol.1990.01870040046011
11. Yardley L, Masson E, Verschuur C, Haacke N, Luxon L. Symptoms, anxiety and handicap in dizzy patients: development of the vertigo symptom scale. *J Psychosom Res.* (1992) 36:731–41. doi: 10.1016/0022-3999(92)90131-K
12. Best C, Eckhardt-Henn A, Tschan R, Dieterich M. Psychiatric morbidity and comorbidity in different vestibular vertigo syndromes. Results of a prospective longitudinal study over one year. *J Neurol.* (2009) 256:58–65. doi: 10.1007/s00415-009-0038-8
13. Godemann F, Schabowska A, Naetebusch B, Heinz A, Ströhle A. The impact of cognitions on the development of panic and somatoform disorders: a prospective study in patients with vestibular neuritis. *Psychol Med.* (2006) 36:99–108. doi: 10.1017/S0033291705005921
14. Godemann F, Siefert K, Hantschke-Brüggemann M, Neu P, Seidl R, Ströhle A, et al. What accounts for vertigo one year after neuritis vestibularis - anxiety or a dysfunctional vestibular organ? *J Psychiatr Res.* (2005) 39:529–34. doi: 10.1016/j.jpsychires.2004.12.006
15. Piker EG, Jacobson GP, McCaslin DL, Grantham SL. Psychological comorbidities and their relationship to self-reported handicap in samples of dizzy patients. *J Am Acad Audiol.* (2008) 19:337–47. doi: 10.3766/jaaa.19.4.6
16. Cheng C, Inder K, Chan SW-C. Coping with multiple chronic conditions: an integrative review. *Nurs Health Sci.* (2020) 22:486–497. doi: 10.1111/nhs.12695
17. Prell T, Finn S, Zipprich HM, Axer H. What predicts improvement of dizziness after multimodal and interdisciplinary day care treatment? *J Clin Med.* (2022) 11:2005. doi: 10.3390/jcm11072005
18. Andersson E. The Hospital Anxiety and Depression Scale: homogeneity of the subscales. *Soc Behav Pers.* (1993) 21:197–204. doi: 10.2224/sbp.1993.21.3.197
19. Tschan R, Wiltink J, Best C, Bense S, Dieterich M, Beutel ME, et al. Validation of the German version of the Vertigo Symptom Scale (VSS) in patients with organic or somatoform dizziness and healthy controls. *J Neurol.* (2008) 255:1168–75. doi: 10.1007/s00415-008-0863-1
20. Eid M, Gollwitzer M, Schmitt M. *Statistik und Forschungsmethoden*. Beltz (2010).
21. Neuhauser HK. [Epidemiology of dizziness and vertigo]. *Nervenarzt.* (2009) 80:887–94. doi: 10.1007/s00115-009-2738-9
22. Ruthberg JS, Rasendran C, Kocharyan A, Mowry SE, Otteson TD. The economic burden of vertigo and dizziness in the United States. *J Vestib Res.* (2021) 31:81–90. doi: 10.3233/VES-201531
23. Wang X, Strobl R, Holle R, Seidl H, Peters A, Grill E, et al. Vertigo and dizziness cause considerable more health care resource use and costs: results from the KORA FF4 study. *J Neurol.* (2019) 266:2120–8. doi: 10.1007/s00415-019-09386-x
24. Weidt S, Bruehl AB, Moergeli H, Straumann D, Hegemann S, Büchi S, et al. Graphic representation of the burden of suffering in dizziness patients. *Health Qual Life Outcomes.* (2014) 12:184. doi: 10.1186/s12955-014-0184-2
25. Wassermann A, Finn S, Axer H. Age-associated characteristics of patients with chronic dizziness and vertigo. *J Geriatr Psychiatry Neurol.* (2021) 35:580–5. doi: 10.1177/08919887211036185
26. Prell T, Finn S, Axer H. How healthcare utilization due to dizziness and vertigo differs between older and younger adults. *Front Med.* (2022) 9:852187. doi: 10.3389/fmed.2022.852187
27. Lamont RA, Swift HJ, Abrams D. A review and meta-analysis of age-based stereotype threat: negative stereotypes, not facts, do the damage. *Psychol Aging.* (2015) 30:180–93. doi: 10.1037/a0038586
28. Meisner BA. A meta-analysis of positive and negative age stereotype priming effects on behavior among older adults. *J Gerontol B Psychol Sci Soc Sci.* (2012) 67:13–7. doi: 10.1093/geronb/gbr062
29. Westerhof GJ, Miche M, Brothers AF, Barrett AE, Diehl M, Montepare JM, et al. The influence of subjective aging on health and longevity: a meta-analysis of longitudinal data. *Psychol Aging.* (2014) 29:793–802. doi: 10.1037/a0038016
30. Hehman JA, Bugental DB. Responses to patronizing communication and factors that attenuate those responses. *Psychol Aging.* (2015) 30:552–60. doi: 10.1037/pag0000041
31. Levy BR, Leifheit-Limson E. The stereotype-matching effect: greater influence on functioning when age stereotypes correspond to outcomes. *Psychol Aging.* (2009) 24:230–3. doi: 10.1037/a0014563
32. Levy BR, Slade MD, Kasl SV. Longitudinal benefit of positive self-perceptions of aging on functional health. *J Gerontol B Psychol Sci Soc Sci.* (2002) 57:409–17. doi: 10.1093/geronb/57.5.P409
33. Wurm S, Tesch-Römer C, Tomasik MJ. Longitudinal findings on aging-related cognitions, control beliefs, and health in later life. *J Gerontol B Psychol Sci Soc Sci.* (2007) 62:156–64. doi: 10.1093/geronb/62.3.P156
34. Levy BR, Slade MD, Chung PH, Gill TM. Resiliency over time of elders' age stereotypes after encountering stressful events. *J Gerontol B Psychol Sci Soc Sci.* (2015) 70:886–90. doi: 10.1093/geronb/gbu082
35. Eckhardt-Henn A, Best C, Bense S, Breuer P, Diener G, Tschan R, et al. Psychiatric comorbidity in different organic vertigo syndromes. *J Neurol.* (2008) 255:420–8. doi: 10.1007/s00415-008-0697-x
36. Eckhardt-Henn A, Dieterich M. Psychiatric disorders in otoneurology patients. *Neurol Clin.* (2005) 23:731–49. doi: 10.1016/j.ncl.2005.01.008
37. Nagarkar AN, Gupta AK, Mann SB. Psychological findings in benign paroxysmal positional vertigo and psychogenic vertigo. *J Otolaryngol.* (2000) 29:154–8.
38. Lindell E, Karlsson T, Kollén L, Johansson M, Finizia C. Benign paroxysmal positional vertigo and vestibular impairment among older adults with dizziness. *Laryngoscope Investig Otolaryngol.* (2021) 6:488–95. doi: 10.1002/lio2.566

Conflict of Interest: The authors declare that the research was conducted in the absence of any commercial or financial relationships that could be construed as a potential conflict of interest.

Publisher's Note: All claims expressed in this article are solely those of the authors and do not necessarily represent those of their affiliated organizations, or those of the publisher, the editors and the reviewers. Any product that may be evaluated in this article, or claim that may be made by its manufacturer, is not guaranteed or endorsed by the publisher.

Copyright © 2022 Prell, Mendorf and Axer. This is an open-access article distributed under the terms of the Creative Commons Attribution License (CC BY). The use, distribution or reproduction in other forums is permitted, provided the original author(s) and the copyright owner(s) are credited and that the original publication in this journal is cited, in accordance with accepted academic practice. No use, distribution or reproduction is permitted which does not comply with these terms.

frontiers | Frontiers in Neurology

ORIGINAL RESEARCH
published: 15 July 2022
doi: 10.3389/fneur.2022.944001

Auditory Manifestations of Vestibular Migraine

Suming Shi[1,2†], *Dan Wang*[1,2†], *Tongli Ren*[1,2] *and Wuqing Wang*[1,2*]

[1] ENT Institute and Otorhinolaryngology Department, Affiliated Eye and ENT Hospital, Fudan University, Shanghai, China,
[2] NHC Key Laboratory of Hearing Medicine (Fudan University), Shanghai, China

Objectives: To investigate the auditory features of patients with vestibular migraine (VM) and to analyze the possible relevant factors of hearing loss.

Methods: A total of 166 patients with VM were enrolled. Demographic variables, age of onset, disease course, distribution of vestibular attacks, characteristics of hearing loss, and the coexistence of related disorders, such as visual aura, familial history, motion sickness, nausea, headache, photophobia, otalgia, tinnitus, aural fullness, and phonophobia, were analyzed and compared.

Results: Patients with VM can manifest otalgia (8.4%), tinnitus (51.8%), aural fullness (41%), and phonophobia (31.9%). Of 166 patients, the prevalence of VMw was 21.1% ($n = 35$). Patients with VMw mainly manifested mild and easily reversible low-frequency hearing loss. The proportions of tinnitus and aural fullness were significantly larger in patients with VMw than that in patients with VMo ($P < 0.05$). The duration of vestibular symptoms was significantly shorter in patients with VMw ($P < 0.05$). However, the age of onset, disease course, gender, frequency of vestibular attacks, the coexistence of visual aura, familial history, motion sickness, nausea, headache, photophobia, otalgia, and phonophobia had no significant difference between the two groups.

Conclusion: Auditory symptoms were common in patients with VM. The hearing loss of VM was characterized by a mild and easily reversible low-frequency hearing loss, accompanied by higher proportions of tinnitus and aural fullness, and a shorter duration of vestibular symptoms compared with patients with VMo.

Keywords: vestibular migraine, auditory symptoms, hearing loss, tinnitus, aural fullness

OPEN ACCESS

Edited by:
Su-Lin Zhang,
Huazhong University of Science and Technology, China

Reviewed by:
Aynur Özge,
Mersin University, Turkey
Soumit Dasgupta,
Alder Hey Children's Hospital, United Kingdom

***Correspondence:**
Wuqing Wang
wwuqing@eent.shmu.edu.cn

†These authors have contributed equally to this work

Specialty section:
This article was submitted to Neuro-Otology, a section of the journal Frontiers in Neurology

Received: *14 May 2022*
Accepted: *17 June 2022*
Published: *15 July 2022*

Citation:
Shi S, Wang D, Ren T and Wang W (2022) Auditory Manifestations of Vestibular Migraine. Front. Neurol. 13:944001. doi: 10.3389/fneur.2022.944001

INTRODUCTION

Vestibular migraine (VM) is one of the most common causes of recurrent vertigo, with a high prevalence of 1∼2.7% in individuals. It causes significant morbidity with loss of work hours and is considered to be the seventh most disabling disease worldwide. However, VM remains under-recognized because of the broad spectrum of its manifestations.

Clinicians frequently come across patients with migraine symptoms and dizziness, many other audiovestibular symptoms are associated with migraine, including tinnitus (1), aural fullness (2), otalgia (3), sudden sensorineural hearing loss (SSNHL) (4–6), and fluctuating hearing loss (7). However, the detailed characteristics of auditory symptoms and the factors related to hearing loss are far from clear. The more details found regarding the characteristics of auditory manifestations of VM, the easier the VM is recognized.

Therefore, we reviewed 166 patients with VM to evaluate the auditory symptoms and to analyze the possible relevant factors of hearing loss. Moreover, in consideration of the difficulty of distinguishing VM from the early Meniere's disease (MD), in addition to clinical symptoms, gadolinium (Gd) contrast-enhanced MRI was used to visualize endolymphatic hydrops (ELH) and to exclude early MD and other vestibular disorders in this study (8).

METHODS

Patients

A total of 166 patients with VM were included from April 2016 to April 2017. The criteria used to enroll patients fulfilled the VM diagnostic criteria formulated by the Committee for Classification of Vestibular Disorders of the Bárány Society (9) (**Supplementary Table 1**). Systematic history inquiry, neurotologic evaluations, including an electric otoscope, audiometry, tympanometry, and other tests when needed were performed. Other vestibular disorders and headaches were excluded. Moreover, to distinguish VM from other vestibular disorders, especially for MD, Gd contrast-enhanced MRI was conducted for all patients enrolled. The clinical manifestations, including presenting age, onset age, disease course, gender, distribution of vestibular attacks and coexisting visual aura, headache, photophobia, familial history, motion sickness, nausea, otalgia, tinnitus, aural fullness, phonophobia, and hearing loss, were collected and compared. For migraine aura, although many patients report typical visual symptoms, like spreading visual scintillations followed by scotoma, others describe less well-defined symptoms, like visual blurring or distortion. Sometimes, typical symptoms follow an atypical spatial or temporal course. Some aura symptoms like aphasia are also often difficult to distinguish from word-finding difficulty due to cognitive fogging. Moreover, patients with visual symptoms are always accompanied by other aura symptoms. Therefore, the migraine aura enrolled in our study was mainly focused on the visual aura. The distribution of vestibular attacks consists of the frequency of vestibular attacks (within 1 year) and duration of vestibular attacks (most frequent). Ethics approval for this retrospective study was obtained from the Ethical Committees of the Eye, Ear, Nose, and Throat Hospital in Shanghai, China.

Gd Injection and MRI Acquisition

In total, 166 patients with VM were subjected to the bilateral intratympanic Gd injection (8) or intravenous injection of a double dose (0.4 mL/kg body weight) of Gd-HP-DO3A. Then, MRI was performed 4 h later. For the IV method, all patients underwent an IV injection of a double dose (0.4 mL/kg body weight) of Gd-HP-DO3A; 4 h later, MRI was performed. For the IV method, all scans were performed on a 3T MRI scanner (Verio; Siemens Healthcare, Erlangen, Germany) using a 32-channel phased-array receive-only coil. T2-space and 3D real-IR sequence MRIs were applied for collecting images. The parameters were as follows: voxel size = 0.17 × 0.17 × 0.6 mm; scan time = 15 min and 20 s, repetition time = 6,000 ms, echo time = 181 ms, inversion time = 1,850 ms, slice thickness = 0.6 mm, field of view = 160 × 160 mm, and matrix size = 768 × 768. The patients with MD and other organic lesions were excluded.

Pure Tone Audiometry Test

Hearing thresholds were tested in all patients at the first visit. The hearing thresholds at low frequency (125, 250, and 500 Hz), medium frequency (1k, 2k Hz), and high frequency (4k, 8k Hz) were evaluated to discover details. All patients conducted a PTA test 1 month later. The threshold below 20 dB HL was considered normal.

Statistical Analysis

Statistical analyses were performed using SPSS Statistics 17 software (IBM, Chicago, IL, USA) package. Data are presented as $\bar{x} \pm$ SD. The Spearman/Pearson correlation coefficient, the Mann-Whitney *U* test, an independent samples *t*-test, the chi-square test, and Fisher's exact test were used for data analyses. Differences were considered to be statistically significant when $p < 0.05$.

Ethical Consideration

The institutional review boards of the authors' institutions approved this study.

RESULTS

Demographics

The group consisted of 131 (78.9%) women and 35 (21.1%) men, with a visiting age of 42.5 ± 14.9 (6–76) years, onset age of 35.7 ± 14.4 (3–71) years, and a disease course of 81.6 ± 121.4 months. Among 166 individuals, 124 (74.7%) cases were diagnosed as VM, 42 (25.3%) cases were diagnosed as probable VM, 23 (13.9%) cases coexisted with visual aura, 91 (54.8%) cases had a family history of VM, 112 (67.5%) cases had motion sickness, 113 (68.1%) cases had nausea, 69 (41.6%) cases had a headache, 35 (21.1%) cases had hearing loss, 14 (8.4%) cases had otalgia, 86 (51.8%) cases had tinnitus, 68 (41%) cases had aural fullness, 53 (31.9%) cases had phonophobia, and 39 (23.5%) cases had photophobia (**Table 1**).

As **Table 2** shows, there are 77.9% (102/131) female and 22.1% (29/131) male patients with VMo, and 82.9% (29/35) female and 17.1% (6/35) male patients with VMw, with no significant gender difference between the two groups ($P = 0.520$). The onset age of the disease tended to be younger in patients with VMw (31.8 ± 14.1 years) than that in those with VMo (36.8 ± 14.3 years); however, it was not significantly different ($P = 0.051$). The average disease duration from the vestibular onset in patients with VMw (99.2 ± 144.8 months) was longer than the duration in patients with VMo (76.5 ± 113.3 months); however, it was statistically insignificant ($P = 0.976$). The proportions of definite and probable VM were similar between the two groups ($P = 0.708$).

Comorbidities

There is no significant difference in the prevalence of coexisting visual aura, headache, photophobia, family history of VM,

TABLE 1 | Demographic and clinical characteristics of enrolled patients ($n = 166$).

Variables	Values
Presenting age, yr, mean±SD	42.5 ± 14.9
Onset age, yr, mean±SD	35.7 ± 14.4
Disease duration, m, mean±SD	81.6 ± 121.4
Gender, *n* (%)	
Female	131 (78.9)
Male	35 (21.1)
Definite VM, *n* (%)	124 (74.7)
Probable VM, *n* (%)	42 (25.3)
Visual aura, *n* (%)	23 (13.9)
Headache, *n* (%)	69 (41.6)
Photophobia, *n* (%)	39 (23.5)
Family history of vertigo, *n* (%)	91 (54.8)
Motion sickness, *n* (%)	112 (67.5)
Nausea, *n* (%)	113 (68.1)
Hearing loss, *n* (%)	35 (21.1)
Unilateral	29 (17.5)
Bilateral	6 (3.6)
Otalgia, *n* (%)	14 (8.4)
Tinnitus, *n* (%)	86 (51.8)
Aural fullness, *n* (%)	68 (41.0)
Phonophobia, *n* (%)	53 (31.9)

TABLE 2 | Clinical features of patients with VM.

	VMo ($n = 131$)	VMw ($n = 35$)	*P*-value
Presenting age (y)	43.2 ± 14.8	40.1 ± 15.0	0.244
Onset age (y)	36.8 ± 14.3	31.8 ± 14.1	0.051
Disease course (m)	76.5 ± 113.3	99.2 ± 144.8	0.976
Gender, n (%)			
Female	102 (77.9)	29 (82.9)	0.520
Male	29 (22.1)	6 (17.1)	
Vestibular migraine, *n* (%)			
Definite	97 (74.0)	27 (77.1)	0.708
Probable	34 (26.0)	8 (22.9)	
Visual aura, *n* (%)	16 (12.2)	7 (20.0)	0.236
Headache, *n* (%)	15 (42.9)	54 (41.2)	0.862
Photophobia, *n* (%)	9 (25.7)	30 (22.9)	0.727
Family history of VM, *n* (%)	74 (56.5)	17 (48.6)	0.403
Motion sickness, *n* (%)	90 (68.7)	22 (62.9)	0.512
Nausea, *n* (%)	93 (71.0)	20 (57.1)	0.118
Otalgia, *n* (%)	10 (7.6)	4 (11.4)	0.473
Tinnitus, *n* (%)	58 (44.3)	28 (80.0)	0.000**
Aural fullness, *n* (%)	37 (28.2)	31 (88.6)	0.000**
Phonophobia, *n* (%)	41 (31.3)	12 (34.3)	0.736

*VMo, VM without hearing loss; VMw, VM with hearing loss. **$p < 0.01$.*

motion sickness, and nausea between the two groups ($P > 0.05$) (**Table 2**). Twenty-eight cases (80%) had tinnitus in the VMw group, whereas the number was 58 cases (44.3%) in the VMo group; this difference was significantly different ($P = 0.000$) (**Table 2**). The proportion of patients with a history of aural fullness was significantly larger in the VMw group (31, 88.6%) than that in the VMo group (37, 28.2%) ($P = 0.000$) (**Table 2**). Four cases (11.4%) had otalgia in the VMw group, and 10 cases (7.6%) in the VMo group ($P = 0.473$) (**Table 2**). Twelve (34.3%) cases had phonophobia in the VMo group, and 41 cases (31.3%) in the VMw group ($P = 0.736$) (**Table 2**).

As **Table 3** shows, 92.9% (13/14) of cases had otalgia on one side, 7.1% (1/14) of cases on both sides; 58.1% (50/86) of cases has tinnitus on one side, 41.9% (36/86) of cases on both sides; 79.7% (55/68) of cases had aural fullness on one side, and 20.3% (13/68) of cases on both sides.

TABLE 3 | Affected sides of auditory symptoms.

Symptoms	VM, % (n/N)
Hearing loss	
Unilateral	82.9 (29/35)
Bilateral	17.1 (6/35)
Otalgia	
Unilateral	92.9 (13/14)
Bilateral	7.1 (1/14)
Tinnitus	
Unilateral	58.1 (50/86)
Bilateral	41.9 (36/86)
Aural fullness	
Unilateral	79.7 (55/68)
Bilateral	20.3 (13/68)

VM, vestibular migraine.

Distribution of Vestibular Attacks

The vestibular attacks included vertigo, dizziness, and lightheadedness. The frequency of vestibular attacks and their duration are illustrated in **Table 4**. No significant difference was noted in the frequency of vestibular attacks between the two groups ($P = 0.537$). The frequency of 1 month-1 year and 1 week-1 month tends to be more common in both groups; the frequency of > 1 year was the least in both groups. The duration of VM was not confined to 5 min-72 h, while some cases can last for <5 min. The duration of vestibular attacks tends to be shorter in the VMw group (VMw, 16/35, 45.7%, <5 min; VMo, 35/131, 26.7%, and <5 min) ($P = 0.031$).

Cochlear Function

The PTA tests were conducted for all patients and repeated 1 month later. Of the 35 patients with hearing loss, 6 cases (17.1%) had bilateral hearing loss, and 29 cases (82.9%) had unilateral hearing loss (**Table 3**). Twenty-seven cases had low-frequency hearing loss (125, 250, and 500 Hz), 3 cases had low-frequency (125, 250, and 500 Hz) and medium-frequency (1k, 2k Hz) hearing loss, and 5 cases had low-frequency (125, 250, and 500 Hz) and high-frequency (4k, 8k Hz) hearing loss. Within 1 month, hearing loss from low to medium frequency completely

TABLE 4 | Distribution of vestibular attacks.

Attacks, *n* (%)	VMo, *n* = 131	VMw, *n* = 35	*P*-value
Frequency			
<1 day	21 (16.0)	6 (17.1)	0.537
1 day∼1 week	15 (11.5)	2 (5.7)	
1 week∼ 1 month	26 (19.8)	11 (31.4)	
1 month∼1 year	60 (45.8)	13 (37.1)	
>1 year	9 (6.9)	2 (5.7)	
Duration			
<1 min	33 (25.2)	13 (37.1)	0.031*
1 min∼5 min	2 (1.5)	3 (8.6)	
5 min∼72 h	96 (73.3)	19 (54.3)	

*VMo, VM without hearing loss; VMw, VM with hearing loss. *p < 0.05.*

transitioned for all patients. The hearing loss at high frequency had no change. Audiograms of a patient with VMw were shown (**Supplementary Figure 1**).

As shown in **Table 5**, patients with VMw were mainly manifested with mild- to low-frequency hearing loss. The average hearing thresholds of the patients with VMw were significantly higher than that of the VMo at frequencies of 125, 250, and 500 Hz ($P = 0.000$), while no significant difference was noted at low frequencies and high frequencies between the two groups ($P > 0.05$) (**Table 5**).

Image Findings

To distinguish VMw from other vestibular disorders and observe the distribution of ELH in patients with VM, all enrolled patients were subjected to the 3T-MRI. Other organic lesions were excluded. All patients ($n = 166$, 100%) had no ELH in both ears, including 131 cases with VMo and 35 cases with VMw.

DISCUSSION

The study identified the auditory features of patients with VM and analyzed the possible relevant factors for hearing loss. These results can be summarized as follows:

Auditory symptoms were common in patients with VM. The hearing loss of VM was characterized by a mild and easily reversible low-frequency hearing loss, accompanied by a higher proportion of tinnitus and aural fullness, and a shorter duration of the vestibular symptom. Moreover, to ensure the accuracy of the diagnosis of VM, a 3-T MRI was used to exclude other vestibular disorders, including MD at an early stage. No ELH was noted in all patients.

Similar to other subtypes of migraine, VM has a female preponderance, with a reported female-to-male ratio of 1.5∼5 to 1, the ratio is 3.7:1 in our study. The median ages of VM symptoms are mid-30–40 s (10–12); our data showed the onset age of 35.7 ± 14.4 (3–71) years, and 2 cases were under 4 years old. VM is the most common vestibular affliction in children (13), its onset may be younger but is often not recognized until children are old enough to properly describe their symptoms. In 41.6% of cases, vestibular and migraine symptoms began concurrently, which was similar to the previous study (42.7%) (14). The proportion of photophobia (23.5%) was lower in our study compared with previous research (15, 16). Apart from the headache, vestibular symptoms, photophobia, and phonophobia, patients with VM may experience visual aura. Visual aura occurred in 13.9% of our patients, it was lower than that observed elsewhere (one-quarter to one-third) (11, 15, 17, 18). Numerous studies over the years have documented familial aggregation of patients with migraine, and it is considered to be a genetic disease (19). Likewise, about 40∼90% of patients with VM had a family history, and our result of 54.8% was within the range. Motion sickness is a well-recognized comorbidity in migraine (20). Around two-thirds of patients with migraine have life-long sensitivity to motion sickness and many have spontaneous bouts of motion sickness without exposure to motion. Similarly, motion sickness was endorsed by most of our patients (67.5%). However, motion sickness is also associated with gravitational sensor dysfunction, examination of vestibular-evoked myogenic potentials, and subjective visual vertical would be useful in a further study. Nausea is also a common accompanying symptom of VM; 68.1% of cases coexisted with nausea during VM attacks in our data, and the prevalence can be higher (80.2%) (15).

The VM was considered closely related to auditory symptoms, including hearing loss, tinnitus, aural fullness, and phonophobia. However, the characteristics of cochlear symptoms are far from clear. The incidence of hearing loss in migraine varied from 3.3 to 14% (21–23), and our data were 21.1%, which may indicate that the prevalence of hearing impairment in VM may be higher. A transient and reversible unilateral or bilateral hearing loss during a migraine attack and the intermittent period have been mentioned in some studies (1, 4–6, 24, 25). Our data showed only 6 cases (3.6%) had bilateral hearing loss, and 29 cases (17.5%) had unilateral hearing loss. Mild and reversible low-frequency (125, 250, and 500 Hz) hearing loss was noted in our patients, Fluctuating hearing loss, tinnitus, and aural pressure may occur in vestibular migraine, but the hearing loss does not typically progress to severe hearing loss over the years in VM compared to MD, the auditory features helped distinguish VM from MD (22, 26, 27), idiopathic SSNHL, and other vestibular disorders. It is also worth mentioning that different treatments were applied according to the symptoms of the patients. Patients with apparent incentives and with infrequent and tolerable attacks do not need pharmacological treatment. Acute attacks can be ameliorated in some patients with antiemetic drugs, such as diphenhydramine, meclizine, and metoclopramide. Frequent attacks may warrant pharmacological prophylaxis with metoprolol, amitriptyline, topiramate, valproic acid, or flunarizine. Patients with insomnia, anxiety, or depression were given symptomatic treatment. Therefore, the hearing loss recovered after treatment or spontaneously requires further research. The mechanism of hearing loss remains unclear, several theories have been proposed: (1) Vasospasms associated with migraine in small arterioles within the cochlea and the labyrinth can induce the endolymphatic hydrops (6, 26, 28). However, our study found no cochlear or vestibular hydrops in our patients. To exclude the possibility of overlap of MD and VM, patients with obvious ELH have been excluded.

TABLE 5 | Auditory thresholds of patients with VM.

Frequency(Hz)/ Threshold(dB)	125	250	500	1k	2k	4k	8k
VMo	17.5 ± 4.1	17.3 ± 3.6	16.3 ± 3.5	16.2 ± 3.9	16.4 ± 5.4	16.4 ± 5.6	21.5 ± 11.9
VMw	32.5 ± 9.5	34.3 ± 12.2	28.8 ± 11.5	20 ± 9.0	18.3 ± 7.3	16.8 ± 8.5	21.4 ± 12.9
P-value	0.000**	0.000**	0.000**	0.051	0.192	0.679	0.880

*VMo, VM without hearing loss; VMw, VM with hearing loss. **$p < 0.01$.*

Moreover, it has been reported that the sensitivity of MRI scans is 50% with a different technique and probably less (29), therefore, further studies are needed. (2) Some inflammations and neurotransmitters involved in the pathogenesis of migraine affect the inner ear and the central auditory system (30). (3) A genetic deficiency of ion channels would be related to VM. Furthermore, channels expressed both in the inner ear and in the brain could affect peripheral and central auditory dysfunction (26, 31).

During a migraine attack, not only the auditory system may get damaged and hearing loss may be initiated, but also the central sensitization in the context of migraine will produce excessively high and distorted auditory signals in the central compensation, leading to tinnitus, otalgia, aural fullness, and phonophobia more likely to be perceived (32, 33). The proportion of tinnitus was reported to be 7.5∼50% among cochlear symptoms of migraine, our data were similar (51.8%). Patients with classic migraine are more likely to report ear pain than patients with other types of headaches, and patients with otalgia are more likely to report headaches than patients who do not have otalgia (3, 34). However, the proportion of otalgia (8.4%) was much less than tinnitus. The underlying mechanism may be that the sensation in the ear is under the control of afferents from the trigeminal nerve. Moreover, idiopathic SSNHL rarely had otalgia, which may be used to distinguish it from VM with hearing loss. The prevalence of aural fullness and phonophobia were 41 and 31.9%, respectively in our patients. Migraine features were commonly associated with aural fullness (2, 35, 36) and phonophobia, which was also possibly attributed to the activation of the trigeminal nerve and central hypersensitivity. Moreover, aural fullness is correlated with low-frequency hearing loss. However, some patients complaining of aural fullness had no increased hearing thresholds in our study. However, the cochlear function was evaluated only by the PTA test in our study, but an objective way of demonstrating cochlear function would have been otoacoustic emissions.

To explore the clinically related factors of hearing loss, we compared the gender, onset age, disease course, visual aura, motion sickness, family history, headache, photophobia, otalgia, tinnitus, aural fullness, phonophobia, and frequency and duration of vestibular attacks between patients with and without hearing loss. The onset age of the vestibular attacks tends to be younger in patients with VMw (31.8 ± 14.1 years) than that in patients with VMo (36.8 ± 14.3 years); however, it was not significantly different ($P = 0.051$). Further studies are needed to verify this point. The proportion of tinnitus was significantly higher in the VMw group than that of the VMo group. On one hand, it is widely accepted that tinnitus is initiated by hearing loss that subsequently causes abnormal hyperexcitability and neural synchronization in the central auditory system. On the other hand, during a migraine attack, not only the auditory system may be damaged and acute tinnitus may be initiated but also the central sensitization in the context of migraine will produce excessively high and distorted auditory signals in the central compensation (32, 33), which is more likely to be perceived. The higher prevalence of aural fullness in the VMw group may also be a result of the low-frequency hearing loss and the central sensitization. Unilateral auditory symptoms were predominant in the 166 patients with VM (5).

The frequency of vestibular attacks has individual variations, and frequencies of 1 week∼1 month and 1 month∼1 year were common in two groups. However, no evidence indicated that frequent vestibular attacks were correlated with hearing loss. The most frequent duration of vestibular attacks was minutes to hours (37), the percentage of seconds to ∼5 min in the VMw group was significantly higher than that in the VMo group. However, the underlying mechanism still needs exploration. We speculated that the vestibular function in VM with hearing loss might be more sensitive to tiny movement, which can manifest as transient attacks. Furthermore, similar to cochlear migraine proposed by several scholars (7), the cochlear system might be preferentially affected, causing a hearing loss but with a quick vestibular recovery. Further studies and more comprehensive vestibular function tests were needed.

Our research still leaves much to be desired. First, other auditory tests have not been performed except PTA. Second, patients with VM have individual variations, the proposed clinical diagnostic criteria of VM were not able to capture all patients, including patients with cochlear migraine (7). Third, vestibular functions were not analyzed. Moreover, migraine and MD might be inherited as a symptom cluster (38), and distinguishing VM from MD is still difficult. Therefore, it still needs further research.

CONCLUSION

In conclusion, auditory symptoms, including tinnitus, aural fullness, phonophobia, and otalgia were common in patients with VM. The hearing impairment of patients with VM was mainly manifested as low frequency and easily reversible hearing loss. In patients with VMw, they were accompanied

by a higher proportion of tinnitus and aural fullness and a shorter duration of vestibular attacks. To explore the correlated clinical factors of hearing loss, further studies are warranted.

DATA AVAILABILITY STATEMENT

The original contributions presented in the study are included in the article/**Supplementary Material**, further inquiries can be directed to the corresponding author.

ETHICS STATEMENT

Ethics approval for this retrospective study was obtained from the Ethical Committees of the Eye, Ear, Nose, & Throat Hospital in Shanghai, China. Written informed consent to participate in this study was provided by the participants' legal guardian/next of kin.

AUTHOR CONTRIBUTIONS

SS: drafting the manuscript. SS and DW: analysis and/or interpretation of data. SS, DW, and TR: acquisition of data. WW: design of study and revising the manuscript critically for important intellectual content. All authors contributed to the article and approved the submitted version.

FUNDING

This study was supported by the National Natural Science Foundation of China (No. 82101222) and the Natural Science Foundation of Shanghai (No. 20ZR1409600).

SUPPLEMENTARY MATERIAL

The Supplementary Material for this article can be found online at: https://www.frontiersin.org/articles/10.3389/fneur.2022.944001/full#supplementary-material

REFERENCES

1. Hwang J, Tsai S, Liu T, Chen Y, Lai J. Association of tinnitus and other cochlear disorders with a history of migraines. *JAMA Otolaryngol Head Neck Surg.* (2018) 144:712. doi: 10.1001/jamaoto.2018.0939
2. Moshtaghi O, Ghavami Y, Mahboubi H, Sahyouni R, Haidar Y, Ziai K, et al. Migraine-related aural fullness: a potential clinical entity. *Otolaryngol Head Neck Surg.* (2018) 158:100–2. doi: 10.1177/0194599817739255
3. Anttila P, Metsahonkala L, Mikkelsson M, Helenius H, Sillanpaa M. Comorbidity of other pains in schoolchildren with migraine or nonmigrainous headache. *J Pediatr.* (2001) 138:176–80. doi: 10.1067/mpd.2001.112159
4. Viirre ES, Baloh RW. Migraine as a cause of sudden hearing loss. *Headache.* (1996) 36:24–8. doi: 10.1046/j.1526-4610.1996.3601024.x
5. Evans RW, Ishiyama G. Migraine with transient unilateral hearing loss and tinnitus. *Headache.* (2009) 49:756–8. doi: 10.1111/j.1526-4610.2008.01075.x
6. Arslan Y, Arslan IB, Aydin H, Yagiz O, Tokucoglu F, Cukurova I. The etiological relationship between migraine and sudden hearing loss. *Otol Neurotol.* (2017) 38:1411–4. doi: 10.1097/MAO.0000000000001617
7. Lai J, Liu T. Proposal for a new diagnosis for cochlear migraine. *JAMA Otolaryngol Head Neck Surg.* (2018) 144:185. doi: 10.1001/jamaoto.2017.2427
8. Sun W, Guo P, Ren T, Wang W. Magnetic resonance imaging of intratympanic gadolinium helps differentiate vestibular migraine from Meniere disease. *Laryngoscope.* (2017) 127:2382–8. doi: 10.1002/lary.26518
9. Lempert T, Olesen J, Furman J, Waterston J, Seemungal B, Carey J, et al. Vestibular migraine: diagnostic criteria. *J Vestib Res.* (2012) 22:167–72. doi: 10.3233/VES-2012-0453
10. Dieterich M, Brandt T. Episodic vertigo related to migraine (90 cases): vestibular migraine? *J Neurol.* (1999) 246:883–92. doi: 10.1007/s004150050478
11. Neuhauser HK, Radtke A, von Brevern M, Feldmann M, Lezius F, Ziese T, et al. Migrainous vertigo: prevalence and impact on quality of life. *Neurology.* (2006) 67:1028–33. doi: 10.1212/01.wnl.0000237539.09942.06
12. Power L, Shute W, McOwan B, Murray K, Szmulewicz D. Clinical characteristics and treatment choice in vestibular migraine. *J Clin Neurosci.* (2018) 52:50–3. doi: 10.1016/j.jocn.2018.02.020
13. Wang A, Zhou G, Lipson S, Kawai K, Corcoran M, Brodsky JR. Multifactorial characteristics of pediatric dizziness and imbalance. *Laryngoscope.* (2021) 131:E1308–14. doi: 10.1002/lary.29024
14. Winterkorn JM, Kupersmith MJ, Wirtschafter JD, Forman S. Brief report: treatment of vasospastic amaurosis fugax with calcium-channel blockers. *N Engl J Med.* (1993) 329:396–8. doi: 10.1056/NEJM199308053290604
15. Beh SC, Masrour S, Smith SV, Friedman DI. The spectrum of vestibular migraine: clinical features, triggers, and examination findings. *Headache.* (2019) 59:727–40. doi: 10.1111/head.13484
16. Teggi R, Colombo B, Albera R, Asprella LG, Balzanelli C, Batuecas CA, et al. Clinical features, familial history, and migraine precursors in patients with definite vestibular migraine: the VM-phenotypes projects. *Headache.* (2018) 58:534–44. doi: 10.1111/head.13240
17. Neuhauser H, Leopold M, von Brevern M, Arnold G, Lempert T. The interrelations of migraine, vertigo, and migrainous vertigo. *Neurology.* (2001) 56:436–41. doi: 10.1212/WNL.56.4.436
18. Hsu LC, Wang SJ, Fuh JL. Prevalence and impact of migrainous vertigo in mid-life women: a community-based study. *Cephalalgia.* (2011) 31:77–83. doi: 10.1177/0333102410373152
19. Baloh RW. Genes and migraine. *Drugs Today (Barc).* (2004) 40:577–88. doi: 10.1358/dot.2004.40.7.850476
20. Kuritzky A, Ziegler DK, Hassanein R. Vertigo, motion sickness and migraine. *Headache.* (1981) 21:227–31. doi: 10.1111/j.1526-4610.1981.hed2105227.x
21. Harno H, Hirvonen T, Kaunisto MA, Aalto H, Levo H, Isotalo E, et al. Subclinical vestibulocerebellar dysfunction in migraine with and without aura. *Neurology.* (2003) 61:1748–52. doi: 10.1212/01.WNL.0000098882.82690.65
22. Battista RA. Audiometric findings of patients with migraine-associated dizziness. *Otol Neurotol.* (2004) 25:987–92. doi: 10.1097/00129492-200411000-00021
23. Dash AK, Panda N, Khandelwal G, Lal V, Mann SS. Migraine and audiovestibular dysfunction: is there a correlation? *Am J Otolaryngol.* (2008) 29:295–9. doi: 10.1016/j.amjoto.2007.09.004
24. Lipkin AF, Jenkins HA, Coker NJ. Migraine and sudden sensorineural hearing loss. *Arch Otolaryngol Head Neck Surg.* (1987) 113:325–6. doi: 10.1001/archotol.1987.01860030101018
25. Lee H, Whitman GT, Lim JG, Yi SD, Cho YW, Ying S, et al. Hearing symptoms in migrainous infarction. *Arch Neurol.* (2003) 60:113–6. doi: 10.1001/archneur.60.1.113
26. Radtke A, von Brevern M, Neuhauser H, Hottenrott T, Lempert T. Vestibular migraine: long-term follow-up of clinical symptoms and vestibulo-cochlear findings. *Neurology.* (2012) 79:1607–14. doi: 10.1212/WNL.0b013e31826e264f
27. Xue J, Ma X, Lin Y, Shan H, Yu L. Audiological findings in patients with vestibular migraine and migraine: history of migraine may be a cause of low-tone sudden sensorineural hearing loss. *Audiol Neurootol.* (2020) 25:209–14. doi: 10.1159/000506147
28. Blodow A, Heinze M, Bloching MB, von Brevern M, Radtke A, Lempert T. Caloric stimulation and video-head impulse testing in Meniere's

disease and vestibular migraine. *Acta Otolaryngol.* (2014) 134:1239–44. doi: 10.3109/00016489.2014.939300
29. Conte G, Lo RF, Calloni SF, Sina C, Barozzi S, Di Berardino F, et al. MR imaging of endolymphatic hydrops in Meniere's disease: not all that glitters is gold. *Acta Otorhinolaryngol Ital.* (2018) 38:369–76. doi: 10.14639/0392-100X-1986
30. Kirkim G, Mutlu B, Olgun Y, Tanriverdizade T, Keskinoglu P, Guneri EA, et al. Comparison of Audiological Findings in Patients with Vestibular Migraine and Migraine. *Turk Arch Otorhinolaryngol.* (2017) 55:158–61. doi: 10.5152/tao.2017.2609
31. Baloh RW. Neurotology of migraine. *Headache.* (1997) 37:615–21. doi: 10.1046/j.1526-4610.1997.3710615.x
32. Volcy M, Sheftell FD, Tepper SJ, Rapoport AM, Bigal ME. Tinnitus in migraine: an allodynic symptom secondary to abnormal cortical functioning? *Headache.* (2005) 45:1083–7. doi: 10.1111/j.1526-4610.2005.05193_2.x
33. Langguth B, Hund V, Landgrebe M, Schecklmann M. Tinnitus patients with comorbid headaches: the influence of headache type and laterality on tinnitus characteristics. *Front Neurol.* (2017) 8:440. doi: 10.3389/fneur.2017.00440
34. Kuttila SJ, Kuttila MH, Niemi PM, Le Bell YB, Alanen PJ, Suonpaa JT. Secondary otalgia in an adult population. *Arch Otolaryngol Head Neck Surg.* (2001) 127:401–5. doi: 10.1001/archotol.127.4.401
35. Neff BA, Staab JP, Eggers SD, Carlson ML, Schmitt WR, Van Abel KM, et al. Auditory and vestibular symptoms and chronic subjective dizziness in patients with Meniere's disease, vestibular migraine, and Meniere's disease with concomitant vestibular migraine. *Otol Neurotol.* (2012) 33:1235–44. doi: 10.1097/MAO.0b013e31825d644a
36. Risbud A, Muhonen EG, Tsutsumi K, Martin EC, Abouzari M, Djalilian HR. Migraine features in patients with isolated aural fullness and proposal for a new diagnosis. *Otol Neurotol.* (2021) 42:1580–4. doi: 10.1097/MAO.0000000000003324
37. Cha YH, Lee H, Santell LS, Baloh RW. Association of benign recurrent vertigo and migraine in 208 patients. *Cephalalgia.* (2009) 29:550–5. doi: 10.1111/j.1468-2982.2008.01770.x
38. Cha YH, Kane MJ, Baloh RW. Familial clustering of migraine, episodic vertigo, and Meniere's disease. *Otol Neurotol.* (2008) 29:93–6. doi: 10.1097/mao.0b013e31815c2abb

Conflict of Interest: The authors declare that the research was conducted in the absence of any commercial or financial relationships that could be construed as a potential conflict of interest.

Publisher's Note: All claims expressed in this article are solely those of the authors and do not necessarily represent those of their affiliated organizations, or those of the publisher, the editors and the reviewers. Any product that may be evaluated in this article, or claim that may be made by its manufacturer, is not guaranteed or endorsed by the publisher.

Copyright © 2022 Shi, Wang, Ren and Wang. This is an open-access article distributed under the terms of the Creative Commons Attribution License (CC BY). The use, distribution or reproduction in other forums is permitted, provided the original author(s) and the copyright owner(s) are credited and that the original publication in this journal is cited, in accordance with accepted academic practice. No use, distribution or reproduction is permitted which does not comply with these terms.

frontiers | Frontiers in Neuroscience

TYPE Review
PUBLISHED 26 July 2022
DOI 10.3389/fnins.2022.956200

Check for updates

OPEN ACCESS

EDITED BY
Su-Lin Zhang,
Huazhong University of Science and Technology, China

REVIEWED BY
Jose Antonio Lopez-Escamez,
Universidad de Granada, Spain
Sarath Vijayakumar,
Creighton University, United States
Angel Ramos De Miguel,
University of Las Palmas de Gran Canaria, Spain

*CORRESPONDENCE
Shuxia Qian
shuxia_630@163.com

SPECIALTY SECTION
This article was submitted to Perception Science, a section of the journal Frontiers in Neuroscience

RECEIVED 30 May 2022
ACCEPTED 27 June 2022
PUBLISHED 26 July 2022

CITATION
Huang S and Qian S (2022) Advances in otolith-related protein research. *Front. Neurosci.* 16:956200. doi: 10.3389/fnins.2022.956200

COPYRIGHT
© 2022 Huang and Qian. This is an open-access article distributed under the terms of the Creative Commons Attribution License (CC BY). The use, distribution or reproduction in other forums is permitted, provided the original author(s) and the copyright owner(s) are credited and that the original publication in this journal is cited, in accordance with accepted academic practice. No use, distribution or reproduction is permitted which does not comply with these terms.

Advances in otolith-related protein research

Shouju Huang[1,2] and Shuxia Qian[2]*

[1]The Fourth School of Clinical Medicine, Zhejiang Chinese Medical University, Hangzhou, China, [2]Department of Neurology, The Second Affiliated Hospital of Jiaxing University, Jiaxing, China

Otoliths are biological crystals formed by a layer of calcium carbonate crystal that adhere to the ciliary surface of the utricular and saccular receptors in the vestibule of all vertebrates inner ear, enabling the utricle and saccule to better perceive the changes in linear and gravitational acceleration. However, the molecular etiology of otolith related diseases is still unclear. In this review, we have summarized the recent findings and provided an overview of the proteins that play important roles in otolith formation and maintenance (Otoconin-90, Otolin-1, Otolith Matrix Protein-1, Cochlin, Otogelin, α-Tectorin, β-Tectorin, Otopetrin-1, and Otopetrin-2, PMCA2, etc.), providing new insight for the prevention and management of benign paroxysmal positional vertigo (BPPV) with basis for otolith-related proteins as potential biomarkers of vestibular disease.

KEYWORDS

otolith, development, formation and maintenance, otolith-related protein, benign paroxysmal positional vertigo

Preface

The inner ear consists of the cochlea and vestibular organs, where the cochlea is responsible for hearing while the vestibular organs perceive the movement of the head, essential for spatial orientation and body balance (Yang et al., 2018). The vestibular organ on each side contains three semicircular canals and two otolith organs (utricle and saccule). The otolithic receptors are distributed on the maculae of the utricle and saccule (Curthoys et al., 2017; **Figure 1**). Henceforth, the correct formation, fixation and maintenance of the vestibular otolith are necessary to maintain optimal vestibular function and preserve the sense of balance (Boyle and Varelas, 2021). Research has shown that protein fragments must express collagen OC90 (Otoconin-90) and Otolin to induce the structural formation of the otolith crystal (Kao et al., 2017). Therefore, in order to understand the role of otolith in the course of vestibular disease, it is essential to scrutinize the protein and molecular mechanisms underlying the formation and maintenance of otolith (Kao et al., 2017). In this article, combined with the latest findings of zebrafish model, we have reviewed the important otolith related proteins in the formation and maintenance of otolith and their possible contribution in the pathogenesis of vestibular diseases.

Otolith formation

Unlike bones and teeth which are mainly formed from carbonate hydroxyapatite, otoliths are mainly composed of calcium carbonate crystals (Ross et al., 1976). Otoliths are formed in the late stages of embryonic development and mature shortly after birth, and then remain basically stable (Moreland et al., 2014). Normal otolith formation requires: (1) Correct induction and formation of utricle and saccule; (2) Standardization and differentiation of sensory maculae, sensory cells and Supporting cells; (3) Establishment of correct ionic environment to allow the normal output and processing of matrix proteins and ions; (4) Production and export of otolith matrix protein and membrane; (5) Assembly of the protein core by free floating matrix protein; and (6) Local increase in calcium ion and carbonate concentrations to initiate the formation of crystals on otoliths. The above elements must appear in a specific order and in the correct form at a specific point in time (Hughes et al., 2006). During the growth of otoliths, the adhesion between biomineralized otoliths and cysts and maculae must be maintained and this is achieved through the otolith membrane (Stooke-Vaughan et al., 2015). The key regulator of otolith morphogenesis is considered to be matrix protein. The inhibition of otolith growth may be due to the reduction of calcium carbonate deposition or the lack of matrix protein, or both (Mulry and Parham, 2020). So far, the molecular process of otolith formation and maintenance is still unclear. Eight proteins specific to inner ear are known: Otolin-1, Otoconin 90/95, Prestin, Otoacorin, Otoglin, α-tectorin, β-Tectorin, and Cochlin (Mulry and Parham, 2020; **Table 1**). There are three main groups of proteins involved in otolith biomineralization: (1) Otolith matrix protein, such as OC90, Otolin-1, OMP-1, Cochlin, etc.; (2) Otolith anchoring protein, the otolith membrane is composed of Otolin and five non-collagenous glycoproteins (Otoglin, Otoglin-like, Otancorin, α-Tectorin, and β-tectorin) and KSPG, which may be primarily associated with otolith anchoring (Tian et al., 2020); (3) Otolith regulatory protein, such as Plasma membrane calcium ATPase isomer 2 (PMCA2), Carbonic anhydrase (CA), Otoptin1 and Otoptin-2, NOx (nitrous oxides), etc. (Tian et al., 2020).

Important factors affecting the formation and maintenance of otoliths

Otolith development and the proteins involved in otolith development

Otoconin-90

Otolithic proteins play the role of building matrix in the process of biomineralization and directly control crystal size and polymorph selection (Weigele et al., 2016). During the development of otolith, the organic matrix is formed before the deposition of calcium carbonate. Gene targeting technology has proved that collagen OC90 (otoconin-90) is necessary for the formation of otolith (Zhao et al., 2007). OC90 is the main matrix protein of mammalian calcified otolith: It retains the ability of calcium binding and is extremely acidic, so that calcium or $CaCO_3$ can bind. In the absence of OC90, the matrix-bound calcium on the surface of the vestibular maculae is greatly reduced. In both *in vivo* and *in vitro* studies, OC90 has shown to promote the nucleation and growth of $CaCO_3$ crystals (Lundberg et al., 2015). Some studies have reported that OC90 deficiency leads to the formation of giant otoliths and that OC90 knockout mouse have reduced balance despite normal hearing (Zhao et al., 2008). Bi et al. (2021) showed that Otoconin-90 levels were significantly higher in subjects with BPPV, that serum otoconin-90 levels were an independent risk factor for benign paroxysmal positional vertigo, and that Otoconin-90 may be a potential biomarker for the development of BPPV.

Otolin-1

Otolin-1, a scaffold protein for otoliths, is found in the extracellular matrix of the inner ear and contains a C1q-like structural domain that forms a stable trimer in the presence of calcium ions and is responsible for Ca^{2+} trimerization and binding (Hołubowicz et al., 2017, 2021). OC90 can bind to Otolin-1 and build a protein-rich matrix that serves as a scaffold for subsequent calcium carbonate deposition (Thiessen et al., 2019). Studies have shown that it is particularly involved in the correct positioning of otoliths in fish, so the correct fixation of otoliths on sensory vesicular maculae is necessary. Otolin-1 was not detected in the utricle, so we speculate that it may be a saccule-specific protein linker between the otolith and the otolith membrane (Weigele et al., 2015). Furthermore, Otolin-1 and OC90 can synergistically regulate calcite crystal morphology *in vitro* and contribute to the formation of otolith-like morphology (Moreland et al., 2014). It has been shown that serum Otolin levels reflect otolith status, that Otolin-1 levels are significantly higher in subjects with BPPV, and that Otolin-1 may be a potential biomarker for the pathogenesis of BPPV (Wu et al., 2020). It was also found that both parathyroid hormone and total calcium levels affect the otolin-1 levels of patients with primary hyperfunction of parathyroid, suggesting that calcium dysregulation caused by primary hyperparathyroidism may contribute to otolith catabolism by affecting Otolin-1 levels, and may be associated with inner ear diseases such as BPPV (Mckenna et al., 2020). Assessment of Otolin-1 levels during or shortly after acute BPPV episodes should be considered in future studies (Wu et al., 2020).

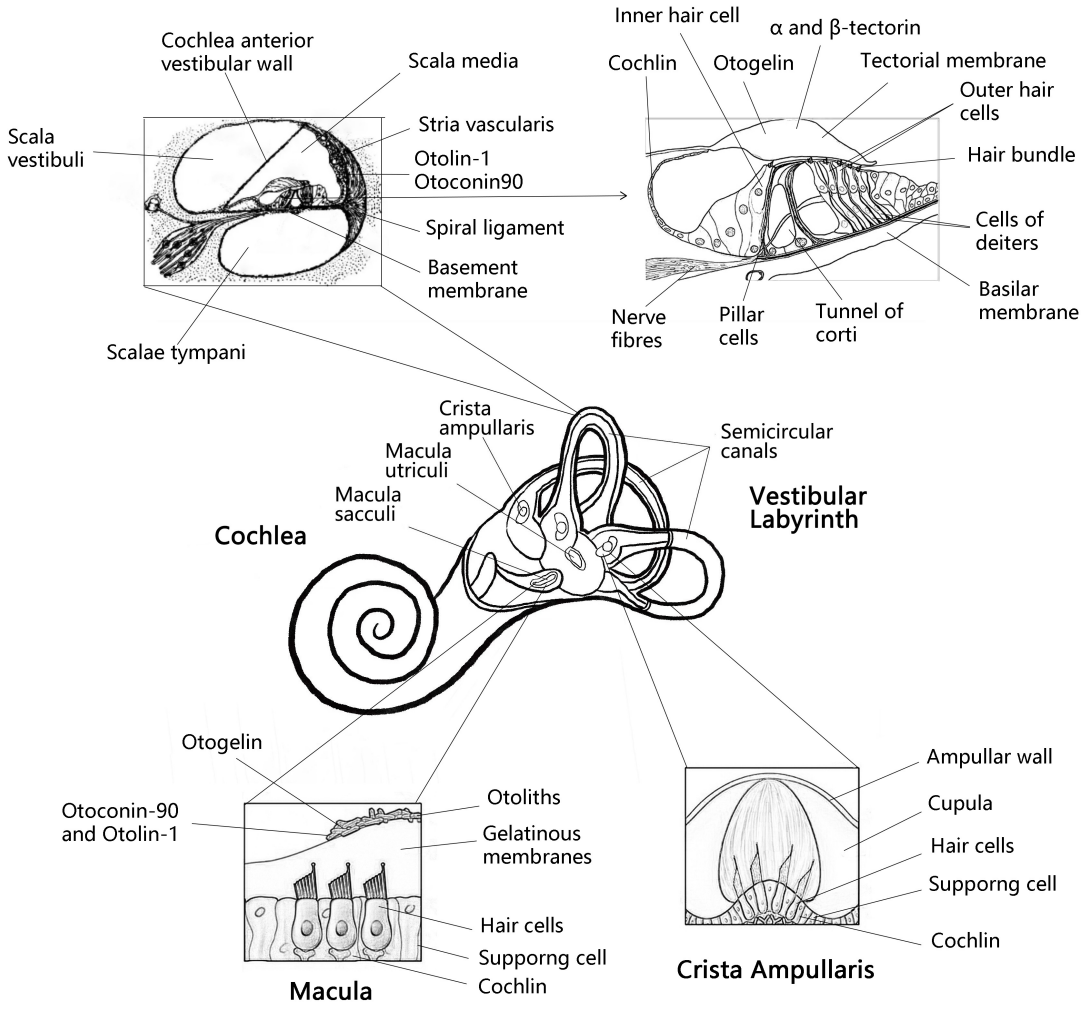

FIGURE 1
Anatomy the vestibular labyrinth and organ of Corti with labeled structures and locations of inner otolith-related proteins. Anatomy of the vestibular labyrinth with labeled structures and locations of inner ear-exclusive proteins. Adapted from Encyclopaedia Britannica, Inc. 1997, by Jack Dumala.

Otolith matrix protein-1

The cDNA homolog of OMP-1, zomp-1, was found to be necessary for normal otolith growth in the saccule of the adult inner ear by a zebrafish model. OMP-1 is synthesized by most epithelial cells outside the sensory patches (Murayama et al., 2005). In the saccule of *Oreochromis mossambicus*, OMP-1 expression is restricted to the dorsal and ventral reticular areas of the macula sacculi, with the sensory portion lacking expression; In the utricule, OMP-1 was present in the median centripetal meshwork area and lateral centrifugal meshwork area (Weigele et al., 2015). OMP-1 is also the major calcium-binding protein in fish otoliths, and the expression pattern of OMP-1 is directly correlated with the shape of the otolith, and alterations in this expression pattern may lead to impaired locomotion. As fish typically exhibit locomotor behavior after transfer from Earth gravity to microgravity, they can be used as a model system for higher vertebrates (Weigele et al., 2015).

Cochlin

Cochlin is expressed in the cochlea and vestibule; normal cochlin expression is evenly distributed in the utricle and the matrix of the ampulla ridge (inner ear protein). Cochlin is involved in clearing bacterial infections in the inner ear, regulating immunity by physically capturing pathogens in the drum stage and recruiting innate immune cells to protect the normal inner ear structure from inflammatory damage (Rhyu et al., 2020). Overexpression of cochlin in the early stage of Meniere's disease may be one of the causes of intractable Meniere's disease (Calzada et al., 2012). Verdoodt et al. (2021) found that the loss of Cochlin had a protective effect on hearing threshold after noise exposure in a Cochlin knockout mouse model, but the mutation of cochlin gene encoding cochlin protein can lead to DFNA9, an autosomal dominant non-syndromic sensorineural deafness with vestibular involvement. Cochlin, which is defective in

TABLE 1 Overview of otolith-related proteins.

Otolith-related proteins or molecules	Location	Role in otolith development and maintenance	Clinical significance
Otoconin-90	Located in the supporting cells of the organ of Corti and the vestibular macula (Lundberg et al., 2015)	The main matrix protein of otoliths, promotes otolith nucleation and growth (Lundberg et al., 2015)	Elevated serum OC90 levels in patients with benign paroxysmal positional vertigo (Bi et al., 2021); Reduced balance in knockout mice (Zhao et al., 2008)
Otolin-1	Located in the supporting cells of the organ of Corti and the vestibular macula (Hołubowicz et al., 2021)	Otolith scaffolding protein, is involved in the formation and correct positioning of the otolith and its correct anchoring to the sensory macula (Weigele et al., 2015)	Elevated serum Ootolin-1 levels in patients with benign paroxysmal positional vertigo (Wu et al., 2020)
Otolith Matrix Protein-1 (OMP-1)	Expressed in the cochlea and vestibular organs (mainly the utricle and saccule) (Weigele et al., 2015)	Maintains normal otolith growth and is directly related to otolith shape (Murayama et al., 2005)	Associated with movement disorders (Weigele et al., 2015)
Cochlin	Expressed in the cochlea and vestibule (mainly in spiral ligament, spiral bone and spiral rim of the inner ear) (Rhyu et al., 2020)	Main otolith constituent, determinant of calcium carbonate crystalline formation (Leventea et al., 2021)	Its overexpression is associated with Ménière's disease (Calzada et al., 2012); associated with conductive hearing loss and vestibular dysfunction (Leventea et al., 2021; Verdoodt et al., 2021); diagnosis of exolymphatic fistula (Xiong et al., 2020); diagnosis of exolymphatic fistula
Otogelin	Expression in the cochlea and vestibule (Avan et al., 2019)	Anchoring of the otolith (Schraders et al., 2012; Whitfield, 2020); stabilization of the cochlear covering membrane (Avan et al., 2019)	Deficiency leading to otolith detachment and instability of the cochlear covering membrane; OTOG mutation leading to DFNB18B hereditary deafness (Avan et al., 2019)
α-tectorin and β-tectorin	Non-collagenous glycoprotein component of the Cochlear Covering Membrane (TM) (Andrade et al., 2016)	Adherence of TM to the spiral rim and to the stereocilia of the outer hair cells of the cochlea (Andrade et al., 2016) Determinants of otolith formation (Asgharzade et al., 2011)	Deficiency can lead to varying degrees of hearing loss (Asgharzade et al., 2017) β-tectorin deficiency can lead to imbalance (Zou et al., 2006)
Otopetrin1 and Otopetrin-2	Expression in the cochlea and vestibule (Kim et al., 2010; Tu et al., 2018; Khan et al., 2019; Lopez et al., 2019)	Maintains nucleus formation, and growth of otoliths (Kim et al., 2010); a proton-selective channel involved in gravity sensing in the vestibular system	Lack of otopetrin-1 knockout in mice leads to vestibular dysfunction (Khan et al., 2019).
PMCA2	High level of expression in vestibular and outer hair cells (Han et al., 2019)	Maintains otolith formation, and growth (Xu et al., 2021); is a calmodulin-sensitive plasma membrane calcium ATPase.	PMCA2w/a missense mutation causes deafness and balance disorders in humans (Bortolozzi and Mammano, 2018)
Nox (NADPH oxidases)	Expression in the cochlea and vestibule (Kiss et al., 2006; Xu et al., 2021)	The main otolith components and factors necessary for calcium carbonate crystallization (Xu et al., 2021)	The absence of NOX3 enhances hearing recovery after noise trauma (Rousset et al., 2022)
CA (carbonic anhydrase)	Expression in the cochlea and vestibule (Tohse and Mugiya, 2001; Matsumoto et al., 2017; Liu et al., 2022)	Maintaining the right pH to promote otolith development and regulate otolith growth (Tohse et al., 2006; Matsumoto et al., 2017)	CA inhibitors can cause hearing loss, and inhibit calcification of otoliths (Tohse and Mugiya, 2001; Liu et al., 2022)

human hearing and vestibular disorders, and DFNA9, is secreted by small specialized areas of vestibular system epithelia whereby cells secrete Cochlin to the ear lumen and base of the basal lamina. Cochlin secreted from the base diffuses along the basal surface of vestibular epithelium, and is apically secreted and integrated into otolith. Cochlin apical secretion defects can lead to abnormal otolith crystallization and behavioral defects. Cochlin is the main otolith component and the determinant of the crystalline form of calcium carbonate (Leventea et al., 2021). Xiong et al. (2020) detected cochin- tomoprotein (CTP) in the middle ear, the shortest isoform of cochlin, which is an endolymph-specific protein that is not expressed in blood, cerebrospinal fluid and saliva, but is highly expressed in inner ear lymph fluid and can be used as a diagnostic biochemical marker for endolymphatic fistula.

Otolith anchoring proteins and otolith functional development

Otogelin

Otogelin is a non-collagenous component of the cell-free gel structure covering the sensory epithelium of the inner ear, including the covering membrane (TM) in the cochlea, the membranes of the utricule and saccule, and the cell-free material at the apical part of the semicircular canal jugular in the vestibular organ (Avan et al., 2019). The sensory epithelium

of the cochlea (organ of Corti) is covered by a cell-free structure, the TM, which contains two types of sensory cells: inner hair cells and outer hair cells. The outer hair cells are the mechanical actuators of the cochlea and their function consists of anchoring their tallest stereocilia to the covering membrane. The long, immobile motile cilia on the hair cells tether the otolith, and a small number of motile cilia at the poles of the utricle contribute to the accuracy of otolith tethering, but neither the presence nor the movement of the cilia is necessary for this process. Instead, otolith tethering is dependent on the presence of hair cells and the function of Otogelin (Whitfield, 2020). It has been shown that Otogelin also plays an important role in otolith seeding in zebrafish, revealing that Otogelin may play an important anchoring role in otolith formation (Stooke-Vaughan et al., 2015). Otogelin and Otogelin-like are TM proteins associated with secreted epithelial mucins, and defects in either result in DFNB18B and DFNB84B hereditary deafness, both of which are respectively characterized by congenital mild to moderate hearing impairment (Avan et al., 2019). In addition, mutations in the OTOG gene encoding Otogelin cause moderate hearing impairment, which may be associated with vestibular dysfunction in humans (Schraders et al., 2012).

α-tectorin and β-tectorin

Both α-tectorin and β-tectorin are non-collagenous glycoprotein components of the cochlear covering membrane (TM). α-tectorin and β-tectorin form a dense matrix within the TM and are used to cross-link type II collagen fibers to adhere the TM to the helical rim (Andrade et al., 2016). In addition, the maintenance of otolith adhesion to sensory maculae was found to be dependent on α-tectorin in zebrafish, and this adhesion process is essential for otolith growth (Stooke-Vaughan et al., 2015). In humans, mutations in the TECTA gene, which encodes alpha-tectorin, cause moderate to severe hearing loss (Asgharzade et al., 2017). Studies have shown that β-tectorin knockouts in zebrafish show balance defect due to disrupted otolith formation and result in severe defects in otolith formation and function in the inner ear, thus suggesting that β-tectorin can affect otolith formation (Asgharzade et al., 2011). However, the underlying molecular mechanisms need to be further investigated. Furthermore, β-tectorin is not only essential for the development of the inner ear, but also normal auditory function. Mutations in its gene can also lead to hearing loss (Zou et al., 2006).

Other factors that regulate and maintain otolith development

Otopetrin-1 and otopetrin-2

Tu et al. (2018) identified Otopetrin1 (Otop1), a proton-selective channel involved in gravity sensing in the vestibular system, as a protein essential for otolith development. It has been shown that Otop1 knockout mice lack functional otoliths and that this leads to vestibular dysfunction (Khan et al., 2019). Past reports have shown that Otop1 is expressed in the extra-striatal region of the mouse saccule and utricle and that Otop1 is enriched in calcium to maintain otolith nucleation, growth, and maintenance (Kim et al., 2010). The otolith is rich in calcium for nuclear formation, growth, and maintenance. During otolith mineralization, Otop1 acts as a receptor for extracellular calcium concentrations near the vestibular support cells, responding to ATP in the endolymph to increase intracellular calcium levels. Its mutation leads to phenotypic imbalance and selective involvement in otolith damage, and Otop1 is likely to function similarly in the human saccule (Lopez et al., 2019). In mouse and human vestibular hair cells, Otop1, Otop2, and Otop3 may function as proton channels (Tu et al., 2018). The differential expression of Otop2 in human saccular-supporting cells suggests an important role in the dynamic balance of vestibular sensory periphery and otolith maintenance, although further studies are needed (Lopez et al., 2019). However, further research is needed. In conclusion, Otop1 is an essential protein for otolith development and maintenance, and Otop2 may play the same role as Otop1 in otolith maintenance (Lopez et al., 2019). Otop2 may play the same role as Otopetrin1 in otolith maintenance.

Plasma membrane calcium ATPase isomer 2

Plasma membrane calcium ATPase (PMCA) is a calmodulin-sensitive plasma membrane calcium ATPase. The lack of otolith formation is more likely due to inhibition of Ca^{2+} transport and $CaCO_3$ deposition. The PMCA isoform ATP2b1a is an active calcium transporter protein that is essential for normal development and function of the inner ear in zebrafish larvae, and knockout of ATP2b1a in embryos results in larvae exhibiting homeostasis defects, reduced otolith proliferation, ectopic otolith localization and occasional fusion (Han et al., 2019). The PMCA2 pump is expressed at high levels in vestibular and outer hair cells in the static cilia and parietal membrane. It pumps Ca^{2+} out of the cell at a relatively high and constant rate. Inner ear hair cells detect acoustic stimuli, inertia, or gravity through the deflection of their apical stereocilia. The current consensus is that the deflection of the stereocilia bundle toward the higher stereocilia increases the tension in the terminal link and that this mechanical stimulus is transmitted to the cation-selective mechano-transduction (MET) channel located at the top of the stereocilia and opened to allow cation influx into the cell, where Ca^{2+} entering through the MET channel is sequestered by the buffer in the stereocilia and then passed PMCA2w/a pump to and from the endolymph. the PMCA2w/a variant is thought to increase calcium ions near the hair bundle and may be related to the complexity of decidual structures on hair cells in the vestibular system, where the pump also contributes to otolith formation and maintenance (Bortolozzi and Mammano, 2018). PMCA2w/a

missense mutations cause deafness and homeostasis disorders in humans (Bortolozzi and Mammano, 2018).

NOx (Nicotinamide adenine dinucleotide phosphate oxidases)

Nicotinamide adenine dinucleotide phosphate (NADPH) oxidases (NOx) represent an important family of enzymes that produce reactive oxygen species (ROS) in a regulated manner for host oxidative defense and redox-based signaling (Schiffers et al., 2021). The activity of NOx is regulated by partners such as p22phox, NOx organizers (Noxo1, p47phox, and p40phox), and NOx activators (Noxa1 and p67phox). Noxo1 mRNA is widely expressed in the embryonic inner ear. It has been demonstrated that ROS production by Noxo1-dependent vestibular oxidases is essential for otolith formation, and the absence of the calcium carbonate component in otoliths of Noxo1 mutants suggests that the process of otolithogenesis is impaired (Kiss et al., 2006). Both the inner ear vestibule and cochlea have high levels of NOX3 mRNA expression, and OC90 and NADPH oxidase Nox3, an essential regulatory protein for otolith formation, are functionally interconnected and enhance each other's functions, which are essential for otolith formation and maintenance (Xu et al., 2021). It is unclear how NOx and its associated proteins mediate otolith formation. The major proteins of otoliths (e.g., OC90) may bind to phospholipids in the vesicle membrane of globules (Ca^{2+}-rich vesicles) in an HCO_3^- rich environment and undergo conformational changes triggered by ROS generated by NOx3 located in the vesicle plasma membrane. This promotes the nucleation of calcite crystals from calcium supplied by the vesicles and bicarbonate ions from endolymph. In conclusion, Nox is a major otolith component and essential for calcium carbonate crystal formation. However, NOX-derived ROS are also implicated in the pathophysiology of sensorineural hearing loss. The absence of functional NOX3 enhances the recovery phase of hearing after noise trauma. This opens an interesting clinical window for pharmacological or molecular interventions aimed at preventing noise-induced hearing loss (Rousset et al., 2022).

Carbonic anhydrase

Carbonic anhydrase (CA), which catalyzes the hydration of CO_2 to produce bicarbonate and protons, has been proposed to regulate potassium homeostasis and cochlear potential in the mammalian cochlea. There are 16 known mammalian CA isozymes (Wu et al., 2013). These CA isoforms play a central role in the transport of calcium, protons, and bicarbonate ions, and thus regulates optimal pH regulation and fluid balance in the inner ear (Tohse et al., 2006). Carbonic anhydrase (CA) may also regulate otolith development and maintenance by providing $HCO3^-$ and maintaining proper pH. CA is expressed in inner ear hair cells and catalyzes the formation of endolymph from carbonate ions for otolith calcification. Studies have reported that treatment of zebrafish embryos with the carbonic anhydrase inhibitor sulforaphane inhibits otolith formation (Matsumoto et al., 2017). The CA inhibitor ethoxyzolamide inhibits the accumulation of bicarbonate in the endolymph and otolith, inhibits otolith calcification, and induces apoptosis of inner ear hair cells. Apoptosis of hair cells can lead to varying degrees of hearing loss (Tohse and Mugiya, 2001; Liu et al., 2022).

Discussion

This review summarizes the inner ear proteins associated with the development and maintenance of otolith and describes the progress in the study of otolith-related proteins and their association with vestibular-related diseases. Little is known about the molecular processes involved in otolith maintenance and human vestibular pathology. Slow and progressive otolith degeneration is part of the normal aging process and can lead to severe balance disorders resulting in falls in the elderly (Agrawal et al., 2012). Otolith degeneration can be caused by ototoxic drugs, infection, trauma and aging. To date, several otolith-related proteins have been investigated and these otolith-related proteins have been studied at the cellular and subcellular levels to show that otoliths begin to degenerate in the fifth decade (Ross et al., 1976). Therefore, determining the protein composition of otoliths in the human saccule and utricle and studying their changes with age and disease can help to clarify the etiology of vestibular pathologies (Lopez et al., 2019). In this review, aggregated data present a clearer picture of otolith-associated proteins in vestibular disorders.

Otolithic proteins associated with benign paroxysmal positional vertigo

Benign paroxysmal positional vertigo is one of the most common otoconia-related balance disorders, and there are no laboratory indicators available to determine the diagnosis of BPPV (Wu et al., 2020). In contrast, recent studies have found that Otoconin-90 can be quantitatively detected in peripheral blood and suggest that Otoconin-90 can be used as a biomarker for BPPV and has clinical significance for the diagnosis of certain patients with BPPV, such as elderly or posttraumatic patients who have difficulty performing diagnostic postural maneuvers, or patients who had nystagmu or satypical symptoms (Bi et al., 2021). In addition, serum otolin-1 is quantifiable in BPPV patients, with elevated levels of Otolin-1 in BPPV patients, who are sensitive to BPPV (Yadav et al., 2021), high serum otolin-1 levels associated with increased risk of BPPV recurrence (Fan et al., 2022). A case-control study found that serum levels of otolin-1 were significantly higher in patients with BPPV than in patients with non-BPPV (IIrugu et al., 2021). Furthermore, high levels of serum Otolin-1 (>299.45 pg/ml)

can be used as a biomarker to differentiate patients with BPPV from healthy controls, suggesting that serum Otolin-1 could be used as a biomarker for BPPV episodes and could be used clinically to promote better management of BPPV (Wu et al., 2020). From a clinical perspective, biomarkers of otolith degeneration can help as a potential diagnostic modality, therapeutic target, and predictive, and therapeutic response monitoring (Yadav et al., 2021).

Otolithic proteins associated with Meniere's disease and hearing loss

Human missense mutations in Cochlin are related to autosomal dominant hearing loss (DFNA9) (Robertson et al., 1998; Py et al., 2013). Consistent with Cochlin determining $CaCO_3$ crystallization, Cochlin mutations in both human and mouse cause vestibular malfunction (Khetarpal et al., 1991; Jones et al., 2011), while some human mutations also result in vertigo (Khetarpal et al., 1991). Notably, most of the mutations in Cochlin are dominant missense mutations in the N-terminal factor C homolog and result in a form of Cochlin with deposition in the vestibular and cochlear labyrinths (Robertson et al., 1998). There are data suggesting that Cochlin is overexpressed in the vestibular endorgans of subjects with persistent Ménière's disease (Calzada et al., 2012) and in autoimmune inner ear disease (Pathak et al., 2013), which may contribute to the dysregulation of the environmental balance within the inner ear in Ménière's disease (Calzada et al., 2012). While α-tectorin is involved in the pathophysiology of Ménière's disease, the shift code deletion of the TECTA gene may be involved in TM formation through altered GPI-anchored signaling leading to an altered clinical phenotype (Roman-Naranjo et al., 2022). Mutations in the human TECTA gene encoding alpha-tectorin cause hearing loss (Asgharzade et al., 2017). Missense mutations in PMCA2w/a cause deafness and balance disorders in humans (Bortolozzi and Mammano, 2018). Mutations in the OTOG gene encoding Otogelin in humans result in moderate hearing impairment (Schraders et al., 2012). Interestingly, one study found that 15 of 46 Ménière's disease families (33%) showed at least one rare missense variant in the OTOG gene, a finding that supports OTOG as an associated gene in familial Ménière's disease and lays the foundation for genetic testing for Ménière's disease (Roman-Naranjo et al., 2020). These findings provide new ideas for genetic testing in patients with comorbid hearing loss in vestibular disease, allowing for the detection of the Cochlin, OTOG, PMCA2, and TECTA genes. If these disorders are detected in a timely manner, early intervention in balance disorders or reduction in the degree of hearing loss can be achieved.

Understanding the function of otolith-associated proteins may provide new ideas for the prevention and diagnosis of vestibular disease and provide a basis for otolith-associated proteins as potential biomarkers of vestibular disease and for conducting corresponding genetic testing. Nevertheless, further research is needed to determine the role of many of the newly identified proteins (Parham and Dyhrfjeld-Johnsen, 2016). Nevertheless, there are indeed certain limitations to our studies, one of the fixed limitations of search-based studies being that the search terms limit them. In this particular area, not all researchers mentioned the term "otolith-related protein" in the keywords, study titles, or conclusions of their publications.

In the future, it is hoped that more otolith-related proteins will be studied and newer diagnostic or therapeutic ideas will be brought to clinic. It is important to be able to determine the use and utility of each otolithic protein in specific vestibular disorders, as well as to combine functional biomarkers and include evoked potentials of hearing and balance-related tests such as vestibular evoked myogenic potentials (VEMPs), posturography, and rotational chair responses which may provide new insights into the diagnosis, treatment or prognosis of vestibular diseases including Meniere's disease and BPPV. Revisiting the otolith-associated proteins, focusing on the most clinically applicable studies to fill in the knowledge gaps, and linking them to vestibular disorders related diseases, and exploring possible biomarkers and genetic tests, may be the future direction of this research.

Author contributions

SH: data curation and writing – original draft, review and editing. SQ: supervision and funding acquisition. Both authors contributed to the article and approved the submitted version.

Funding

This study was supported by Zhejiang Basic Public Welfare Research Program (LGF20H090020).

Conflict of interest

The authors declare that the research was conducted in the absence of any commercial or financial relationships that could be construed as a potential conflict of interest.

Publisher's note

All claims expressed in this article are solely those of the authors and do not necessarily represent those of their affiliated organizations, or those of the publisher, the editors and the reviewers. Any product that may be evaluated in this article, or claim that may be made by its manufacturer, is not guaranteed or endorsed by the publisher.

References

Agrawal, Y., Zuniga, M. G., Davalos-Bichara, M., Schubert, M. C., Walston, J. D., Hughes, J., et al. (2012). Decline in semicircular canal and otolith function with age. *Otol. Neurotol.* 33, 832–839.

Andrade, L. R., Salles, F. T., Grati, M., Manor, U., and Kachar, B. (2016). Tectorins crosslink type II collagen fibrils and connect the tectorial membrane to the spiral limbus. *J. Struct. Biol.* 194, 139–146. doi: 10.1016/j.jsb.2016.01.006

Asgharzade, S., Tabatabaiefar, M. A., Modarressi, M. H., Ghahremani, M. H., Reiisi, S., Tahmasebi, P., et al. (2017). A novel TECTA mutation causes ARNSHL. *Int. J. Pediatr. Otorhinolaryngol.* 92, 88–93.

Asgharzade, S., Tabatabaiefar, M. A., Modarressi, M. H., Ghahremani, M. H., Reiisi, S., Tahmasebi, P., et al. (2011). Zona pellucida domain-containing protein β-tectorin is crucial for zebrafish proper inner ear development. *PLoS One* 6:e23078. doi: 10.1371/journal.pone.0023078

Avan, P., Le Gal, S., Michel, V., Dupont, T., Hardelin, J. P., and Petit, C. (2019). Otogelin, otogelin-like, and stereocilin form links connecting outer hair cell stereocilia to each other and the tectorial membrane. *Proc. Natl. Acad. Sci. U.S.A.* 116, 25948–25957. doi: 10.1073/pnas.1902781116

Bi, J., Liu, B., Zhang, Y., and Zhou, Q. (2021). Study on the bone metabolism indices and otoconin-90 in benign paroxysmal positional vertigo. *Otol. Neurotol.* 42, e744–e749. doi: 10.1097/MAO.0000000000003087

Bortolozzi, M., and Mammano, F. (2018). PMCA2 pump mutations and hereditary deafness. *Neurosci. Lett.* 663, 18–24.

Boyle, R., and Varelas, J. (2021). Otoconia structure after short- and long-duration exposure to altered gravity. *J. Assoc. Res. Otolaryngol.* 22, 509–525. doi: 10.1007/s10162-021-00791-6

Calzada, A. P., Lopez, I. A., Beltran Parrazal, L., Ishiyama, A., and Ishiyama, G. (2012). Cochlin expression in vestibular endorgans obtained from patients with Meniere's disease. *Cell Tissue Res.* 350, 373–384. doi: 10.1007/s00441-012-1481-x

Curthoys, I. S., MacDougall, H. G., Vidal, P. P., and de Waele, C. (2017). Sustained and transient vestibular systems: a physiological basis for interpreting vestibular function. *Front. Neurol.* 8:117. doi: 10.3389/fneur.2017.00117

Fan, Z., Hu, Z., Han, W., Lu, X., Liu, X., and Zhou, M. (2022). High serum levels of Otolin-1 in patients with benign paroxysmal positional vertigo predict recurrence. *Front. Neurol.* 13:841677. doi: 10.3389/fneur.2022.841677

Han, J., Liu, K., Wang, R., Zhang, Y., and Zhou, B. (2019). Exposure to cadmium causes inhibition of otolith development and behavioral impairment in zebrafish larvae. *Aquat. Toxicol.* 214:105236. doi: 10.1016/j.aquatox.2019.105236

Hołubowicz, R., Ożyhar, A., and Dobryszycki, P. (2021). Natural mutations affect structure and function of gC1q domain of otolin-1. *Int. J. Mol. Sci.* 22:9085. doi: 10.3390/ijms22169085

Hołubowicz, R., Wojtas, M., Taube, M., Kozak, M., Ożyhar, A., and Dobryszycki, P. (2017). Effect of calcium ions on structure and stability of the C1q-like domain of otolin-1 from human and zebrafish. *FEBS J.* 284, 4278–4297. doi: 10.1111/febs.14308

Hughes, I., Thalmann, I., Thalmann, R., and Ornitz, D. M. (2006). Mixing model systems: using zebrafish and mouse inner ear mutants and other organ systems to unravel the mystery of otoconial development. *Brain Res.* 1091, 58–74. doi: 10.1016/j.brainres.2006.01.074

IIrugu, D. V. K., Singh, A., Yadav, H., Verma, H., Kumar, R., Abraham, R. A., et al. (2021). Serum otolin-1 as a biomarker for benign paroxysmal positional vertigo: a case-control study. *J. Laryngol. Otol.* 135, 589–592.

Jones, S. M., Robertson, N. G., Given, S., Giersch, A. B., Liberman, M. C., and Morton, C. C. (2011). Hearing and vestibular deficits in the Coch(-/-) null mouse model: comparison to the Coch(G88E/G88E) mouse and to DFNA9 hearing and balance disorder. *Hear. Res.* 272, 42–48. doi: 10.1016/j.heares.2010.11.002

Kao, W., Parnes, L., and Chole, R. (2017). Otoconia and otolithic membrane fragments within the posterior semicircular canal in benign paroxysmal positional vertigo. *Laryngoscope* 127, 709–714.

Khan, S., Della Santina, C., and Migliaccio, A. (2019). Angular vestibuloocular reflex responses in Otop1 mice. I. Otolith sensor input is essential for gravity context-specific adaptation. *J. Neurophysiol.* 121, 2291–2299. doi: 10.1152/jn.00811.2018

Khetarpal, U., Schuknecht, H. F., Gacek, R. R., and Holmes, L. B. (1991). Autosomal dominant sensorineural hearing loss. Pedigrees, audiologic findings, and temporal bone findings in two kindreds. *Arch. Otolaryngol. Head Neck Surg.* 117, 1032–1042.

Kim, E., Hyrc, K. L., Speck, J., Lundberg, Y. W., Salles, F. T., and Kachar, B. (2010). Regulation of cellular calcium in vestibular supporting cells by otopetrin 1. *J. Neurophysiol.* 104, 3439–3450. doi: 10.1152/jn.00525.2010

Kiss, P. J., Knisz, J., Zhang, Y., Baltrusaitis, J., Sigmund, C. D., Thalmann, R., et al. (2006). Inactivation of NADPH oxidase organizer 1 results in severe imbalance. *Curr. Biol.* 16, 208–213. doi: 10.1016/j.cub.2005.12.025

Leventea, E., Zhu, Z., Fang, X., Nikolaeva, Y., Markham, E., Hirst, R. A., et al. (2021). Ciliopathy genes are required for apical secretion of Cochlin, an otolith crystallization factor. *Proc. Natl. Acad. Sci. U.S.A.* 118:e2102562118. doi: 10.1073/pnas.2102562118

Liu, H., Giffen, K. P., Chen, L., Henderson, H. J., Cao, T. A., Kozeny, G. A., et al. (2022). Molecular and cytological profiling of biological aging of mouse cochlear inner and outer hair cells. *Cell Rep.* 39:110665. doi: 10.1016/j.celrep.2022.110665

Lopez, I. A., Ishiyama, G., Acuna, D., and Ishiyama, A. (2019). Otopetrin-2 immunolocalization in the human macula utricle. *Ann. Otol. Rhinol. Laryngol.* 128, 96S–102S. doi: 10.1177/0003489419834952

Lundberg, Y. W., Xu, Y., Thiessen, K. D., and Kramer, K. L. (2015). Mechanisms of otoconia and otolith development. *Dev. Dyn.* 244, 239–253.

Matsumoto, H., Fujiwara, S., Miyagi, H., Nakamura, N., Shiga, Y., Ohta, T., et al. (2017). Carbonic anhydrase inhibitors induce developmental toxicity during zebrafish embryogenesis, especially in the inner ear. *Mar. Biotechnol.* 19, 430–440. doi: 10.1007/s10126-017-9763-7

Mckenna, K., Rahman, K., and Parham, K. (2020). Otoconia degeneration as a consequence of primary hyperparathyroidism. *MedHypotheses* 144:109982. doi: 10.1016/j.mehy.2020.109982

Moreland, K. T., Hong, M., Lu, W., Rowley, C. W., Ornitz, D. M., De Yoreo, J. J., et al. (2014). In vitro calcite crystal morphology is modulated by otoconial proteins otolin-1 and otoconin-90. *PLoS One* 9:e95333. doi: 10.1371/journal.pone.0095333

Mulry, E., and Parham, K. (2020). Inner ear proteins as potential biomarkers. *Otol. Neurotol.* 41, 145–152.

Murayama, E., Herbomel, P., Kawakami, A., Takeda, H., and Nagasawa, H. (2005). Otolith matrix proteins OMP-1 and Otolin-1 are necessary for normal otolith growth and their correct anchoring onto the sensory maculae. *Mech. Dev.* 122, 791–803. doi: 10.1016/j.mod.2005.03.002

Parham, K., and Dyhrfjeld-Johnsen, J. (2016). Outer Hair cell molecular protein, prestin, as a serum biomarker for hearing loss: proof of concept. *Otol. Neurotol.* 37, 1217–1222. doi: 10.1097/MAO.0000000000001164

Pathak, S., Hatam, L. J., Bonagura, V., and Vambutas, A. (2013). Innate immune recognition of molds and homology to the inner ear protein, cochlin, in patients with autoimmune inner ear disease. *J. Clin. Immunol.* 33, 1204–1215. doi: 10.1007/s10875-013-9926-x

Py, B. F., Gonzalez, S. F., Long, K., Kim, M. S., Kim, Y. A., and Zhu, H. (2013). Cochlin produced by follicular dendritic cells promotes antibacterial innate immunity. *Immunity* 38, 1063–1072. doi: 10.1016/j.immuni.2013.01.015

Rhyu, H. J., Bae, S. H., Jung, J., and Hyun, Y. M. (2020). Cochlin-cleaved LCCL is a dual-armed regulator of the innate immune response in the cochlea during inflammation. *BMB Rep.* 53, 449–452. doi: 10.5483/BMBRep.2020.53.9.104

Robertson, N. G., Lu, L., Heller, S., Merchant, S. N., Eavey, R. D., McKenna, M., et al. (1998). Mutations in a novel cochlear gene cause DFNA9, a human nonsyndromic deafness with vestibular dysfunction. *Nat. Genet.* 20, 299–303. doi: 10.1038/3118

Roman-Naranjo, P., Gallego-Martinez, A., Soto-Varela, A., Aran, I., Moleon, M. D. C., Espinosa-Sanchez, J. M., et al. (2020). Burden of rare variants in the OTOG gene in familial Meniere's disease. *Ear. Hear.* 41, 1598–1605. doi: 10.1097/AUD.0000000000000878

Roman-Naranjo, P., Parra-Perez, A. M., Escalera-Balsera, A., Soto-Varela, A., Gallego-Martinez, A., Aran, I., et al. (2022). Defective α-tectorin may involve tectorial membrane in familial Meniere disease. *Clin. Transl. Med.* 12:e829. doi: 10.1002/ctm2.829

Ross, M. D., Peacor, D., Johnsson, L. G., and Allard, L. F. (1976). Observations on normal and degenerating human otoconia. *Ann. Otol. Rhinol. Laryngol.* 85, 310–326.

Rousset, F., Nacher-Soler, G., Kokje, V. B. C., Sgroi, S., Coelho, M., Krause, K. H., et al. (2022). NADPH oxidase 3 deficiency protects from noise-induced sensorineural hearing loss. *Front. Cell Dev. Biol.* 22:832314. doi: 10.3389/fcell.2022.832314

Schiffers, C., Reynaert, N. L., Wouters, E. F. M., and van der Vliet, A. (2021). Redox dysregulation in aging and COPD: role of NOX enzymes and implications for antioxidant strategies. *Antioxidants* 10:1799. doi: 10.3390/antiox10111799

Schraders, M., Ruiz-Palmero, L., Kalay, E., Oostrik, J., del Castillo, F. J., Sezgin, O., et al. (2012). Mutations of the gene encoding otogelin are a cause of autosomal-recessive nonsyndromic moderate hearing impairment. *Am. J. Hum. Genet.* 91, 883–889. doi: 10.1016/j.ajhg.2012.09.012

Stooke-Vaughan, G. A., Obholzer, N. D., Baxendale, S., Megason, S. G., and Whitfield, T. T. (2015). Otolith tethering in the zebrafish otic vesicle requires Otogelin and α-Tectorin. *Development* 142, 1137–1145. doi: 10.1242/dev.116632

Thiessen, K. D., Grzegorski, S. J., Chin, Y., Higuchi, L. N., Wilkinson, C. J., Shavit, J. A., et al. (2019). Zebrafish otolith biomineralization requires polyketide synthase. *Mech. Dev.* 157, 1–9. doi: 10.1016/j.mod.2019.04.001

Tian, Q., Gu, H. H., Feng, M. Y., and Zhuang, J. H. (2020). [A review of the role of otolithic regulatory proteins in otoconial forming and maintaining]. *Chin. J. Otorhinolaryngol. Head Neck Surgery* 55, 549–553. doi: 10.3760/cma.j.cn115330-20190529-00363

Tohse, H., and Mugiya, Y. (2001). Effects of enzyme and anion transport inhibitors on in vitro incorporation of inorganic carbon and calcium into endolymph and otoliths in salmon Oncorhynchus masou. *Comp. Biochem. Physiol. A Mol. Integr. Physiol.* 128, 177–184. doi: 10.1016/s1095-6433(00)00287-7

Tohse, H., Murayama, E., Ohira, T., Takagi, Y., and Nagasawa, H. (2006). Localization and diurnal variations of carbonic anhydrase mRNA expression in the inner ear of the rainbow trout Oncorhynchus mykiss. *Comp. Biochem. Physiol. B Biochem. Mol. Biol.* 145, 257–264. doi: 10.1016/j.cbpb.2006.06.011

Tu, Y. H., Cooper, A. J., Teng, B., Chang, R. B., Artiga, D. J., Turner, H. N., et al. (2018). An evolutionarily conserved gene family encodes proton-selective ion channels. *Science* 359, 1047–1050. doi: 10.1126/science.aao3264

Verdoodt, D., Peeleman, N., Szewczyk, K., Van Camp, G., Ponsaerts, P., and Van Rompaey, V. (2021). Cochlin deficiency protects aged mice from noise-induced hearing loss. *Int. J. Mol. Sci.* 22:11549. doi: 10.3390/ijms222111549

Weigele, J., Franz-Odendaal, T. A., and Hilbig, R. (2015). Spatial expression of otolith matrix protein-1 and otolin-1 in normally and kinetotically swimming fish. *Anat. Rec.* 298, 1765–1773. doi: 10.1002/ar.23184

Weigele, J., Franz-Odendaal, T. A., and Hilbig, R. (2016). Not all inner ears are the same: otolith matrix proteins in the inner ear of sub-adult cichlid fish, oreochromis mossambicus, reveal insights into the biomineralization process. *Anat. Rec.* 299, 234–245. doi: 10.1002/ar.23289

Whitfield, T. T. (2020). Cilia in the developing zebrafish ear. *Philos. Trans. R. Soc. Lond B Biol. Sci.* 375:20190163.

Wu, L., Sagong, B., Choi, J. Y., Kim, U. K., and Bok, J. (2013). A systematic survey of carbonic anhydrase mRNA expression during mammalian inner ear development. *Dev. Dyn.* 242, 269–280. doi: 10.1002/dvdy.23917

Wu, Y., Han, W., Yan, W., Lu, X., Zhou, M., Li, L., et al. (2020). Increased otolin-1 in serum as a potential biomarker for idiopathic benign paroxysmal positional vertigo episodes. *Front. Neurol.* 11:367. doi: 10.3389/fneur.2020.00367

Xiong, X., Yu, J., and Sun, Y. (2020). [The diagnostic value of cochlin-tomoprotein in perilymphatic fistula]. *Lin Chung Er Bi Yan Hou Tou Jing Wai Ke Za Zhi* 34, 857–861. Chinese,

Xu, Y., Yang, L., Zhao, X., Zhang, Y., Jones, T. A., and Jones, S. M. (2021). Functional cooperation between two otoconial proteins Oc90 and Nox3. *J. Vestib. Res.* 31, 441–449. doi: 10.3233/VES-201591

Yadav, H., Irugu, D., Ramakrishanan, L., Singh, A., Abraham, R., Sikka, K., et al. (2021). An evaluation of serum Otolin-1 & Vitamin-D in benign paroxysmal positional vertigo. *J. Vestib. Res.* 31, 433–440.

Yang, L., Xu, Y., Zhang, Y., Vijayakumar, S., Jones, S. M., and Lundberg, Y. Y. W. (2018). Mechanism underlying the effects of estrogen deficiency on otoconia. *J. Assoc. Res. Otolaryngol.* 19, 353–362. doi: 10.1007/s10162-018-0666-8

Zhao, X., Jones, S. M., Yamoah, E. N., and Lundberg, Y. W. (2008). Otoconin-90 deletion leads to imbalance but normal hearing: a comparison with other otoconia mutants. *Neuroscience* 153, 289–299. doi: 10.1016/j.neuroscience.2008.01.055

Zhao, X., Yang, H., Yamoah, E. N., and Lundberg, Y. W. (2007). Gene targeting reveals the role of Oc90 as the essential organizer of the otoconial organic matrix. *Dev. Biol.* 304, 508–524. doi: 10.1016/j.ydbio.2007.01.013

Zou, P., Muramatsu, H., Sone, M., Hayashi, H., Nakashima, T., and Muramatsu, T. (2006). Mice doubly deficient in the midkine and pleiotrophin genes exhibit deficits in the expression of the β-tectorin gene and in auditory response. *Lab. Invest.* 86, 645–653. doi: 10.1038/labinvest.3700428

frontiers | Frontiers in Neurology

TYPE Original Research
PUBLISHED 22 August 2022
DOI 10.3389/fneur.2022.978442

Check for updates

OPEN ACCESS

EDITED BY
Jian-hua Zhuang,
Shanghai Changzheng Hospital, China

REVIEWED BY
Taisheng Chen,
Tianjin First Central Hospital, China
Tzu-Pu Chang,
Tzu Chi University, Taiwan

*CORRESPONDENCE
Peixia Wu
13524844652@163.com
Wenyan Li
wenyan_li2000@126.com

†These authors have contributed equally to this work and share first authorship

SPECIALTY SECTION
This article was submitted to Neuro-Otology, a section of the journal Frontiers in Neurology

RECEIVED 26 June 2022
ACCEPTED 02 August 2022
PUBLISHED 22 August 2022

CITATION
Yu J, Wan Y, Zhao J, Huang R, Wu P and Li W (2022) Normative data for rotational chair considering motion susceptibility.
Front. Neurol. 13:978442.
doi: 10.3389/fneur.2022.978442

COPYRIGHT
© 2022 Yu, Wan, Zhao, Huang, Wu and Li. This is an open-access article distributed under the terms of the Creative Commons Attribution License (CC BY). The use, distribution or reproduction in other forums is permitted, provided the original author(s) and the copyright owner(s) are credited and that the original publication in this journal is cited, in accordance with accepted academic practice. No use, distribution or reproduction is permitted which does not comply with these terms.

Normative data for rotational chair considering motion susceptibility

Jiaodan Yu[1†], Yi Wan[1†], Jieli Zhao[1†], Ruonan Huang[1], Peixia Wu[1,2*] and Wenyan Li[1,3,4,5*]

[1]Ear Nose Throat (ENT) Institute and Department of Otorhinolaryngology, Eye and ENT Hospital, State Key Laboratory of Medical Neurobiology and Ministry of Education Frontiers Center for Brain Science, Fudan University, Shanghai, China, [2]Nursing Department of Eye and ENT Hospital, Fudan University, Shanghai, China, [3]Institutes of Biomedical Sciences, Fudan University, Shanghai, China, [4]National Health Commission Key Laboratory of Hearing Medicine, Fudan University, Shanghai, China, [5]The Institutes of Brain Science and the Collaborative Innovation Center for Brain Science, Fudan University, Shanghai, China

Objective: Rotational Chair Test (RCT) is considered one of the most critical measures for vestibular functionality, which generally includes the sinusoidal harmonic acceleration test (SHAT), velocity step test (VST), and visual suppression (VS). The purpose of this study was to establish normal values for different age groups on the RCT and investigate whether motion susceptibility, such as with a history of motion sickness or migraine, has any effects on test metrics.

Methods: One hundred and nine subjects aged from 20 to 59 years who were free from neurotological and vestibular disorders were enrolled. According to the history of motion sickness or migraine, participants were divided into four groups: the motion sickness (MS) group ($n = 13$), the migraine group ($n = 8$), comorbidity group ($n = 11$), and the control group ($n = 77$). The 77 subjects without any history of MS and migraine were then further separated into four age groups: youth group (20–29 years), young and middle-aged group (30–39 years), middle-age group (40–49 years), and middle-age and elderly group (50–59 years). All participants underwent SHAT, VST, and VS, and a comprehensive set of metrics including gain, phase, asymmetry, time constant (TC), and Fixation Index were recorded.

Results: Regarding the VST and VS, no significant differences were observed either across the four groups (MS, migraine, comorbidity, and control group) or four age categories within the control group. For SHAT, VOR gain at the frequency of 0.01 Hz, VOR phase from 0.08 to 0.64 Hz, and asymmetry at 0.01, 0.16, and 0.64 Hz indicated significant differences among various age groups ($P < 0.05$ for all comparisons). The VOR phase lead was lower in the migraine and comorbidity group than that in the control group at 0.64 Hz ($P = 0.027$, $P = 0.003$, respectively).

Conclusions: Age slightly affects the result of SHAT, but not for VST and VS. VOR gain is more susceptible to aging at low frequency, while the phase is opposite. Subjects with both migraine and motion sickness show abnormal

velocity storage mechanisms. Phase bias should be considered when assessing motion susceptibility with the RCT. SHAT is more sensitive than VST in terms of reflecting motion susceptibility.

KEYWORDS

sinusoidal harmonic acceleration test (SHAT), velocity step test (VST), visual suppression (VS), rotational chair test, motion sickness (MS), velocity storage mechanism (VSM)

Introduction

It is well known that the peripheral vestibular system has frequency characteristics. The daily head movement frequency ranged from 0.05 to 6 Hz (1). Within this frequency range, the vestibular-ocular reflex (VOR) plays a vital role in maintaining visual stability. In past decades, videonystagmography (VNG) and the video head impulse test (v-HIT) have been commonly used to assess the vestibular system. But they both have their limitations. For example, the caloric test is equivalent to stimulating the vestibular system by adopting an aphysiological frequency range from 0.003 to 0.008 Hz. Moreover, it is unsuitable for the pediatric population and those with otologic surgery or meatal atresia (2). The v-HIT is a quantitative measure for assessing VOR with high-frequency (1–6 Hz) but is not adaptive for individuals with limited neck motion (1). The rotational chair test is complementary to the caloric test and v-HIT. The rotational chair test can test a broader range of frequencies from 0.01 to 0.64 Hz, provides a gold standard for diagnosis of bilateral vestibulopathy (BVP), and serves as a better choice for pediatric populations who cannot tolerate caloric irrigation test (3–5). Although the rotational chair test is less sensitive to acute unilateral peripheral disorders than the caloric test and v-HIT, it can assess vestibular compensatory status by analyzing parameters (1, 6). However, the normative data of the rotational chair test needs further study, and whether the parameters are age-related remains controversial.

Motion sickness (MS) is physiological vertigo commonly seen in the general population, but its susceptibility and severity vary between individuals. During exposure to vehicle motion or complicated and virtual vision, MS generally occurs with symptoms such as nausea, vomiting, and dizziness (7). The most cited pathogenesis for MS is the sensory conflict and neural mismatch hypothesis (8). Previous research reported that motion sickness and migraine are reciprocally connected. It is evident that migraine people increase motion sickness susceptibility (9, 10). Motion sickness susceptibility is related to VOR's spatial-temporality through activating the velocity storage mechanism (VSM) (11–13). In theory, motion sickness susceptibility generally shows lower phase lead and higher time constants (14). However, the empirical data are lacking. To fill that gap, this study aims to investigate what parameters of RCT differ in subjects with or without a history of motion sickness or migraine, or both.

The purposes of this study are divided into two parts. The first is establishing normal values for different age groups on the rotational chair test. Then, the second aim is to compare the control, MS, migraine and comorbidity groups, providing inspiration when assessing vestibular functionality by rotatory chair test.

Materials and methods

Subjects

This research study was conducted from June 2020 to March 2021. This study was approved by the Institute Review Board of Fudan University Eye Ear Nose and Throat Hospital (Reference Number 2020087). To create a representative sample of the general population, we recruited 109 subjects free from neurotological and vestibular disorders. Exclusion criteria included a history of otologic surgery or head injuries, cerebrovascular diseases, and systemic disorders. The subjects were asked to fill out a questionnaire about whether they had motion sickness and a history of migraine. Thirteen subjects reported having only motion sickness and 8 subjects had only a history of migraine. There were 11 patients who had both motion sickness and migraine. The remaining 77 subjects were assigned to four age groups: youth group (20–29 years), young and middle-aged group (30–39 years), middle-age group (40–49 years), and middle-age and elderly group (50–59 years). All subjects were told to refrain from eating for 2 h before the testing.

Rotational chair test

A rotational chair test was performed using the VertiChair (ZT-CHAIR-I, Shanghai ZEHNIT Medical Technology Co., Ltd., Shanghai, China). Two technicians performed all the tests using a standardized protocol available before this study's start.

The whole rotational chair system can implement a sinusoidal harmonic acceleration test, velocity step test, and visual suppression. The subjects were seated in the rotational chair with a safety belt in the completely dark room. The goggles were placed on the subject's faces and were tightened to the head with an elastic band to avoid slipping. The head was restrained and tilted forward 30° so that horizontal semicircular canals could be stimulated effectively. The subjects were told to keep alert and their eyes open throughout the whole testing procedure. When necessary, the operating technician communicates verbally to help the subjects maintain a constant awareness.

Sinusoidal harmonic acceleration test

The chair was rotated with sinusoidal waves at various range of frequencies (0.01, 0.02, 0.04, 0.08, 0.16, 0.32, and 0.64 Hz). The maximum velocity is 50 degrees/s. During the sinusoid rotation, the primary outcome variables were gain, phase, and asymmetry. The gain is calculated by dividing the eyes' slow component velocity by the chair's velocity. It can't orientate the vestibular lesion side but reflect the system's overall responsiveness. The phase reflects the temporal relationship between head movement and eye movement. It's called phase lead, reflecting the eye movements lead to head movement. If eye trace is ahead of head trace, phase lead will be a negative value. Otherwise, it will get a positive phase value called phase lag. The asymmetry reflects the difference in intensity of nystagmus of leftwards and rightwards directions.

$$y_{\text{eye}} = A_{\text{eye}} * \sin(\omega_{\text{eye}}\text{t} - \varphi_{\text{eye}})$$
$$y_{\text{head}} = A_{\text{head}} * \sin\left(\omega_{\text{head}}t - \varphi_{\text{head}}\right)$$
$$\text{phase} = \varphi_{\text{eye}} - \varphi_{\text{head}}$$

y: the real-time speed of the fitted sine curve; A: the maximum speed (°/s); ω: rotational angular velocity; φ: the initial phase shift in degree.

$$\text{Asymmetry} = (\text{a} - \text{b})/(\text{a} + \text{b}) \times 100\%$$

a: maximum right-beating slow phase average eye velocities; b: maximum left-beating slow phase eye velocities.

Velocity step test

Firstly, the chair has attained a velocity (90 degrees/s) with a constant acceleration (3 degrees/s^2) in a clockwise direction. Constant acceleration causes nystagmus to occur. Although the subject's whole body was rotated, the right horizontal semicircular canal was stimulated in the acceleration process. Then, the chair was operated at 90 degrees/s for 1 min. As the chair was rotated constantly, nystagmus decayed exponentially. Finally, the chair was decelerated to 0 degrees/s in 1 s. The nystagmus that we recorded occurred in the opposite direction. The rotation in the clockwise direction stopped suddenly was equal to stimulation of the left semicircular canal. The whole procedure was then repeated in a counterclockwise direction. Two parameters were also measured during the velocity step test. They were post-rotary gain and time constant (TC). The gain is the ratio of the eyes' maximum SPV to the chair's velocity. The TC is the time for the VOR response to decay 37% of the maximum SPV.

Visual suppression

The subjects were rotated sinusoidally at a single frequency for three cycles with a peak velocity of 50 degrees/s. After that, subjects were instructed to fixate on the laser dot that appears on the Googles. The average VOR gain with a laser dot was compared with that without a laser dot. The Fixation Index (FI) was calculated by dividing gain with laser dot by gain without laser dot and then multiplying 100.

Statistical analysis

The IBM SPSS Statistics version 26.0 for Mac was used for statistical analysis. We first examined whether the data were normal distribution. Normality of quantitative variables was performed using the Shapiro-Wilk test. Data were described as mean, standard deviation (SD), Inter Quartile Range (IQR), or percentages. We examined whether the parameters were affected by gender by using a t-test. Four age groups were compared using a one-way analysis of variance (ANOVA). For not normally distributed variables, the Kruskal-Wallis test was used instead of the ANOVA. Pearson correlation coefficient was used to analyze the correlation between parameters of SHAT and age. Considering the effect of age on SHAT, multiple-factors ANOVA was applied to compare the difference in phase for four groups (motion sickness, migraine, comorbidity, and control). *Post-hoc* comparisons with Least-Significance-Difference Method (LSD) were used. One-way ANOVA was used to explore the difference between groups for VAT and VS. The P-value < 0.05 was considered significant.

Results

Demographics of subjects

A total of 109 subjects aged from 20 to 59 years participated in this study. Thirteen out of 109 subjects had only motion sickness and 8 out of 109 subjects had only migraine. Eleven subjects with both motion sickness and migraine thus served as the comorbidity group. In the MS group, 10 subjects were female, and 3 were male. In the Migraine group, 6 subjects were female, and 2 were male. In the comorbidity group, 7

TABLE 1 Demographics of the subjects.

Age groups	*N*	Mean age ± SD	Sex [*n* (%)]	
			Male	Female
20–29	22	25.86 ± 2.47	9 (41)	13 (49)
30–39	13	33.77 ± 2.20	8 (62)	5 (38)
40–49	24	45.13 ± 3.22	11 (46)	13 (54)
50–59	18	54.06 ± 2.71	5 (28)	13 (72)
Total	77	39.79 ± 11.26	33 (43)	44 (57)

TABLE 2 Demographics of the four groups.

Groups	*n*/*N*	Mean age ± SD	Male	Female
Motion sickness	13/109	29.62 ± 9.32	3	10
Migraine	8/109	33.13 ± 10.32	2	6
Comorbidity	11/109	27.73 ± 4.54	4	7
Control	77/109	39.79 ± 11.26	33	44

Comorbidity group indicated the subjects have both migraine and motion sickness.

were female and 4 were male. The remaining 77 subjects were stratified by four age groups: 20–29 years ($n = 22$), 30–39 years ($n = 13$), 40–49 years ($n = 24$), 50–59 years ($n = 18$). The demographics of the subjects are detailed in Tables 1, 2.

SHAT

Three parameters of SHAT across the four age groups are shown in Table 3. The parameters at each frequency confirmed as normal distribution were compared with one-way ANOVA, whereas others were compared with the Kruskal-Wallis test. Gain of 0.01 Hz significantly differed across four age groups ($P = 0.044$). Phases of 0.08, 0.16, 0.32, and 0.64 Hz exhibited significant differences in four age groups ($P_{0.08} = 0.019$, $P_{0.16} = 0.001$, $P_{0.32} < 0.001$, $P_{0.64} < 0.001$, respectively). Asymmetry significantly differed at 0.01, 0.16, and 0.64 Hz among the various age groups ($P_{0.01} = 0.031$, $P_{0.16} = 0.01$, $P_{0.64} = 0.005$, respectively). No significant differences in gender were observed. There were mild correlations between age and three parameters. The gain at 0.01 and 0.02 Hz was positively related to the age ($r_{0.01} = 0.334$, $P_{0.01} = 0.004$; $r_{0.02} = 0.248$, $P_{0.02} = 0.032$). The phase values from 0.16 to 0.64 Hz was negatively correlated with age ($r_{0.16} = -0.374$, $P_{0.16} = 0.001$; $r_{0.32} = -0.475$, $P_{0.32} < 0.001$; $r_{0.64} = -0.549$, $P_{0.64} < 0.001$, respectively). Because the sign of phase indicated whether the phase was leading or lagging. The phase lead values from 0.16 to 0.64 Hz correlate with age clinically. The asymmetry at 0.01, 0.16, and 0.64 Hz was negatively correlated with age ($r_{0.01} = -0.263$, $P_{0.01} = 0.023$; $r_{0.16} = -0.261$, $P_{0.16} = 0.025$; $r_{0.64} = -0.331$, $P_{0.64} = 0.004$, respectively).

When adjusted for the age, multiple-factors ANOVA indicated that no significant difference was observed among the four groups (motion sickness, migraine, comorbidity and control) at frequency from 0.01 to 0.32 Hz for phase. However, *Post-hoc* comparisons indicated that there was a statistically significant difference at 0.64 Hz for phase between migraine and control groups ($P = 0.027$). Phase lead of the migraine group is lower than that in the control group. Between the comorbidity and control groups, statistically significant difference in phase at 0.64 Hz exists ($P = 0.003$). Phase lead of comorbidity is lower than that in the control group. Significant difference for phase at 0.64 Hz was not observed between MS group and control group whereas was found between MS group and comorbidity group ($P = 0.041$). Likewise, phase lead of comorbidity group was lower than MS group and it was the lowest of the four groups. Figure 1 shows the phase difference of each frequency.

VST and VS

Post-rotary gain and TC as parameters of VST and FI as a parameter of VS were analyzed. No significant age differences were found for the VST and VS ($P > 0.05$). For VS, our results indicated normative values for FI were <52.0% on the right side and <47.2% on the left side. Table 4 presents the normative data of VST in the control group and comparison across the MS, migraine, comorbidity and control group. The results indicated no significant differences exists among the four groups ($P > 0.05$ for all comparisons). There was also no significant difference in VS for the four groups.

Discussion

The rotational chair is a physiological way to evaluate horizontal semicircular canal function. In this study, we sought to understand if the parameters were age-related and to build a normative dataset for different age groups. Our study shows that the difference of age groups for gain only exists at 0.01 Hz of SHAT. Moreover, it is positively related to age at 0.01 Hz even though the correlation coefficient was moderate. During the rotation, the most nauseating frequency is 0.1 Hz because it lasts the longest time and is a big challenge to keep alert, which explains why the gain values of lower frequency are less stable.

Moreover, the subjects' age range is 20–60 years old, and not equal distribution of subjects is in each group. So far, the relationship between VOR and age has been controversial. In some studies, the gain is relatively stable until an older age and is hardly affected by aging (15–18). In contrast, Chan et al. demonstrated VOR gain differences with age for the rotational chair test. They reported that the gain of SHAT across all

TABLE 3 SHAT normative values of four age groups.

Frequency (Hz)	Parameters	Age groups (years)				*P*
		20–29	30–39	40–49	50–59	
0.01	Gain	0.30 ± 0.08	0.27 ± 0.11	0.36 ± 0.14	0.38 ± 0.12	0.044*
	Phase	−44.86 ± 5.84	−45.08 ± 5.54	−41.62 ± 7.22	−43.81 ± 7.48	0.324
	Asymmetry	10.48 ± 10.78	12.46 ± 14.05	2.42 ± 12.16	4.19 ± 9.53	0.031*
0.02	Gain	0.37 ± 0.13	0.35 ± 0.14	0.42 ± 0.14	0.43 ± 0.12	0.189
	Phase	−26.86 ± 7.89	−24.69 ± 4.77	−21.87 ± 5.61	−24.20 ± 4.09	0.056
	Asymmetry	3.82 ± 9.45	3.69 ± 11.29	1.50 ± 12.36	−1.80 ± 7.13	0.392
0.04	Gain	0.44 ± 0.14	0.43 ± 0.14	0.47 ± 0.15	0.48 ± 0.12	0.395
	Phase	−11.95 ± 8.79	−13.00 ± 3.52	−13.46 ± 6.18	−14.50 ± 4.26	0.682
	Asymmetry	(−3.00, 6.50)	(−2.00, 18.00)	(−8.75, 9.75)	(−2.75, 8.00)	0.545
0.08	Gain	0.47 ± 0.15	0.41 ± 0.11	0.46 ± 0.17	0.54 ± 0.14	0.134
	Phase	−3.90 ± 4.92	−4.54 ± 4.43	−2.54 ± 7.09	−8.12 ± 4.29	0.019*
	Asymmetry	2.48 ± 10.23	3.23 ± 10.13	0.92 ± 9.82	−0.18 ± 8.52	0.749
0.16	Gain	0.47 ± 0.19	0.42 ± 0.11	0.47 ± 0.20	0.51 ± 0.15	0.614
	Phase	(−5.50, 4.00)	(−0.75, 9.50)	(−6.00, 2.00)	(−11.50, −1.75)	0.001*
	Asymmetry	(−4.00, 11.50)	(0.25, 15.50)	(−13.00, 8.00)	(−9.25, 5.00)	0.013*
0.32	Gain	0.54 ± 0.21	0.51 ± 0.17	0.48 ± 0.20	0.52 ± 0.19	0.539
	Phase	(−2.75, 2.75)	(−5.50, 5.00)	(−16.25, −0.75)	(−17.25, −5.50)	<0.001*
	Asymmetry	(−4.00, 6.75)	(−1.25, 8.50)	(−5.00, 7.00)	(−7.25, 3.25)	0.235
0.64	Gain	0.69 ± 0.19	0.62 ± 0.20	0.63 ± 0.21	0.69 ± 0.14	0.520
	Phase	(−8.00, 0.00)	(−6.50, 1.00)	(−29.00, −3.00)	(−37.00, −12.00)	<0.001*
	Asymmetry	3.81 ± 8.38	6.00 ± 6.71	−0.62 ± 6.83	−2.72 ± 7.14	0.005*

Bold fonts indicate that data of parameters were presented as Inter Quartile Range.
*Statistically significant according to Kruskal-Wallis test or one-way ANOVA ($p < 0.05$).

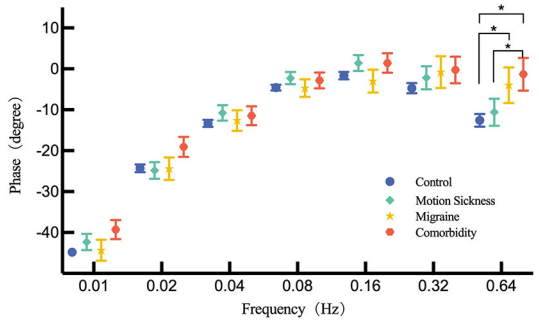

FIGURE 1
Comparison of the phase across MS group, migraine group, comorbidity group and control group for each frequency by multiple-factors ANOVA. Corrected phase values are presented by mean and standard error. The asterisk (*) indicates a significant difference exists.

the frequencies was inversely correlated to age (4). However, McGarvie et al. demonstrated that gains have a slightly negative relationship with age from the sixth-decade (16).

Similarly, Kim and Kim reported that the gain declined as age increased over 70 years for horizontal semicircular canal (17). Likewise, our data suggests gain varies significantly with age at 0.01 Hz under 60 years, which is inconsistent with the age range of the above studies. Gain is susceptible to the subjects' nervousness and alertness (19). In our study, we tried to ensure the subjects were constantly alert throughout the testing procedure.

Generally, when the head is rotated, the eyes move in the opposite direction with the same speed and angle to keep the visual steady. But they are not always at the same time and have a time delay. Phase highly corresponded to TC of VOR is measured to reflect the timing relationship between head movement and eye movement. The phase is a more reliable variable than the gain because it's steady and reproducible (20). This study indicated that phase angle decreased from phase leading to phase lag as the frequency increases in normal control. Our data also showed differences in phase existing from 0.08 to 0.64 Hz for all age groups, and phase lead values was found to be correlated with the age from 0.16 to 0.64 Hz. It may be linked to the velocity storage time constant. Previous studies demonstrated that age-dependent changes in the human VOR, especially decreasing time constant, which was explained by

TABLE 4 Comparison for velocity step test for the control group, motion sickness group, migraine group, and comorbidity group.

	Parameters	Control	Motion sickness	Migraine	Comorbidity	*P*
CW	Post-rotary gain	0.63 ± 0.13	0.57 ± 0.18	0.68 ± 0.12	0.73 ± 0.18	0.060
	TC	14.33 ± 3.96	14.51 ± 5.06	14.15 ± 3.73	14.90 ± 4.96	0.976
CCW	Post-rotary gain	0.62 ± 0.15	0.57 ± 0.14	0.62 ± 0.10	0.69 ± 0.12	0.317
	TC	14.85 ± 3.75	12.10 ± 4.21	14.39 ± 4.85	14.46 ± 4.32	0.330

MS, motion sickness; CW, clock-wise; CCW, counter clock-wise; TC, time constant.

Bayesian optimal adaptation in the velocity storage occurring in response to the death of motion-sensing hair cells (21, 22). Asymmetry involves a comparison between the SPV to the right and leftward, indicating skewness within the peripheral vestibular system, which is often seen in unilateral peripheral vestibular lesion cases.

The second paradigm of the rotational chair test is VST. Gain and TC are the main parameters. Like SHAT, the gain of VST is associated with TC to explain vestibular functionality. To reduce the equipment wastage rate, post-rotatory TC is measured in our laboratory instead of per-rotatory. The stimulated semicircular canal is the opposite side of the rotation direction. A mathematical model has been proposed between TC of VST and phase of SHAT (23). As the phase lead increases, TC decreases. Though both reflect whether the VSM is normal or not, TC can be used to localize a lesion while phase not.

The last paradigm of the rotational chair test is VS. Differ from SHAT and VST, failure responses of VS usually suggest a lesion of central origin. The abnormal range of the Fixation Index is generally thought to be cerebellar involved. Lotfi et al. reported that children with attention deficit and hyperactivity disorder showed higher VOR gain but lower fixation abilities due to a lesion involving the middle cerebellum (24). Our study finds no correlation between age and parameters for VST and VS, indicating that both are steady and not affected by age.

The prolongation of an afferent signal existing VOR responses is achieved by velocity storage mechanism (VSM) (11, 12). In other words, VSM regulates the phase of the VOR system. The value of phase is influenced by the peripheral vestibular system and central nervous system. Peripheral dysfunction with pathologic damage results in abnormal information input to VSM, so phase lead may be beyond the normal range. Brainstem lesions may generate phase abnormally given that VSM is located in the brainstem. The pathological mechanism of MS is closely related to VSM by delaying the signals from the peripheral vestibule to the medial vestibular nucleus (25, 26). We expected differences in rotational chair test parameters between healthy groups and individuals with MS. The Barany Society presented diagnostic criteria for MS, including the observable signs or symptoms of gastrointestinal disturbance and thermoregulatory disruption, dizziness, and headache during exposure to physical motion (27). Clement and Reschke found no correlation between VOR gain and level of MS; however, they found that the lower the phase lead, the more severe the MS (14).

Previous literature showed the severity of symptoms was not related to the intensity of physical motion but impacted by stimulus frequency in MS susceptible individuals, which was usually triggered by low-frequency vertical, angular, and rotation motion (28). Irmak et al. used sinusoidal fore-aft motions to determine frequency responses among individuals with MS (29). They found individual variability in motion frequency sensitivity but no significant effect at the group level. In the present study, we found no significant differences between MS group and control group. This may be due to the fact that level of MS is mild. However, phase lead of comorbidity group which have both motion sickness and migraine was significantly lower than that of the control group. Moreover, some articles indicated that migraine was often associated with MS and enhanced symptoms with each other. They may share a common neural pathway involving the brainstem and serotonin modulation (9, 10). Therefore, the motion susceptibility of subjects with both motion sickness and migraine may be the most severe. But no significant difference was revealed in the TC of VST for comorbidity and control groups. Based on this finding, we speculate that phase is more sensitive to TC in assessing VSM.

It is reported that migraine is one of the leading causes of disability and affects people's life and work. The pathological theory of migraine has focused on the brainstem as a source of neurovascular disturbances (30). Evidence showed vestibular migraine patients were hypersensitive to self-motion and enhanced susceptibility to motion sickness during rotation (31). Murdin et al. demonstrated that both VM and migraine increased motion sickness susceptibility and were no different when assessed by Sickness Rating and short from Motion Sickness Susceptibility Questionnaire (32). However, how would migraineurs behave on chair rotary motions and whether they present differences in objective parameters remain unknown. We investigated motion sickness susceptibility differences objectively by measuring phase and TC. We found a significant difference in phase lead 0.64 Hz between the migraine and control groups. A series of studies have shown that velocity

storage of semicircular canal signals is a critical factor for susceptibility to motion sickness. Receiving motion stimulation and having decayed symptoms is a prolonged period for individuals with motion sickness susceptibility. Longer time constants of the vestibular velocity store have been suggested to correlate with heighten motion sickness susceptibility (7, 33). So, it's not hard to understand that phase lead is lower for them.

But interestingly, no significant difference in TC of VST was observed. Our data supported that migraine is generally associated with high susceptibility during rotating motions, especially at higher frequencies. Unlike many previous studies, this study involved participants' susceptibility to motion, indicating SHAT is more sensitive to VST though they both reflect the performances of VSM.

Study limitation

The study is limited to a single-center study. Due to a lack of volunteers, we have not established the normative values for younger than 20 and older than 60 years old. The sample size of MS, migraine and comorbidity groups is limited and age distribution was uneven. Future research should be undertaken to build a more comprehensive normative range.

Conclusion

A small effect of age exists in SHAT. Gain is more susceptible to age at low frequency, while the phase is the opposite. No age difference exists in VST and VS. Subjects with both migraine and motion sickness show abnormal VSM and their motion susceptibility may be the most severe. When assessing their vestibular function with the rotational chair test, we should consider the bias of phase. According to our results, SHAT is more sensitive to VST in terms of reflecting motion susceptibility.

Data availability statement

The original contributions presented in the study are included in the article/Supplementary material, further inquiries can be directed to the corresponding authors.

Ethics statement

The studies involving human participants were reviewed and approved by Institute Review Board of Fudan University Eye Ear Nose and Throat Hospital (Reference Number 2020087). The patients/participants provided their written informed consent to participate in this study.

Author contributions

WL and PW designed the study. JY and YW performed the study and wrote the manuscript. JZ and RH collected and analyzed the data for the study. All authors contributed to the article and approved the submitted version.

Funding

This work was supported by the National Key R&D Program of China (No. 2022ZD0205400), the grant from the Science and Technology Commission of Shanghai (19441917100 and 20S31907000), the National Natural Science Foundation of China (Nos. 81922018 and 81771011), and the Three-year Action Plan of Shanghai Shenkang Hospital Development Center to Promote Clinical Skills and Clinical Innovation in Municipal Hospitals (SHDC2020CR3050B).

Acknowledgments

We want to express our deep gratitude to the subjects who participated in this study.

Conflict of interest

The authors declare that the research was conducted in the absence of any commercial or financial relationships that could be construed as a potential conflict of interest.

Publisher's note

All claims expressed in this article are solely those of the authors and do not necessarily represent those of their affiliated organizations, or those of the publisher, the editors and the reviewers. Any product that may be evaluated in this article, or claim that may be made by its manufacturer, is not guaranteed or endorsed by the publisher.

Supplementary material

The Supplementary Material for this article can be found online at: https://www.frontiersin.org/articles/10.3389/fneur.2022.978442/full#supplementary-material

References

1. Zuniga SA, Adams ME. Efficient use of vestibular testing. *Otolaryngol Clin North Am.* (2021) 54:875–91. doi: 10.1016/j.otc.2021.05.011

2. Shepard NT, Jacobson GP. The caloric irrigation test. *Handb Clin Neurol.* (2016) 137:119–31. doi: 10.1016/B978-0-444-63437-5.00009-1

3. Gimmon Y, Schubert MC. Vestibular testing-rotary chair and dynamic visual acuity tests. *Adv Otorhinolaryngol.* (2019) 82:39–46. doi: 10.1159/000490270

4. Chan FM, Galatioto J, Amato M, Kim AH. Normative data for rotational chair stratified by age. *Laryngoscope.* (2016) 126:460–3. doi: 10.1002/lary.25497

5. Strupp M, Kim JS, Murofushi T, Straumann D, Jen JC, Rosengren SM, et al. Bilateral vestibulopathy: diagnostic criteria consensus document of the classification committee of the barany society. *J Vestib Res.* (2017) 27:177–89. doi: 10.3233/VES-170619

6. Arriaga MA, Chen DA, Cenci KA. Rotational chair (Roto) instead of electronystagmography (Eng) as the primary vestibular test. *Otolaryngol Head Neck Surg.* (2005) 133:329–33. doi: 10.1016/j.otohns.2005.05.002

7. Golding JF. Motion sickness. *Handb Clin Neurol.* (2016) 137:371–90. doi: 10.1016/B978-0-444-63437-5.00027-3

8. Keshavarz B, Golding JF. Motion sickness: current concepts and management. *Curr Opin Neurol.* (2022) 35:107–12. doi: 10.1097/WCO.0000000000001018

9. Marcus DA, Furman JM, Balaban CD. Motion sickness in migraine sufferers. *Expert Opin Pharmacother.* (2005) 6:2691–7. doi: 10.1517/14656566.6.15.2691

10. Cuomo-Granston A, Drummond PD. Migraine and motion sickness: what is the link? *Prog Neurobiol.* (2010) 91:300–12. doi: 10.1016/j.pneurobio.2010.04.001

11. Nooij SAE, Pretto P, Bulthoff HH. More vection means more velocity storage activity: a factor in visually induced motion sickness? *Exp Brain Res.* (2018) 236:3031–41. doi: 10.1007/s00221-018-5340-1

12. Bertolini G, Ramat S, Laurens J, Bockisch CJ, Marti S, Straumann D, et al. Velocity storage contribution to vestibular self-motion perception in healthy human subjects. *J Neurophysiol.* (2011) 105:209–23. doi: 10.1152/jn.00154.2010

13. Bertolini G, Ramat S. Velocity storage in the human vertical rotational vestibulo-ocular reflex. *Exp Brain Res.* (2011) 209:51–63. doi: 10.1007/s00221-010-2518-6

14. Clement G, Reschke MF. Relationship between motion sickness susceptibility and vestibulo-ocular reflex gain and phase. *J Vestib Res.* (2018) 28:295–304. doi: 10.3233/VES-180632

15. Matino-Soler E, Esteller-More E, Martin-Sanchez JC, Martinez-Sanchez JM, Perez-Fernandez N. Normative data on angular vestibulo-ocular responses in the yaw axis measured using the video head impulse test. *Otol Neurotol.* (2015) 36:466–71. doi: 10.1097/MAO.0000000000000661

16. McGarvie LA, MacDougall HG, Halmagyi GM, Burgess AM, Weber KP, Curthoys IS. The video head impulse test (Vhit) of semicircular canal function - age-dependent normative values of vor gain in healthy subjects. *Front Neurol.* (2015) 6:154. doi: 10.3389/fneur.2015.00154

17. Kim TH, Kim MB. Effect of aging and direction of impulse in video head impulse test. *Laryngoscope.* (2018) 128:E228–E33. doi: 10.1002/lary.26864

18. Pogson JM, Taylor RL, Bradshaw AP, McGarvie L, D'Souza M, Halmagyi GM, et al. The human vestibulo-ocular reflex and saccades: normal subjects and the effect of age. *J Neurophysiol.* (2019) 122:336–49. doi: 10.1152/jn.00847.2018

19. Matta FV, Enticott JC. The effects of state of alertness on the vestibulo-ocular reflex in normal subjects using the vestibular rotational chair. *J Vestib Res.* (2004) 14:387–91. doi: 10.3233/VES-2004-14504

20. Li CW, Hooper RE, Cousins VC. Sinusoidal harmonic acceleration testing in normal humans. *Laryngoscope.* (1991) 101:192–6. doi: 10.1288/00005537-199102000-00016

21. Karmali F, Whitman GT, Lewis RF. Bayesian optimal adaptation explains age-related human sensorimotor changes. *J Neurophysiol.* (2018) 119:509–20. doi: 10.1152/jn.00710.2017

22. Madhani A, Lewis RF, Karmali F. How peripheral vestibular damage affects velocity storage: a causative explanation. *J Assoc Res Otolaryngol.* (2022). doi: 10.1007/s10162-022-00853-3 [Online Ahead of Print].

23. Wall C, III. The sinusoidal harmonic acceleration rotary chair test theoretical and clinical basis. *Neurol Clin.* (1990) 8:269–85. doi: 10.1016/S0733-8619(18)30355-4

24. Lotfi Y, Rezazadeh N, Moossavi A, Haghgoo HA, Rostami R, Bakhshi E, et al. Rotational and collic vestibular-evoked myogenic potential testing in normal developing children and children with combined attention deficit/hyperactivity disorder. *Ear Hear.* (2017) 38:e352–e8. doi: 10.1097/AUD.0000000000000451

25. Jacobson GP, McCaslin DL, Patel S, Barin K, Ramadan NM. Functional and anatomical correlates of impaired velocity storage. *J Am Acad Audiol.* (2004) 15:324–33. doi: 10.3766/jaaa.15.4.6

26. Previc FH. Intravestibular balance and motion sickness. *Aerosp Med Hum Perform.* (2018) 89:130–40. doi: 10.3357/AMHP.4946.2018

27. Cha YH, Golding JF, Keshavarz B, Furman J, Kim JS, Lopez-Escamez JA, et al. Motion sickness diagnostic criteria: consensus document of the classification committee of the barany society. *J Vestib Res.* (2021) 31:327–44. doi: 10.3233/VES-200005

28. Leung AK, Hon KL. Motion sickness: an overview. *Drugs Context.* (2019) 8:2019-9-4. doi: 10.7573/dic.2019-9-4

29. Irmak T, de Winkel KN, Pool DM, Bulthoff HH, Happee R. Individual motion perception parameters and motion sickness frequency sensitivity in fore-aft motion. *Exp Brain Res.* (2021) 239:1727–45. doi: 10.1007/s00221-021-06093-w

30. Peters GL. Migraine overview and summary of current and emerging treatment options. *Am J Manag Care.* (2019) 25:S23–34.

31. Wurthmann S, Naegel S, Roesner M, Nsaka M, Scheffler A, Kleinschnitz C, et al. Sensitized rotatory motion perception and increased susceptibility to motion sickness in vestibular migraine: a cross-sectional study. *Eur J Neurol.* (2021) 28:2357–66. doi: 10.1111/ene.14889

32. Murdin L, Chamberlain F, Cheema S, Arshad Q, Gresty MA, Golding JF, et al. Motion sickness in migraine and vestibular disorders. *J Neurol Neurosurg Psychiatry.* (2015) 86:585–7. doi: 10.1136/jnnp-2014-308331

33. Lackner JR. Motion sickness: more than nausea and vomiting. *Exp Brain Res.* (2014) 232:2493–510. doi: 10.1007/s00221-014-4008-8

frontiers | Frontiers in Neuroscience

TYPE Original Research
PUBLISHED 24 August 2022
DOI 10.3389/fnins.2022.990682

Check for updates

OPEN ACCESS

EDITED BY
Jian-hua Zhuang,
Shanghai Changzheng Hospital, China

REVIEWED BY
Chuyi Tan,
Feinstein Institute for Medical Research, United States
Brenda Cabrera Mendoza,
Yale University, United States
Jun Wang,
Huazhong University of Science and Technology, China

*CORRESPONDENCE
Chunxiang Qin
chunxiangqin@csu.edu.cn

SPECIALTY SECTION
This article was submitted to Perception Science, a section of the journal Frontiers in Neuroscience

RECEIVED 10 July 2022
ACCEPTED 01 August 2022
PUBLISHED 24 August 2022

CITATION
Xiao G, Wang H, Hu J, Liu L, Zhang T, Zhou M, Li X and Qin C (2022) Estimating the causal effect of frailty index on vestibular disorders: A two-sample Mendelian randomization. *Front. Neurosci.* 16:990682. doi: 10.3389/fnins.2022.990682

COPYRIGHT
© 2022 Xiao, Wang, Hu, Liu, Zhang, Zhou, Li and Qin. This is an open-access article distributed under the terms of the Creative Commons Attribution License (CC BY). The use, distribution or reproduction in other forums is permitted, provided the original author(s) and the copyright owner(s) are credited and that the original publication in this journal is cited, in accordance with accepted academic practice. No use, distribution or reproduction is permitted which does not comply with these terms.

Estimating the causal effect of frailty index on vestibular disorders: A two-sample Mendelian randomization

Gui Xiao[1,2], Hu Wang[2], Jiaji Hu[2], Li Liu[1,2], Tingting Zhang[1,2], Mengjia Zhou[1,2], Xingxing Li[1,2] and Chunxiang Qin[1,2]*

[1]Department of Health Management, The Third Xiangya Hospital, Central South University, Changsha, China, [2]Xiangya School of Nursing, Central South University, Changsha, China

Background: Frailty index and vestibular disorders appear to be associated in observational studies, but causality of the association remains unclear.

Methods: A two-sample Mendelian randomization (MR) study was implemented to explore the causal relationship between the frailty index and vestibular disorders in individuals of European descent. A genome-wide association study (GWAS) of frailty index was used as the exposure ($n = 175, 226$), whereas the GWAS of vestibular disorders was the outcome ($n = 462{,}933$). MR Steiger filtering method was conducted to investigate the causal effect of the frailty index on vestibular disorders. An inverse variance weighted (IVW) approach was used as the essential approach to examine the causality. Additionally, the MR-Egger methods, the simple mode analysis, the weighted median analysis, and the weighted mode analysis were used as supplementary methods. The MR-PRESSO analysis, the MR-Egger intercept analysis, and Cochran's Q statistical analysis also were used to detect the possible heterogeneity as well as directional pleiotropy. To evaluate this association, the odds ratio (OR) with 95% confidence intervals (CIs) was used. All statistical analyses were performed in R. The STROBE-MR checklist for the reporting of MR studies was used in this study.

Results: In total, 14 single nucleotide polymorphisms (SNPs) were identified as effective instrumental variables (IVs) in the two sample MR analyses. The significant causal effect of the frailty index on vestibular disorders was demonstrated by IVW method [OR 1.008 (95% CI 1.003, 1.013), $p = 0.001$]. Results from the various sensitivity analysis were consistent. The "leave-one-out" analysis indicated that our results were robust even without a single SNP. According to the MR-Egger intercept test [intercept $= -0.000151$, SE $= 0.011$, $p = 0.544$], genetic pleiotropy did not affect the results. No heterogeneity was detected by Cochran's Q test. Results of MR Steiger directionality test indicated the accuracy of our estimate of the potential causal direction (Steiger $p < 0.001$).

Conclusion: The MR study suggested that genetically predicted frailty index may be associated with an increased risk of vestibular disorders. Notably, considering the limitations of this study, the causal effects between frailty

index and vestibular disorders need further investigation. These results support the importance of effectively managing frailty which may minimize vestibular disorders and improve the quality of life for those with vestibular disorders.

KEYWORDS

frailty index, vestibular disorders, Mendelian randomization, dizziness, vertigo

Introduction

The vestibular disorders (VDs) include a variety of syndromes or (and) diseases arising from disfunction of the inner ear, vestibulocochlear nerve, or central vestibule (Strupp et al., 2020). The symptoms of vestibular disorders involve vertigo, dizziness, and imbalance, which have a strong impact on the daily life and health (Bisdorff et al., 2015). There is a high incidence of vestibular disorders. According to data from the 2001–2004 National Health and Nutrition Examination Surveys (n = 5,086), 35.4% of US adults aged 40 years and older had vestibular dysfunction (Agrawal et al., 2009). The prevalence of dizziness was 16.70% in South Korea according to data from the 2009 to 2010 Korea National Health and Nutrition Examination Surveys, which were cross-sectional surveys of the South Korean civilian, non-institutionalized population aged 40 years and older (n = 3,267) (Koo et al., 2015). Studies have shown that dizziness and vertigo are highly prevalent in the community over the past decade. Dizziness (including vertigo) affects about 15% to over 20% of adults yearly in large population-based studies (Neuhauser, 2016). It is estimated that vestibular disorders pose a substantial burden on the healthcare system because of the high prevalence and severity of symptoms (Kobel et al., 2021). Moreover, vestibular disorders are among the most relevant contributors to the burden of disability among older adults living in the community and associated with immobility, limitations of activities of daily living and decreased participation (Regauer et al., 2020). Studies have focused on factors or diseases associated with vestibular disorders, such as gender, age, hyperglycemia and hypertension, thyroid function abnormalities, abnormal lipid metabolism, and abnormal sex hormone levels (Grill et al., 2016; Bronstein and Dieterich, 2019; Brandt and Dieterich, 2020). Vestibular disorders have been associated with these factors or diseases, but the causal link has not been fully established. Understanding the potential association between vestibular disorders and related diseases or factors, and the underlying mechanisms may facilitate the individualized management and early interventions of patients with vestibular disorders.

Frailty refers to a complex clinical syndrome with the characteristics of a decrease in physiological capacity across multiple organs or systems, as well as an increase in susceptibility to stress (Dent et al., 2019). Frailty increases the risk of hospitalizations, iatrogenic complications, falls and fractures, lower quality of life, and early mortality and other health problems in older people (Vermeiren et al., 2016; Cesari et al., 2017; Junius-Walker et al., 2018; Yang et al., 2018). Frailty index is widely accepted as one operationalization of frailty (Martin and O'Halloran, 2020). The frailty index is a continuous measurement based on the rate of the number of health defects due to aging to all the number of defects considered (Kojima et al., 2018; Palliyaguru et al., 2019). Defects can be manifested as symptoms, signs, diseases, disabilities, laboratory abnormalities, radiographic abnormalities, and social characteristics. The frailty index measurements take into account diverse aspects of health contemporaneously and are highly predictive of a variety of pernicious consequences, such as functional degenerating, physical disabilities, falls, death and morbidity (Theou et al., 2016; Bersani et al., 2020). Thus, the frailty index is a highly sensitive method for representing frailty. Evidence from numerous epidemiological research proved that frailty increases the dizziness risk (de Moraes et al., 2011, 2013; Gomez et al., 2011; Kammerlind et al., 2016). However, the relationship remains doubtful as a result of contrary causality and confounding factors. A randomized controlled trial (RCT) is regarded as the reliable method of demonstrating the causal relationship between frailty index and vestibular disorders (Eichler et al., 2021). Regrettably, it is not usually feasible to conduct RCT because of the complexities of methodology, financial restrictions, and/or difficulty of collecting sufficient samples (Evans and Davey Smith, 2015; Gupta et al., 2017).

Mendelian randomization (MR) analysis is a useful epidemiological research strategy for assessing causal relationships. In MR, genetic variants are used as instrumental variables (IVs) for assessing the causal effect between exposure and outcome. With MR, genotypes can be unbiasedly estimated as they are determined at conception and they are generally not confounded by other factors such as reverse causation (Bowden and Holmes, 2019). Due to this huge advantage, MR has been widely applied in recent years to infer causality from publicly available GWAS summary statistics (Hartwig et al., 2017; Choi et al., 2020; Wang et al., 2022). Herein, a two-sample MR approach was implemented to assess the potential causal effect of frailty index on vestibular disorders in the study.

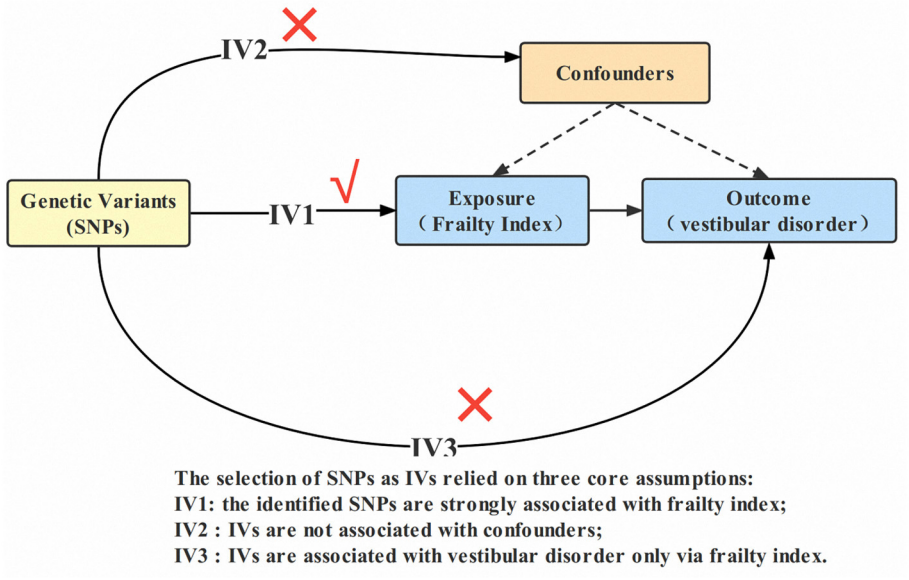

FIGURE 1
Design of the two-sample Mendelian randomization study. IVs, instrumental variables; SNP, single nucleotide polymorphism.

Materials and methods

MR design and data source

The general design of this MR research can be found in Figure 1. The study methods were compliant with the STROBE-MR checklist (Skrivankova et al., 2021). The complete GWAS summary statistics for the frailty index can be downloaded from the GWAS catalog checklist. (https://www.ebi.ac.uk/gwas/downloads/summary-statistics; study accession GCST90020053). A detailed description of the exposures and outcomes of the GWAS used in the MR study can be found in Supplementary Table 1.

Frailty index GWAS dataset

The GWAS involving 175, 226 European ancestry individuals were used to generate the exposure dataset for frailty index. (https://gwas.mrcieu.ac.uk/datasets/ebi-a-GCST90020053/). Notably, Atkins et al. (2021) reported the most comprehensive exploration of genetic influences on the frailty index so far, by performing a genome-wide association study (GWAS) meta-analysis of the frailty index data in European descent UK Biobank participants ($n = 164{,}610$, 60–70 years old) and Swedish Twin Gene participants ($n = 10{,}616$, 41–87 years old). For UK Biobank and Twin Gene, frailty indexes were calculated using 49 or 44 self-reported items on symptoms, disabilities, and diagnosed diseases. The 49 self-reported baseline data variables were used to calculate the frailty index for UK Biobank. Physiological and mental health variables, including symptoms, disabilities, and diagnosed diseases, were reported by participants at baseline (see Supplementary Table 2 for details of the frailty index components included). The 44 deficits were used to calculate the TwinGene's frailty index (see Supplementary Table 3 for details of the frailty index components included). Of the 49 items used in UK Biobank, 29 of these have approximate items in TwinGene. In total, 14 loci were related with the frailty index ($p < 5^{*}10^{-8}$).

Vestibular disorders GWAS dataset

In terms of the GWAS outcome datasets, vestibular disorders were taken from a different independent study that included 462,933 individuals (4,012 cases and 458,921 controls) of European ancestry (https://gwas.mrcieu.ac.uk/datasets/ukb-b-5188/). The GWAS summary data for vestibular disorders was obtained from the MRC-IEU Open GWAS data infrastructure, available through the UK Biobank (Elsworth et al., 2020). UK Biobank is a large, population-based prospective cohort study that enables health-related research. It has already been described in detail how the study will be designed and who will be participating in it. Over 500,000 participants were recruited between 2006 and 2010 for the UK Biobank. The participants provided detailed data *via* questionnaires and verbal interviews, as well as phenotypic data and biological samples. The assessment of vestibular disorders visit comprised electronic

signed consent; a self-completed touch-screen questionnaire; brief computer-assisted interview (Sudlow et al., 2015).

Selection of instrumental variables (IVs)

There are three assumptions that must be satisfied by the IVs used in MR analysis: (1) IVs must be relevant to exposure (i.e., frailty index); (2) IVs must be independent of any confounding factor; and (3) IVs are associated with outcome (i.e., vestibular disorders) only *via* exposure (i.e., frailty index) (Burgess et al., 2013). As a first step, the independent genetic variants (SNPs) with significant genome-wide associations ($p < 5 \times 10^{-8}$) for frailty index were identified as IVs. Then, independent variants were identified using a clumping procedure implemented in R software, in which a linkage-disequilibrium threshold of $r^2 < 0.001$ within a 10,000 kb window in the European 1,000 Genomes Project Phase 3 reference panel was set (Machiela and Chanock, 2015; Myers et al., 2020). The LD of chosen SNPs strongly related to frailty should meet some criteria, for example, $r^2 < 0.001$ and distance >10,000 kb (Myers et al., 2020). From the chosen instrumental SNPs, palindromic SNPs with middle allele frequency were removed (A palindromic SNP is a SNP with the A/T or G/C allele, whereas the "middle allele frequency" are from 0.01 to 0.30). MR Steiger filters are used to exclude SNPs with the incorrect causal direction. Due to their low confidence level, SNPs with a minor allele frequency <0.01 were also eliminated from the original GWAS. Finally, we calculated the explained variance (R^2) and F statistic parameters to determine whether the identified IVs were powerful enough. Generally, IVs (SNPs) with F-statistic parameters <10 are considered weak instruments (Burgess et al., 2017).

MR analyses

Wald ratios were computed to calculate the causal impact of exposure on site-specific outcome mediated by instrumental SNPs (Yu et al., 2015). To calculate the strength of the association between frailty index and vestibular disorders, inverse variance weighted (IVW) approach was used as the essential analysis method in our study. In addition, MR-Egger method, weighted median method, and simple mode method were conducted as supplementary methods (Qi and Chatterjee, 2019). Odds ratios (OR) were used to measure causal effects. in addition, it was calculated using Cochran's Q statistic in order to estimate the heterogeneity of each SNP (Cohen et al., 2015; Wang, 2022). In order to assess the bias caused by ineffective IVs and the possibility of horizontal pleiotropy, MR-Egger intercepts and MR-PRESSO were used (Bowden et al., 2015; Burgess and Thompson, 2017; Verbanck et al., 2018). A "leave-one-out" sensitivity analysis was also conducted in order to determine if a single SNP affected the results (Burgess and Thompson, 2017). Moreover, we used the MR Steiger directionality test to examine whether the results we found followed the direction in our hypothesis. To adjust for confounders, a multivariable MR analysis was performed after MR analysis (Burgess and Thompson, 2015). In this multivariable MR analysis, genetic variants associated with at least one exposure were included, and a multivariable IVW procedure was used to estimate the causal relationship (Burgess and Thompson, 2015). Atkins et al. demonstrated that multiple traits are associated with the risk of frailty, including body mass index (BMI), C-reactive protein (CRP), inflammatory bowel disease (IBD), and smoking initiation (Atkins et al., 2021; Liu et al., 2022). As a result, we included the four covariates in the following multivariable analysis. BMI genetic variants were obtained from the GIANT consortium (Locke et al., 2015). The genetic variants for CRP were obtained from Wojcik et al. (2019). Genetic variants for IBD were obtained from the IIBDGC consortium (Liu et al., 2015). Genetic variants for smoking were obtained from the GSCAN consortium (Liu et al., 2019). Notably, all analyses were conducted using Two Sample MR 0.5.6 and MR-PRESSO packages in R (version 4.2.0, the R Foundation for Statistical Computing, Vienna, Austria). Statistical significance was determined by $p < 0.05$ with two-tailed tests. An FDR correction based on Benjamini-Hochberg was implemented to correct for multiple comparisons (Reiss et al., 2012).

Results

Strength of the instrumental variables

A two-sample MR analysis was applied to examine the causal association between frailty index and vestibular disorders. The generated IVs including 14 SNPs could explain 0.318% of the variance of their corresponding frailty index. In addition, the minimum F statistic of these IVs was 30, suggesting that all IVs were sufficiently effective for the MR analysis (F statistic >10). There were 14 SNPs involved in our analyses, as shown in Table 1.

MR and sensitivity analyses

According to fixed-effect IVW estimates, frailty index significantly contributed to an increased risk of vestibular disorders [OR 1.008 (95% CI 1.003, 1.013), $p = 0.001$] (shown in Table 2; Figures 2, 3). For the IVW method, Cochran's Q statistic was 11.75 ($p = 0.466$), suggesting a low level of heterogeneity and relative reliability of the causal effect. Additionally, weighted median analysis [OR 1.010 (95% CI 1.003, 1.017), $p = 0.005$], simple mode analysis [OR 1.009 (95% CI 0.998, 1.020), $p = 0.162$], weighted mode analysis [OR 1.011 (95% CI 1.002, 1.021),

TABLE 1 The characteristics of 14 SNPs and their genetic associations with frailty index and vestibular disorders.

SNP	Chr	EA	OA	EAF	*F*-statistics	SNP-frailty index association			SNP-vestibular disorders association		
						Beta	SE	*p*-value	Beta	SE	*p*-value
rs10891490	11	C	T	0.5915	31	−0.0188	0.0034	2.00E-08	−0.000407302	0.000196225	0.03
rs12739243	1	C	T	0.2206	37	−0.0242	0.004	1.28E-09	0.000339685	0.000233882	0.15
rs1363103	5	C	T	0.38	32	−0.0191	0.0034	2.23E-08	2.02E-05	0.000199038	0.92
rs17612102	15	C	T	0.5933	30	0.0187	0.0034	2.85E-08	6.23E-05	0.000196554	0.75
rs2071207	3	C	T	0.478	32	−0.0187	0.0033	1.47E-08	−0.000154846	0.000192738	0.42
rs2396766	7	A	G	0.4725	37	0.0201	0.0033	1.22E-09	0.000251141	0.000193096	0.19
rs3959554	15	G	A	0.4177	31	0.0189	0.0034	1.74E-08	0.00015428	0.000195434	0.43
rs4146140	10	T	C	0.3811	34	−0.0198	0.0034	6.83E-09	−2.96E-05	0.000199535	0.88
rs4952693	2	T	C	0.3734	33	−0.0194	0.0034	1.47E-08	−3.85E-05	0.000199655	0.85
rs56299474	8	A	C	0.1733	30	0.0241	0.0044	3.94E-08	−4.98E-05	0.00025414	0.84
rs583514	3	C	T	0.5111	36	0.0199	0.0033	1.65E-09	0.000195733	0.000192951	0.31
rs8089807	18	T	C	0.1866	33	−0.0248	0.0043	6.50E-09	−0.000436891	0.000248114	0.07
rs82334	4	C	A	0.3177	41	−0.0223	0.0035	3.13E-10	−0.000355566	0.000207515	0.08
rs9275160	6	A	G	0.3397	119	0.0382	0.0035	7.18E-28	0.000475587	0.00020293	0.01

SNP, single nucleotide polymorphism; Chr, chromosome; EA, effect allele; OA, other allele; EAF, frequency of effect allele; SE, standard error.

TABLE 2 Association of frailty index with vestibular disorders using various methods.

Methods	OR	LCI	UCI	*p*-value
Fixed-effect IVW	1.00784921	1.00297777	1.01274430	0.001**
Weighted median	1.00965905	1.00297798	1.01638462	0.005**
Simple mode	1.00865773	0.99721538	1.02023138	0.162
Weighted mode	1.01137620	1.00185004	1.02099293	0.030*
MR-Egger	1.01455225	0.99311915	1.03644791	0.209

**p < 0.01; *p < 0.05; OR, odds ratio; LCI, lower confidence interval; UCI, upper; IVW, inverse-variance weighted.

$p = 0.036$], and MR-Egger analysis [OR 1.015 (95% CI 0.993, 1.036), $p = 0.209$] also indicated comparable results (Table 2; Figure 2). MR analysis turned out to be reliable according to the results based on the "leave-one-out" analysis (shown in Figure 4; Supplementary Table 4). The horizontal pleiotropy between IVs and outcomes was investigated using MR-Egger regression, but no significant intercept was found [intercept = −0.000151, SE = 0.011, $p = 0.544$] (shown in Table 3). Furthermore, MR-PRESSO results indicated that horizontal pleiotropy did not exist in the MR study ($p = 0.491$). Based on the funnel plot results (shown in Supplementary Figure 1), there was neither horizontal pleiotropy nor heterogeneity in our MR study. Results of the MR Steiger directionality test indicated the accuracy of our estimate of the causal direction (Steiger $p < 0.001$). The estimated causal effect of frailty index on vestibular disorders may be still significant after adjustment for BMI (OR = 1.006, 95% CI 1.000–1.012, FDR-corrected $p = 0.035$), CRP (OR = 1.008, 95% CI 1.003–1.012, FDR-corrected $p = 0.0007$), IBD (OR = 1.006, 95% CI 1.000–1.012, FDR-corrected $p = 0.035$) and smoking (OR = 1.008, 95% CI 1.004–1.012, FDR-corrected $p = 0.0007$) (shown in Supplementary Tables 5, 6). As a consequence, we found that the frailty index may be causally related to vestibular disorders.

Discussion

Based on the summary level data from large GWAS, we implemented the two-sample MR study with the purpose of investigating the causal association between frailty index and vestibular disorders. We found a causality between genetically predicted frailty index and vestibular disorders in our analysis. The sensitivity analyses showed consistent estimates, indicating that there was minimal horizontal pleiotropy and the association was robust. According to our knowledge, this is the first MR study to evaluate the potential causality of frailty index and vestibular disorders.

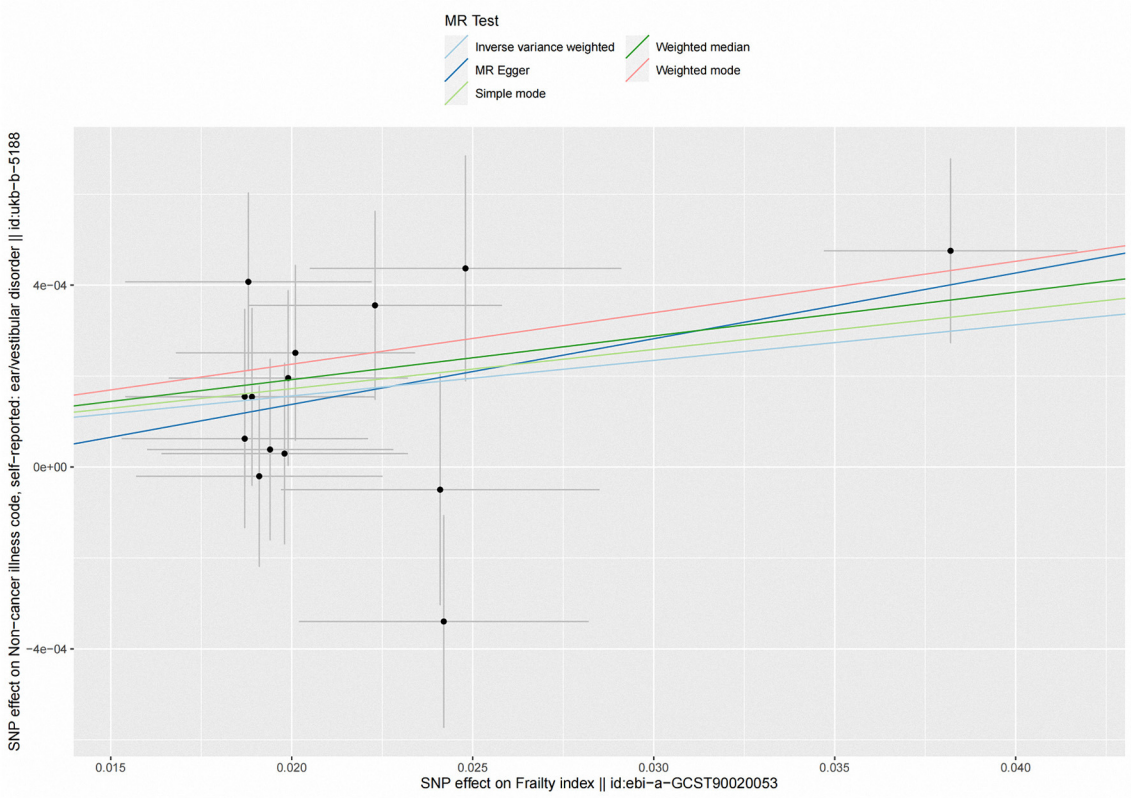

FIGURE 2
Scatter plot of the effects of genetic variants on frailty index and vestibular disorders. The slopes of the solid lines denote the magnitudes of the associations estimated from the MR analyses. MR, Mendelian randomization; SNP, single-nucleotide polymorphism.

Vestibular disorders are mainly characterized by dysfunction of the vestibular system, involving body posture and motion perception, eye movement control, posture, gait, and spatial positioning. According to the proposed structure of the international classification of vestibular disorders (ICVD), there are four layers about vestibular disorders: symptoms and signs; clinical syndromes; diseases/disorders; and pathophysiologic mechanisms. Four categories of vestibular symptoms are described by the ICVD: vertigo, dizziness, vestibulovisual symptoms, and postural symptoms (Bisdorff et al., 2015). Vertigo and dizziness are one of the most common complaints in patients with vestibular disorders. In a previous study, researchers have found that patients with intractable dizziness are more likely to develop frailty (Gomez et al., 2011). According to research, community-dwelling elderly adults with frailty are much more likely to experience dizziness. Furthermore, Researchers have discovered that older adults who report dizziness tend to be physically frail, have more chronic diseases and sensory impairments (de Moraes et al., 2011, 2013; Gomez et al., 2011; Kammerlind et al., 2016). Dizziness, unsteadiness, or lightheadedness is associated with frailty, and in fully adjusted models, frailty was still related to dizziness, unsteadiness, or lightheadedness (O'Connell et al., 2015; Goshtasbi et al., 2020). Because of the limitations of observational epidemiological studies in eliminating bias (for example, reverse causation and confounding factors), while observational studies have reported a relationship between frailty and vestibular disease, little is known about their causal relationship.

The results of our study suggested that vestibular disorders may be independently affected by the genetic liability to frailty index. Notably, Atkins et al. (2021) demonstrated that multiple traits including BMI, CRP, IBD, and smoking initiation are associated with the risk of frailty (Liu et al., 2022). In this study, multivariable MR analysis including the four traits was undertaken in order to evaluate the causal relationship between genetically predicted frailty index and the risk of vestibular disorders. The results indicate that frailty index may be still associated with an increased risk of vestibular disorders after adjustment for BMI, CRP, IBD and smoking. According to the results of the systematic review and meta-analysis conducted by Yuan et al. (2021) obesity or underweight is associated with an increased risk of frailty in community-dwelling older adults. Studies also found that frailty are associated with CRP and IBD (Soysal et al., 2016; Kochar et al., 2021). Smoking is one of the

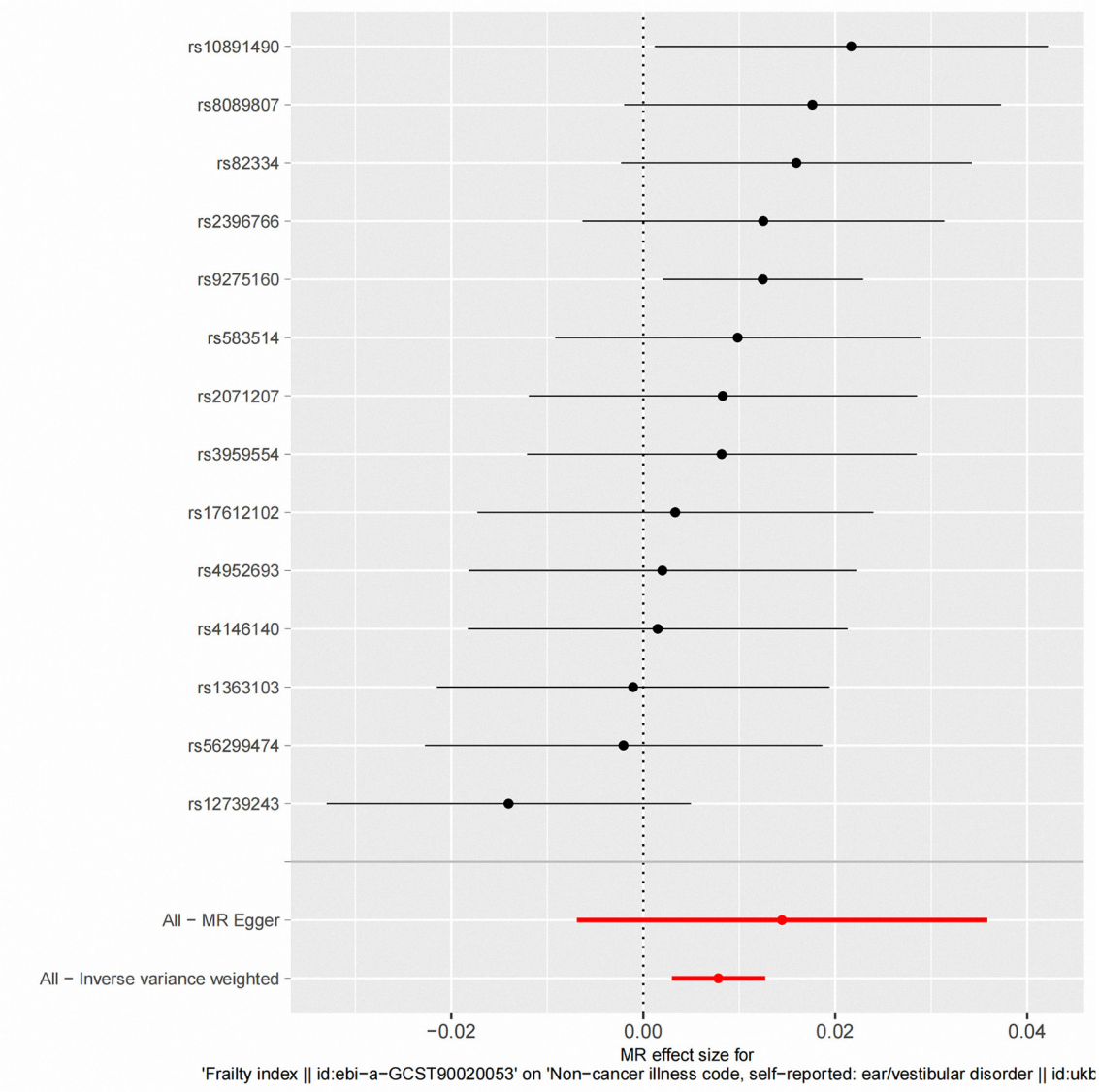

FIGURE 3
Fixed-effect IVW analysis of the causal association between frailty index and vestibular disorders. The black dots and bars indicate the causal estimate and 95% CI using each SNP. The red dot and bar indicate the overall estimate and 95% CI meta-analyzed by fixed-effect IVW method. IVW, inverse-variance weighted; HI, hearing impairment; CI, confidence interval; SNP, single nucleotide polymorphism.

main causes of health problems worldwide and can also lead to an increased risk of frailty. In addition, smoking-associated frailty may be linked to epigenetic changes (Gao et al., 2017). Notably, it is necessary to conduct further research to replicate our findings in relation to frailty and vestibular disorders due to the potential confounders.

The mechanisms involved in frailty resulting in vestibular disease are complex and poorly understood. Frailty is a complicated and prevalent age-related clinical syndrome characterized by a decline in physiological capacities across multiple organs or (and) systems (Vermeiren et al., 2016; Cesari et al., 2017; Dent et al., 2019). There is a close connection between aging and frailty (Mitnitski et al., 2017). A number of studies have demonstrated that vestibular function declines with aging (Brosel et al., 2016). It is believed that the central vestibular system, vision, and proprioception slowly deteriorate with aging, contributing to vestibular compensation mechanisms degrading. The vestibular system is revealed to lose neural cells with aging through anatomical studies (Bouccara et al., 2018; Krager, 2018; Vanspauwen, 2018). It is becoming increasingly clear that biological aging (vs. chronological aging) contributes to the development of chronic diseases and physical frailty at

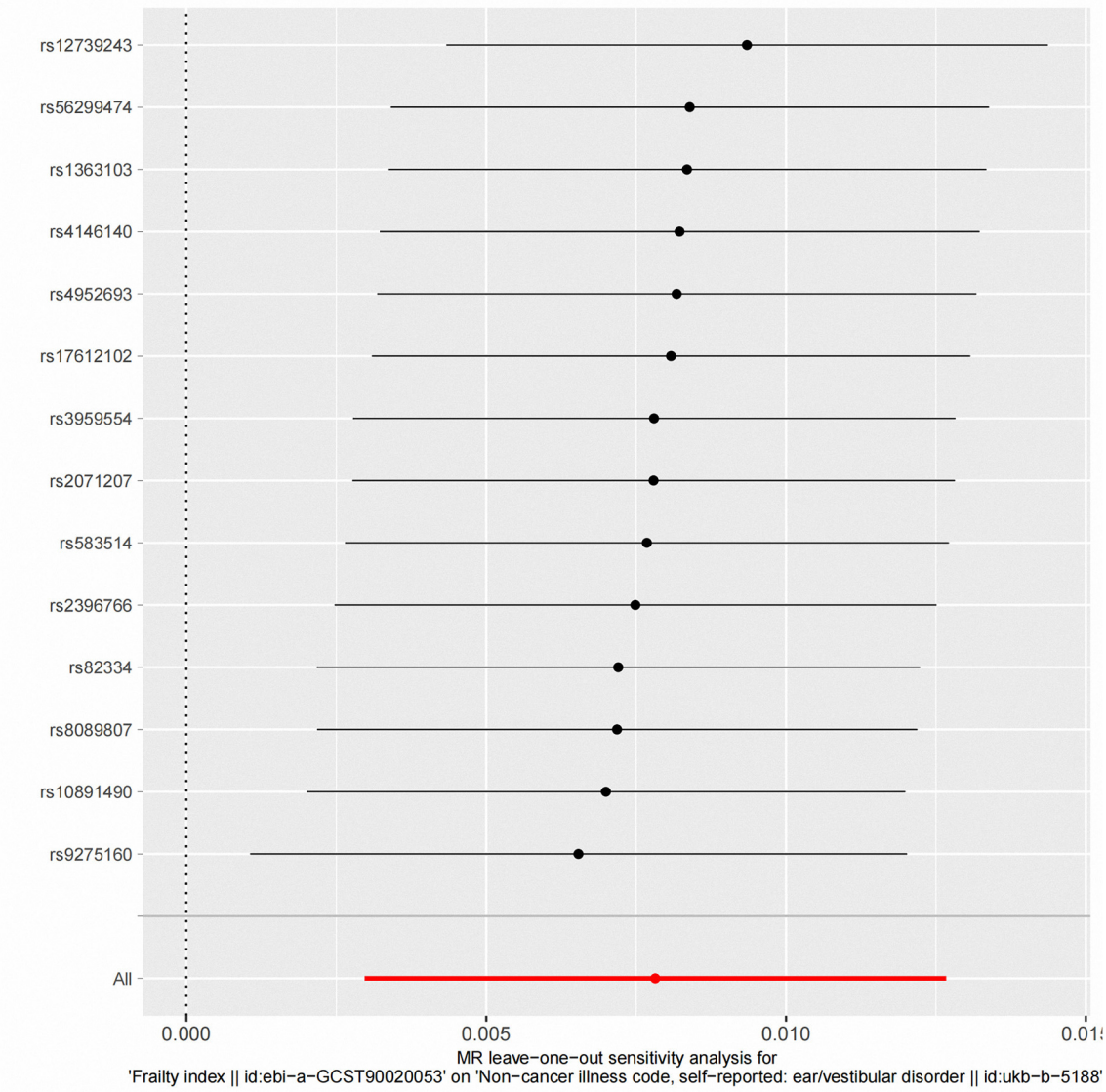

FIGURE 4
"Leave-one-out" analysis of the causal association of frailty Index and vestibular disorders. The black dots and bars indicate the causal estimate and 95% CI when an SNP was removed in turn. The red dot and bar indicate the overall estimate and 95% CI using the fixed-effect IVW method; CI, confidence interval; SNP, single nucleotide polymorphism; IVW, inverse-variance weighted.

TABLE 3 MR-Egger intercept test results of the association between frailty index and vestibular disorders.

Estimates	SE	LCI	UCI	*p*-value
−0.000151	0.011	−0.007	0.036	0.544

the molecular and cellular level which can lead to decline and death (Fougere et al., 2017). Furthermore, a cross-sectional study has shown that frailty is independently associated with mortality and prolonged hospital stays following vestibular schwannoma resection (Dicpinigaitis et al., 2021; Tang et al., 2022). Compared with advanced patient age alone, frailty may be more accurate for predicting vestibular schwannoma resection outcomes. Health-related outcomes are more likely to be determined by frailty than by age, and targeted interventions may prevent or mitigate frailty (de Labra et al., 2015; Wilson et al., 2015; Bray et al., 2016). Frailty starts before age 65 in many studies, and not all older people develop frailty, despite their advanced age (Dent et al., 2019). Most intervention trials involve older people, despite the fact that frailty can affect people at any age (especially if comorbid conditions are present). Frailty index is an important indicator of accelerated biological aging (when the organism exceeds its actual age). Research has proved the frailty index

score was a remarkable predictor of morbidity and mortality in chronologically young orthopedic trauma patients (Kojima et al., 2018; Grabovac et al., 2019). Notably, the prevalence of frailty and prefrailty was 45.9% in the young adults in a previous study (Yasuda, 2021). A growing number of young people suffer from benign paroxysmal positional vertigo (BPPV, one of the most primary vestibular disorders), in which frailty is one of the risk factors for BPPV in young people (Wang et al., 2021). Therefore, in addition to vestibular degeneration associated with frailty, more mechanisms need to be explored as frailty becomes younger.

There are several strengths to the study. It is the first report using summary level data from large GWASs to confirm the potential causal relationship between frailty index and vestibular disorders. In order to verify the hypothesis, several sensitivity analyses were carried out. Additionally, multivariate analysis was performed in order to adjust for confounding factors. And to a certain extent make our results more reliable. However, there are several limitations in our MR analysis. First, given the classification of the original data, we could not further subdivide the pressure type of vestibular disorders, and thus we could only analyze the vestibular disorders as a whole. Second, although Mendelian randomization has been shown to be a powerful method to assess the causality between frailty index and vestibular disorders, the two-sample MR analysis only provides an estimate of the putative causal effect, and further studies are required to estimate a direct causal effect of frailty on vestibular disorders. Third, a reverse causal association (effect of vestibular disorders on frailty) was not evaluated in this study. The fourth limitation is that the GWAS data were compiled for individuals of European descent, which means that the population at large might not be fully represented by our results. Fifth, the two GWAS datasets are from European populations, there will be an overlap of samples. Over-fitting and instrument bias become more pronounced as overlap between samples increases, similar to those observed in one-sample MR. Last, the two European samples could differ substantially according to population characteristics such as socio-economic background, which also could affect the interpretation of causal estimates.

Conclusion

In our study, we found that vestibular disorders may be causally related to frailty index. Notably, considering the limitations of this study, the causal effects between frailty index and vestibular disorders need further investigation. These results support the importance of effectively managing frailty which may minimize vestibular disorders and improve the quality of life for those with vestibular disorders.

Data availability statement

The original contributions presented in the study are included in the article/Supplementary material, further inquiries can be directed to the corresponding author/s.

Author contributions

GX and CQ conceptualized and designed the study. GX, HW, and JH prepared and analyzed the data and drafted the manuscript. LL, TZ, MZ, and XL contributed to interpretation and editing of the manuscript. All authors contributed to the article and approved the submitted version.

Funding

This work was supported by the National Natural Science Foundation of China (Grant Number 72074225), the Philosophy and Social Science Foundation of Hunan Province (Grant Number 19YBA351), and the Key R&D Plan of Hunan Province (Grant Number 2020SK2089). The funding sources played no role in conducting the research and preparing the article.

Acknowledgments

We would like to thank the Xiangya Center for Evidence-Based Practice & Healthcare Innovation: A Joanna Briggs Institute Affiliated Group of Central South university for statistical assistance.

Conflict of interest

The authors declare that the research was conducted in the absence of any commercial or financial relationships that could be construed as a potential conflict of interest.

Publisher's note

All claims expressed in this article are solely those of the authors and do not necessarily represent those of their affiliated organizations, or those of the publisher, the editors and the reviewers. Any product that may be evaluated in this article, or claim that may be made by its manufacturer, is not guaranteed or endorsed by the publisher.

Supplementary material

The Supplementary Material for this article can be found online at: https://www.frontiersin.org/articles/10.3389/fnins.2022.990682/full#supplementary-material

References

Agrawal, Y., Carey, J. P., Della Santina, C. C., Schubert, M. C., and Minor, L. B. (2009). Disorders of balance and vestibular function in US adults: data from the National Health and Nutrition Examination Survey, 2001–2004. *Arch. Intern. Med.* 169, 938–944. doi: 10.1001/archinternmed.2009.66

Atkins, J. L., Jylhava, J., Pedersen, N. L., Magnusson, P. K., Lu, Y., Wang, Y., et al. (2021). A genome-wide association study of the frailty index highlights brain pathways in ageing. *Aging Cell.* 20, e13459. doi: 10.1111/acel.13459

Bersani, F. S., Canevelli, M., Cesari, M., Maggioni, E., Pasquini, M., Wolkowitz, O. M., et al. (2020). Frailty Index as a clinical measure of biological age in psychiatry. *J. Affect Disord.* 268, 183–187. doi: 10.1016/j.jad.2020.03.015

Bisdorff, A. R., Staab, J. P., and Newman-Toker, D. E. (2015). Overview of the international classification of vestibular disorders. *Neurol. Clin.* 33, 541–550. doi: 10.1016/j.ncl.2015.04.010

Bouccara, D., Rubin, F., Bonfils, P., and Lisan, Q. (2018). [Management of vertigo and dizziness]. *Rev. Med. Interne.* 39, 869–874. doi: 10.1016/j.revmed.2018.02.004

Bowden, J., Davey Smith, G., and Burgess, S. (2015). Mendelian randomization with invalid instruments: effect estimation and bias detection through Egger regression. *Int. J. Epidemiol.* 44, 512–525. doi: 10.1093/ije/dyv080

Bowden, J., and Holmes, M. V. (2019). Meta-analysis and mendelian randomization: a review. *Res. Synth. Methods.* 10, 486–496. doi: 10.1002/jrsm.1346

Brandt, T., and Dieterich, M. (2020). 'Excess anxiety' and 'less anxiety': both depend on vestibular function. *Curr. Opin. Neurol.* 33, 136–141. doi: 10.1097/WCO.0000000000000771

Bray, N. W., Smart, R. R., Jakobi, J. M., and Jones, G. R. (2016). Exercise prescription to reverse frailty. *Appl. Physiol. Nutr. Metab.* 41, 1112–1116. doi: 10.1139/apnm-2016-0226

Bronstein, A. M., and Dieterich, M. (2019). Long-term clinical outcome in vestibular neuritis. *Curr. Opin. Neurol.* 32, 174–180. doi: 10.1097/WCO.0000000000000652

Brosel, S., Laub, C., Averdam, A., Bender, A., and Elstner, M. (2016). Molecular aging of the mammalian vestibular system. *Ageing Res. Rev.* 26, 72–80. doi: 10.1016/j.arr.2015.12.007

Burgess, S., Butterworth, A., and Thompson, S. G. (2013). Mendelian randomization analysis with multiple genetic variants using summarized data. *Genet. Epidemiol.* 37, 658–665. doi: 10.1002/gepi.21758

Burgess, S., Small, D. S., and Thompson, S. G. A. (2017). Review of instrumental variable estimators for Mendelian randomization. *Stat. Methods Med. Res.* 26, 2333–2355. doi: 10.1177/0962280215597579

Burgess, S., and Thompson, S. G. (2015). Multivariable Mendelian randomization: the use of pleiotropic genetic variants to estimate causal effects. *Am. J. Epidemiol.* 181, 251–260. doi: 10.1093/aje/kwu283

Burgess, S., and Thompson, S. G. (2017). Interpreting findings from Mendelian randomization using the MR-Egger method. *Eur. J. Epidemiol.* 32, 377–389. doi: 10.1007/s10654-017-0255-x

Cesari, M., Calvani, R., and Marzetti, E. (2017). Frailty in older persons. *Clin. Geriatr. Med.* 33, 293–303. doi: 10.1016/j.cger.2017.02.002

Choi, Y., Lee, S. J., Spiller, W., Jung, K. J., Lee, J. Y., Kimm, H., et al. (2020). Causal associations between serum bilirubin levels and decreased stroke risk: a two-sample mendelian randomization study. *Arterioscler. Thromb. Vasc. Biol.* 40, 437–445. doi: 10.1161/ATVBAHA.119.313055

Cohen, J. F., Chalumeau, M., Cohen, R., Korevaar, D. A., Khoshnood, B., Bossuyt, P. M., et al. (2015). Cochran's Q test was useful to assess heterogeneity in likelihood ratios in studies of diagnostic accuracy. *J. Clin. Epidemiol.* 68, 299–306. doi: 10.1016/j.jclinepi.2014.09.005

de Labra, C., Guimaraes-Pinheiro, C., Maseda, A., Lorenzo, T., and Millan-Calenti, J. C. (2015). Effects of physical exercise interventions in frail older adults: a systematic review of randomized controlled trials. *BMC Geriatr.* 15, 154. doi: 10.1186/s12877-015-0155-4

de Moraes, S. A., Soares, W. J., Ferriolli, E., and Perracini, M. R. (2013). Prevalence and correlates of dizziness in community-dwelling older people: a cross sectional population based study. *BMC Geriatr.* 13, 4. doi: 10.1186/1471-2318-13-4

de Moraes, S. A., Soares, W. J., Rodrigues, R. A., Fett, W. C., Ferriolli, E., Perracini, M. R., et al. (2011). Dizziness in community-dwelling older adults: a population-based study. *Braz. J. Otorhinolaryngol.* 77, 691–699. doi: 10.1590/S1808-86942011000600003

Dent, E., Martin, F. C., Bergman, H., Woo, J., Romero-Ortuno, R., Walston, J. D., et al. (2019). Management of frailty: opportunities, challenges, and future directions. *Lancet.* 394, 1376–1386. doi: 10.1016/S0140-6736(19)31785-4

Dicpinigaitis, A. J., Kalakoti, P., Schmidt, M., Gurgel, R., Cole, C., Carlson, A., et al. (2021). Associations of baseline frailty status and age with outcomes in patients undergoing vestibular schwannoma resection. *JAMA Otolaryngol. Head Neck Surg.* 147, 608–614. doi: 10.1001/jamaoto.2021.0670

Eichler, H. G., Pignatti, F., Schwarzer-Daum, B., Hidalgo-Simon, A., Eichler, I., Arlett, P., et al. (2021). Randomized controlled trials versus real world evidence: neither magic nor myth. *Clin. Pharmacol. Ther.* 109, 1212–1218. doi: 10.1002/cpt.2083

Elsworth, B., Lyon, M., Alexander, T., Liu, Y., Matthews, P., Hallett, J., et al. (2020). The MRC IEU Open GWAS data infrastructure. *bioRxiv* 08, 244293. doi: 10.1101/2020.08.10.244293

Evans, D. M., and Davey Smith, G. (2015). Mendelian randomization: new applications in the coming age of hypothesis-free causality. *Ann. Rev. Genom. Hum. Genet.* 16, 327–350. doi: 10.1146/annurev-genom-090314-050016

Fougere, B., Boulanger, E., Nourhashemi, F., Guyonnet, S., and Cesari, M. (2017). Chronic inflammation: accelerator of biological aging. *J. Gerontol. A Biol. Sci. Med. Sci.* 72, 1218–1225. doi: 10.1093/gerona/glw240

Gao, X., Zhang, Y., Saum, K. U., Schottker, B., Breitling, L. P., Brenner, H., et al. (2017). Tobacco smoking and smoking-related DNA methylation are associated with the development of frailty among older adults. *Epigenetics.* 12, 149–156. doi: 10.1080/15592294.2016.1271855

Gomez, F., Curcio, C. L., and Duque, G. (2011). Dizziness as a geriatric condition among rural community-dwelling older adults. *J. Nutr. Health Aging.* 15, 490–497. doi: 10.1007/s12603-011-0050-4

Goshtasbi, K., Abouzari, M., Soltanzadeh-Zarandi, S., Sarna, B., Lee, A., Hsu, F. P. K., et al. (2020). The association of age, body mass index, and frailty with vestibular schwannoma surgical morbidity. *Clin. Neurol. Neurosurg.* 197, 106192. doi: 10.1016/j.clineuro.2020.106192

Grabovac, I., Haider, S., Mogg, C., Majewska, B., Drgac, D., Oberndorfer, M., et al. (2019). Frailty status predicts all-cause and cause-specific mortality in community dwelling older adults. *J. Am. Med. Dir. Assoc.* 20, 1230–1235. doi: 10.1016/j.jamda.2019.06.007

Grill, E., Penger, M., and Kentala, E. (2016). Health care utilization, prognosis and outcomes of vestibular disease in primary care settings: systematic review. *J. Neurol.* 263 Suppl 1, S36–44. doi: 10.1007/s00415-015-7913-2

Gupta, V., Walia, G. K., and Sachdeva, M. P. (2017). 'Mendelian randomization': an approach for exploring causal relations in epidemiology. *Public Health.* 145, 113–119. doi: 10.1016/j.puhe.2016.12.033

Hartwig, F. P., Borges, M. C., Horta, B. L., Bowden, J., and Davey Smith, G. (2017). Inflammatory biomarkers and risk of schizophrenia: a 2-sample mendelian randomization study. *JAMA Psychiatr.* 74, 1226–1233. doi: 10.1001/jamapsychiatry.2017.3191

Junius-Walker, U., Onder, G., Soleymani, D., Wiese, B., Albaina, O., Bernabei, R., et al. (2018). The essence of frailty: a systematic review and qualitative synthesis on frailty concepts and definitions. *Eur. J. Intern. Med.* 56, 3–10. doi: 10.1016/j.ejim.2018.04.023

Kammerlind, A. S., Ernsth Bravell, M., and Fransson, E. I. (2016). Prevalence of and factors related to mild and substantial dizziness in community-dwelling older adults: a cross-sectional study. *BMC Geriatr.* 16, 159. doi: 10.1186/s12877-016-0335-x

Kobel, M. J., Wagner, A. R., Merfeld, D. M., and Mattingly, J. K. (2021). Vestibular thresholds: a review of advances and challenges in clinical applications. *Front. Neurol.* 12, 643634. doi: 10.3389/fneur.2021.643634

Kochar, B., Orkaby, A. R., Ananthakrishnan, A. N., and Ritchie, C. S. (2021). Frailty in inflammatory bowel diseases: an emerging concept. *Therap. Adv. Gastroenterol.* 14, 17562848211025474. doi: 10.1177/17562848211025474

Kojima, G., Iliffe, S., and Walters, K. (2018). Frailty index as a predictor of mortality: a systematic review and meta-analysis. *Age Ageing.* 47, 193–200. doi: 10.1093/ageing/afx162

Koo, J. W., Chang, M. Y., Woo, S. Y., Kim, S., and Cho, Y. S. (2015). Prevalence of vestibular dysfunction and associated factors in South Korea. *BMJ Open.* 5, e008224. doi: 10.1136/bmjopen-2015-008224

Krager, R. (2018). Assessment of vestibular function in elderly patients. *Curr. Opin. Otolaryngol. Head Neck Surg.* 26, 302–306. doi: 10.1097/MOO.0000000000000476

Liu, J. Z., van Sommeren, S., Huang, H., Ng, S. C., Alberts, R., Takahashi, A., et al. (2015). Association analyses identify 38 susceptibility loci for inflammatory bowel disease and highlight shared genetic risk across populations. *Nat. Genet*. 47, 979–986. doi: 10.1038/ng.3359

Liu, M., Jiang, Y., Wedow, R., Li, Y., Brazel, D. M., Chen, F., et al. (2019). Association studies of up to 1.2 million individuals yield new insights into the genetic etiology of tobacco and alcohol use. *Nat. Genet*. 51, 237–244. doi: 10.1038/s41588-018-0307-5

Liu, W., Zhang, L., Fang, H., Gao, Y., Liu, K., Li, S., et al. (2022). Genetically predicted frailty index and risk of stroke and Alzheimer's disease. *Eur. J. Neurol*. 29, 1913–1921. doi: 10.1111/ene.15332

Locke, A. E., Kahali, B., Berndt, S. I., Justice, A. E., Pers, T. H., Day, F. R., et al. (2015). Genetic studies of body mass index yield new insights for obesity biology. *Nature*. 518, 197–206. doi: 10.1038/nature14177

Machiela, M. J., and Chanock, S. J. (2015). LDlink: a web-based application for exploring population-specific haplotype structure and linking correlated alleles of possible functional variants. *Bioinformatics*. 31, 3555–3557. doi: 10.1093/bioinformatics/btv402

Martin, F. C., and O'Halloran, A. M. (2020). Tools for assessing frailty in older people: general concepts. *Adv. Exp. Med. Biol*. 1216, 9–19. doi: 10.1007/978-3-030-33330-0_2

Mitnitski, A. B., Rutenberg, A. D., Farrell, S., and Rockwood, K. (2017). Aging, frailty and complex networks. *Biogerontology*. 18, 433–446. doi: 10.1007/s10522-017-9684-x

Myers, T. A., Chanock, S. J., and Machiela, M. J. (2020). LDlinkR: an R package for rapidly calculating linkage disequilibrium statistics in diverse populations. *Front. Genet*. 11, 157. doi: 10.3389/fgene.2020.00157

Neuhauser, H. K. (2016). The epidemiology of dizziness and vertigo. *Handb. Clin. Neurol*. 137, 67–82. doi: 10.1016/B978-0-444-63437-5.00005-4

O'Connell, M. D., Savva, G. M., Fan, C. W., and Kenny, R. A. (2015). Orthostatic hypotension, orthostatic intolerance and frailty: the Irish longitudinal study on aging-TILDA. *Arch. Gerontol. Geriatr*. 60, 507–513. doi: 10.1016/j.archger.2015.01.008

Palliyaguru, D. L., Moats, J. M., Di Germanio, C., Bernier, M., and Cabo, D. (2019). Frailty index as a biomarker of lifespan and healthspan: Focus on pharmacological interventions. *Mech. Ageing Dev*. 180, 42–48. doi: 10.1016/j.mad.2019.03.005

Qi, G., and Chatterjee, N. (2019). Mendelian randomization analysis using mixture models for robust and efficient estimation of causal effects. *Nat. Commun*. 10, 1941. doi: 10.1038/s41467-019-09432-2

Regauer, V., Seckler, E., Muller, M., and Bauer, P. (2020). Physical therapy interventions for older people with vertigo, dizziness and balance disorders addressing mobility and participation: a systematic review. *BMC Geriatr*. 20, 494. doi: 10.1186/s12877-020-01899-9

Reiss, P. T., Schwartzman, A., Lu, F., Huang, L., and Proal, E. (2012). Paradoxical results of adaptive false discovery rate procedures in neuroimaging studies. *Neuroimage*. 63, 1833–1840. doi: 10.1016/j.neuroimage.2012.07.040

Skrivankova, V. W., Richmond, R. C., Woolf, B. A. R., Yarmolinsky, J., Davies, N. M., Swanson, S. A., et al. (2021). Strengthening the reporting of observational studies in epidemiology using mendelian randomization: the STROBE-MR statement. *JAMA*. 326, 1614–1621. doi: 10.1001/jama.2021.18236

Soysal, P., Stubbs, B., Lucato, P., Luchini, C., Solmi, M., Peluso, R., et al. (2016). Inflammation and frailty in the elderly: a systematic review and meta-analysis. *Ageing Res. Rev*. 31, 1–8. doi: 10.1016/j.arr.2016.08.006

Strupp, M., Dlugaiczyk, J., Ertl-Wagner, B. B., Rujescu, D., Westhofen, M., Dieterich, M., et al. (2020). Vestibular disorders. *Dtsch. Arztebl. Int*. 117, 300–310. doi: 10.3238/arztebl.2020.0300

Sudlow, C., Gallacher, J., Allen, N., Beral, V., Burton, P., Danesh, J., et al. (2015). UK biobank: an open access resource for identifying the causes of a wide range of complex diseases of middle and old age. *PLoS Med*. 12, e1001779. doi: 10.1371/journal.pmed.1001779

Tang, O. Y., Bajaj, A. I., Zhao, K., Rivera Perla, K. M., Ying, Y. M., Jyung, R. W. et al. (2022). Association of patient frailty with vestibular schwannoma resection outcomes, machine learning development of a vestibular schwannoma risk stratification. *Score*. 22, 98. doi: 10.1227/neu.0000000000001998

Theou, O., Tan, E. C. K., Bell, J. S., Emery, T., Robson, L., Morley, J. E., et al. (2016). Frailty levels in residential aged care facilities measured using the frailty index and FRAIL-NH scale. *J. Am. Geriatr. Soc*. 64, E207–E12. doi: 10.1111/jgs.14490

Vanspauwen, R. (2018). Dizziness and (Fear of) Falling in The Elderly: A Few Facts. *J Int. Adv. Otol*. 14, 1–2. doi: 10.5152/iao.2018.0201815

Verbanck, M., Chen, C. Y., Neale, B., and Do, R. (2018). Detection of widespread horizontal pleiotropy in causal relationships inferred from Mendelian randomization between complex traits and diseases. *Nat. Genet*. 50, 693–698. doi: 10.1038/s41588-018-0099-7

Vermeiren, S., Vella-Azzopardi, R., Beckwee, D., Habbig, A. K., Scafoglieri, A., Jansen, B., et al. (2016). Frailty and the prediction of negative health outcomes: a meta-analysis. *J. Am. Med. Dir. Assoc*. 17, 1163.e1-e17. doi: 10.1016/j.jamda.2016.09.010

Wang, A., Zhou, G., Kawai, K., O'Brien, M., Shearer, A. E., Brodsky, J. R., et al. (2021). Benign paroxysmal positional vertigo in children and adolescents with concussion. *Sports Health*. 13, 380–386. doi: 10.1177/1941738120970515

Wang, J., Liu, D., Tian, E., Guo, Z. Q., Chen, J. Y., Kong, W. J., et al. (2022). Is hearing impairment causally associated with falls? evidence from a two-sample Mendelian randomization study. *Front. Neurol*. 13, 876165. doi: 10.3389/fneur.2022.876165

Wang, R. (2022). Mendelian randomization study updates the effect of 25-hydroxyvitamin D levels on the risk of multiple sclerosis. *J. Transl. Med*. 20, 3. doi: 10.1186/s12967-021-03205-6

Wilson, M. G., Beland, F., Julien, D., Gauvin, L., Guindon, G. E., Roy, D., et al. (2015). Interventions for preventing, delaying the onset, or decreasing the burden of frailty: an overview of systematic reviews. *Syst. Rev*. 4, 128. doi: 10.1186/s13643-015-0110-7

Wojcik, G. L., Graff, M., Nishimura, K. K., Tao, R., Haessler, J., Gignoux, C. R., et al. (2019). Genetic analyses of diverse populations improves discovery for complex traits. *Nature*. 570, 514–518. doi: 10.1038/s41586-019-1310-4

Yang, X., Lupon, J., Vidan, M. T., Ferguson, C., Gastelurrutia, P., Newton, P. J., et al. (2018). Impact of frailty on mortality and hospitalization in chronic heart failure: a systematic review and meta-analysis. *J. Am. Heart Assoc*. 7, e008251. doi: 10.1161/JAHA.117.008251

Yasuda, T. (2021). Identifying preventative measures against frailty, locomotive syndrome, and sarcopenia in young adults: a pilot study. *J. Phys. Ther. Sci*. 33, 823–827. doi: 10.1589/jpts.33.823

Yu, Z., Demetriou, M., and Gillen, D. L. (2015). Genome-wide analysis of gene-gene and gene-environment interactions using closed-form wald tests. *Genet. Epidemiol*. 39, 446–455. doi: 10.1002/gepi.21907

Yuan, L., Chang, M., and Wang, J. (2021). Abdominal obesity, body mass index and the risk of frailty in community-dwelling older adults: a systematic review and meta-analysis. *Age Ageing*. 50, 1118–1128. doi: 10.1093/ageing/afab039

frontiers | Frontiers in Neuroscience

TYPE Original Research
PUBLISHED 24 August 2022
DOI 10.3389/fnins.2022.957617

Check for updates

OPEN ACCESS

EDITED BY
Tino Prell,
University Hospital in Halle, Germany

REVIEWED BY
Dongzhen Yu,
Shanghai Jiao Tong University, China
Antonio Pirodda,
University of Bologna, Italy

*CORRESPONDENCE
Taisheng Chen
fch_cts@sina.com
Wei Wang
wwei1106@hotmail.com

SPECIALTY SECTION
This article was submitted to Perception Science, a section of the journal Frontiers in Neuroscience

RECEIVED 31 May 2022
ACCEPTED 01 August 2022
PUBLISHED 24 August 2022

CITATION
Zhang X, Deng Q, Liu Q, Wen C, Wang W and Chen T (2022) The horizontal and vertical components of nystagmus evoked by the supine roll test in horizontal semicircular canal canalolithiasis.
Front. Neurosci. 16:957617.
doi: 10.3389/fnins.2022.957617

COPYRIGHT
© 2022 Zhang, Deng, Liu, Wen, Wang and Chen. This is an open-access article distributed under the terms of the Creative Commons Attribution License (CC BY). The use, distribution or reproduction in other forums is permitted, provided the original author(s) and the copyright owner(s) are credited and that the original publication in this journal is cited, in accordance with accepted academic practice. No use, distribution or reproduction is permitted which does not comply with these terms.

The horizontal and vertical components of nystagmus evoked by the supine roll test in horizontal semicircular canal canalolithiasis

Xueqing Zhang[1,2,3,4,5], Qiaomei Deng[1,2,3,4,5], Qiang Liu[1,2,3,4,5], Chao Wen[1,2,3,4,5], Wei Wang[1,2,3,4,5]* and Taisheng Chen[1,2,3,4,5]*

[1]Department of Otorhinolaryngology Head and Neck Surgery, Tianjin First Central Hospital, Tianjin, China, [2]Institute of Otolaryngology of Tianjin, Tianjin, China, [3]Key Laboratory of Auditory Speech and Balance Medicine, Tianjin, China, [4]Key Medical Discipline of Tianjin (Otolaryngology), Tianjin, China, [5]Quality Control Centre of Otolaryngology, Tianjin, China

Objective: The characteristics of horizontal and vertical components of nystagmus evoked by the supine roll test in patients with horizontal semicircular canal canalolithiasis (HSC-Can) were analyzed, according to Ewald's first law. It provided a basis for the study of human horizontal semicircular canal function and structure, objective diagnosis, and treatment of benign paroxysmal positional vertigo (BPPV).

Materials and methods: The records of patients that had been tested with 2-dimensional videonystagmography (2D-VNG) were reviewed between June 2019 and June 2021. The intensity and direction of horizontal and vertical nystagmus elicited by the supine roll test were analyzed in 189 patients with idiopathic HSC-Can.

Results: All the 189 patients with HSC-Can were induced horizontal nystagmus with the same direction as head-turning (geotropic) in the supine roll test, of which 119 patients (63.96%) had a weak vertical upward component of nystagmus on the affected and unaffected sides, 57 patients (30.16%) had a vertical downward component of nystagmus on the affected side and/or the unaffected side, and 13 patients (6.88%) had no vertical component of nystagmus on both the sides. The intensity values of the horizontal component on the affected and unaffected sides were 42.14 ± 24.78 (range: 6.26–138.00°/s) and 17.48 ± 10.91°/s (range: 2.40–53.83°/s), with a ratio of 2.96 ± 2.17:1, representing a significant difference ($p < 0.001$). We analyzed the characteristics of horizontal and vertical components in 119 patients with HSC-Can (57 L-HSC-Can and 62 R-HSC-Can) on the supine roll test. The intensity values of the horizontal component on the affected and unaffected sides were 43.17 ± 23.76 (range: 8.60–124.51°/s) and 17.98 ± 10.99°/s (range: 2.40–53.83°/s), and the intensity values of the

vertical component on the affected and unaffected sides were 10.65 ± 8.46 (range: 1.90–50.83°/s) and 4.81 ± 3.45°/s (range: 0.30–20.43°/s), representing a significant difference between groups ($p < 0.001$). Among 119 patients with HSC-Can who had a vertical upward component on both the affected and unaffected sides in the supine roll test, unilateral weakness (UW) was normal in 53 cases and abnormal in 51 cases, and 15 cases did not undergo the caloric test. We compared the horizontal and vertical components of nystagmus induced on the affected and unaffected sides in the supine roll test in 53 patients with normal UW and 51 patients with abnormal UW, and the difference was not statistically significant.

Conclusion: There is mostly a vertical upward component based on the horizontal component in HSC-Can, and the direction and intensity characteristics of nystagmus accord with Ewald's first law, which can provide a basis for the study of human HSC function and structure, objective diagnosis, and treatment of BPPV.

KEYWORDS

Ewald's laws, horizontal semicircular canal, canalolithiasis, video nystagmography, vertical component, BPPV

Introduction

Benign paroxysmal positional vertigo (BPPV), the most common perivestibular disease, has gained consensus on the pathogenesis of canalolithiasis and cupulolithiasis (von Brevern et al., 2015; Kim et al., 2021). Based on this theory and Ewald's law, the diagnostic guidelines for BPPV and various repositioning therapy methods have achieved good clinical diagnosis and treatment effects for most patients (Lou et al., 2020; Power et al., 2020; Abdulovski and Klokker, 2021). The research on the characteristics and mechanism of nystagmus also has attracted attention (Chen et al., 2013; Jafarov et al., 2020; Yu et al., 2021). Previous studies on horizontal semicircular canal canalolithiasis (HSC-Can) nystagmus mainly discussed the characteristics of horizontal nystagmus in the supine roll test (Vats, 2021; Zhang et al., 2021). According to Ewald's first law, the plane of the eye movement is the same as that of the stimulated semicircular canal. Therefore, HSC-Can nystagmus is not simple horizontal nystagmus, but positional nystagmus with horizontal components and weak vertical components. However, there are still few studies on the horizontal and vertical components of HSC-Can nystagmus and their relationship. The purpose of this study was to record and analyze the direction and intensity characteristics of the horizontal and vertical components of nystagmus induced by the supine roll test in patients with HSC-Can by using 2-dimensional videonystagmography (2D-VNG) and to further explore its mechanism, to provide a basis for the study of human HSC function and structure, objective diagnosis, and treatment of BPPV.

Materials and methods

Subjects

This prospective study involved the assessment of 189 patients with HSC-Can, examined at the Ear, Nose, and Throat (ENT) Department of MY Hospital, Tianjin First Central Hospital, between June 2019 and June 2021. Of 189 patients, 83 patients had L-HSC-Can, and 106 patients had R-HSC-Can. All the subjects provided informed consent before their inclusion in the study. The study procedures were approved by the Ethics Committee of the Tianjin First Central Hospital.

Inclusion criteria

(1) Patients with a history of positional vertigo as a predominant symptom, or associated with other complaints, such as dizziness, nausea, and vomiting.

(2) Patients diagnosed with geotropic HSC-Can, according to the benign paroxysmal positional vertigo: Diagnostic criteria (Brevern et al., 2015).

(3) No abnormalities were found in brain CT and MRI.

Exclusion criteria

(1) Patients with apogeotropic HSC-Can, superior semicircular canal canalolithiasis (SSC-Can), posterior

semicircular canal canalolithiasis (PSC-Can), multiple canal canalolithiasis, cupulolithiasis, spontaneous, or other types of positional nystagmus.

(2) Patients with Meniere's disease (MD), vestibular neuritis (VN), sudden deafness (SD), Ramsay Hunt syndrome, labyrinthitis, or other peripheral diseases.

(3) Patients with head trauma, vestibular migraine, stroke, and other central vestibular vertigo and balance disorders.

Materials and methods

We obtained a detailed medical history, focusing primarily on the type of vertigo, including the onset of symptoms, and their severity, duration, and associated factors. Induction of nystagmus and corresponding parameters were observed and recorded using 2-dimensional videonystagmography (2D-VNG; France Synapsys) in the supine roll tests. The supine roll test was used to diagnose HSC-Can and consisted of turning the head from the supine to lateral position (left or right) when the patient was lying down in a supine position, with the head maintained at a 30° upward angle. The procedure was undertaken in line with the clinical practice guidelines (Bhattacharyya et al., 2017).

The direction and intensity of nystagmus, including horizontal and vertical components, were recorded in the left and right head positions on the supine roll test. According to Synapsys parameters, left and right nystagmus are considered horizontal phases, while the fast phase upward was defined as right nystagmus, and the fast phase downward was defined as left nystagmus. Vertical nystagmus includes upward and downward nystagmus, and the fast phase upward was defined as upbeat nystagmus, and the fast phase downward was defined as downbeat nystagmus. The peak slow-phase velocity within 5 s from the onset of nystagmus was recorded as the intensity of nystagmus.

In 189 patients with HSC-Can after the supine roll test, 159 of them underwent the caloric test, the other 30 cases did not undergo the caloric test. The unilateral weakness (UW) $\geq$ 25% is abnormal.

Analysis

We compared the parameters of horizontal and vertical components of nystagmus elicited by the supine roll test. IBM SPSS Statistics 22 (IBM SPSS, Turkey) and JASP 0.16.3 (JASP, Netherlands) were used for statistical analyses. The quantitative data are presented as mean ± SD values and plotted using GraphPad Prism version 5 (GraphPad, San Diego, California, United States). Statistically significant differences were determined by an unpaired Student's *t*-test. A value of $P < 0.05$ and Cohen's $d \geq 0.8$ were considered statistically significant.

Results

General demographic characteristics of subjects

Patients with HSC-Can (45 men and 144 women) ranged from 18 to 83 years (mean 53.92 years). Of these, 83 patients with left HSC-Can (20 men and 63 women) ranged in age from 26 to 74 years (mean 53.20 years), and 106 patients with right HSC-Can (25 men and 81 women) ranged in age from 18 to 83 years (mean 54.48 years). Demographic data for left HSC-Can and right HSC-Can are shown in **Table 1**. There were no significant differences in age or sex ratio between the two groups ($p > 0.05$).

Horizontal and vertical components of nystagmus evoked by the supine roll test in patients with horizontal semicircular canal canalolithiasis

All the 189 patients with HSC-Can were induced horizontal nystagmus with the same direction as head-turning (geotropic) in the supine roll test, of which 119 patients (63.96%) had a weak vertical upward nystagmus (**Figure 1**), 57 patients (30.16%) had vertical downward nystagmus on the affected side and/or the unaffected side, and 13 patients (6.88%) had no vertical nystagmus on both the sides. The intensity values of horizontal nystagmus on the affected and unaffected sides were 42.14 ± 24.78 (range: 6.26–138.00°/s) and 17.48 ± 10.91°/s (range: 2.40–53.83°/s), with a ratio of 2.96 ± 2.17:1, representing a significant difference ($p < 0.001$, Cohen's $d = 1.228$; **Figure 2A**). This is consistent with our previous results (Zhang et al., 2021).

This study induced a weak vertical upward nystagmus in 119 of 189 (62.96%) patients with HSC-Can on the affected and unaffected sides in the supine roll test. A total of 57 patients (30.16%) had vertical downward nystagmus on the affected side

TABLE 1 Demographic features of subjects in the L- and R-HSC-Can groups.

Group feature	L-HSC-Can	R-HSC-Can	HSC-Can
Number	83	106	189
Age (years)*	53.20 ± 12.58	54.48 ± 13.81	53.92 ± 13.26
Sex (M: F)*	20 : 63	25 : 81	45 : 144

HSC-Can, horizontal semicircular canal canalolithiasis; L-HSC-Can, Left HSC-Can; R-HSC-Can, Right HSC-Can; M, male; F, female; *$p > 0.05$.

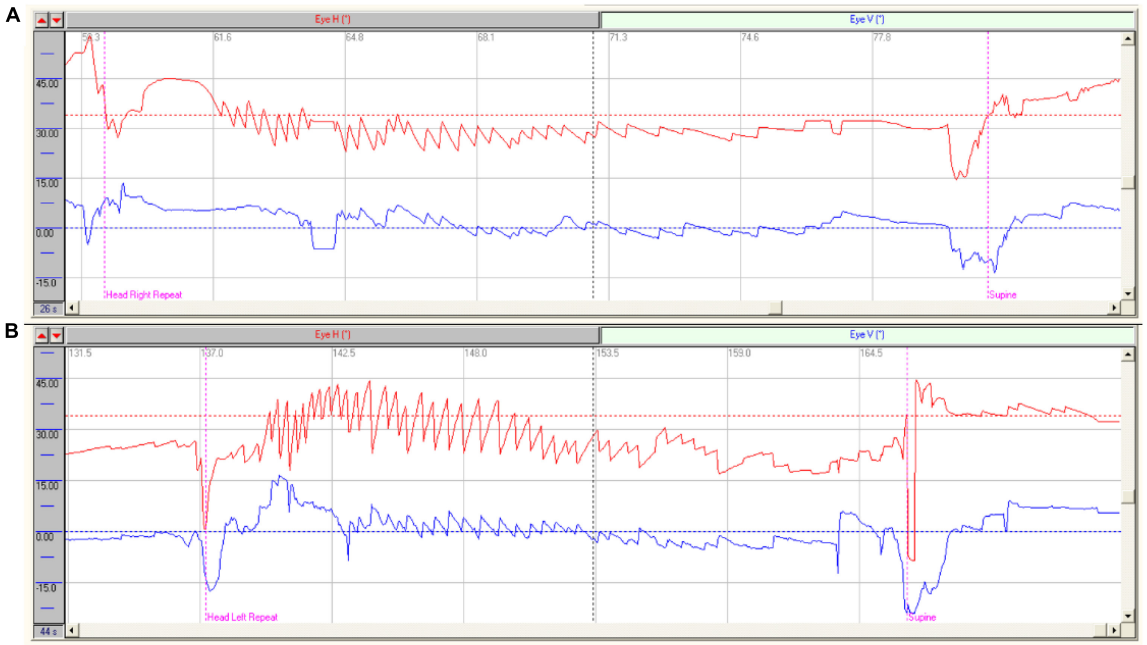

FIGURE 1
Characteristics of nystagmus in patients with HSC-Can. **(A)** Characteristics of nystagmus in a patient with R-HSC-Can: Right horizontal positional nystagmus (37.90°/s, red), accompanied by a weak vertical upward nystagmus (10.10°/s, blue) on the head-right position; **(B)** Characteristics of nystagmus in a patient with L-HSC-Can: Left horizontal positional nystagmus (39.80°/s, red), accompanied by a weak vertical upward nystagmus (10.30°/s, blue) on the head-left position.

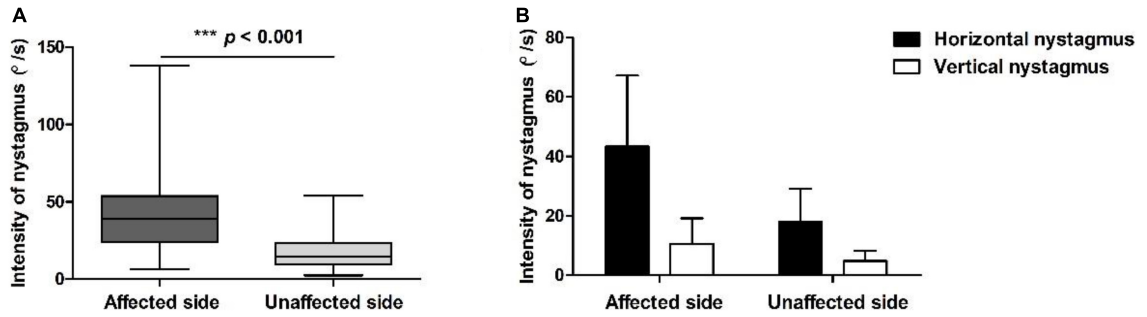

FIGURE 2
Positional nystagmus on the affected and unaffected sides in patients with HSC-Can. **(A)** The intensity values of horizontal nystagmus in 189 patients with HSC-Can on the affected and unaffected sides were 42.14 ± 24.78 (range: 6.26–138.00°/s) and 17.48 ± 10.91°/s (range: 2.40–53.83°/s), with a ratio of 2.96 ± 2.17:1, respectively ($p < 0.001$, Cohen's $d = 1.228$). **(B)** The horizontal and vertical nystagmus in 119 patients with HSC-Can on the supine roll test. The intensity values of horizontal nystagmus on the affected and unaffected sides were 43.17 ± 23.76 (range: 8.60–124.51°/s) and 17.98 ± 10.99°/s (range: 2.40–53.83°/s), and the intensity values of vertical nystagmus on the affected and unaffected sides were 10.65 ± 8.46 (range: 1.90–50.83°/s) and 4.81 ± 3.45°/s (range: 0.30–20.43°/s), representing a significant difference between groups ($p < 0.001$, Cohen's $d \geq 0.8$).

and/or the unaffected side, among which, 12 cases had a weak vertical downward nystagmus on both the sides, 32 cases had vertical upward nystagmus on one side and vertical downward nystagmus on the other side, 13 cases had vertical nystagmus on one side and no vertical nystagmus on the other side, and the rest 13 cases had no vertical nystagmus on both the sides (Table 2).

Considering that the cause of vertical downward nystagmus is unknown, we excluded 57 patients with HSC-Can with vertical downward nystagmus and 13 patients with HSC-Can with no vertical nystagmus, and only analyzed the characteristics of horizontal and vertical nystagmus in 119 patients with HSC-Can (57 L-HSC-Can and 62 R-HSC-Can) on the supine roll test (Figure 2B). The intensity values of horizontal nystagmus on the affected and unaffected sides were 43.17 ± 23.76 (range: 8.60–124.51°/s) and 17.98 ± 10.99°/s (range: 2.40–53.83°/s), and the intensity values of vertical nystagmus on the

TABLE 2 The vertical component of nystagmus evoked by the supine roll test on the affected and unaffected sides in 189 patients with HSC-Can.

Head position		Affected side		
	Vertical component	Up (cases,%)	Down (cases,%)	No (cases,%)
Unaffected side	*Up (cases,%)*	119/189, (62.96%)	16/189, (8.47%)	2/189, (1.06%)
	Down (cases,%)	16/189, (8.47%)	12/189, (6.34%)	2/189, (1.06%)
	No (cases,%)	6/189, (3.17%)	3/189, (1.59%)	13/189, (6.88%)

Up, vertical upward nystagmus; Down, vertical downward nystagmus, No, no vertical nystagmus.

TABLE 3 Comparisons of horizontal and vertical nystagmus evoked by the supine roll test on the affected and unaffected sides in 119 patients with HSC-Can.

	Horizontal (°/s)	Vertical (°/s)	*t*-value	*P*-value	Cohen's *d* (95%CI)
Affected side	43.17 ± 23.76	10.65 ± 8.46	17.89	<0.001	1.626
Unaffected side	17.98 ± 10.99	4.81 ± 3.45	15.66	<0.001	1.423
t-value	14.24	6.92			
p-value	<0.001	<0.001			
Cohen's *d* (95%CI)	1.294	0.804			

affected and unaffected sides were 10.65 ± 8.46 (range: 1.90–50.83°/s) and 4.81 ± 3.45°/s (range: 0.30–20.43°/s), representing a significant difference between groups ($p < 0.001$, Cohen's $d \geq 0.8$; Table 3).

Nystagmus of horizontal semicircular canal canalolithiasis and the function of horizontal semicircular canal

Among 189 patients with HSC-Can, 159 cases completed the caloric test, including 82 cases with normal UW and 77 cases with abnormal UW, and 30 cases did not undergo the caloric test. In the 119 patients with HSC-Can who had a vertical upward component of nystagmus on the affected and unaffected sides in the supine roll test, 104 patients of them underwent the caloric test, UW was abnormal in 53 cases and normal in 51 cases, and the other 9 cases did not undergo the caloric test. There were no statistically significant differences in horizontal and vertical components of nystagmus between normal and abnormal UW cases on the affected and unaffected sides in the supine roll test (Table 4).

TABLE 4 Comparisons of horizontal and vertical nystagmus evoked by the supine roll test on the affected and unaffected sides in patients with HSC-Can with normal and abnormal UW.

		Abnormal UW (51 cases)	Normal UW (53 cases)	t-value	*P*-value
Affected side	H (°/s)	46.41 ± 24.96	41.46 ± 22.83	1.06	0.29
	V (°/s)	11.85 ± 9.98	9.50 ± 6.18	1.45	0.15
Unaffected side	H (°/s)	18.46 ± 12.36	16.92 ± 9.98	0.70	0.48
	V (°/s)	5.12 ± 3.78	4.71 ± 3.51	0.57	0.57

UW, unilateral weakness; H, the intensity of horizontal component; V, the intensity of vertical component.

Discussion

Multiple semicircular canals are involved in unilateral peripheral vestibular diseases (a single semicircular canal is rare), and the spontaneous nystagmus resulting is mostly horizontal or torsional. The relationship between the direction of spontaneous nystagmus and the injured semicircular canal is not completely clear. The reason that there is still a lack of vestibular detection technology to fully evaluate each semicircular canal. Nystagmus of HSC-Can, a single factor stimulus response induced from a single HSC, has the physiological properties of a single HSC. It is also the best way to analyze the characteristics of HSC nystagmus through HSC-Can based on Ewald's laws (Zhang et al., 2021).

We analyzed the characteristics of horizontal and vertical components of nystagmus evoked by the supine roll test in 189 patients with HSC-Can, and found that there was mostly a vertical upward component based on the horizontal component in HSC-Can. The direction and intensity characteristics of HSC-Can nystagmus accord with Ewald's first law and the anatomical characteristics of HSC at about 30° from the horizontal plane. Moreover, there was no significant difference in horizontal and vertical components of nystagmus between normal and abnormal UW subjects in affected- and unaffected-head position of the supine roll test, which further suggests that the nystagmus of HSC-Can can reflect the anatomical and physiological characteristics of HSC and provide a basis for the study of HSC function, objective diagnosis, and treatment of BPPV.

With the in-depth study of BPPV and the application of VNG, the diagnosis and treatment of BPPV have gradually developed from subjective analysis to objective positioning (Zhu et al., 2021). Previous studies on HSC-Can nystagmus mostly focused on the analysis of horizontal nystagmus (Vats, 2021; Zhang et al., 2021). The direction and intensity of horizontal nystagmus induced by the supine roll test were measured by subjective visual measurement or objective quantitative method. Based on VNG technology, the development from

single horizontal nystagmus to two-dimensional nystagmus will be also one of the research focus of HSC-Can nystagmus. Further exploring the characteristics of horizontal and vertical components of HSC-Can nystagmus will help to deeply understand the physiological characteristics of human HSC and provide a basis for clinical research of HSC-Can.

The caloric test, a routine vestibular function test, detects the low-frequency vestibulo-ocular reflex (VOR) function of the HSC through different temperature stimulations, which can induce horizontal nystagmus with or without weak vertical nystagmus. The vertical nystagmus induced in caloric testing may be due to the local stimulation of temperature that affects multiple semicircular canals ipsilaterally (anterior, horizontal, and posterior semicircular canals), and may also be related to the presence of central lesions in the patient (Chen et al., 2007). In addition, research has shown the simultaneous occurrence of a non-thermoconvective mechanism, which theoretically could answer for about one-third of the total caloric response. It has been assumed that this latter mechanism underlies the caloric nystagmus induced in microgravity (Stahle, 1990). Therefore, it is not suitable to analyze the anatomical angle and gravity relationship of HSC through the characteristics of nystagmus induced by caloric test. Otoconia are only a single factor stimulation to HSC-Can-induced nystagmus, and are completely derived from the gravity effect. At present, any other clinical vestibular test method is difficult to simulate, and simple unilateral HSC damage is rare in clinical methods. Therefore, HSC-Can is an excellent physiological stimulation model of HSC in humans.

In HSC-Can, gravity induces the rolling of the otoconia from the posterior arm of the HSC toward the ampulla on the affected side, driving the endolymph to the ampulla, while the otoconia roll to the canal from the ampulla driving the endolymph away from the ampulla (Martellucci et al., 2020; Zhang et al., 2020). This results in a single stimulus to the HSC without involving the anterior and posterior semicircular canals. According to Ewald's first law, the plane of eye movement in the aVOR is the same as that of the stimulated semicircular canal. The nystagmus in patients with HSC-Can has horizontal and vertical components, and we speculate that this may be caused by the angle between the HSC and the horizontal plane.

A total of 189 patients with HSC-Can were included in this study, of which 119 patients (62.96%) were induced with left/right horizontal nystagmus (geotropic nystagmus), accompanilane (about 30 ? above the horizontal plane).ed by a weak vertical upward nystagmus on the affected and unaffected sides in the supine roll test. The other 70 cases (37.04%) had horizontal nystagmus consistent with HSC-Can nystagmus, while the forms of vertical nystagmus were different. We suspected that 70 patients who had vertical downward nystagmus or no vertical nystagmus might have heterophoria (Barton and Ranalli, 2021), which needs to be further studied in the future. The vertical component of nystagmus in 119 cases (62.96%) was upward when the head was positioned on both the affected and unaffected sides. This finding was related to the direction of nystagmus—always toward the side with higher vestibular tension. Taking R-HSC-Can as an example, when the patient moved from supine to right head position, the otoconia of the right HSC rolled toward the ampulla, resulting in excitatory stimulation. Right horizontal nystagmus accompanied by a vertical upward component can be induced (**Figure 1A**), and its direction was consistent with the HSC plane (about 30° above the horizontal plane). Therefore, the supine roll test induced horizontal nystagmus accompanied by a weak vertical upward component. When the patient turned to the left head position, the otoconia of the right HSC rolled away from the ampulla to produce inhibitory stimulation, and the tension of the left HSC increased. A weak left horizontal nystagmus accompanied by a vertical upward component can be induced (**Figure 1B**), and its direction was consistent with the left HSC plane (about 30° above the horizontal plane).

In the other 70 cases (37.04%), the horizontal component of nystagmus accorded with the characteristics of HSC-Can nystagmus. However, the vertical component had different forms, including several different situations: vertical downward nystagmus on the affected side and vertical upward nystagmus on the unaffected side; vertical upward nystagmus on the affected side and vertical downward nystagmus on the unaffected side; vertical downward nystagmus on both the affected and unaffected sides; and no vertical nystagmus on the affected and/or unaffected side. For HSC-Can, the vertical component of nystagmus induced by otoconia rolling is correlated with the spatial orientation of the horizontal semicircular canal, and there is no otoconia stimulation of the posterior semicircular canal. Nystagmus of HSC-Can is a comprehensive vector of the horizontal component and vertical upward component. When the direction and intensity of the vertical component change, it is speculated that the patients with HSC-Can may have other semicircular canal or otolithic lesions, or be related to the patients' heterophoria (Barton and Ranalli, 2021).

Our previous study showed that HSC-Can could demonstrate Ewald's law in the human body and be used as a physiological stimulus model to obtain a deeper understanding of the characteristics of the human HSC (Zhang et al., 2021). The intensity and direction of HSC-Can nystagmus are mainly related to the stimulation effect of the rolling otoconia induced by gravity. Nystagmus is based on the functional existence of the involved HSC, and may also be affected by other factors, such as the function of ASC, PSC, or otolith organ. Our study showed that among 119 patients with HSC-Can, 51 patients had abnormal UW and 53 patients had normal UW, which were similar to previous reports (Bi et al., 2019). However, there was no significant difference in horizontal and vertical components of nystagmus between normal and abnormal UW subjects in affected- and unaffected-head position of the supine roll test,

which further suggests that the nystagmus of HSC-Can can reflect the anatomical and physiological characteristics of HSC.

Questions to be studied

Following the BPPV diagnostic criteria, a systematic vestibular examination was not carried out for patients with HSC-Can, such as vestibular evoked myogenic potential (VEMP) and multifrequency tests of three semicircular canals. The influence from otoliths lesion and other frequency lesions of the three semicircular canals for nystagmus of HSC-Can cannot be excluded. Therefore, the reason why the vertical component of nystagmus was not upward in 70 of 189 cases cannot be clearly explained yet. On the contrary, the presence of a vertical downward component, or the nystagmus does not conform to Ewald's first law in HSC-Can that should be further studied whether is revealed HSC-Can combined with other semicircular canals or otolith organ lesions.

Conclusion

In this study, the direction and intensity characteristics of horizontal and vertical components of HSC-Can nystagmus evoked by the supine roll test were recorded and analyzed. The results showed that most of them had vertical upward components except horizontal components, suggesting that HSC-Can has the characteristics of the human HSC physiological effect model. The nystagmus follows Ewald's first law, which can provide a basis for the study of HSC function and objective diagnosis and treatment of HSC-Can and semicircular canal-related diseases.

Data availability statement

The raw data supporting the conclusions of this article will be made available by the authors, without undue reservation.

Ethics statement

The studies involving human participants were reviewed and approved by this study was approved by the Institutional Review Board of Tianjin First Central Hospital (Tianjin, China). The patients/participants provided their written informed consent to participate in this study.

Author contributions

WW and TC performed the study design. XZ, QD, QL, and CW acquired and analyzed the data. XZ and TC drafted the manuscript. All authors data interpretation and critical revision of the manuscript.

Funding

This study was supported by the Tianjin Key Medical Discipline Construction Project (TJYXZDXK-046A) and the Tianjin Health Research Project (TJWJ2022QN027), (TJWJ2022QN028), (21JCQNJC01670), (21JCQNJC01780), (21JCQNJC01770), (TJWJ2021QN012), (ZC20010), (ZC20061), (KJ20136), and (KJ20133). The sponsors had no role in study design, data collection, analysis, interpretation, or manuscript writing.

Conflict of interest

The authors declare that the research was conducted in the absence of any commercial or financial relationships that could be construed as a potential conflict of interest.

Publisher's note

All claims expressed in this article are solely those of the authors and do not necessarily represent those of their affiliated organizations, or those of the publisher, the editors and the reviewers. Any product that may be evaluated in this article, or claim that may be made by its manufacturer, is not guaranteed or endorsed by the publisher.

References

Abdulovski, S., and Klokker, M. (2021). Repositioning chairs in the diagnosis and treatment of benign paroxysmal positional vertigo - A systematic review. *J. Int. Adv. Otol.* 17, 353–360. doi: 10.5152/iao.2021.9434

Barton, J. J. S., and Ranalli, P. J. (2021). Vision therapy: Occlusion, prisms, filters, and vestibular exercises for mild traumatic brain injury. *Surv. Ophthalmol.* 66, 346–353. doi: 10.1016/j.survophthal.2020.08.001

Bhattacharyya, N., Gubbels, S. P., Schwartz, S. R., Edlow, J. A., El-Kashlan, H., Fife, T., et al. (2017). Clinical practice guideline: Benign paroxysmal positional Vertigo (Update). *Otolaryngol. Head Neck Surg.* 156, S1–S47. doi: 10.1177/0194599816689667

Bi, J., Liu, B., Zhang, Y., Duan, J., and Zhou, Q. (2019). Caloric tests in clinical practice in benign paroxysmal positional vertigo. *Acta Otolaryngol.* 139, 671–676. doi: 10.1080/00016489.2019.1614220

Brevern, M. V., Bertholon, P., Brandt, T., Fife, T., Imai, T., Nuti, D., et al. (2015). Benign paroxysmal positional vertigo: Diagnostic criteria. *J. Vestib. Res.* 25, 105–117.

Chen, F. Y., Chen, T. S., Wen, C., Li, S. S., Lin, P., Zhao, H., et al. (2013). [Objective characteristics of nystagmus in horizontal semicircular canal benign paroxysmal positional vertigo]. *Zhonghua Er Bi Yan Hou Tou Jing Wai Ke Za Zhi* 48, 622–627.

Chen, T. S., Song, W., Ma, Y. X., and Lu, H. H. (2007). Analysis of inverted and perverted nystagmus during air caloric testing. *Chin. J. Otol.* 5, 277–280.

Jafarov, S., Hizal, E., Bahcecitapar, M., and Ozluoglu, L. N. (2020). Upright positioning-related reverse nystagmus in posterior canal benign paroxysmal positional vertigo and its effect on prognosis. *J. Vestib. Res.* 30, 195–201. doi: 10.3233/VES-200700

Kim, H. J., Park, J., and Kim, J. S. (2021). Update on benign paroxysmal positional vertigo. *J. Neurol.* 268, 1995–2000. doi: 10.1007/s00415-020-10314-7

Lou, Y., Cai, M., Xu, L., Wang, Y., Zhuang, L., and Liu, X. (2020). Efficacy of BPPV diagnosis and treatment system for benign paroxysmal positional vertigo. *Am. J. Otolaryngol.* 41:102412. doi: 10.1016/j.amjoto.2020.102412

Martellucci, S., Malara, P., Castellucci, A., Pecci, R., Giannoni, B., Marcelli, V., et al. (2020). Upright BPPV protocol: Feasibility of a new diagnostic paradigm for lateral semicircular canal benign paroxysmal positional vertigo compared to standard diagnostic maneuvers. *Front. Neurol.* 11:578305. doi: 10.3389/fneur.2020.578305

Power, L., Murray, K., and Szmulewicz, D. J. (2020). Characteristics of assessment and treatment in Benign Paroxysmal Positional Vertigo (BPPV). *J. Vestib. Res.* 30, 55–62. doi: 10.3233/VES-190687

Stahle, J. (1990). Controversies on the caloric response. From Barany's theory to studies in microgravity. *Acta Otolaryngol* 109, 162–167. doi: 10.3109/00016489009107430

Vats, A. K. (2021). Lying-Down Nystagmus (LDN) - When a lateralizing sign of secondary importance attains ascendancy in the diagnosis of Horizontal Semicircular Canal Benign Paroxysmal Positional Vertigo (HSC-BPPV). *Ann. Indian Acad. Neurol.* 24, 401–404. doi: 10.4103/aian.AIAN_322_20

von Brevern, M., Bertholon, P., Brandt, T., Fife, T., Imai, T., Nuti, D., et al. (2015). Benign paroxysmal positional vertigo: Diagnostic criteria. *J. Vestib. Res.* 25, 105–117. doi: 10.3233/VES-150553

Yu, J., Gu, Y., Meng, G., Zhu, X., Wang, W., Liu, X., et al. (2021). Nystagmus parameters of supine roll test correlates with prognosis after repositioning maneuver in horizontal semicircular canal benign paroxysmal positional vertigo. *Front. Neurol.* 12:790430. doi: 10.3389/fneur.2021.790430

Zhang, S. L., Tian, E., Xu, W. C., Zhu, Y. T., and Kong, W. J. (2020). Light cupula: To be or not to be? *Curr. Med. Sci.* 40, 455–462. doi: 10.1007/s11596-020-2199-8

Zhang, X., Bai, Y., Chen, T., Wang, W., Han, X., Li, S., et al. (2021). A show of Ewald's Law: I horizontal semicircular canal benign paroxysmal positional vertigo. *Front. Neurol.* 12:632489. doi: 10.3389/fneur.2021.632489

Zhu, Y., He, X., Hu, M., Mao, C., Liu, Z., Yang, X., et al. (2021). Objective findings in patients with multi-canal benign paroxysmal positional vertigo. *Ear Nose Throat J.* 2021:1455613211066679. doi: 10.1177/01455613211066679

frontiers | Frontiers in Neuroscience

TYPE Original Research
PUBLISHED 24 August 2022
DOI 10.3389/fnins.2022.983427

Check for updates

OPEN ACCESS

EDITED BY
Sulin Zhang,
Huazhong University of Science and Technology, China

REVIEWED BY
Binbin Xiong,
Zhuhai Hospital of Integrated of Traditional Chinese Medicine and Western Medicine, China
Francesco Comacchio,
Regional Specialized Vertigo Center Veneto Region, Italy

*CORRESPONDENCE
Lingzhi Kong
konglingzhi@blcu.edu.cn
Yixin Zhao
zhaoyixin16@163.com
Tongxiang Diao
tongx@foxmail.com
Xin Ma
13581709195@163.com

†These authors have contributed equally to this work

SPECIALTY SECTION
This article was submitted to Perception Science, a section of the journal Frontiers in Neuroscience

RECEIVED 01 July 2022
ACCEPTED 29 July 2022
PUBLISHED 24 August 2022

CITATION
Wang M, Liu J, Kong L, Zhao Y, Diao T and Ma X (2022) Subjective tinnitus patients with normal pure-tone hearing still suffer more informational masking in the noisy environment. *Front. Neurosci.* 16:983427. doi: 10.3389/fnins.2022.983427

COPYRIGHT
© 2022 Wang, Liu, Kong, Zhao, Diao and Ma. This is an open-access article distributed under the terms of the Creative Commons Attribution License (CC BY). The use, distribution or reproduction in other forums is permitted, provided the original author(s) and the copyright owner(s) are credited and that the original publication in this journal is cited, in accordance with accepted academic practice. No use, distribution or reproduction is permitted which does not comply with these terms.

Subjective tinnitus patients with normal pure-tone hearing still suffer more informational masking in the noisy environment

Mengyuan Wang[1], Jinjun Liu[1], Lingzhi Kong[2*†], Yixin Zhao[3*†], Tongxiang Diao[3*†] and Xin Ma[3*†]

[1]School of Psychology, Beijing Normal University, Beijing, China, [2]School of Communication Sciences, Beijing Language and Culture University, Beijing, China, [3]Department of Otolaryngology, Head and Neck Surgery, People's Hospital, Peking University, Beijing, China

Subjective tinnitus patients experience more hearing difficulties than normal peers in complex hearing environments, even though most of these patients have normal pure-tone hearing thresholds. Using speech recognition tasks under different masking conditions can provide insight into whether the effects of tinnitus are lateralized and the mechanisms behind the effects. By simulating sound field recordings, we obtain a target speech sentence that can be perceived as presented on one side and noise or speech masking with or without spatial separation from it. Our study used the virtual sound field technique to investigate the difference in speech recognition ability between chronic subjective tinnitus patients and a normal-hearing control group under the four masking conditions (speech-spectrum noise masking or two-talker speech masking, with or without perceived spatial separation). Experiment 1 showed no differences for target speech perceived location (left or right), which rules out a lateralization of the effect of tinnitus patients. Experiment 2 further found that although tinnitus patients had weaker performance than normal people in very complex auditory scenarios, when the spatial cue of the target speech exists, they can make good use of this cue to make up for the original processing disadvantage and achieve a similar performance as the normal-hearing group. In addition, the current study distinguished the effects of informational masking and energetic masking on speech recognition in patients with tinnitus and normal hearing. The results suggest that the impact of tinnitus on speech recognition in patients is more likely to occur in the auditory center rather than the periphery.

KEYWORDS

subjective tinnitus, tinnitus mechanisms, informational masking, energetic masking, spatial cues

Introduction

Subjective tinnitus is a perception of phantom sound heard by a person in the absence of any external physical stimulation (Roberts et al., 2010). The prevalence of tinnitus in adults varies across various studies (McCormack et al., 2016), ranging from 5.1 to 42.7%, which is likely influenced by the phrasing of the question. Most often, subjective tinnitus is associated with aging, hearing loss, head trauma and noise exposure (Baguley et al., 2013). In addition to hearing-loss peers, approximately 10% of tinnitus patients have normal hearing sensitivity, defined as pure-tone thresholds less than 25 dB HL at 0.25, 0.5, 1, 2, 4, and 8 kHz (Theodoroff and Folmer, 2013). For tinnitus patients with hearing loss, the mechanisms of their tinnitus can usually be related to a functional loss of hair cells in the inner ear and neuronal activities in the auditory nervous system (Noreña, 2015; Ma et al., 2021). However, does the central auditory system function abnormally in tinnitus patients with normal pure-tone hearing? At present, some researchers have explored the evidence of chronic tinnitus through cortical auditory evoked potentials, brain signal variability and delayed memory (Cardon et al., 2022), but the underlying mechanism is still unclear. Furthermore, is there any effect on speech recognition performance under different masking conditions? Thus, our study included individuals with tinnitus and normal hearing to explore the effect of subjective tinnitus on speech recognition in masking.

Speech recognition, especially in reverberant noisy environments, is an important ability in people's daily lives. Speech recognition in noise (SIN) is a complicated multifaceted process, including bottom-up sensory encoding of target speech from the peripheral to the central auditory system and compensatory sensorimotor integration, supported by higher-level cognitive functions such as working memory and selective attention (Du et al., 2014; Coffey et al., 2017; Zhang et al., 2021). Many previous studies have found that people with hearing difficulties, such as elderly individuals (Anderson et al., 2013), children (Litovsky, 2005) and patients with a history of idiopathic sudden sensorineural hearing loss (ISSHL) (Diao et al., 2022), have poorer performance with SIN. There are two types of interference in such a process that make speech recognition difficult: energetic masking and informational masking (Freyman et al., 1999; Wu et al., 2005; Villard and Kidd, 2019). Energy masking is the disturbance of maskers that induces neural activity in the auditory periphery and reduces the reception of target information. Informational masking is the interference generated by the information contained in the masking sound, mainly affecting higher-level cognitive processing. Due to the different ways in which the two types of masking affect speech recognition, people can use some cognitive cues (such as spatial separation from target to masking) to release from information masking greatly but not energy masking significantly. Freyman et al. (1999), in his classical experimental paradigm, produced energy masking through noise and used two or more talkers' speaking to cause informational masking.

At the same time, it is true that some tinnitus patients suffer from hearing loss or that older individuals report hearing difficulty in their daily lives (Vielsmeier et al., 2016; Ivansic et al., 2017). For patients with normal hearing, does tinnitus alone have an impact on their speech recognition? Several studies have involved SIN in tinnitus patients with normal hearing. However, there is no consistent conclusion among studies on the performance of tinnitus patients. Some of these studies have found that the speech recognition performance of tinnitus patients is worse than that of normal people of the same age (Huang et al., 2007; Hennig et al., 2011; Ryu et al., 2012; Jain and Sahoo, 2014; Moon et al., 2015; Gilles et al., 2016). Other studies have found that tinnitus patients have lesser performances in speech recognition only under individual task conditions and no significant difference from the normal population under other conditions (Tai and Husain, 2018; Zeng et al., 2020). Some studies have evaluated the association of factors such as tinnitus loudness, THI score, otoacoustic emissions, auditory brain stem responses (ABR) and the ability to discriminate the sound spectrum with SIN performance and found no significant correlation (Gilles et al., 2016; Tai and Husain, 2018). Notably, two studies have found differences in speech recognition performance in both ears of tinnitus patients (Moon et al., 2015; Tai and Husain, 2018). Such results, which are different from other studies, seem to predict the possibility of the lateralization of auditory processing in patients with tinnitus. The experimental paradigms used in these studies are quite different.

There may be two reasons for the discrepancies in previous research results. On the one hand, tinnitus is a very heterogeneous symptom, and there are many individual differences among patients. In previous studies, the type of tinnitus, the duration of symptoms, and the age of the patients were different. These factors may be the reasons for individual differences and affect the performance of speech recognition tasks. On the other hand, different experimental paradigms have various sensitivities to differences in listener auditory processing and speech recognition performance. For example, a measure named QuickSIN (Quick Speech in Noise test), which syntactically corrects sentences with low semantic cues, is more sensitive to performance differences between normal-hearing and hearing-impaired groups than the BKB-SIN (Bamford–Kowal–Bench SIN) and the hearing in noise test (HINT), which use meaningful sentences (Wilson et al., 2007). Additionally, previous studies found that attention, fatigue and other factors are considered important mediating factors between tinnitus and its impact (Andersson and Westin, 2008), and subjects need to invest more cognitive resources in some experimental paradigms but less in others. Therefore, the effect of tinnitus on speech recognition remains understudied, contributing

to a lack of understanding of the mechanisms of tinnitus with normal hearing.

In summary, the current study focused on two issues worth investigating: whether there are interaural differences in speech recognition performance in tinnitus patients with normal hearing and whether tinnitus patients with normal hearing have difficulty in speech recognition compared to healthy adults. To reduce the heterogeneity of the tinnitus patient population, we focused the study population on relatively young patients with chronic subjective tinnitus who had symptoms for more than 6 months and tried to select patients with bilateral tinnitus. We investigated the patients' SIN performance under speech-spectrum noise and two-talker speech using a perceived spatial separation paradigm (Wu et al., 2005). Additionally, spatial separation between target and interference is an important cognitive cue for listeners in SIN recognition, so we considered spatial separation an experimental factor. In Experiment 1, we sought to verify the existence of interaural differences of the patients by comparing the SIN performance on one side and the other as the target sound is perceived. In Experiment 2, we compared speech recognition performance in tinnitus patients with normal hearing and healthy adults. In Experiment 2, we compared speech recognition performance in tinnitus patients with normal hearing and healthy adults with matched age, gender and education level. This is conducive to more clearly showing the effect of tinnitus and provides a scientific research basis for exploring the mechanisms of tinnitus with normal hearing.

Experiment 1

Materials and methods

Participants

Eight tinnitus patients (3 females and 5 males, mean age = 29.2 years) who met the following criteria participated in our research. They all had bilateral subjective tinnitus that persisted for more than 6 months, with normal hearing thresholds (≤20 dB HL) at audiometric frequencies from 250 to 8,000 Hz (the only exception was one patient who had a hearing threshold of 30 dB at 8,000 Hz). Institutional Review Board of the Faculty of Psychology, BNU approved the study (202206260076) and all participants provided written informed consents.

Apparatus and stimuli

A set of special Chinese nonsense sentences the same as the sentences used by Wang et al. (2018) were used as the target sentences. The sentences were semantically anomalous but syntactically correct, and their English translations are partially similar to the English nonsense sentences used by Freyman et al. (1999). For example, the English translation of a sentence is "A frog always sets up your cup." Each sentence consists of six Chinese words, with two characters for each word and one syllable for each character, and has three keywords within them: subject, predicate, and object. Target sentences were spoken by a young female talker (Talker A) at a stable rate, and the duration of a sentence was approximately 2 s.

The speech masker was a 47-s loop of digitally combined continuous recordings of Chinese nonsense sentences spoken by two different young female talkers (Talkers B and C). The noise masker was a stream of steady-state speech-spectrum noise, whose spectrum was representative of the average spectrum of the target sentences.

The acoustic signals were recorded by two microphones placed on the two sides of a simulated head and presented binaurally through ATH-MSR7 headphones driven by a desktop computer. When recording sound stimuli, we put the target speech on one side (90° relative to the front of the simulated head) and then put the masking on the same side or opposite side of the target speech. In this way, we controlled the contents and loudness of the acoustic signals that participants received the same on the two sides, and participants perceived the target on only one side according to the "precedence" effect (although the sounds were delivered to each side) (Li et al., 2005). Maskers were perceived in the same way so we could control whether there was a spatial separation of targets and maskers. Target-speech sounds were presented at an SPL of 56 dBA. The SPLs of the maskers were adjusted to produce five signal-to-noise ratios (SNRs) (−12, −8, −4, 0, 4 dB), and four consequent SNRs were used according to the performance of a participant in practice trials.

Design and procedure

Experiment 1 had four within-subject factors: masker type (noise masker, speech masker), the side from which the participants perceived the target (left, right), perceived spatial separation (colocation, separation) and SNRs (four consequent levels from −12, −8, −4, 0, 4 dB). Fifteen target sentences were used in each condition, and 480 trials were used for each participant.

Stimuli were presented by *Presentation* program. In each trial, the participant pressed the "space" bar on the keyboard to start the masker sound. Approximately 1 s later, a single target sentence was presented with the masker. Then, the masker was gated off as soon as the target ended. Participants were asked to vocally repeat the whole target sentence they heard as much as possible soon after the acoustic signals stopped. The number of correctly identified syllables in the keyword was recorded by the experimenter. There was a set of practice trials of each condition before the formal experiment.

Data analysis

A logistic psychometric function (Eq. 1) was fit to the mean data across the four SNR levels for each participant, where y is the probability of the correct identification of keywords, x is

the SNR corresponding to y, μ is the SNR corresponding to 50% correct on the psychometric function, and σ determines the slope of the psychometric function:

$$y = \frac{1}{1 + e^{-\sigma(x-\mu)}} \quad (1)$$

Results

Figure 1 shows the psychometric functions of SIN perception performance on both target-perceived sides under two types of masking conditions, noise masking and speech masking. Through these functions, we could calculate the SIN perception threshold values of 50% correct (μ, in dB) in the SNR for tinnitus patients under each condition. Paired sample *t*-tests showed that the SIN perception thresholds of the two sides from which the participants perceived the target were not significant under each condition (noise masking colocation, $t = 0.243$, $p = 0.815$; speech masking colocation, $t = 0.866$, $p = 0.415$; noise masking separation, $t = 0.159$, $p = 0.879$; speech masking separation, $t = 0.012$, $p = 0.997$). These results did not support interaural differences in speech recognition in patients with tinnitus and normal hearing, suggesting that the performance is consistent between the left and right sides.

Discussion

The results of the current study support the absence of interaural differences in speech perception performance in patients with tinnitus, consistent with most previous studies on SIN perception in tinnitus patients and normal-hearing adults. As mentioned above, two previous studies have found interaural differences in speech recognition in patients with tinnitus (Moon et al., 2015; Tai and Husain, 2018). Moon et al. (2015) considered unilateral tinnitus patients with hearing loss or normal hearing and found that tinnitus-affected ears showed poorer SRTs than non-tinnitus ears in SIN performance. There are differences in the groups and questions that Moon's study and our study focused on, so the differences in results are explainable. More notably, Study of Tai and Husain (2018) found a right-ear advantage for SIN recognition in patients with non-lateralized tinnitus and normal hearing but not in the control group. Some researchers believe that there is truly a right-ear advantage in SIN perception because the left hemisphere dominates speech and language, and conduction of the right ear can efficiently conduct signals to the left hemisphere (Kimura, 2011). Past research on older adults also found a right-ear advantage in their SIN recognition, and the advantage seemed to increase with normal aging and age-related hearing loss (Jerger et al., 1994; Roup, 2011). In the view of some researchers, right-ear advantage, or in other words left-ear disadvantage, was due to a decline in cognitive functions or a loss in efficiency of interhemispheric transfer at the corpus callosum (Jerger et al., 1994; Roup, 2011). The participants from study of Tai and Husain were 43.86 years on average, and they were more likely to be affected by age-related difficulty in speech perception than patients in the current study. Therefore, the current results should be plausible for the group of participants in this study, the younger population with bilateral tinnitus and normal hearing.

Based on the above results and previous research viewpoints, we had sufficient reasons to believe that there was no interaural difference in speech recognition among the tinnitus patients participating in the experiment. Therefore, the possibility of SIN recognition lateralization would no longer be considered in Experiment 2.

Experiment 2

Materials and methods

Participants

Tinnitus group

On the basis of continuing to use the results of the 8 participants in Experiment 1, two new tinnitus patients were recruited, and finally, a total of 10 patients participated in the experiment (4 females and 6 males, mean age = 29.4 years). They all had subjective tinnitus (9 of them were bilateral, and one had only right-sided tinnitus) that persisted for more than 6 months, with normal hearing thresholds (≤20 dB HL) at audiometric frequencies from 125 to 8,000 Hz (the only exception was one patient who had a hearing threshold of 30 dB at 8,000 Hz). Institutional Review Board of the Faculty of Psychology, BNU approved the study (202206260076) and all participants provided written informed consents.

Normal-hearing adults (NH group)

Ten normal-hearing adults (4 females and 6 males, mean age = 29.4 years) were recruited and matched with each TN group patient for age, sex and education level. They had normal hearing thresholds (≤ 20 dB HL) at audiometric frequencies from 250 to 8,000 Hz (the only exception was one patient who had a hearing threshold of 25 dB at 8,000 Hz), without a history of tinnitus or other hearing disorders. There was no significant group difference between the hearing thresholds of the right ear for both groups, $F(1, 18) = 4.239$, $p = 0.054$. The hearing thresholds of the left ear for the tinnitus group were significantly higher than those for control group, $F(1, 18) = 5.979$, $p < 0.05$. The hear thresholds at left ear for the tinnitus group were significantly higher than those for the control group only at

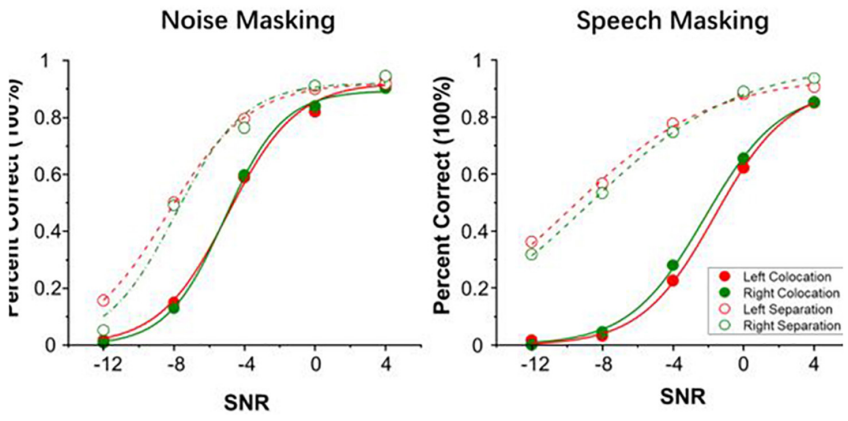

FIGURE 1
Group mean percent of correct as a function of signal-to-noise ratio (SNR) in noise masking condition **(left panel)** and speech masking condition **(right panel)**. Red lines represent when targets were perceived from the left. Green lines represent when targets were perceived from the right.

250 Hz (mean difference: 5.5 dB, $p < 0.01$) and 1,000 Hz (mean difference: 4.5 dB, $p < 0.05$).

Stimuli, procedure and data analysis

The material is the same as in Experiment 1. Affected by the COVID-19 epidemic and needing to simplify the experimental process, we used only the stimulus material in which the targets were perceived by participants on the left. The process and data analysis are also the same as in Experiment 1.

Design

Experiment 2 had three within-subject factors: masker type (noise masker, speech masker), perceived spatial separation (colocation, separation) and SNRs (four consequent levels from -12, -8, -4, 0, 4 dB). In addition, there was a between-subject factor: group (tinnitus patients, normal-hearing adults). Fifteen target sentences were used in each condition, and 240 trials were used for each participant.

Results

Figure 2 shows the group mean percent correct as a function of SNR and the SIN perception threshold (μ, in dB) computed by the psychometric function under two types of masking conditions, noise masking, and speech masking. The thresholds μ are presented separately in Figure 3.

According to Figure 3, a set of independent sample *t*-tests showed that the SIN perception threshold μ of the NH group was significantly lower than that of the TN group only under speech masking's colocation condition ($t = 2.460$, $p = 0.024$) and marginally significant under noise masking's colocation condition ($t = 1.836$, $p = 0.083$) but not under noise masking's separation condition ($t = 0.926$, $p = 0.367$) or speech masking's separation condition ($t = 0.689$, $p = 0.500$). These results indicate that patients performed significantly worse than normal-hearing peers under speech masking without spatial separation cues and performed as well as their peers under the other conditions.

Discussion

The results of Experiment 2 found that tinnitus patients perform poorer in SIN perception under speech masking without spatial separation cues than their normal-hearing peers. In fact, people often encounter the situation of recognizing target speech in the scene of multisound source interference, including noise, and speech masking in daily life. In such conditions, listeners were affected by both energetic masking and informational masking so that their speech recognition was more difficult than when masked only by noise. The results of Experiment 2 showed that in the absence of additional perceptual cues, tinnitus patients with normal hearing showed more difficulty under speech masking and little difficulty under noise masking. It can be said that they had weaker performance than normal people only under the most difficult conditions. In addition, patients in the TN group could perform as well as adults in the NH group if they received spatial separation cues in SIN recognition.

The current study distinguished the effects of informational masking and energetic masking well on SIN recognition in patients with tinnitus and normal hearing. Under noise masking conditions, listeners were disturbed only by energetic masking, which affected SIN recognition primarily in the auditory periphery (Freyman et al., 1999; Wu et al., 2005). At this time, the patients' performances were close to those of normal-hearing adults, indicating that the tinnitus patients did not receive more interference from the auditory

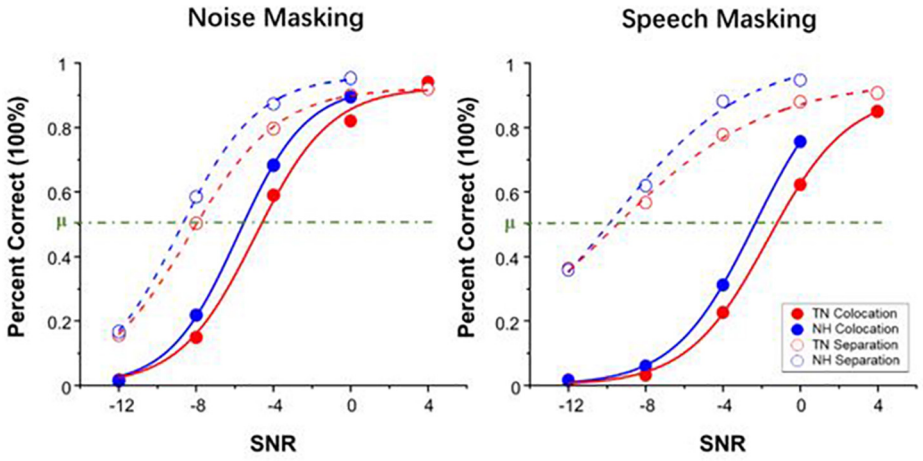

FIGURE 2
Group mean percent of correct as a function of signal-to-noise ratio (SNR) in noise masking condition **(left panel)** and speech masking condition **(right panel)**. Red and blue represent the data of the TN group and NH group, respectively.

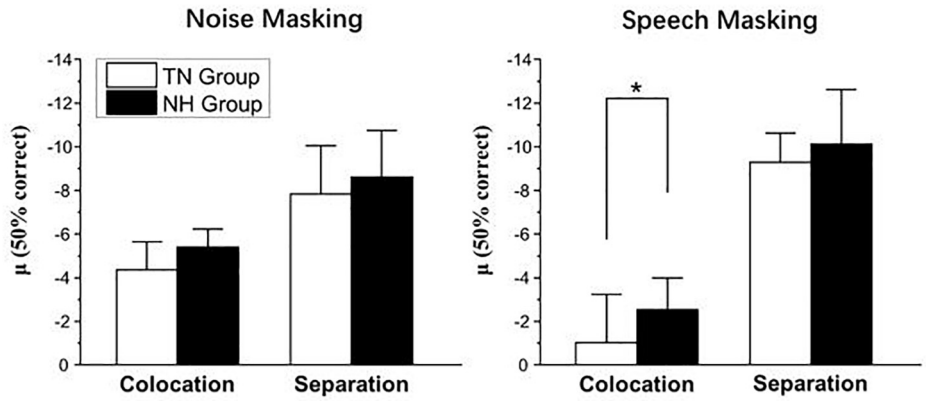

FIGURE 3
Participants' SIN perception threshold μ in noise masking condition **(left panel)** and speech masking condition **(right panel)**. *$p < 0.05$.

periphery. This result matched the patients' normal pure-tone hearing ability. Informational masking was introduced into the condition of speech masking, and the patients showed significant SIN recognition difficulties compared to normal-hearing adults. This result suggested that tinnitus patients were more disturbed by informational masking than normal adults in the auditory center and higher-level cognitive processing. This result is also consistent with the findings in the study by Cardon et al. (2022) that patients with tinnitus differ from normal adults in cortical auditory evoked potentials, brain signal variability and delayed memory.

There are several putative mechanisms of tinnitus pathophysiology which originated from previous animal research. These mechanisms show that tinnitus is related to "aberrant" neural activity (that is not produced by physically measurable sounds from the environment) that is generated at some level of the auditory system (Cima et al., 2019). In most cases, tinnitus is believed to be associated with some degree of cochlear damage and such damage may not be detected by a standard audiogram. Correspondingly, there are some researchers posing many central mechanisms that can account for the generation of the tinnitus-related activity (Eggermont and Roberts, 2004). However, the central mechanism of tinnitus mostly points to the population with hearing loss, and the central mechanism of tinnitus in these patients with normal hearing is more controversial. In Experiment 2, patients experienced more disturbances in central auditory processing and slightly more peripheral disturbances than their peers. The current study results, to some extent, provide a reference for the etiology or subtype classification of tinnitus patients with normal hearing. Their performance suggested

that their SIN recognition difficulties originate primarily in the auditory centers, which are more inclined to suggest that tinnitus patients have the influence of related activities at the central level.

There did not appear to be a decline in tinnitus patients' ability to use spatial separation cues. With the help of cognitive cues, their speech recognition performance can be as good as that of normal-hearing adults. This suggests that patients with tinnitus are more dependent on cognitive cues to some extent. Most of the time, they do not experience many distractions or are aided by enough cognitive cues, and their speech recognition performance can be unaffected by tinnitus. However, in some difficult auditory situations, they may show more difficulty than normal-hearing peers.

General discussion

The current study considered interaural differences in the speech perception performance of tinnitus patients with normal hearing under noise masking and speech masking with spatial separation or not in Experiment 1 and compared the performance between tinnitus patients and normal-hearing adults in Experiment 2. First, we found no interaural differences in tinnitus patients in each condition, refuting the effects of tinnitus with lateralization. Then, we found that tinnitus patients had significantly more difficulties in SIN recognition than normal-hearing adults under speech masking without spatial separation cues but performed as well as normal people with spatial separation cues.

The manifestations of normal-hearing tinnitus patients are similar to those of other hearing-difficulty groups, such as elderly individuals (Anderson et al., 2013; Zhang et al., 2021) and cured ISSHL patients (Diao et al., 2022), who experience difficulties under both types of masking without spatial cues and could release from masking in SIN recognition to a great extent *via* cognitive cues. From the perspective of the auditory processing mechanism, this again proved that SIN, especially in reverberant noisy environments, was a complex cognitive process including sensory input from the auditory periphery and top-down cognitive processing. Our experiments considered the distinction between energy masking and information masking and found that the increased disturbances in these patients did not come from the periphery. Whether the increased disturbances they receive at higher levels come from tinnitus' integration of attention, speech recognition strategies, or the integration of the auditory center can be investigated in future studies.

In addition, in some previous studies, the age range of the tinnitus group was larger, and there were some elderly tinnitus groups, so researchers have explored age-related tinnitus (Heeren et al., 2014; Tai and Husain, 2018, 2019; Zeng et al., 2020). However, the effect of aging seems uncertain in the tinnitus population because the effects of aging on cognitive processing or control and on auditory processing are almost concomitant. The participants in our study were all under the age of 40 and belonged to a younger group, so we could relatively simply reflect the effect of tinnitus on SIN recognition processing and ignore the age factor. The present results provide a good indication that tinnitus causes speech recognition difficulties in patients, although it does not produce pure-tone hearing impairment. In follow-up studies of the auditory processing mechanism of tinnitus patients, it may be considered to include elderly tinnitus patients for age grouping and to use experimental techniques that better reflect the ability of auditory center integration (for example, functional brain imaging technology). Additionally, the study participant population was fixed as chronic normal-hearing tinnitus patients. In fact, tinnitus symptoms have many possibilities, acute or chronic, and a complex relationship with hearing impairment (Ma et al., 2021).

Data availability statement

The raw data supporting the conclusions of this article will be made available by the authors, without undue reservation.

Ethics statement

The studies involving human participants were reviewed and approved by Institutional Review Board of the Faculty of Psychology, BNU. The patients/participants provided their written informed consent to participate in this study.

Author contributions

MW contributed to the design of the study, the analysis, interpretation of the data, and drafting the manuscript. JL contributed to the acquisition, analysis of the data, and the writing of the manuscript. LK contributed to the interpretation of the data and the final version of the manuscript. YZ contributed to the recruitment of participants and theoretical support for tinnitus symptoms. TD contributed to the recruitment of participants and reviewed the final draft very carefully. XM contributed to the theoretical support for tinnitus symptoms. All authors contributed to the article and approved the submitted version.

Funding

This study was supported by Peking University Educational Reform Foundation (2299000138), the Peking University

People's Hospital Scientific Research Development Funds (RDL2021–14), the Peking University People's Hospital Scientific Research Development Funds (RDY2021–25), the Beijing Social Science Foundation (19YYC020), and the National Natural Sciences Foundation of China (31800962).

Conflict of interest

The authors declare that the research was conducted in the absence of any commercial or financial relationships that could be construed as a potential conflict of interest.

Publisher's note

All claims expressed in this article are solely those of the authors and do not necessarily represent those of their affiliated organizations, or those of the publisher, the editors and the reviewers. Any product that may be evaluated in this article, or claim that may be made by its manufacturer, is not guaranteed or endorsed by the publisher.

References

Anderson, S., White-Schwoch, T., Parbery-Clark, A., and Kraus, N. (2013). A dynamic auditory-cognitive system supports speech-in-noise perception in older adults. *Hear. Res.* 300, 18–32. doi: 10.1016/j.heares.2013.03.006

Andersson, G., and Westin, V. (2008). Understanding tinnitus distress: introducing the concepts of moderators and mediators. *Int. J. Audiol.* 47(Suppl. 2), S106–S111. doi: 10.1080/14992020802301670

Baguley, D., Mcferran, D., and Hall, D. (2013). Tinnitus. *Lancet* 382, 1600–1607. doi: 10.1016/S0140-6736(13)60142-7

Cardon, E., Vermeersch, H., Joossen, I., Jacquemin, L., Mertens, G., Vanderveken, O., et al. (2022). Cortical auditory evoked potentials, brain signal variability and cognition as biomarkers to detect the presence of chronic tinnitus. *Hear. Res.* 420:108489. doi: 10.1016/j.heares.2022.108489

Cima, R. F. F., Mazurek, B., Haider, H., Kikidis, D., and Hoare, D. J. (2019). A multidisciplinary european guideline for tinnitus: diagnostics, assessment, and treatment. *HNO* 67, 10–42. doi: 10.1007/s00106-019-0633-7

Coffey, E., Chepesiuk, A., Herholz, S. C., Sylvain, B., and Zatorre, R. J. (2017). Neural correlates of early sound encoding and their relationship to speech-in-noise perception. *Front. Neurosci.* 11:479. doi: 10.3389/fnins.2017.00479

Diao, T., Duan, M., Ma, X., Liu, J., and Wang, M. (2022). The impairment of speech perception in noise following pure tone hearing recovery in patients with sudden sensorineural hearing loss. *Sci. Rep.* 12:882. doi: 10.1038/s41598-021-03847-y

Du, Y., Buchsbaum, B. R., Grady, C. L., and Alain, C. (2014). Noise differentially impacts phoneme representations in the auditory and speech motor systems. *Proc. Natl. Acad. Sci. U.S.A.* 111, 7126–7131. doi: 10.1073/pnas.1318738111

Eggermont, J. J., and Roberts, L. E. (2004). The neuroscience of tinnitus. *Trends Neurosci.* 27, 676–682. doi: 10.1016/j.tins.2004.08.010

Freyman, R. L., Helfer, K. S., Mccall, D. D., and Clifton, R. K. (1999). The role of perceived spatial separation in the unmasking of speech. *J. Acoust. Soc. Am.* 106, 3578–3588. doi: 10.1121/1.428211

Gilles, A., Schlee, W., Rabau, S., Wouters, K., Fransen, E., and Van de Heyning, P. (2016). Decreased speech-in-noise understanding in young adults with tinnitus. *Front. Neurosci.* 10:288. doi: 10.3389/fnins.2016.00288

Heeren, A., Maurage, P., Perrot, H., De Volder, A., Renier, L., Araneda, R., et al. (2014). Tinnitus specifically alters the top-down executive control sub-component of attention: evidence from the attention network task. *Behav. Brain Res.* 269, 147–154. doi: 10.1016/j.bbr.2014.04.043

Hennig, T. R., Costa, M. J., Urnau, D., Becker, K. T., and Schuster, L. C. (2011). Recognition of speech of normal-hearing individuals with tinnitus and hyperacusis. *Arq. Int. Otorrinolaringol.* 15, 21–28. doi: 10.1590/S1809-48722011000100003

Huang, C., Lee, H., Chung, K., Chen, H., Shen, Y., and Wu, J. (2007). Relationships among speech perception, self-rated tinnitus loudness and disability in tinnitus patients with normal puretone thresholds of hearing. *ORL* 69, 25–29. doi: 10.1159/000096713

Ivansic, D., Guntinas-Lichius, O., Müller, B., Volk, G. F., and Dobel, C. (2017). Impairments of speech comprehension in patients with tinnitus—a review. *Front. Aging Neurosci.* 9:244. doi: 10.3389/fnagi.2017.00224

Jain, C., and Sahoo, J. P. (2014). The effect of tinnitus on some psychoacoustical abilities in individuals with normal hearing sensitivity. *Int. Tinnitus J.* 19, 28–35.

Jerger, J., Chmiel, R., Allen, J., and Wilson, A. (1994). Effects of age and gender on dichotic sentence identification. *Ear Hear.* 15, 274–286. doi: 10.1097/00003446-199408000-00002

Kimura, D. (2011). From ear to brain. *Brain Cogn* 76, 214–217. doi: 10.1016/j.bandc.2010.11.009

Li, L., Qi, J., He, Y., Alain, C., and Schneider, B. A. (2005). Attribute capture in the precedence effect for long-duration noise sounds. *Hear. Res.* 202, 235–247. doi: 10.1016/j.heares.2004.10.007

Litovsky, R. Y. (2005). Speech intelligibility and spatial release from masking in young children. *J. Acoust. Soc. Am.* 117, 3091–3099. doi: 10.1121/1.1873913

Ma, X., Li, J., Lai, J., and Yu, L. (2021). An integrated physical regulation theory and classification of acute tinnitus. *Curr. Med. Sci.* 41, 84–86. doi: 10.1007/s11596-021-2322-5

McCormack, A., Edmondson-Jones, M., Somerset, S., and Hall, D. (2016). A systematic review of the reporting of tinnitus prevalence and severity. *Hear. Res.* 337, 70–79. doi: 10.1016/j.heares.2016.05.009

Moon, I. J., Won, J. H., Kang, H. W., Kim, D. H., An, Y. H., and Shim, H. J. (2015). Influence of tinnitus on auditory spectral and temporal resolution and speech perception in tinnitus patients. *J. Neurosci.* 35, 14260–14269. doi: 10.1523/JNEUROSCI.5091-14.2015

Noreña, A. J. (2015). Revisiting the cochlear and central mechanisms of tinnitus and therapeutic approaches. *Audiol. Neurotol.* 20, 53–59. doi: 10.1159/000380749

Roberts, L. E., Eggermont, J. J., Caspary, D. M., Shore, S. E., and Kaltenbach, J. A. (2010). Ringing ears: the neuroscience of tinnitus. *J. Neurosci.* 30, 14972–14979. doi: 10.1523/JNEUROSCI.4028-10.2010

Roup, C. M. (2011). Dichotic word recognition in noise and the right-ear advantage. *J. Speech Lang. Hear. Res.* 54, 292–297. doi: 10.1044/1092-4388(2010/09-0230)

Ryu, I. S., Ahn, J. H., Lim, H. W., Joo, K. Y., and Chung, J. W. (2012). Evaluation of masking effects on speech perception in patients with unilateral chronic tinnitus using the hearing in noise test. *Otol. Neurotol.* 33, 1472–1476. doi: 10.1097/MAO.0b013e31826dbcc4

Tai, Y., and Husain, F. (2018). Right-ear advantage for speech-in-noise recognition in patients with nonlateralized tinnitus and normal hearing sensitivity. *J. Assoc. Res. Otolaryngol.* 19, 211–221. doi: 10.1007/s10162-017-0647-3

Tai, Y., and Husain, F. (2019). The role of cognitive control in tinnitus and its relation to speech-in-noise performance. *J. Audiol. Otol.* 23, 1–7. doi: 10.7874/jao.2018.00409

Theodoroff, S. M., and Folmer, R. L. (2013). Repetitive transcranial magnetic stimulation as a treatment for chronic tinnitus: a critical review. *Otol. Neurotol.* 34, 199–208. doi: 10.1097/MAO.0b013e31827b4d46

Vielsmeier, V., Kreuzer, P., Haubner, F., Steffens, T., Semmler, P., Kleinjung, T., et al. (2016). Speech comprehension difficulties in chronic tinnitus and its relation to hyperacusis. *Front. Aging Neurosci.* 8:293. doi: 10.3389/fnagi.2016.00293

Villard, S., and Kidd, G. (2019). Effects of acquired aphasia on the recognition of speech under energetic and informational masking conditions. *Trends Hear.* 23, 1–22. doi: 10.1177/2331216519884480

Wang, M., Kong, L., Zhang, C., Wu, X., and Li, L. (2018). Speaking rhythmically improves speech recognition under "cocktail-party" conditions. *J. Acoust. Soc. Am.* 143, EL255–EL259. doi: 10.1121/1.5030518

Wilson, R. H., McArdle, R. A., and Smith, S. L. (2007). An evaluation of the BKB-SIN, HINT, QuickSIN, and WIN materials on listeners with normal hearing and listeners with hearing loss. *J. Speech Lang. Hear. Res.* 50, 844–856. doi: 10.1044/1092-4388(2007/059)

Wu, X., Wang, C., Jing, C., Qu, H., and Li, W. (2005). The effect of perceived spatial separation on informational masking of chinese speech. *Hear. Res.* 199, 1–10. doi: 10.1016/j.heares.2004.03.010

Zeng, F. G., Richardson, M., and Turner, K. (2020). Tinnitus does not interfere with auditory and speech perception. *J. Neurosci.* 40, 6007–6017. doi: 10.1523/JNEUROSCI.0396-20.2020

Zhang, L., Fu, X. Y., Luo, D., Xing, L., and Du, Y. (2021). Musical experience offsets age-related decline in understanding speech-in-noise: type of training does not matter, working memory is the key. *Ear Hear.* 42, 258–270. doi: 10.1097/AUD.0000000000000921

frontiers | Frontiers in Neurology

ORIGINAL RESEARCH
published: 26 August 2022
doi: 10.3389/fneur.2022.921133

Bilateral Dysfunction of Otolith Pathway in Patients With Unilateral Idiopathic BPPV Detected by ACS-VEMPs

Xiaorong Niu[1†], Peng Han[1†], Maoli Duan[2], Zichen Chen[1], Juan Hu[3], Yanfei Chen[3], Min Xu[3], Pengyu Ren[3] and Qing Zhang[3,4*]*

[1] Department of Otorhinolaryngology Head and Neck Surgery, First Affiliated Hospital of Xi'an Jiaotong University, Xi'an, China, [2] Department of Otolaryngology Head and Neck Surgery, Department of Clinical Science, Intervention and Technology, Karolinska University Hospital, Karolinska Institute, Stockholm, Sweden, [3] Department of Otorhinolaryngology Head and Neck Surgery, Ear Institute, Second Affiliated Hospital of Xi'an Jiaotong University, Xi'an, China, [4] Department of Otorhinolaryngology Head and Neck Surgery, Xinhua Hospital, Shanghai Jiaotong University School of Medicine, Shanghai Jiaotong University School of Medicine Ear Institute, Shanghai Key Laboratory of Translational Medicine on Ear and Nose Diseases, Shanghai, China

OPEN ACCESS

Edited by:
Leonardo Manzari,
MSA ENT Academy Center, Italy

Reviewed by:
David Bächinger,
University Hospital Zürich, Switzerland
Niraj Singh,
All India Institute of Speech and Hearing (AIISH), India

***Correspondence:**
Qing Zhang
zhqent@163.com
Pengyu Ren
reaping2006@126.com

[†] These authors have contributed equally to this work and share first authorship

Specialty section:
This article was submitted to Neuro-Otology, a section of the journal Frontiers in Neurology

Received: 15 April 2022
Accepted: 16 June 2022
Published: 26 August 2022

Citation:
Niu X, Han P, Duan M, Chen Z, Hu J, Chen Y, Xu M, Ren P and Zhang Q (2022) Bilateral Dysfunction of Otolith Pathway in Patients With Unilateral Idiopathic BPPV Detected by ACS-VEMPs. Front. Neurol. 13:921133. doi: 10.3389/fneur.2022.921133

Objective: To observe the functional status of the otolith pathway in patients with unilateral idiopathic benign paroxysmal positional vertigo (BPPV) by combining air-conducted sound elicited cervical vestibular-evoked myogenic potential (ACS-cVEMP) and ocular vestibular-evoked myogenic potential (ACS-oVEMP).

Methods: One hundred and eighty patients with BPPV were recruited for conventional cVEMP and oVEMP tests. The abnormal rates of VEMPs were compared between BPPV patients and control participants.

Results: The abnormal rates of cVEMP and oVEMP in BPPV patients were 46.7% (84/180) and 57.2% (103/180) in affected ears, respectively, and 45.0% (81/180) and 56.7% (102/180) in unaffected ears, respectively; both were significantly higher than the abnormal rates of cVEMP and oVEMP in normal control ears. Compared with normal subjects, the cVEMP response rate was lower in affected and unaffected ears in BPPV patients. The abnormal rates of cVEMP and oVEMP were 48.1% (76/158) and 57.6% (91/158) in patients with posterior semicircular canal BPPV, and 36.4% (8/22) and 54.5% (12/22) in lateral semicircular canal BPPV. There was no significant difference in VEMP abnormalities between posterior semicircular canal BPPV and lateral semicircular canal BPPV.

Conclusion: The prevalence of abnormal cVEMPs and oVEMPs in both affected and unaffected ears of patients with BPPV was significantly higher than that observed in the control group. The pathological mechanism of unilateral idiopathic BPPV may be associated with bilateral degeneration of otolith pathways.

Keywords: air-conducted sound, benign paroxysmal positional vertigo, cervical vestibular-evoked myogenic potential, ocular vestibular-evoked myogenic potential, vestibular function

INTRODUCTION

Benign paroxysmal positional vertigo (BPPV) is characterized by recurrent spells of vertigo triggered by changes in head position with respect to gravity. BPPV is one of the most common peripheral vestibular disorders leading to vertigo. BPPV is caused by the otoconia being dislodged from the macula into the semicircular canals. Most cases of BPPV are idiopathic in origin and probably result from degeneration of the macula (1).

Vestibular-evoked myogenic potentials (VEMPs) are used as clinical tests of the otolith pathway, including the saccule and utricle. Cervical VEMP (cVEMP) is recorded from the surface of the sternocleidomastoid muscle (SCM) and reflects the function of the saccule and inferior vestibular nerve. Ocular VEMP (oVEMP) is recorded from the skin surface of the inferior oblique muscle and reflects the function of the utricle and the superior vestibular nerve input pathway (2). Patients with BPPV have abnormal VEMPs in affected ears, and the prevalence of abnormal VEMPs is higher in recurrent BPPV (3, 4). A meta-analysis by Chen et al. (5) revealed that several distinctive characteristics of cVEMP tests exist in BPPV patients compared to healthy controls, including longer latency of p13, a lower amplitude of p13-n23, and a higher proportion of absent responses (5). Some researchers have found that oVEMP is more often abnormal in BPPV patients as compared to cVEMP, leading to speculation that utricular dysfunction may be more common than saccular dysfunction (6, 7). Seo et al. (8) found that reduced oVEMP may originate from the partial degeneration of utricular hair cells. Conversely, augmented oVEMP in the affected ears is thought to originate from hypermobility of the stereocilia due to the detachment of otoconia within the utricle. The results of oVEMP do not appear to be related to the recovery from symptoms (8), although some studies report an increase in oVEMP amplitude on the affected side after a successful repositioning procedure, supporting the hypothesis of the return of otoconia into the area of the utricular macula (9, 10). Singh et al. (3) suggested that a large asymmetry ratio is the most potent characteristic of oVEMP in BPPV. In addition, another study found that abnormalities of cVEMP and oVEMP in the unaffected ears of BPPV patients were significantly higher than in the control group (11). Differences in findings between existing studies indicate the need for more studies. Therefore, we used both cVEMP and oVEMP tests elicited by air-conducted sound (ACS) to fully assess the functional status of the otolith pathway in patients with BPPV and aimed to get a more credible result using a larger sample population.

MATERIALS AND METHODS

Patient Selection

Patients with unilateral idiopathic BPPV who visited the Department of Otorhinolaryngology of the Second Affiliated Hospital of Xi'an Jiaotong University from May 2012 to May 2015 were enrolled in this study. We included only patients with their first attack of idiopathic BPPV. The diagnosis of BPPV was based on: (1) a history of episodes of vertigo with changes in head position relative to gravity; (2) vertigo associated with characteristic nystagmus provoked by the Dix-Hallpike test or roll test; (3) absence of identifiable central nervous system disorders that could explain positional vertigo and nystagmus; and (4) absence of any history of neurotological or vestibular disorders, such as Ménière's disease, labyrinthitis, sudden deafness, vestibular neuritis, migraine, and head trauma. Exclusion criteria included: (1) tympanic membrane perforation or conductive/sensorineural hearing loss caused by any outer/middle/inner ear diseases; (2) symptoms of other cranial nerve damage; (3) bilateral onset or multiple semicircular canal involvement; (4) a previous history of craniocerebral trauma, otitis media, or a history of middle or inner ear surgery (12, 13). No patient underwent any form of treatment for BPPV before their participation in this study. Participants underwent a detailed history collection, physical examination, positional tests, and basic hearing tests to exclude other vestibular diseases.

A total of 180 patients (180 affected ears and 180 unaffected ears) were enrolled in the BPPV group, including 65 males and 115 females aged 16–90 years (mean age = 54.38 ± 14.33 years). There were 92 patients affected on the left side ($n = 180$, 51.1%) and 88 patients affected on the right side ($n = 180$, 48.9%); 158 patients had posterior semicircular canal BPPV and 22 patients had lateral semicircular canal BPPV. The details of clinic data are given in **Table 1**. We also recruited 57 age and gender-matched healthy subjects (114 ears, aged 22–83 years, mean age: 52.37 ± 15.18 years; 21 men) without a history of previous ear disease or dizziness to serve as controls, after confirming normal findings with a neurological examination and pure tone audiogram. All 180 patients and 57 healthy subjects underwent audiometry, ACS-cVEMP, and ACS-oVEMP tests. The study was approved by the regional ethical committee of the Second Affiliated Hospital of Xi'an Jiaotong University. Each participant signed an informed consent form for participation.

cVEMP and oVEMP Recording

To record cVEMP, a supine position was assumed by the subject. There were five electrodes placed on the subject: two active electrodes in the middle of each SCM, two reference electrodes on each sternoclavicular joint, and a ground electrode above the midline of the forehead. Inter-electrode impedance should not exceed 5 kΩ. When receiving tone bursts through an inserted earphone, the subject had to lift her/his head off the pillow in the midline in order to activate the SCM (14). We monitored the background SCM contraction levels, and the instrument only recorded cVEMP responses at a set EMG range of 50–200 μV.

For the recording of oVEMP, a supine position was also assumed. The detailed method of the oVEMP test was laid out in our earlier article (15). Five electrodes were placed on the body surface. Two active electrodes were in line with each pupil and 2 cm below the lower lid margin. Two reference electrodes were below each active electrode at a distance of 1 cm. A ground

Abbreviations: BPPV, benign paroxysmal positional vertigo; VEMP, vestibular evoked myogenic potential; SCM, sternocleidomastoid; cVEMP, cervical VEMP; oVEMP, ocular VEMP; ACS, air-conducted sound; BCV, bone-conducted vibration; EMG, electromyogram.

TABLE 1 | The clinic data of 180 patients with benign paroxysmal positional vertigo (BPPV).

Age groups	*n*	Sex (*n*)		Sides (*n*)		Clinic types (*n*)	
		M	F	Left	Right	PSC	LSC
≤30	10	5	5	10	0	10	0
31–50	58	19	39	30	28	53	5
51–70	88	30	58	45	43	71	17
>70	24	11	13	7	17	24	0
Total	180	65	115	92	88	158	22

PSC, posterior semicircular canal; LSC, lateral semicircular canal.

electrode was located on the midline of the forehead. Inter-electrode impedance should not exceed 5 kΩ. When receiving tone bursts through a calibrated insert earphone, each subject had to gaze upward at a fixed point on the wall with a vertical visual angle of ∼30–35°. The recording instrument and the setting of ACS stimulus in the cVEMP and oVEMP tests were the same. The subjects received a 500 Hz short tone burst (rise/fall time = 1 ms; plateau time = 2 ms) through an insert earphone. A GN Otometrics (Taastrup, Denmark) ICS Chartr EP analyzer was used to amplify the electromyographic signal from the stimulated side. The stimulation rate was 5/s. The average response to each of the 50 stimuli was calculated twice and recorded bilaterally. To check whether a VEMP could be elicited in the subject and waveforms could be identified, the default starting intensity of the stimulus was set as 131 dB Sound Pressure Level (SPL). Then stimulus intensity was decreased in steps of 10 dB when VEMPs were present and increased by 5 dB when VEMPs were absent (15).

Observation Index for cVEMP and oVEMP

The oVEMP and cVEMP were reproducible short-latency biphasic waveforms. A waveform unrecognizable or unrepeatable was regarded as an absent response. The threshold of the VEMP (dB SPL) was the lowest stimulus intensity leading to an identifiable and repeatable biphasic wave. The parameters, such as amplitude (μV) and p1 and n1 latencies (ms) of oVEMP and cVEMP, were measured at a stimulus of 131 dB SPL. The p1 and n1 latencies were measured as the difference between 0 ms and the time of maximal p1 and n1 peaks. The vertical distance between the peaks of p1 and n1 was amplitude.

Normal values in different age groups, including threshold (dB SPL), p1 and n1 latencies (ms), and amplitude (μV) at a stimulus of 131 dB SPL of oVEMP and cVEMP were recorded in our earlier article (15). Normal ranges of those parameters were calculated as mean ± 2 SD in different age groups. Abnormalities were defined as the absence of VEMPs and recorded parameter values outside of the normal ranges.

Statistical Analysis

Data were analyzed using SPSS Statistics 18.0. The χ^2 test was used to compare the rate of abnormalities and the response rate between the BPPV group and the normal control group. The rate of abnormalities and the response rate between the affected ears and the unaffected ears of the BPPV group were analyzed with the McNemar test. For continuous variables, parameters, such as thresholds, p1 and n1 latencies, and amplitude, the Kolmogorov–Smirnov test was used to test for normal distribution. Between the BPPV group and the normal control group, the independent-samples *t*-test was used for normal distributions, and the Mann–Whitney U test was used for non-normal distributions. Between the affected ears and unaffected ears of the BPPV group, the paired-samples *t*-test was used for normal distributions, and the Wilcoxon signed-rank test was used for non-normal distributions. The level of statistical significance was set at $p < 0.05$.

RESULTS

Comparison of Abnormal Rates of ACS-VEMPs Among the Affected Ears, the Unaffected Ears of BPPV, and Controls

The abnormal rates of cVEMP and oVEMP in the affected ears of 180 patients with BPPV were 46.7% (84/180) and 57.2% (103/180), respectively. In the unaffected ears, abnormal rates for cVEMP and oVEMP were 45.0% (81/180) and 56.7% (102/180), respectively. The abnormal rates of cVEMP and oVEMP were 23.7% (27/114) and 43.0% (49/114) in the 114 normal control ears tested (114 ears of 57 healthy subjects). The details of abnormal parameters of cVEMP/oVEMP in affected, unaffected, and control ears are depicted in **Table 2**.

Abnormal rates of cVEMP and oVEMP were significantly higher in the affected ears of BPPV patients than those in normal control ears ($\chi^2_{\text{cVEMP}} = 15.687$, $p < 0.01$; $\chi^2_{\text{oVEMP}} = 5.668$, $p < 0.05$). The unaffected ears of BPPV patients similarly had abnormal rates of cVEMP and oVEMP, higher than those in normal control ears ($\chi^2_{\text{cVEMP}} = 13.646$, $p < 0.01$; $\chi^2_{\text{oVEMP}} = 5.232$, $p < 0.01$) (**Table 3**; **Figure 1**). The abnormal rates of cVEMP or oVEMP between the affected ears and unaffected ears in patients with BPPV did not differ (McNemar test, $p > 0.05$). The results suggest that the abnormal rates of cVEMP and oVEMP are significantly increased bilaterally in patients with BPPV.

TABLE 2 | Abnormal parameters of vestibular-evoked myogenic potentials (VEMPs) in affected, unaffected and control ears.

Groups	Abnormal oVEMP (n)								Abnormal cVEMP (n)						
	n	Absent	T↑	T↑ n1↓	T↑ n1↑	T↓	T↓A↑	n1↑	*n*	Absent	T↑	T↓	T↓A↑	T↓p1↓	p1↑
Affected ears	103	88	0	1	1	3	4	6	84	75	0	2	0	1	6
Unaffected ears	102	90	1	1	0	0	0	10	81	74	2	2	0	0	3
Control ears	49	45	0	0	0	0	1	3	27	22	0	0	1	0	4

T: Threshold; n1: n1 latency; A: Amplitude; p1: p1 latency; ↑: increase; ↓: decrease.

TABLE 3 | Comparison of abnormal rates of cervical vestibular-evoked myogenic potential (cVEMP) and ocular vestibular-evoked myogenic potential (oVEMP) among different groups.

Groups	Ears (*n*)		
	Affected (180)	Unaffected (180)	Controls (114)
cVEMP	46.7% (84/180)*	45.0% (81/180)*	23.7% (27/114)
oVEMP	57.2% (103/180)#	56.7% (102/180)#	43.0% (49/114)

$^{*}p < 0.01$, $^{\#}p < 0.05$, Compared with the normal controls, χ^2 test.

Comparison of Parameters of ACS-VEMPs Among the Affected Ears, Unaffected Ears of BPPV, and Controls

Among 180 patients with BPPV, cVEMP was recorded in 105 (58.3%) affected ears of BPPV patients (aged 16–79 years, mean age = 50.77 ± 13.95 years), and in 106 (58.9%) unaffected ears (aged 16–84 years, mean = 50.86 ± 13.60 years), respectively. Among 114 normal control ears, cVEMP was recorded in 92 (80.7%) ears (aged 22–83 years, mean = 50.42 ± 15.43 years). The average parameters of each group, such as thresholds, p1 and n1 latencies, inter-peak latency, and amplitude, are shown in **Table 4**.

The response rate of cVEMP in the affected ears of BPPV patients ($\chi^2 = 15.796$, $p < 0.01$) and that in the unaffected ears of BPPV patients ($\chi^2 = 15.101$, $p < 0.01$) were significantly lower than that in normal control ears. The affected and unaffected ears of BPPV patients did not differ in cVEMP response rate (McNemar test, $p > 0.05$). There were no significant differences in cVEMP threshold, p1 latency, n1 latency, or amplitude in affected/unaffected ears of BPPV patients vs. normal control ears ($p > 0.05$, independent-samples *t*-test), and in the affected vs. unaffected ears of BPPV patients ($p > 0.05$, paired-samples *t*-test) (**Table 4**; **Figure 2**).

Parameters of oVEMP were similarly compared in affected and unaffected ears of BPPV patients and normal control ears. Among 180 BPPV patients, an oVEMP was recorded in 92 (51.1%) affected ears of BPPV patients (aged 16–77 years, mean = 49.24 ± 13.91 years), and in 90 (50.0%) unaffected ears of BPPV patients (aged 16–74 years, mean = 47.72 ± 13.13 years), respectively. Among the 114 normal control ears, oVEMP was recorded in 69 (60.5%) cases (aged 22–83 years, mean = 46.59 ± 14.50 years). The average parameters of each group, such as thresholds, p1 and n1 latencies, inter-peak latency, and amplitude, are shown in **Table 5**.

The response rate of oVEMP did not differ in the affected/unaffected ears of BPPV patients *vs.* normal control ears (χ^2 test, $p > 0.05$), and in the affected ears vs. unaffected ears in patients with BPPV (McNemar test, $p > 0.05$). There were no significant differences in oVEMP threshold, p1 latency, n1 latency, or amplitude between the affected/unaffected ears of BPPV patients and normal control ears ($p > 0.05$, independent-samples *t*-test), and between the affected ears and unaffected ears in patients with BPPV ($p > 0.05$, paired-samples *t*-test), respectively (**Table 5**; **Figure 3**).

Comparison of Abnormal Rates of ACS-VEMPs Between Different Types of BPPV

Among 180 patients with unilateral BPPV, there were 158 cases of posterior semicircular canal BPPV (age range = 16–90 years, mean age = 54.54 ± 14.94 years). In this group, the abnormal rate of cVEMP was 48.1% (76/158), and the abnormal rate of oVEMP was 57.6% (91/158). The remaining 22 cases were of lateral semicircular canal BPPV (age range = 34–69 years, mean age = 53.27 ± 8.89 years). For this group, the abnormal rate of cVEMP was 36.4% (8/22), and the abnormal rate of oVEMP was 54.5% (12/22). A χ^2 test was performed, and abnormal rates of cVEMP and oVEMP did not differ significantly between the posterior semicircular canal BPPV group and the lateral semicircular canal BPPV group ($\chi^2_{cVEMP} = 1.069$, $p > 0.05$; $\chi^2_{oVEMP} = 0.073$, $p > 0.05$) (**Table 6**).

DISCUSSION

From 17 to 42% of patients with vertigo ultimately were diagnosed with BPPV, making BPPV the most frequent peripheral system cause of vertigo, in general, and the most common cause of vestibular organ-related vertigo, in particular (16, 17). One cross-sectional research from Europe reported a 2.4% lifetime prevalence of BPPV and 10.7 to 64 cases per 100,000 per year incidence (18, 19). The peak incidence of the disorder occurs between the fifth and sixth decades of life. Women are disproportionately affected, with a ratio of 2–3 to 1 compared to men (17, 18). Among the three semicircular canals, the posterior canal variant is the most common type of BPPV (80–90%). Horizontal canal

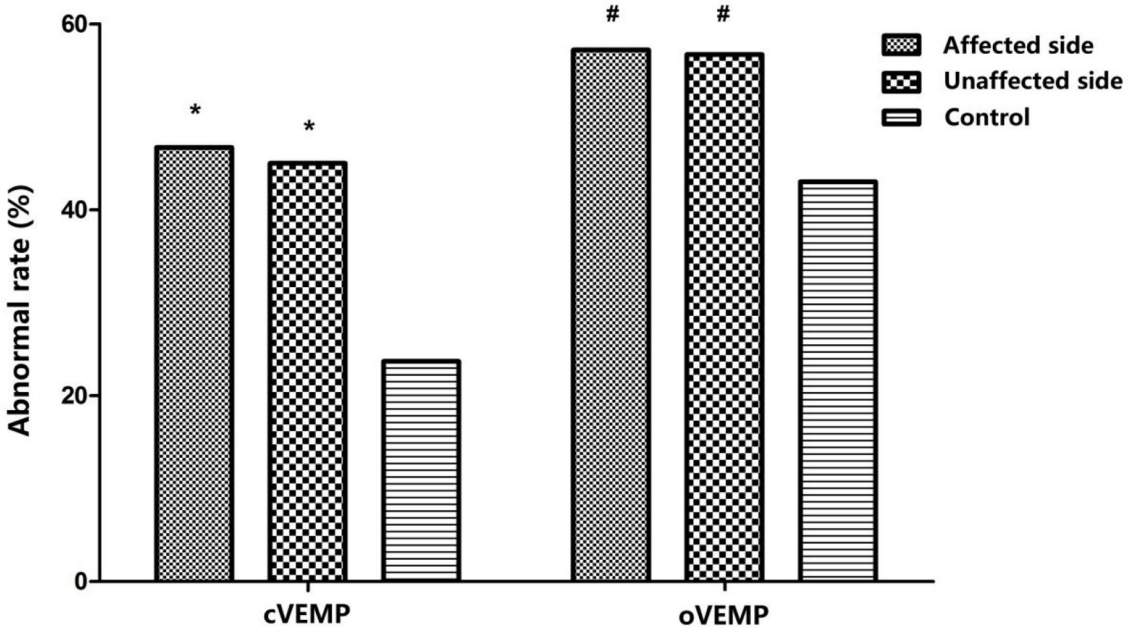

FIGURE 1 | Comparison of abnormal rates of cervical vestibular-evoked myogenic potential (cVEMP) and ocular vestibular-evoked myogenic potential (oVEMP) among affected ears and unaffected ears in the benign paroxysmal positional vertigo (BPPV) group and normal control ears; $^{*}p < 0.01$, $^{\#}p < 0.05$, compared with normal control ears. $p_{\text{affected,cVEMP}} < 0.001$, $p_{\text{unaffected,cVEMP}} < 0.001$; $p_{\text{affected,oVEMP}} = 0.17$, $p_{\text{unaffected,oVEMP}} = 0.22$.

TABLE 4 | Comparison of cervical vestibular-evoked myogenic potential (cVEMP) parameters among affected, unaffected, and control ears.

Groups	Ears		
	Affected	**Unaffected**	**Controls**
Response rate	58.3%*	58.9%*	80.7%
	(105/180)	(106/180)	(92/114)
p1 latency (ms)	16.22 ± 2.49	16.09 ± 2.35	16.70 ± 2.20
n1 latency (ms)	23.41 ± 2.52	23.37 ± 2.61	23.79 ± 2.28
p1-n1 interval (ms)	7.15 ± 1.83	7.32 ± 1.83	7.09 ± 1.78
Amplitude (μV)	138.13 ± 83.56	151.89 ± 98.61	152.10 ± 78.69
Threshold (dB SPL)	123.19 ± 5.76	123.26 ± 5.94	122.36 ± 5.65

**Compared with the normal controls, $p < 0.01$, χ^2 test.*

and superior canal BPPV represent only 10–20% and 3% of cases, respectively (20–22). To avoid confounding factors from multicanal and bilateral cases, our study included only patients with BPPV present in a single semicircular canal. The age distribution, sex ratio and proportion of clinical types of all included BPPV patients were similar to those in previous reports.

Earlier histopathologic research by Dix and Hallpike (23) and Schuknecht (24) suggested that BPPV may be caused by the displacement of utricular otoconia. Then, Moriarty et al. (25) and Naganuma et al. (26) found the basophilic cupular deposits in human temporal bones. Later, a study of 186 temporal bones aged from newborn to 10 years showed that the occurrence of the basophilic cupular deposits, which have been clinically associated with BPPV, was lower in children. Also, the granular particles in basophilic deposits were indistinguishable from otoconia observed on the otoconial membrane of the utricular macula. They speculated that aging of the vestibular labyrinth could be the cause of the accumulation of deposits. In recent work by Kao et al. (27), a scanning electron micrograph of the posterior semicircular canal from patients with intractable BPPV found free-floating otoconia linked to a gelatinous matrix by linking filaments. The free-floating particles leading to BPPV are thought to be otoconia dislodged from the utricle (1, 28). BPPV is typically caused by degeneration of the utricular macula and is idiopathic in origin (1). VEMPs are routinely used as clinical tests of saccule and utricle function. VEMPs abnormalities in BPPV have been reported in several pieces of research, and the prevalence was higher in recurrent BPPV (7, 29–31).

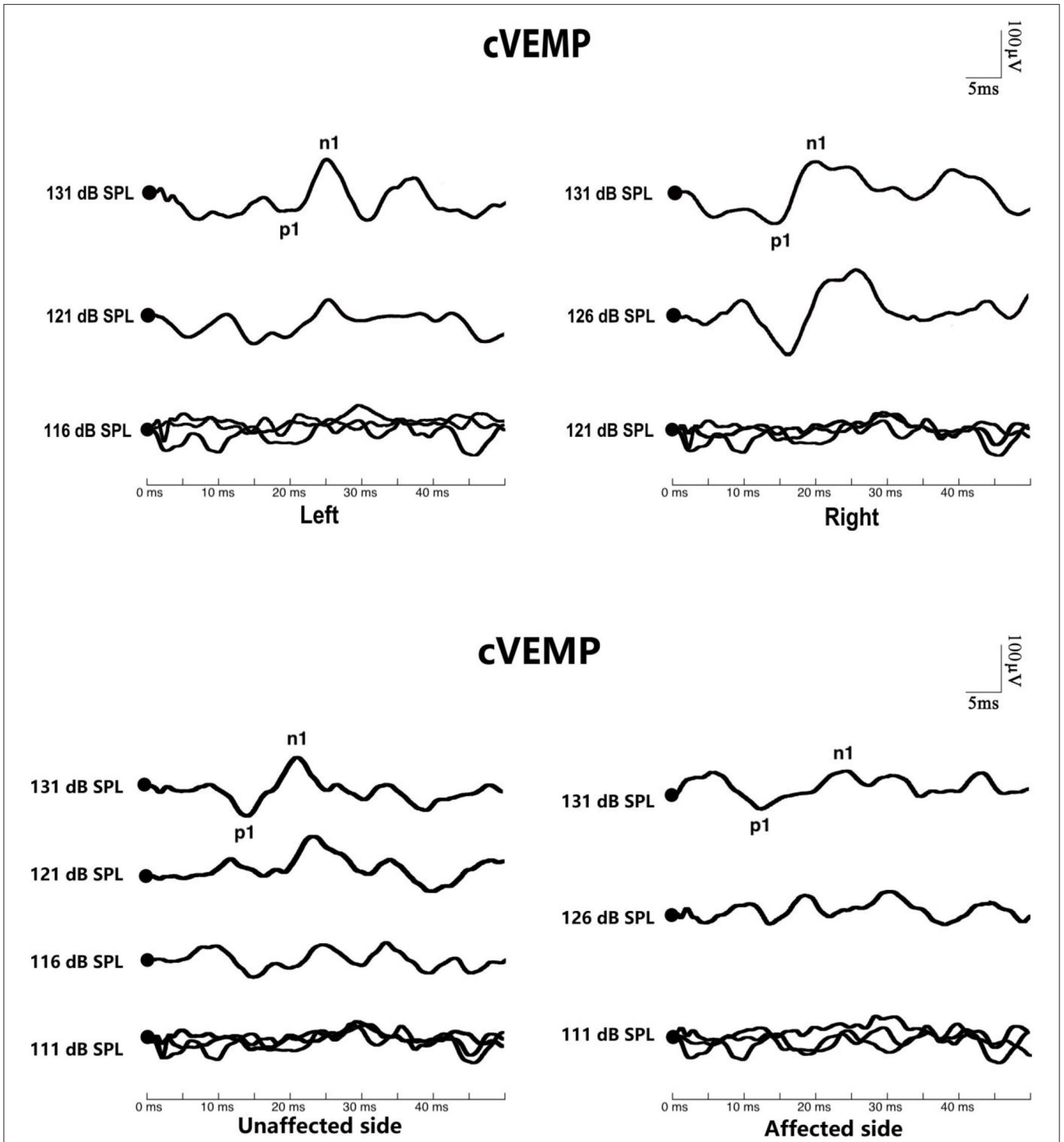

FIGURE 2 | Cervical vestibular-evoked myogenic potential (cVEMP) waves of patients with benign paroxysmal positional vertigo (BPPV). The top picture shows the cVEMP response of a normal subject. The bottom picture shows the cVEMP response of a patient with BPPV.

Ocular vestibular-evoked myogenic potential (oVEMP) responses were reported as having more association with BPPV than cVEMP, the interpretation being that the utricle is considered to play a more important role than the saccule, because of the anatomical relation with the semicircular canals (SCCs) (7). Nakahara et al. (7) found abnormal oVEMPs and

TABLE 5 | Comparison of ocular vestibular-evoked myogenic potential (oVEMP) parameters among affected, unaffected, and control ears.

Groups	Ears		
	Affected	**Unaffected**	**Controls**
Response rate	51.1% (92/180)	50.0% (90/180)	60.5% (69/114)
n1 latency (ms)	10.34 ± 0.88	10.44 ± 1.06	10.51 ± 0.76
p1 latency (ms)	14.96 ± 1.67	15.11 ± 1.66	14.89 ± 1.48
p1-n1 interval (ms)	4.62 ± 1.37	4.66 ± 1.31	4.38 ± 1.32
Amplitude (μV)	5.46 ± 4.21	4.91 ± 3.46	5.01 ± 3.27
Threshold (dB SPL)	123.93 ± 5.65	124.11 ± 4.83	123.03 ± 5.31

cVEMPs in 66.7% and 16.7% of posterior SCC BPPV patients, respectively. They considered that the higher incidence of abnormal oVEMPs suggested dislodgement of otoconia from the utricular macula led to utricular dysfunction (7). Kim et al. (11) showed that the abnormal rates of both cVEMP and oVEMP were significantly higher in patients with BPPV than in healthy controls. Our results that show the proportions of abnormal cVEMP and oVEMP in the affected ears of BPPV patients were significantly higher than that in normal control ears are consistent with those of Kim et al. (11) and indicate that BPPV patients have decreased function of both saccular and utricular pathways compared with normal healthy individuals.

At the same time, we found no significant difference between affected ears and unaffected ears in the BPPV group for abnormal rates of cVEMP or oVEMP. However, when compared to the control group, unaffected ears in the BPPV group showed significantly higher abnormal rates of cVEMP and oVEMP. Similar results have been reported by other investigators. For example, Nakahara et al. (7) found that 75% of patients with abnormal oVEMPs showed bilaterally abnormal responses. Kim et al. (11) reported significantly higher abnormal rates of cVEMP and oVEMP on both the unaffected and affected sides of BPPV patients. This suggests that even when BPPV patients have only unilateral clinical symptoms, dysfunction of saccular and utricular pathways may occur bilaterally. BPPV is considered to be caused by the detachment of otoconia from the macula of the utricle. However, increasing evidence suggests that both the utricle and the saccule could be affected by the macular degenerative process (32–36). Although the pathology of the detachment of the otoconia is not yet fully understood, it was thought that a decrease in the gelatinous layer of the otolithic membrane could be caused by degenerative changes, and that may lead to spontaneous dislodgment of the otoconia from the utricular or saccular macula (30, 37). With aging, the otoconia get pitted, fissured, penetrated, and eventually broken into fragments (38). Osteopenia, osteoporosis, and vitamin D deficiency may also cause deranged calcium metabolism in the vestibular organs and may be related to the incidence of BPPV (39). Thus, it appears that macular degenerative changes, caused by increasing age or abnormal calcium metabolism, lead to BPPV and that this contributes to the development of bilateral otolith dysfunction. When this occurs, the otoconia can fall off the macula on either side and enter the semicircular canal, causing clinical symptoms on the corresponding side.

Abnormalities in VEMPs in this study included the absence of a waveform and recorded parameter values outside the normal range for the age group. The response rates of cVEMPs in the affected and unaffected ears of patients with BPPV were significantly lower than in normal control ears. The response rate of oVEMP did not differ in the affected/unaffected ears of BPPV patients *vs.* normal control ears. This may be related to the low response of ACS-oVEMP being affected by age. The waveform of oVEMP was elicited in only 60.5% of normal control ears. There were no significant differences in oVEMP threshold, p1 latency, n1 latency, or amplitude between the affected/unaffected ears of BPPV patients and normal control ears, and between the affected ears and unaffected ears in patients with BPPV, respectively. The abnormalities of VEMPs elicited by ACS in patients with BPPV presented mainly as an absence of response. The recorded waveform of BPPV patients was similar to that of normal control ears. Different results have been reported in the past in this regard. Some studies have found that the waveform parameters of VEMPs in patients with BPPV have prolonged latency, amplitude reduction, and abnormal asymmetry ratio (AR) value (3, 4). Similar to our study, Singh et al. (40) found that the latency or amplitude did not differ between healthy individuals and those with BPPV.

Yetiser et al. (29) and Singh et al. (40) noted that the abnormality of cVEMP is not related to which semicircular canal is affected in BPPV patients. Kim et al. (11) compared the abnormal rates of cVEMP and oVEMP between 47 patients with posterior semicircular canal BPPV and 51 patients with lateral semicircular canal BPPV and found no significant differences (11). In the current study, the abnormal rates of cVEMPs and oVEMPs similarly did not differ between different types of BPPV.

Gacek (34) proposed that BPPV may result from a morphological change associated with the aging labyrinth that leads to cupular deposits. He proposed that the inhibitory

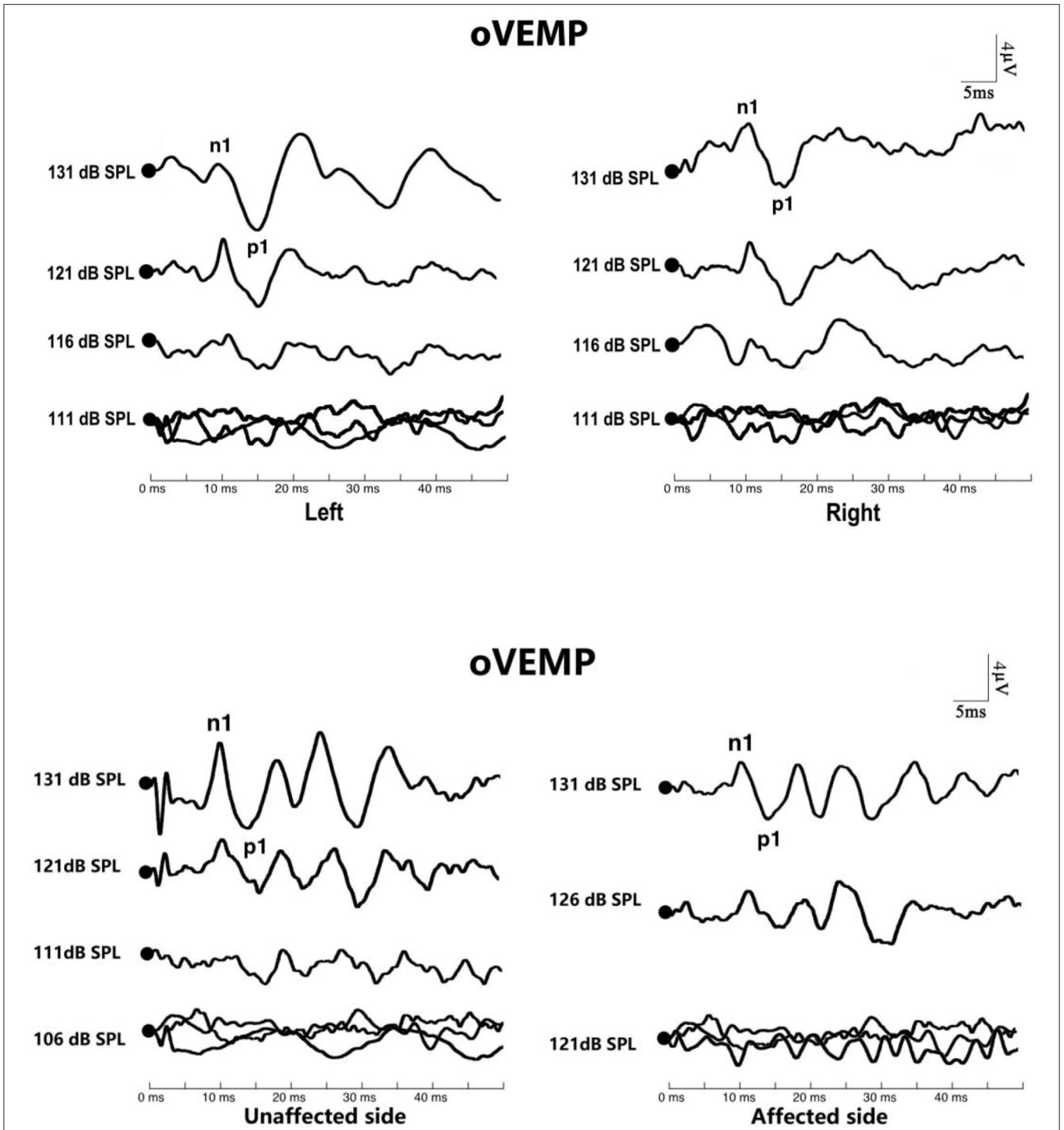

FIGURE 3 | Ocular vestibular-evoked myogenic potential (oVEMP) in affected ears with benign paroxysmal positional vertigo (BPPV). The top picture shows the oVEMP response of a normal subject. The bottom picture shows the oVEMP response of a patient with BPPV.

action of otolith organs to canal activation was lost due to the degeneration of otolith neurons and that this explains the brief canal response induced by the positional stimulus. He further proposed that the inadequate inhibition in the saccular macula may lead to nystagmus of posterior canal BPPV, while decreased utricular inhibition of lateral canal activation may be presented in lateral canal BPPV (34). We speculate that this concept may offer a better explanation for patients with chronic BPPV, refractory BPPV, and subjective BPPV. In contrast, our findings do not support the above hypotheses.

TABLE 6 | Comparison of abnormal rates of vestibular-evoked myogenic potentials (VEMPs) between two types of benign paroxysmal positional vertigo (BPPV).

Groups	Semicircular canal BPPV (*n*)	
	Posterior (158)	Horizontal (22)
cVEMP	48.1% (76/158)	36.4% (8/22)
oVEMP	57.6% (91/158)	54.5% (12/22)

CONCLUSION

The occurrence of abnormal cVEMP or oVEMP in both affected and unaffected ears of patients with BPPV was significantly higher than that observed in the ears of the control group, indicating that otolith pathway dysfunction occurs bilaterally and simultaneously in both saccular and utricular pathways. Thus, the pathological mechanism of unilateral idiopathic BPPV may be associated with bilateral degeneration of otolith pathways. The affected side of those with BPPV that creates symptoms may occur at random or may be related to physical factors, such as sleeping position and anatomical structure of the inner ear.

LIMITATIONS

The ACS-oVEMP we used may be more sensitive than BCV-oVEMP in detecting disease but is associated with more false-positive (abnormal) results. We also have a portion of older subjects, though control subjects were not significantly different in age compared with BPPV subjects. Furthermore, ACS VEMPS can be affected by even minor air-bone gaps. It must be admitted that we should be cautious in interpreting absent ACS-oVEMPs, especially in patients with hearing loss and elderly patients. Therefore, although we have the preliminary results above, oVEMP and whether specific differences arise from the use of BCV or ACS stimulation could be the focus of further studies.

DATA AVAILABILITY STATEMENT

The raw data supporting the conclusions of this article will be made available by the authors, without undue reservation.

ETHICS STATEMENT

The studies involving human participants were reviewed and approved by Regional Ethical Committee of the Second Affiliated Hospital of Xi'an Jiaotong University. Written informed consent to participate in this study was provided by the participants' legal guardian/next of kin.

AUTHOR CONTRIBUTIONS

XN and PH wrote the manuscript. PR, MX, and QZ provided the idea for the study and reviewed and edited the manuscript. MD reviewed and edited the manuscript. ZC, YC, and JH collected the clinical data. All authors contributed to the article and approved the submitted version.

FUNDING

This study was funded by the Natural Science Foundation of China (Nos. 81803317, 81970891, and 82171137), Natural Science Foundation of Shaanxi Province (No. 2019JQ-957), The Key International Cooperation Project of Shaanxi Province (No. 2020-KWZ-019), and Fundamental Research Funds for the Central Universities, China (No. xjj2018094).

ACKNOWLEDGMENTS

The authors thank the healthy volunteers who participated in this study.

REFERENCES

1. You P, Instrum R, Parnes L. Benign paroxysmal positional vertigo. *Laryngoscope Investig Otolaryngol.* (2019) 4:116–23. doi: 10.1002/lio2.230
2. Murofushi T. Clinical application of vestibular evoked myogenic potential (VEMP). *Auris Nasus Larynx.* (2016) 43:367–76. doi: 10.1016/j.anl.2015.12.006
3. Singh NK, Apeksha K. Efficacy of cervical and ocular vestibular-evoked myogenic potentials in evaluation of benign paroxysmal positional vertigo of posterior semicircular canal. *Eur Arch Otorhinolaryngol.* (2016) 273:2523–32. doi: 10.1007/s00405-015-3867-3
4. Yang WS, Kim SH, Lee JD, Lee WS. Clinical significance of vestibular evoked myogenic potentials in benign paroxysmal positional vertigo. *Otol Neuroto.* (2008) 29:1162–6. doi: 10.1097/MAO.0b013e31818a0881
5. Chen G, Yu G, Li Y, Zhao X, Dai X, Wang G. Cervical vestibular evoked myogenic potentials in benign paroxysmal positional vertigo: a systematic review and meta-analysis. *Front Neurol.* (2019) 10:1043. doi: 10.3389/fneur.2019.01043
6. Xu H, Liang FY, Chen L, Song XC, Tong MC, Thong JF, et al. Evaluation of the utricular and saccular function using oVEMPs and cVEMPs in BPPV patients. *J Otolaryngol Head Neck Surg.* (2016) 45:12. doi: 10.1186/s40463-016-0125-7
7. Nakahara H, Yoshimura E, Tsuda Y, Murofushi T. Damaged utricular function clarified by oVEMP in patients with benign paroxysmal positional vertigo. *Acta Otolaryngol.* (2013) 133:144–9. doi: 10.3109/00016489.2012.720030
8. Seo T, Saka N, Ohta S, Sakagami M. Detection of utricular dysfunction using ocular vestibular evoked myogenic potential in patients with benign paroxysmal positional vertigo. *Neurosci Lett.* (2013) 550:12–6. doi: 10.1016/j.neulet.2013.06.041
9. Mendes T, Maslovara S, Vceva A, Butkovic Soldo S. Role of vestibular evoked myogenic potentials as an indicator of recovery in patients with benign paroxysmal positional vertigo. *Acta Clin Croat.* (2017) 56:756–64. doi: 10.20471/acc.2017.56.04.25
10. Bremova T, Bayer O, Agrawal Y, Kremmyda O, Brandt T, Teufel J, et al. Ocular VEMPs indicate repositioning of otoconia to the utricle after successful liberatory maneuvers in benign paroxysmal positioning vertigo. *Acta Otolaryngol.* (2013) 133:1297–303. doi: 10.3109/00016489.2013.829922

11. Kim EJ, Oh SY, Kim JS, Yang TH, Yang SY. Persistent otolith dysfunction even after successful repositioning in benign paroxysmal positional vertigo. *J Neurol Sci.* (2015) 358:287–93. doi: 10.1016/j.jns.2015.09.012
12. Bhattacharyya N, Gubbels SP, Schwartz SR, Edlow JA, El-Kashlan H, Fife T, et al. Clinical practice guideline: benign paroxysmal positional vertigo (Update). *Otolaryngol Head Neck Surg.* (2017) 156 (Suppl. 3):S1–47. doi: 10.1177/0194599816689667
13. Bhattacharyya N, Baugh RF, Orvidas L, Barrs D, Bronston LJ, Cass S, et al. Clinical practice guideline: benign paroxysmal positional vertigo. *Otolaryngol Head Neck Surg.* (2008) 139 (Suppl. 4):S47–81. doi: 10.1016/j.otohns.2008.08.022
14. Sheykholeslami K, Murofushi T, Kaga K. The effect of sternocleidomastoid electrode location on vestibular evoked myogenic potential. *Auris Nasus Larynx.* (2001) 28:41–3. doi: 10.1016/S0385-8146(00)00091-2
15. Zhang Q, Xu X, Niu X, Hu J, Chen Y, Xu M. [Effects of aging on air-conducted sound elicited ocular vestibular- evoked myogenic potential and cervical vestibular-evoked myogenic potential]. *Zhonghua Er Bi Yan Hou Tou Jing Wai Ke Za Zhi.* (2014) 49:897–901. doi: 10.3760/cma.j.issn.1673-0860.2014.11.005
16. Hanley K, O'Dowd T, Considine N. A systematic review of vertigo in primary care. *Br J Gen Pract.* (2001) 51:666–71.
17. Katsarkas A. Benign paroxysmal positional vertigo (BPPV): idiopathic versus post-traumatic. *Acta Otolaryngol.* (1999) 119:745–9. doi: 10.1080/00016489950180360
18. Kim JS, Zee DS. Clinical practice. Benign paroxysmal positional vertigo. *N Engl J Med.* (2014) 370:1138–47. doi: 10.1056/NEJMcp1309481
19. von Brevern M, Radtke A, Lezius F, Feldmann M, Ziese T, Lempert T, et al. Epidemiology of benign paroxysmal positional vertigo: a population based study. *J Neurol Neurosurg Psychiatry.* (2007) 78:710–5. doi: 10.1136/jnnp.2006.100420
20. Anagnostou E, Kouzi I, Spengos K. Diagnosis and treatment of anterior-canal benign paroxysmal positional vertigo: a systematic review. *J Clin Neurol.* (2015) 11:262–7. doi: 10.3988/jcn.2015.11.3.262
21. Hornibrook J. Benign paroxysmal positional vertigo (BPPV): history, pathophysiology, office treatment and future directions. *Int J Otolaryngol.* (2011) 2011:835671. doi: 10.1155/2011/835671
22. Parnes LS, Agrawal SK, Atlas J. Diagnosis and management of benign paroxysmal positional vertigo (BPPV). *CMAJ.* (2003) 169:681–93.
23. Dix MR, Hallpike CS. The pathology symptomatology and diagnosis of certain common disorders of the vestibular system. *Proc R Soc Med*. (1952) 45:341–54. doi: 10.1177/003591575204500604
24. Schuknecht HF. *Pathology of the Ear*. Philadelphia: Lea and Febiger (1993). p. 529–39.
25. Moriarty B, Rutka J, Hawke M. The incidence and distribution of cupular deposits in the labyrinth. *Laryngoscope.* (1992) 102:56–9. doi: 10.1288/00005537-199201000-00011
26. Naganuma H, Kohut RI Ryu JH, Tokumasu K, Okamoto M, Fujino A, et al. Basophilic deposits on the cupula: preliminary findings describing the problems involved in studies regarding the incidence of basophilic deposits on the cupula. *Acta Otolaryngol Suppl.* (1996) 524:9–15. doi: 10.3109/00016489609124341
27. Kao WT, Parnes LS, Chole RA. Otoconia and otolithic membrane fragments within the posterior semicircular canal in benign paroxysmal positional vertigo. *Laryngoscope.* (2017) 127:709–14. doi: 10.1002/lary.26115
28. Furman JM, Cass SP. Benign paroxysmal positional vertigo. *N Engl J Med.* (1999) 341:1590–6. doi: 10.1056/NEJM199911183412107
29. Yetiser S, Ince D, Gul M. An analysis of vestibular evoked myogenic potentials in patients with benign paroxysmal positional vertigo. *Ann Otol Rhinol Laryngol.* (2014) 123:686–95. doi: 10.1177/0003489414532778
30. Lee JD, Park MK, Lee BD, Lee TK, Sung KB, Park JY. Abnormality of cervical vestibular-evoked myogenic potentials and ocular vestibular-evoked myogenic potentials in patients with recurrent benign paroxysmal postitional vertigo. *Acta Otolaryngol.* (2013) 133:150–3. doi: 10.3109/00016489.2012.723823
31. Krempaska S, Koval J. The role of vestibular evoked myogenic potentials (VEMPs) in vestibulopathy diagnostics. *Bratisl Lek Listy.* (2012) 113:301–6. doi: 10.4149/BLL_2012_070
32. Longo G, Onofri M, Pellicciari T, Quaranta N. Benign paroxysmal positional vertigo: is vestibular evoked myogenic potential testing useful? *Acta Otolaryngol.* (2012) 132:39–43. doi: 10.3109/00016489.2011.619570
33. Hong SM, Park DC, Yeo SG, Cha CI. Vestibular evoked myogenic potentials in patients with benign paroxysmal positional vertigo involving each semicircular canal. *Am J Otolaryngol.* (2008) 29:184–7. doi: 10.1016/j.amjoto.2007.07.004
34. Gacek RR. Pathology of benign paroxysmal positional vertigo revisited. *Ann Otol Rhinol Laryngol.* (2003) 112:574–82. doi: 10.1177/000348940311200702
35. Honrubia V, Baloh RW, Harris MR, Jacobson KM. Paroxysmal positional vertigo syndrome. *Am J Otol.* (1999) 20:465–70.
36. Welling DB, Parnes LS, O'Brien B, Bakaletz LO, Brackmann DE, Hinojosa R. Particulate matter in the posterior semicircular canal. *Laryngoscope.* (1997) 107:90–4. doi: 10.1097/00005537-199701000-00018
37. Kim JS, Oh SY, Lee SH, Kang JH, Kim DU, Jeong SH, et al. Randomized clinical trial for geotropic horizontal canal benign paroxysmal positional vertigo. *Neurology.* (2012) 79:700–7. doi: 10.1212/WNL.0b013e3182648b8b
38. Jang YS, Hwang CH, Shin JY, Bae WY, Kim LS. Age-related changes on the morphology of the otoconia. *Laryngoscope.* (2006) 116:996–1001. doi: 10.1097/01.mlg.0000217238.84401.03
39. Jeong SH, Kim JS. Impaired calcium metabolism in benign paroxysmal positional vertigo: a topical review. *J Neurol Phys Ther.* (2019) 43 (Suppl. 2):S37–41. doi: 10.1097/NPT.0000000000000273
40. Singh NK, Sinha SK, Govindaswamy R, Kumari A. Are cervical vestibular evoked myogenic potentials sensitive to changes in the vestibular system associated with benign paroxysmal positional vertigo? *Hear Balance Commun.* (2014) 12:20–6. doi: 10.3109/21695717.2014.883208

Conflict of Interest: The authors declare that the research was conducted in the absence of any commercial or financial relationships that could be construed as a potential conflict of interest.

Publisher's Note: All claims expressed in this article are solely those of the authors and do not necessarily represent those of their affiliated organizations, or those of the publisher, the editors and the reviewers. Any product that may be evaluated in this article, or claim that may be made by its manufacturer, is not guaranteed or endorsed by the publisher.

Copyright © 2022 Niu, Han, Duan, Chen, Hu, Chen, Xu, Ren and Zhang. This is an open-access article distributed under the terms of the Creative Commons Attribution License (CC BY). The use, distribution or reproduction in other forums is permitted, provided the original author(s) and the copyright owner(s) are credited and that the original publication in this journal is cited, in accordance with accepted academic practice. No use, distribution or reproduction is permitted which does not comply with these terms.

frontiers | Frontiers in Neurology

TYPE Original Research
PUBLISHED 13 September 2022
DOI 10.3389/fneur.2022.964217

Check for updates

OPEN ACCESS

EDITED BY
Sulin Zhang,
Huazhong University of Science and Technology, China

REVIEWED BY
Pedro Marques,
University of Porto, Portugal
Daogong Zhang,
Shandong Provincial ENT Hospital, China

*CORRESPONDENCE
Wuqing Wang
wwuqing@eent.shmu.edu.cn

SPECIALTY SECTION
This article was submitted to Neuro-Otology, a section of the journal Frontiers in Neurology

RECEIVED 08 June 2022
ACCEPTED 25 July 2022
PUBLISHED 13 September 2022

CITATION
Shi S, Li W, Wang D, Ren T and Wang W (2022) Characteristics of clinical details and endolymphatic hydrops in unilateral and bilateral Ménière's disease in a single Asian group. *Front. Neurol.* 13:964217. doi: 10.3389/fneur.2022.964217

COPYRIGHT
© 2022 Shi, Li, Wang, Ren and Wang. This is an open-access article distributed under the terms of the Creative Commons Attribution License (CC BY). The use, distribution or reproduction in other forums is permitted, provided the original author(s) and the copyright owner(s) are credited and that the original publication in this journal is cited, in accordance with accepted academic practice. No use, distribution or reproduction is permitted which does not comply with these terms.

Characteristics of clinical details and endolymphatic hydrops in unilateral and bilateral Ménière's disease in a single Asian group

Suming Shi[1,2], Wenquan Li[3], Dan Wang[1,2], Tongli Ren[1,2] and Wuqing Wang[1,2]*

[1]ENT Institute and Otorhinolaryngology Department, Eye & ENT Hospital of Fudan University, Shanghai, China, [2]NHC Key Laboratory of Hearing Medicine, Fudan University, Shanghai, China, [3]Department of Otolaryngology, The Second Affiliated Hospital of Soochow University, Soochow, China

Objectives: To elucidate the characteristics of the clinical details and endolymphatic hydrops (EH) in bilateral Ménière's disease (BMD).

Methods: A total of 545 patients with definite MD were enrolled. Demographic variables; the age of onset; disease course; inner ear function; the coexistence of related disorders such as migraine, delayed MD, drop attacks, and autoimmune diseases; familial history; and characteristics of EH were analyzed.

Results: In the study population, the prevalence of BMD was 15.4%. The disease duration of BMD (84.0 ± 89.6 months) was significantly longer than that of unilateral MD (UMD, 60.1 ± 94.0 months) ($P = 0.001$). As evaluated by hearing thresholds and cervical and ocular vestibular evoked myogenic potentials, inner ear functions were more deteriorated in BMD ($P < 0.05$) than in UMD. The proportions of delayed MD and a family history of vertigo were significantly larger in BMD ($P < 0.05$). EH was observed in 100% of cases on the clinically affected side and 6.1% of cases on the unaffected side.

Conclusion: A low prevalence of BMD, longer disease duration, higher frequencies of delayed MD, and family history of vertigo in patients with BMD were significant findings observed in the present study. All affected ears presented with EH, and a low percentage of unaffected sides presented with EH.

KEYWORDS

bilateral Ménière's disease, unilateral Ménière's disease, clinical characteristics, endolymphatic hydrops, delayed Ménière's disease

Introduction

Ménière's disease (MD) is a complex condition of the inner ear and the most common cause of episodic vertigo combined with fluctuating hearing loss, tinnitus, and aural fullness. The precise etiology is currently unknown. Unilateral MD (UMD) accounts for the majority of MD cases, and bilateral MD (BMD) has the classic symptoms of UMD combined with disequilibrium and oscillopsia from bilateral vestibular hypofunction and communication difficulties from bilateral hearing loss (1). BMD can have a profound

impact on the patient's quality of life, and treatment options are very limited. To date, the frequency and related factors of BMD remain unclear, especially concerning ethnic differences in epidemiology (2, 3).

Most cases of BMD present with both ears affected sequentially, with initial unilateral symptoms evolving toward bilateral disease (1); unfortunately, the causes are not exactly known. To date, an epidemiological association between MD and migraine has been reported, and some studies proposed the hypothesis that MD is a migraine-related phenomenon. Autoimmune pathologies are considered to be related to MD, including autoimmune arthritis (4) and thyroid diseases (5). A familial predisposition to the development of MD has also been described (6), especially for BMD (7, 8), and ethnic differences were shown in epidemiologic and genetic features (9). In addition, patients with BMD were reported to have a higher frequency of delayed MD (9). The concept of delayed MD is not different from delayed endolymphatic hydrops (DEH). Because the formation of EH was unclear, delayed MD might be more reasonable. However, whether these factors are related to BMD remains unclear, and most pertinent studies had limited data or were population-based research conducted in Western countries.

The pathological hallmark of MD is endolymphatic hydrops (EH) (10). Recently, extensive use of gadolinium (Gd) contrast-enhanced MRI has enabled the depiction of EH. Therefore, all patients included in our study underwent Gd contrast-enhanced MRI because of two reasons. First, it is worthwhile to improve the diagnostic accuracy of definite MD. Second, it is beneficial for investigating the characteristics of EH in BMD.

Therefore, we performed a prospective analysis of 545 patients with definite MD to investigate the characteristics of clinical details and EH of bilateral MD and the factors associated with bilateral MD.

Materials and methods

Patients

A total of 545 patients (274 men, 271 women; mean age 51.1 years, SD = 13.6 years) were included from February 2016 to September 2021. The patients enrolled in the study fulfilled the the definite MD diagnostic criteria formulated by the Classification Committee of the Bárány Society. Moreover, all patients underwent 3-T MRI. Neurotologic evaluations were performed, including an electric otoscope, audiometry, and tympanometry. Demographic variables, age of onset, disease course, inner ear functions, the coexistence of related disorders, such as migraine, delayed MD, drop attacks, systemic autoimmune diseases, and familial history of vertigo, and characteristics of EH were analyzed and compared. The enrolled patients with delayed MD had been suffering from longstanding (>2 years) unilateral severe or profound hearing loss, and cases with fluctuating hearing loss, mild or moderate hearing loss, were excluded though the time passes years before the occurrence of vertigo. The medical ethics committee of the Eye, Ear, Nose, and Throat Hospital of Fudan University approved this study, and all patients signed an intravenous Gd contrast operation consent form.

IT or IV Gd injection and MRI acquisition

Intratympanic Gd injection (IT method) and intravenous injection (IV method) were used to visualize EH in MD. In total, 74 patients underwent the bilateral IT method (11), and 471 patients underwent IV injection for a double dose (0.4 mL/kg body weight) of Gd-HP-DO3A. For the IV method, MRI was performed 4 h after the injection, and scans were performed on a 3T MRI scanner (Verio; Siemens Healthcare, Erlangen, Germany) using a 32-channel phased array receive-only coil. The parameters applied were as follows: voxel size = 0.17 × 0.17 × 0.6 mm, scan time = 15 min and 20 s, repetition time = 6,000 ms, echo time = 181 ms, inversion time = 1,850 ms, slice thickness = 0.6 mm, field of view = 160 × 160 mm, and matrix size = 768 × 768. The 3T MR imaging was used to demonstrate EH and to exclude vestibular schwannoma or other causes of vertigo and hearing loss.

Caloric test

The bithermal caloric test was performed in a dark room and conducted with an open-loop GN Otometrics Type 1068 air irrigator combined with an electronystagmography system (both Otometrics, Taastrup, Denmark). Patients were asked to lie in a supine position with their head and back inclined at 30° from the horizontal position. Nystagmus was bilaterally evoked and recorded after irrigation of the external auditory canal with an airflow of 8 L/min at 23°C (cool) and 49°C (warm), in the following order: cool left, cool right, warm left, and warm right. The duration of each irrigation was 60 s, and the interval between two irrigations was 5 min. The maximum slow-phase velocities elicited by cool and warm air on both sides were compared, and an abnormal result of the caloric test was noted when unilateral weakness was indicated by a value difference >25%.

Vestibular-evoked myogenic potential test

We ensured that each patient was cooperative, could contract sternocleidomastoid muscles, and had no air-bone gaps. The VEMP test was performed on patients in a supine

position in a sound-proof room with a temperature of 25°C. Using air-conducted sounds, a total of 120 auditory stimuli (short tone bursts, 500 Hz) were applied to each ear *via* calibrated insert headphones. Rise/fall time and plateau time were set at 2 ms each. A Bio-Logic Navigator PRO system (Version.7.0.0 of Biologic Auditory Evoked Potential software) was used to amplify the electromyographic signals, and electrical activity was bandpass filtered (10–1,500 Hz). To keep the electrode impedance below 5 kX, the skin was pretreated with a facial scrub. An initial intensity of 95 dB nHL was applied as the initial intensity to confirm a VEMP response and was changed afterward in decrements or increments of 5 dB nHL until VEMPs were not detectable. Response thresholds were defined as the minimum stimulus intensities of the characteristic waveform. For all patients with increased threshold, delayed latency or lack of response were regarded as "abnormal VEMP response."

Cervical vestibular evoked myogenic potential test

White, blue, and red electrodes (serving as the non-inverting, inverting, and common electrodes, respectively) were placed on the lower part of the suprasternal fossa, the center of the ipsilateral sternocleidomastoid muscle (SCM), which is the same as the stimulating side, and the center of the contralateral SCM, respectively. The SCM electrodes could be switched automatically, so position adjustments of the electrodes were not necessary when the test was repeated on the opposite side. Patients were required to raise their heads for an SCM contraction when they heard a sound or saw a signal from the examiner. The elicitation of cVEMP was confirmed when the characteristic P13-N23 (positive-negative waveform, negative being upward) appeared. An absence of cVEMP was noted when the typical waveforms could not be elicited or were unrepeatable. The normal value of the cVEMP threshold was set at 75 ± 5 dB nHL.

Ocular vestibular evoked myogenic potential test

The blue and red electrodes (the inverting and common electrodes, respectively) were placed on the pretreated skin about 1 cm beneath the right and left eyes, respectively. When recording on the left side, the white electrode (the non-inverting electrode) was placed 2 cm below the blue one; while recording on the right side, the white electrode was placed 2 cm below the red one. There was no need to reposition the blue and red electrodes because those beneath the eyes could be switched automatically. Patients were required to gaze 30° upward from the vertical position when they heard a sound or saw a gesture from the examiner. The elicitation of oVEMP was confirmed when the characteristic N10-P15 appeared (negative-positive waveform, negative being upward). An absence of oVEMP was established when the typical waveforms could not be elicited or were unrepeatable. The normal value for the oVEMP threshold was determined as 80 ± 5 dB nHL.

TABLE 1 Demographic and clinical characteristics of enrolled patients ($n = 545$).

Variables	Values
Visiting age, yr, mean±SD	51.1 ± 13.6
Onset age, yr, mean±SD	45.6 ± 14.3
Disease duration, m, mean±SD	65.1 ± 93.6
Gender, *n* (%)	
Women	271 (49.7)
Men	274 (50.3)
Affected ear, *n* (%)	
Unilateral	461 (84.6)
Bilateral	84 (15.4)
Comorbid migraines, *n* (%)	71 (13.0)
Family history of vertigo, *n* (%)	33 (6.1)
Delayed MD, *n* (%)	36 (6.6)
Drop attack, *n* (%)	15 (2.8)
Systemic autoimmune diseases, *n* (%)	1 (0.2)

Pure tone audiometry test

Hearing thresholds before Gd intravenous injection were tested in all patients. Hearing thresholds at 250, 500, 1,000, 2,000, and 4,000 Hz were evaluated.

Statistical analysis

Statistical analyses were performed using SPSS Statistics 17 software (IBM, Chicago, IL, USA) package. Data were presented as x ± SD. The Mann-Whitney *U* test, the independent samples *t*-test, the chi-square test, and Fisher's exact test were used for data analyses. Differences were considered to be statistically significant with a p-value <0.05.

Results

Demographics

The group consisted of 271 women and 274 men with a first-visit age of 51.1 ± 13.6 years, an age at onset of 45.6 ± 14.3 years, and a disease course of 65.1 ± 93.6 months. A total of 461 (84.6%) out of 545 enrolled patients had UMD, and 84 (15.4%) out of 545 patients had BMD (Table 1). Of 545 patients, 71 (13.0%) had comorbid migraines, 33 (6.1%) had a family

TABLE 2 Comparison of unilateral MD versus bilateral MD.

Variables	UMD ($n = 461$)	BMD ($n = 84$)	*P*-Value
Visiting age, yr, mean±SD	50.9 ± 13.4	51.9 ± 14.6	0.331
Onset age, yr, mean±SD	45.9 ± 14.1	44.2 ± 15.3	0.322
Disease duration, m, mean±SD	60.1 ± 94.0	84.0 ± 89.6	0.001**
Gender, *n* (%)			
Women	232 (50.3)	39 (46.4)	0.511
Men	229 (49.7)	45 (53.6)	
Comorbid migraines, *n* (%)	59 (12.8)	12 (14.3)	0.710
Family history of vertigo, *n* (%)	22 (4.8)	11 (13.1)	0.003**
Delayed MD, *n* (%)	24 (5.2)	12 (14.3)	0.002**
Drop attack, *n* (%)	12 (2.6)	3 (3.6)	0.618
Systemic autoimmune diseases, *n* (%)	0	1 (1.2)	0.019*
Canal weakness, %			
First involved ear	67.1	69.0	0.840[†]
Second involved ear	0	20.7	0.000**[§]
Abnormal cVEMP response, %			
First involved ear	82.2	100.0	0.045*[†]
Second involved ear		84.2	0.071[§]
Abnormal oVEMP response, %			
First involved ear	82.2	100.0	0.045*[†]
Second involved ear		100.0	1[§]
Hearing threshold, dB, HL, mean±SD			
First involved ear	56.5 ± 23.1	67.5 ± 28.9	0.019*[†]
Second involved ear		45.8 ± 20.0	0.000**[§]

Hearing threshold = average of 250, 500, 1,000, 2,000, 4,000 Hz. [†] A *P*-value in the comparison between the affected ear in UMD and the first involved ear in BMD. [§] A *P*-value in the comparison between the first and second involved ears in BMD. UMD, unilateral Ménière's disease; BMD, bilateral Ménière's disease. *$P < 0.05$. **$P < 0.01$.

history of vertigo, 36 (6.6%) had delayed MD, 15 (2.8%) had drop attacks, and only 1 (0.2%) had a systemic autoimmune disease (Table 1).

As seen in Table 2, 50.3% (232/461) of patients with UMD were women and 49.7% (229/461) were men, and 46.4% (40/84) of the patients with BMD were women and 53.6% (46/84) men, with no significant sex difference between the two groups ($P = 0.511$). Patients with BMD tended to be younger at the onset of the disease (44.2 ± 15.3 years) than those with UMD (45.9 ± 14.1 years); however, it was not significantly different ($P = 0.322$). The disease duration from the onset of the first involved ear of patients with BMD (84.0 ± 89.6 months) was significantly longer than that of the first involved ear of patients with UMD (60.1 ± 94.0 months) ($P = 0.001$).

Cochlear and vestibular function

The average hearing thresholds of the first involved ear in patients with BMD (67.5 ± 28.9 dB HL) were significantly higher than those of the affected side in patients with UMD (56.5 ± 23.1 dB HL, $P = 0.019$) (Table 2). In patients with BMD, the mean hearing thresholds of the first involved ear (67.5 ± 28.9 dB HL) were significantly higher than those of the second involved ear (45.8 ± 20.0 dB HL) ($P < 0.001$) (Table 2).

Caloric testing was performed in 167 patients with UMD and 29 patients with BMD. Caloric weakness was not significantly different between the first involved ear in the BMD group (20/29, 69%) and the affected ear in the UMD group (112/167, 67.1%) ($P = 0.084$). In patients with BMD, the caloric weakness in the first involved ear was significantly more deteriorated than that in the second involved ear (6/29, 20.7%) ($P < 0.001$) (Table 2). cVEMP and oVEMP were performed in 146 patients with UMD and 19 patients with BMD. The proportion of the first involved ears with abnormal response in cVEMP recordings was significantly higher in patients with BMD (BMD, 19/19, 100%; UMD, 120/146, 82.2%) ($P = 0.045$) (Table 2). The difference was not significant between the initially involved side (19/19, 100%) and the second involved side (16/19, 84.2%) in patients with BMD ($P = 0.071$). The proportion of the first involved ears with abnormal response in oVEMP recordings was significantly higher in patients with BMD (BMD, 19/19, 100%;

UMD, 120/146, 82.2%) ($P = 0.045$) (Table 2). The difference was not significant between the initially involved side (19/19, 100%) and the second involved side (19/19, 100%) in patients with BMD ($P > 0.05$). Overall, cochlear and vestibular functions were more deteriorated in the first involved ear of patients with BMD than those in the affected ear of patients with UMD.

Comorbidities

There was no significant difference in the prevalence of comorbid migraines between the two groups (UMD, 12.8%; BMD, 14.3%) ($P = 0.710$) (Table 2). In the UMD group, 22 patients (4.8%) had family members with vertigo, whereas the BMD group had 11 patients (13.1%) who had family members with vertigo; this difference was significantly different ($P = 0.003$) (Table 2). However, family members with vertigo had not yet been diagnosed with MD. The proportion of patients with delayed MD was significantly larger in the BMD group (BMD, 14.3%; UMD, 5.2%) ($P = 0.002$) (Table 2). Twelve patients (2.6%) in the UMD group had drop attacks, and three patients (3.6%) in the BMD group had drop attacks ($P = 0.618$) (Table 2). Only one patient with BMD was diagnosed with rheumatic polymyopathy (Table 2).

Image findings

All patients ($n = 545$, 100%) had EH in the affected ears, including 461 cases with unilateral MD and 84 cases with bilateral MD. Among these 461 patients with UMD, 21 patients (4.6%) had EH on the contralateral side, including 11 patients with only cochlear EH, 3 patients with only vestibular EH, and 7 patients with both cochlear and vestibular EH. The extent of EH on the contralateral side was mild (Figure 1). Of the 21 cases, 9 cases had unexplained hearing loss. Notably, all ears with symptoms of hearing loss, aural fullness, or tinnitus were regarded as symptomatic. For the 84 cases with bilateral MD, all ears (168 ears) had EH, and the proportion of EH in the second involved ear of patients with BMD was significantly larger than that in the contralateral side of patients in the UMD group ($P < 0.05$) (Table 3).

Discussion

We enrolled a large number of MD patients, and all patients were diagnosed by clinical criteria and MRI, ensuring the diagnostic accuracy of definite MD. The results were more persuasive compared with previous studies. Additionally, we analyzed the clinical characteristics, cochlear and vestibular functions, and features of EH of UMD and BMD, aiming to comprehensively explore the characteristics of BMD and the associated factors for the development of BMD.

The overall prevalence of BMD was 15.4%, and this value was within the range of 5.4–29% in the Asian population, as reported in previous studies (9, 12–14). The prevalence of BMD of 2–47% in the Caucasian population was higher, as reported in a previous study (15), which might indicate ethnic diversity in epidemiology (2, 3). No gender difference (man:woman = 274:271) was noted among the 545 patients, and the female preponderance in some previous studies might involve patients with vestibular migraine. Patients with BMD had a longer disease course than those with UMD; bilateral involvement occurred through metachronous progression, and the second ear was involved more than 5–10 years after the onset of first ear involvement (1, 15). The comorbid rate of migraine in MD was reported to be 22–56%, which was higher than that reported in the general population (6–17%) (16, 17). However, the prevalence rates (UMD, 12.8%; BMD, 14.3%) were lower in our study. The definite MD in the patients enrolled in our study was diagnosed by clinical features and EH, which accurately ruled out other vestibular disorders, especially easily misdiagnosed vestibular migraine. The proportion of family history of vertigo was higher in patients with BMD in our study (BMD, 13.1%; UMD, 4.8%). Genetic mechanisms have been suggested as a mechanism of detecting MD, especially for BMD. Several genes, including FAM136A, DTNA, PRKCB, SEMA3D, OTOG, and DPT (18), have been suggested but no single gene has been validated. A higher prevalence of familial MD in patients with BMD has also been reported in some studies, but other studies took a different issue (2, 9, 19). The proportion of patients with delayed MD was significantly larger in the BMD group, and the result was similar to that of a previous study (9). The underlying mechanism remains unclear, and the autoimmune pathology might involved (20, 21), predisposing ears to EH subsequently. Moreover, it also indicates that attention should be paid to delayed MD, which has the potential to become BMD. No significant difference was noted in the proportion of drop attacks between patients with BMD (3.6%) and patients with UMD (2.6%). The frequency of drop attacks varied from 3 to 19% in different studies, and it was reported to be a common phenomenon in MD, which occurred even in mild MD and complicated with syncope (22). Autoimmune pathologies were considered to be related to MD (23); however, only one patient with BMD was diagnosed with rheumatic polymyopathy, a kind of systemic autoimmune disease. Nevertheless, we cannot entirely exclude the possibility of other potential autoimmune pathologies. Cochlear and vestibular functions deteriorated more in the first involved ear of patients with BMD than in the affected side of those with UMD. The longer disease duration of patients with BMD may be the main reason. The better results of hearing thresholds and vestibular functions in the second

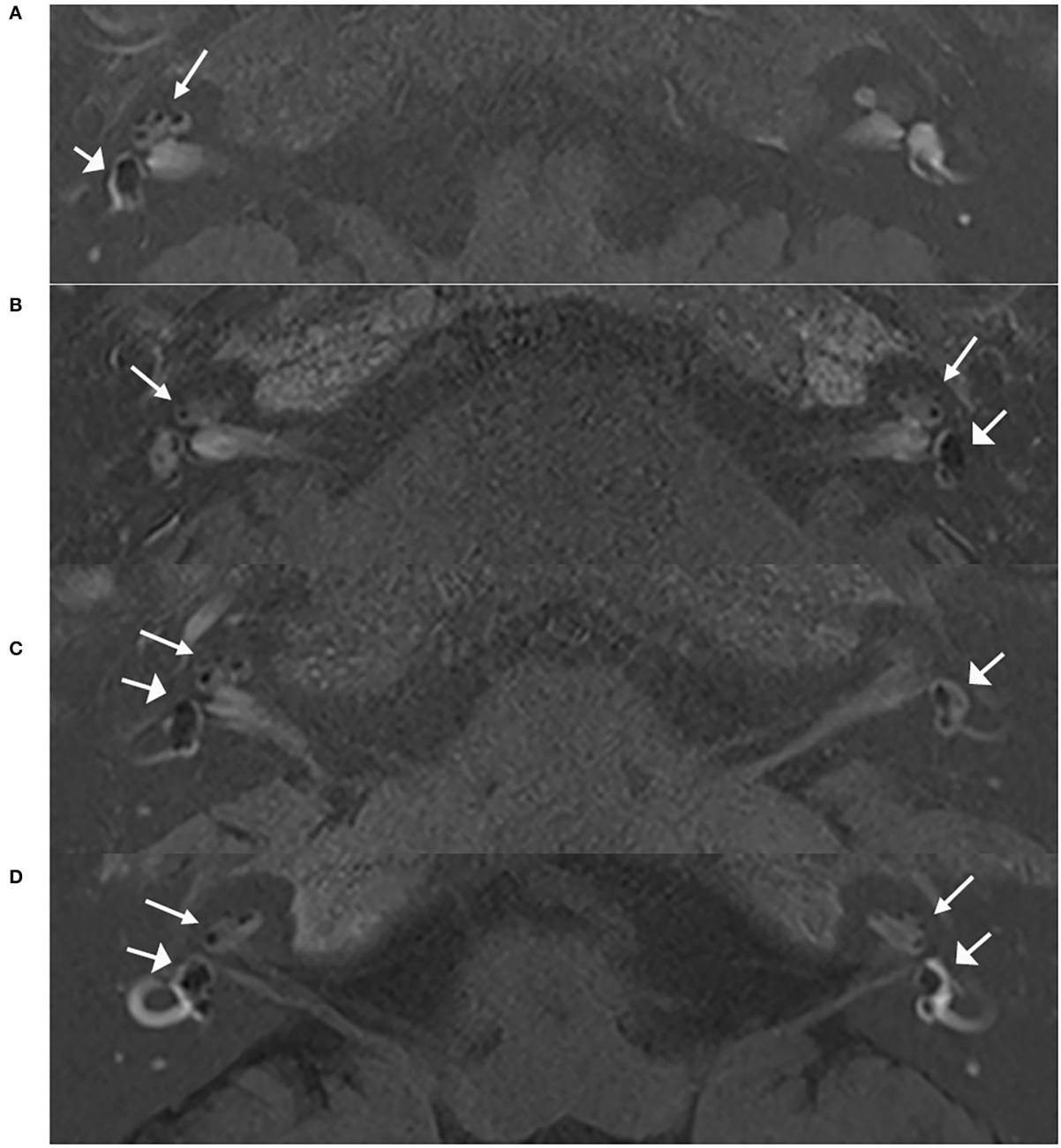

FIGURE 1
MRI scans of patients with unilateral and bilateral ELH. Images of 3D real IR performed 4 h after intravenous Gd injection. **(A)** Vestibular and cochlear ELH on the right side in a patient with unilateral MD; **(B)** Vestibular and cochlear ELH on the left side and cochlear ELH on the contralateral side in a patient with unilateral MD; **(C)** Vestibular and cochlear ELH on the right side and vestibular ELH on the contralateral side in a patient with unilateral MD; **(D)** Vestibular and cochlear ELH on the bilateral ears in a patient with bilateral MD. MD, Ménière's disease. Cochlea (thin arrows) and vestibule (broad arrows).

involved ear compared with the first involved ear may further indicate the metachronous process of bilateral involvement in BMD (9). The high proportions of abnormal VEMP and the caloric tests in the second involved ear of BMD also suggest bilateral involvement (24).

All patients underwent the IT or IV method. Both methods were useful techniques for the clarification of the inner ear clinical condition through a statistical analysis of signal-intensity differences in the perilymph fluid. Of the two methods, the IV method was less invasive and ascertained the presence of

TABLE 3 Percentages of endolymphatic hydrops in UMD and BMD.

ELH, *n* (%)	UMD (*n* = 461)	BMD (*n* = 84)	*P*-Value
First involved ear	461 (100)	84 (100)	/
Contralateral ear	21 (4.6)	84 (100)	0.000**†

† A *P*-value in the comparison between the clinically silent ear in UMD and the second involved ear in BMD. UMD, unilateral Ménière's disease; BMD, bilateral Ménière's disease. ** $P < 0.01$.

EH in the bilateral labyrinth. All the 545 patients presented with EH in the affected ears. On the nonaffected side of the patients with UMD, 28 cases (6.1%) had EH, and the extent of EH in the nonaffected ears seemed to be lighter. Gu et al. (25) showed that all eight patients with bilateral definite MD had bilateral EH. Wu et al. (26) evaluated EH of both sides in 54 patients with unilateral definite MD and reported that all ears had EH on the affected sides and that nine ears had EH on the nonaffected side. Morimoto et al. reported that 48% of the cochlea and 55% of the vestibule showed EH on the nonaffected side (27). These results might indicate that EH is the hallmark of UMD and BMD, and it seems that symptoms of MD are present even after the development of EH. The percentage of EH on the nonaffected side was lower in our study (4.6%). Due to ethnic differences and different disease durations, temporary symptoms of hearing loss, aural fullness, or tinnitus might be overlooked. Moreover, it was reported that the sensitivity of MRI scans is 50% with a different technique and probably less (28), which might be a factor of the different percentage of EH. To determine whether there is a possibility of developing bilateral MD in patients with bilateral EH in unilateral MD, a longitudinal study is needed.

Our research still has some limitations. Because it was a retrospective study, not every patient was evaluated with the same vestibular tests. Therefore, more prospective studies are needed.

Conclusion

Overall, a lower prevalence of BMD, longer disease duration, and higher frequencies of delayed MD and family history of vertigo were found in patients with BMD compared with patients with UMD. A low frequency of systemic autoimmune diseases was found in both patients with UMD and BMD. The variables of gender, comorbid migraines, and drop attacks were not significantly different between patients with BMD and UMD. All patients presented with EH on the affected ears, and a low percentage of unaffected ears presented with EH. These findings will provide information about the development of BMD. In addition, for UMD patients with those risk factors, serious considerations before aggressive treatment for the first involved ear were needed.

Data availability statement

The original contributions presented in the study are included in the article/supplementary material, further inquiries can be directed to the corresponding author.

Ethics statement

The studies involving human participants were reviewed and approved by the Medical Ethics Committee of the Eye, Ear, Nose, and Throat Hospital of Fudan University approved this study, and all patients signed an intravenous Gd contrast operation consent form. Written informed consent to participate in this study was provided by the participants' legal guardian/next of kin.

Author contributions

WW provided approval for publication of the content. WW and SS agreed to be accountable for all aspects of the work in ensuring that questions related to the accuracy or integrity of any part of the work are appropriately investigated and resolved. SS drafting the work or revising it critically for important intellectual content. SS, WL, DW, and TR made substantial contributions to the conception or design of the work, the acquisition, analysis, and interpretation of data for the work. All authors contributed to the article and approved the submitted version.

Funding

This study was supported by the National Natural Science Foundation of China (Nos. 82101222 and 81670933) and the Natural Science Foundation of Shanghai (No. 20ZR1409600).

Conflict of interest

The authors declare that the research was conducted in the absence of any commercial or financial relationships that could be construed as a potential conflict of interest.

Publisher's note

All claims expressed in this article are solely those of the authors and do not necessarily represent those of their affiliated organizations, or those of the publisher, the editors and the reviewers. Any product that may be evaluated in this article, or claim that may be made by its manufacturer, is not guaranteed or endorsed by the publisher.

References

1. Nabi S, Parnes L S. Bilateral Meniere's diseaseJ. *Curr Opin Otolaryngol Head Neck Surg.* (2009) 175:356–62. doi: 10.1097/MOO.0b013e3283304cb3

2. Lee JM, Kim MJ, Jung J, Kim HJ, Seo YJ, Kim SH. Genetic aspects and clinical characteristics of familial Meniere's disease in a South Korean populationJ. *Laryngoscope.* (2015) 1259:2175–80. doi: 10.1002/lary.25207

3. Ohmen JD, White CH Li X, Wang J, Fisher LM, Zhang H, et al. Genetic evidence for an ethnic diversity in the susceptibility to Meniere's diseaseJ. *Otol Neurotol.* (2013) 347:1336–41. doi: 10.1097/MAO.0b013e3182868818

4. Caulley L, Quimby A, Karsh J, Ahrari A, Tse D, Kontorinis G. Autoimmune arthritis in Meniere's disease: A systematic review of the literatureJ. *Semin Arthritis Rheum.* (2018) 481:141–7. doi: 10.1016/j.semarthrit.2017.11.008

5. Kim SY, Song YS, Wee JH, Min C, Yoo DM, Choi HG. Association between Meniere's disease and thyroid diseases: a nested case-control studyJ. *Sci Rep.* (2020) 101:18224. doi: 10.1038/s41598-020-75404-y

6. Morrison A W, Johnson K J. Genetics molecular biology and Meniere's diseaseJ. *Otolaryngol Clin North Am.* (2002) 353:497–516. doi: 10.1016/S0030-6665(02)00018-X

7. Requena T, Gazquez I, Moreno A, Batuecas A, Aran I, Soto-Varela A, et al. Allelic variants in TLR10 gene may influence bilateral affectation and clinical course of Meniere's diseaseJ. *Immunogenetics.* (2013) 655:345–55. doi: 10.1007/s00251-013-0683-z

8. Lopez-Escamez JA, Saenz-Lopez P, Acosta L, Moreno A, Gazquez I, Perez-Garrigues H, et al. Association of a functional polymorphism of PTPN22 encoding a lymphoid protein phosphatase in bilateral Meniere's diseaseJ. *Laryngoscope.* (2010) 1201:103–7. doi: 10.1002/lary.20650

9. Suh MJ, Jeong J, Kim HJ, Jung J, Kim SH. Clinical Characteristics of Bilateral Meniere's Disease in a Single Asian Ethnic GroupJ. *Laryngoscope.* (2019) 1295:1191–6. doi: 10.1002/lary.27423

10. Hallpike C S, Cairns H. Observations on the Pathology of Meniere's Syndrome: Section of OtologyJ. *Proc R Soc Med.* (1938) 3111:1317–36. doi: 10.1177/003591573803101112

11. Sone M, Yoshida T, Morimoto K, Teranishi M, Nakashima T, Naganawa S. Endolymphatic hydrops in superior canal dehiscence and large vestibular aqueduct syndromesJ. *Laryngoscope.* (2016) 1266:1446–50. doi: 10.1002/lary.25747

12. Shojaku H, Watanabe Y, Yagi T, Takahashi M, Takeda T, Ikezono T, et al. Changes in the characteristics of definite Meniere's disease over time in Japan: a long-term survey by the Peripheral Vestibular Disorder Research Committee of Japan, formerly the Meniere's Disease Research Committee of JapanJ. *Acta Otolaryngol.* (2009) 1292:155–60. doi: 10.1080/00016480802112587

13. Kitahara M, Matsubara H, Takeda T, Yazawa Y. Bilateral Meniere's diseaseJ. *Adv Otorhinolaryngol.* (1979) 25:117–21. doi: 10.1159/000402927

14. Shojaku H, Watanabe Y, Mizukoshi K, Kitahara M, Yazawa Y, Watanabe I, et al. Epidemiological study of severe cases of Meniere's disease in Japan. *J Acta Otolaryngol.* (1995) 2:415–8. doi: 10.3109/00016489509125286

15. Huppert D, Strupp M, Brandt T. Long-term course of Meniere's disease revisitedJ. *Acta Otolaryngol.* (2010) 1306:644–51. doi: 10.3109/00016480903382808

16. Ghavami Y, Mahboubi H, Yau AY, Maducdoc M, Djalilian HR. Migraine features in patients with Meniere's diseaseJ. *Laryngoscope.* (2016) 1261:163–8. doi: 10.1002/lary.25344

17. Ray J, Carr SD, Popli G, Gibson WP. An epidemiological study to investigate the relationship between Meniere's disease and migraineJ. *Clin Otolaryngol.* (2016) 416:707–10. doi: 10.1111/coa.12608

18. Arweiler-Harbeck D, Horsthemke B, Jahnke K, Hennies HC. Genetic aspects of familial Meniere's diseaseJ. *Otol Neurotol.* (2011) 324:695–700. doi: 10.1097/MAO.0b013e318216074a

19. Nonoyama H, Tanigawa T, Tamaki T, Tanaka H, Yamamuro O, Ueda H. Evidence for bilateral endolymphatic hydrops in ipsilateral delayed endolymphatic hydrops: preliminary results from examination of five casesJ. *Acta Otolaryngol.* (2014) 1343:221–6. doi: 10.3109/00016489.2013.850741

20. Harris J P, Aframian D. Role of autoimmunity in contralateral delayed endolymphatic hydrops. *Am J Otol.* (1994) 156:710–6.

21. Suzuki M, Hanamitsu M, Kitanishi T, Kohzaki H, Kitano H. Autoantibodies against inner ear proteins in patients with delayed endolymphatic hydrops and unilateral juvenile deafness. *Acta Otolaryngol.* (2006) 1262:117–21. doi: 10.1080/00016480500266008

22. Kutlubaev MA, Xu Y, Manchaiah V, Zou J, Pyykko I. Vestibular drop attacks in Meniere's disease: A systematic review and meta-analysis of frequency, correlates and consequences. *J Vestib Res.* (2022) 322:171–82. doi: 10.3233/VES-201514

23. Hietikko E, Sorri M, Mannikko M, Kotimaki J. Higher prevalence of autoimmune diseases and longer spells of vertigo in patients affected with familial Meniere's disease: a clinical comparison of familial and sporadic Meniere's disease. *Am J Audiol.* (2014) 232:232–7. doi: 10.1044/2014_AJA-13-0060

24. Huang C H, Young Y H. Bilateral Meniere's disease assessed by an inner ear test battery. *Acta Otolaryngol.* (2015) 1353:233–8. doi: 10.3109/00016489.2014.962184

25. Gu X, Fang ZM, Liu Y, Huang ZW, Zhang R, Chen X. Diagnostic advantages of intratympanically gadolinium contrast-enhanced magnetic resonance imaging in patients with bilateral Meniere's disease. *Am J Otolaryngol.* (2015) 361:67–73. doi: 10.1016/j.amjoto.2014.10.003

26. Wu Q, Dai C, Zhao M, Sha Y. The correlation between symptoms of definite Meniere's disease and endolymphatic hydrops visualized by magnetic resonance imaging. *Laryngoscope.* (2016) 1264:974–9. doi: 10.1002/lary.25576

27. Morimoto K, Yoshida T, Sugiura S, Kato M, Kato K, Teranishi M, et al. Endolymphatic hydrops in patients with unilateral and bilateral Meniere's disease. *Acta Otolaryngol.* (2017) 1371:23–8. doi: 10.1080/00016489.2016.1217042

28. Conte G, Lo RF, Calloni SF, Sina C, Barozzi S, Di Berardino F, et al. MR imaging of endolymphatic hydrops in Meniere's disease: not all that glitters is gold. *Acta Otorhinolaryngol Ital.* (2018) 384:369–76. doi: 10.14639/0392-100X-1986

frontiers | Frontiers in Neurology

TYPE Original Research
PUBLISHED 15 September 2022
DOI 10.3389/fneur.2022.997367

Check for updates

OPEN ACCESS

EDITED BY
Sulin Zhang,
Huazhong University of Science and Technology, China

REVIEWED BY
Daogong Zhang,
Shandong Provincial ENT Hospital, China
Zhaomin Fan,
Shandong Provincial ENT Hospital, China

*CORRESPONDENCE
Yi Li
alinaliyi@163.com

SPECIALTY SECTION
This article was submitted to Neuro-Otology, a section of the journal Frontiers in Neurology

RECEIVED 18 July 2022
ACCEPTED 29 August 2022
PUBLISHED 15 September 2022

CITATION
Wang T, Liu H, He DZ and Li Y (2022) Occlusion of two semicircular canals does not disrupt normal hearing in adult mice. *Front. Neurol.* 13:997367. doi: 10.3389/fneur.2022.997367

COPYRIGHT
© 2022 Wang, Liu, He and Li. This is an open-access article distributed under the terms of the Creative Commons Attribution License (CC BY). The use, distribution or reproduction in other forums is permitted, provided the original author(s) and the copyright owner(s) are credited and that the original publication in this journal is cited, in accordance with accepted academic practice. No use, distribution or reproduction is permitted which does not comply with these terms.

Occlusion of two semicircular canals does not disrupt normal hearing in adult mice

Tianying Wang[1], Huizhan Liu[2], David Z. He[2] and Yi Li[1]*

[1]Department of Otorhinolaryngology-Head and Neck Surgery, Beijing Tongren Hospital, Capital Medical University, Beijing, China, [2]Department of Biomedical Sciences, Creighton University School of Medicine, Omaha, NE, United States

Vertigo is a debilitating disease affecting 15–20% of adults worldwide. Vestibular peripheral vertigo is the most common cause of vertigo, often due to Meniere's disease and benign paroxysmal positional vertigo. Although some vertigo symptoms can be controlled by conservative treatment and/or vestibular rehabilitation therapy, these treatments do not work for some patients. Semicircular canal occlusion surgery has proven to be very effective for these patients with intractable vertigo. However, its application is limited due to concern that the procedure will disrupt normal hearing. In this study, we investigated if occlusion of two semicircular canals would jeopardize auditory function by comparing auditory function and hair cell morphology between the surgical and contralateral ears before and after the surgery in a mouse model. By measuring the auditory brainstem response and distortion product otoacoustic emission 4 weeks post-surgery, we show that auditory function does not significantly change between the surgical and contralateral ears. In addition, confocal imaging has shown no hair cell loss in the cochlear and vestibular sensory epithelia, and scanning electron microscopy also indicates normal stereocilia morphology in the surgical ear. More importantly, the endocochlear potential measured from the surgical ear is not significantly different than that seen in the contralateral ear. Our study suggests that occlusion of two semicircular canals does not disrupt normal hearing in the mouse model, providing a basis to extend the procedure to patients, even those with normal hearing, benefitting more patients with intractable vertigo attacks.

KEYWORDS

semicircular canal occlusion, vertigo, auditory function, endocochlear potential, mice

Introduction

Vertigo has a high incidence rate worldwide, affecting between 15 and 20% of adults each year. Its prevalence rises with age, especially in adults over the age of 60. Long-term vertigo causes mood changes and leads to other serious consequences, such as falls, varying degrees of disability, and accidental deaths (1, 2).

Vestibular peripheral vertigo is the most common cause of vertigo, accounting for 71% of all vertigo patients (2, 3). Among them, Meniere's disease accounts for ~1.0–1.6%, and 34% of vertigo patients with benign paroxysmal positional

vertigo. These patients often require vestibular rehabilitation therapy and/or other conservative treatment to control vertigo symptoms (4–6). However, these treatments are often ineffective for some patients with intractable vertigo attacks.

Semicircular canal occlusion (SCO) is considered to be an effective treatment of vertigo in patients who are not responsive to conservative treatments. SCO is a surgical operation in which the endolymphatic flow is blocked by bone wax, bone shavings, fascia, biological glue or a laser after drilling in the bony wall of the semicircular canal (7, 8). At present, posterior semicircular canal occlusion (PSCO) is most commonly used in the treatment of benign paroxysmal positional vertigo, and its curative effect has been affirmed. In recent years, PSCO, combined with lateral semicircular canal occlusion (LSCO) and three semicircular canals occlusion, have also been used in treatment of Meniere's disease, and its effectiveness has been recognized (9). However, SCO has also been reported to cause hearing loss in some patients, while no hearing loss has been observed in other patients (9, 10). The controversy surrounding SCO's potential side effects on auditory function has limited the treatment's availability to patients with intractable vertigo attacks, and have moderate to severe hearing loss (9–13). Therefore, determining whether SCO is safe for maintaining auditory function is essential to further expand SCO's availability for patients with other forms of vertigo, such as vestibular peripheral vertigo.

The goal of our study is to investigate if SCO would disrupt the auditory function. We examined auditory function, hair cell morphology, and endocochlear potential (EP) in a mouse model to determine if normal hearing is still retained after a surgical procedure that blocks the two semicircular canals (i.e., combination of PSCO and LSCO). If the SCO surgery is observed to have a minimal impact on the auditory function of animal models, our experiments will provide a stronger basis for extending the treatment to patients with normal hearing, benefitting a wider range of patients suffering from intractable vertigo attacks.

Materials and methods

Animals

C57BL/6 mice with both sexes at 4 weeks of age were used for experiments. The care and usage of mice were approved by the Animal Ethics Review Committee of Beijing Capital Medical University.

Surgery

Animals were anesthetized through an intraperitoneal injection of ketamine HCl (120 mg/kg) and xylazine HCl (7 mg/kg). After anesthesia administration, the animal was placed on a preheated pad with a preset temperature of 37°C. The canalostomy procedure, including locating and exposing the posterior semicircular canal (PSC) and lateral semicircular canal (LSC) in neonatal and adult mice, has been previously described in detail (14). The surgery was performed only on one ear. Two small holes were made on PSC and LSC, respectively, using a miniature electric drill. After the small hole was drilled in the bony wall of LSC and PSC, translucent tissue and endolymph leakage were observed. The two holes were then blocked with a piece of muscle tissue and surgical bone wax. The left or right ear was randomly selected as the surgical ear and the contralateral ear was used as control.

Measurement of auditory brainstem response and distortion product otoacoustic emission

ABRs were used to determine hearing threshold. ABRs were recorded using a Tucker-Davis Technologies workstation with SigGen32 software (Tucker-Davis Technologies Inc., Alachua, FL, USA) in a sound-isolated chamber as previously described (15). Mice were anesthetized and placed on a temperature-controlled heating pad. Tone pips with frequencies of 4, 8, 12, 16, 22, 32, 40, and 50 kHz were delivered to the ear canal with an EC1 electrostatic speaker (Tucker-Davis Technologies, Alachua, FL, USA). ABR signals were collected with subcutaneous platinum needle electrodes placed at the vertex, mastoid prominence, and leg. Response signals were amplified (100,000x), filtered, and acquired by TDT RZ6 (Tucker-Davis Technologies). Each averaged response was based on 1,024 stimulus repetitions. The ABR threshold was defined visually as the lowest sound pressure level at which any wave of the four waves (wave I to wave IV) was detected above the noise level at each frequency of the tone.

Two EC1 electrostatic speakers (Tucker-Davis Technologies) were used for the measurement of DPOAE threshold. Two tone bursts with different frequencies (f_1 and f_2, with $f_2/f_1 = 1.2$ and the f_2 level 10 dB lower than the f_1 level) were delivered to the ear canal from the speakers through a coupler. The sound pressure obtained from the microphone in the ear-canal was amplified and computed from averaged waveforms of ear-canal sound pressure using the Fast-Fourier transforms. The DPOAE component at the frequency of $2f_1$-f_2 was measured in response to the two-tone bursts. The DPOAE threshold is defined as the f_1 sound pressure level (measured in decibels) required to produce a repeatable response above the noise level at the frequency of $2f_1$-f_2 (16).

Recording of EP

Details for recording EP are described elsewhere (17, 18). In brief, tracheotomy was performed in the ventral position

after anesthesia. The tympanic bulla was opened after tissue and musculature overlying the bulla were removed. A glass capillary pipette electrode (10 MΩ) filled with 3 mM KCl was mounted on a hydraulic micromanipulator. The tip of the pipette electrode was in contact with the round window. With the help of micromanipulator, the electrode was advanced through the round window membrane toward the organ of Corti. After the tip of the microelectrode penetrated through the window membrane and was in the scala tympani, the baseline was adjusted to zero. The microelectrode was then advanced through the region of the organ of Corti on the basilar membrane. When the microelectrode passed through the organ of Corti, a negative DC potential was recorded. A stable positive DC potential (i.e., the EP) was observed when the micropipette entered the scala media. Axopatch 200B amplifier (Molecular Devices, San Jose, CA, USA) was used to record EP. The EP response was amplified under current-clamp mode and acquired by software pClamp 9.2 (Molecular Devices). The sampling frequency was 1 kHz.

Immunostaining of cochlear and vestibular hair cells and hair cell count

After measuring auditory function, mice were euthanized through CO2 inhalation, and then decapitated to remove the temporal bones. Under a dissecting microscope, a hole was poked at the apex of the cochlea. The round and oval windows were opened with a needle. The temporal bones were fixed in 4% paraformaldehyde in PBS for 2h. After rinsing three times with PBS, the inner ear, containing both the cochlea and vestibular end organs (utricle, saccule and crista), was decalcified in 10% EDTA solution for 1.5 h. The bony wall was then removed and the organ of Corti and vestibular end organs were all dissected out. The auditory and vestibular sensory epithelia were treated with 0.3% Triton X-100 (Sigma-Aldrich, St. Louis, MO, USA) and 5% normal goat serum (ZSGB-BIO, Beijing, China) in PBS for 2h at room temperature. The samples were then incubated at 4°C overnight with the anti-MYO7A antibody (diluted 1:300, Proteus BioSciences Inc., Ramona, CA, USA). After rinsing in PBS, the samples were incubated with secondary antibody tagged with Alexa Fluor 488 (diluted 1:300; Invitrogen, Carlsbad, CA, USA) for 2h at room temperature. Alexa Fluor 594-conjugated phalloidin (diluted 1:300; Invitrogen) was used for labeling F-actin. After rinsing with PBS, samples were mounted on glass slides with Fluoromount-G (Southern Biotech, Birmingham, AL, USA) and examined using a Leica scanning confocal microscope (TCS SP8 II; Leica Microsystems, Wetzlar, Germany). ImageJ (https://imagej.nih.gov/ij/) was used for imaging analysis.

For cochlear hair cell count, images from apical, mid and basal turn regions (each with 400 μm in length) were captured, and IHCs and OHCs were counted separately from confocal images off-line, as described previously (19). For counting hair cells in utricle and saccule from captured confocal images off-line, protocols described previously were used (20). Three cochleae and three utricles and saccules from three animals were used for cell count.

Semicircular canal histology

The temporal bone tissues were placed in cold 4% paraformaldehyde solution for 24 h, and then in 10% EDTA solution for 3 days. After dehydration in graded concentrations of ethanol, the sample was embedded in graded concentrations of celloidin. Serial sections of the temporal bones were individually cut along the long axis of the two semicircular canals (PSC and LSC) at a thickness of 20 μm. The sections were transferred from an 80% ethanol storage solution and then stained with H and E.

Scanning electron microscopy

The cochleae from the surgical ear were fixed for 24 h in a solution of 2.5% glutaraldehyde and 0.1 M sodium cacodylate buffer (pH 7.4) containing 2 mM $CaCl_2$. The cochlear wall was removed upon decalcification in 10% EDTA solution for 24 h. The cochleae were then post-fixed for 1 h with 1% OsO_4 in 0.1 M sodium cacodylate buffer and washed. The cochleae were dehydrated *via* an ethanol series, critical point dried from CO_2 and sputter-coated with gold. The morphology of the HCs was examined in a FEI Quanta 200 scanning electron microscope (ThermoFisher, Hillsboro, OR, USA) and photographed.

Statistical analyses

Data are expressed as means ± standard errors. Student's *t*-test was used to determine statistical significance between two conditions (control and surgical ears or right and left ears) in hair cell counts or EP change. Two-way ANOVA with multiple *t*-tests using the Holm–Sidak correction for multiple comparisons was also used to determine statistical significance. $P \leq 0.05$ was regarded as significant.

Results

Due to the inaccessibility to the superior semicircular canal during surgery in mice, LSC and PSC were chosen to be blocked in our study (Figure 1A). Tone-evoked ABR thresholds of the mice's bilateral ears were determined before the surgery (designated as Day 1 in Figure 1B) and 4 weeks after the surgery.

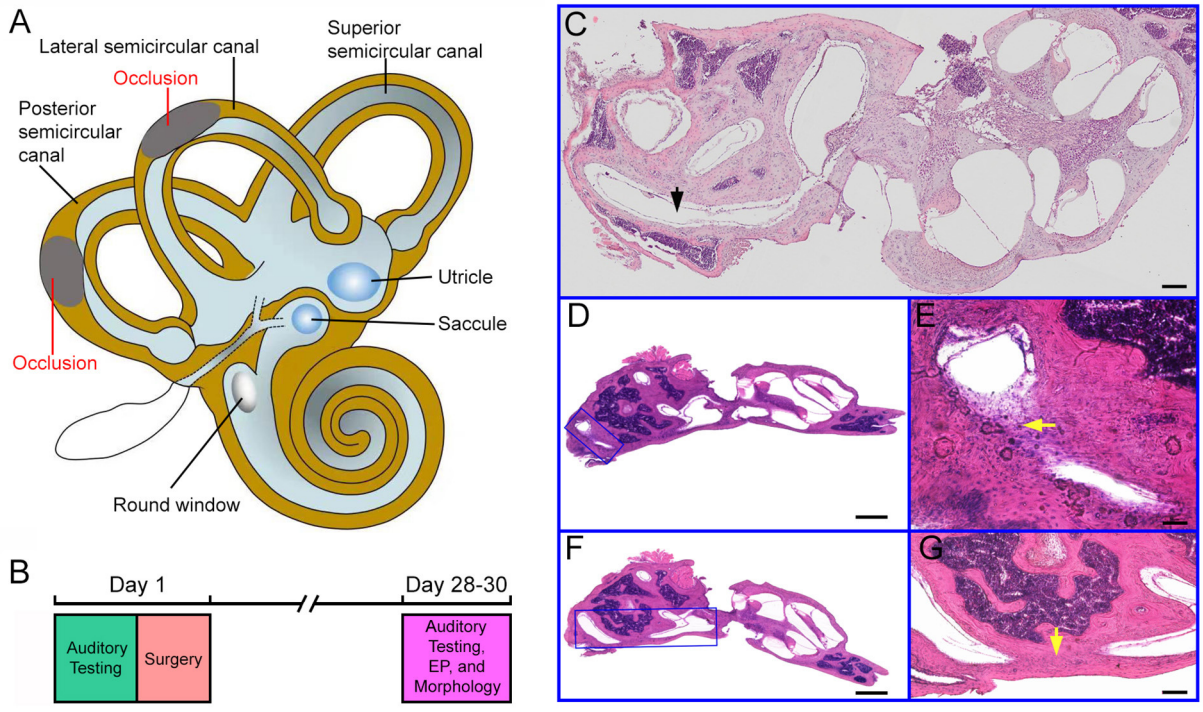

FIGURE 1
Experimental design and histology of the cochlea and semicircular canals. **(A)** Schematic drawing of the inner ear with the cochlea, the vestibule and the semicircular canals. Occlusions of the lateral and posterior semicircular canals are indicated in the drawing. **(B)** Experimental design and timeline for the surgery and assessment of auditory function and hair cell morphology. **(C)** Cross section (H and E staining) of the inner ear from a control ear. The lateral semicircular canal is marked in the picture. Bar: 50 μm. **(D)** Cross section of the inner ear from a surgical ear with posterior semicircular canal blocked. The area with occlusion is marked with a blue frame. **(E)** High magnification view of the area shown in **(D)**. The area with occlusion is marked by a yellow arrow. **(F)** Image of cross section of the inner ear from a surgical ear with lateral semicircular canal blocked. The area with occlusion is marked with a blue frame. **(G)** High magnification view of the area shown in **(F)**. The area with occlusion is marked by a yellow arrow. Bar for **(D,F)**: 200 μm. Bar for **(E,G)**: 50 μm.

Four weeks after the surgery ABR and EP were measured and the inner ear morphology was examined, as the experimental design is outlined in Figure 1B.

To determine if the surgery successfully blocked the LSC and PSC, we examined LSC and PSC morphology in celloidin-embedded serial sections. For comparison, morphology of the control ear was also examined. Figures 1C–G shows some representative images of H and E staining of the semicircular canals from the two ears. Figure 1C shows a section of the cochlea and vestibule from a control ear. As shown, the PSC is continuous with no tissue blocking the canal. Figures 1D,F show sections of the surgical ear with LSCO and PSCO at 4 weeks after the surgery. At higher magnification, fibrinous and cellular material was seen in the LSC (Figure 1E) and PSC (Figure 1G) lumen at the surgical site. We examined the morphology of LSC and PSC of the surgical ears in all mice and only those whose LSC and PSC were both blocked were included for analysis.

Cochlear and vestibular hair cell morphology

Confocal microscopy was used to examine hair cell status in the cochlea 4 weeks after surgery. Figure 2A show confocal images of hair cells in the three cochlear locations (apical, middle, and basal turn regions) from the surgical and contralateral ears. One row of inner hair cells (IHCs) and three rows of outer hair cells (OHCs) can be seen with no obvious signs of missing hair cells. The number of hair cells in the three cochlear locations from surgical and contralateral ears was counted and the mean of IHC and OHC count is presented in Figure 2B, respectively. We compared the hair cell count between surgical and contralateral ear at these locations and no statistical difference was found ($n = 3$, $P > 0.05$). We also used scanning electron microscopy to examine stereocilia morphology of hair cells in the surgical ear. Figure 2C shows two representative SEM micrographs obtained from the apical and

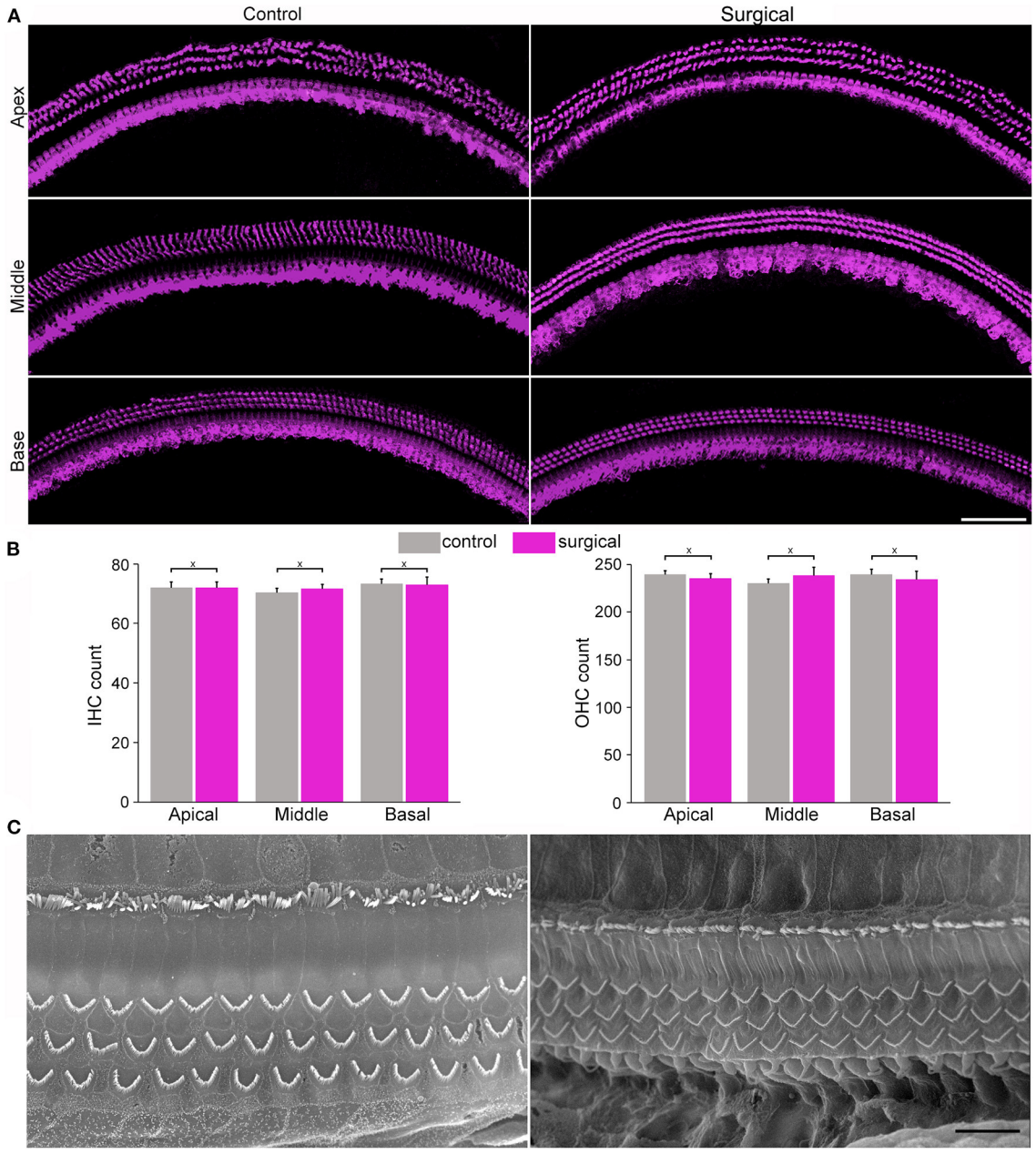

FIGURE 2
Images from confocal and scanning electron microscopy and morphology of cochlear hair cells and stereocilia. **(A)** Representative confocal images of hair cells from apical, mid- and basal regions of the cochleae from control and surgical ears with occlusion 28 days after surgery (surgical ear was used in all subsequent figures to represent occlusion of two semicircular canals). Bar: 75 μm. **(B)** IHC and OHC count from control and surgical ears. Data are presented as the mean ± SD, $n = 3$. X represents no statistical significance between the two groups ($p = 0.83$, 0.35 and 0.86 for apical, middle and basal turn for IHC count, respectively. $p = 0.34$, 0.22, and 0.44 for apical, middle and basal OHC count, respectively). **(C)** Representative SEM micrographs of stereocilia bundles of hair cells from apical and basal turns of the surgical ear. Bar: 10 μm.

basal turn regions. The stereocilia appear to be normal with no signs of degeneration, such as fusion and loss.

Vestibular hair cell morphology was examined in the surgical ear to determine if blockage of the lateral and posterior canals causes degeneration of hair cells in utricle, saccule and crista. Confocal microscopy was used to examine hair cell morphology. Figure 3A shows confocal images of anti-MYO7A antibody-labeled hair cells in utricle and saccule of surgical and contralateral (control) ears. The number of hair cells in utricle and saccule was counted and compared between surgical and

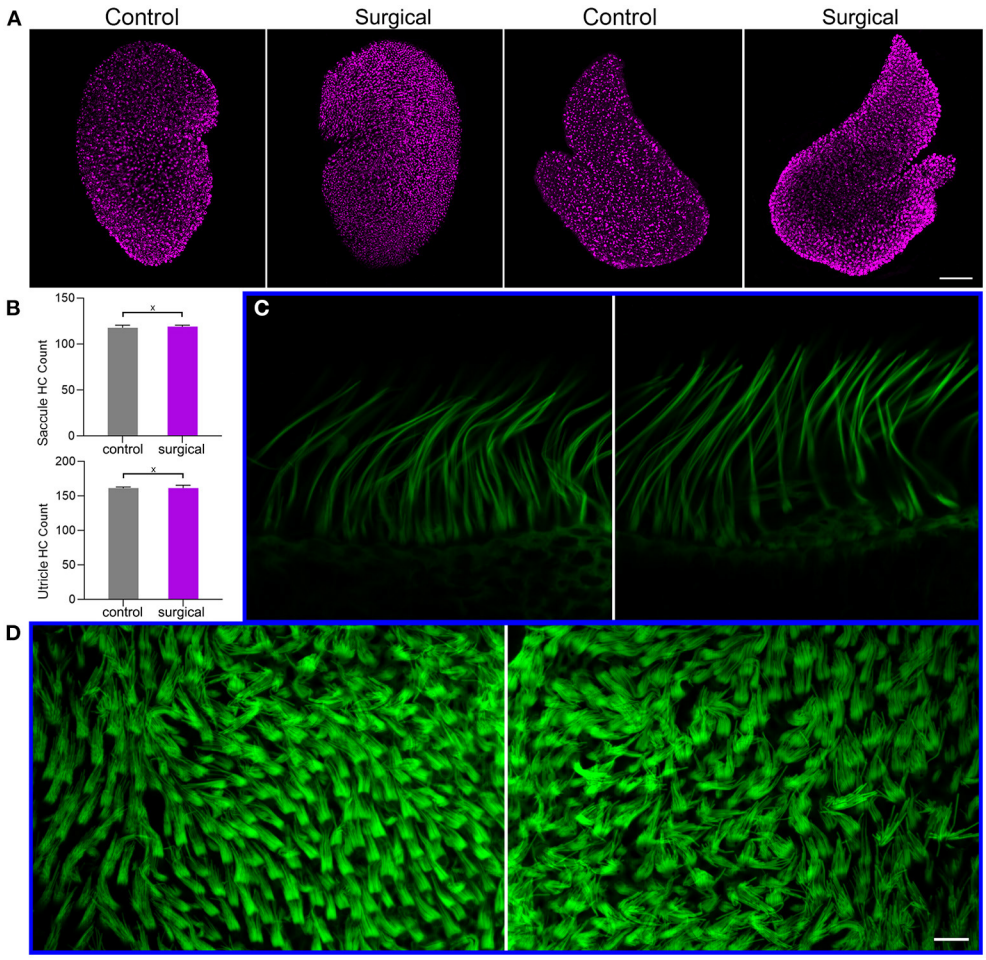

FIGURE 3
Hair cell and stereocilia status after occlusion of lateral-posterior semicircular canals. **(A)** Confocal images of utricle and saccule hair cells in control and surgical ears. Hair cells were labeled with anti-MYO7A antibody. Bar: 75 μm. **(B)** Hair cell count in utricle and saccule of control and surgical ears. X marks no statistical significance between control and surgical ears ($p = 0.35$ and 0.48 for saccule and utricle hair cell count, respectively). Data are presented as the mean ± SD, $n = 3$. **(C)** Confocal images of stereocilia bundles of crista hair cells from control (left panel) and surgical (right panel) ears. **(D)** Confocal images of utricle hair cell stereocilia control (left panel) and surgical (right panel) ears. Bar: 10 μm for **(C,D)**.

control ears. The mean count is presented in Figure 3B. No statistical significance was found between control and surgical ears. We did not count the hair cell number in crista as it is not easy to accurately count hair cells in crista in the surface mount (whole mount) preparation. But we examined stereocilia bundle morphology of hair cells in crista (Figure 3C) and utricle (Figure 3D) in the control and surgical ears. As shown, the stereocilia bundles appear to be normal with no signs of loss and degeneration.

ABR and DPOAE thresholds

To determine if SCO leads to hearing loss, we measured ABR and DPOAE thresholds. Figures 4A,B show the mean ABR and DPOAE thresholds measured from the left and right ears from six mice before the surgery. The ABR and DPOAE thresholds (at each frequency) of the two ears were not observed to be not statistically different ($P > 0.05$ for ABR and DPOAE, $n = 6$). Figures 4C,D show the mean ABR and DPOAE thresholds measured from the surgical ear before and 4 weeks after the surgery. No significant difference in either ABR or DPOAE threshold was found ($P > 0.05$ for ABR and DPOAE, respectively, $n = 6$). We also compared ABR and DPOAE thresholds between the surgical and contralateral ears after surgery, in order to minimize the possible effect of age-related hearing loss on our measurement. As shown in Figures 4E,F, no significant difference in either ABR or DPOAE threshold is found ($p > 0.05$ for ABR and DPOAE, respectively, $n = 6$).

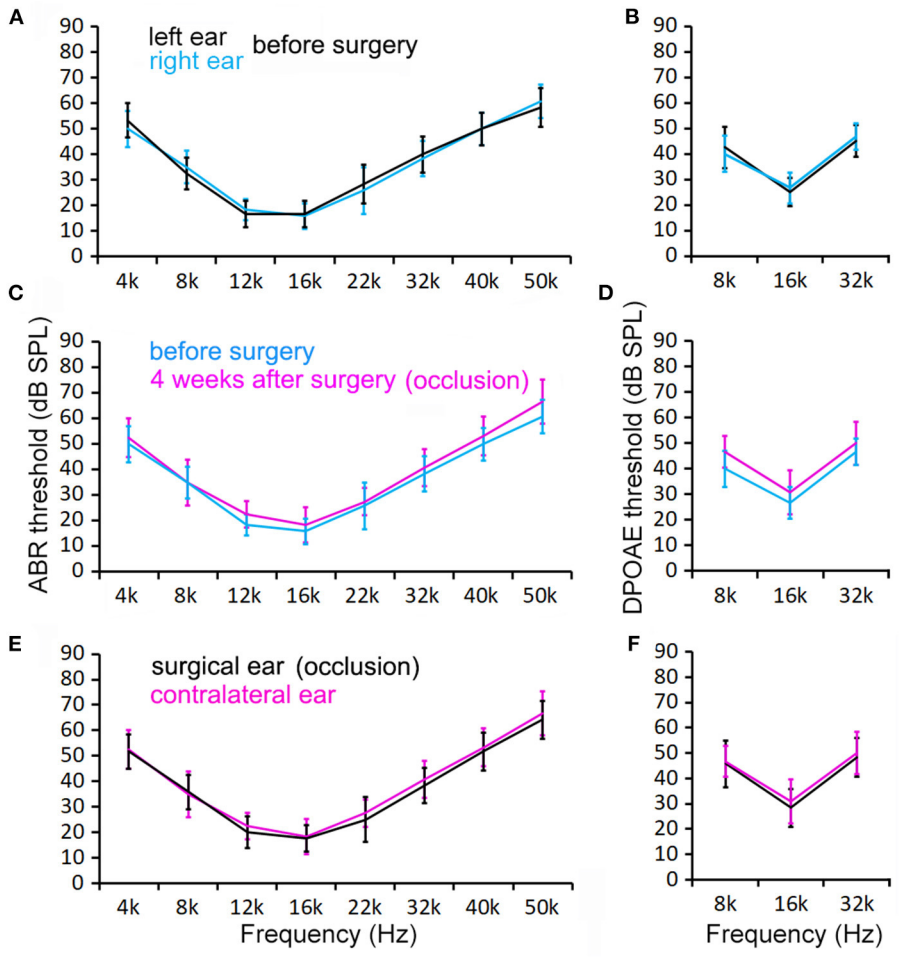

FIGURE 4
ABR and DPOAE thresholds measured from control and surgical ears before and 4 weeks after surgery. **(A,B)** ABR and DPOAE thresholds of the right and left ears before surgery. No statistical significance in thresholds is found at any of these frequencies ($p > 0.05$, $n = 6$). **(C,D)** ABR and DPOAE thresholds of the ears before and after occlusion. No statistical significance in thresholds is found at any of these frequencies ($p > 0.05$, $n = 6$). **(E,F)** Control and surgical ears at 4 weeks after surgery. No statistical significance in thresholds is found at any of these frequencies ($p > 0.05$, $n = 6$). Two-way ANOVA with multiple t-tests using the Holm–Sidak correction for multiple comparisons was also used to determine statistical significance.

EP measured from surgical ear

The endolymph within the scala media exhibits a constant ~80-mV positive polarization with respect to the perilymph (21). This positive potential or EP provides a driving force for hair cell mechanotransduction. We measured EP to determine if SCO would affect EP magnitude as endolymph dynamic in the endolymph compartment might have been altered by blockage of the two semicircular canals. We took the round window approach to measure EP (17, 18), as shown in Figure 5A. Figure 5B exhibits two examples of EP measured from the surgical and contralateral ears 4 weeks after the surgery. The negative potential shown in the figure reflects the organ of Corti potential, while the positive potential is the EP (22). As displayed, the EP magnitude is similar between the two ears. We measured EP from the surgical and contralateral ears from six mice and the mean EP magnitude is presented in Figure 5C. The EP magnitude is 98.3 ± 6.3 mV for the surgical ear and 96.7 ± 5.6 mV for the contralateral ear. No statistical significance ($p = 0.71$, $n = 6$) was found between the two ears after the surgery.

Discussion

It has been known for a long time that surgically obstructing posterior semicircular canal is an effect way to treat benign positional vertigo (8–10, 13, 23). The main risk of such an operation was the potential damage to hearing. The first

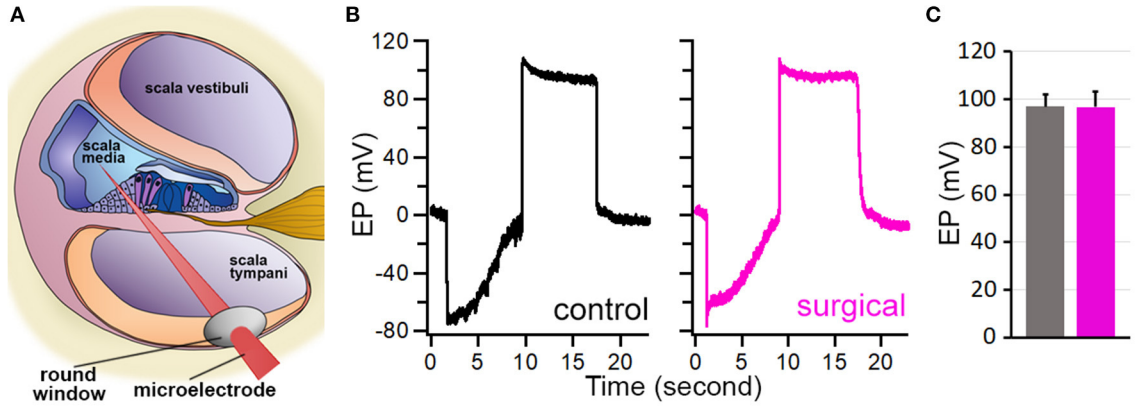

FIGURE 5
EP measured from control and surgical ears. **(A)** Schematic drawing of EP measurement. **(B)** Representative EP measured from control and surgical ears. **(C)** Mean ± SD of EPs measured from control and surgical ears. No statistical difference was found ($p = 0.72$, $n = 6$).

report of a successful posterior canal occlusion for posterior canal benign positional vertigo was in two patients with profound deafness (8), and a year later in five patients with normal hearing (7). In a different study, 53 patients underwent posterior canal occlusion and all 53 were cured of their benign positional vertigo. Nine suffered some symptomatic permanent hearing loss between 20 to 25 dB at low to high frequencies (10). Experimental semicircular canal plugging has long been performed in animal models for research purposes (24–29). Plugging individual semicircular canals reduces only the activity of affected crista without influencing the function of the remaining vestibular labyrinth in cats (26) and squirrel monkeys (30). Parnes and McClure (27) examined the auditory function of guinea pigs by measuring ABR before and after plugging posterior semicircular canal. They found ABR thresholds were not affected. However, the results are not entirely consistent since ABR thresholds were reported to be elevated in some human and animal studies (7, 9, 24). The exact reason of why hearing was affected in some animals and human patients was unknown (31), however, damage during surgery and/or different ways to plug the canal may have played a role (24, 31).

In the present study we show that ABR and DPOAE thresholds measured from the ear with occlusion of lateral and posterior semicircular canals were not significantly elevated when compared to the pre-operative thresholds and thresholds of the contralateral ear. Although previous studies also examined auditory function after SCO, our study differs from previous studies. First, we examined auditory function after two canals (PSC and LSC) were plugged. In most previous studies, only one canal, often PSC, was plugged. Second, we measured EP to determine if occlusion of two canals would affect EP. Although one study also measured EP after three canals were blocked in a guinea pig model, the EP was only monitored for a short period of time right after the surgery (25). No long-term effect of canal obstruction was examined. Third, our study is more comprehensive; we not only measured ABR and DPOAE thresholds and examined hair cell morphology and stereocilia ultrastructure, but also measured EP. Most previous studies only measured ABR threshold and/or examined cochlear hair cell morphology.

Transient loss of hearing and vestibular function has been seen in patients and animal models after SCO procedures (7, 9, 10, 32). We did not examine auditory function in the first few days after the surgery as our focus was on the long-term effect. However, we observed circular behavior in some mice, suggesting a transient effect on the vestibular function. The circular behavior disappeared in 3 to 5 days after surgery in mice used in our study, suggesting compensation and adaption to angular acceleration in two ears. We note that the absence of circular behavior does not necessarily mean that the response to rotational movements is not affected, as the goal of occlusion of semicircular canals is to reduce stimulation to crista hair cells to treat intractable vertigo symptoms.

There are two limitations to our study. The first limitation is that our conclusion that SCO exhibited no obvious effect on auditory function was only based on observations made in a period of 4 weeks after the surgery. Therefore, it is unclear if the procedure would have any negative impact on long-term auditory function. As obstruction of the canals is certain to lead to change in endolymph flow, it is yet to be determined if such change could eventually lead to endolymphatic hydrops (29). The second limitation is that we did not examine vestibular function after SCO surgery in our animal models. Permanent impairment of semicircular canal function was observed in the cat (26), guinea pig (33) and human (34). In guinea pigs, vestibulo-ocular reflex to high acceleration impulsive head rotations was lost following a unilateral lateral semicircular canal occlusion and no adaptive plasticity was found (33). Interestingly, in clinical studies the majority of patients who received posterior canal occlusion surgery did not show signs

of loss of balance (10). However, incomplete occlusion or ossification of SCs was the principal cause of vertigo recurrence in Meniere's disease patients who underwent triple semicircular canal plugging (32).

In summary, our results revealed that the plugging two semicircular canals does not lead to detectable hearing loss. Hair cell morphology in the cochlea and vestibule appears to be normal with no signs of hair cell degeneration and loss. EP also shows no significant change despite change in the endolymph fluid movement in the canal. The fact that normal hearing is preserved in the mouse model with obstruction of two canals suggest that SCO procedure does not disrupt auditory function. The procedure can be extended to human patients with normal hearing to treat benign positional vertigo after vestibular function and balance of the patient are also considered in decision making about SCO surgery.

Data availability statement

The raw data supporting the conclusions of this article will be made available by the authors, without undue reservation.

Ethics statement

The animal study was reviewed and approved by Animal Care Committee of Beijing Tongren Hospital.

Author contributions

TW performed the experiments, analyzed the data, and wrote the manuscript. HL and DH performed some experiments. YL and DH designed the experiments, analyzed the data, and revised and finalized the manuscript. All authors contributed to the article and approved the submitted version.

Funding

This work was supported by National Natural Science Foundation of China grants #81870718 and #81770996 to YL.

Acknowledgments

We acknowledge the use of the Imaging Core Facility at the Capital Medical University for confocal imaging and SEM. We would like to thank Disha Chandra from Creighton University for reading and commenting on the manuscript.

Conflict of interest

The authors declare that the research was conducted in the absence of any commercial or financial relationships that could be construed as a potential conflict of interest.

Publisher's note

All claims expressed in this article are solely those of the authors and do not necessarily represent those of their affiliated organizations, or those of the publisher, the editors and the reviewers. Any product that may be evaluated in this article, or claim that may be made by its manufacturer, is not guaranteed or endorsed by the publisher.

References

1. Kim H, Lee S, Kim J. Risk of injury after emergency department visit for acute peripheral vertigo: a matched-cohort study. *Clin Exp Emerg Med.* (2020) 7:176–82. doi: 10.15441/ceem.19.064

2. Neuhauser H, Leopold M, Brevern M, von Arnold G, Lempert T. The interrelations of migraine, vertigo, and migrainous vertigo. *Neurology.* (2001) 56:436–41. doi: 10.1212/WNL.56.4.436

3. Zuma e Maia F, Ramos BF, Cal R, Brock CM, Mangabeira Albernaz PL, Strupp M. Management of Lateral Semicircular Canal Benign Paroxysmal Positional Vertigo. *Front Neurol.* (2020) 11:1040. doi: 10.3389/fneur.2020.01040

4. Berryhill WE, Graham MD. Chemical and physical labyrinthectomy for Meniere's disease. *Otolaryngol Clin North Am.* (2002) 35:675–82. doi: 10.1016/S0030-6665(02)00025-7

5. Hall CD, Herdman SJ, Whitney SL, Anson ER, Carender WJ, Hoppes CW, et al. Vestibular rehabilitation for peripheral vestibular hypofunction: an updated clinical practice guideline from the academy of neurologic physical therapy of the american physical therapy association. *J Neurol Phys Ther.* (2022) 46:118–77. doi: 10.1097/NPT.0000000000000382

6. Quaranta A, Aloisi A, De Benedittis G, Scaringi A. Intratympanic therapy for ménière's disease: high-concentration gentamicin with round-window protection. *Ann N Y Acad Sci.* (1999) 884:410–24. doi: 10.1111/j.1749-6632.1999.tb08658.x

7. Parnes LS, McClure JA. Posterior semicircular canal occlusion in the normal hearing ear. *Otolaryngol Neck Surg.* (1991) 104:52–7. doi: 10.1177/019459989110400111

8. Parnes LS, McClure JA. Posterior semicircular canal occlusion for intractable benign paroxysmal positional vertigo. *Ann Otol Rhinol Laryngol.* (1990) 99:330–4. doi: 10.1177/000348949009900502

9. Beyea JA, Agrawal SK, Parnes LS. Transmastoid semicircular canal occlusion: a safe and highly effective treatment for benign paroxysmal positional vertigo and superior canal dehiscence. *Laryngoscope.* (2012) 122:1862–6. doi: 10.1002/lary.23390

10. Ahmed RM, Pohl DV, MacDougall HG, Makeham T, Halmagyi GM. Posterior semicircular canal occlusion for intractable benign positional vertigo: outcome in 55 ears in 53 patients operated upon over 20 years. *J Laryngol Otol.* (2012) 126:677–82. doi: 10.1017/S0022215112000758

11. Lin KF, Bojrab DI, Fritz CG, Vandieren A, Babu SC. Hearing outcomes after surgical manipulation of the membranous labyrinth during superior semicircular canal dehiscence plugging or posterior semicircular canal occlusion. *Otol Neurotol.* (2021) 42:806–14. doi: 10.1097/MAO.0000000000003100

12. Maas BDPJ, van der Zaag-Loonen HJ, van Benthem PPG, Bruintjes TD. Effectiveness of canal occlusion for intractable posterior canal benign paroxysmal positional vertigo: a systematic review. *Otolaryngol Neck Surg.* (2020) 162:40–9. doi: 10.1177/0194599819881437

13. Stultiens JJA, Guinand N, Van Rompaey V, et al. The resilience of the inner ear—vestibular and audiometric impact of transmastoid semicircular canal plugging. *J Neurol.* (2021). doi: 10.1007/s00415-021-10693-5

14. Guo JY, He L, Qu TF, Liu YY, Liu K, Wang GP, et al. Canalostomy as a surgical approach to local drug delivery into the inner ears of adult and neonatal mice. *J Vis Exp.* (2018) 135:57351. doi: 10.3791/57351

15. Zhang Q, Liu H, McGee J, Walsh EJ, Soukup GA, He DZZ. Identifying MicroRNAs involved in degeneration of the organ of corti during age-related hearing loss. *PLoS ONE.* (2013) 8:e62786. doi: 10.1371/journal.pone.0062786

16. Liu H, Giffen KP, Chen L, Henderson HJ, Cao TA, Kozeny GA, et al. Molecular and cytological profiling of biological aging of mouse cochlear inner and outer hair cells. *Cell Rep.* (2022) 39:110665. doi: 10.1016/j.celrep.2022.110665

17. Li Y, Liu H, Zhao X, He DZ. Endolymphatic potential measured from developing and adult mouse inner ear. *Front Cell Neurosci.* (2020) 14:584928. doi: 10.3389/fncel.2020.584928

18. Zhang Q, Liu H, Soukup GA, He DZZ. Identifying MicroRNAs involved in aging of the lateral wall of the cochlear duct. *PLoS ONE.* (2014) 9:12. doi: 10.1371/journal.pone.0112857

19. Liu H, Giffen KP, Grati M, Morrill SW, Li Y, Liu X, et al. Transcription co-factor LBH is necessary for the survival of cochlear hair cells. *J Cell Sci.* (2021) 134:jcs.254458. doi: 10.1242/jcs.254458

20. Guo J-Y, He L, Chen Z-R, Liu K, Gong S-S, Wang G-P. AAV8-mediated Atoh1 overexpression induces dose-dependent regeneration of vestibular hair cells in adult mice. *Neurosci Lett.* (2021) 747:135679. doi: 10.1016/j.neulet.2021.135679

21. Von Bekesy G. Resting potentials inside the cochlear partition of the guinea pig. *Nature.* (1952) 169:241–2. doi: 10.1038/169241a0

22. Woolf NK, Ryan AF, Harris JP. Development of mammalian endocochlear potential: normal ontogeny and effects of anoxia. *Am J Physiol-Regul Integr Comp Physiol.* (1986) 250:R493–8. doi: 10.1152/ajpregu.1986.250.3.R493

23. Zhu Q, Liu C, Lin C, Chen X, Liu T, Lin S, et al. Efficacy and safety of semicircular canal occlusion for intractable horizontal semicircular benign paroxysmal positional vertigo. *Ann Otol Rhinol Laryngol.* (2015) 124:257–60. doi: 10.1177/0003489414556307

24. Antonelli PJ, Bouchard KR, Kartush JM, Kubilis PS. Triple semicircular canal occlusion in the guinea pig. *Otolaryngol Neck Surg.* (1997) 117:509–15. doi: 10.1016/S0194-5998(97)70023-8

25. Kobayashi T, Shiga N, Hozawa K, Hashimoto S, Takasaka T. Effect on cochlear potentials of lateral semicircular canal destruction. *Arch Otolaryngol Neck Surg.* (1991) 117:1292–5. doi: 10.1001/archotol.1991.01870230108018

26. Money KE, Scott JW. Functions of separate sensory receptors of nonauditory labyrinth of the cat. *Am J Physiol-Leg Content.* (1962) 202:1211–20. doi: 10.1152/ajplegacy.1962.202.6.1211

27. Parnes LS, McClure JA. Effect on brainstem auditory evoked responses of posterior semicircular canal occlusion in guinea pigs. *J Otolaryngol.* (1985) 14:145–50.

28. Yakushin SB, Kolesnikova OV, Cohen B, Ogorodnikov DA, Suzuki J-I, Della Santina CC, et al. Complementary gain modifications of the cervico-ocular (COR) and angular vestibulo-ocular (aVOR) reflexes after canal plugging. *Exp Brain Res.* (2011) 210:549–60. doi: 10.1007/s00221-011-2558-6

29. Yin S, Yu D, Li M, Wang J. Triple semicircular canal occlusion in guinea pigs with endolymphatic hydrops. *Otol Neurotol.* (2006) 27:78–85. doi: 10.1097/01.mao.0000170535.42023.96

30. Paige GD. Vestibuloocular reflex and its interactions with visual following mechanisms in the squirrel monkey. I Response characteristics in normal animals. *J Neurophysiol.* (1983) 49:134–51. doi: 10.1152/jn.1983.49.1.134

31. Yin S, Yu D, Chen Z, Cao Z, Wang J. Important factors for the hearing loss caused by the triple semicircular canal occlusion in guinea pigs. *Otol Neurotol.* (2007) 28:513–9. doi: 10.1097/mao.0b013e318033f020

32. Zhang D, Lv Y, Han Y, Sun G, Li Y, Li X, et al. Revision surgery after triple semicircular canal plugging and morphologic changes of vestibular organ. *Sci Rep.* (2019) 9:19397. doi: 10.1038/s41598-019-55810-7

33. Gilchrist DP, Curthoys IS, Burgess AM, Cartwright AD, Jinnouchi K, MacDougall HG, et al. Semicircular canal occlusion causes permanent VOR changes. *Neuroreport.* (2000) 11:2527–31. doi: 10.1097/00001756-200008030-00036

34. Aw ST, Halmagyi GM, Pohl DV, Curthoys IS, Yavor RA, Todd MJ. Compensation of the human vertical vestibulo-ocular reflex following occlusion of one vertical semicircular canal is incomplete. *Exp Brain Res.* (1995) 103:471–5. doi: 10.1007/BF00241506

frontiers | Frontiers in Neuroscience

TYPE Original Research
PUBLISHED 20 September 2022
DOI 10.3389/fnins.2022.986860

Check for updates

OPEN ACCESS

EDITED BY
Hubertus Axer,
Jena University Hospital, Germany

REVIEWED BY
Thomas A. Stoffregen,
University of Minnesota Twin Cities, United States
Jose Antonio Lopez-Escamez,
Universidad de Granada, Spain

*CORRESPONDENCE
Jin Hu
hujin19771110@163.com

SPECIALTY SECTION
This article was submitted to Perception Science, a section of the journal Frontiers in Neuroscience

RECEIVED 05 July 2022
ACCEPTED 31 August 2022
PUBLISHED 20 September 2022

CITATION
Meng D, Zhou X, Hu T, Zheng J, Jin T, Gao H and Hu J (2022) Study of clinical correlation of motion sickness in patients with vestibular migraine. *Front. Neurosci.* 16:986860. doi: 10.3389/fnins.2022.986860

COPYRIGHT
© 2022 Meng, Zhou, Hu, Zheng, Jin, Gao and Hu. This is an open-access article distributed under the terms of the Creative Commons Attribution License (CC BY). The use, distribution or reproduction in other forums is permitted, provided the original author(s) and the copyright owner(s) are credited and that the original publication in this journal is cited, in accordance with accepted academic practice. No use, distribution or reproduction is permitted which does not comply with these terms.

Study of clinical correlation of motion sickness in patients with vestibular migraine

Danyang Meng[1], Xuyou Zhou[1], Tianye Hu[2], Jialian Zheng[3], Tingyu Jin[1], Han Gao[1] and Jin Hu[1]*

[1]Department of Neurology, Affiliated Hospital of Jiaxing University, Jiaxing, China, [2]Department of Traditional Chinese Medicine and Acupuncture, Affiliated Hospital of Jiaxing University, Jiaxing, China, [3]Department of Physical Examination Center, Affiliated Hospital of Jiaxing University, Jiaxing, China

Objective: In this study, clinical data from vestibular migraine (VM) patients and healthy control populations were collected to analyze the clinical data of VM patients, especially the history of motion sickness, and to understand their clinical characteristics.

Methods: According to VM diagnostic criteria, 140 patients diagnosed with confirmed VM (cVM) and probable VM (pVM) who attended the outpatient and inpatient ward of Jiaxing First Hospital between August 2017 and June 2021, as well as 287 healthy check-ups in the health management center, were analyzed and compared in terms of age, gender, and previous history of motion sickness.

Results: A comparison of clinical data related to VM patients and the control population showed that there were more women in the VM group ($P < 0.01$) and that patients in the VM group were older ($P < 0.05$) and had a higher prevalence of history of motion sickness history ($P < 0.01$). Analysis after matching gender and age revealed that patients in the cVM group were older than those in the pVM group ($P < 0.05$), but the proportion of motion sickness was lower than in the pVM group ($P < 0.05$). The age of the patients in the cVM group was mainly distributed around 50 years of age, following a normal distribution, whereas the age distribution of the patients in the pVM group did not have a significant trend of age concentration and was distributed at all ages.

Conclusion: The history of motion sickness is significant in patients with VM and may be a potential suggestive factor for the diagnosis of VM.

KEYWORDS

vestibular migraine, motion sickness, vertigo, clinical diagnosis, correlation

Introduction

Vestibular migraine (VM) is the second most common cause of recurrent vertigo or dizziness and is clinically second to benign paroxysmal positional vertigo as a subtype of migraine (Mallampalli et al., 2021; Krishnan and Carey, 2022). The typical vestibular symptoms of VM are spontaneous vertigo, positional vertigo, and head motion intolerance, as well as increased visuomotor sensitivity and spatial disorientation (Zaleski-King and Monfared, 2021; Shen and Qi, 2022).

The Migraine Classification Subcommittee of the International Headache Society (IHS) proposed in 2018 that the diagnosis of VM is based on recurrent vestibular symptoms, a history of migraine, a temporal association between vestibular symptoms and migraine symptoms, and the exclusion of other causes of vestibular symptoms (2018).

The latest proposed diagnostic criteria divide the VM into confirmed VM (cVM) and probable VM (pVM), and the diagnosis is based mainly on the clinical manifestations of the patient, lacking specific examination means and objective indicators. According to this criterion, only about 20% of patients have received a relatively accurate diagnosis (Li et al., 2021; Mallampalli et al., 2021). And the first five episodes of dizziness or vertigo in patients with VM were not diagnosed. Motion sickness is a series of physiological reactions caused by abnormal external exercise stimulation, including nausea, vomiting, cold sweat, dizziness, and other symptoms. In daily life, motion sickness often occurs in the process of taking airplanes, ships, cars, and other vehicles, which affects people's normal life and work (Koch et al., 2018; Cohen et al., 2019; Keshavarz and Golding, 2022). In this article, we analyze the correlation between VM patients and their history of motion sickness to provide more clinical guidance significance for the early diagnosis of VM.

Materials and methods

Ethics statement

The study was approved by the Institutional Review Board of the Affiliated Hospital of Jiaxing University, Jiaxing City. Informed consent was obtained from patients and healthy subjects.

Study population

One hundred and forty patients with a diagnosis of VM and pVM and 287 people who underwent health checks, who were seen in outpatient clinics and inpatient ward of the Department of Neurology, Affiliated Hospital of Jiaxing University between August 2017 and June 2021, were selected and divided into experimental and control groups. Clinical data such as age, gender, and previous history of motion sickness were collected from both groups and the data were analyzed, summarized and compared.

Inclusion criteria: (1) adults aged 18–80 years; (2) diagnostic criteria for cVM patients and pVM patients met the diagnostic criteria of the International Classification of Headache Disorders, 3rd edition, Olesen et al. (2018) and the BARANY Criteria (Lempert et al., 2012); (3) all patients underwent neurological and neurotological examinations, including an evaluation of nystagmus and assessments of limb ataxia and balance to confirm the absence of a central lesion. Magnetic resonance imaging (MRI) was also conducted for differential diagnosis; and (4) average communication skills for filling out the questionnaire. Exclusion criteria: (1) patients with VM who also had other types of vertigo disorders such as central vertigo, benign paroxysmal positional vertigo, etc.; (2) pregnancy; (3) mental illness; and (4) severe systemic diseases (including hepatic failure, uremia, heart failure, and rheumatic immune diseases).

Methods

The retrospective study designs

The study participants were divided into a VM group and a healthy physical examination group (control group), and the VM group was further divided into two groups: the cVM group and the pVM group. Various clinical data including age, sex, and previous history of motion sickness were collected from all participants. We conducted further screening for the sample by referring to Golding questionnaire (Golding, 2006) to determine the history of motion sickness and the data were presented with or without motion sickness. The calculation of sample size was done using an online sample size calculators.[1] The sample size used in the present study was appropriate based on the result of sample size calculation ($\alpha = 0.05$, $\beta = 0.2$). This study was approved by the Ethics Committee of the Affiliated Hospital of Jiaxing University.

Statistical analysis

The measurement data were presented as mean ± standard deviation ($M \pm SD$) and the count data was presented as a number. SPSS software (version 25.0) was used for the statistical analysis of the collected data. The count data were compared using the chi-square (χ^2) test. The measurement data were first tested for normality and data that conformed to a normal distribution were compared using the independent samples t-test. $P < 0.05$ was considered statistically significant.

1 https://sample-size.net/

Results

Analysis of clinical data from the vestibular migraine and control groups

There were 31 males and 109 females in the VM group and 142 males and 145 females in the control group, respectively. After the Chi-square test, the gender difference between the two groups was statistically significant (χ^2 = 29.173, $P < 0.0001$, Table 1).

The age of the patients in the VM group was 46.24 ± 12.88 years and the age of the people in the control group was 42.29 ± 14.12 years. Data between the two groups showed a statistical difference in age between the two groups ($t = -2.792$, $P = 0.005$, Table 1).

There were 91 and 66 individuals with a history of motion sickness and 49 and 221 individuals without a history of motion sickness in the VM and control groups, respectively. The results between the two groups were statistically different ($\chi^2 = 71.408$, $P < 0.0001$, Table 1).

Analysis of clinical data of the vestibular migraine and control groups after age and gender matching

Since there were statistical differences in age and gender between the VM group and the control group, and the number of people in the control group was much larger than that in the VM group, 84 individuals in the control group were removed to rematch the two groups.

After rematching age and gender, there were 64 men and 142 women in the control group, and the gender difference between the two groups was not statistically significant compared to the VM group (χ^2 = 3.334, P = 0.068, Table 2). The age of the control group after rematching was 42.29 ± 14.12 years, which was not statistically different compared to the control group (t = 1.567, P = 0.068, Table 2). There were 18 and 188 people with and without a history of motion sickness in the control groups, and it is statistically significant compared to the VM group ($\chi^2 = 122.273$, $P < 0.001$, Table 2).

Analysis of clinical data of the confirmed vestibular migraine and probable vestibular migraine groups

After the VM group, the patients were subgrouped into cVM and pVM groups, we performed normality tests for different age groups, and the results showed that the age distribution of the patients in the cVM group was mainly distributed around 50 years of age, which was consistent with a normal distribution, while the age distribution of the patients in the pVM group did not show a significant age concentration trend and was distributed in all age groups (Figure 1).

There were 11 males and 36 females in the cVM group, and 20 males and 73 females in the pVM group, respectively, and the gender difference between the two groups was not statistically significant (χ^2 = 0.065, P = 0.798, Table 3). The age of the patients in the cVM group was 49.61 ± 9.03 years and the age of the patients in the pVM group was 44.52 ± 14.18 years. The age between the two groups showed a statistical difference ($t = -2.578$, P = 0.011, Table 3). There were 24 and 67 individuals with a history of motion sickness and 23 and 26 individuals without a history of motion sickness in the cVM and pVM groups, respectively. The results between the two groups were statistically different ($\chi^2 = 6.04$, $P = 0.014$, Table 3).

Discussion

With the increasingly standardized diagnosis and treatment of vertigo and dizziness disorders, VM is receiving increasing attention from clinicians. Clinical work has identified many patients with VM who are undiagnosed during the first five episodes of dizziness and are eventually diagnosed with VM as the number of episodes increases over time. Therefore, the early diagnosis of patients with VM is a difficult problem that needs to be addressed in clinical work. Studies have shown that, there is auditory dysfunction at the lower frequencies in VM patients and the cochlear dysfunction of the peripheral auditory system (Xue et al., 2020). Besides, compared with migraine patients, the incidence of tinnitus was significantly increased in the VM group (Kirkim et al., 2017). Abnormal oculomotor functions are commonly observed in patients with VM (Fu et al., 2021). Previous studies have focused on the potential relationship and mechanism between migraine with vestibular symptoms and motion sickness. In our study, we have refined the classification, studies VM, and the cVM and pVM scales. Depicting their age distribution and differences in the incidence of motion sickness. Some studies have shown (Antal et al., 2005) that the visual cortex of migraine patients exhibits increased excitability, so the increase in motion perception may be caused by hyperexcitability of the visual cortex. Patients with VM have vestibular dysfunction with elevated perceptual thresholds, and their thresholds increase further after complex visual stimuli. Based on this finding, it has been hypothesized (Wurthmann et al., 2021) that the interaction between the visual and vestibular cortex may contribute to the occurrence of migraine and visual vertigo of VM, while during the interictal period, VM patients have reduced motor perception thresholds and show a marked susceptibility to motion sickness, which may indicate an increased level of vestibular processing. Previous studies (Winnick et al., 2018; Bednarczuk et al., 2019) have shown the presence of abnormal spatial location and sensory

TABLE 1 Clinical data of the VM and control groups.

	VM group	Control group	χ^2/T-value	*P*-value
Gender (male/female)	31/109	142/145	29.173	0.0001
Age (years)	46.24 ± 12.88	42.29 ± 14.12	−2.792	0.005
Motion sickness (yes/no)	91/49	66/221	71.408	0.0001

TABLE 2 Clinical data of the VM and control groups after age and gender matching.

	VM group	Control group	χ^2/T-value	*P*-value
Gender (male/female)	31/109	64/142	3.334	0.068
Age (years)	46.24 ± 12.88	44.48 ± 14.90	1.567	0.068
Dizziness or vertigo (yes/no)	91/49	18/188	122.273	<0.001

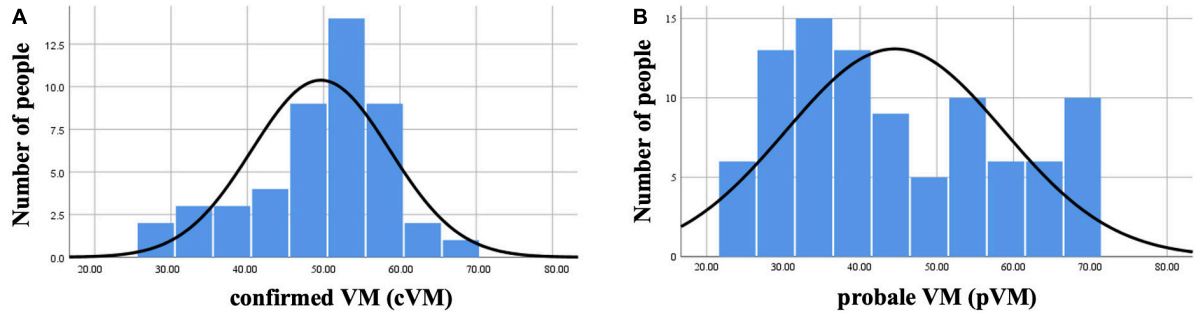

FIGURE 1
Histogram of the age distribution of VM in the cVM group and the pVM group. **(A)** Histogram of the age distribution of the cVM group. **(B)** Histogram of the age distribution of the pVM group.

TABLE 3 Clinical data of the cVM and pVM groups.

	cVM group	pVM group	χ^2/T-value	*P*-value
Gender (male/female)	11/36	20/73	0.065	0.798
Age (years)	49.61 ± 9.03	44.52 ± 14.18	2.578	0.011
Dizziness or vertigo (yes/no)	24/23	67/26	6.04	0.014

integration in patients with VM. Several other fMRI studies (Russo et al., 2014; Shin et al., 2014) have identified interactions between vestibular and visual cortical areas and activation of vestibular thalamocortical pathways during VM episodes. These findings could suggest that the occurrence of VM is related to vestibular, somatosensory, and visual information, and VM could be considered a complex disorder caused by multiple disorders of sensory integration. A small number of patients have reported visual aura, but more detailed data for analysis are difficult to obtain. Perhaps patients with aura have a higher prevalence of motion sickness, which deserves further investigation.

Various serum factors such as 5-hydroxytryptamine (5-HT), calcitonin gene-related peptide (CGRP), and Mg^{2+} have been found to be associated with VM (van Dongen et al., 2017; Wang et al., 2020; Zhang et al., 2020). Furthermore, some cytokines, such as interleukin-1β, CCL3, CCL22, and CXCL1, have also been found to be valuable in the diagnosis of VM (Flook et al., 2019). However, there is no single experimental index that can diagnose VM, serologically or with various cytokines, so it is not easy to find relatively specific indexes among many laboratory indexes. In some studies, subjective scales and motion sickness susceptibility questionnaires have reached similar conclusions, with more people susceptible to motion sickness in the migraine group than in the normal control group (Jeong et al., 2010). Similarly, we hope that in the future, motion sickness can be used as an accessible predictor to assist in the early diagnosis of VM.

Clinically relevant influences are more easily accessible than laboratory indicators. Some triggers such as sleep deprivation, stress, irregular diet, flickering light, odor stimuli, food, weather changes, and menstrual cycle have been suggested to be present

in patients with VM (Neuhauser et al., 2001; Baier et al., 2009; Andress-Rothrock et al., 2010). Several studies have shown that about half of patients with VM have a family history of the disease (Oh et al., 2001; Lee et al., 2008; Teggi et al., 2018; Huang et al., 2020). The prediction of models using clinical factors and laboratory indicators in patients with VM to diagnose VM has also been reported in the literature (Zhou et al., 2020). However, fewer studies have been reported on the interrelationship between virtual reality and motion sickness. Previous studies have reported that compared with Meniere's disease, benign paroxysmal positional vertigo or vestibular neuritis, migraine patients are more likely to have motion sickness. It is therefore hypothesized that the pathways involved in motion sickness and migraine are central rather than peripheral (Cuomo-Granston and Drummond, 2010). It has been suggested that although patients with VM have an increased susceptibility to motion sickness in general, this is not different from migraine (Murdin et al., 2015). However, other studies have further refined the symptoms of migraine patients, and migraine patients with dizziness/vertigo have more severe motion sickness than migraine patients without dizziness/vertigo and normal controls, which is similar to our results (Jeong et al., 2010). A study of motion sickness and VM showed that in a college student population, approximately half of those with motion sickness had VM in combination, while the prevalence of VM in those without motion sickness was only 30% (Abouzari et al., 2020), but the population involved in this study was in their 20s and was a motion sickness-centered study, making its clinical value relatively limited.

There are limited researches on the clinical differences between cVM and pVM, and some studies suggest that the patient groups' characteristics were most pronounced for definite diagnoses (Oh et al., 2021), and there are other studies that support this conclusion, suggesting that utriculo-ocular pathway dysfunction is more frequent in VM than pVM (Fujimoto et al., 2020). In addition to these discussions between cVM and pVM, some studies suggest that the current criteria of VM is questionable and needs to be further refined and expanded (Dominguez-Duran et al., 2021; Chae et al., 2022). The results of this study showed that women with cVM were approximately 3–4 times more likely than male patients, and their age matched a normal distribution, with a high prevalence in middle-aged women around 50 years of age, which is consistent with previous studies (Dieterich and Brandt, 1999). However, the age distribution of pVM patients does not have an obvious age concentration trend and is distributed in all age stages, with a relatively higher prevalence in young and middle-aged women. The age distribution of patients with pVM, which is rarely reported in previous studies, may be related to the fact that the clinical diagnosis of patients with VM requires longer follow-up and the increased frequency of attacks near menopause and the presence of other conditions that are consistent with the diagnosis, so that the age would tend to be around 50 years. In contrast, pVM, because it requires relatively few conditions for diagnosis, requires a shorter follow-up period, and is diagnosed when patients are much younger. Previous statistical analysis shows a significant increase in the diagnosis of pVM with increasing age and a decrease in VM diagnosis. The type of vestibular symptoms varies according to the age of onset of VM. This conclusion may have been limited by the sample size and the investigators set a temporal cut-off of 60 years old, based on the evidence of the radical decrease in the onset of migraine attacks from the age of 50 (Ori et al., 2020). Furthermore, this study also found that patients with pVM had a higher rate of motion sickness, 72.04%, compared to 51.06% of patients in the cVM group and 23.00% in the control group. cVM patients with motion sickness were consistent with the study by Wurthmann et al. (2021). However, motion sickness in pVM patients as well as in the normal control population was also investigated in this study, and age and sex matched analysis revealed a statistically significant comparison between the proportion of the VM group and the physical examination group with a history of motion sickness.

Migraine is considered to be a neurological disorder. Due to the unpredictability of migraine and the lack of reliable and acceptable ways to trigger a typical migraine, it is difficult to examine patients during migraine attacks, especially to detect subtle neuronal activity or neurotransmitter levels (Marcus et al., 2005). However, motion sickness provides a reproducible phenomenon, allowing easy study in the research laboratory. Our research suggests a high correlation between motion sickness and VM, which can be used as one of the clinical predictors of early onset in patients with VM. Some studies believe that the diagnosis of motion sickness diagnosis is mainly clinical, based on the history of a triggering situation (imposed or perceived motion) and typical symptoms and signs of motion sickness such as nausea, headache, blurred vision, non-vertiginous dizziness, drowsiness, spatial disorientation, difficulty concentrating, and sometimes vomiting., etc. The diagnosis can be facilitated if there is a prior history of motion sickness, especially following the exposure to similar events, while laboratory testing is usually not necessary (Leung and Hon, 2019). It is worth noting that in studies of EDA (electrodermal activity), the participants were divided into groups based on whether they had Graybiel scores of 0 or $\geq$1 for all seven Graybiel diagnostic criteria (nausea, skin color, cold sweating, increased salivation, drowsiness, pain, and central nervous system). And the results showed that there was no difference in scores of 0 and $\geq$1 for autonomic symptoms except cold sweat and salivation, which suggested that self-reports may not be as accurate as we expect (Tamura et al., 2018). In 2021, signs and symptoms related to motion accounted for the majority of the diagnostic conditions in the Barany criteria. However, there have been studies evaluating bodily stability in different diseases using direct quantitative measures of movement (Cohen et al., 2014; Lubetzky et al., 2021).

The quantitative kinematics of postural activity differ between persons who are susceptible to motion sickness, and those who are not. These differences exist during exposure to nauseogenic motion stimuli but, critically, also exist in the absence of such exposure. That is, measures of "ordinary body sway" can be used to predict the risk of motion sickness for individuals (Koslucher et al., 2016; Weech et al., 2018). The same effect has been observed in the case of mild traumatic brain injury (Chen et al., 2013). These indicators make the diagnosis of motion sickness seem more traceable than the signs and symptoms in the diagnostic criteria, and may further predict VM. Criteria was introduced in the manuscript to diagnose cVM and pVM, and according to the inclusion and exclusion criteria, the included patients with cVM and pVM were consistent with moderate or severe intensity, lasting 5 min to 72 h. Although the difference between cVM and pVM is the migration history or migration features during the episode in the criteria, it should be noted that the severity and duration of symptoms (dizziness and headache) may interfere with outcomes. In the future, we will also combine other influencing factors to conduct multifactorial impact analysis and model construction to guide VM for early clinical diagnosis. In addition, there are a series of new directions on the diagnosis and treatment of VM, including functional magnetic resonance imaging (fMRI), combined treatment with different antidepressants, which provide inspiration for the rehabilitation and prevention of vestibular function, and we will carry out a variety of new studies related to VM to further explore these contents. Most of episodic or progressive syndromes show familial clustering (Roman-Naranjo et al., 2018). To explore the familial genetics of VM, we established the Vertigo Diagnosis and Treatment Consortium. As a large public hospital, we work closely with the county hospitals and community hospitals to provide them with equipment and share technology. At present, these processes are still being improved, and we hope to collect more data and conduct multicenter studies on VM family history in the future.

Data availability statement

The raw data supporting the conclusions of this article will be made available by the authors, without undue reservation.

Ethics statement

The studies involving human participants were reviewed and approved by the Ethics Committee of the Affiliated Hospital of Jiaxing University. Written informed consent for participation was not required for this study in accordance with the national legislation and the institutional requirements.

Author contributions

JH designed and developed this study and performed the analysis. DM and JH drafted and edited the manuscript. JZ and TH contributed to conception of the study. XZ, TJ, and HG collected the data. DM performed the interpretation. All authors contributed to the article and approved the submitted version.

Funding

This work was supported by the Young Talents Fund project of Zhejiang Provincial TCM Sci-Tech Plan (2021ZQ084) and the Jiaxing Public Welfare Research Program (2019AD32180).

Conflict of interest

The authors declare that the research was conducted in the absence of any commercial or financial relationships that could be construed as a potential conflict of interest.

Publisher's note

All claims expressed in this article are solely those of the authors and do not necessarily represent those of their affiliated organizations, or those of the publisher, the editors and the reviewers. Any product that may be evaluated in this article, or claim that may be made by its manufacturer, is not guaranteed or endorsed by the publisher.

References

Abouzari, M., Cheung, D., Pham, T., Goshtasbi, K., Sarna, B., Tajran, S., et al. (2020). The relationship between vestibular migraine and motion sickness susceptibility. *Otol. Neurotol.* 41, 1116–1121.

Andress-Rothrock, D., King, W., and Rothrock, J. (2010). An analysis of migraine triggers in a clinic-based population. *Headache* 50, 1366–1370. doi: 10.1111/j.1526-4610.2010.01753.x

Antal, A., Temme, J., Nitsche, M. A., Varga, E. T., Lang, N., and Paulus, W. (2005). Altered motion perception in migraineurs: evidence for interictal cortical hyperexcitability. *Cephalalgia* 25, 788–794. doi: 10.1111/j.1468-2982.2005.00949.x

Baier, B., Winkenwerder, E., and Dieterich, M. (2009). "Vestibular migraine": effects of prophylactic therapy with various drugs. A retrospective study. *J. Neurol.* 256, 436–442. doi: 10.1007/s00415-009-0111-3

Bednarczuk, N. F., Bonsu, A., Ortega, M. C., Fluri, A. S., Chan, J., Rust, H., et al. (2019). Abnormal visuo-vestibular interactions in vestibular migraine: a cross sectional study. *Brain* 142, 606–616. doi: 10.1093/brain/awy355

Chae, R., Krauter, R., Pasquesi, L. L., and Sharon, J. D. (2022). Broadening the vestibular migraine diagnosis criteria: a prospective cohort study on vestibular migraine subtypes. *J. Vestib. Res.* [Online ahead of print]. doi: 10.3233/VES-210117.

Chen, Y. C., Tseng, T. C., Hung, T. H., Hsieh, C. C., Chen, F. C., and Stoffregen, T. A. (2013). Cognitive and postural precursors of motion sickness in adolescent boxers. *Gait Posture* 38, 795–799. doi: 10.1016/j.gaitpost.2013.03.023

Cohen, B., Dai, M., Yakushin, S. B., and Cho, C. (2019). The neural basis of motion sickness. *J. Neurophysiol.* 121, 973–982. doi: 10.1152/jn.00674.2018

Cohen, H. S., Mulavara, A. P., Peters, B. T., Sangi-Haghpeykar, H., and Bloomberg, J. J. (2014). Standing balance tests for screening people with vestibular impairments. *Laryngoscope* 124, 545–550. doi: 10.1002/lary.24314

Cuomo-Granston, A., and Drummond, P. D. (2010). Migraine and motion sickness: what is the link? *Prog. Neurobiol.* 91, 300–312. doi: 10.1016/j.pneurobio.2010.04.001

Dieterich, M., and Brandt, T. (1999). Episodic vertigo related to migraine (90 cases): vestibular migraine? *J. Neurol.* 246, 883–892. doi: 10.1007/s004150050478

Dominguez-Duran, E., Domenech-Vadillo, E., Becares-Martinez, C., Montilla-Ibanez, M. A., Alvarez-Morujo de Sande, M. G., Gonzalez-Aguado, R., et al. (2021). Exploring the frontiers of vestibular migraine: a case series. *J. Vestib. Res.* 31, 91–99. doi: 10.3233/VES-201559

Flook, M., Frejo, L., Gallego-Martinez, A., Martin-Sanz, E., Rossi-Izquierdo, M., Amor-Dorado, J. C., et al. (2019). Differential proinflammatory signature in vestibular migraine and meniere disease. *Front. Immunol.* 10:1229. doi: 10.3389/fimmu.2019.01229

Fu, W., Wang, Y., He, F., Wei, D., Bai, Y., Han, J., et al. (2021). Vestibular and oculomotor function in patients with vestibular migraine. *Am. J. Otolaryngol.* 42:103152. doi: 10.1016/j.amjoto.2021.103152

Fujimoto, C., Kamogashira, T., Takenouchi, S., Kinoshita, M., Sugasawa, K., Kawahara, T., et al. (2020). Utriculo-ocular pathway dysfunction is more frequent in vestibular migraine than probable vestibular migraine. *J. Neurol.* 267, 2340–2346. doi: 10.1007/s00415-020-09851-y

Golding, J. F. (2006). Motion sickness susceptibility. *Auton. Neurosci.* 129, 67–76.

Huang, T. C., Wang, S. J., and Kheradmand, A. (2020). Vestibular migraine: an update on current understanding and future directions. *Cephalalgia* 40, 107–121. doi: 10.1177/0333102419869317

Jeong, S. H., Oh, S. Y., Kim, H. J., Koo, J. W., and Kim, J. S. (2010). Vestibular dysfunction in migraine: effects of associated vertigo and motion sickness. *J. Neurol.* 257, 905–912. doi: 10.1007/s00415-009-5435-5

Keshavarz, B., and Golding, J. F. (2022). Motion sickness: current concepts and management. *Curr. Opin. Neurol.* 35, 107–112. doi: 10.1097/WCO.0000000000001018

Kirkim, G., Mutlu, B., Olgun, Y., Tanriverdizade, T., Keskinoglu, P., Guneri, E. A., et al. (2017). Comparison of audiological findings in patients with vestibular migraine and migraine. *Turk. Arch. Otorhinolaryngol.* 55, 158–161. doi: 10.5152/tao.2017.2609

Koch, A., Cascorbi, I., Westhofen, M., Dafotakis, M., Klapa, S., and Kuhtz-Buschbeck, J. P. (2018). The neurophysiology and treatment of motion sickness. *Dtsch. Arztebl. Int.* 115, 687–696. doi: 10.3238/arztebl.2018.0687

Koslucher, F., Haaland, E., and Stoffregen, T. A. (2016). Sex differences in visual performance and postural sway precede sex differences in visually induced motion sickness. *Exp. Brain Res.* 234, 313–322. doi: 10.1007/s00221-015-4462-y

Krishnan, P. S., and Carey, J. P. (2022). Vestibular migraine: clinical aspects and pathophysiology. *Otolaryngol. Clin. North Am.* 55, 531–547. doi: 10.1016/j.otc.2022.02.003

Lee, H., Jen, J. C., Cha, Y. H., Nelson, S. F., and Baloh, R. W. (2008). Phenotypic and genetic analysis of a large family with migraine-associated vertigo. *Headache* 48, 1460–1467. doi: 10.1111/j.1526-4610.2007.01002.x

Lempert, T., Olesen, J., Furman, J., Waterston, J., Seemungal, B., Carey, J., et al. (2012). Vestibular migraine: diagnostic criteria. *J. Vestib. Res.* 22, 167–172. doi: 10.3233/VES-2012-0453

Leung, A. K., and Hon, K. L. (2019). Motion sickness: an overview. *Drugs Context* 8:2019-9-4. doi: 10.7573/dic.2019-9-4.

Li, M., Xu, X., Qi, W., Liang, Y., Huang, Y., and Huang, H. (2021). Vestibular migraine: the chameleon in vestibular disease. *Neurol. Sci.* 42, 1719–1731. doi: 10.1007/s10072-021-05133-1

Lubetzky, A. V., Aharoni, M. M. H., Arie, L., and Krasovsky, T. (2021). People with persistent postural-perceptual dizziness demonstrate altered postural strategies in complex visual and cognitive environments. *J. Vestib. Res.* 31, 505–517. doi: 10.3233/VES-201552

Mallampalli, M. P., Rizk, H. G., Kheradmand, A., Beh, S. C., Abouzari, M., Bassett, A. M., et al. (2021). Care gaps and recommendations in vestibular migraine: an expert panel summit. *Front. Neurol.* 12:812678. doi: 10.3389/fneur.2021.812678

Marcus, D. A., Furman, J. M., and Balaban, C. D. (2005). Motion sickness in migraine sufferers. *Expert Opin. Pharmacother.* 6, 2691–2697. doi: 10.1517/14656566.6.15.2691

Murdin, L., Chamberlain, F., Cheema, S., Arshad, Q., Gresty, M. A., Golding, J. F., et al. (2015). Motion sickness in migraine and vestibular disorders. *J. Neurol. Neurosurg. Psychiatry* 86, 585–587. doi: 10.1136/jnnp-2014-308331

Neuhauser, H., Leopold, M., von Brevern, M., Arnold, G., and Lempert, T. (2001). The interrelations of migraine, vertigo, and migrainous vertigo. *Neurology* 56, 436–441. doi: 10.1212/wnl.56.4.436

Oh, A. K., Lee, H., Jen, J. C., Corona, S., Jacobson, K. M., and Baloh, R. W. (2001). Familial benign recurrent vertigo. *Am. J. Med. Genet.* 100, 287–291. doi: 10.1002/ajmg.1294

Oh, S. Y., Dieterich, M., Lee, B. N., Boegle, R., Kang, J. J., Lee, N. R., et al. (2021). Endolymphatic hydrops in patients with vestibular migraine and concurrent meniere's disease. *Front. Neurol.* 12:594481. doi: 10.3389/fneur.2021.594481

Olesen, J., Dodick, D. W., Ducros, A., and Evers, A. (2018). Headache classification committee of the international headache society (ihs) the international classification of headache disorders, 3rd edition. *Cephalalgia* 38, 1–211. doi: 10.1177/0333102417738202

Ori, M., Arra, G., Caricato, M., Freccia, R., Frati, F., De Bonis, T., et al. (2020). Age-related features in vestibular migraine onset: a multiparametric analysis. *Cephalalgia* 40, 1605–1613. doi: 10.1177/0333102420951505

Roman-Naranjo, P., Gallego-Martinez, A., and Lopez Escamez, J. A. (2018). Genetics of vestibular syndromes. *Curr. Opin. Neurol.* 31, 105–110. doi: 10.1097/WCO.0000000000000519

Russo, A., Marcelli, V., Esposito, F., Corvino, V., Marcuccio, L., Giannone, A., et al. (2014). Abnormal thalamic function in patients with vestibular migraine. *Neurology* 82, 2120–2126. doi: 10.1212/WNL.0000000000000496

Shen, Y., and Qi, X. (2022). Update on diagnosis and differential diagnosis of vestibular migraine. *Neurol Sci.* 43, 1659–1666. doi: 10.1007/s10072-022-05872-9

Shin, J. H., Kim, Y. K., Kim, H. J., and Kim, J. S. (2014). Altered brain metabolism in vestibular migraine: comparison of interictal and ictal findings. *Cephalalgia* 34, 58–67. doi: 10.1177/0333102413498940

Tamura, A., Iwamoto, T., Ozaki, H., Kimura, M., Tsujimoto, Y., and Wada, Y. (2018). Wrist-worn electrodermal activity as a novel neurophysiological biomarker of autonomic symptoms in spatial disorientation. *Front. Neurol.* 9:1056. doi: 10.3389/fneur.2018.01056

Teggi, R., Colombo, B., Albera, R., Asprella Libonati, G., Balzanelli, C., Batuecas Caletrio, A., et al. (2018). Clinical features, familial history, and migraine precursors in patients with definite vestibular migraine: the vm-phenotypes projects. *Headache* 58, 534–544. doi: 10.1111/head.13240

van Dongen, R. M., Zielman, R., Noga, M., Dekkers, O. M., Hankemeier, T., van den Maagdenberg, A. M., et al. (2017). Migraine biomarkers in cerebrospinal fluid: a systematic review and meta-analysis. *Cephalalgia* 37, 49–63. doi: 10.1177/0333102415625614

Wang, F., Wang, J., Cao, Y., and Xu, Z. (2020). Serotonin-norepinephrine reuptake inhibitors for the prevention of migraine and vestibular migraine: a systematic review and meta-analysis. *Reg. Anesth. Pain Med.* 45, 323–330. doi: 10.1136/rapm-2019-101207

Weech, S., Varghese, J. P., and Barnett-Cowan, M. (2018). Estimating the sensorimotor components of cybersickness. *J. Neurophysiol.* 120, 2201–2217. doi: 10.1152/jn.00477.2018

Winnick, A., Sadeghpour, S., Otero-Millan, J., Chang, T. P., and Kheradmand, A. (2018). Errors of upright perception in patients with vestibular migraine. *Front. Neurol.* 9:892. doi: 10.3389/fneur.2018.00892

Wurthmann, S., Naegel, S., Roesner, M., Nsaka, M., Scheffler, A., Kleinschnitz, C., et al. (2021). Sensitized rotatory motion perception and increased susceptibility to motion sickness in vestibular migraine: a cross-sectional study. *Eur. J. Neurol.* 28, 2357–2366. doi: 10.1111/ene.14889

Xue, J., Ma, X., Lin, Y., Shan, H., and Yu, L. (2020). Audiological findings in patients with vestibular migraine and migraine: history of migraine may be a cause of low-tone sudden sensorineural hearing loss. *Audiol. Neurootol.* 25, 209–214. doi: 10.1159/000506147

Zaleski-King, A., and Monfared, A. (2021). Vestibular migraine and its comorbidities. *Otolaryngol. Clin. North Am.* 54, 949–958. doi: 10.1016/j.otc.2021.05.014

Zhang, Y., Zhang, Y., Tian, K., Wang, Y., Fan, X., Pan, Q., et al. (2020). Calcitonin gene-related peptide facilitates sensitization of the vestibular nucleus in a rat model of chronic migraine. *J. Headache Pain* 21:72. doi: 10.1186/s10194-020-01145-y

Zhou, C., Zhang, L., Jiang, X., Shi, S., Yu, Q., Chen, Q., et al. (2020). A novel diagnostic prediction model for vestibular migraine. *Neuropsychiatr. Dis. Treat.* 16, 1845–1852. doi: 10.2147/NDT.S255717

frontiers | Frontiers in Neurology

TYPE Original Research
PUBLISHED 23 September 2022
DOI 10.3389/fneur.2022.925883

Check for updates

OPEN ACCESS

EDITED BY
Lisheng Yu,
Peking University People's Hospital, China

REVIEWED BY
Yi Ju,
Beijing Tiantan Hospital, Capital Medical University, China
Wei Sun,
University at Buffalo, United States

*CORRESPONDENCE
Ning Yu
yuning@301hospital.org
Qing Sun
2504511479@qq.com

SPECIALTY SECTION
This article was submitted to Neuro-Otology, a section of the journal Frontiers in Neurology

RECEIVED 22 April 2022
ACCEPTED 22 June 2022
PUBLISHED 23 September 2022

CITATION
Chen YX, Sun HJ, Mu XT, Jiang C, Wang HB, Zhang QH, Qu YY, Li J, Zhou LL, Zhao LZ, Yu N and Sun Q (2022) Intracranial tumors mimicking benign paroxysmal positional vertigo: A case series.
Front. Neurol. 13:925883.
doi: 10.3389/fneur.2022.925883

COPYRIGHT
© 2022 Chen, Sun, Mu, Jiang, Wang, Zhang, Qu, Li, Zhou, Zhao, Yu and Sun. This is an open-access article distributed under the terms of the Creative Commons Attribution License (CC BY). The use, distribution or reproduction in other forums is permitted, provided the original author(s) and the copyright owner(s) are credited and that the original publication in this journal is cited, in accordance with accepted academic practice. No use, distribution or reproduction is permitted which does not comply with these terms.

Intracranial tumors mimicking benign paroxysmal positional vertigo: A case series

Yuan Xing Chen[1,2], Han Jun Sun[1,2], Xue Tao Mu[3], Chao Jiang[2], Hui Bing Wang[1,2], Qing Hua Zhang[1,2], Yuan Yi Qu[1,2], Jian Li[1,2], Ling Ling Zhou[1,2], Long Zhu Zhao[1,2], Ning Yu[1,2]* and Qing Sun[1,2]*

[1]Department of Otolaryngology-Head and Neck Surgery, The Six Medical Center of Chinese PLA General Hospital, Beijing, China, [2]Department of Otolaryngology Head and Neck Surgery, Chinese PLA General Hospital, National Clinical Research Center for Otolaryngology Diseases, Beijing, China, [3]Department of Radiology, The Third Medical Center of Chinese PLA General Hospital, Beijing, China

Background: A few intracranial lesions may present only with positional vertigo which are very easy to misdiagnose as benign paroxysmal positional vertigo (BPPV); the clinicians should pay more attention to this disease.

Objectives: To analyze the clinical characteristics of 6 patients with intracranial tumors who only presented with positional vertigo to avoid misdiagnosing the disease.

Material and methods: Six patients with intracranial tumors who only presented with positional vertigo treated in our clinic between May 2015 to May 2019 were reviewed, and the clinical symptoms, features of nystagmus, imaging presentation, and final diagnosis of the patients were evaluated.

Results: All patients presented with positional vertigo and positional nystagmus induced by the changes in head position or posture, including one case with downbeating nystagmus in a positional test, two cases with left-beating nystagmus, one case with apogeotropic nystagmus in a roll test, one case with right-beating nystagmus, and one case with left-beating and upbeating nystagmus. Brain MRI showed the regions of the tumors were in the vermis of the cerebellum, the fourth ventricle, the lateral ventricle, and the cerebellar hemisphere.

KEYWORDS

positional vertigo, intracranial tumor, nystagmus, mimicking, benign

Positional vertigo is a transient vertigo attack caused by gravity-related changes in head position or posture (after reaching the new head position). It can be divided into peripheral and central types. Generally, peripheral vertigo is the most common symptom (1). Benign paroxysmal positional vertigo (BPPV) is a typical peripheral vertigo, and its incidence is the highest in vertigo and dizziness diseases, accounting for 17–30% of vertigo cases (2, 3). Central paroxysmal positional vertigo (CPPV) is a position-related vertigo attack caused by a central disease. It was first described by Riesco-Macllure in 1957 (4) and is gradually concerned by more and more colleagues in neurotology and ophthalmology because it can cause serious consequences. Most

patients of CPPV are accompanied by other neurological localization symptoms, which are easy to identify clinically. However, rare isolated paroxysmal positional vertigo or patients of CPPV accompanied by isolated nystagmus, are easily misdiagnosed as BPPV, and treated by repositioning maneuvers, which could delay treatment. CPPV has been reported to be related to various lesions involving the posterior fossa (such as infarction, bleeding, tumor, or demyelinating disease) (5–8). However, isolated CPPV caused only by intracranial tumors is rare. Isolated CPPV are mostly case or series reports, and there are no bulk case reports. This paper collected six patients with positional vertigo caused by intracranial tumors treated in our department from May 2015 to May 2019, focusing on the characteristics of nystagmus in position tests and the location of intracranial tumors. The report is as follows (Table 1).

Case series

Case report 1

A 27 year old woman presented with more than 2 years history of episodic vertigo which often occurred when changing from lying position to sitting position, or from sitting position to lying position, and turning around quickly, accompanied by mild nausea. She denied any vomiting, headache, diplopia, choking cough in drinking water, dysarthria, ear symptoms such as tinnitus, ear tightness, and hearing loss, and she had clear consciousness when the episodic vertigo occurred, which often lasted for 1–2 min each time. She was initially diagnosed with BPPV in another hospital, but repositioning maneuvers for BPPV failed to relieve her symptoms. There was no progress in the disease in the past 2 years. She did not pay attention to it and did not conduct further examination. There was no spontaneous nystagmus in the examination in our hospital, and the visual eye movement, video head impulse testing, and Romberg test were normal. She had vertical downbeating nystagmus when changing from sitting position to supine position for more than 1 min in a positional test. In a roll test and Dix-Hallpike (DH) test, vertical downbeating nystagmus occurred at all positions and lasted for more than 1 min. Brain MRI showed the regions of the tumors were in the vermis of the cerebellum, which was considered as low-grade glioma, and there was no significant change in brain MRI at 8 months after diagnosis in the follow-up.

Case report 2

A 29 year old woman presented with a 3-month history of positional vertigo, provoked by rolling in bed to the left

TABLE 1 Clinical data of six intracranial tumor patients.

Case	Sex	Age	course of disease	Side events/type of nystagmus/duration			Diseased region	Diagnosis
				DH	Lying down position	Roll test		
1	w	27 y	2 years	Bilateral down-beating >1 min	Downbeating >1min	Bilateral downbeating >1 min	The vermis of the cerebellum	Low-grade glioma
2	w	29 y	3 months			Bilateral apogeotropic >1 min	The fourth ventricle	Medulloblastoma
3	m	54 y	1 months	Bilateral leftbeating >1 min	Leftbeating >1 min	Bilateral left-beating >1 min	The vermis of the cerebellum	Missing visits
4	m	65 y	17 years	Left Leftbeating >1min		Left Leftbeating >1min	The right lateral ventricle	Choroid plexus
5	m	53 y	2 years	Bilateral rightbeating >1 min	Rightbeating >1 min	Bilateral rightbeating >1 min	The cerebellar hemisphere and the vermicompost	hemangiobla-stomas
6	m	39 y	1 week	Left left-beating <1 min	Upbeating left torsional <1 min		The cerebellar hemisphere	Lung cancer metastasis

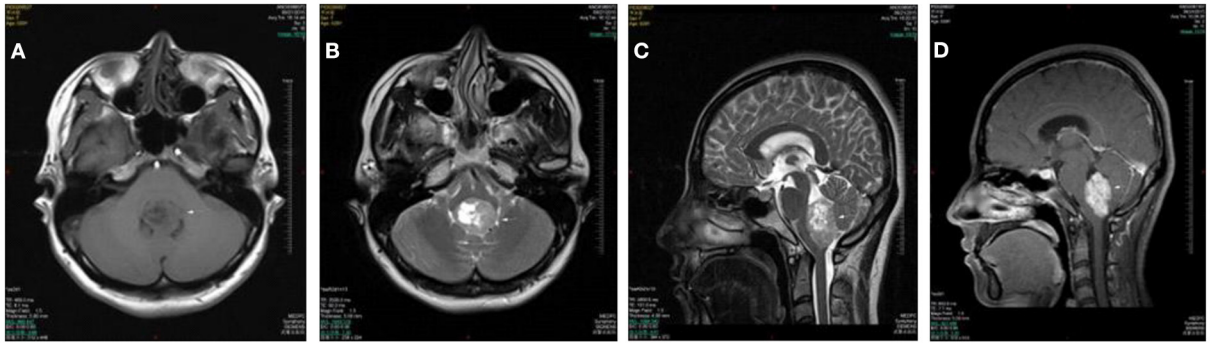

FIGURE 1
Case 2: medulloblastoma of the fourth ventricle. Axial T1WI **(A)** and Axial T2WI **(B)** show a lobulated mass in the fourth ventricle with heterogeneously iso- to hypointense signal T1WI and iso- to hyperintense signal on T2WI. The lesion extrudes posteroinferiorly through the foramen of Magendie on sagittal T2WI **(C)**. The lesion shows a moderate heterogeneous enhancement on postcontrast axial T1WI with fat saturation **(D)**.

and right, which was mild (Figure 1). She denied any nausea, vomiting, amaurosis fugax, diplopia, dysarthria, fear of light and sound, ear symptoms such as tinnitus, ear tightness, and hearing loss. The positional vertigo often lasted for several seconds. Her past medical history was that of migraine. She was initially diagnosed with BPPV, but repositioning maneuvers for BPPV failed to relieve her symptoms. There was no spontaneous nystagmus in the examination in our hospital, and the visual eye movement, video head impulse testing, and Romberg test were normal. The sharpened Romberg test was performed to the left. She presented with apogeotropic nystagmus induced in the roll test when rolling to left and right, which the slow phase velocity was $<6^{\circ}$/s and lasted for more than 1 min. Brain MRI showed the regions of the tumors were in the fourth ventricle which had undergone resection and radiotherapy in another hospital. The pathological diagnosis was medulloblastoma. The positional vertigo and ambiguous speech disappeared after the operation.

Case report 3

A 54 year old man presented with more than 1 month history of positional vertigo which often occurred when changing from lying position to sitting position or from sitting position to lying position. He denied any nausea, vomiting, headache, amaurosis fugax, diplopia, dysarthria, fear of light and sound, ear symptoms such as tinnitus, ear tightness, and hearing loss. He was relieved for several seconds and had recurrent attacks. He was initially diagnosed with BPPV in another hospital, but repositioning maneuvers for BPPV failed to relieve his symptoms. There was no spontaneous nystagmus in the examination in our hospital, and the visual eye movement, video head impulse testing, and Romberg test were normal. He had left-beating nystagmus when changing from sitting position to supine position for more than 1 min in a positional test. In a roll test and DH test, left-beating nystagmus occurred at all positions and lasted for more than 1 min. Brain MRI showed the regions of the tumors were in the vermis of the cerebellum, and metastatic tumor could not be ruled out. The patient went to another hospital for treatment without further follow-up.

Case report 4

A 65 year old man presented with a 17-year history of positional vertigo which was often provoked by rolling in bed to the left and right, sometimes accompanied by mild headache. He denied any obvious visual rotation, nausea, vomiting, amaurosis fugax, diplopia, dysarthria, fear of light and sound, ear symptoms such as tinnitus, ear tightness, and hearing loss. He was relieved for more than 10 s. He had no significant medical history. There was no spontaneous nystagmus in the examination in our hospital, and the visual eye movement, video head impulse testing, and Romberg test were normal. He had left-beating nystagmus in the left DH test and the left roll test and lasted for more than 1 min. Brain MRI showed the regions of the tumors were in the lateral ventricle which was like a circle and had long T1 and long T2 signals. The tumor was considered as choroid plexus after the neurosurgical consultation. There was no significant change in brain MRI at seven months after diagnosis in the follow-up.

Case report 5

A 53 year old man presented with more than 2 years history of dizziness which often occurred accompanied by top-heavy and unstable walking (Figure 2). He presented with more than 3 months history of positional vertigo, worsened by rolling in

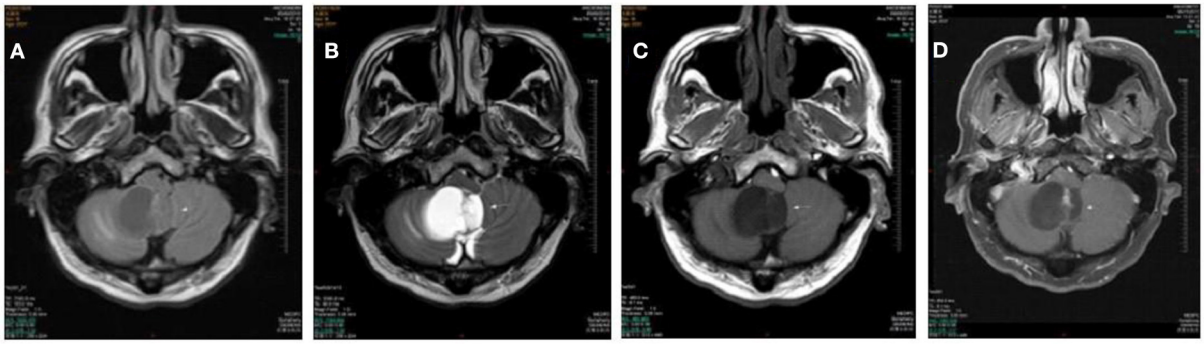

FIGURE 2
Cases 5: cerebellar hemangioblastomas. Axial T1WI **(A)**, axial T2WI **(B)**, and axial FLAIR **(C)** show a cyst mass in the cerebellar hemisphere and vermis with the marked hypointense signal on T1WI, the hyperintense signal on axial T2WI, and iso- and hypointense on FLAIR. The lesion shows septum and nodule enhancement on postcontrast axial T1WI with fat saturation **(D)**.

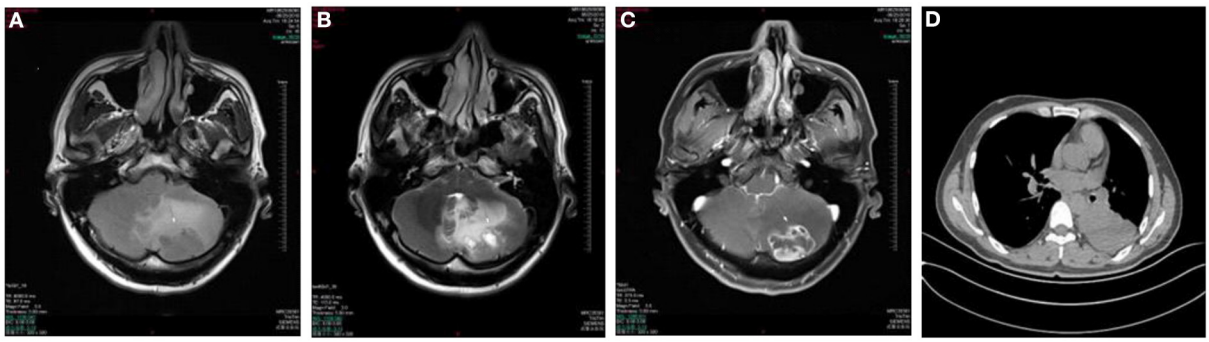

FIGURE 3
Case 6: metastasis of the left cerebellar hemisphere. Axial T1WI **(A)** and Axial T2WI **(B)** show irregular lesion and surrounding edema in the left cerebellar hemisphere with the heterogeneously hypointense signal on T1WI and marked hyperintense signal on T2WI relative to the normal parenchyma of the cerebellum. The lesion shows ring-enhancement on postcontrast axial T1WI with fat saturation **(C)**. Chest CT shows a soft tissue attenuation mass in the lower left lung **(D)**.

bed to the left, accompanied by visual rotation and mild nausea. He denied any vomiting, headache, amaurosis fugax, diplopia, dysarthria, hearing loss, fear of light and sound. He was relieved for tens of seconds. His past medical history was that of bilateral tinnitus for more than 10 years, which did not change every time the vertigo attacked. The bilateral tinnitus was not diagnosed and treated because it was mild and had little impact on daily life. There was no spontaneous nystagmus in the examination in our hospital, and the visual eye movement, video head impulse testing, and Romberg test were normal. The sharpened Romberg test was with unstable walking. He had right-beating nystagmus when changing from sitting position to supine position for more than 1 min in a positional test. In a roll test and DH test, right-beating nystagmus occurred at all positions and lasted for more than 1 min. Brain MRI showed the regions of the tumors were in the cerebellar hemisphere and vermis, which was considered as hemangioblastomas. The patient went to another hospital for treatment without further follow-up.

Case report 6

A 39 year old man presented with a 1-week history of episodic vertigo which was provoked by changing the head position, accompanied by mild headache and nausea (Figure 3). He denied any vomiting, amaurosis fugax, diplopia, dysarthria, hearing loss, fear of light and sound. He was relieved for several s. He was diagnosed with left lung cancer 6 months ago and underwent left lung resection in the last month. There was no spontaneous nystagmus in the examination in our hospital, and the visual eye movement, video head impulse testing, and Romberg test were normal. He had upbeating left torsional nystagmus when changing from sitting position to supine position for <1 min in positional test. He had left-beating nystagmus in the left DH test that lasted for <1 min. Brain MRI showed the regions of the tumors were in the left cerebellar hemisphere which was considered the brain metastasis of

lung cancer. He was transferred to the oncology department for radiotherapy.

Discussion

Clinically, patients with positional vertigo as the primary complaint are prevalent, most of them are BPPV; CPPV is only a minority. Intracranial tumors, often with hidden onset, can be seen in all ages. Whether the patients with an intracranial tumor only present positional vertigo depends on the region and extent of involvement of the lesion. If the lesion is small and the functional area is not involved, there may be no clinical symptoms; if the lesion is large and the other functional areas are affected, it may be accompanied by central nervous system symptoms and signs, such as double vision, facial numbness, limb numbness, dysphonia, dysphagia, etc., which is easier to identify clinically; if the lesion is relatively limited and only involves the vestibular conduction pathway, it only manifests as position-related vertigo, dizziness, and imbalance, which is easily misdiagnosed clinically. The six patients in this group showed sole positional vertigo with positional nystagmus without other central nervous system symptoms. Before the diagnosis, three patients were misdiagnosed for BPPV and were treated with repositioning maneuvers.

CPPV caused by intracranial tumors mainly violates the vestibular conduction pathway. The lesions are mostly located in the dorsal lateral part of the fourth ventricle, the dorsal part of the cerebellum, the cerebellar nodules, and the cerebellar lingual lobe (9, 10). The function of the glomus nodule is to process vertical and horizontal otolith signals. The positional nystagmus may be induced if the tumor involves the glomus nodule. However, this lesion causes vertical nystagmus and other neurological symptoms, including periodic alternating nystagmus, gaze induced nystagmus, and ataxia. Besides the semicircular canal, the cerebellar nodules and the cerebellar lingual lobe are also connected with otolith organs, which control the regulation of vestibular ocular reflex. If the lesion only involves the cerebellar nodules and the cerebellar lingual lobe, it does not cause other neurological symptoms, and the nystagmus caused is not only vertical (8, 11, 12). The lesion regions of the six patients in this group, except for case 2 whose lesion was located in the lateral ventricle, were common sites with CPPV symptom, including one case in the fourth ventricle, two cases in the cerebellar vermis, and two cases in both the cerebellar hemisphere and the cerebellar vermis. The tumors in the lateral ventricle theoretically do not cause positional nystagmus, and the patient had no significant medical history and there were no other lesions in the examination in our hospital. However, the same nystagmus was induced in positional tests during the past three times. The positional nystagmus may not be caused by direct stimulation of the vestibular system by tumor. During head position change, the flow of cerebrospinal fluid is blocked by the mass and reflux, indirectly stimulating the vestibular center and causing positional vertigo. However, the follow-up needs to continue to track whether the patient has new lesions. Common pathological types of intracranial tumors inducing CPPV include neurogenic tumors, meningiomas, gliomas, metastases, etc. There was one case of low-grade glioma, one case of medulloblastoma, one case of choroid plexus, one case of hemangioblastomas, one case of lung cancer metastasis and one case of lost follow-up in the group. There was no number of cases of one pathological type being the majority.

Since the clinical incidence of CPPV is low, Cranial CT or craniocerebral MRI is not a routine examination for patients with positional vertigo. If patients do not present with central nervous system symptoms, nystagmus in positional tests is often the first breakthrough. Central paroxysmal positional nystagmus (CPPN) associated with central lesions is often different from the nystagmus in BPPV and it has its independent characteristics. CPPN usually has no latency, can appear in multiple positions, has no noticeable change in strength, and has no attenuation in the fixation test. CPPN cannot be explained by the theory of canalith flow (9, 13, 14). In 2017 (15), Macdonald summarized the nystagmus characteristics of 82 CPPV patients in 28 articles. The results are as follows: (1) CPPV patients often have nystagmus in the DH test, roll test, head suspension test, and other examinations; (2) Among the patients with positive DH test, about 60% are positive on both sides, of which 47.5% are vertical nystagmus; (3) Most of the nystagmus induced by the DH test and head suspension test lasts for <30 s, roll test Induced nystagmus lasts for <1 min for geotropic nystagmus and >1 min for apogeotropic nystagmus; (4) Most CPPN has no latency, fatigue, and fixation suppression disappears. In our six cases, the head suspension test was not performed, and the nystagmus in the supine position was observed in the roll test. The summary is as follows: (1) Case 1, 3, and 5 induced the nystagmus in the same direction at all positions. Case 1 was vertical downbeating nystagmus. Case 3 and 5 were horizontal-beating nystagmus. Case 4 had left-beating nystagmus in the left DH test and the left roll test. Case 2 presented with apogeotropic nystagmus induced in a roll test. Case 6 had upbeating left torsional nystagmus when changing from sitting position to supine position in positional test and left-beating nystagmus in the left DH test. (2) Case 2 had apogeotropic direction-changing positional nystagmus induced by the roll test and was treated with canalith repositioning procedures (CRP). Nystagmus analysis showed the slow phase velocity of the bilateral nystagmus in the roll test was $<6^{\circ}$/s, which was not consistent with the characteristic of nystagmus in BPPV, as in the other five cases. (3) The duration of nystagmus in case 6 was <1 min, the other five cases were more than 1 min, and it had no characteristics of

becoming stronger and weaker. The analysis is as follows: (1) All patients showed induced nystagmus in at least two positions, and in four of the patients, nystagmus did not change with positional changes. The reason may be that the lesion was located in the center and there was no flow of semicircular canal stones in patients with BPPV after postural change; it was only manifested as the asymmetry of sensory signals in bilateral vestibular center, which induced specific nystagmus through specific conduction pathways. (2) The duration of nystagmus in five patients was more than 1 min, and there was no visible fatigue, which was not consistent with the characteristics of nystagmus described by Macdonald, but was consistent with the characteristics of central nystagmus. (3) Only one patient showed the induced vertical nystagmus, one patient had the induced torsional nystagmus at one position, and four patients had horizontal nystagmus. Vertical nystagmus is not a common type in our cases. It may be because of the small number of cases in our study. (4) One patient had apogeotropic direction-changing positional nystagmus induced by the roll test and the slow phase velocity of the bilateral nystagmus was $<6^{\circ}$/s. The nystagmus on one side was not significantly stronger than the nystagmus on the other side, which was not consistent with the characteristic of nystagmus in classical BPPV.

CPPV needs to be differentiated from other diseases, first of which is BPPV. For most patients with BPPV, the characteristics of nystagmus are consistent with the canalith theory, and the treatment effect is good. Next is the relatively rare cupulolithiasis of the horizontal semicircular canal BPPV. Its nystagmus often has no incubation period, easy fatigue, and has a great duration (16), in addition, the effect of CRP is relatively weak. In particular, clinicians should avoid misdiagnosis and missed diagnosis. In vestibular migraine (VM), most VM patients can present with positional vertigo during the onset period, about 1% of VM patients show isolated positional vertigo (7) because it is a central nervous system disease. Its nystagmus can also show the characteristics of central nystagmus, which may be confused with CPPV, but VM is often accompanied by symptoms such as headache, photophobia, phobia, and migraine characteristics such as family history and motion sickness (17), which can help identify the correct diagnosis. For vestibular paroxysmia (VP), which is caused by the compression of the eighth cranial nerve, rare in the clinic, and can be manifested as stereotyped and positional vertigo. The experimental treatment with carbamazepine is effective for collaborative diagnosis, and brain MRI is used to differentiate VP from the intracranial tumor (18).

Although CPPV is rare in the clinic, once it is a missed diagnosis, it may cause serious consequences. When patients complain of positional vertigo, nystagmus characteristics are inconsistent with BPPV, and CRP is invalid, etc. we should think of the possibility of CPPV, take a craniocerebral MRI examination promptly, determine if there are intracranial lesions, and get timely and appropriate treatments.

Conclusions and significance

When presenting with nystagmus features that are not consistent with BPPV, patients should receive a brain MRI examination to distinguish BPPV from intracranial diseases.

Data availability statement

The original contributions presented in the study are included in the article/supplementary material, further inquiries can be directed to the corresponding author/s.

Ethics statement

The studies involving human participants were reviewed and approved by the Ethics Committee of the Chinese PLA General Hospital (S2020-465-01). The patients/participants provided their written informed consent to participate in this study. Written informed consent was obtained from the individual(s) for the publication of any potentially identifiable images or data included in this article.

Author contributions

QS and NY designed the experimental paradigm, summarized the results, and wrote the article. YC collected the clinical cases. HS, XM, CJ, HW, QZ, YQ, JL, LLZ, and LZZ examined the patients, like hearing examination, vestibular function examination, and imaging examination. All authors contributed to the article and approved the submitted version.

Funding

This research was supported by Beijing Natural Science Foundation (7222185), National Foundation (2020YFC2004001), and NSFC (81470700).

Conflict of interest

The authors declare that the research was conducted in the absence of any commercial or financial relationships that could be construed as a potential conflict of interest.

Publisher's note

All claims expressed in this article are solely those of the authors and do not necessarily represent those of their affiliated organizations, or those of the publisher, the editors and the reviewers. Any product that may be evaluated in this article, or claim that may be made by its manufacturer, is not guaranteed or endorsed by the publisher.

References

1. Bertholon P, Tringali S, Faye MB, Antoine JC, Martin C. Prospective study of positional nystagmus in 100 consecutive patients. *Ann Otol Rhinol Laryngol.* (2006) 115:587–94. doi: 10.1177/000348940611500804

2. Von Brevern M, Radtke A, Lezius F, Feldmann M, Ziese T, Lempert T, et al. Epidemiology of benign paroxysmal positional vertigo: a population based study. *J Neurol Neurosurg Psychiatry.* (2007) 78:710–5. doi: 10.1136/jnnp.2006.100420

3. Strupp M, Dieterich M, Brandt T. The treatment and natural course of peripheral and central vertigo. *Dtsch Arztebl Int.* (2013) 110:505–11. doi: 10.3238/arztebl.2013.0505

4. Shoman N, Longridge N. Cerebellar vermis lesions and tumors of the fourth ventricle in patients with positional and positioning vertigo and nystagmus. *J Laryngol Otology.* (2007) 121:166. doi: 10.1017/S0022215106004063

5. Habek M, Gabelić T, Pavliša G, Brinar VV. Central positioning upbeat nystagmus and vertigo due to pontine stroke. *J Clin Neurosci.* (2011) 18:977–8. doi: 10.1016/j.jocn.2010.11.021

6. Johkura K. Central paroxysmal positional vertigo: isolated dizziness caused by small cerebellar hemorrhage. *Stroke.* (2007) 38:c26–27. doi: 10.1161/STROKEAHA.106.480319

7. Power L, Murray K, Bullus K, Drummond KJ, Trost N, Szmulewicz DJ. Central conditions mimicking benign paroxysmal positional vertigo: a case series. *J Neurol Phys Ther.* (2019) 43:186–91. doi: 10.1097/NPT.0000000000000276

8. Gregorius FK, Crandall PH, Baloh RW. Positional vertigo with cerebellar astrocytoma. *Surg Neurol.* (1976) 6:83–286.

9. Tian J. Paroxysmal positional vertigo:identification of benign and non-benign. *Am J Speech Lang Pathol.* (2013) 21:102–5.

10. Chang MB, Bath AP, Rutka JA. Are all atypical positional nystagmus patterns reflective of central pathology? *J Otolaryngol.* (2001) 30:280–2. doi: 10.2310/7070.2001.19532

11. Cho BH, Kim SS, Choi YJ, Lee SH. Central positional nystagmus associated with cerebellar tumors: Clinical and topographical analysis. *J Neurol Sci.* (2017) 373:147–51. doi: 10.1016/j.jns.2016.12.050

12. Beynon GJ, Baguley DM, Moffat DA, Irving RM. Positional vertigo as a first symptom of a cerebellopontine angle cholesteatoma: case report. *Ear Nose Throat J.* (2000) 79:508–10. doi: 10.1177/014556130007900709

13. Lee HJ, Kim ES, Kim M, Chu H, Ma HI, Lee JS. Isolated horizontal positional nystagmus from a posterior fossa lesion, Ann. *Neurol.* (2014) 76:905–10. doi: 10.1002/ana.24292

14. Clack TD, McGillicuddy JE, Wolf GT. Labyrinthine functional tests and a case of midline cerebellar teratoma, Am. *J Otolaryngol.* (1988) 9:481–8.

15. Xia X, Bai Y, Zhou Y, Yang Y, Xu R, Gao X. Central positional nystagmus: a systematic literature review. *Front Neurol.* (2017) 8:141. doi: 10.3389/fneur.2017.00141

16. Von Brevern M, Bertholon P, Brandt T, Fife T, Imai T, Nuti D, et al. Benign paroxysmal positional vertigo: diagnostic criteria. *J Vestib Res.* (2015) 25:105–17. doi: 10.3233/VES-150553

17. Murdin L, Chamberlain F, Cheema S, Arshad Q, Gresty M, Golding J, et al. The role of motion sickness susceptibility in vestibular disorders and migraine. *J Neurol.* (2013) 260:S27–8.

18. Brandt T, Strupp M, Dieterich M. Vestibularparoxysmia: a treatable neurovascular cross-compression syndrome. *J Neurology.* (2016) 263:90–6. doi: 10.1007/s00415-015-7973-3

frontiers | Frontiers in Neurology

TYPE Brief Research Report
PUBLISHED 26 September 2022
DOI 10.3389/fneur.2022.1000318

Check for updates

OPEN ACCESS

EDITED BY
Jian-hua Zhuang,
Shanghai Changzheng Hospital, China

REVIEWED BY
Nicolas Perez-Fernandez,
University Clinic of Navarra, Spain
Chih Chung Chen,
Chang Gung University, Taiwan

*CORRESPONDENCE
Sofia Waissbluth
sofia.waissbluth@gmail.com

SPECIALTY SECTION
This article was submitted to Neuro-Otology, a section of the journal Frontiers in Neurology

RECEIVED 22 July 2022
ACCEPTED 07 September 2022
PUBLISHED 26 September 2022

CITATION
Waissbluth S, Sepúlveda V, Leung J-S and Oyarzún J (2022) Caloric and video head impulse test dissociated results in dizzy patients. *Front. Neurol.* 13:1000318. doi: 10.3389/fneur.2022.1000318

COPYRIGHT
© 2022 Waissbluth, Sepúlveda, Leung and Oyarzún. This is an open-access article distributed under the terms of the Creative Commons Attribution License (CC BY). The use, distribution or reproduction in other forums is permitted, provided the original author(s) and the copyright owner(s) are credited and that the original publication in this journal is cited, in accordance with accepted academic practice. No use, distribution or reproduction is permitted which does not comply with these terms.

Caloric and video head impulse test dissociated results in dizzy patients

Sofia Waissbluth*, Valeria Sepúlveda, Jai-Sen Leung and Javier Oyarzún

Department of Otolaryngology, Pontificia Universidad Católica de Chile, Santiago, Chile

Introduction: We are now able to detect abnormalities for any semicircular canal with the use of the video head impulse test (vHIT). Prior to the vHIT, the gold standard for unilateral canal paresis of the lateral canal was considered the caloric test. Clinical cases where the caloric test and vHIT are discordant are not uncommon.

Methods: Retrospective study. All consecutive cases of dizziness seen from 11/2020 to 12/2021 for which the patient underwent both caloric and vHIT tests performed within 10 days, were reviewed. Patients with discordant results were included. We evaluated the caloric response, vHIT gains for all canals and saccades, with and without gain abnormalities.

Results: We included 74 cases of dizziness with dissociated results. The most common finding was a normal caloric response with abnormal vHIT results (60.8%); the main abnormal finding on vHIT was the presence of saccades. In this group, 37.7% of patients had normal gains and refixation saccades. In addition, the most found low gain was for the posterior canal. The main diagnosis in this group was vestibular migraine. For the group with unilateral caloric paresis and normal vHIT gain in the lateral canal, the main diagnosis was Ménière's disease.

Discussion: The most common disorders with discordant results were Ménière's disease and vestibular migraine. The caloric test and vHIT are complementary and combining both tests provide greater clinical information. Further research is needed to understand refixation saccades with normal gains.

KEYWORDS

vertigo, dizziness, caloric test, video head impulse test, vestibular disease

Introduction

Recent evidence has shown that vestibular assessment with the caloric test and the video head impulse test (vHIT) can be discordant or dissociated (1). While both tests evaluate lateral semicircular canal function, they have important differences and limitations. The caloric test uses a non-physiological stimulus (≈0.006 Hz) to test the lateral canal and superior vestibular nerve while the vHIT tests the vestibulo-ocular reflex (VOR) at a high acceleration (≈2.5 Hz), considered a physiological stimulus of

head rotation (2). It also provides information about all semicircular canals, superior and inferior vestibular nerve function, and overt and covert saccades (3). Prior to the implementation of the vHIT, the caloric test was considered the gold standard for testing lateral canal function. However, it is now understood that because these two tests evaluate at different frequencies and have different stimuli, they are complementary (4).

A recent study by Lee et al. reports that discordant results can be seen in approximately one out of every six patients with dizziness. However, this is considering that only horizontal vHITs were included in the analyses (5). They observed that the main diagnoses for patients with an abnormal caloric test but normal vHIT were Ménière's disease and vestibular neuritis/labyrinthitis. Similar findings were observed as a result of a systematic review and meta-analysis regarding discordant results in patients with chronic dizziness (4). As for an abnormal vHIT and normal caloric test, Lee et al. observed this finding in a variety of central and peripheral lesions (5).

The current study was undertaken to evaluate the etiology of patients with dizziness that underwent caloric testing and vHIT on the same day (or within 10 days), evaluate the patterns on vHIT for all semicircular canals, and the presence of refixation saccades.

Methods

All consecutive cases of dizziness seen at the Pontificia Universidad Católica de Chile healthcare center from November 2020 until December 2021 for which the patient underwent both the caloric and vHIT tests, were reviewed. Inclusion criteria consisted of cases for which both tests were performed on the same day, or within 10 days. Cases were excluded if they had incomplete charts or if the tests were performed at another health care center. During this time period, 166 cases had both tests performed, however, 46 were excluded because the time period between both tests exceeded 10 days. A total of 120 cases were analyzed, of which, 46 were eliminated as both tests were concordant, hence, we finally included 74 cases of dizziness with dissociated results. This study was approved by the local Ethics Committee of the Pontificia Universidad Católica de Chile.

Bithermal caloric testing was performed with caloric stimuli consisting of alternate binaural irrigations with an air irrigator, with cold and hot temperatures (24 and 48°C) for 1 min. Nystagmus was recorded with videonystagmography (VisualEyes™ 525, Interacoustics) and peak slow-phase velocity was documented. Canal paresis was defined as a difference of ≥25% between both sides and was calculated using Jongkees' formula (6).

For vHIT testing, the right eye was recorded, and all three canals were evaluated (Otometrics ICS® Impulse). During testing, subjects were fitted with the goggles, seated and asked to look at an eye-level target on the wall which is at a 1-meter distance. Following calibration, the examiner standing behind the patient, placed their hands on the participant's head and performed repeated head impulses which were randomized, in velocity and direction, in the plane of the tested semicircular canal. Head impulses (150–300°/s) were continued until 20 head impulses were adequate (artifact-free) for each tested canal. All head impulses were completed by experienced practitioners. Parameters of abnormality were as follows: lateral canal VOR gain < 0.8; vertical canal VOR gain < 0.7; and/or presence of corrective saccades (covert and/or overt) in any canal. The gain was calculated as the ratio of the area under the eye velocity and head velocity curve.

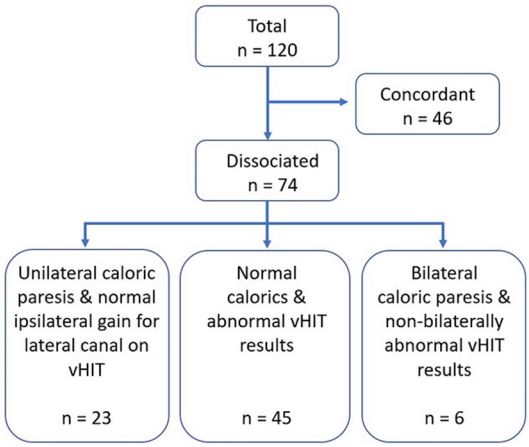

FIGURE 1
Flowchart of study participants.

Results were considered discordant when: (1) normal caloric test and abnormal vHIT results (low gain in any canal and/or saccades in any canal), (2) unilateral canal paresis on caloric test with normal gain for the lateral canal on vHIT, and low gains for the posterior or anterior canals and/or ipsilateral and contralateral saccades, and (3) bilateral canal paresis on caloric test with normal gains for the lateral canals bilaterally on vHIT, and low gains for the posterior or anterior canals and/or saccades.

Depending on the history and clinical presentation, other tests were performed when considered necessary such as pure-tone audiometry, vestibular evoked myogenic potentials and brain MRI with or without posterior fossa protocol.

Results

Seventy-four cases of dizziness with dissociated results were evaluated (Figure 1). Patients were 58.6 ± 15.5 years on average, median of 59 years and range 10–85 years; 75.7% were women.

TABLE 1 Normal caloric test and abnormal vHIT results.

	Normal caloric test ($n = 45$)	
vHIT low gains ($n = 32$)		
In any canal	32	71%
Lateral canal low gain	18	40%
Lateral canal low gain—bilateral	5/18	
Posterior canal low gain	25	56%
Posterior canal low gain—bilateral	12 / 25	
Anterior canal low gain	0	0%
vHIT saccades ($n = 45$)		
In any canal	45	100%
Lateral canal	18	40%
Posterior canal	25	56%
Anterior canal	4	9%

The most common finding was presenting normal caloric testing with abnormal vHIT results ($n = 45$, 60.8%) followed by unilateral caloric paresis and normal vHIT gains for the lateral canal ($n = 23$). Six cases had bilateral canal paresis on caloric testing yet did not show abnormal bilateral vHIT gains for the lateral canals.

For the group with normal caloric testing with abnormal vHIT results, average gains for the lateral, posterior and anterior canals on the right side were: 0.93 ± 0.13, 0.74 ± 0.15 and 0.84 ± 0.16, and on the left side: 0.85 ± 0.14, 0.72 ± 0.19, and 0.78 ± 0.11, respectively. Overall, 71% of cases showed a low gain in any of the six canals, and 100% exhibited saccades in any canal (Table 1). The most commonly found low gain was for the posterior canal (56%), followed by the lateral canal (40%). Also, the most commonly found saccades were for the posterior canal (56%) followed by the lateral canal (40%). Although the percentages of low gains and saccades are coincidentally the same for the lateral and posterior canals, the saccades do not, however, necessarily correspond with the canal with low gain. When assessing per canal, we observed that 37.7% of canals had normal gains and refixation saccades, 37.7% had low gains with refixation saccades and 24.4% had low gains without any saccades. In this group, the most common diagnoses were vestibular migraine (53%) followed by vestibular neuritis (16%) (Figure 2A). No patient in this category had a low gain in an anterior canal and only four cases exhibited saccades for that canal.

For the group with caloric paresis and dissociated findings on vHIT (Table 2), unilateral canal paresis was observed in 23 cases and bilateral paresis in six cases. Average caloric paresis was 36.7 ± 12.9%. For the unilateral canal paresis cases, ipsilateral and contralateral saccades for the lateral canal was the most common finding on vHIT. Only three cases had a low gain for the posterior canal on the same side. This last finding was also observed for bilateral paresis cases ($n = 6$) where posterior canal low gain, ipsi- or contralaterally, were observed ($n = 4$). In this group, the most common diagnoses were Ménière's disease (34%) followed by vestibular migraine (28%) (Figure 2B).

A few other aspects that were also evaluated was the presence of spontaneous nystagmus and directional preponderance on caloric testing. Fifteen patients had spontaneous nystagmus; five had Ménière's disease, five had vestibular migraine, three had a central etiology, one had vestibular neuritis and one had a labyrinthine infarction. Eight of these patients had caloric paresis and dissociated findings on vHIT, six had spontaneous horizontal nystagmus beating away from the affected side, but two had nystagmus toward the affected side and these patients had Ménière's disease. Seven had normal caloric testing with abnormal vHIT results, with a myriad of combinations; low gains and/or saccades, unilateral or bilateral, involving any canal. Only two cases had a directional preponderance on caloric testing (≥40%), one had a lateral semicircular canal dysplasia and one had vestibular migraine.

Because the most common diagnosis in this cohort was Ménière's disease, we decided to look into enhanced eye velocity on vHIT testing since prior evidence has suggested that this may be a result of endolymphatic hydrops. Twenty-six patients had a VOR >1 for the lateral canal (average gain: 1.07 ± 0.06). Interestingly, all were for the rightward head impulse, and of these, six were bilateral. This directional bias has been previously described for area under the curve gains (i.e., Otometrics®) with a consistent directional bias, with gains being larger in the ipsilateral direction of the eye used to measure gain (right eye in this case) (7). Thirteen had vestibular migraine and five had Ménière's disease. We did not encounter any cases with VOR gains >1.29, a recently described cutoff value based on gains obtained from healthy subjects (8).

As various patients had normal gains with saccades, we decided to analyze this group of patients as well. Overall, 22 patients had normal gains on vHIT and saccades in at least one canal; 14 patients had a normal caloric response and eight had unilateral caloric paresis. Ninety percent had saccades in the lateral canal. This most common diagnoses for these patients was vestibular migraine (54.5%), followed by vestibular neuritis (22.7%).

Discussion

With the introduction of the vHIT in clinical practice, we are now able to detect abnormalities for any semicircular canal and clearly view overt and covert saccades. Prior to the vHIT, the gold standard for unilateral canal paresis of the lateral canal was considered the caloric test, as well as rotatory chair, mostly for bilateral paresis. As we now understand the intricacies and importance of testing different frequencies, we have come across clinical cases where the caloric and vHIT are not concordant, and it is not uncommon to have one of the two tests with

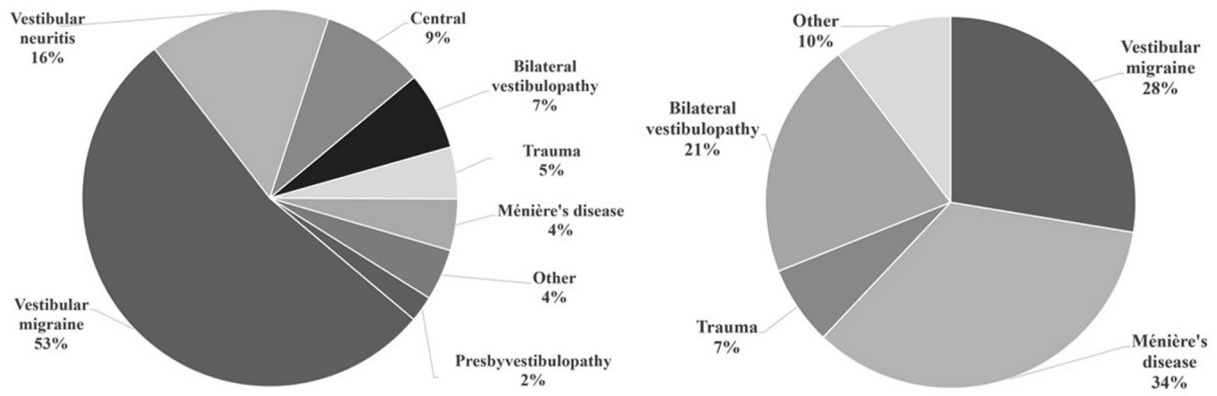

FIGURE 2
Otoneurological diagnoses of the included participants. **(A)** Normal caloric test and abnormal vHIT results. Common diagnoses in this category were vestibular migraine and vestibular neuritis (acute unilateral vestibulopathy). **(B)** Caloric paresis with dissociated vHIT findings. Common diagnoses in this category were Ménière's disease and vestibular migraine.

TABLE 2 Caloric paresis and dissociated findings on vHIT.

Unilateral caloric paresis ($n = 23$)		
vHIT ipsilateral low gain ($n = 3$)		
Lateral canal	0	0%
Posterior canal	3	13%
Anterior canal	0	0%
vHIT ipsilateral saccades ($n = 9$)		
Lateral canal only	6	26%
Lateral and posterior canals	3	13%
Anterior canal	0	0%
vHIT contralateral saccades ($n = 8$)		
Lateral canal only	6	26%
Posterior canal only	2	9%
Anterior canal	0	0%
Bilateral caloric paresis ($n = 6$)		
vHIT lateral canal low gain - bilateral	0	0%
vHIT lateral canal low gain - unilateral	2	33%
vHIT posterior canal low gain - unilateral or bilateral	4	67%
vHIT anterior canal low gain	0	0%
Saccades in any canal	5	83%

abnormalities while the other is normal. With our criteria for discordant results, we observed that 74 out of 120 clinical cases had some degree of discordance, being the most frequent presentation that of a normal caloric test with abnormal vHIT results (60.8%), and that within this group, all patients had saccades in at least one canal (Table 1). Recently, Li et al. also evaluated discordance rates in 65 patients, and they observed that 55 patients had caloric weakness with a normal horizontal vHIT. However, they also observed that 36.4% had corrective saccades on the abnormal caloric side (9). Their conclusions are based on the horizontal canals, and therefore differ from ours, since they report that an abnormal caloric test with negative horizontal vHIT was mostly found.

The most common otoneurological disorders with discordant results were Ménière's disease and vestibular migraine. All these cases were diagnosed based on the consensus documents of the Classification Committee of the Bárány Society (10, 11). These happen to also be the most common causes of spontaneous episodic vestibular syndrome. We observed that the most common diagnosis for unilateral canal paresis with dissociated vHIT results was Ménière's disease; this is consistent with recently published data (12–15). It appears that the caloric test is more sensitive for detecting vestibular abnormalities in Ménière's disease, however, concomitant use of the vHIT enables the clinician to detect abnormal gains in vertical canals (16), and also demonstrates the presence of overt and covert saccades. This is of interest because both tests provide different types of information. It is believed that the caloric test in Ménière's disease is abnormal as a result of the physical enlargement of the membranous labyrinth by endolymphatic hydrops with a resulting localized convective flow that dissipates hydrostatic pressure across the cupula, and causes the cupular and hair cell deflection to be reduced (1). This is a non-physiological stimulus to test the lateral canal and superior vestibular nerve and does not provide information about saccades. On the other hand, the vHIT tests the VOR at a high acceleration, considered a physiological stimulus (2). Considering the hydrostatic temperature dissipation hypothesis previously mentioned, an increase in the semicircular duct diameter would have little effect on the response of the canal to

angular acceleration stimulation (1, 3). This is compatible with the current findings and previously published data regarding caloric test and vHIT discrepancies in Ménière's disease.

While 34% of cases in the unilateral canal paresis with dissociated vHIT results group had Ménière's disease, 28% had vestibular migraine. This was also the most common diagnosis in the normal caloric test and abnormal vHIT results group. While vestibular migraine is a clinical diagnosis, a variety of examination findings and vestibular test abnormalities, both ictal and interictal, have been reported (17, 18). Most studies evaluating both test results in vestibular migraine report greater hypofunction on caloric testing vs. vHIT abnormalities (14, 19–22), and discordant results have been observed (14, 15, 21). However, some authors considered vHIT as abnormal when there was a low canal gain and saccades (22), or reported the vHIT as abnormal when the gain was low for the lateral canal (14). Mahringer and Rambold evaluated patients with caloric paresis to assess discordance with vHIT results (21). They analyzed cases with a pathological unilateral weakness on caloric testing (absolute value $\geq$ 25%). Of the 18 patients with vestibular migraine, two had a pathological unilateral vHIT. On the other hand, Janiak-Kiszka et al. recently evaluated 33 patients with vestibular migraine and none had caloric paresis (23). Potential explanations for our results could be that (1) The patients included were seen at their initial presentation and perhaps with a longer follow-up, results would vary as it has been suggested that vestibulo-cochlear dysfunction progresses slowly in some patients with vestibular migraine (24), (2) We only included patients with discordant results, and (3) The sample size is too small to take into account the great variability seen in vestibular tests for vestibular migraine.

Yilmaz et al. reported that 18% of patients with vestibular migraine with normal caloric testing had abnormal vHIT results; and so, this is not a rare finding (14). Interestingly, the main abnormal finding on vHIT when the caloric test was normal, was the presence of saccades. In this group, we observed that 37.7% had normal gains and refixation saccades. ElSherif et al. observed that 18.8% of patients with vestibular migraine had saccades with normal VOR gains (25), while Yollu et al. report that 52.4% of VM patients had saccades, and 28% had an abnormal gain for any canal (26). In our cohort, vestibular migraine was the most frequent diagnosis with normal gains with saccades in at least one canal, followed by vestibular neuritis. For the latter, evidence has shown that vHIT gains tend to recover while saccades can be detected at follow-up when gains have already recovered. Hence, it is not uncommon to observe saccades in the lateral canal in a patient who experienced vestibular neuritis in the months prior (27).

The pathophysiology of vestibular migraine is still unclear, but recent advances in structural and functional imaging have shown altered connectivity patterns in these patients (28–30). Structurally, it has been described that patients with vestibular migraine have a selective gray matter volume increase in the frontal and occipital regions, as well as of the left thalamus (31). When stimulated with ear irrigation, a significant increase in thalamic activation has been observed with functional MRI (fMRI) (30). Other findings on fMRI have been enhanced functional connectivity between the auditory network and the salience network and decreased functional connectivity in the bilateral medial cingulate gyrus and paracingulate gyrus within the sensorimotor network (28). The debate is ongoing as to whether vestibular migraine is a functional central vestibular disease, with or without structural changes, or whether the origin is mostly central or peripheral. Findings suggest that there may be an increased sensitivity to vestibular sensory processing (28), and an abnormal brain sensitization leading to altered multimodal sensory integration and processing cortical areas in these patients (31). Also, there is evidence for the existence of an interconnected trigemino-vestibular neuro-circuitry, which includes connections between the trigeminal system, the vestibular nuclei and the vestibulocerebellum (32). Interestingly, a small, proof-of-concept study, has shown that external trigeminal nerve stimulation produces some relief of vestibular migraine attacks (32).

The reason for saccades with normal gain values in vestibular migraine remains to be determined. Interestingly, Pérez-Fernández and Eza-Nuñez evaluated patients with dizziness with vHIT in order to evaluate whether refixation saccades alone had a localizing value when lateral canal gain was normal. Of the 36 patients included in their study, 29 had Ménière's disease and overall, the caloric test was abnormal in 60% (33).

Our study has limitations. It is a retrospective study which can have a selection bias. Our sample size is considered small because the main diagnoses were episodic vestibular syndromes that vary based on ictal/interictal presentations or attacks, hence, a larger sample would provide further information. Our subsample of bilateral vestibulopathy was too small to assess discordance. Also, we do not have access to, or have results for, rotary chair testing, which would have provided further details regarding lateral canal function.

Data availability statement

The raw data supporting the conclusions of this article will be made available by the authors, without undue reservation.

Ethics statement

The studies involving human participants were reviewed and approved by Ethics Committee of the Pontificia Universidad Católica de Chile. Written informed consent for participation

was not required for this study in accordance with the national legislation and the institutional requirements.

Author contributions

SW designed the study and wrote the first draft of the manuscript. SW and VS evaluated and collected data and performed data analyses. J-SL and JO collected data. All authors contributed to the article and approved the submitted version.

Funding

This work was supported by the Fondo Nacional de Desarrollo Científico y Tecnológico (FONDECYT-ANID) grant 11201142 for SW.

Conflict of interest

The authors declare that the research was conducted in the absence of any commercial or financial relationships that could be construed as a potential conflict of interest.

Publisher's note

All claims expressed in this article are solely those of the authors and do not necessarily represent those of their affiliated organizations, or those of the publisher, the editors and the reviewers. Any product that may be evaluated in this article, or claim that may be made by its manufacturer, is not guaranteed or endorsed by the publisher.

Supplementary material

The Supplementary Material for this article can be found online at: https://www.frontiersin.org/articles/10.3389/fneur.2022.1000318/full#supplementary-material

SUPPLEMENTARY FIGURE 1
vHIT result for a patient with Ménière's disease. The patient had a caloric paresis of the right side (30%), however, the vHIT showed a decreased gain for the left lateral canal (0.74) and covert saccades for the lateral canals.

SUPPLEMENTARY FIGURE 2
vHIT result for a patient with vestibular neuritis. The patient had a normal caloric response, however, the vHIT showed decreased gains for the left lateral (0.67) and posterior (0.66) canals, and overt saccades for the left lateral canal.

References

1. McGarvie LA, Curthoys IS, MacDougall HG, Halmagyi GM. What does the dissociation between the results of video head impulse versus caloric testing reveal about the vestibular dysfunction in Ménière's disease? *Acta Otolaryngol.* (2015) 135:859–65. doi: 10.3109/00016489.2015.1015606

2. Maire R, van Melle G. Vestibulo-ocular reflex characteristics in patients with unilateral Ménière's Disease. *Otol Neurotol.* (2008) 29:693–8. doi: 10.1097/MAO.0b013e3181776703

3. Halmagyi GM, Chen L, MacDougall HG, Weber KP, McGarvie LA, Curthoys IS. The video head impulse test. *Front Neurol.* (2017) 8:258. doi: 10.3389/fneur.2017.00258

4. Vallim MGB, Gabriel GP, Mezzalira R, Stoler G, Chone CT. Does the video head impulse test replace caloric testing in the assessment of patients with chronic dizziness? A systematic review and meta-analysis. *Braz J Otorhinolaryngol.* (2021) 87:733–41. doi: 10.1016/j.bjorl.2021.01.002

5. Lee JY, Kwon E, Kim HJ, Choi JY, Oh HJ, Koo JW, et al. Dissociated results between caloric and video head impulse tests in dizziness: prevalence, pattern, lesion location, and etiology. *J Clin Neurol.* (2020) 16:277–84. doi: 10.3988/jcn.2020.16.2.277

6. Strupp M, Magnusson M. Acute unilateral vestibulopathy. *Neurol Clin.* (2015) 33:669–85. doi: 10.1016/j.ncl.2015.04.012

7. Janky KL, Patterson JN, Shepard NT, Thomas MLA, Honaker JA. Effects of device on video head impulse test (vHIT) gain. *J Am Acad Audiol.* (2017) 28:778–85. doi: 10.3766/jaaa.16138

8. Curthoys IS, Manzari L, Rey-Martinez J, Dlugaiczyk J, Burgess AM. Enhanced eye velocity in head impulse testing-a possible indicator of endolymphatic hydrops. *Front Surg.* (2021) 8:666390. doi: 10.3389/fsurg.2021.666390

9. Li X, Ling X, Li Z, Song N, Ba X, Yang B, et al. Clinical characteristics of patients with dizziness/vertigo showing a dissociation between caloric and video head impulse test results. *Ear Nose Throat J.* (2022) 1455613221113790. doi: 10.1177/01455613221113790. [Epub ahead of print].

10. Lempert T, Olesen J, Furman J, Waterston J, Seemungal B, Carey J, et al. Vestibular migraine: diagnostic criteria. *J Vestib Res.* (2012) 22:167–72. doi: 10.3233/VES-2012-0453

11. Lopez-Escamez JA, Carey J, Chung WH, Goebel JA, Magnusson M, Mandalà M, et al. Diagnostic criteria for Menière's disease. *J Vestib Res.* (2015) 25:1–7. doi: 10.3233/VES-150549

12. Sanyelbhaa H, Refaat N, Zein-Elabedein A. Sensitivity of caloric test versus video head impulse test for detection of vestibulo-ocular reflex abnormalities in Meniere's disease. *Egypt J Ear Nose Throat Allied Sci.* (2022) 23:1–5. doi: 10.21608/ejentas.2021.77335.1371

13. Young AS, Nham B, Bradshaw AP, Calic Z, Pogson JM, Gibson WP, et al. Clinical, oculographic and vestibular test characteristics of Ménière's disease. *J Neurol.* (2022) 269:1927–44. doi: 10.1007/s00415-021-10699-z

14. Yilmaz MS, Egilmez OK, Kara A, Guven M, Demir D, Elden SG. Comparison of the results of caloric and video head impulse tests in patients with Meniere's disease and vestibular migraine. *Eur Arch Otorhinolaryngol.* (2021) 278:1829–34. doi: 10.1007/s00405-020-06272-5

15. Hannigan IP, Welgampola MS, Watson SRD. Dissociation of caloric and head impulse tests: a marker of Meniere's disease. *J Neurol.* (2021) 268:431–9. doi: 10.1007/s00415-019-09431-9

16. Cordero-Yanza JA, Arrieta Vázquez EV, Hernaiz Leonardo JC, Mancera Sánchez J, Hernández Palestina MS, Pérez-Fernández N. Comparative study between the caloric vestibular and the video-head impulse tests in unilateral Menière's disease. *Acta Otolaryngol.* (2017) 137:1178–82. doi: 10.1080/00016489.2017.1354395

17. Beh SC, Masrour S, Smith SV, Friedman DI. The spectrum of vestibular migraine: clinical features, triggers, and examination findings. *Headache.* (2019) 59:727–40. doi: 10.1111/head.13484

18. Young AS, Nham B, Bradshaw AP, Calic Z, Pogson JM, D'Souza M, et al. Clinical, oculographic, and vestibular test characteristics of vestibular migraine. *Cephalalgia.* (2021) 41:1039–52. doi: 10.1177/03331024211006042

19. Fu W, Wang Y, He F, Wei D, Bai Y, Han J, et al. Vestibular and oculomotor function in patients with vestibular migraine. *Am J Otolaryngol.* (2021) 42:103152. doi: 10.1016/j.amjoto.2021.103152

20. Yoo MH, Kim SH, Lee JY, Yang CJ, Lee HS, Park HJ. Results of video head impulse and caloric tests in 36 patients with vestibular migraine and 23

patients with vestibular neuritis: a preliminary report. *Clin Otolaryngol.* (2016) 41:813–7. doi: 10.1111/coa.12556

21. Mahringer A, Rambold HA. Caloric test and video-head-impulse: a study of vertigo/dizziness patients in a community hospital. *Eur Arch Otorhinolaryngol.* (2014) 271:463–72. doi: 10.1007/s00405-013-2376-5

22. Blödow A, Heinze M, Bloching MB, von Brevern M, Radtke A, Lempert T. Caloric stimulation and video-head impulse testing in Ménière's disease and vestibular migraine. *Acta Otolaryngol.* (2014) 134:1239–44. doi: 10.3109/00016489.2014.939300

23. Janiak-Kiszka J, Nowaczewska M, Wierzbiński R, Kazmierczak W, Kazmierczak H. The visual-ocular and vestibulo-ocular reflexes in vestibular migraine. *Otolaryngol Pol.* (2021) 76:21–8. doi: 10.5604/01.3001.0015.5711

24. Radtke A, von Brevern M, Neuhauser H, Hottenrott T, Lempert T. Vestibular migraine: long-term follow-up of clinical symptoms and vestibulo-cochlear findings. *Neurology.* (2012) 79:1607–14. doi: 10.1212/WNL.0b013e31826e264f

25. ElSherif M, Reda MI, Saadallah H, Mourad M. Video head impulse test (vHIT) in migraine dizziness. *J Otol.* (2018) 13:65–7. doi: 10.1016/j.joto.2017.12.002

26. Yollu U, Uluduz DU, Yilmaz M, Yener HM, Akil F, Kuzu B, et al. Vestibular migraine screening in a migraine-diagnosed patient population, and assessment of vestibulocochlear function. *Clin Otolaryngol.* (2017) 42:225–33. doi: 10.1111/coa.12699

27. Psillas G, Petrou I, Printza A, Sfakianaki I, Binos P, Anastasiadou S, et al. Video head impulse test (vHIT): value of gain and refixation saccades in unilateral vestibular neuritis. *J Clin Med.* (2022) 11:3467. doi: 10.3390/jcm11123467

28. Li ZY Si LH, Shen B, Yang X. Altered brain network functional connectivity patterns in patients with vestibular migraine diagnosed according to the diagnostic criteria of the Bárány Society and the International Headache Society. *J Neurol.* (2022) 269:3026–36. doi: 10.1007/s00415-021-10868-0

29. Shin JH, Kim YK, Kim HJ, Kim JS. Altered brain metabolism in vestibular migraine: comparison of interictal and ictal findings. *Cephalalgia.* (2014) 34:58–67. doi: 10.1177/0333102413498940

30. Russo A, Marcelli V, Esposito F, Corvino V, Marcuccio L, Giannone A, et al. Abnormal thalamic function in patients with vestibular migraine. *Neurology.* (2014) 82:2120–6. doi: 10.1212/WNL.0000000000000496

31. Messina R, Rocca MA, Colombo B, Teggi R, Falini A, Comi G, et al. Structural brain abnormalities in patients with vestibular migraine. *J Neurol.* (2017) 264:295–303. doi: 10.1007/s00415-016-8349-z

32. Beh SC. External trigeminal nerve stimulation: potential rescue treatment for acute vestibular migraine. *J Neurol Sci.* (2020) 408:116550. doi: 10.1016/j.jns.2019.116550

33. Perez-Fernandez N, Eza-Nuñez P. Normal gain of VOR with refixation saccades in patients with unilateral vestibulopathy. *J Int Adv Otol.* (2015) 11:133–7. doi: 10.5152/iao.2015.1087

frontiers | Frontiers in Neurology

TYPE Original Research
PUBLISHED 26 September 2022
DOI 10.3389/fneur.2022.967323

Check for updates

OPEN ACCESS

EDITED BY
Lisheng Yu,
Peking University People's Hospital, China

REVIEWED BY
Fang Liu,
Beijing Hospital, China
Athanasia Warnecke,
Hannover Medical School, Germany
Pedro Marques,
University of Porto, Portugal

*CORRESPONDENCE
Shengnan Ye
kzb13645016830@163.com

†These authors have contributed equally to this work and share first authorship

SPECIALTY SECTION
This article was submitted to Neuro-Otology, a section of the journal Frontiers in Neurology

RECEIVED 12 June 2022
ACCEPTED 22 August 2022
PUBLISHED 26 September 2022

CITATION
Xiao H, Guo X, Cai H, Lin J, Lin C, Fang Z and Ye S (2022) Magnetic resonance imaging of endolymphatic hydrops in Ménière's disease: A comparison of the diagnostic value of multiple scoring methods. *Front. Neurol.* 13:967323. doi: 10.3389/fneur.2022.967323

COPYRIGHT
© 2022 Xiao, Guo, Cai, Lin, Lin, Fang and Ye. This is an open-access article distributed under the terms of the Creative Commons Attribution License (CC BY). The use, distribution or reproduction in other forums is permitted, provided the original author(s) and the copyright owner(s) are credited and that the original publication in this journal is cited, in accordance with accepted academic practice. No use, distribution or reproduction is permitted which does not comply with these terms.

Magnetic resonance imaging of endolymphatic hydrops in Ménière's disease: A comparison of the diagnostic value of multiple scoring methods

Heng Xiao[1†], Xiaojing Guo[1†], Huimin Cai[1], Jianwei Lin[1], Chenxin Lin[1], Zheming Fang[2] and Shengnan Ye[1*]

[1]Department of Otorhinolaryngology Head and Neck Surgery, Fujian Otorhinolaryngology Institute, The First Affiliated Hospital of Fujian Medical University, Fuzhou, China, [2]Departments of Imaging, The First Affiliated Hospital of Fujian Medical University, Fuzhou, China

Objectives: To compare three methods of scoring endolymphatic hydrops in patients with Ménière's disease in order to assess the correlation between endolymphatic hydrops and auditory characteristics.

Methods: A retrospective study of 97 patients with unilateral definite Ménière's disease (DMD) who underwent contrast-enhanced three-dimensional fluid attenuated inversion recovery (3D FLAIR) MRI. Each patient was scored by the Inner Ear Structural Assignment Method (IESAM), the Saccule to utricle area ratio (SURI), and the Four Stage Vestibular Hydrops Grading (FSVH), according to their corresponding axial images. Cohen's Kappa and intra-class correlation coefficient were used for consistency testing, combined with binary logistic regression analysis, to compare the sensitivity and specificity of the three methods. The degree of hydrops in different stages of MD was compared. The correlation between endolymphatic hydrops in the inner ear sub-units and hearing thresholds was further analyzed.

Results: The intra- and inter-reader reliability for the scoring of endolymphatic hydrops were excellent. The IESAM had a high diagnostic value for identifying definite Ménière's disease (sensitivity: 86.6%, specificity: 97.9%). The hearing thresholds were correlated with the degree of endolymphatic hydrops. Stages 3 and 4 were more significant for the severity of hydrops than stage 1. Within the subgroups of the Ménière's disease patients, compared with the non-hydrops group and the pure vestibular hydrops (V group), the cochlear combined vestibular hydrops group (CV group) had significantly higher auditory thresholds. The amplitude ratio of electrocochleogram was significantly higher in the affected ear than in the healthy ear.

Conclusion: The IESAM is a more sensitive and specific diagnostic scoring method for the diagnosis of DMD. Diagnostic imaging may improve the

detection of inner ear hydrops which is correlated with severity of hearing loss. A comprehensive evaluation of the inner ear sub-unit structures maybe necessary.

KEYWORDS

Ménière's disease, magnetic resonance imaging, endolymphatic hydrops, inner ear structure assignment method, auditory function

Introduction

Ménière's disease (MD) is an inner ear disorder characterized by spontaneous vertigo attacks, fluctuating sensorineural hearing loss (SNHL), tinnitus and/or aural fullness (1). Ménière's disease is most common between the ages of 40 and 60 years, with approximately 50 to 200 per 100,000 adults affected, and a serious impact on the quality of life of affected patients (2). In 2015, the Bárány Association developed simplified diagnostic criteria for MD (3), including two categories: definite and probable MD. At present, the diagnosis of MD is largely based on symptomatology, especially in the early stages of the disease, where symptoms may be atypical and even, in some cases, where the main symptoms overlap with the clinical symptoms of other diseases, such as vestibular migraine (4, 5).

The main pathological feature of MD is endolymphatic hydrops (EH) (6, 7). Currently, gadolinium imaging of the inner ear provides the basis for visualizing endolymphatic hydrops *in vivo* (8). In the last decade or so, the use of magnetic resonance imaging (MRI) for the diagnosis of EH has become increasingly widespread. Endolymphatic hydrops scoring systems and methods are also increasingly available, however, there is still no consensus on the visual scoring of endolymphatic hydrops in Ménière's disease. Therefore, we compared the three most commonly used endolymphatic hydrops scoring methods in the world, evaluating their diagnostic capacity for Ménière's disease as well as the correlation between endolymphatic hydrops and auditory functions.

Materials and methods

Patients

From January 2010 to January 2022, a total of 482 patients with symptoms of vertigo, tinnitus, aural fullness, and fluctuating hearing loss underwent gadolinium-enhanced magnetic resonance imaging of the inner ear for the presence of endolymphatic hydrops at our institution.

After obtaining approval from the institutional regulatory board and obtaining written informed consent from the participants, patients were treated according to the routine standard of care. Patients were fully informed prior to tympanic injection, and they could choose to perform bilateral or affected-sided injections at their own discretion. Almost all patients opted for bilateral imaging. The exclusion criteria included (1) bilateral Ménière's disease; (2) a history of previous ear surgery; (3) external or middle ear lesions, large vestibular aqueduct syndrome, or other congenital cochlear malformations; (4) having central vertigo, severe neurological, or psychiatric disorders; and (5) poor contrast imaging; (6) patients in whom MRI was contraindicated. Among them, eight cases of poor imaging were excluded. The clinical diagnosis was made according to the diagnostic criteria for MD established by the Bárány Association in 2015 (3). A total of 97 patients with unilateral definite Ménière's disease (DMD) were included, retrospectively analyzed in conjunction with clinical data. All patients had unilateral disease with the contralateral side being the healthy ear, and bilateral imaging was performed to facilitate binaural comparison. The contralateral normal ear served as a control. The age range was 15–67 years (42 ± 12), female/male = 58:39.

Imaging acquisition

Gadolinium-diethylenetriaminepentaacetic acid (Gd-DTPA) dimer injection as contrast agent, diluted eight-fold in saline, was administered bilaterally to the tympanic membrane in all 97 patients. After injection, the patient's head was rotated 45° contralaterally and held for 30 min. Twenty four hours later, a three-dimensional fluid-attenuated inversion recovery MRI was performed using a 3 T unit. All MRI examinations were performed using a Verio 3.0T 16 channel head machine (Siemens, Erlangen, Germany), repetition time 6,000 ms, echo time 132 ms, spatial resolution 0.5 × 0.5 × 0.5 mm, isotropic acquisition, scan time = 4 min 16 s. Simultaneous isotropic 3-dimensional-sampling refinement was compared with application optimization using different flip angle evolution (3D-SPC) inversion recovery for fluid decay inversion recovery [repetition time = 6,000 ms, echo time = 388 ms, inversion time (TI) = 2,100 ms, scan time = 5 min 32 s, spatial resolution = 0.7 × 0.7 × 0.7 mm].

TABLE 1 Scoring criteria of IESAM in 3D-SPC-FLAIR images*.

Appearance†	Cochlea			Vestibule	Semicircular canals		
	Base	Middle	Apex		Superior	Horizontal	Posterior
Not visible[a]	0	0	0	0	0	0	0
Partially visible[b]	1	1	1	3	1	1	1
Completely visible[c]	2	2	2	6	2	2	3

*Time of inversion (TI) = 2,100 ms.
†On 3D-SPC-FLAIR images.
[a]Absence of high-signal contrast medium.
[b]Failure to show high-signal image of entire cochlear canal, or high-signal image of cochlear canal limited to tympanic or vestibular scale, or interrupted high-signal images of semicircular canals, or incomplete high-signal image of vestibule.
[c]All labyrinth structures completely visible.

Inner ear analysis

The images were independently assessed by a radiologist and a senior otolaryngologist with more than 5 years of experience in EH imaging review blinded to the clinical findings and the side. The three structures of the inner ear, including the cochlea, vestibule, and semicircular canals, were grouped according to their involvement. All subjects with involvement of only the cochlear region were defined as type C pathological changes, vestibular involvement only and semicircular canals involvement only as type V and Sc, respectively. Similarly, simultaneous cochlear and vestibular involvement was labeled as CV-type, cochlear and semicircular involvement as CSc-type, vestibular and semicircular involvement as VSc-type, and if cochlear, vestibular, and semicircular regions were all involved, patients were labeled as CVSc-type. If no endolymphatic hydrops were detected, the patient was regarded as type N.

Inner ear structure assignment method

The degree of gadolinium contrast (high signal) filling in the perilymphatic space of the affected ear was observed and assessed. The three structures of the cochlea, vestibule and semicircular canals were assigned different scores according to the following conventions: no filling, partial filling and full filling (non-visible, partially visible, fully visible). A full score of 18 points indicated that there was no endolymphatic hydrops. The lower the scores, the more severe the endolymphatic hydrops, as shown in Table 1 (9). Binary logistic regression combined with subject operating characteristic curve analysis was used to assess the diagnostic capacity of the Inner Ear Structural Assignment Method (IESAM) model for detection of endolymphatic hydrops based on the scores of the three structures of the inner ear.

Saccule to utricle area ratio

Using MRI data of the temporal bone region, we graded the EH according to the saccule morphology proposed by Attyé et al. (10). Using the lower part of the vestibule (i.e. 2 mm below the horizontal semicircular canal) as the reference plane. If the saccule area was greater than or equal to the utricle area, i.e., saccule to utricle area ratio (SURI) $\geq$1, this suggested the presence of endolymphatic hydrops, which was then classified into Grade 1 or Grade 2 according to whether or not the saccule morphology was visible (Figure 1).

Four stage vestibular hydrops grading

The EH was graded using the four stage vestibular hydrops grading system first proposed by Bernaerts et al. (11). The reference plane for vestibular hydrops is the plane of the lower part of the vestibule (i.e., 2 mm below the horizontal semicircular canal; Figure 1). The four stages of vestibular hydrops are graded as follows:

(i) Normal vestibule: saccule and utricle area are clearly separated; saccule are smaller than utricle and occupy less than half of the vestibular area.
(ii) Grade I: saccule becomes equal to or larger than utricle, but has not yet fused with utricle.
(iii) Grade II: there is a confluence of the saccule and utricle with still a peripheral rim enhancement of the perilymphatic space.
(iv) Grade III: perilymphatic enhancement is not visible and there is a full obliteration of the bony vestibule.

Auditory function

Pure-tone audiometry was conducted for all patients. The audiometer model used was the OB922 (Madsen, Denmark). Tests were performed in a standard sound isolation shielded

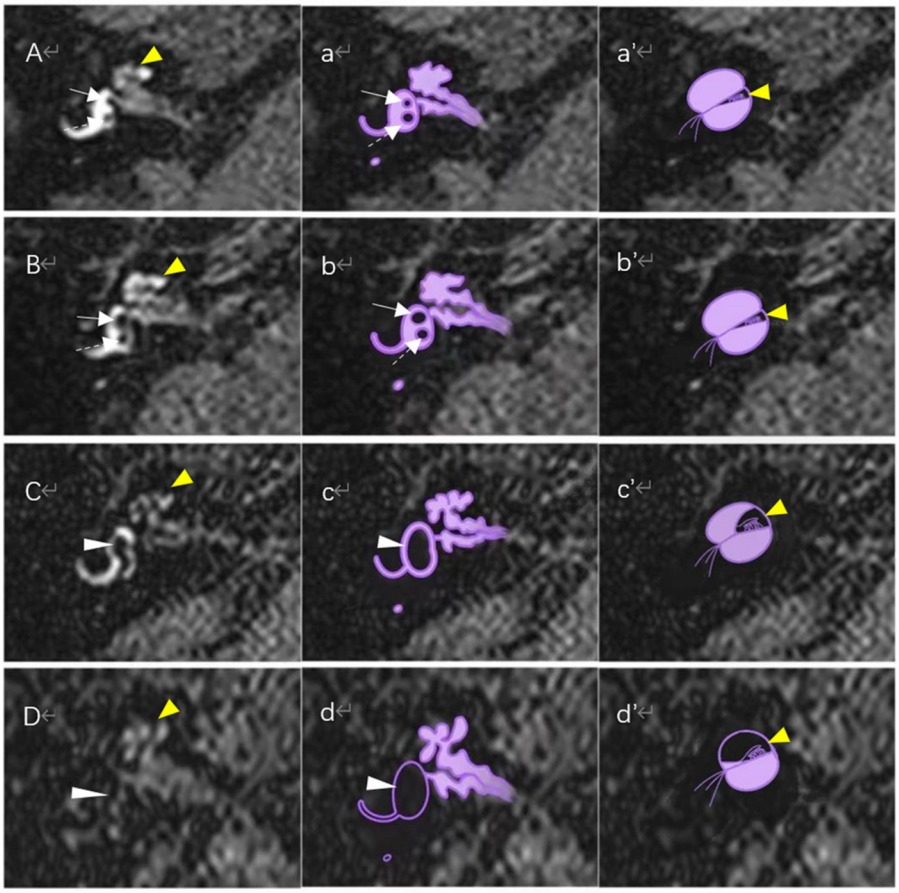

FIGURE 1
Magnetic resonance imaging of different degrees of endolymphatic hydrops on the axial reference plane of the lower vestibular and schematic diagram of the corresponding vestibular and cochlear endolymphatic hydrops. **(A)** Normal vestibule and normal cochlea: Saccule (white solid-line arrow) and utricle (white dotted arrow) are distinctly separated, and the saccule area is smaller than the area of the utricle; no enlargement of the scala media (yellow arrowhead). **(B)** FSVH grade I (or SURI grade 1) and normal cochlea: saccule (white solid-line arrow) appeared equal or larger than the utricle (white dotted arrow), but is not yet confluent with the utricle; no enlargement of the sacala media (yellow arrowhead). **(C)** FSVH grade II (or SURI grade 2): There is a confluence of the saccule and utricle (white arrowhead) with still a peripheral rim enhancement of the perilymphatic space. The scala media expands toward the vestibular scala vestibuli, which is still visible. **(D)** FSVH grade III (or SURI grade 2): The saccule and utricle are fused (white arrowhead) and peripheral ectolymphatic enhancement is no longer visible; the scala media is enlarged toward the scala vestibuli,which is barely visible. **(a–d)** are schematic diagrams of vestibular hydrops corresponding to **(A–D)**, respectively. **(a′-d′)** are schematic diagrams of cochlear hydrops corresponding to **(A–D)**, respectively.

room, and the pure tone hearing thresholds of six frequencies in the range of 0.25–8 kHz were measured. PTA thresholds were calculated as the mean value of the four frequency hearing thresholds of 500 Hz, 1 kHz, 2 kHz, and 4 kHz. The mean hearing thresholds of low frequency (250 Hz), middle frequency (500 Hz—2 kHz), and high frequency (4–8 kHz) hearing thresholds were calculated separately. According to the AAO-HNS guideline for PTA-based MD stages (12), participants fell into four groups: 16, 21, 53 and 7 cases in Stage I (PTA $\leq$ 25 dBHL), II (PTA 26–40 dBHL), III (PTA 41–70 dBHL), and IV (PTA $\geq$71 dBHL), respectively.

The electrocochleogram (ECochG) test apparatus was an American Nicolay brainstem evoked potentiometer, used in a standard acoustically isolated shielded room with click sound stimulation. The following parameters were set: period 100 μs, scan time 10 ms, filter range 10–3,000 Hz, gain 100 k, polarity alternating wave, rate 11.1 times/s, intensity 95 dBnHL.The recording electrode was placed in the center of the tight tympanic membrane, the ground electrode was placed in the brow, and the reference electrode was placed in the contralateral mastoid process. Diagnostic basis: -SP/AP ratio $\geq$0.4 was considered abnormal (13).

Statistical analysis

Data were analyzed using IBM SPSS Statistics 26.0 software and R software (3.6.3 version). Data for categorical

TABLE 2 Clinical features of all patients.

	MD ($n = 97$)	HC ($n = 97$)
Age, mean (SD)	42.0 (11.9)	42.0 (11.9)
Sex, *n* (%)		
Male	39 (40.2%)	39 (40.2%)
Female	58 (59.8%)	58 (59.8%)
Affected ear, *n* (%)		
Left	62 (63.9%)	62 (63.9%)
Right	35 (36.1%)	35 (36.1%)
Hearing threshold, mean (SD)		
LF	48.9 (17.1)	17.8 (5.6)
MF	45.6 (19.0)	16.8 (4.4)
HF	50.1 (21.7)	19.5 (11.3)
PTA	45.7 (18.6)	17.4 (4.8)
Type of hydrops pathology*, *n* (%)		
C	3 (3.1%)	0 (0%)
V	22 (22.7%)	2 (2.1%)
Sc	0 (0%)	2 (2.1%)
CV	34 (35.1%)	0 (0%)
CSc	0 (0%)	2 (2.1%)
VSc	3 (3.1%)	2 (2.1%)
CVSc	24 (24.7%)	0 (0%)
N	11 (11.3%)	89 (91.8%)

*Classification based on the site of endolymphatic hydrops involvement on imaging.
LF, low frequency; MF, medium frequency; HF, high frequency; PTA, pure-tone average; C only cochlear involvement; V only vestibular involvement; Sc only semicircular canals involvement; CV, simultaneous cochlear and vestibular involvement; CSc, simultaneous cochlear and semicircular canals involvement; VSc, simultaneous vestibular and semicircular canals involvement; CVSc, cochlear, vestibular, and semicircular regions were all involved; N, no endolymphatic hydrops.

and parametric variables were expressed as percentages and mean ± standard deviation (SD) or median (P25, P75), respectively. Data from normal and skewed distributions were compared using analysis of variance (ANOVA) and Mann–Whitney *U*-test, respectively. The intra- and inter-reader reliability of endolymphatic hydrops levels were estimated using Cohen's kappa and Intra-class correlation coefficients (ICC). The sensitivity and specificity of each endolymphatic hydrops scoring methods were calculated. The area under the ROC curve for three scoring methods and the differences in the degree of endolymphatic hydrops between MD stages were performed using the Bonferroni correction to adjust for the multiple comparisons. The correlation between endolymphatic hydrops and auditory function was determined using Spearman's correlation. Tukey HSD *post hoc* test was used to adjust for multiple comparisons of hearing thresholds across groups. $p < 0.05$ was considered statistically significant.

Results

Clinical features of all patients are illustrated in Table 2. The intra- and inter-reader reliability of endolymphatic hydrops scores were good ($0.94 <$ kappa < 0.96, ICC $= 0.98$; Table 3).

Of the three endolymphatic hydrops scoring methods, the IESAM displayed the highest diagnostic efficacy. Across all MD patients, the sensitivity and specificity of IESAM were 86.6 and 97.9%, respectively (Figure 2). Table 3 lists the sensitivity and specificity of each assessment method to correctly diagnose MD. The difference in the area under the ROC curve between IESAM and SURI or Four Stage Vestibular Hydrops Grading (FSVH) diagnostic methods was statistically significant in MD patients (adjusted p value < 0.05), and the difference in the area under the ROC curve between SURI and FSVH was not statistically significant (adjusted p value > 0.05; Table 4).

Of the 97 patients with Ménière's disease, IESAM was used to analyze the correlation between endolymphatic hydrops scores and the auditory function. The different frequency hearing thresholds (low, medium and high) were negatively correlated with the total scores of endolymphatic hydrops (Figure 3, $p < 0.05$). After staging of 97 patients according to guidelines, there was a statistically significant difference in the distribution of endolymphatic hydrops among the four stages ($H = 18.77$, $p < 0.001$). The Bonferroni method was used to correct the significance level, and the results showed that the severity of hydrops in stage 3 and stage 4 was greater than that in stage 1, and the difference was statistically significant (adjusted p value $= 0.001$, adjusted p value $= 0.006$, respectively; Supplementary Table 1). There were no statistically significant differences in the degree of intramuscular hydrops between the remaining groups (adjusted p-value > 0.05). As shown in Figure 4, the results showed that across the four subgroups of low-frequency, mid-frequency, high-frequency, and PTA, the hearing thresholds of CV type was significantly higher than that of N type patients, and the differences were statistically significant (Tukey HSD test, $p <0.001$, $p = 0.001$, $p = 0.003$, $p < 0.001$, respectively). But there was no statistical difference between N and V type pure tone hearing thresholds (adjusted $p > 0.05$). Across the three subgroups of low-frequency, mid-frequency, and PTA, the differences in CV-type and V-type hearing thresholds were statistically significant (Figure 4, Tukey HSD test, $p = 0.004$, $p = 0.004$, and $p = 0.011$, respectively), and in the H-PTA subgroup, the differences in CV-type and V-type hearing thresholds were not statistically significant ($p = 0.317$).

Among the 97 patients with MD, there were 43 patients with EcochG examination. The amplitude ratio of EcochG was significantly higher in the affected ear than in the healthy ear (Mann–Whitney *U*-test, $p < 0.001$). The Spearman correlation analysis indicated that there was no correlation between the degree of endolymphatic hydrops in the affected ear and EcochG

TABLE 3 Sensitivity and specificity of three scoring methods for the diagnosis of Ménière's disease by magnetic resonance endolymphatic hydrops imaging.

Scoring methods	Sensitivity	specificity	AUC	95% CI	Inter-reader reliability	Intra-reader reliability
IESAM[a]	86.6	97.9	0.94	0.90–0.98	0.98	0.98
SURI[b]	84.5	94.8	0.90	0.86–0.95	0.96	0.95
FSVH[b]	84.5	93.8	0.90	0.8–50.95	0.95	0.94

[a]Consistency testing of quantitative data using ICC.
[b]Consistency testing of categorical data using Cohen's kappa.
FSVH, four stages of vestibular hydrops grading; IESAM, inner ear structure assignment method; SURI, Saccule to utricle area ratio.

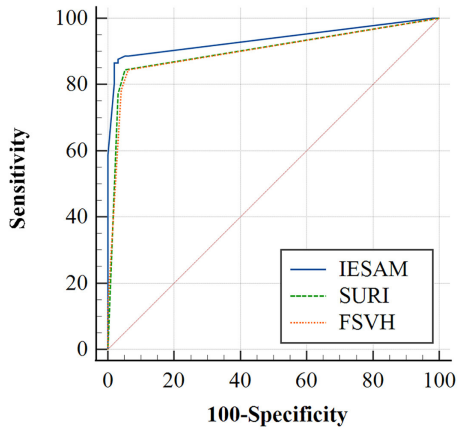

FIGURE 2
Receiver operating characteristic curves for three scoring methods of endolymphatic hydrops with definite Ménière's disease.

amplitude ratio ($r = -0.229$, $p = 0.166$). There was no correlation between cochlear hydrops, vestibular hydrops and ECochG amplitude ratio ($r = -0.314$, $p = 0.055$, $r = -0.099$, $p = 0.555$, respectively).

Discussion

There are many scoring methods of endolymphatic hydrops with Ménière's disease, visual assessment methods provide clinicians with convenient tools to determine the presence of endolymphatic hydrops, among these methods is the IESAM scoring method first proposed by Fang et al. (9), the SURI method described by Attyé et al. (10) and the FSVHS method proposed by Bernaerts et al. (11). We compared the sensitivity and specificity of the three scoring methods in the diagnosis of DMD. Kappa values >0.80 and ICC values >0.75 were generally considered to have good agreement (14), this study demonstrated high inter-reader and intra-reader reliability. Among these scoring methods, IESAM demonstrated optimal imaging diagnostic capacity for the detection of DMD. Our study showed that delayed gadolinium contrast-enhanced 3DFLAIR magnetic resonance imaging is a reliable and accurate technique for the diagnosis of endolymphatic hydrops using a variety of scoring methods. This is the first study to summarize and compare the top, commonly used assessments for diagnostic imaging of endolymphatic hydrops.

Our present study indicated that the IESAM was the better diagnostic imaging method for DMD among the three, with a sensitivity and specificity of 86.6 and 97.9%, respectively. This is consistent with the previous findings of Fang et al. (9). We subsequently hypothesized that the different stages of endolymphatic hydrop development in patients with Ménière's disease affect all three structures of the cochlea, vestibule, and semicircular canals of the inner ear. A comprehensive assessment of the implicated sites of endolymphatic hydrops was performed, with particular attention to the three sub-unit structures of the cochlea, vestibule, and semicircular canals. The pathogenesis of endolymphatic hydrops in Ménière is currently unclear, and a comprehensive assessment of the structure of the inner ear sub-units will facilitate future step-by-step studies of the mechanisms of Ménière's disease in conjunction with imaging and clinical features. We therefore posit that IESAM scoring method may aid in the clinical diagnosis of MD, though more robust testing is additionally required in future studies.

The total scores of endolymphatic hydrops was negatively correlated with the low-, mid- and high-frequency hearing thresholds, suggesting that the severity of hearing loss may indirectly reflect the severity of endolymphatic hydrops. We hypothesize that because endolymphatic hydrops often start in the cochlea and progresses to the saccule, the lesion worsens when the saccule compliance decreases, shedding the saccule otolith and causing obstruction of ductus reuniens (15). As the degree of endolymphatic hydrops increases, it affects the function of inner and outer hair cells as well as the ionic concentration of endolymphatic fluid. The subsequent failure of endolymphatic regulation in the inner ear leads to cochlear damage, such as loss of short cilia in outer and inner hair cells, early changes in spiral ligament fibroblasts or changes in cell morphology- causing hearing loss. This supports the correlation between the severity of endolymphatic hydrops and hearing. This is consistent with the findings of Kahn et al. (16).

TABLE 4 Multiple comparison of the area under the ROC curve of the three imaging scoring methods.

Group i	Group j	Difference between areas	*z* statistic	*p*-Value	95% confidence interval
IESAM	SURI	0.0329	2.585	**0.0097***	0.00797 to 0.0579
IESAM	FSVH	0.0354	2.722	**0.0065***	0.00991 to 0.0609
SURI	FSVH	0.00244	0.486	0.6272	−0.00742 to 0.0123

*Bonferroni correction adjusted p-value and "significant" results. Bold value represents statistically significant p-value adjusted < 0.05.

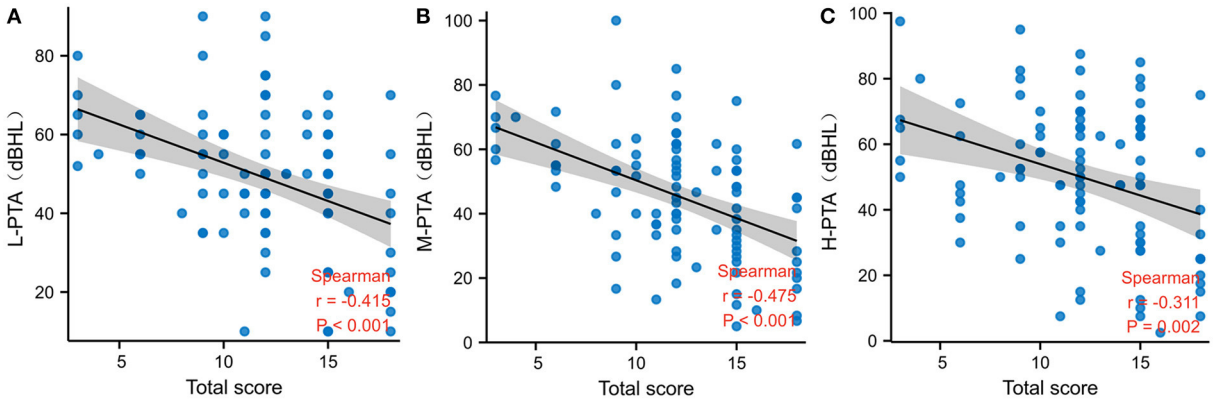

FIGURE 3
Correlation between IESAM total scores and pure tone hearing thresholds in the Ménière's patients. **(A)** Negative correlation between low-frequency hearing thresholds and total scores; **(B)** Negative correlation between mid-frequency hearing thresholds and total scores; **(C)** Negative correlation between high-frequency hearing thresholds and total scores. L-PTA low frequency pure tone hearing thresholds; M-PTA medium frequency pure tone hearing thresholds; H-PTA high frequency pure tone hearing thresholds.

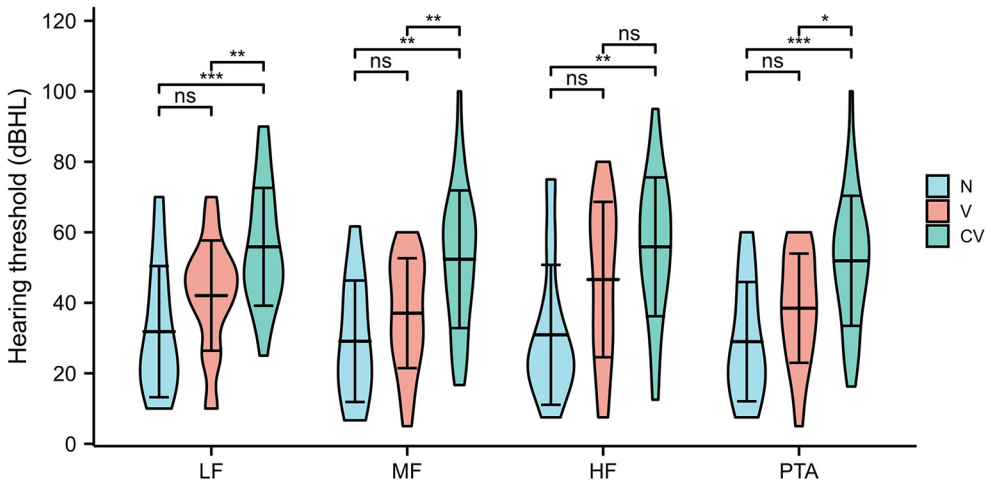

FIGURE 4
Relationship between different types of hydrops and hearing thresholds at each frequency in Ménière's patients. LF, Low Frequency, MF, Medium Frequency, HF, High Frequency, *N,* no endolymphatic hydrops, V only vestibular region with endolymphatic hydrops, CV cochlear and vestibular hydrops. Ns, $p \geq 0.05$; *$p \leq 0.05$; **$p < 0.01$; ***$p < 0.001$. *p*-values were adjusted by the Tukey HSD method for multiple comparisons.

The result indicated that the different frequency hearing thresholds (low, medium and high) were correlated with the total scores of endolymphatic hydrops, while the *p* -value was insignificant. According to the stages of diagnostic criteria for MD by AAO-HNS, We found that the PTA of stage 3 and stage 4 was significantly higher than that of stage 1. With the

development of hydrops, its influence on the inner ear is more significant, however, MD with mild hearing loss did not show any difference in the degree of hydrops. We speculate that this may be related to the compliance of inner ear subunits. The degree of hydrops in the inner ear increases with the MD stage, and the corresponding pressure in the inner ear membrane labyrinth increases. When the buffering effect of the inner membrane labyrinth is destroyed, it will cause hydrops in the corresponding subunit structure, resulting in more severe hearing loss or vertigo symptoms (17, 18). We further evaluated pure-tone hearing thresholds differences between various groups of Ménière's patients with differentially affected inner ear sub-units. The results of the this study suggest that the CV sub group displayed significantly higher hearing thresholds at all frequencies compared to the MD patients with normative inner-ear structures (N) group. This is consistent with what has been observed clinically. The CV group displayed significantly higher hearing thresholds at low and mid frequencies compared to the V group, suggesting that hearing impairment is more pronounced in Ménière's disease when the cochlea is involved in endolymphatic hydrops. In the cochlea, the most severe endolymphatic fluid accumulation occurs first in the apical turn of the cochlea, followed by the middle and basal turns. As the basilar membrane in the cochlea vibrates in response to an acoustic stimulus, the outer hair cells amplify the stimulus and transmit fluid vibrations to the sound-sensitive inner hair cells. The location of the maximum basilar membrane vibration depends on the frequency of the detected sound. Low-frequency waves are predominantly distributed in the apical turn of the cochlea, while high-frequency waves mainly affect the basal turn of the cochlea. The basilar membrane at the apex of the cochlea is wider and softer than the basilar membrane at the bottom of the cochlea (1). The result is that the expansion of the basement membrane in the EH begins with the apical turn and its corresponding hearing loss. Therefore, cochlear hydrops is often associated with hearing loss. These results were consistent with the previous findings of Zhang et al. (19, 20).

The more commonly used diagnostic method to determine endolymphatic hydrops in Ménière's disease patients is the electrophysiologically-based EcochG, whose diagnostic criteria are: -SP/AP $\geq$0.4. Pressure changes in the endolymphatic fluid cause the basement membrane to move toward the Scala tympani, generating -SP due to asymmetric basement membrane vibrations. Varying degrees of membranous labyrinth hydrops increase the amplitude of the alternating short sound-induced negative summation potential (SP), leading to an increase in the -SP/AP amplitude ratio ($\geq$0.4). In the present study, the amplitude ratio of EcochG was significantly higher in the affected ear than in the healthy ear, suggesting an abnormality in the affected cochlea, which is consistent with the previous findings (21). Our study showed that there was no correlation between the degree of endolymphatic hydrops and EcochG amplitude ratio in the affected ear. We believe that the amplitude ratio may correlate with the severity and site of endolymphatic hydrops. While this study indicated that the degree of cochlear hydrops did not correlate with the amplitude ratio. So we consider that this may be related to the relatively low sample of vestibular function studies performed in this cohort, a limitation of this study which will be further improved in subsequent studies.

In our study, we excluded 8 patients with poor contrast imaging. We assume that these eight patients may have poor permeability of round window membrane (22, 23), or it is quite possible that the perilymphatic space in severe EH patients is extremely compressed, leading to a significant reduction in the diffusion route of Gd-DTPA. As a result, the perilymph could not be visualized, so we excluded these. In addition, one of the limitations of the current study is the retrospective design and the tertiary care hospital, where patients were only examined according to their need for disease diagnosis. Thus, not all patients underwent ECochG test, with the exception of pure tone audiometry. Another limitation was the small number of cases of ECochG test in this study. In addition, long-term follow-up data for longitudinal evaluation was outside the scope of the current study, which we expect to improve in a follow-up study.

Conclusion

The IESAM is a imaging assessment method with optimal sensitivity and specificity for the diagnosis of DMD. Diagnostic imaging may improve the detection of endolymphatic hydrops and subsequently indirectly reflect the severity of hearing loss. A comprehensive evaluation of the inner ear sub-unit structure maybe necessary.

Data availability statement

All datasets generated for this study are included in the article/Supplementary material, further inquiries can be directed to the corresponding author.

Ethics statement

The studies involving human participants were reviewed and approved by the Ethics Committee of the First Affiliated Hospital of Fujian Medical University. The patients/participants provided their written informed consent to participate in this study.

Author contributions

HX, XG, and SY designed and coordinated the study. HX and XG analyzed the data and wrote the manuscript. HC,

JL, and CL supervised the data collection. HX, XG, and ZF performed the data collection. HX and SY interpreted findings and reviewed the manuscript. All authors contributed to the article and approved the submitted version.

Acknowledgments

The authors would like to express thank to the patients and their families for their cooperation.

Conflict of interest

The authors declare that the research was conducted in the absence of any commercial or financial relationships that could be construed as a potential conflict of interest.

Publisher's note

All claims expressed in this article are solely those of the authors and do not necessarily represent those of their affiliated organizations, or those of the publisher, the editors and the reviewers. Any product that may be evaluated in this article, or claim that may be made by its manufacturer, is not guaranteed or endorsed by the publisher.

Supplementary material

The Supplementary Material for this article can be found online at: https://www.frontiersin.org/articles/10.3389/fneur.2022.967323/full#supplementary-material

References

1. Nakashima T, Pyykkö I, Arroll M, Casselbrant M, Foster C, Manzoor N, et al. Meniere's disease. *Nat Rev Dis Primers.* (2016) 2:16028. doi: 10.1038/nrdp.2016.28

2. Basura G, Adams M, Monfared A, Schwartz S, Antonelli P, Burkard R, et al. Clinical practice guideline: Ménière's disease executive summary. *Otolaryngol Head Neck Surg.* (2020) 162:415–34. doi: 10.1177/0194599820909439

3. Lopez-Escamez J, Carey J, Chung W, Goebel J, Magnusson M, Mandalà M, et al. Diagnostic criteria for Menière's disease. *J Vestib Res.* (2015) 25:1–7. doi: 10.3233/VES-150549

4. Dlugaiczyk J, Habs M, Dieterich M. Vestibular evoked myogenic potentials in vestibular migraine and Menière's disease: cVEMPS make the difference. *J Neurol.* (2020) 267:169–80. doi: 10.1007/s00415-020-09902-4

5. Dlugaiczyk J, Lempert T, Lopez-Escamez J, Teggi R, von Brevern M, Bisdorff A. Recurrent vestibular symptoms not otherwise specified: clinical characteristics compared with vestibular migraine and Menière's disease. *Front Neurol.* (2021) 12:674092. doi: 10.3389/fneur.2021.674092

6. Hallpike C, Cairns H. Observations on the pathology of Ménière's syndrome: (section of otology). *Proc R Soc Med.* (1938) 31:1317–36. doi: 10.1177/003591573803101112

7. Semaan M, Megerian C. Contemporary perspectives on the pathophysiology of Meniere's disease: implications for treatment. *Curr Opin Otolaryngol Head Neck Surg.* (2010) 18:392–8. doi: 10.1097/MOO.0b013e32833d3164

8. Nakashima T, Naganawa S, Sugiura M, Teranishi M, Sone M, Hayashi H, et al. Visualization of endolymphatic hydrops in patients with Meniere's disease. *Laryngoscope.* (2007) 117:415–20. doi: 10.1097/MLG.0b013e31802c300c

9. Fang Z, Chen X, Gu X, Liu Y, Zhang R, Cao D, et al. A new magnetic resonance imaging scoring system for perilymphatic space appearance after intratympanic gadolinium injection, and its clinical application. *J Laryngol Otol.* (2012) 126:454–9. doi: 10.1017/S0022215112000060

10. Attyé A, Eliezer M, Boudiaf N, Tropres I, Chechin D, Schmerber S, et al. Mri of endolymphatic hydrops in patients with meniere's disease: a case-controlled study with a simplified classification based on saccular morphology. *Eur Radiol.* (2017) 27:3138–46. doi: 10.1007/s00330-016-4701-z

11. Bernaerts A, Vanspauwen R, Blaivie C, van Dinther J, Zarowski A, Wuyts F, et al. The value of four stage vestibular hydrops grading and asymmetric perilymphatic enhancement in the diagnosis of Menière's disease on MRI. *Neuroradiology.* (2019) 61:421–9. doi: 10.1007/s00234-019-02155-7

12. Committee on hearing and equilibrium guidelines for the diagnosis and evaluation of therapy in Menière's disease. American Academy of Otolaryngology-Head and Neck Foundation, Inc. *Otolaryngol Head Neck Surg.* (1995) 113:181–5. doi: 10.1016/S0194-5998(95)70102-8

13. Ge X, Shea J. Transtympanic electrocochleography: a 10-year experience. *Otol Neurotol.* (2002) 23:799–805. doi: 10.1097/00129492-200209000-00032

14. Fleiss JL, Cohen J. The equivalence of weighted kappa and the intraclass correlation coefficient as measures of reliability. *Educ Psychol Meas.* (2016) 33:613–9. doi: 10.1177/001316447303300309

15. Hornibrook J, Mudry A, Curthoys I, Smith C. Ductus reuniens and its possible role in Menière's disease. *Otol Neurotol.* (2021) 42:1585–93. doi: 10.1097/MAO.0000000000003352

16. Kahn L, Hautefort C, Guichard J, Toupet M, Jourdaine C, Vitaux H, et al. Relationship between video head impulse test, ocular and cervical vestibular evoked myogenic potentials, and compartmental magnetic resonance imaging classification in Menière's disease. *Laryngoscope.* (2020) 130:E444–52. doi: 10.1002/lary.28362

17. Attyé A, Eliezer M, Medici M, Tropres I, Dumas G, Krainik A, et al. In vivo imaging of saccular hydrops in humans reflects sensorineural hearing loss rather than Meniere's disease symptoms. *Eur Radiol.* (2018) 28:2916–22. doi: 10.1007/s00330-017-5260-7

18. Pender D. Membrane stress in the human labyrinth and meniere disease: a model analysis. *Int Arch Otorhinol.* (2015) 19:336–42. doi: 10.1055/s-0035-1549157

19. Zhang W, Hui L, Zhang B, Ren L, Zhu J, Wang F, et al. The correlation between endolymphatic hydrops and clinical features of meniere disease. *Laryngoscope.* (2021) 131:E144–E50. doi: 10.1002/lary.28576

20. Yang S, Zhu H, Zhu B, Wang H, Chen Z, Wu Y, et al. Correlations between the degree of endolymphatic hydrops and symptoms and audiological test results in patients with Menière's disease: a reevaluation. *Otol Neurotol.* (2018) 39:351–6. doi: 10.1097/MAO.0000000000001675

21. He B, Zhang F, Zheng H, Sun X, Chen J, Chen J, et al. The correlation of a 2d volume-referencing endolymphatic-hydrops grading system with extra-tympanic electrocochleography in patients with definite Ménière's disease. *Front Neurol.* (2020) 11:595038. doi: 10.3389/fneur.2020.595038

22. Yoshioka M, Naganawa S, Sone M, Nakata S, Teranishi M, Nakashima T. Individual differences in the permeability of the round window: evaluating the movement of intratympanic gadolinium into the inner ear. *Otol Neurotol.* (2009) 30:645–8. doi: 10.1097/MAO.0b013e31819bda66

23. Shi H, Li Y, Yin S, Zou J. The predominant vestibular uptake of gadolinium through the oval window pathway is compromised by endolymphatic hydrops in ménière's disease. *Otol Neurotol.* (2014) 35:315–22. doi: 10.1097/mao.0000000000000196

frontiers | Frontiers in Neurology

TYPE Original Research
PUBLISHED 27 September 2022
DOI 10.3389/fneur.2022.987076

Check for updates

OPEN ACCESS

EDITED BY
Sulin Zhang,
Huazhong University of Science and Technology, China

REVIEWED BY
Jae-Hwan Choi,
Pusan National University Yangsan Hospital, South Korea
Haibo Shi,
Shanghai Jiao Tong University, China

*CORRESPONDENCE
Jun Hu
dochj@163.com

SPECIALTY SECTION
This article was submitted to Neuro-Otology, a section of the journal Frontiers in Neurology

RECEIVED 05 July 2022
ACCEPTED 09 August 2022
PUBLISHED 27 September 2022

CITATION
Cheng Y, Zheng J, Zhan Y, Liu C, Lu B and Hu J (2022) Identification of hub genes and pathophysiological mechanism related to acute unilateral vestibulopathy by integrated bioinformatics analysis.
Front. Neurol. 13:987076.
doi: 10.3389/fneur.2022.987076

COPYRIGHT
© 2022 Cheng, Zheng, Zhan, Liu, Lu and Hu. This is an open-access article distributed under the terms of the Creative Commons Attribution License (CC BY). The use, distribution or reproduction in other forums is permitted, provided the original author(s) and the copyright owner(s) are credited and that the original publication in this journal is cited, in accordance with accepted academic practice. No use, distribution or reproduction is permitted which does not comply with these terms.

Identification of hub genes and pathophysiological mechanism related to acute unilateral vestibulopathy by integrated bioinformatics analysis

Yajing Cheng, Jianrong Zheng, Ying Zhan, Cong Liu, Bihua Lu and Jun Hu*

Department of Neurology, Peking University Shenzhen Hospital, Shenzhen, China

Background: Although many pathological mechanisms and etiological hypotheses of acute unilateral vestibulopathy (AUVP) have been reported, but the actual etiology remains to be elucidated.

Objective: This study was based on comprehensive bioinformatics to identify the critical genes of AUVP and explore its pathological mechanism.

Methods: Gene expression profiles of AUVP and normal samples were collected from GSE146230 datasets of the Gene Expression Omnibus (GEO) database. Weighted gene co-expression network analysis (WGCNA) was constructed, and the WGCNA R-package extracted significant modules. The limma R-package was applied to identify differentially expressed genes (DEGs). The common genes of practical modules and DEGs were screened for GO and KEGG pathways analysis. The protein–protein interaction (PPI) layout and hub genes validation was created by Cytoscape software using the link from the STRING database. The functions of hub genes were predicted through the CTD (comparative genetics database).

Results: A total of 332 common genes were screened from practical modules and DEGs. Functional enrichment analysis revealed that these genes were predominantly associated with inflammation and infection. After construction of PPI, expressions of hub genes, and drawing ROC curves, LILRB2, FPR1, AQP9, and LILRA1 are highly expressed in AUVP ($p < 0.05$) and have a certain diagnostic efficacy for AUVP (AUC > 0.7), so they were selected as hub genes. The functions of hub genes suggested that the occurrence of AUVP may be related to inflammation, necrosis, hepatomegaly, and other conditions in CTD.

Conclusion: LILRB2, FPR1, AQP9, and LILRA1 may play essential roles in developing AUVP, providing new ideas for diagnosing and treating AUVP.

KEYWORDS

acute unilateral vestibulopathy, inflammation, immune response, bioinformatics analysis, hub genes

Introduction

Acute unilateral vestibulopathy (AUVP), also known as vestibular neuritis, is an acute peripheral vestibular syndrome characterized by acute unilateral loss of peripheral vestibular function without sensitive central nervous system or acute audiological symptoms or signs (1). It is the third most common peripheral vestibular disease after benign paroxysmal positional vertigo (BPPV) and Meniere's disease (2). There were no unified diagnostic criteria for AUVP, so there is no compelling new epidemiological study (3). The onset age of AUVP is usually 30–60 years old (1, 4, 5), and the distribution peak is 40–50 years old (1, 4). It is reported that the annual incidence rate of AUVP is 3.5–15.5 per 100,000 people (1, 4), the recurrence rate is 1.9% (6)—10.7% (7), and approximately 4–9.8% of adult patients and 3.3% of children are treated for acute unilateral vestibular loss (8). Although it is thought to be caused by viral inflammation or potential viral reactivation in vestibular nerve ganglia, the exact cause of vestibular neuritis is unclear (2). Therefore, the treatment methods for AUVP are various, such as corticosteroids, antiviral drugs, and vestibular rehabilitation training (2), but the treatment effects were not satisfactory.

The Committee for the Classification of Vestibular Disorders of the Bárány Society divides the diagnostic criteria of AUVP into four categories: 1. "Acute Unilateral Vestibulopathy," 2. "Acute Unilateral Vestibulopathy in Evolution," 3. "Probable Acute Unilateral Vestibulopathy" and 4. "History of Acute Unilateral Vestibulopathy" (1). The diagnosis of AUVP is based on the patient's medical history, bedside examination, and laboratory evaluation. It is worth noting that since there is no precise detection method for AUVP, its diagnosis needs to exclude central lesions and various other peripheral vestibular disorders. In addition, a pathological examination is a gold standard for diagnosis, but it is not easy to implement clinically. Thus, there is still a lack of ideal indicators in clinical practice. The viral hypothesis of AUVP that Bell's palsy and some types of acute hearing loss are likely to be related to viral infection, has not been confirmed so far (9–12). It has been reported that an autopsy of patients with AUVP showed neuroinflammatory vestibular degeneration (13). It is speculated that HSV-1, as a concurrent factor damaging the immune system, replicates and induces inflammation and edema, resulting in secondary cell damage to vestibular ganglion cells and axons in bone canals, which may also explain the therapeutic effect of steroids in the acute phase of AUVP (1). However, these findings have not confirmed the relationship between inflammation and virus hypothesis and AUVP. Therefore, improving understanding of the molecular mechanisms of AUVP is necessary to predict prognosis and develop therapeutic strategies targeting target genes.

With the rapid development and application of the gene chip and sequencing technology, NCBI (National Center for Biotechnology Information) established the GEO (Gene Expression Omnibus, https://www.ncbi.nlm.nih.gov/geo/) database in 2000 and maintained it. The GEO database collates high-throughput genomic data uploaded by researchers around the world. It is an international repository that archives and freely distributes high-throughput gene expression data (14). Through this database, researchers can easily download all kinds of sequencing data to study tumors, cerebrovascular diseases, neurodegenerative diseases, basic molecular biology, cardiovascular diseases, neuro-otology, and other fields (15–17). At present, research on AUVP has been reported and the original sequencing data have been uploaded (18). Therefore, using an online platform to integrate and analyze the existing high-throughput data can help to mine new biological targets, and provide big data support for follow-up experimental research. WGCNA is a commonly used high-throughput data analysis method to mine module information by analyzing the similarity of gene expression (19). Compared with previous clustering methods, WGCNA clustering has more biological significance. It not only focuses on differentially expressed genes (DEGs) but also makes full use of data information to transform thousands of genes and traits into several gene modules associated with clinical traits, thus eliminating the problem of multiple hypothesis test correction, and the results are more reliable.

This study aims to screen for critical biological processes and essential genes related to the development of AUVP based on a comprehensive bioinformatics analysis. We downloaded the gene expression profiles of AUVP and normal blood samples. After determining the common genes of significant modules and differentially expressed genes (DEGs) between diseased samples and healthy subjects, a cluster analysis and a functional enrichment analysis of common genes were carried out to explore the biological pathways in the processes of AUVP. In addition, the protein-protein interaction (PPI) network of common genes was constructed to find the potentially critical genes in developing AUVP. The hub genes were identified by drawing ROC curves. Finally, the functions of hub genes were predicted through the Comparative Toxicogenomics Database (CTD). The identified hub genes may play an essential role in developing AUVP. These findings provide a reference for exploring the pathological mechanism of AUVP.

Materials and methods

Data collection and data preprocessing

The keywords "Acute Unilateral Vestibulopathy," "vertigo," and "Vestibulopathy" were searched through the GEO database. Finally, the data set related to AUVP was selected as GSE146230 (18), including 10 control group samples and 10 AUVP patient

samples. Before analyzing the dataset, we need to screen the gene probe in the dataset. First, if the gene probe does not have a corresponding gene, the expression of this gene probe will be excluded; if one gene probe corresponds to multiple genes, the face of this gene probe will be banned. If one gene has two or more gene probes, the average expression of all the probes corresponding to the gene in each sample will be retained (20). As a result, 18,782 genes were included and will be further analyzed.

Gene co-expression network construction and identification of key modules

When constructing the weighted gene co-expression network, the "SD" function in R software was used to calculate the standard deviation of each gene and arrange it in descending order. Genes with the top 5,000 highest standard deviations were obtained for further analysis. Pearson's correlation coefficient among 5,000 genes was calculated to measure the degree of co-expression among genes. The network topology was analyzed through the "picksoftthreshold" function in the WGCNA package of R software. A hierarchical clustering tree of network modules was performed, and the number of modules was determined using the "cutreeDynamic" function with a minimum size module of 30 genes. Finally, we used the Dynamic Tree Cut approach to merge highly correlated modules using a height cut of 0.25 (21). Co-expression modules are represented by module colors, noted in the first row of the horizontal color bar. The correlation coefficients cor and *P*-values of gene modules and groups were calculated according to Pearson's correlation and visualized in the form of heatmap through the "labeledheatmap" function. The smaller the *p*-value and the larger the cor, the stronger correlation between AUVP and the gene module is, and the gene module was selected as the key module.

Identification of DEGs

First, we used the principal component analysis (PCA) to verify the reliable data and eliminate the system error for further analysis (22). The DEGs between patients with AUVP and control samples were screened by the R language "Limma" package. The selection criteria of DEGs was: $|\log2FC| > 0.3$, and p (T-test, Empirical Bayes methods) < 0.05 (23, 24). Fold Change (FC) represents the considerable differences between DEGs. The "ggplot2" package of R language was used to visualize the DEGs.

Screening of candidate genes in AUVP

An intersection of genes in the essential module and DEGs would be obtained by the "ggplot2" package, and the acquired genes were the crucial genes of AUVP.

Functional enrichment analysis

A functional enrichment analysis can divide hundreds of genes into different pathways and reduce the complexity of the analysis. The KEGG pathway analysis and the GO enrichment analysis of upregulated genes and downregulated genes in DEGs, modules, and common genes were carried out by using "cluster Profiler" of the R language, respectively (23). The GO enrichment analysis covered three aspects of biology namely Biological Process (BP), Cellular Component (CC), and Molecular Function (MF). In this study, $p < 0.05$ was selected as the screening condition, and the top pathways were chosen to explore the biological signal pathways and bodily functions of genes.

Construction of PPI

The STRING (25) (STRING, http://string.embl.de/) database aims to collect, score, and integrate all publicly available sources of protein-protein interaction information, and complement these with computational predictions. PPI is an essential component of the biological network, which plays a vital role in cell fate determination, signal transduction, and other life processes. It is also a vital link to the occurrence and development of disease. A total of 332 DEGs were introduced into the STRING database to construct the PPI network of key genes in AUVP. The PPI network was analyzed and visualized by Cytoscape software (http://www.cytoscape.org/), and the CytoHubba plug-in analyzed the genes in the PPI network.

Screening of hub genes

According to the four scoring algorithms, including the maximum neighborhood component (MNC), the density of maximum neighborhood component (DMNC), the maximal clique centrality (MCC), and the Degree of the CytoHubba plug-in, each gene in the PPI network is scored. The genes were ranked according to the level of each score (23). The top 20 genes were selected in each algorithm, and the shared genes of the four scoring algorithms were identified as hub genes.

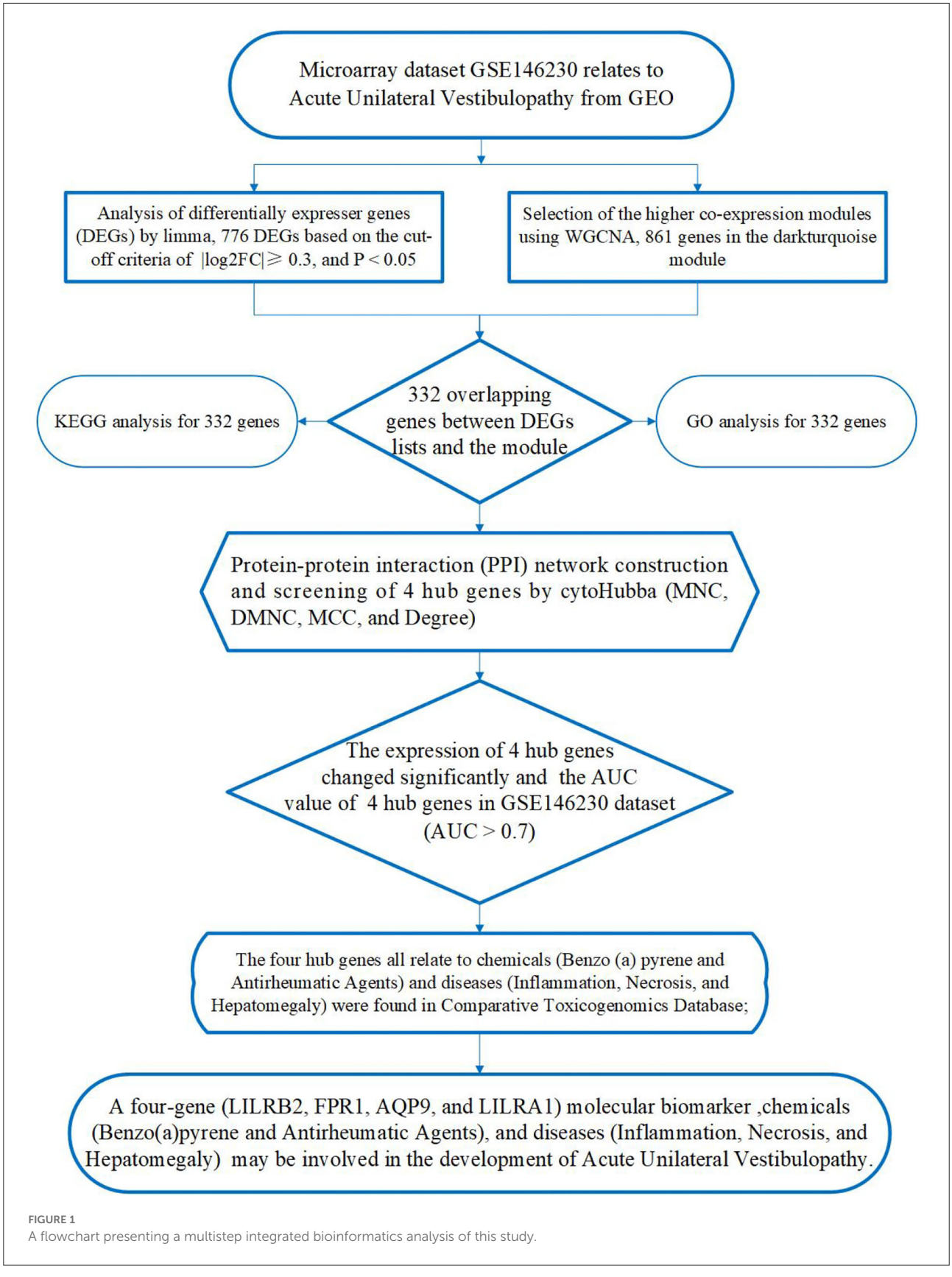

FIGURE 1
A flowchart presenting a multistep integrated bioinformatics analysis of this study.

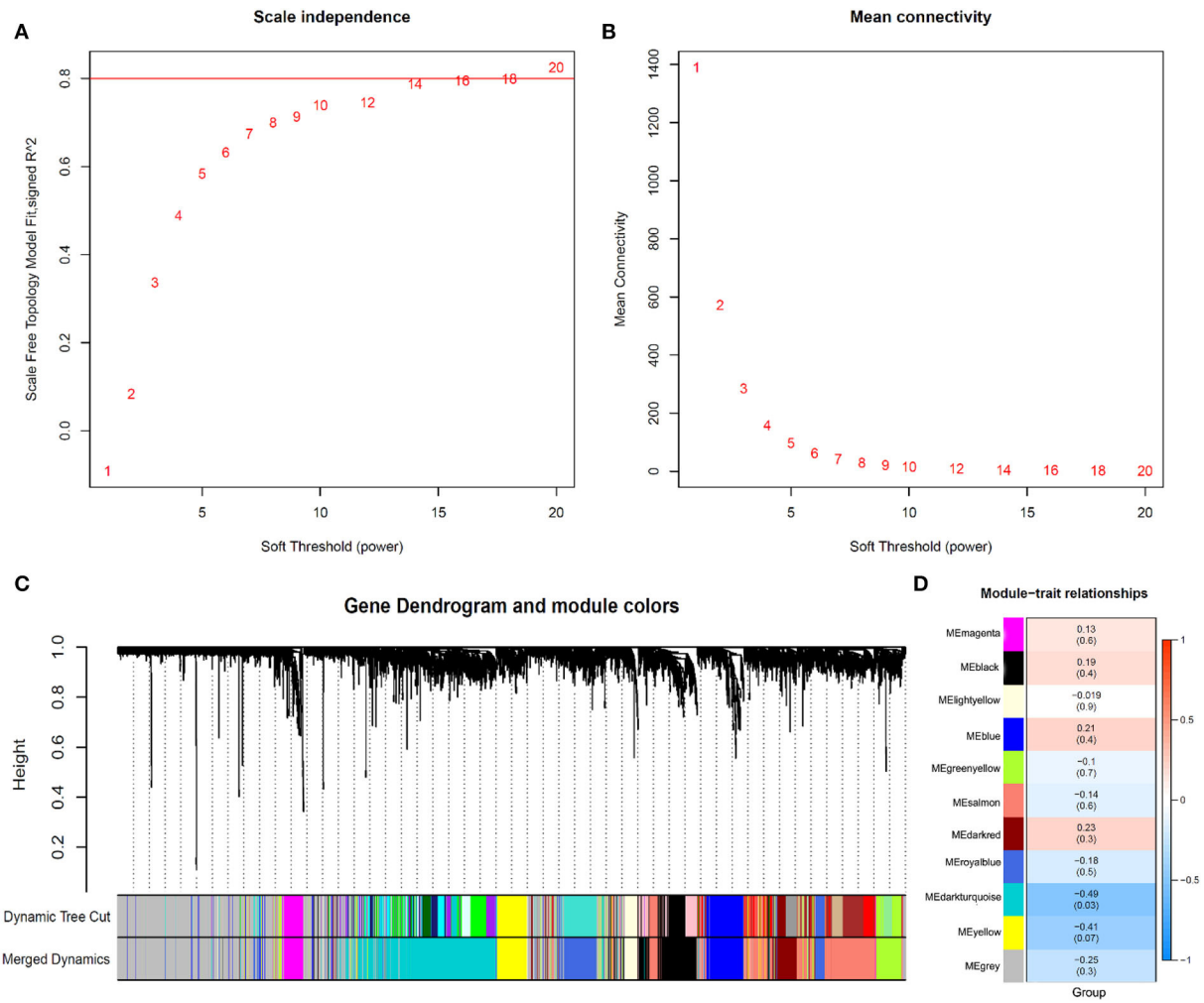

FIGURE 2
Identification of modules associated with the clinical subtypes of AUVP. **(A)** Analysis of the scale-free fit index for different soft-thresholding power. **(B)** Analysis of the mean connectivity for different soft-thresholding power. **(C)** Dendrogram of all differentially expressed genes clustered. **(D)** Heatmap of the correlation between gene modules and clinical information of AUVP.

Gene expression values of the hub genes in AUVP

To evaluate the clinical value of four hub genes, we used one independent GEO cohort as a validation dataset. The *T*-test analyzed the differences in expression patterns of four hub genes between patients with AUVP and normal samples, and the violin plot using the ggplot2 (V3.3.1) package in the R (V4.0.0) was used for visualization.

Receiver operating characteristic curve analysis of hub genes

The "pROC" and "ggplot2" packages of R language were used to analyze and visualize the hub gene's ROC curve and compare the hub gene's diagnostic efficiency in patients with AUVP (26). The area value (AUC) under the ROC curve is 0.5–1. The closer the AUC is to 1, the better the diagnostic effect. AUC has lower accuracy when 0.5–0.7, AUC has certain accuracy when 0.7–0.9, and AUC has higher accuracy when it is above 0.9.

Exploring the common functions of hub genes in the comparative toxicogenomics database

CTD, a robust and publicly available database, was used to find relevant disease associations. To explore the biological function of hub genes, the role of hub genes was predicted by using the CTD from two aspects of chemicals and diseases related to hub genes (27).

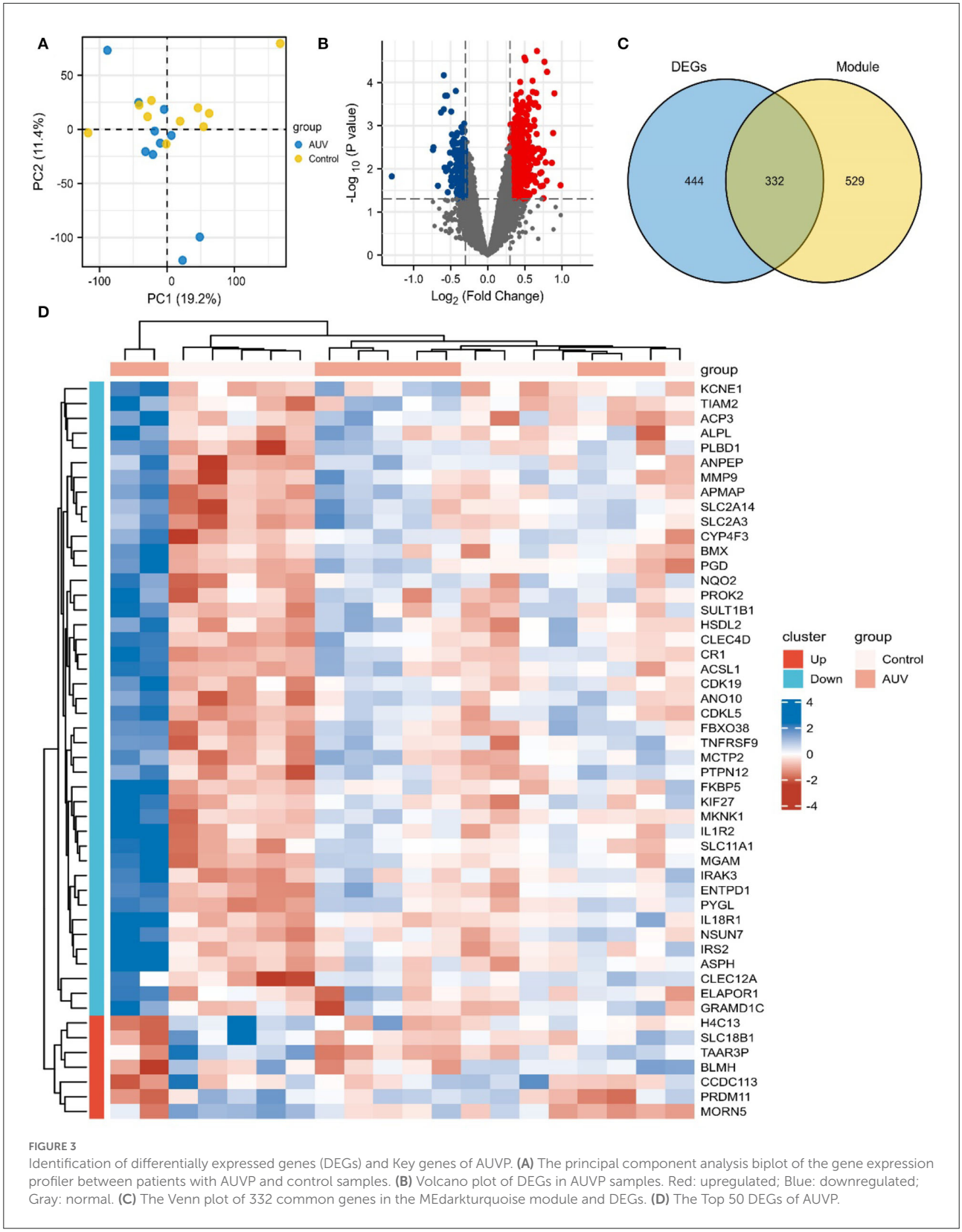

FIGURE 3
Identification of differentially expressed genes (DEGs) and Key genes of AUVP. **(A)** The principal component analysis biplot of the gene expression profiler between patients with AUVP and control samples. **(B)** Volcano plot of DEGs in AUVP samples. Red: upregulated; Blue: downregulated; Gray: normal. **(C)** The Venn plot of 332 common genes in the MEdarkturquoise module and DEGs. **(D)** The Top 50 DEGs of AUVP.

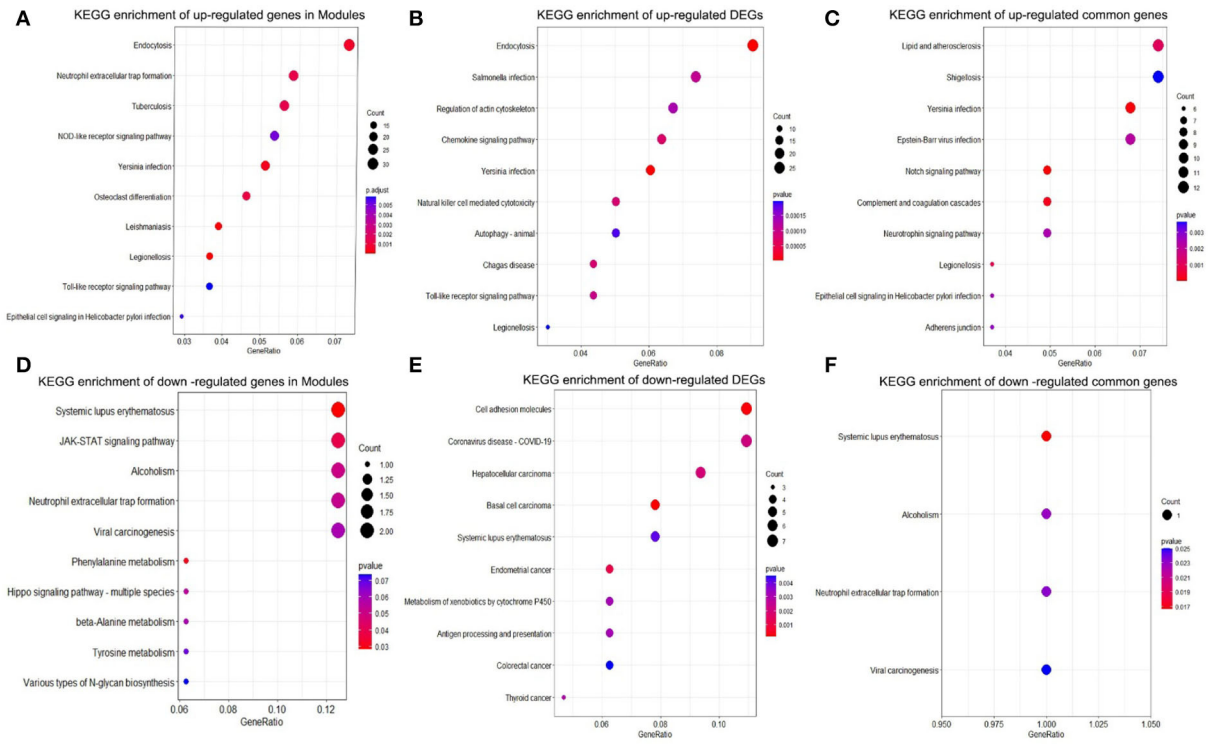

FIGURE 4
KEGG pathway enrichment analysis. **(A)** Top 10 KEGG pathway enrichment results of upregulated genes in the modules. **(B)** Top 10 KEGG pathway enrichment results of upregulated DEGs. **(C)** Top 10 KEGG pathway enrichment results of upregulated common genes. **(D)** Top 10 KEGG pathway enrichment results of downregulated genes in the modules. **(E)** Top 10 KEGG pathway enrichment results of downregulated DEGs. **(F)** KEGG pathway enrichment results in downregulated common genes. KEGG, Kyoto encyclopedia of genes and genomes; DEGs, differentially expressed gene.

Statistical analyses

WGCNA (version 1.69) and limma (version 1.9.6) was running in R (version 4.0.2) with the default statistics parameter and cut-off values specified in each section. $p < 0.05$ was defined as statistically significant.

Results

Figure 1 presents a multistep integrated bioinformatics analysis of this study.

Weighted co-expression network construction and key module identification

The β ($\beta = 20$, R2 $= 0.89$) value was selected to ensure the constructed scale-free co-expression network (Figures 2A,B). After successfully constructing the scale-free co-expression network, using the algorithm recognition module of the dynamic cut tree, the gene expression value in the module is very similar. After the highly similar modules were merged, a total of 11 co-expression modules were identified, while the gray module retained the genes that were not co-expressed (Figure 2C). After the module was cut, the grouping was combined with each module, and the heat map of the correlation between the module and the group was calculated using the "labeled heatmaps" function of the WGCNA package. The results showed that the correlation between the MEdarkturquoise module and patients with AUVP was the greatest, and the *p*-value was the smallest, so there was a significant correlation between the MEdarkturquoise module and patients with AUVP (Figure 2D). The 861 genes in the MEdarkturquoise module will be analyzed.

Identification of DEGs

In this study, the quality control (QC) of data was assessed by the principal component analysis (PCA) (Figure 3A). The DEGs between patients with AUVP and control samples were screened by the R language "limma" package. The selection criteria of DEGs are: $|\log2FC| > 0.3$, $p < 0.05$. As shown in Figure 3B, 776 differential genes were obtained, including

615 upregulated and 161 downregulated genes, red indicates upregulated genes, blue indicates downregulated genes, and gray indicates non-differential genes.

The "ggplot2" package of R software was used to intersect the genes in the key modules and DEGs, and 332 key genes of AUVP were obtained (Figure 3C). The "ComplexHeatmap" package of R language was used to visualize the expression level of the Top 50 DEGs (Figure 3D).

TABLE 1 KEGG analysis of upregulated common genes in AUVP.

ID	Description	Count	*p*-value
hsa04330	Notch signaling pathway	8	0.0000191
hsa05135	Yersinia infection	11	0.0000825
hsa04610	Complement and coagulation cascades	8	0.000267237
hsa05134	Legionellosis	6	0.000877613
hsa05417	Lipid and atherosclerosis	12	0.001148697
hsa05169	Epstein-Barr virus infection	11	0.002235012
hsa04722	Neurotrophin signaling pathway	8	0.002467031
hsa05120	Epithelial cell signaling in *Helicobacter pylori* infection	6	0.002566374
hsa04520	Adherens junction	6	0.002758126
hsa05131	Shigellosis	12	0.003666819

Functional enrichment analysis

The KEGG pathway was analyzed to explore the biological function of upregulated genes and downregulated genes in DEGs, modules, and common genes. As shown in Figures 4A–C, the up regulated genes in DEGs, modules, and common genes were mainly enriched in Yersinia infection, Neutrophil extracellular trap formation, Epstein-Barr virus infection, complement and coagulation cascades, neurotrophin signaling pathway, legionellosis, and epithelial cell signaling in the *Helicobacter pylori* infection (Table 1). The downregulated genes in DEGs, modules, and common genes were mainly enriched in systemic lupus erythematosus, alcoholism, neutrophil extracellular trap formation, and viral carcinogenesis (Figures 4D–F; Supplementary Table S1). In addition, after the GO analysis of upregulated genes and downregulated genes in DEGs, modules, and common genes, it was found that these genes were mainly enriched in biological functions related to

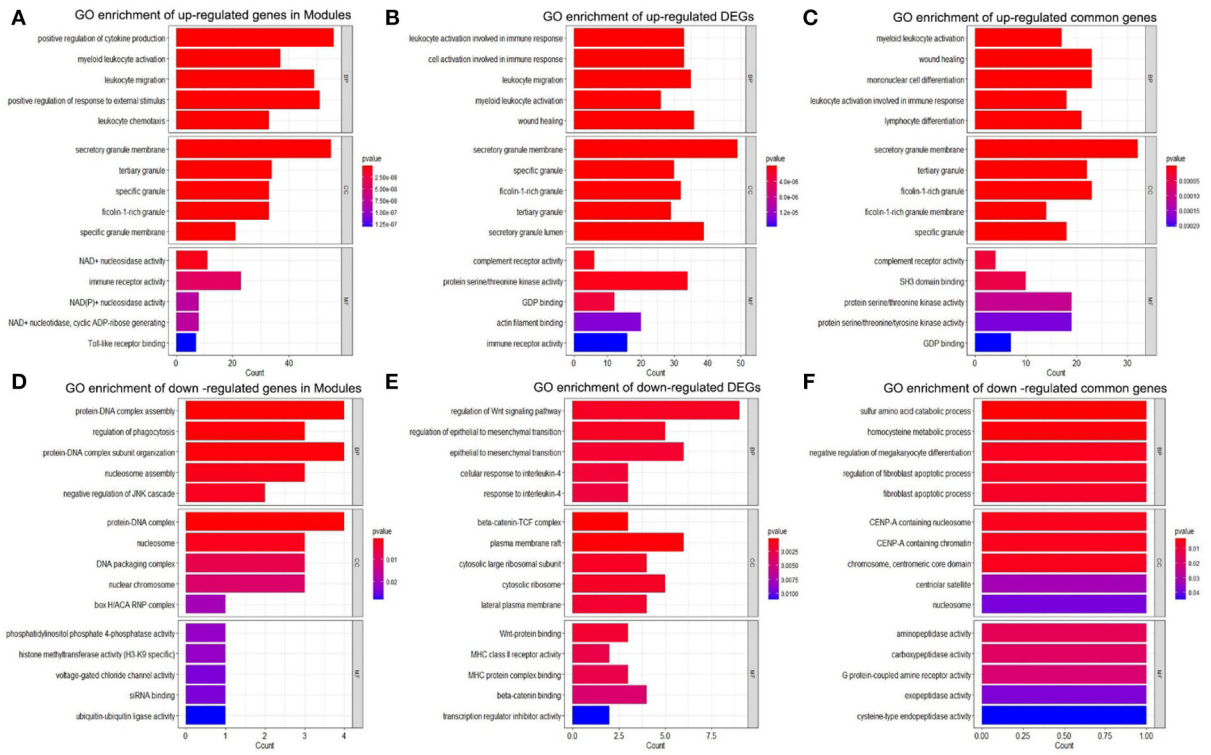

FIGURE 5
GO enrichment analysis. **(A)** GO enrichment of upregulated genes in the modules. **(B)** GO enrichment of upregulated DEGs. **(C)** GO enrichment of upregulated common genes. **(D)** GO enrichment of downregulated genes in Modules. **(E)** GO enrichment of downregulated DEGs. **(F)** GO enrichment of downregulated common genes. DEGs, differentially expressed genes; GO, gene ontology.

TABLE 2 GO analysis of upregulated common genes in AUVP.

ID	Ontology	Description	Count	*p*-value
GO:0002274	BP	Myeloid leukocyte activation	17	2.07E-07
GO:0042060	BP	Wound healing	23	4.47E-07
GO:1903131	BP	Mononuclear cell differentiation	23	5.25E-07
GO:0002366	BP	Leukocyte activation involved in immune response	18	8.16E-07
GO:0030098	BP	Lymphocyte differentiation	21	9.60E-07
GO:0030667	CC	Secretory granule membrane	32	7.12E-17
GO:0070820	CC	Tertiary granule	22	2.29E-14
GO:0101002	CC	Ficolin-1-rich granule	23	3.08E-14
GO:0101003	CC	Ficolin-1-rich granule membrane	14	6.59E-13
GO:0042581	CC	Specific granule	18	1.10E-10
GO:0004875	MF	Complement receptor activity	4	3.29E-05
GO:0017124	MF	SH3 domain binding	10	4.45E-05
GO:0004674	MF	Protein serine/threonine kinase activity	19	0.000108993
GO:0004712	MF	Protein serine/threonine/tyrosine kinase activity	19	0.000174533
GO:0019003	MF	GDP binding	7	0.000204491

inflammation and regulation of immune response. The GO analysis of upregulated genes in DEGs, modules, and common genes was primarily enriched in myeloid leukocyte activation, leukocyte activation involved in immune response, lymphocyte differentiation, secretory granule membrane, tertiary granule, complement receptor activity, and immune receptor activity (Figures 5A–C; Table 2). The GO analysis of downregulated genes in DEGs, modules, and common genes was mainly concentrated in the cell growth process metabolic pathway and so on (Figures 5D–F; Supplementary Table S2).

Construction of PPI and screening hub genes identification

In this study, 332 key genes of AUVP were introduced into the online STRING database to construct the interaction between differential gene proteins. The PPI network between 332 genes had 156 nodes and 232 edges (Figure 6A). The CytoHubba plug-in of Cytoscape software was used to screen the hub genes among the 332 key genes of AUVP. According to the four scoring algorithms of MNC, DMNC, MCC and Degree of the CytoHubba plug-in, each gene in the PPI network was scored, and the genes were sorted according to the score of each algorithm. The first 20 genes are selected in each algorithm (Figures 6B–E), and the genes obtained by intersection are determined to be the hub genes of AUVP. Finally, four hub genes were obtained (Figure 6F). Pearson's correlation coefficient and correlation significance p-value among four hub genes are shown in Figure 6G.

Hub genes identification

The expression patterns of 4 hub genes between AUVP patients and normal samples demonstrated that LILRB2, FPR1, AQP9, and LILRA1 were increased in AUVP ($p < 0.05$) (Figures 7A–D). ROC curve analysis was performed with the "pROC" package to compare the diagnostic efficacy of four hub genes in patients with AUVP. LILRB2, FPR1, AQP9, and LILRA1 have sure accuracy in diagnosing AUVP ($0.9 > AUC > 0.7$, Figures 7E–H). More details of the four hub genes are listed in Table 3. Therefore, LILRB2, FPR1, AQP9, and LILRA1 can be used as hub genes in the pathogenesis of AUVP.

Exploring the common functions of hub genes in the comparative toxicogenomics database

We can access this information by searching for target genes and looking up the chemicals and disease linked to the four hub genes in the CTD. The four hub genes were related to chemicals Benzo(a)pyrene and antirheumatic agents (Figure 7I). In addition, inflammation, necrosis, and hepatomegaly have strong links with the four hub genes in CTD (Figure 7J). This indicated that chemicals [benzo(a)pyrene and antirheumatic agents] and diseases (inflammation, necrosis, and hepatomegaly) play a significant role in the initiation and progression of the AUVP.

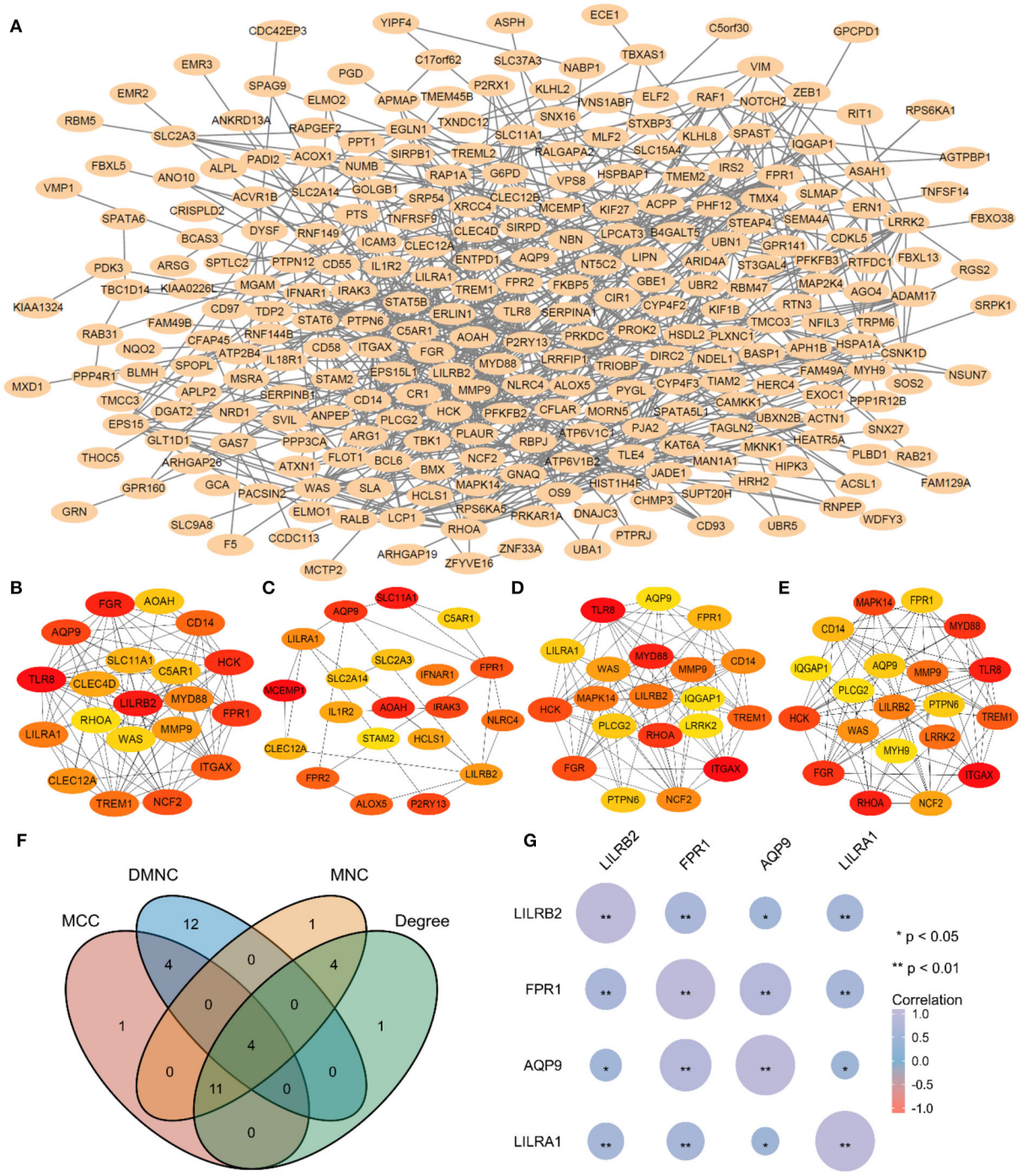

FIGURE 6
Hub genes identification. **(A)** Construction of PPI using 332 genes. **(B)** The Top 20 gene of MNC algorithm in PPI. **(C)** The Top 20 genes of DMNC algorithm in PPI. **(D)** The Top 20 genes of MCC algorithm in PPI. **(E)** The Top 20 genes of Degree algorithm in PPI. **(F)** The Venn plot of the intersection between four algorithms. **(G)** Pearson's correlation coefficient and correlation significance *p*-value among four hub genes of AUVP. MNC, maximum neighborhood component; DMNC, density of maximum neighborhood component; MCC, maximal clique centrality.

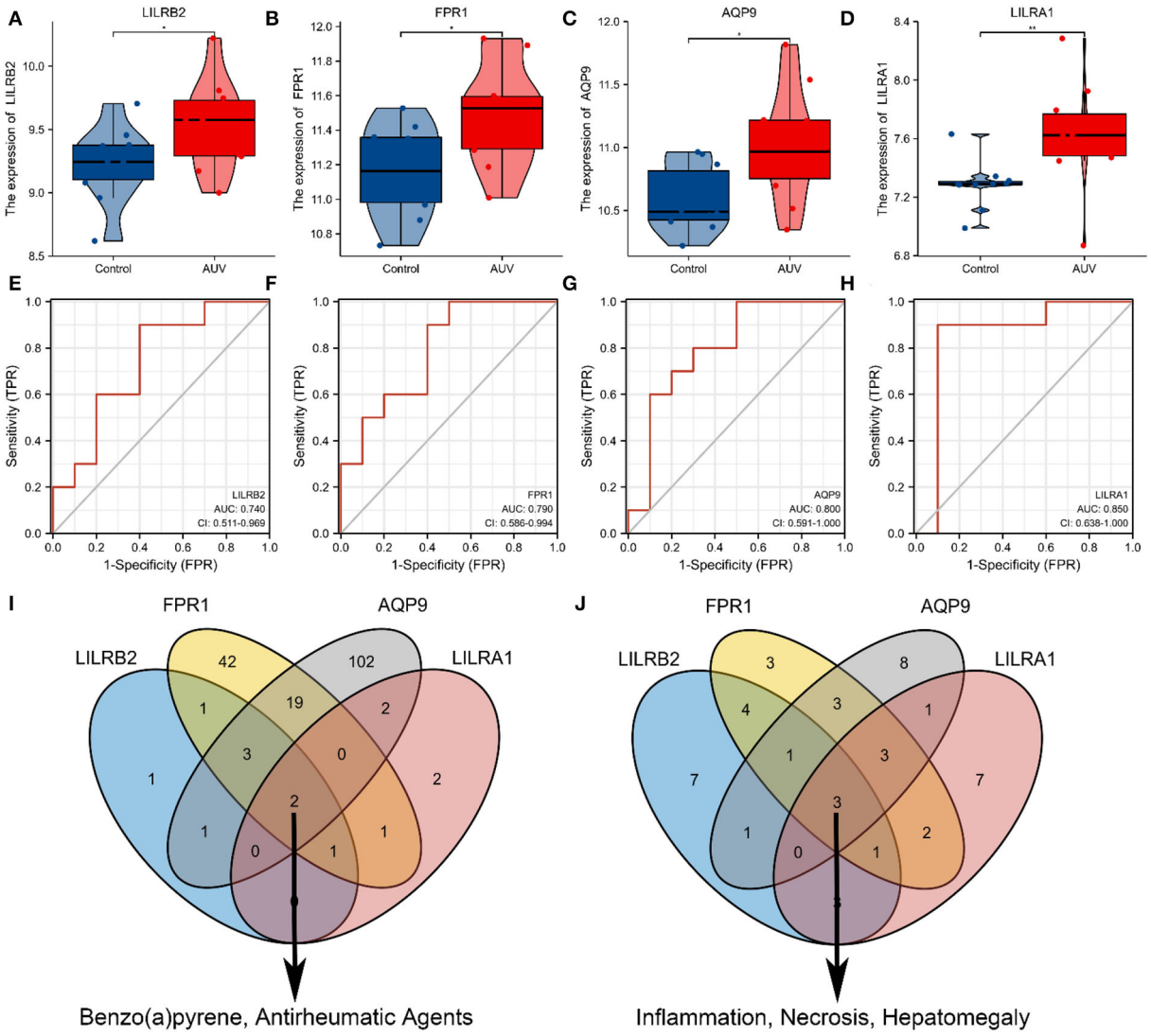

FIGURE 7
Exploring the functions of four hub genes. **(A)** Expression of LILRB2 mRNA among Normal and AUVP. **(B)** Expression of FPR1 mRNA among Normal and AUVP. **(C)** Expression of AQP9 mRNA among Normal and AUVP. **(D)** Expression of LILRA1 mRNA among Normal and AUVP. **(E)** ROC curve validated the sensitivity and specificity of LILRB2 as a predictive biomarker for AUVP prognosis. **(F)** ROC curve validated the sensitivity and specificity of FPR1 as a predictive biomarker for AUVP prognosis. **(G)** ROC curve validated the sensitivity and specificity of AQP9 as a predictive biomarker for AUVP prognosis. **(H)** ROC curve validated the sensitivity and specificity of LILRA1 as a predictive biomarker for AUVP prognosis. **(I)** The Venn plot of the four hub genes related to chemicals in the CTD. **(J)** The Venn plot of the four hub genes related to diseases in the CTD (*$p < 0.05$; **$p < 0.01$; ns, the difference is not statistically significant; CTD, Comparative Toxicogenomics Database).

Discussion

AUVP is the third inducing factor of secondary functional dizziness, second only to BPPV and vestibular migraine (1). Although many physiological and pathological mechanisms and etiological hypotheses of AUVP have been reported, the true etiology of AUVP is still unknown. Therefore, it is urgent and necessary to improve the understanding of the molecular mechanisms of AUVP and develop therapeutic strategies that aim at the targeting gene. First, the dataset of AUVP samples was analyzed by WGCNA R-package to obtain the relationship between the twelve gene expression modules and the clinical phenotype (group). It was found that the MEdarkturquoise module had the most considerable significant difference among all modules. Another method was used to perform the DEGs on the samples by the "limma" package, and 776 DEGs were screened. The common genes of the MEdarkturquoise module and 776 DEGs would be further analyzed. KEGG pathway analysis results suggest that the pathologies of AUVP may probably be associated with bacterial and viral infection

TABLE 3 The hub genes in Acute Unilateral Vestibulopathy.

Gene	GeneCards identifier*	Full name of the gene	Gene-related diseases*
LILRB2	GC19M066340	Leukocyte Immunoglobulin Like Receptor B2	Hymenolepiasis
FPR1	GC19M051745	Formyl Peptide Receptor 1	Susceptibility To Localized Juvenile Periodontitis; Periodontitis, Aggressive; Pulmonary Coin Lesion; Diamond-Blackfan Anemia 2 (DBA2); Aggressive Periodontitis.
AQP9	GC15P058138	Aquaporin 9	Hydrarthrosis; Polyhydramnios; Infective Endocarditis; Bullous Keratopathy; Constipation.
LILRA1	GC19P054593	Leukocyte Immunoglobulin Like Receptor A1	Immune System

*From the GeneCards database (www.genecards.org).

pathways. The results of GO analysis indicated that AUVP might be related to the inflammatory response and regulation of immune response. Then constructed PPI network and four hub genes were identified by the Cytoscape software using four scoring algorithms of the CytoHubba plugin (MNC, DMNC, MCC, and Degree). It is reported that biological networks are heterogeneous, so it is reasonable to use more than one method of CytoHubba to screen the hub genes, and it was also found that the essential proteins filtered by the four algorithms of MNC, DMNC, MCC, and Degree have a better performance on the precision than the other methods (28). ROC curve analysis suggests that four hub genes have certain accuracy in diagnosing AUVP ($0.9 > AUC > 0.7$). Finally, the four hub genes of AUVP identified by the two methods were LILRB2, FPR1, AQP9, and LILRA1. Therefore, we believe that the four hub genes and inflammation play a vital role in the pathogenesis of AUVP. Next, the four hub genes will be used as the entry point to explore the role of inflammation in the pathogenesis of AUVP.

As for the viral infection of vestibular neuronitis, some researchers believe that viruses causing upper respiratory tract infection, such as influenza virus, adenovirus, herpes simplex virus (HSV), cytomegalovirus, Epstein Barr virus, and parainfluenza virus, are related to vestibular neuronitis because 43 and 46% of patients with vestibular neuronitis have shown previous or concurrent viral infection of the upper respiratory tract (29). HSV-1 is the most common cause of vestibular nerve and ganglion virus infection among them. The autopsy showed that HSV-1 DNA, $CD8^+$T lymphocytes, cytokines, and chemokines were present in two-thirds of human vestibular ganglia (30), and injection of HSV-1 into a mouse model resulted in vestibular dysfunction of infected vestibular ganglion cells, such as vestibular neuritis (9, 30). Vestibular neuro virus infection or anterior vestibular artery ischemia is cause of vestibular neuritis. In addition, recent studies on the immune-mediated mechanism as the etiology of vestibular neuritis have been reported (9, 29, 30); the immune imbalance between T-helper cells and T- suppressor cells is associated with vestibular neuritis, similar to that observed in multiple sclerosis (9, 29). In addition, the functional enrichment analysis results of this study suggest that bacterial and viral infections are associated with AUVP development, including Epstein-Barr virus infection, Yersinia infection, legionellosis, and epithelial cell signaling in *Helicobacter pylori* infection. Inflammation and regulation of immune response also have been involved in the initiation and progression of AUVP. Therefore, the inflammation and immune response caused by virus infection may play an essential role in the pathogenesis of AUVP.

The previous study of the GSE146230 dataset has shown that the neutrophil-mediated immune pathway promotes AUVP development by mediating thrombotic changes and inflammation in vestibular organs with one bioinformatics method (18). In the current study, bioinformatic analyses were performed two times using two independent methods, and four hub genes were identified and validated. Among them, LILRA1 (CD86i, LIR6), a group I receptor that binds to HLA-C free heavy chains, has a lower affinity than LILRB1 and LILRB2 (31). The expression of LILRA1 is found on monocytes and macrophages. Anti-LILRA1 monoclonal antibody (clone m467) does not bind neutrophils (32). Additionally, LILRA1-specific peptides were not detectable in most proteomics studies of neutrophil-derived products. This indicates neutrophils expressed no or very little LILRA1 (33). LILRB2 (LIR2, CD85d, and ILT4), which contains four Ig-like domains, is a receptor for classical and non-classical HLA-I molecules (34–37). One study localized the expression of LILRB2 to particles. It showed that neutrophils were stimulated with fMLP, PS, or TNF α, resulting in upregulation of LILRB2 expression, which was accompanied by exocytosis of granules (38). The degranulation and phagocytosis of neutrophils were inhibited by cross-linking LILRB2 and HLA-G (38). During mid-and late-activation phases of the neutrophil lifecycle, LILRB2 modulates immune responses (33). FPR1 and its variants FPR like 1 (FPRL1) plays a critical role in cell proliferation, angiogenesis, and signaling pathways of neuroinflammation (39). In recent years, many pharmacological studies have demonstrated that FPR1 can effectively control neuroinflammation by inhibiting

the production of various proinflammatory mediators, such as TNF-α and IL-1β, otherwise inducing IL-10 and IL-1RA expression (40). In the course of demyelination, FPR1 causes and maintains glial cell activation. Therefore, FPR1 is an essential component of innate immunity in chronic degenerative diseases such as multiple sclerosis (41). AQP9 seems responsible for neutrophil migration, as Aqp9-KO mice show reduced neutrophil migration to fMLP (42, 43). Patients with systemic inflammatory response syndrome (SIRS) show increased AQP9 expression in neutrophils compared to healthy controls (42, 44). It has been reported that AQP9 expression in astrocytes, ependymocytes, tanycytes, endothelial cells of pial vessels, and dopaminergic neurons of the midbrain in the CNS (45, 46). Although there were few research reports on the role of four hub genes in AUVP, as discussed above, we found that all four hub genes are related to inflammation in the CTD database. Therefore, the four hub genes are also related to neutrophils, modulate immune responses, and express on immune cells. They could be used as the entry point to explore the role of inflammation, immune responses, and Immune cells in the development of AUVP.

Furthermore, our research also has some limitations. The four hub genes screened in this study have not been verified by experiments, for the time being, we will use four hub genes as a breakthrough point to design a new topic and study the specific role of four hub genes in AUVP. Our analysis results are based on a small sample size, which may not provide sufficient evidence to support our hypothesis. More samples need to be further studied to determine the accuracy of hub genes in the diagnosis of AUVP and the relationship between hub genes level and future treatment patterns, and to determine the immune and inflammation-related pathological mechanisms behind AUVP.

Conclusion

To sum up, the vestibular neurons are damaged following bacterial and viral infection. Then inflammation and immune responses are activated as well as immune proteins like LILRB2, FPR1, AQP9, and LILRA1 are produced in patients with AUVP to regulate their immune responses. However, the related mechanism still needs to be further explored. Although some reports suggest that viral infection is more critical in AUVP, we believe that bacterial infection may be equally important in the pathogenesis of AUVP. Therefore, the inflammation and immune response play a vital role in developing AUVP. Though it is still not clear about the specific position and mechanism of four hub genes in AUVP, the high expression levels suggest that they would be an essential target for AUVP diagnosis and treatment.

Data availability statement

The original contributions presented in the study are included in the article/Supplementary material, further inquiries can be directed to the corresponding author.

Author contributions

JH and YC designed the study. YC carried out the bioinformatic analysis and wrote the manuscript. JZ, YZ, CL, and BL reviewed and revised the manuscript. All authors read and approved the final manuscript.

Conflict of interest

The authors declare that the research was conducted in the absence of any commercial or financial relationships that could be construed as a potential conflict of interest.

Publisher's note

All claims expressed in this article are solely those of the authors and do not necessarily represent those of their affiliated organizations, or those of the publisher, the editors and the reviewers. Any product that may be evaluated in this article, or claim that may be made by its manufacturer, is not guaranteed or endorsed by the publisher.

Supplementary material

The Supplementary Material for this article can be found online at: https://www.frontiersin.org/articles/10.3389/fneur.2022.987076/full#supplementary-material

References

1. Strupp M, Bisdorff2 A, Furman J, Hornibrook J, Jahn K, Maire R, et al. Acute unilateral vestibulopathy/vestibular neuritis: diagnostic criteria. *J Vestib Res.* (2021) 1–18. doi: 10.3233/VES-220201

2. Bae CH, Na HG, Choi YS. Current diagnosis and treatment of vestibular neuritis: a narrative review. *J Yeungnam Med Sci.* (2022) 39:81–8. doi: 10.12701/yujm.2021.01228

3. Neuhauser HK. The epidemiology of dizziness and vertigo. *Handb Clin Neurol*. (2016) 137:67–82. doi: 10.1016/B978-0-444-63437-5.00005-4

4. Adamec I, Krbot Skoric M, Handzic J, Habek M. Incidence, seasonality and comorbidity in vestibular neuritis. *Neurol Sci*. (2015) 36:91–5. doi: 10.1007/s10072-014-1912-4

5. Depondt M. Vestibular neuronitis. Vestibular paralysis with special characteristics. *Acta Otorhinolaryngol Belg*. (1973) 27:323–59.

6. Huppert D, Strupp M, Theil D, Glaser M, Brandt T. Low recurrence rate of vestibular neuritis: a long-term follow-up. *Neurology*. (2006) 67:1870–1. doi: 10.1212/01.wnl.0000244473.84246.76

7. Kim YH, Kim KS, Kim KJ, Choi H, Choi JS, Hwang IK. Recurrence of vertigo in patients with vestibular neuritis. *Acta Otolaryngol*. (2011) 131:1172–7. doi: 10.3109/00016489.2011.593551

8. Wiener-Vacher SR, Quarez J, Priol AL. Epidemiology of vestibular impairments in a pediatric population. *Semin Hear*. (2018) 39:229–42. doi: 10.1055/s-0038-1666815

9. Le TN, Westerberg BD, Lea J. Vestibular neuritis: recent advances in etiology, diagnostic evaluation, and treatment. *Adv Otorhinolaryngol*. (2019) 82:87–92. doi: 10.1159/000490275

10. Baloh RW. Clinical practice. Vestibular neuritis. *N Engl J Med*. (2003) 348:1027–32. doi: 10.1056/NEJMcp021154

11. Gacek RR, Gacek MR. The three faces of vestibular ganglionitis. *Ann Otol Rhinol Laryngol*. (2002) 111:103–14. doi: 10.1177/000348940211100201

12. Baloh RW, Ishyama A, Wackym PA, Honrubia V. Vestibular neuritis: clinical-pathologic correlation. *Otolaryngol Head Neck Surg*. (1996) 114:586–92. doi: 10.1016/S0194-5998(96)70251-6

13. Schuknecht HF. *Pathology of the Ear*. Phildelphia, PA: Lea & Febinger (1993).

14. Barrett T, Wilhite SE, Ledoux P, Evangelista C, Kim IF, Tomashevsky M, et al. NCBI GEO: archive for functional genomics data sets–update. *Nucleic Acids Res*. (2013) 41:D991–5. doi: 10.1093/nar/gks1193

15. Sun Y, Zhang D, Sun G, Lv Y, Li Y, Li X, et al. RNA-sequencing study of peripheral blood mononuclear cells in sporadic Meniere's disease patients: possible contribution of immunologic dysfunction to the development of this disorder. *Clin Exp Immunol*. (2018) 192:33–45. doi: 10.1111/cei.13083

16. Flook M, Frejo L, Gallego-Martinez A, Martin-Sanz E, Rossi-Izquierdo M, Amor-Dorado JC, et al. Differential proinflammatory signature in vestibular migraine and meniere disease. *Front Immunol*. (2019) 10:1229. doi: 10.3389/fimmu.2019.01229

17. Choi K-D, Oh EH, Kim HS, Kim H-S, Park J-Y, Choi SY, et al. Transcriptional down-regulation of major histocompatibility complex as a possible pathogenesis for Meniere's disease. *Front Neurol*. (2022) 13:938740. doi: 10.3389/fneur.2022.938740

18. Oh EH, Rhee JK, Shin JH, Cho JW, Kim DS, Park JY, et al. Neutrophil-mediated immune response as a possible mechanism of acute unilateral vestibulopathy. *J Vestib Res*. (2020) 30:363–374. doi: 10.3233/VES-200044

19. Langfelder P, Horvath S. WGCNA: an R package for weighted correlation network analysis. *BMC Bioinformatics*. (2008) 9:559. doi: 10.1186/1471-2105-9-559

20. Peng WF, Bai F, Shao K, Shen LS, Li HH, Huang S. The key genes underlying pathophysiology association between the type 2-diabetic and colorectal cancer. *J Cell Physiol*. (2018) 233:8551–7. doi: 10.1002/jcp.26440

21. Wang CCN, Li CY, Cai JH, Sheu PC, Tsai JJP, Wu MY, et al. Identification of prognostic candidate genes in breast cancer by integrated bioinformatic analysis. *J Clin Med*. (2019) 8:1160. doi: 10.3390/jcm8081160

22. Yang H, Wang Z, Gong L, Huang G, Chen D, Li X, et al. A nove hypoxia-related gene signature with strong predicting ability in non-small-cell lung cancer identified by comprehensive profiling. *Int J Genomics*. (2022) 2022:8594658. doi: 10.1155/2022/8594658

23. Cheng Y, Sun M, Wang F, Geng X, Wang F. Identification of hub genes related to Alzheimer's disease and major depressive disorder. *Am J Alzheimers Dis Other Demen*. (2021) 36:15333175211046123. doi: 10.1177/15333175211046123

24. Ritchie ME, Phipson B, Wu D, Hu Y, Law CW, Shi W, et al. limma power differential expression analyses for RNA-sequencing and microarray studies. *Nucleic Acids Res*. (2015) 43:e47. doi: 10.1093/nar/gkv007

25. Szklarczyk D, Gable AL, Lyon D, Junge A, Wyder S, Huerta-Cepas J, et al. STRING v11: protein-protein association networks with increased coverage, supporting functional discovery in genome-wide experimenta datasets. *Nucleic Acids Res*. (2019) 47:D607–13. doi: 10.1093/nar/gky1131

26. Xu S, Liu D, Cui M, Zhang Y, Zhang Y, Guo S, et al. Identification of hub genes for early diagnosis and predicting prognosis in colon adenocarcinoma. *Biomed Res Int*. (2022) 2022:1893351. doi: 10.1155/2022/1893351

27. Nguyen HD, Kim MS. The protective effects of curcumin on metabolic syndrome and its components: *in-silico* analysis for genes, transcription factors, and microRNAs involved. *Arc Biochem Biophys*. (2022) 727:109326. doi: 10.1016/j.abb.2022.109326

28. Hegi ME, Liu L, Herman JG, Stupp R, Wick W, Weller M, et al. Correlation of O6-methylguanine methyltransferase (MGMT) promoter methylation with clinical outcomes in glioblastoma and clinical strategies to modulate MGMT activity. *J Clin Oncol*. (2008) 26:4189–99. doi: 10.1200/JCO.2007.11.5964

29. Greco A, Macri GF, Gallo A, Fusconi M, De Virgilio A, Pagliuca G, et al. Is vestibular neuritis an immune related vestibular neuropathy inducing vertigo? *J Immunol Res*. (2014) 2014:459048. doi: 10.1155/2014/459048

30. Jeong SH, Kim HJ, Kim JS. Vestibular neuritis. *Semin Neurol*. (2013) 33:185–94. doi: 10.1055/s-0033-1354598

31. Jones DC, Kosmoliaptsis V, Apps R, Lapaque N, Smith I, Kono A, et al. HLA class I allelic sequence and conformation regulate leukocyte Ig-like receptor binding. *J Immunol*. (2011) 186:2990–7. doi: 10.4049/jimmunol.1003078

32. Tedla N, Bandeira-Melo C, Tassinari P, Sloane DE, Samplaski M, Cosman D, et al. Activation of human eosinophils through leukocyte immunoglobulin-like receptor 7. *Proc Natl Acad Sci USA*. (2003) 100:1174–9. doi: 10.1073/pnas.0337567100

33. Lewis Marffy L, McCarthy AJ. Leukocyte immunoglobulin-like receptors (LILRs) on human neutrophils: modulators of infection and immunity. *Front Immunol*. (2020) 11:857. doi: 10.3389/fimmu.2020.00857

34. Shiroishi M, Kajikawa M, Kuroki K, Ose T, Kohda D, Maenaka K. Crystal structure of thehuman monocyte-activating receptor, "Group 2" leukocyte Ig-like receptor A5 (LILRA5/LIR9/ILT11). *J Biol Chem*. (2006) 281:19536–44. doi: 10.1074/jbc.M603076200

35. Willcox BE, Thomas LM, Bjorkman PJ. Crystal structure of HLA-A2 bound to LIR-1, a host and viral major histocompatibility complex receptor. *Nat Immunol*. (2003) 4:913–9. doi: 10.1038/ni961

36. Lepin EJ, Bastin JM, Allan DS, Roncador G, Braud VM, Mason DY, et al. Functional characterization of HLA-F and binding of HLA-F tetramers to ILT2 and ILT4 receptors. *Eur J Immunol*. (2000) 30:3552–61. doi: 10.1002/1521-4141(200012)30:12<3552::AID-IMMU3552>3.0.CO;2-L

37. Navarro F, Llano M, Bellon T, Colonna M, Geraghty DE, Lopez-Botet M. The ILT2(LIR1) and CD94/NKG2A NK cell receptors respectively recognize HLA-G1 and HLA-E molecules co- expressed on target cells. *Eur J Immunol*. (1999) 29:277–83. doi: 10.1002/(SICI)1521-4141(199901)29:01<277::AID-IMMU277>3.0.CO;2-4

38. Baudhuin J, Migraine J, Faivre V, Loumagne L, Lukaszewicz AC, Payen D, et al. Exocytosis acts as a modulator of the ILT4-mediated inhibition of neutrophil functions. *Proc Natl Acad Sci USA*. (2013) 110:17957–62. doi: 10.1073/pnas.1221535110

39. Cattaneo F, Guerra G, Ammendola R. Expression and signaling of formyl-peptide receptors in the brain. *Neurochem Res*. (2010) 35:2018–26. doi: 10.1007/s11064-010-0301-5

40. Calvello R, Cianciulli A, Porro C, Moda P, De Nuccio F, Nicolardi G, et al. Formyl peptide receptor (FPR)1 modulation by resveratrol in an LPS- induced neuroinflammatory animal model. *Nutrients*. (2021) 13:1418. doi: 10.3390/nu13051418

41. Bihler K, Kress E, Esser S, Nyamoya S, Tauber SC, Clarner T, et al. Formyl peptide receptor 1-mediated glial cell activation in a mouse model of cuprizone-induced demyelination. *J Mol Neurosci*. (2017) 62:232–43. doi: 10.1007/s12031-017-0924-y

42. Rump K, Adamzik M. Function of aquaporins in sepsis: a systematic review. *Cell Biosci*. (2018) 8:10. doi: 10.1186/s13578-018-0211-9

43. Moniaga CS, Watanabe S, Honda T, Nielsen S, Hara-Chikuma M. Aquaporin-9-expressing neutrophils are required for the establishment of contact hypersensitivity. *Sci Rep*. (2015) 5:15319. doi: 10.1038/srep15319

44. Matsushima A, Ogura H, Koh T, Shimazu T, Sugimoto H. Enhanced expression of aquaporin 9 in activated polymorphonuclear leukocytes in patients with systemic inflammatory response syndrome. *Shock*. (2014) 42:322–6. doi: 10.1097/SHK.0000000000000218

45. Trillo-Contreras JL, Ramirez-Lorca R, Villadiego J, Echevarria M. Cellular distribution of brain aquaporins and their contribution to cerebrospinal fluid homeostasis and hydrocephalus. *Biomolecules*. (2022) 12:530. doi: 10.3390/biom12040530

46. Badaut J, Petit JM, Brunet JF, Magistretti PJ, Charriaut-Marlangue C, Regli L. Distribution of aquaporin 9 in the adult rat brain: preferential expression in catecholaminergic neurons and in glial cells. *Neuroscience*. (2004) 128:27–38. doi: 10.1016/j.neuroscience.2004.05.042

frontiers | Frontiers in Neurology

TYPE Original Research
PUBLISHED 12 October 2022
DOI 10.3389/fneur.2022.1030006

Check for updates

OPEN ACCESS

EDITED BY
Sulin Zhang,
Huazhong University of Science and Technology, China

REVIEWED BY
Jose Antonio Lopez-Escamez,
Universidad de Granada, Spain
So Young Kim,
CHA University, South Korea

*CORRESPONDENCE
Dingqiang Huang
Huangdingq666666@163.com

SPECIALTY SECTION
This article was submitted to Neuro-Otology, a section of the journal Frontiers in Neurology

RECEIVED 28 August 2022
ACCEPTED 16 September 2022
PUBLISHED 12 October 2022

CITATION
Zou W, Li Q, Peng F and Huang D (2022) Worldwide Meniere's disease research: A bibliometric analysis of the published literature between 2002 and 2021. *Front. Neurol.* 13:1030006. doi: 10.3389/fneur.2022.1030006

COPYRIGHT
© 2022 Zou, Li, Peng and Huang. This is an open-access article distributed under the terms of the Creative Commons Attribution License (CC BY). The use, distribution or reproduction in other forums is permitted, provided the original author(s) and the copyright owner(s) are credited and that the original publication in this journal is cited, in accordance with accepted academic practice. No use, distribution or reproduction is permitted which does not comply with these terms.

Worldwide Meniere's disease research: A bibliometric analysis of the published literature between 2002 and 2021

Wujun Zou[1], Qian Li[1], Fei Peng[2] and Dingqiang Huang[1]*

[1]Department of Otorhinolaryngology Head and Neck Surgery, Chengdu Second People's Hospital, Chengdu, China, [2]Department of Anesthesia, West China Hospital of Sichuan University, Chengdu, China

Background: In recent years, there has been an increasing number of publications on Meniere's disease. However, there are no bibliometric research on Meniere's disease. The purpose of this study was to find the focus and trends of Meniere's disease research through bibliometric approach.

Methods: Publications related to Meniere's disease in the Web of Science Core Collection (WOSCC) from 2002 to 2021 were collected. The bibliometric approach was used to estimate the searched data. Research foci of the studies were identified using VOSviewer and CiteSpace software.

Results: A total of 1,987 articles meet the inclusion criteria and are included in the study. In the past 20 years, the number of Meniere's disease publications is gradually increasing, especially in the past 3 years. The country with the largest contribution to Meniere's disease research is the United States, followed by Europe and Japan. High-frequency keywords included Meniere's disease, endolymphaic hydrops, vertigo, meniere-disease, inner ear, dizziness, symptoms, hearing, diagnosis, and tentamicin. The analyses of keyword burst direction indicate that evoked myogenic potential, MRI, and committee are emerging research hotspots.

Conclusion: This study provides an objective, systematic, and comprehensive analysis of Meniere's disease-related literature. In addition, we find a dramatic increase in studies in this field over the past 3 years. Evoked myogenic potentials and MRI may become the research hotspots of Meniere's disease in future. This study will help otolaryngologists, neurologists, and audiologists to clarify the research direction and potential hotspots of Meniere's disease and further help clinicians improve patients' prognosis.

KEYWORDS

Meniere's disease, CiteSpace, VOSviewer, bibliometric analysis, hotspot, trend

Introduction

Meniere's disease is characterized by recurrent episodes of spontaneous, usually rotational vertigo, sensorineural hearing loss, tinnitus, and a feeling of fullness or pressure in the affected ear. It is a condition that frequently lasts for decades. It is usually unilateral but may be bilateral. Meniere's disease is most common between

the ages of 30 and 60 years, although younger people may be affected (1–3). Acute episodes can occur in clusters of about 6–11 years, although remission may last many months or even years. In addition, many people with Meniere's disease often have reduced daily activities to avoid triggering the disease. However, limiting daily activities may delay psychological and neurophysiological recovery, prolong the onset of the disease, and increase distress (4, 5).

Despite the availability of various interventions, there is uncertainty surrounding their relative efficacy, thus making it difficult to select the appropriate treatments for Meniere's disease (6, 7). Most treatments provide only temporary relief of symptoms, not the psychiatric symptoms associated with Meniere's disease, such as anxiety, irritability, and depression. Thus, it is imperative to find effective treatments for Meniere's disease.

Bibliometric analysis uses mathematical and statistical methods to analyze basic information on included literature, such as countries/regions, research collaborations, journals, institutions, and authors, and to identify research dynamics in selected areas (8, 9). Bibliometric analysis can be used to predict potential research hotspots by showing changes in research directions at different time points, and it has been used in many research fields (10). Compared with systematic reviews and meta-analysis, bibliometric analysis can comprehensively analyze the current status of research fields and more accurately predict development trends (11). CiteSpace is a Java-based scientific mapping software, and VOSviewer helps to build maps based on web data, both of which were used for analyzing included literature (12). Both CiteSpace and VOSviewer have been used in various fields, such as physical education and healthy urban planning (13, 14).

Bibliometric techniques and visual analysis have not been used to summarize Meniere's disease research. At the same time, there is no research to explore the hotspot of Meniere's disease. In this study, we aim to investigate the research status and hotspots of Meniere's disease in the past 20 years through quantitative analysis. Furthermore, we build a network of authors, institutions, and countries among the researchers. These analyses can bring new perspectives to otolaryngologists and neurologists.

Materials and methods

Data source and search strategy

We carefully searched the Web of Science database for articles about Meniere's disease from 2002 to 2021 and included original articles and review articles. Topic = (Meniere's disease) AND Language = English was the only retrieval strategy. On 1 July 2022, we completed the literature search and data collection. Since there were no exclusion criteria, the search results might include some non-relevant articles. The detail of search procedure is exhibited in Figure 1. Two researchers analyzed the data separately, and if there was a disagreement, a third researcher would be asked to solve the problem. The information includes title, abstract, keywords, author, institution, country, journal, references, and citations.

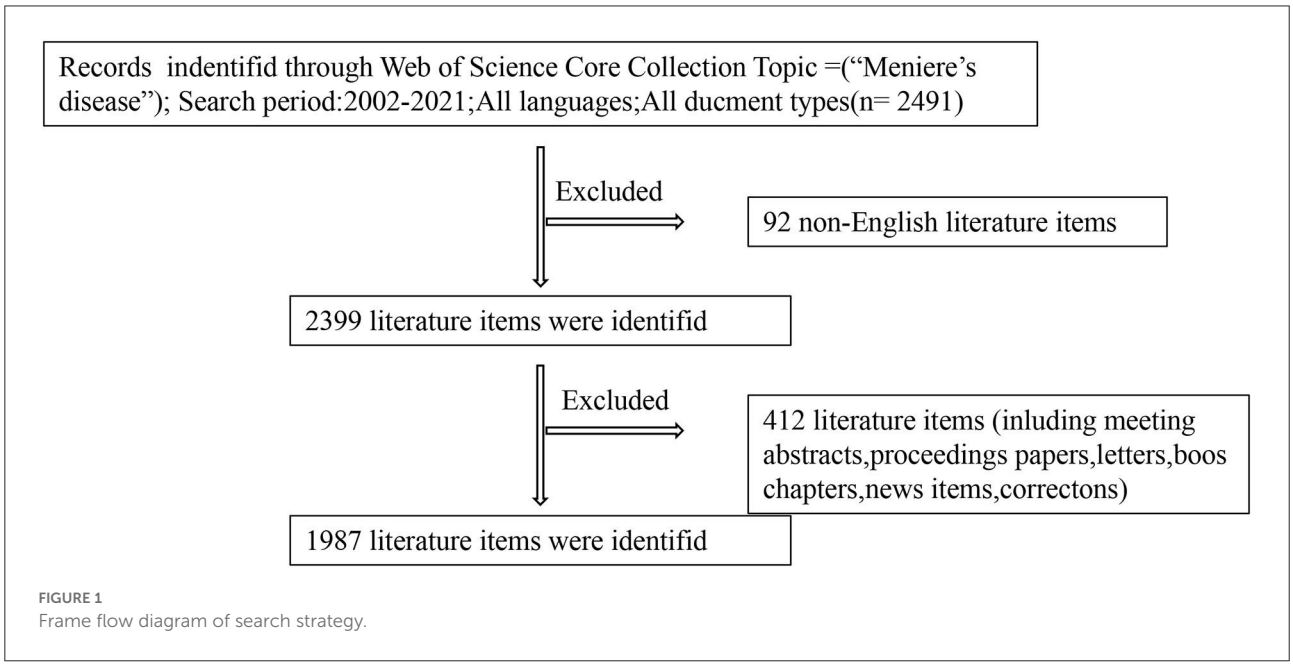

FIGURE 1
Frame flow diagram of search strategy.

Bibliometric analysis

First, the included data were converted to texts, which included basic information such as co-cited articles, keywords, countries, institutions, journals, authors, and network characteristics of keyword burst. Second, the texts were imported into the analysis software including. Finally, the results are presented in tables or figures. The Journal Citation Report 2021 included the H-index, impact factor, and category quartiles. Among them, the H-index is an important indicator for evaluating the scientific impact of journals or articles (15, 16).

To explore the research hotspots of Meniere's disease, we analyzed the included articles by CiteSpace software. The metrics analyzed were publishers, co-cited articles, and most relevant keywords. Different nodes on the network visualization map represent different analyzed objects. The larger nodes indicate more frequent occurrences. Moreover, we analyzed the centrality of the included studies by CiteSpace software, where the more important nodes are represented *via* higher centrality (17). We presented the evolution of research fields

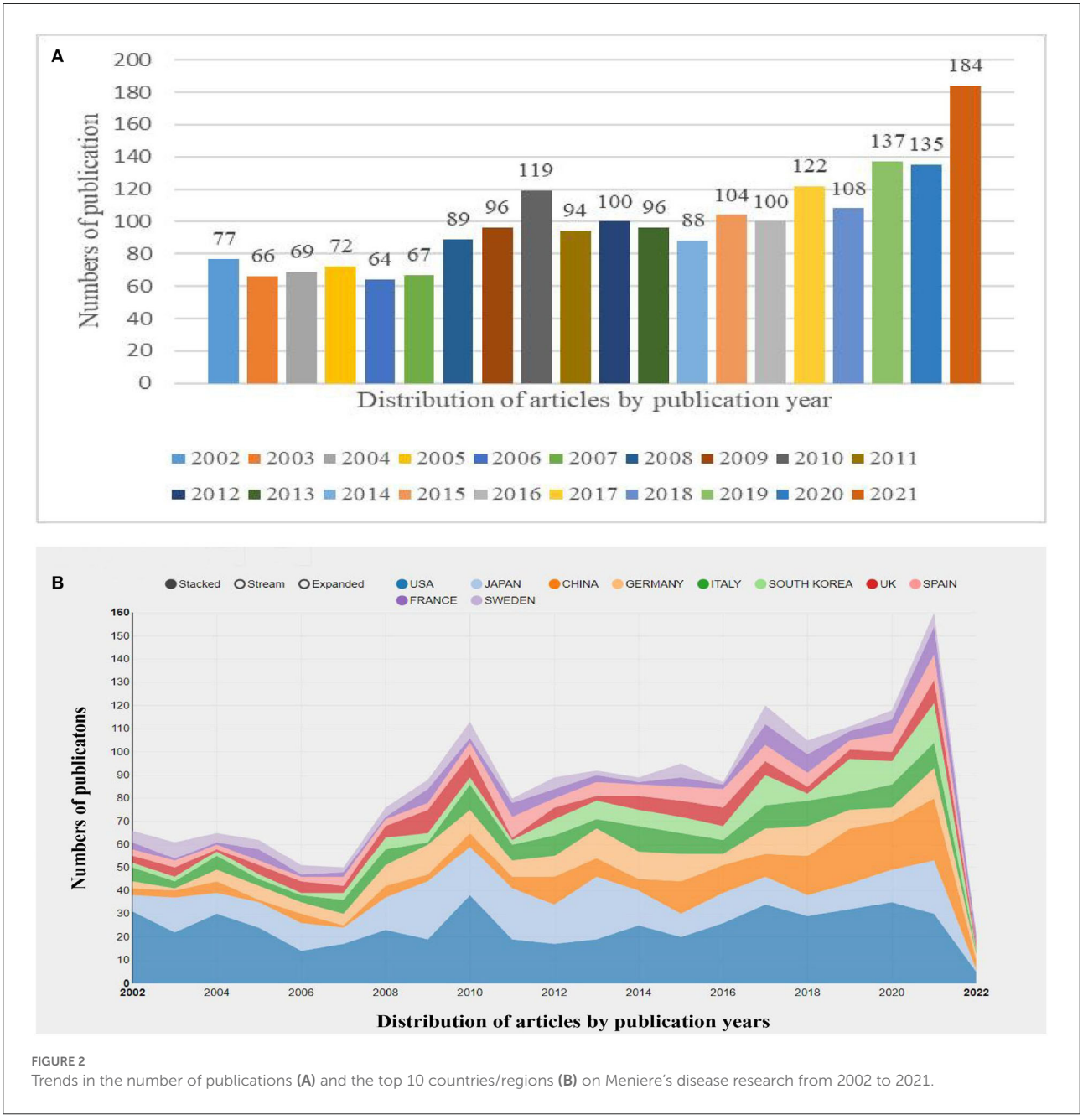

FIGURE 2
Trends in the number of publications **(A)** and the top 10 countries/regions **(B)** on Meniere's disease research from 2002 to 2021.

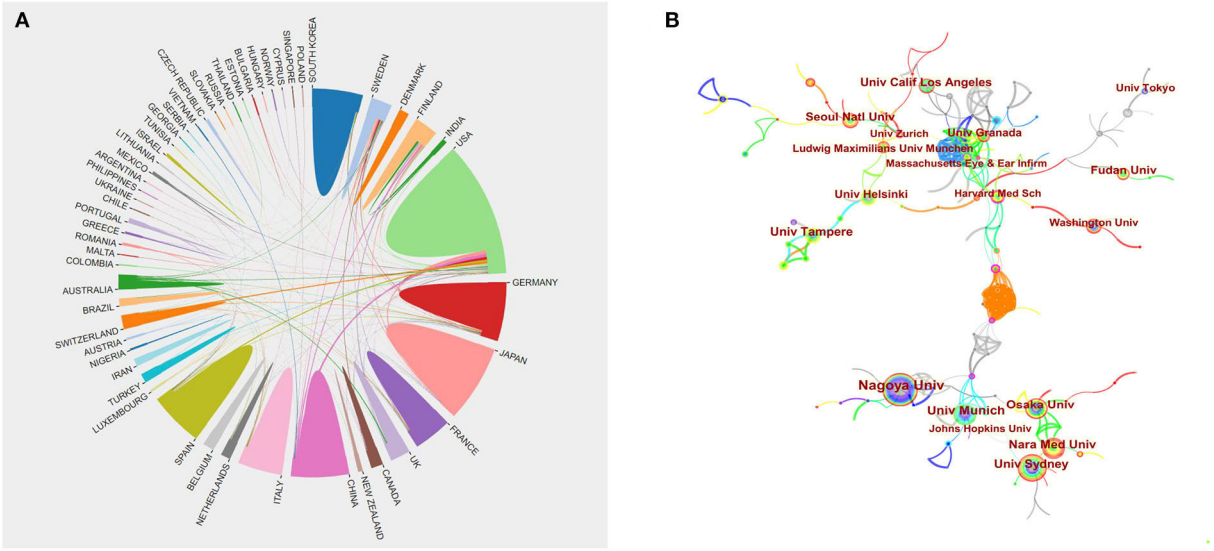

FIGURE 3
Cooperation of countries/regions **(A)** and institutions **(B)** contributed to publications on Meniere's disease research from 2002 to 2021.

and collaborations between different institutions by creating scientific knowledge networks through VOSviewer software followed by predicting potential research hotspots.

VOSviewer software was used to analyze the co-occurrence of keywords. The results were presented as a density map with different color clusters showing the co-occurrence frequency of the keywords which has the potential to predict underlying trends.

Results

Annual outputs and growth trends

Overall, there has been an upward trend in original research on Meniere's disease over the past 20 years, especially in the last 3 years. In the past two decades, researchers have published a total of 1987 studies (Figure 2A). In Meniere's disease research, the United States published the most research results (Figure 2B). In the past 3 years, the number of articles published has increased significantly. In the past decade, research on Meniere's disease has peaked, almost twice as much as in the previous decade.

Distribution of Countries/Regions and Institutions

A network of national collaborations between studies on Meniere's disease is shown in Figure 3A. Table 1 shows the top ten contributing countries. The country with the most published research is the United States (513), followed by Japan (296), Germany (170), China (145), and Italy (142). The United States accounted for about 30% of the total number of published studies. The centrality score is a metric for evaluating the importance of network nodes. The centrality analysis of this study confirms that the United States (0.72) is at the top of the network, followed by Spain (0.35) and France (0.31). Higher centrality means stronger cooperation. The low density of the national cooperation network graph indicates that the research institutions are relatively independent and need to strengthen further cooperation.

TABLE 1 Ranking of top 10 most published countries in Meniere's disease research from 2002 to 2021.

Rank	Articles counts	Centrality	Country
1	513	0.72	USA
2	296	0.00	Japan
3	170	0.04	Germany
4	145	0.04	China
5	142	0.08	Italy
6	120	0.00	South Korea
7	101	0.35	Spain
8	87	0.08	UK
9	86	0.31	France
10	85	0.19	Sweden

The network of institutional collaborations between studies on Meniere's disease is shown in Figure 3B. The top ten institutions include University of Munich (0.02), University of

TABLE 2 Ranking of top 10 institutions for collaboration in Meniere's disease research from 2002 to 2021.

Rank	Articles counts	Centrality	Institutions	Country
1	75	0.02	University of Munich	Germany
2	62	0.01	University of California	USA
3	61	0.09	Nagoya University	Japan
4	54	0.00	UDICE	France
5	47	0.03	Harvard University	USA
6	47	0.03	Tampere University	Finland
7	43	0.09	University of Sydney	Australia
8	38	0.17	Massachusetts Eye and Ear Infirmary	USA
9	38	0.05	Osaka University	Japan
10	35	0.05	University of Navarra	Spain

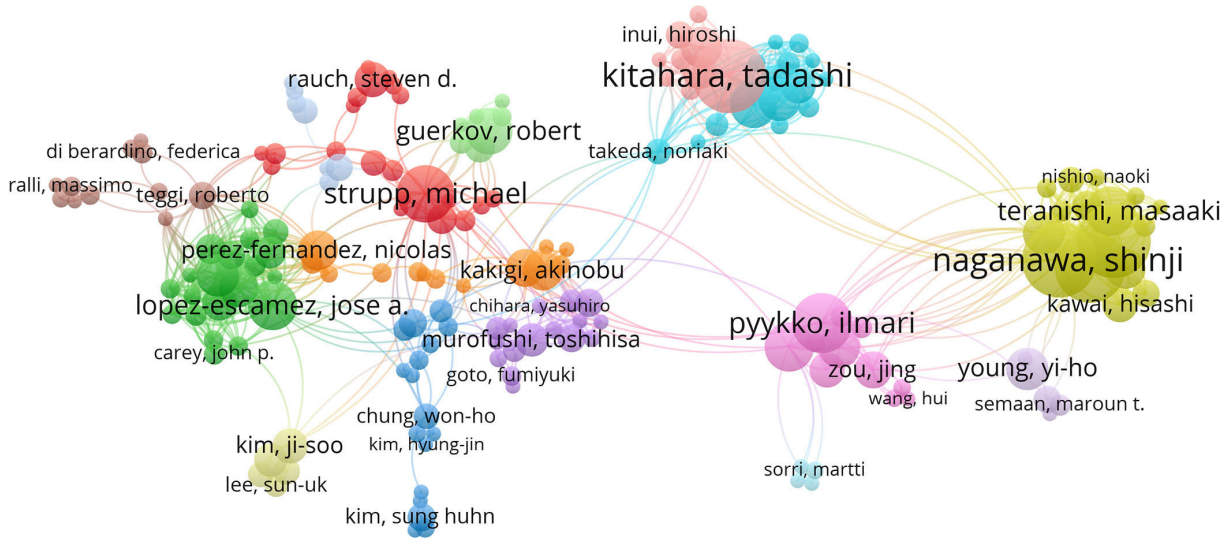

FIGURE 4
Joint mapping of productive authors in Meniere's disease research from 2002 to 2021.

California (0.01), Nagoya University (0.09), Tampere University (0.03), and Harvard University (0.03) (Table 2). The highest centrality is Massachusetts Eye and Ear Infirmary (0.17). The low centrality of all institutions indicates less inter-agency cooperation and further emphasizes the importance of cooperation.

Contributions of authors

VOSviewer was used for visualizing authors (at least five articles and 200 citations) (Figure 4). In the past 20 years, 266 authors have published ≥ five studies on Meniere's disease. Each circle represents a researcher. Some overlapping authors may not be presented. Closed circles represent researchers with closed working relationship.

Table 3 shows the top ten researchers with the most published articles. The most published author is Kitahara T (53 articles, 659 citations), followed by Naganawa S (51 articles, 2,153 citations). In terms of centrality, Nakashima T and Strupp M tied for first place (0.08). The centrality of investigators working on Meniere's disease was all below 0.1, which emphasized that Meniere's disease investigators were less cooperative and needed to strengthen their cooperation with each other.

Journal analyses

Table 4 presents the characteristics of the top ten active journals. Most of the journal's publishers are located in the United States and Europe. The top three journals that

TABLE 3 Ranking of top 10 most published authors in Meniere's disease research from 2002 to 2021.

Rank	Author	Articles Counts	Centrality	Total Citations	Average Citations	H-index
1	Kitahara T	53	0.02	659	12.43	13
2	Naganawa S	51	0.06	2,153	42.22	25
3	Sone M	51	0.07	1,858	36.43	23
4	Nakashima T	50	0.00	2,136	42.72	25
5	Pyykko I	43	0.08	836	19.44	13
6	Lopez-escamez JA	41	0.06	1,720	41.95	22
7	Strupp M	35	0.08	2,292	65.49	23
8	Kentala E	33	0.02	517	15.67	12
9	Teranishi M	30	0.02	1169	38.97	18
10	Gurkov R	28	0.00	760	27.14	17

TABLE 4 Ranking of top 10 journals for number of published articles on Meniere's disease research from 2002 to 2021.

Rank	Journal	Articles counts	Country	Journal citation reports (2021)	Impact factor (2021)	Total cites	Average number of citations	H-index
1	Otology and Neurotology	263	USA	Q3	2.619	5,177	19.68	35
2	Acta Oto-Laryngologica	224	Norway	Q4	1.698	3,159	14.10	26
3	Laryngoscope	104	USA	Q3	2.970	3,033	29.16	30
4	European Archives of Oto-Rhino-Laryngology	91	Germany	Q2	3.236	1,204	13.23	19
5	Otolaryngology-Head And Neck Surgery	62	USA	Q1	5.591	1,257	20.27	20
6	Journal of Laryngology And Otology	56	UK	Q3	2.187	603	10.77	14
7	Frontiers In Neurology	55	Switzerland	Q2	4.086	488	8.87	12
8	Auris Nasus Larynx	51	Netherlands	Q3	2.119	559	10.96	12
9	Annals of Otology Rhinology And Laryngology	43	USA	Q3	1.973	548	12.74	14
10	Audiology And Neuro-Otology	42	USA	Q3	2.213	563	13.40	14

publish Meniere's disease research are Otology and Neurotology, Acta Oto-Laryngologica, and Laryngoscope. Otology and Neurotology publishes the most articles on Meniere's disease. Moreover, Otology and Neurotology had the highest average number of citations (29.16) and the highest H-index (35). Journal Citation Report quartile Q1 included Otolaryngology-Head and Neck Surgery, Q2 contained European Archives of Oto-Rhino-Laryngology and Frontiers In Neurology, Q3 contained Otology and Neurotology, Laryngoscope, Journal of Laryngology And Otology, Auris Nasus Larynx, Annals of Otology Rhinology And Laryngology and Audiology And Neuro-Otology, and Q4 contained Acta Oto-Laryngologica in.

Cluster analysis of keyword co-occurrence related to research hotspots

The titles and keywords of the 1,987 literature included in this study were analyzed *via* VOSviewer software. Figure 5A depicts that the map, which was divided into five clusters, contained only 252 keywords (more than 20 times) and 4,979 keywords totally. The frequency keywords were meniere's disease (998), endolymphaic hydrops (518), vertigo (453), meniere-disease (327), inner-ear (223), dizziness (185), symbols (165), hearing (154), diagnosis (136), and tentamicin (135). Terms with similar research subjects were combined under the same category, with five main clusters: clinical characteristics, mechanisms, diagnosis, management, and pathophysiology of Meniere's disease.

Figure 5B shows the distribution of keywords that appear in order. The order of keywords is determined by the color of the labels. In the first decade, most research focused on mechanisms and pathophysiology, and recent research trends suggest that diagnosis may become a research hotspot.

Moreover, Figure 5C shows that the frequency of occurrence of different keywords is represented by the density of the graph. The higher the density, the warmer the color "closer to yellow." Research hotspots in this field mostly appear in areas with high density.

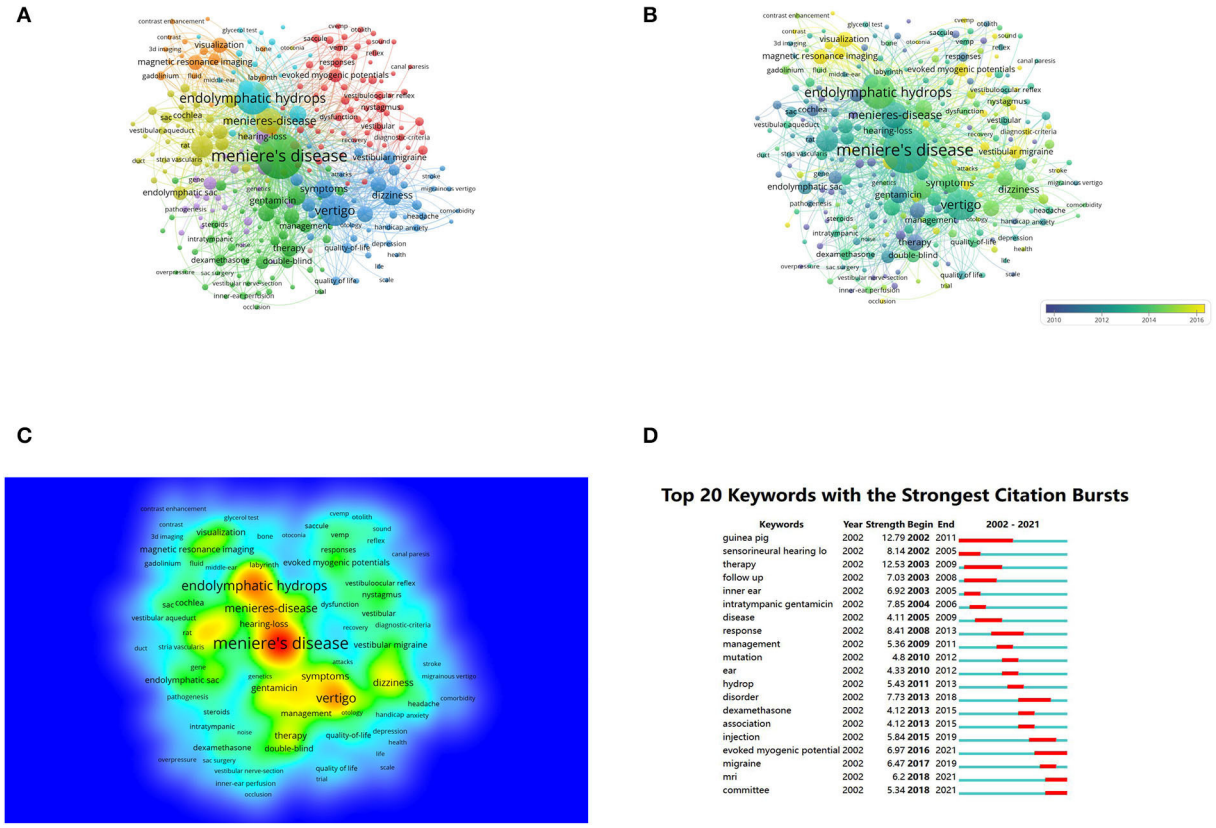

FIGURE 5
Co-occurrence analysis of global research on Meniere's disease based on the WoSCC database from 2002 to 2021. **(A)** Mapping of keywords in the research field. **(B)** Distribution of keywords according to the chronological order of appearance. **(C)** Distribution of keywords according to the mean frequency of appearance. **(D)** Keywords with the strongest citation bursts in Meniere's disease research.

Detection of keyword bursts

By analyzing 1,987 articles retrieved from the WoSCC database, we identified keyword outbreaks from 2002 to 2021 (Figure 5D). A straight line represents the timeline, consisting of blue and (or) red. The red part illustrates the burst period in which length represents the starting and ending year and time span. To focus on research trends in Meniere's disease, we identified keywords with strongest burst. Between 2002 and 2021, guinea pig (12.79) was top one, followed by therapy (12.53), response (8.41), sensorineural hearing loss (8.14), and intratympanic gentamicin (7.85). The analyses of keyword burst direction indicated that evoked myogenic potential (2016–2021), MRI (2018–2021), and committee (2018–2021) were emerging research hotspots.

Analyses of co-cited references

In this study, a co-citation analysis was performed on 25,639 cited references from 1987 articles, and a clustering network graph was obtained based on the analysis of the results. The visual network of the co-cited articles consists of 184 nodes and 204 links (Figure 6A). Cited articles are represented by nodes. The diameter of the node represents the total number of cited articles. Links between nodes indicate how often the citation was cited. The purple ring around the node can be used to connect the stages of the growth of a field. The red around the node represents the referenced "explosive growth".

Moreover, the research hotspots of Meniere's disease can be found by ranking the co-cited articles generated in the co-citation network. There were eight major clusters (Figure 6B). Figure 7 presents a timeline perspective of the cluster plot, supporting the discovery of new research hotspots in Meniere's disease. Table 5 lists the top 10 co-cited articles. The study published by Lopez-Escamez JA (18) in the Journal of Vestibular Research-Equilibrium and Orientation was the most cited (577 citations), followed by the research published by Nakashima T (19) in Laryngoscope (343 citations) and the article published by Merchant SN (20) in Otology and Neurotology (324 citations).

Figure 8 shows the top 20 most cited references. Most of the highly cited references were from ENT or neurology

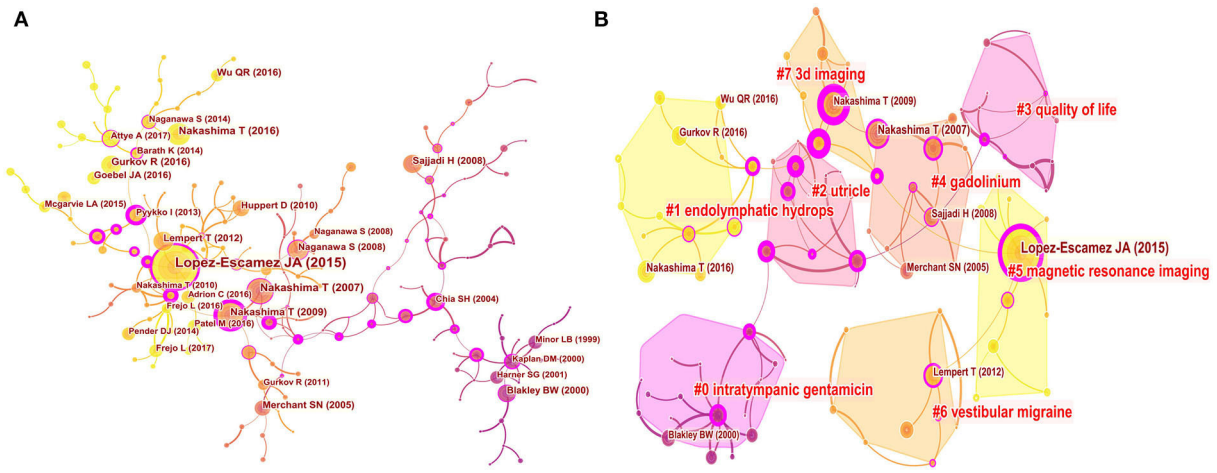

FIGURE 6
Co-cited references map **(A)** and clustered network map of co-cited references **(B)** on Meniere's disease research from 2002 to 2021.

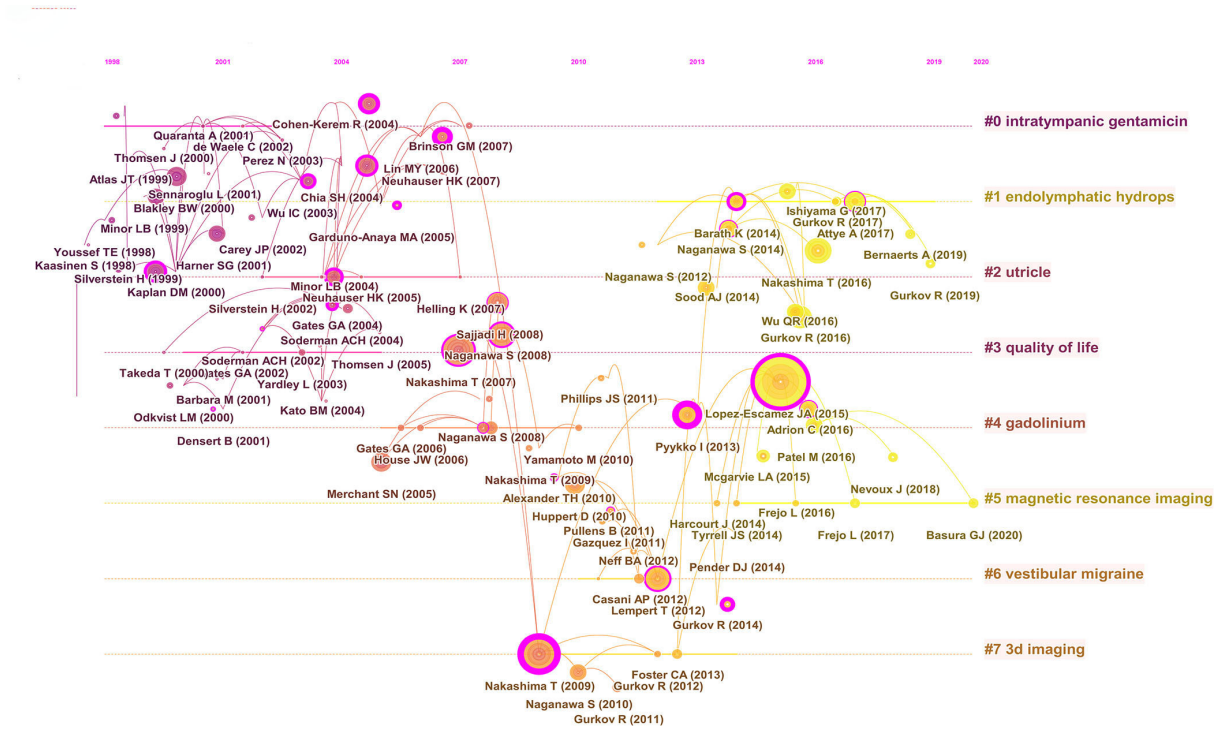

FIGURE 7
Timeline view of co-cited clusters with cluster labels.

publishers. This suggests that Meniere's disease belongs to the intersection of otolaryngology and neurology. The citing journal is on the left, and the cited journal is on the right. There are five main reference paths in Figure 9: three gray paths and two orange paths. The orange path means that studies published in Molecular/Biology/Immunology journals are cited in Molecular/Biology/Immunology/Dermatology/Dentistry/Surgery journals. Studies published in Dermatology/Dentistry/Surgery journals are cited for studies in Molecular/Biology/Genetic, Health/Nursing/Medicine, and psychology/Education/Social journals, as shown by the gray route.

TABLE 5 Top 10 most co-cited references on Meniere's disease research from 2002 to 2021.

Rank	Title	First Author	Year	Journal	Cited Frequency
1	Diagnostic criteria for Meniere's disease	Lopez-Escamez JA	2015	Journal of Vestibular Research-Equilibrium & Orientation	577
2	Visualization of endolymphatic hydrops in patients with Meniere's disease	Nakashima T	2007	Laryngoscope	343
3	Pathophysiology of Meniere's syndrome: Are symptoms caused by endolymphatic hydrops?	Merchant SN	2005	Otology & Neurotology	324
4	Meniere's disease	Sajjadi H	2008	Lancet	255
5	Epidemiology of vertigo	Neuhauser HK	2007	Current Opinion In Neurology	237
6	Migraine and Meniere's disease - Is there a link?	Radtke A	2002	Neurology	221
7	Intratympanic dexamethasone for sudden sensorineural hearing loss after failure of systemic therapy	Haynes DS	2007	Laryngoscope	199
8	Bilateral vestibulopathy: Diagnostic criteria Consensus document of the Classification Committee of the Barany Society	Strupp M	2017	Journal of Vestibular Research-Equilibrium and Orientation	193
9	Causative factors and epidemiology of bilateral vestibulopathy in 255 patients	Zingler VC	2007	Annals of Neurology	174
10	Epidemiology of vertigo, migraine and vestibular migraine	Lempert T	2009	Journal of Neurology	156

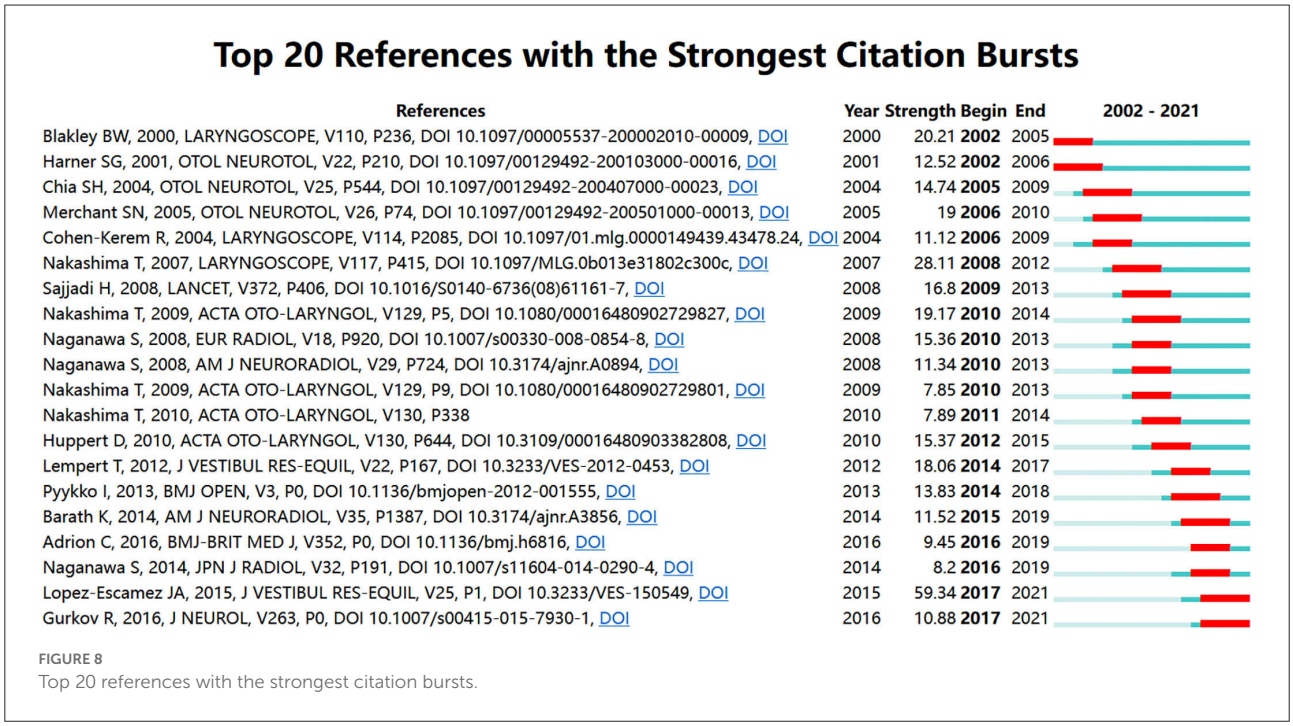

FIGURE 8
Top 20 references with the strongest citation bursts.

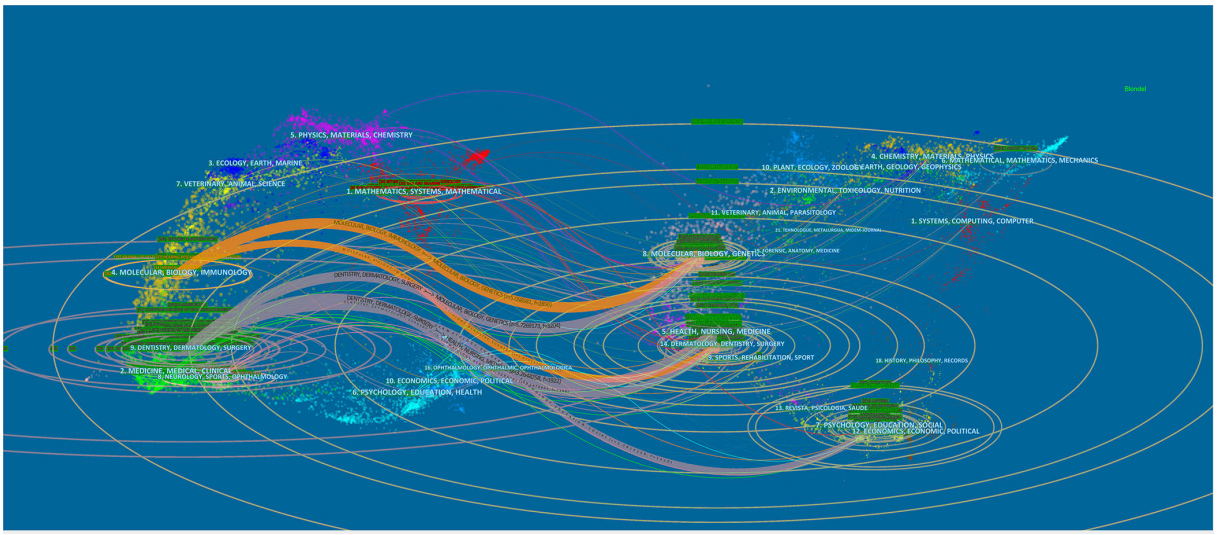

FIGURE 9
Dual-map overlay of journals on Meniere's disease.

Discussion

Meniere's disease is an inner ear disease characterized by endolymphatic hydrops (21). Meniere's disease is often misdiagnosed due to the difficulties to directly see the endolymphatic hydrops and defects with auxiliary testing equipment. Therefore, it is imperative to summarize Meniere's disease research in recent years. Interestingly, this is the only study to analyze the research status of Meniere's disease by quantitative and qualitative bibliometrics, which includes 5,000 articles retrieved from WoSCC. The results confirmed that the total number of publications on Meniere's disease worldwide was gradually increasing over the past 7 years, which suggested the importance in otolaryngology and neurology. The number of articles had increased dramatically over the past 3 years. On the one hand, it may benefit from the improvement of assistive technology and clinical treatment. On the other hand, it may be related to experimental technology and research investment. The United States accounted for 30% of the articles on Meniere's disease. Furthermore, the publishers are mainly located in the United States and Europe. This result confirms that there are good medical conditions in developed countries, especially in European and American countries. At the same time, this result also reflects the urgency of strengthening global cooperation to find effective treatments for Meniere's disease. In addition, China, Japan, and Germany have also published many articles, but these countries lack cooperation with each other, so these countries have relatively low centrality. We suggest that countries should strengthen cooperation to jointly promote the progress of Meniere's disease research which is eventually beneficial for patients. In terms of Meniere's disease research, the top 10 institutions are from USA, Europe, and Japan, which confirm that research in developed countries is far ahead of relatively developing countries. University of Sydney, Massachusetts Eye and Ear Infirmary, and Nagoya University have the strongest collaborations with other institutions. Moreover, it suggests that there should be greater cooperation between institutions with less interaction.

Kitahara T has published the most articles in the field of Meniere's disease. Kitahara T's research focuses on the study of Meniere's disease, mainly including clinical research, diagnostic technology, international consensus, and diagnostic and therapeutic strategies. In addition, Naganawa S, Sone M, Nakashima T, and Pyykko I are the five most published scholars in the past two decades. Naganawa S, Nakashima T, Sone M, and Strupp M were the top four authors with a high H-index. Nonetheless, scholars who have made outstanding contributions to Meniere's disease research are mostly from developed countries, such as the United States, Europe, and Japan. Therefore, enhanced communication and collaboration among researchers around the world will facilitate the development of Meniere's disease research.

Meniere's disease-related articles are mostly published in leading journals in the field of ENT and neurology, including Otology & Neurotology, Acta Oto-Laryngologica, Laryngoscope, European Archives of Oto-Rhino-Laryngology, Otolaryngology-Head and Neck Surgery, Journal of Laryngology And Otology, Frontiers In Neurology, Auris Nasus Larynx, Annals of Otology Rhinology And Laryngology, and Audiology And Neuro-Otology. These journals are recognized as leading journals within the specialty, greatly contributing to the development of ENT and neurology. This trend suggests

that otolaryngologists and neurologists are dedicated to the disease together. Judging from the references cited, researchers are currently focusing more on the clinical management of Meniere's disease. It is worth mentioning that the first most cited reference is the article "Diagnostic Criteria for Meniere's Disease" published by Lopez-Escamez JA (18), which proposes normative diagnostic criteria for Meniere's disease. This is a milestone in the clinical treatment and management of Meniere's disease. At the same time, a dual-map (Figure 8) overlay also confirms that Meniere's disease's research focus has begun to transform from basic research to clinical research. The core of basic research includes Molecular, Biology, and Immunology. Such translation brings great benefits to Meniere's disease patients.

Judging by the frequency of keywords, the epidemiology, pathophysiology, and treatment of Meniere's disease remain as the focus of research. Burst keywords indicate cutting-edge and emerging trends in scientific research. Three frontiers of Meniere's disease research were identified: evoked myogenic potential (2016–2021), MRI (2018–2021), and committee (2018–2021). Meniere's disease is an extremely distressing disease, one of the reasons is that it is easy to be misdiagnosed due to the lack of clear diagnostic criteria. Thanks to the existence of the Committee on Hearing and Equilibrium of the American Academy of Otolaryngology (AAO-CHE), the clinical guidelines of Meniere's disease were clarified, which greatly improved the diagnosis and treatment of Meniere's disease (22). Vestibular evoked myogenic potentials (VEMPs) are short-latency vestibular reflexes primarily driven by otoliths and are often evoked by air-conducted sound (ACS), bone-conducted vibration (BCV), or electrical vestibular stimulation (23, 24), although vestibular function tests alone have limited diagnostic value for Meniere's disease. However, the diagnosis of Meniere's disease still needs a comprehensive evaluation with vestibular function examination (25). In 2007, scholars confirmed the existence of endolymphatic hydrops in Meniere's disease patients using MRI imaging with intratympanic gadolinium (19, 26). Although MRI is not the gold standard for the diagnosis of Meniere's disease, it still contributes to the development of Meniere's disease (27).

The treatment of Meniere's disease has been a challenge for neurologists and otolaryngologists for a long time. The pathogenesis of Meniere's disease is mainly related to idiopathic endolymphatic hydrops in the cochlear duct and vestibular organs (28). Current treatments for Meniere's disease mainly include conservative drugs such as diuretics and betahistine, intratympanic steroids, endolymphatic sac surgery or intratympanic gentamicin, and destructive surgery (29, 30). The onset of clinical symptoms of Meniere's disease is often random, and there may be periods of remission lasting months to years. For the reason, the misdiagnosis, which results in poor outcomes, is common (31). In particular, vestibular migraine (VM) and Meniere's disease overlap in clinical symptoms in patients without hearing loss, and these disorders may co-occur, with some studies estimating a 35% incidence of VM in Meniere's disease patients (32).

We observe that endolymphatic hydrops, genes, and immunology are the focus of research in Meniere's disease. Endolymphatic hydrops is an area of lymphatic fluid accumulation in the inner ear that occupies the perilymphatic space, mostly in the cochlear duct and saccule, and occasionally in the utricle and semicircular canal (21). At present, endolymphatic hydrops can be visualized by injecting gadolinium contrast agent, which increases the diagnostic rate of Meniere's disease (33). Scholars have confirmed that the degree of endolymphatic hydrops is related to the stage of Meniere's disease, low-frequency hearing threshold, EchoG, and VEMP asymmetry ratio (34, 35). Meniere's disease is mostly attributed to endolymphatic hydrops in the inner ear. However, some evidence supports genetic contribution to Meniere's disease. The incidence of Meniere's disease varies in different ethnic backgrounds and geographical regions. In different regions, the incidence of Meniere's disease was 43/100.000 (in Finland), 56/10.000 (in UK), 200/100.000 (in USA), and 17-34.5/100.000 (in Japan) (31, 36, 37). Genetically, variant forms of Meniere's disease include monogenic forms in isolated families and polygenic forms in most familial and sporadic cases. Mutated genes in sporadic cases include GJB2, USH1G, SLC26A4, ESRRB, CLDN14, NTN4, and NOX3 (38). In familial Meniere disease, mutated genes include FAM136A, DTNA, PRKCB, COCH, DPT, SEMA3D, STRC, HMX2, TMEM55B, OTOG, and LSAMP (39). Moreover, multiple rare missense variants in the OTOG gene are related to 33% familial Meniere disease (40). The role of immune mechanisms in the development of MD is also a hot topic. The possible immune mechanisms of Meniere's disease include type I allergy, autoimmunity, circulating immune complexes, and immune genetics. The inner ear might participate in immune responses as autoantigens, including cellular and humoral immunity (41, 42). This allows neurologists and otolaryngologists to obtain more accurate pathogenesis, which can help improve the diagnosis and treatment of Meniere's disease. This will also make precision therapy and targeted therapy possible.

Limitations

Certain limitations should be acknowledged. First, the constant updating of the database may lead to discrepancies between the number of articles retrieved and those included. Second, although the data for bibliometric analysis mainly come from the WoSCC database, some articles from other databases may be missed (43, 44). In addition, the absence of books, chapters, letters, and non-English literature may contribute to the bias of our analysis. Finally, different countries invest differently in Meniere's disease researches, which may

be a potential source of bias. Nonetheless, this study presents the status and trends of Meniere's disease research through bibliometric analysis. Visual analysis of published literature helps researchers quickly understand hotspots and trends in Meniere's research, providing a basis for finding new research directions.

Conclusion

The number of publications in the field of Meniere's disease was steadily increasing over the past two decades. Research on Meniere's disease may become a hotspot in neurology and otolaryngology in future. There are far more articles published in the journals of otolaryngology and neurology than other journals. The United States contributes ∼30% of Meniere's disease publications, which greatly improved the treatment status of Meniere's disease. Meanwhile, China is the only developing country in the top 10 countries that contributed mostly in the relative fields. Therefore, it is urgent to strengthen the collaboration between different research teams. Further research into Meniere's disease will benefit a wide range of patients. Endolymphatic hydrops, pathophysiology, and therapy are the current research hotspots in the field of Meniere's disease.

Data availability statement

The original contributions presented in the study are included in the article/supplementary material, further inquiries can be directed to the corresponding author.

Author contributions

WZ and DH conceived the study. WZ, QL, and FP collected the data. WZ and FP re-examined the data and analyzed the data. WZ wrote the manuscript. FP reviewed and revised the manuscript. All authors contributed to the article and approved the submitted version.

Conflict of interest

The authors declare that the research was conducted in the absence of any commercial or financial relationships that could be construed as a potential conflict of interest.

Publisher's note

All claims expressed in this article are solely those of the authors and do not necessarily represent those of their affiliated organizations, or those of the publisher, the editors and the reviewers. Any product that may be evaluated in this article, or claim that may be made by its manufacturer, is not guaranteed or endorsed by the publisher.

References

1. Sajjadi H, Paparella MM. Meniere's disease. *Lancet.* (2008) 372:406–14. doi: 10.1016/S0140-6736(08)61161-7

2. Harris JP, Alexander TH. Current-day prevalence of Meniere's syndrome. *Audiol Neurootol.* (2010) 15:318–22. doi: 10.1159/000286213

3. Harcourt J, Barraclough K, Bronstein AM. Meniere's disease. *BMJ.* (2014) 349:g6544. doi: 10.1136/bmj.g6544

4. Stephens D, Pyykko I, Varpa K, Levo H, Poe D, Kentala E. Self-reported effects of Meniere's disease on the individual's life: a qualitative analysis. *Otol Neurotol.* (2010) 31:335–8. doi: 10.1097/MAO.0b013e3181bc35ec

5. Arroll M, Dancey CP, Attree EA, Smith S, James T. People with symptoms of Meniere's disease: the relationship between illness intrusiveness, illness uncertainty, dizziness handicap, and depression. *Otol Neurotol.* (2012) 33:816–23. doi: 10.1097/MAO.0b013e3182536ac6

6. James AL, Burton MJ. Betahistine for Meniere's disease or syndrome. *Cochrane Database Syst Rev.* (2001) 2001:CD001873. doi: 10.1002/14651858.CD001873

7. Thirlwall AS, Kundu S. Diuretics for Meniere's disease or syndrome. *Cochrane Database Syst Rev.* (2006) 2006:CD003599.

8. Ma C, Su H, Li H. Global research trends on prostate diseases and erectile dysfunction: a bibliometric and visualized study. *Front Oncol.* (2020) 10:627891. doi: 10.3389/fonc.2020.627891

9. Zhang J, Zhang Y, Hu L, Huang X, Liu Y, Li J, et al. Global trends and performances of magnetic resonance imaging studies on acupuncture: a bibliometric analysis. *Front Neurosci.* (2020) 14:620555. doi: 10.3389/fnins.2020.620555

10. Duong A, Kay J, Khan M, Simunovic N, Ayeni OR. Authorship in the field of femoroacetabular impingement: an analysis of journal publications. *Knee Surg Sports Traumatol Arthrosc.* (2017) 25:94–100. doi: 10.1007/s00167-016-4058-5

11. Zhu H, Zhang Z. Emerging trends and research foci in cataract genes: a bibliometric and visualized study. *Front Genet.* (2021) 12:610728. doi: 10.3389/fgene.2021.610728

12. Zhao Y, Zhang X, Song Z, Wei D, Wang H, Chen W, et al. Bibliometric analysis of ATAC-seq and its use in cancer biology via nucleic acid detection. *Front Med (Lausanne).* (2020) 7:584728. doi: 10.3389/fmed.2020.584728

13. Jia B, Chen Y, Wu J. Bibliometric analysis and research trend forecast of healthy urban planning for 40 years (1981-2020). *Int J Environ Res Public Health.* (2021) 18:18. doi: 10.3390/ijerph18189444

14. Xu D, Zheng Y, Jia Y. The bibliometric analysis of the sustainable influence of physical education for university students. *Front Psychol.* (2021) 12:592276. doi: 10.3389/fpsyg.2021.592276

15. Moffatt DC, Shah P, Wright AE, Zon K, Pine HS. An otolaryngologist's guide to understanding the h-index and how it could affect your future career. *OTO Open.* (2022) 6:2473974X221099499. doi: 10.1177/2473974X221099499

16. Nowak JK, Lubarski K, Kowalik LM, Walkowiak J. H-index in medicine is driven by original research. *Croat Med J.* (2018) 59:25–32. doi: 10.3325/cmj.2018.59.25

17. Luo H, Cai Z, Huang Y, Song J, Ma Q, Yang X, et al. Study on pain catastrophizing from 2010 to 2020: a bibliometric analysis via CiteSpace. *Front Psychol.* (2021) 12:759347. doi: 10.3389/fpsyg.2021.759347

18. Lopez-Escamez JA, Carey J, Chung WH, Goebel JA, Magnusson M, Mandala M, et al. Diagnostic criteria for Meniere's disease. *J Vestib Res.* (2015) 25:1–7. doi: 10.3233/VES-150549

19. Nakashima T, Naganawa S, Sugiura M, Teranishi M, Sone M, Hayashi H, et al. Visualization of endolymphatic hydrops in patients with Meniere's disease. *Laryngoscope.* (2007) 117:415–20. doi: 10.1097/MLG.0b013e31802c300c

20. Merchant SN, Adams JC, Nadol JB. Pathophysiology of Meniere's syndrome: are symptoms caused by endolymphatic hydrops? *Otol Neurotol.* (2005) 26:74–81. doi: 10.1097/00129492-200501000-00013

21. Merchant SN, Rauch SD, Nadol JB. Meniere's disease. *Eur Arch Otorhinolaryngol.* (1995) 252:63–75. doi: 10.1007/BF00168023

22. Stapleton E, Mills R. Clinical diagnosis of Meniere's disease: how useful are the American Academy of Otolaryngology Head and Neck Surgery Committee on Hearing and Equilibrium guidelines? *J Laryngol Otol.* (2008) 122:773–9. doi: 10.1017/S0022215107000771

23. Curthoys IS, Dlugaiczyk J. Physiology, clinical evidence and diagnostic relevance of sound-induced and vibration-induced vestibular stimulation. *Curr Opin Neurol.* (2020) 33:126–35. doi: 10.1097/WCO.0000000000000770

24. Rosengren SM, Colebatch JG, Young AS, Govender S, Welgampola MS. Vestibular evoked myogenic potentials in practice: Methods, pitfalls and clinical applications. *Clin Neurophysiol Pract.* (2019) 4:47–68. doi: 10.1016/j.cnp.2019.01.005

25. Xu M, Chen ZC, Wei XY, Zhang YZ, Yang FY, Zhang C, et al. Evaluation of vestibular evoked myogenic potential, caloric test and cochlear electrogram in the diagnosis of Meniere's disease. *Lin Chung Er Bi Yan Hou Tou Jing Wai Ke Za Zhi.* (2019) 33:704–8.

26. Naganawa S, Sugiura M, Kawamura M, Fukatsu H, Sone M, Nakashima T. Imaging of endolymphatic and perilymphatic fluid at 3T after intratympanic administration of gadolinium-diethylene-triamine pentaacetic acid. *AJNR Am J Neuroradiol.* (2008) 29:724–6. doi: 10.3174/ajnr.A0894

27. Neri G, Tartaro A, Neri L. MRI With intratympanic gadolinium: comparison between otoneurological and radiological investigation in Meniere's disease. *Front Surg.* (2021) 8:672284. doi: 10.3389/fsurg.2021.672284

28. Hallpike CS, Cairns H. Observations on the pathology of Meniere's syndrome: (Section of Otology). *Proc R Soc Med.* (1938) 31:1317–36. doi: 10.1177/003591573803101112

29. Espinosa-Sanchez JM, Lopez-Escamez JA. The pharmacological management of vertigo in Meniere disease. *Expert Opin Pharmacother.* (2020) 21:1753–63. doi: 10.1080/14656566.2020.1775812

30. Nevoux J, Barbara M, Dornhoffer J, Gibson W, Kitahara T, Darrouzet V. Authors' response to the letter on the article: "International consensus (ICON) on treatment of Meniere's disease". *Eur Ann Otorhinolaryngol Head Neck Dis.* (2020) 137:239. doi: 10.1016/j.anorl.2020.01.019

31. Watanabe Y, Mizukoshi K, Shojaku H, Watanabe I, Hinoki M, Kitahara M. Epidemiological and clinical characteristics of Meniere's disease in Japan. *Acta Otolaryngol Suppl.* (1995) 519:206–10. doi: 10.3109/00016489509121906

32. Shin CH, Kim Y, Yoo MH, Kim TS, Park JW, Kang BC, et al. Management of Meniere's disease: how does the coexistence of vestibular migrainE AFFECT OUTCOMES? *Otol Neurotol.* (2019) 40:666–73. doi: 10.1097/MAO.0000000000002176

33. Paskoniene A, Baltagalviene R, Lengvenis G, Beleskiene V, Ivaska J, Markeviciute V, et al. The importance of the temporal bone 3t mr imaging in the diagnosis of Meniere's disease. *Otol Neurotol.* (2020) 41:235–41. doi: 10.1097/MAO.0000000000002471

34. Sun Q, Jiang G, Xiong G, Sun W, Wen W, Wei F. Quantification of endolymphatic hydrops and its correlation with Meniere's disease clinical features. *Clin Otolaryngol.* (2021) 46:1354–61. doi: 10.1111/coa.13847

35. Xie J, Zhang W, Zhu J, Hui L, Li S, Ren L, et al. Differential diagnosis of endolymphatic hydrops between "probable" and "definite" Meniere's disease via magnetic resonance imaging. *Otolaryngol Head Neck Surg.* (2021) 165:696–700. doi: 10.1177/0194599821990680

36. Alexander T, Harris J. Current epidemiology of Meniere's syndrome. *Otolaryngol Clin North Am.* (2010) 43:965–70. doi: 10.1016/j.otc.2010.05.001

37. Kotimäki J, Sorri M, Aantaa E et al. Prevalence of Meniere disease in Finland. *Laryngoscope.* (1999) 109:748–53. doi: 10.1097/00005537-199905000-00013

38. Gallego M, Lopez E. Genetic architecture of Meniere's disease. *Hear Res.* (2020) 397:107872. doi: 10.1016/j.heares.2019.107872

39. Escalera B, Roman N, Lopez E. Systematic review of sequencing studies and gene expression profiling in familial Meniere disease. *Genes (Basel).* (2020) 11. doi: 10.3390/genes11121414

40. Roman N, GallegoM, Soto V, Aran I, Moleon M, Espinosa-Sanchez JM, et al. Burden of rare variants in the OTOG gene in familial Meniere's disease. *Ear Hear.* (2020) 41:1598–605. doi: 10.1097/AUD.0000000000000878

41. Rose N. Autoimmune disease 2002: an overview. *J Investig Dermatol Symp Proc.* (2004) 9:1–4. doi: 10.1111/j.1087-0024.2004.00837.x

42. Tomoda K, Suzuka Y, Iwai H, Yamashita T, Kumazawa T. Menière's disease and autoimmunity: clinical study and survey. *Acta Otolaryngol Suppl.* (1993) 500:31–4. doi: 10.3109/00016489309126174

43. Shao B, Qin YF, Ren SH, Peng QF, Qin H, Wang ZB, et al. Structural and temporal dynamics of mesenchymal stem cells in liver diseases from 2001 to 2021: a bibliometric analysis. *Front Immunol.* (2022) 13:859972. doi: 10.3389/fimmu.2022.859972

44. Sun W, Wan W, Gao Z, Suo T, Shen S, Liu H. Publication trends of research on gallbladder cancer during 2001-2021: a 20-year bibliometric analysis. *Front Oncol.* (2022) 12:932797. doi: 10.3389/fonc.2022.932797

frontiers | Frontiers in Neurology

TYPE Original Research
PUBLISHED 12 October 2022
DOI 10.3389/fneur.2022.984865

Check for updates

OPEN ACCESS

EDITED BY
Lisheng Yu,
Peking University People's Hospital, China

REVIEWED BY
Alexandre Bisdorff,
Hospital Center Emile Mayrisch, Luxembourg
Roberto Teggi,
San Raffaele Hospital (IRCCS), Italy

*CORRESPONDENCE
Xiaoshan Wang
lidou2005@126.com

†These authors have contributed equally to this work

SPECIALTY SECTION
This article was submitted to Neuro-Otology, a section of the journal Frontiers in Neurology

RECEIVED 02 July 2022
ACCEPTED 08 September 2022
PUBLISHED 12 October 2022

CITATION
Tang L, Jiang W and Wang X (2022) New onset episodic vertigo as a presentation of vestibular neuritis. *Front. Neurol.* 13:984865. doi: 10.3389/fneur.2022.984865

COPYRIGHT
© 2022 Tang, Jiang and Wang. This is an open-access article distributed under the terms of the Creative Commons Attribution License (CC BY). The use, distribution or reproduction in other forums is permitted, provided the original author(s) and the copyright owner(s) are credited and that the original publication in this journal is cited, in accordance with accepted academic practice. No use, distribution or reproduction is permitted which does not comply with these terms.

New onset episodic vertigo as a presentation of vestibular neuritis

Lu Tang†, Weiwei Jiang† and Xiaoshan Wang*

Department of Neurology, The Affiliated Brain Hospital of Nanjing Medical University, Nanjing Medical University, Nanjing, China

Objective: Vestibular neuritis (VN) is a common peripheral cause of acute vestibular syndrome, characterized by sustained vertigo and gait instability, persisting from 1 day to several weeks. With the widespread use of comprehensive vestibular function tests, patients with VN and non-sustained vertigo have drawn attention. In this study, we retrospectively analyzed the clinical presentation of patients with VN and episodic vertigo, aiming to expand the atypical clinical features of VN.

Methods: This retrospective study enrolled 58 patients with VN. Among them, 11 patients with more than 3 remissions per day, each lasting over 1 h were assigned to the episodic vertigo (EV) group, and 47 subjects without significant relief into the sustained vertigo (SV) group. Demographic information, clinical manifestations and data of supplementary examinations were collected and statistically analyzed. These patients were followed up 1 year after discharge to gather prognostic information.

Results: The incidence of spontaneous nystagmus (SN) and proportion of severe vertigo (Dizziness Handicap Inventory questionnaire score >60) in the SV group were significantly higher than those in the EV group. Spearman correlation showed that with a longer disease course, the velocity of overt saccade was smaller ($p < 0.05$, $Rs = -0.263$) in all patients with VN.

Conclusion: The non-sustained manifestations in VN overlap with a wider spectrum of other vestibular disorders and stroke-related vertigo, which add an additional layer of complexity to the differential diagnosis of new onset episodic vertigo. By retrospectively analyzing the clinical characteristics and vHIT parameters, our study has expounded on the atypical features and potential pathophysiological mechanism of episodic syndromes in VN. VOR gain and saccades measured by vHIT could be reliable indicators for vestibular rehabilitation process.

KEYWORDS

peripheral vestibular vertigo, vestibular neuritis, video head impulse test (vHIT), new onset episodic vertigo, overt saccades

Introduction

Vestibular neuritis (VN) is characterized by the sudden onset of sustained vertigo and gait instability. These symptoms develop acutely in minutes or hours. VN affects males and females equally, with a peak onset age of 40–50 years (1, 2). It is always accompanied by nausea or vomiting, head motion intolerance, and nystagmus. The sense of imbalance and unsteadiness may linger for weeks (1, 3). As the second common peripheral cause of acute vestibular syndrome next to benign episodic positioning vertigo, VN is diagnosed in 3.2–9% of patients visiting clinics because of dizziness (3). Inflammatory etiology of VN has long been hypothesized on the basis of its association with respiratory tract infections and its frequent occurrence in epidemics (3, 4). Inflammatory activation after infections leads to a systemic reaction reducing microvascular perfusion and vestibular organ infarction, thus causing the loss of vestibular function (5). Possible comorbidity with herpes simplex virus type 1 reactivation or influenza virus infection has also been proposed (6, 7). Nevertheless, evidence of systemic viral infection based on seroconversion remain unconvincing (3).

As defined by the Committee for the Classification of Vestibular Disorders of the Bárány Society, patients are suspected of acute unilateral vestibulopathy / VN when they have prolonged vertigo with unsteadiness, nausea/vomiting and/or oscillopsia for days or weeks, and spontaneous horizontal–torsional nystagmus with the quick phase beating away from the lesion side (8, 9). The diagnosis of VN is generally based on the comprehensive interpretation of clinical symptomatology, laboratory evaluation and reasonable exclusion of other disorders, such as acute central lesions or peripheral audiological vestibular disorders (9, 10). Neurological signs are very important for the diagnosis of VN. Performed by trained specialists, the HINTS exam (Head Impulse, Nystagmus and Test of Skew) is a series of three bedside ocular motor tests that can be used to differentiate central and peripheral symptoms in patients with acute vestibular syndrome (11–14). Head impulse tests (HITs) could identify the function of the six semicircular canals over a high frequency range, which is similar to those of head movements (15–17). With a video-monitoring system, the video HITs (vHITs) provide objective measurement of the vestibular- ocular- reflex (VOR) gains and saccade parameters by capturing eye and head movements (18). Spontaneous nystagmus (SN) suppressed by fixation is an important clinical sign in patients with VN, which is caused by an imbalance average firing rate in the vestibular nerve on both sides (19). Skew deviation is a sign of an abnormal otolith-ocular reflex (OOR). Large amplitude skew deviation and the ocular tilt reaction (OTR) are commonly seen in central lesions (14, 20, 21), but rarely in VN (22).

Vestibular function evaluation is also useful for the diagnosis of VN. For example, caloric tests are used in investigating the function of the horizontal semicircular canal in the low frequency range (∼0.003 Hz), in which a canal paresis (CP) of ≥ 25% is the diagnostic hallmark of VN (10, 23). Other quantitative assessments, such as vestibular evoked myogenic potentials (VEMPs) (24, 25), subjective visual vertical (SVV) (26) and vestibular autorotation test (VAT) (27), are also helpful tools for evaluating the diagnosis and prognosis of VN. Although there is no definite examination for VN, these approaches can help evaluate different portions of the peripheral vestibular system and appear to complement each other.

With the widespread application of neurological examination and vestibular electrophysiology tests, we have previously observed the patients diagnosed with VN experienced episodic vertigo. A few studies have revealed the atypical features in VN, such as transient dizziness or prodromal unsteadiness before severe prolonged vertigo, overturning the general awareness of VN symptoms (3, 28, 29). Reportedly, VN is the third common trigger after benign paroxysmal positional vertigo (BPPV) and vestibular migraine of secondary functional dizziness (9). Nevertheless, appropriate rehabilitation promoted in time could benefit patients with less sequelae and functional disturbance (30, 31). Since transient ischemic attack (TIA) of vertebrobasilar territory could also manifest as recurrent vertigo, we sought to retrospectively analyze the clinical features of VN patients with episodic vertigo, aiming to alert awareness of the diagnostic confusion.

Methods

Participants

A total of 100 patients diagnosed with VN were screened for inclusion from January 2018 to June 2022. They were hospitalized in the Neurology Division Vertigo Center at the Affiliated Brain Hospital of Nanjing Medical University. All subjects were inquired about their symptoms and completed the Chinese version of the original dizziness handicap inventory (DHI) questionnaire at initial visit. We emphasized the symptomatic persistence at rest when taking the semeiology of a case. Patients who met all of the following criteria were enrolled in this study: (1) patients without vertigo history by complaint of a sudden onset of vertigo (more than 24 h); (2) patients with positive first degree vestibular nystagmus and negative skew deviation test; (3) patients without brain lesions according to magnetic resonance imaging (MRI) and diffusion-weighted imaging; (4) patients with either horizontal or vertical vHITs gain value of <0.8 and corrective saccades peak velocity of $>100^{\circ}/s$ (32–34); (5) patients with affected horizontal semicircular canals, vHITs showing corrective saccades on the side of slow-phase SN, and CP of $>25\%$ according to caloric examination. The following patients were excluded: (1) patients

with medical history of diabetes, migraine, vertigo or anxiety; (2) patients with auditory symptoms, such as hearing loss, tinnitus, or ear fullness on either side; and (3) patients without adequate supplementary examinations for this study, including DHI, caloric tests, vHITs and MRI. In total, 58 patients met the inclusion criteria for this study. Patients with more than 3 remissions per day, each lasting over 1 h were assigned to the episodic vertigo (EV) group, and subjects without significant relief into the sustained vertigo (SV) group. The flow chart for screening and grouping patients is shown in Figure 1.

Vestibular function test

Vestibular function tests, composed of nystagmus evaluation, bilateral caloric tests and vHITs, were performed within 2 days after the first visit. All patients were asked to take the tests during the symptomatic phases. An infrared-illuminated, vision-denied video nystagmography (VNG) goggle (VG40, ICS Medical Schaumburg, IL, USA) was used to record the intensity and direction of the slow-phase velocity (SPV) of SN. The SN was captured in darkness in the sitting position without visual fixation, when eyes are pointing straight ahead and laterally to either side. SPV toward the left was defined as positive, and toward right as negative.

Before a caloric test, an otoscope was used in excluding contraindications, such as tympanic membrane perforation. Patients were asked to place their heads on the pillows raised by 30°. Each ear was irrigated with constant airflow at alternating temperatures of 24 °C and 50 °C for 30 s (23). The nystagmus was recorded using an infrared video-based system (CHARTR VNG, ICS Medical Schaumburg, IL, USA). The maximum SPV of the nystagmus was calculated after each irrigation, and Jongkees' formula was used to determine CP.

The high-frequency VOR functions of horizontal and vertical canals were assessed by vHITs, which were applied in all the subjects using ICS impulse system (Otometrics, Denmark). The impulse system includes a pair of goggles with integrated video oculography camera and a half-silvered mirror. The subject's right eye was illuminated by a low-power infrared light-emitting diode, and was reflected into the camera by the mirror. The parameters of eyeball movements were thus recorded. A small sensor placed on the goggles was used to measure head movements of the subjects.

All examinations were performed by a skilled physician who specialized in neurotological testing and vHITs. The patients were asked to gaze at an earth-paralleled target 1.2 m in front during the examination. Firstly, calibration was performed by subjects staring at the left and right laser targets alternately. The horizontal canals were subsequently evaluated after excluding the interference of blinking or eyeballs-swaying. The physician stood behind a patient and turned the patient's head to the left and right unpredictably at a small angle (10°-20°) with an appropriate velocity (150°-200° per second). The movement of the head in the horizontal plane stimulated the lateral semicircular canals, and the movement was only in the atlanto-occipital joint pivoting around the odontoid apophysis axis (35). Next, the physician rotated the subject's head at a 45° angle relative to the trunk to evaluate the vertical semicircular canals. The head impulses were performed downward to stimulate the

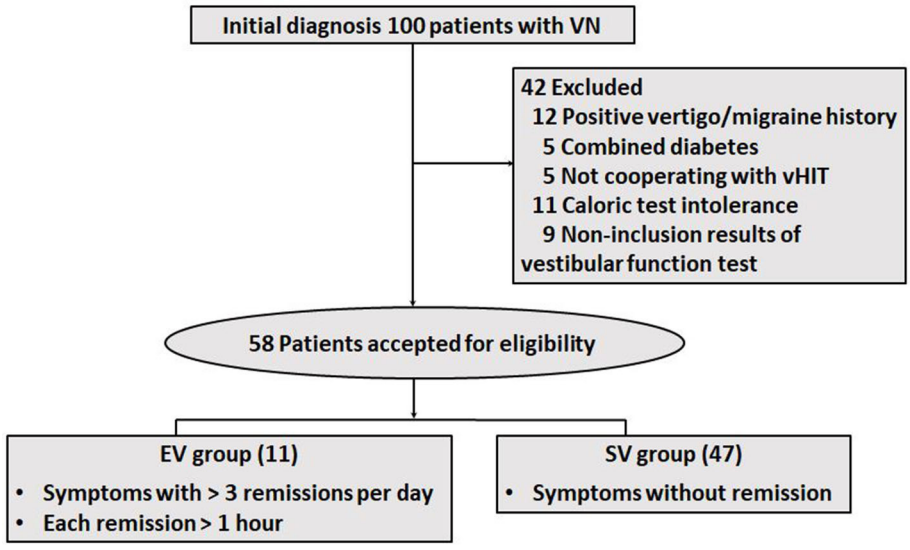

FIGURE 1
Flow chart for enrolling and grouping patients.

anterior canal opposite to the side of rotation, and upward to stimulate the posterior canal at the side of rotation (15). In a full test, 20 impulses were applied to each direction (36).

Statistics

The threshold of statistical significance for differences was set $P < 0.05$ for each test. The Wilcoxon rank sum test was done to analyze ordered categorical data. As for quantitative data, the description was expressed as mean ± standard deviation ($x \pm s$). Student's *t*-test was used to compare the quantitative data when they accorded with a normal distribution and their variance was homogeneous. Otherwise, the Wilcoxon signed rank sum test was used. The rates of the two groups were compared *via* Chi-square test. Correlation analysis was conducted to determine the relevance between variables of overt saccades, VOR gain and DHI score. Statistical analyses were performed using SPSS version 25.0 for Windows (SPSS Inc., Chicago, IL, USA).

Results

We finally enrolled a total of 58 patients who experienced visual rotation or gait instability diagnosed with VN. The patients were composed of 29 males and 29 females, aged 21–83. More than half of them (31 subjects) went to a vertigo clinic within 5 days. The EV group composed of 11 subjects, whose average age was 58.27 ± 15.05, the SV group included 47 subjects, whose average age was 51.04 ± 15.21. In the EV group, 9 patients only had episodic vertigo from the onset to their initial consultation, whereas 2 patients had transient vertigo before the onset of prolonged symptoms. The demographic, and clinical characteristics of the subjects are shown in Tables 1, 2. For the typical vHIT results of the subjects, see Figure 2.

Patients were treated with 40 mg of pulse methylprednisolone, which was reduced by half every 3 days, as well as physical rehabilitation. Oral anxiolytics was initiated for some patients with severe vertigo after consulting the psychiatrist. All the patients were relieved of their symptoms after 2 weeks of treatment. In the first year of follow-up, no patient reported the recurrence of vertigo or gait instability.

Statistical analysis revealed that compared to the EV group, patients in the SV group had significantly higher occurrence of SN and proportion of severe vertigo (DHI questionnaire score > 60). No significant differences were found in gender, age, disease course, prodromal infection history, incidence of covert saccade, impaired vestibular nerve and bilateral VOR difference between the two groups. Since the data of disease course and DHI score accorded with skewed distribution, Spearman correlation analysis was applied to reveal the associations of the overt saccade (latency and velocity), VOR gain and disease course. Statistical analysis reveal that the velocity of overt saccade was negatively correlated with disease course ($P < 0.05$, Rs $= -0.263$) in patients with VN. Detailed statistical results are shown in Table 3 and Figure 3.

Discussion

The typical manifestations of VN include severe prolonged vertigo and SN. With the advancement in vestibular function testing which evaluate different portions of the peripheral vestibular system, the diagnosis of VN is no longer restricted to symptomatology and limited supplementary tests. For example, vHITs permit evaluation of the angular VOR in the plane of all six semicircular canals (15, 28). Other quantitative assessments also provide more indicators other than CP, such as VOR gain, saccades, VEMP response and deflection angle of SVV, to assess the clinical course and prognosis of VN (24, 26, 37). Benefited from advances in vestibular testing, an increasing number of episodic atypical syndromes in VN were therefore recognized. According to Lee (28), approximately a quarter of patients experienced transient dizziness before severe prolonged vertigo. Silvoniemi (3) found that 8.6% of patients with VN had a mild prodromal sensation of unsteadiness 1–7 days before the onset of intensive vertigo. To the best of our knowledge, no study has systematically analyzed the characteristics of VN patients with episodic vertigo. This study presented those 11 (19.0%) patients with VN and episodic sense of vertigo, among whom 2 (3.4 %) had episodic manifestation before the prolonged syndrome onset. Since this study aimed to disclose the episodic syndromes in patients with VN, we assigned the 2 cases into the EV subgroup according to the grouping criteria.

There were 31 patients (53.4 %) enrolled in this study within 5 days from the onset. 12 of whom were re-examined for the vHITs at discharge. However, we did not track their vHITs in the early stages in this study. By sequentially measuring the VOR gains of patients with acute VN, previous studies have found the ipsilesional VOR gains vary after the initial measurement during the week from onset (38, 39). Meanwhile, patients with lower initial VOR gains were less likely to improve on subsequent 3–5 days, and would generate more covert catch-up saccades over time (39).

Compared to those with sustained vertigo, patients with episodic syndrome reported lower incidence of SN. In this study, SN referred to the nystagmus recorded while patients were looking in the straight-ahead (center gaze) position (40). Patients enrolled in this study without SN presented with first degree vestibular nystagmus while gazing at the contralesional side, indicating an acute phase of VN along with other inclusion criteria. According to previous researches, the intensity of SN could be modified in one or more other gaze positions (40). Since SN is the most prominent indicator of static vestibular imbalance, which could determine the severity of

TABLE 1 Demographic, clinical characteristics and vHIT results of the 58 VN patients.

No.	Gender	Age	Global duration of symptoms (days)	Duration of vertigo episodes (hours/day)	Frequency of vertigo episodes (daily)	DHI score	SN	SPV	Lesion	Ipsilesional VOR			Contralesional VOR			Mean latency of OS	Mean velocity of OS	CS
										LC	AC	PC	LC	AC	PC			
1	F	33	14	>5	3–5	56	N	/	R	0.68	0.72	0.60	1.05	0.91	0.73	159.0	149.0	P
2	M	47	3	1–2	2; persistent symptoms set in after 1 day	38	P	1.8	R	0.42	0.57	0.66	0.96	0.93	0.72	283.0	135.7	N
3	F	50	7	> 5	1–2	34	P	−1	L	0.29	0.79	0.94	1.13	0.90	1.12	241.5	244.0	N
4	M	51	10	>5	3–5	72	N	/	L	0.37	0.56	1.00	1.20	0.98	1.18	213.0	261.0	N
5	M	51	24	2–5	2; persistent symptoms set in after 2 days	68	N	/	R	0.53	0.55	0.43	0.85	0.87	0.67	169.0	284.0	P
6	M	54	15	2–5	2–3	14	N	/	R	0.76	0.61	0.85	1.20	0.83	0.83	241.3	180.0	N
7	F	56	7	>5	1–2	60	N	/	L	0.41	0.44	0.99	1.20	0.78	1.07	152.0	162.0	P
8	M	63	7	> 5	3–4	12	N	/	R	0.69	0.54	0.64	1.12	0.75	0.68	292.0	297.0	P
9	M	75	2	>5	2–3	56	P	4	R	0.63	0.62	0.50	0.72	0.89	0.47	248.0	158.0	N
10	F	78	30	1–2	> 5	38	N	/	R	0.35	0.64	0.45	0.88	0.82	0.74	240.0	287.5	N
11	M	83	3	1–2	3–4	28	N	/	L	0.78	0.78	0.59	1.20	1.03	0.51	209.5	226.0	P
12	F	52	2.5	/	/	58	N	/	R	0.72	0.74	0.82	1.20	1.04	0.80	195.5	159.5	P
13	F	53	7	/	/	62	P	−5	L	0.06	0.38	0.24	0.72	0.95	0.44	120.0	118.7	N
14	F	54	3	/	/	68	P	1.2	R	0.60	0.45	0.91	0.88	0.77	0.72	297.0	105.5	N
15	M	32	10	/	/	30	P	−2	L	0.23	0.34	0.48	0.94	0.89	0.70	193.0	192.0	P
16	F	34	2	/	/	64	N	/	R	0.11	0.77	0.74	0.92	0.85	0.82	275.5	272.0	P
17	F	34	10	/	/	60	P	3.2	R	0.43	0.63	0.72	0.89	0.60	0.81	219.5	192.5	N
18	F	38	2	/	/	68	P	1	R	0.40	0.77	1.15	1.02	0.58	0.87	183.0	143.0	N
19	F	42	2	/	/	52	P	3.6	R	0.38	0.31	0.59	1.03	0.93	0.86	247.5	193.0	N
20	F	43	20	/	/	74	P	−4.8	L	0.56	0.43	0.82	0.60	0.91	0.82	258.0	224.0	N
21	M	45	10	/	/	56	N	/	R	1.20	0.87	0.56	1.20	0.85	0.95	286.5	172.0	P

(Continued)

10.3389/fneur.2022.984865

TABLE 1 (Continued)

No.	Gender	Age	Global duration of symptoms (days)	Duration of vertigo episodes (hours/day)	Frequency of vertigo episodes (daily)	DHI score	SN	SPV	Lesion	Ipsilesional VOR			Contralesional VOR			Mean latency of OS	Mean velocity of OS	CS
										LC	AC	PC	LC	AC	PC			
22	M	48	5	/	/	50	P	4	R	0.79	0.48	0.89	1.20	1.00	0.85	254.5	178.5	N
23	M	49	2	/	/	68	P	−4.7	L	0.20	0.30	0.51	0.84	0.58	0.75	278.0	296.0	N
24	F	67	3	/	/	50	N	/	R	0.78	0.73	1.09	1.06	1.06	0.88	116.0	174.0	N
25	F	67	7	/	/	32	N	/	R	0.40	0.44	0.83	0.98	0.94	0.75	376.0	359.0	N
26	M	68	10	/	/	38	P	−3	L	0.77	0.93	0.47	1.12	0.94	0.71	213.0	160.0	N
27	M	73	14	/	/	20	N	/	L	0.65	0.66	0.44	0.87	0.92	0.68	306.0	136.5	N
28	F	59	30	/	/	76	N	/	R	1.07	0.87	0.68	1.11	1.09	0.77	190.0	229.0	N
29	M	75	2	/	/	66	P	5	R	0.77	0.75	0.91	0.81	0.95	0.79	310.0	140.0	N
30	F	76	7	/	/	60	N	/	R	0.52	0.22	0.74	0.97	0.58	0.42	208.0	200.0	N
31	F	83	2	/	/	46	N	/	L	0.78	0.66	0.69	1.19	0.83	0.72	234.0	84.5	N
32	M	64	2	/	/	68	P	−2.4	L	0.44	0.34	0.87	0.81	0.80	0.82	293.5	221.0	P
33	M	53	2.5	/	/	20	P	−3	L	0.25	0.53	0.87	0.82	0.87	0.72	288.5	182.5	N
34	F	67	10	/	/	76	N	/	R	0.74	0.78	0.70	1.04	0.81	0.82	248.5	159.0	N
35	F	61	3	/	/	62	P	3	R	0.50	0.64	0.33	0.75	0.65	0.78	216.0	163.5	P
36	M	30	24	/	/	62	N	/	R	0.67	0.78	0.95	0.88	0.96	1.20	276.0	168.0	P
37	M	61	3	/	/	60	P	2	R	0.36	0.38	0.42	0.85	0.87	0.67	171.0	130.0	N
38	F	57	2.5	/	/	74	P	5	R	0.38	0.43	0.73	1.05	0.89	0.83	338.0	197.0	N
39	M	37	1.2	/	/	68	P	2	R	0.72	0.57	1.05	1.20	1.05	1.13	265.0	274.0	P
40	M	62	3	/	/	30	P	−5	L	0.36	0.41	0.98	0.93	1.11	0.75	252.0	243.3	P
41	F	28	4	/	/	56	P	2	R	0.34	0.70	0.88	0.95	0.94	0.94	341.0	225.0	N
42	M	36	2.5	/	/	70	P	1	R	0.97	1.02	0.83	0.32	0.51	1.11	201.5	225.5	N
43	F	21	1.5	/	/	60	P	5	R	0.32	0.46	0.87	1.03	0.80	0.86	240.0	199.5	P
44	F	57	15	/	/	62	P	1	R	0.55	0.59	0.89	0.88	0.95	0.81	224.5	217.5	N
45	F	36	2	/	/	62	P	2	R	0.67	0.78	0.90	1.02	1.00	0.85	185.0	299.0	N
46	M	58	15	/	/	58	N	/	R	0.80	1.07	0.76	0.47	0.38	0.86	250.0	223.5	P
47	F	48	7	/	/	70	P	3	L	0.87	0.87	0.84	0.57	0.78	0.85	238.0	200.0	N
48	M	53	3	/	/	68	N	/	L	0.45	0.64	0.87	1.07	1.18	0.78	304.0	160.5	P
49	F	26	4	/	/	62	N	/	R	0.78	0.71	0.53	1.04	0.81	0.81	219.3	196.3	N

(Continued)

10.3389/fneur.2022.984865

10.3389/fneur.2022.984865

TABLE 1 (Continued)

No.	Gender	Age	Global duration of symptoms (days)	Duration of vertigo episodes (hours/day)	Frequency of vertigo episodes (daily)	DHI score	SN	SPV	Lesion	Ipsilesional VOR			Contralesional VOR			Mean latency of OS	Mean velocity of OS	CS
										LC	AC	PC	LC	AC	PC			
50	M	64	3	/	/	20	P	−6	L	0.26	0.49	0.51	1.00	0.69	0.63	283.5	168.5	P
51	M	38	2.5	/	/	70	P	−2.8	L	0.63	0.51	1.17	1.20	1.05	1.05	181.0	274.0	P
52	F	30	3	/	/	70	P	−1	L	0.48	0.53	0.78	0.86	1.07	0.70	242.5	170.5	P
53	M	48	32	/	/	76	N	/	L	0.31	0.67	0.65	0.99	1.02	0.81	228.7	147.7	P
54	F	58	22	/	/	38	N	/	R	1.00	0.94	0.92	0.59	0.55	0.49	245.7	158.0	P
55	M	45	14	/	/	60	P	1.4	R	0.48	0.36	0.78	1.09	0.87	0.87	299.3	220.7	P
56	M	60	2	/	/	68	P	−2	L	0.70	0.45	0.80	1.19	1.00	0.72	257.5	167.5	N
57	F	56	7	/	/	42	P	−2.4	L	0.46	0.48	0.56	1.18	0.97	0.73	253.0	178.0	P
58	M	63	1.5	/	/	72	P	−5	L	0.37	0.41	0.73	1.18	1.02	0.77	292.0	272.0	N

F, female; M, male; N, negative; P, positive; LC, Lateral semicircular canal; AC, Anterior semicircular canal; PC, posterior semicircular canal; SN, spontaneous nystagmus in the sitting position; SPV, SPV of SN while looking straight-ahead in the sitting position; OS, overt saccades; CS, covert saccades.

TABLE 2 Clinical characteristics of all patients with vestibular neuritis.

		n %
Gender	Male	29 (50.0)
	Female	29 (50.0)
Age (years)	≤65	47 (81.0)
	>65	11 (19.0)
Course (days)	≤5	31 (53.4)
	>5	27 (46.6)
Episodic vertigo	Positive	11 (19.0)
	Negative	47 (81.0)
History of prodromal infection	Positive	13 (22.4)
	Negative	45 (77.6)
Vestibular symptoms	Dizziness	15 (25.9)
	Oscillopsia	44 (75.9)
	Instability	36 (62.1)
Autonomic symptoms	Nausea	50 (86.2)
	Vomiting	44 (75.9)
Spontaneous nystagmus	Positive	33 (56.9)
	Negative	25 (43.1)
Impaired vestibular nerve	Superior	34 (58.6)
	Inferior	2 (3.4)
	Both	22 (37.9)
Compensatory saccade	Covert	24 (41.4)
	Overt	58 (100)
DHI questionnaire score	Mild to moderate (≤60)	31 (53.4)
	Severe (> 60)	27 (46.6)

clinical symptoms (40, 41), a lower incidence of SN implies a milder lesion of static imbalance and/or an improvement of nerve function after initial loss in patients with episodic syndrome (41). We thus presumed that patients in the EV group either had milder VOR deficiency or abided by more effective strategies of central compensation than those in the SV group.

To assess the behavioral and emotional status, patients were required to complete the DHI questionnaire at initial consultation. In this study, patients in the SV group had significantly higher occurrence of severe vertigo handicap (DHI score > 60) than those in the EV group. In other words, the life quality of patients in the SV group was considerably more likely to be affected by physical disability and psychological stress. This is in line with previous studies that patients with vestibular hypofunctional exhibited increasing incidence of anxiety and depressions (42, 43). In our research, a portion of patients with severe vertigo and emotional dysfunction were administered with oral anxiolytics after consulting the psychiatrist. At the 1-year follow-up, these patients presented no emotional disorders. From a therapeutic point of view, timely psychological treatment or drug intervention should

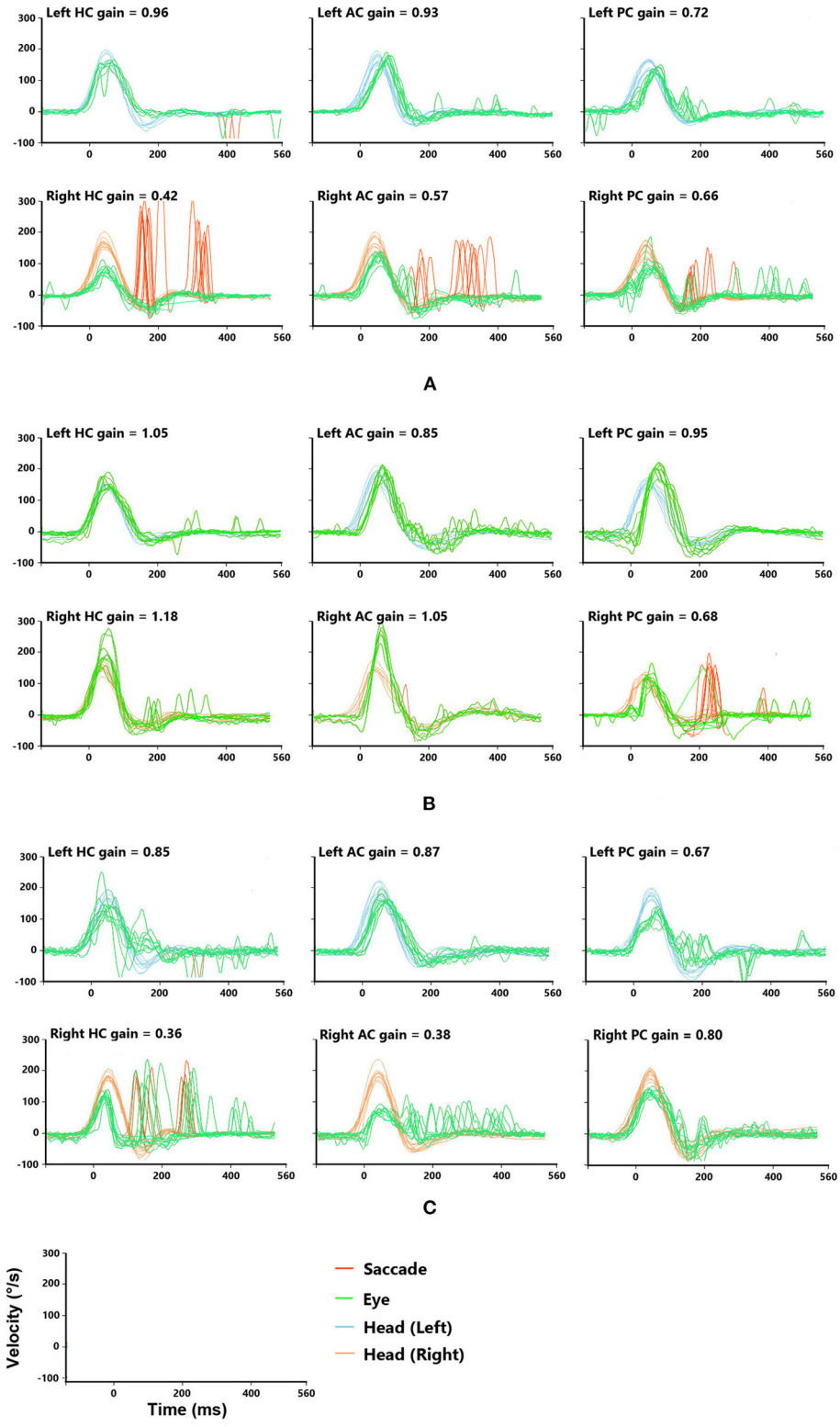

FIGURE 2
Typical vHITs images recorded from patients with episodic vertigo. The sample coordinates (last row) indicate the units of vHITs. **(A)** A patient with damaged superior and inferior vestibular nerves. The vHITs findings showed decreased VOR gains and corrective saccade for the right horizontal semicircular canal (HC) and vertical semicircular canals, including anterior and posterior semicircular canal (AC and PC). **(B)** A patient with damaged inferior vestibular nerve. The vHITs findings showed decreased gains in VOR for the right PC, while that for right the AC and HC was normal. **(C)** A patient with damaged superior vestibular nerve. The vHITs findings showed decreased gains of VOR for the right AC and HC. The VOR for right PC was normal.

TABLE 3 Statistical analysis between patients in the episodic vertigo (EV) group and the sustained vertigo (SV) group.

		EV	SV	t /z/x^2 value	*P* value	OR (95% CI)
Age (years)		58.27 ± 15.05	51.04 ± 15.21	−1.42	0.16	-
Lantency of overt saccade (ms)		234.44 ± 42.88	244.39 ± 53.41	0.58	0.57	-
Velocity of overt saccade (°/s)		186.18 ± 38.82	203.66 ± 57.84	0.95	0.35	-
Disease course (days)		7.00 (3.00, 15.00)	3.50 (2.00, 10.00)	−1.76	0.08	-
Bilateral VOR difference		0.29 ± 0.10	0.28 ± 0.12	−0.24	0.81	-
History of prodromal infection	Positive	3 (27.3 %)	10 (21.3 %)	0.001	0.98	-
	Negative*	8 (72.7 %)	37 (78.7 %)			
Spontaneous nystagmus in straight-ahead position	Positive	2 (18.2 %)	31 (66.0 %)	6.46	***0.01***	8.72 (1.68–45.25)
	Negative*	9 (81.8 %)	16 (34.0 %)			
Covert saccades	Positive	4 (36.4 %)	20 (42.6 %)	0.001	0.97	-
	Negative*	7 (63.6 %)	27 (57.4 %)			
Impaired vestibular nerve	Superior or inferior*	6 (54.5 %)	30 (63.8 %)	0.54	0.83	-
	Both	5 (45.5 %)	17 (36.2 %)			
Gender	male*	7 (63.6 %)	22 (46.8 %)	1.01	0.32	-
	female	4 (36.4 %)	25 (53.2 %)			
DHI questionnaire score	Mild to moderate (≤ 60)*	9 (81.8 %)	22 (46.8 %)	4.39	***0.04***	5.11 (1.00–26.25)
	Severe (> 60)	2 (18.2 %)	25 (53.2 %)			

*The control group in chi-square test. Statistical analysis revealed that patients with spontaneous nystagmus had significantly higher occurrence of sustained vertigo ($P < 0.05$, OR = 8.72). Besides, patients with severe vertigo (DHI questionnaire score > 60 points) had significantly higher occurrence of sustained vertigo ($P < 0.05$, OR = 5.11). *P*-value less than 0.05 are exhibited in bold and italic font.

be considered for patients with high DHI score to prevent emotional disorders.

In our research, two cases had inferior vestibular nerve affected only, and both reported sustained vertigo. The small sample size of inferior neuritis showed limited impact on statistical results. We analyzed the incidence of incomplete vestibular nerve (superior or inferior) impairment between the two groups, and no statistical differences were identified.

Of note, our study revealed that neither the VOR asymmetry between the subgroups showed a difference, nor did the VOR gain correlate with the DHI score in overall patients. Although the quantitative lesion indicators are commonly irrelevant to the intensity of symptoms in clinical practice, negative results without correlations are rarely seen in literature. Limited cases reported that some patients had physical signs of VN, but their ipsilesional VOR gains were in the normal range (39). By sequential head impulse measurements, Palla et al. found that VOR gains toward the ipsilesional side appeared to descend initially and then increased with the course, which was not parallel to the disease progression (38). From another perspective, the DHI questionnaire comprised 25 items with scores ranging from 0 and 100 points. It could be further subdivided into physical, functional, and emotional scores (44). The ipsilesional VOR gains could reflex the intensity of physical symptoms, but not the emotional and functional disabilities. Previous studies have shown that anxiety and dizziness are co-morbid symptoms in a larger percentage of patients (42). Emotion disorders could aggravate clinical symptoms (45–47) and thus impact the DHI score. Further study with multivariate analysis and larger sample size would be helpful to reveal the relationship between symptoms and lesion indicators.

In this study, 24 patients presented with both overt and covert saccades at vHITs, while 34 patients had overt saccades only. The velocity of overt saccades presented a negative correlation with the disease course in overall VN patients. This is in line with a previous study that the velocity of covert and overt saccade could exhibit a gradual decrease during follow-ups, while the latency of them remained unchanged (37). Triggered by the sensory stimulus from the cervico-ocular reflex (COR), covert saccades are considered facilitating dynamic compensation to overcome the inadequate VOR on the ipsilesional side (31, 38, 48). Overt saccades, as secondary catch-up saccades, are generated when the covert saccades fail to drive eye-movements reaching the target during head rotation. In line with previous study, our study found a certain number of patients presenting with covert saccades at early stage of VN (39). Therefore, the incidence and parameters of saccades, covert or overt, are a promising indicator for evaluation of vestibular deficit and central compensation other than VOR (49). We postulated that there could be a different saccadic strategy

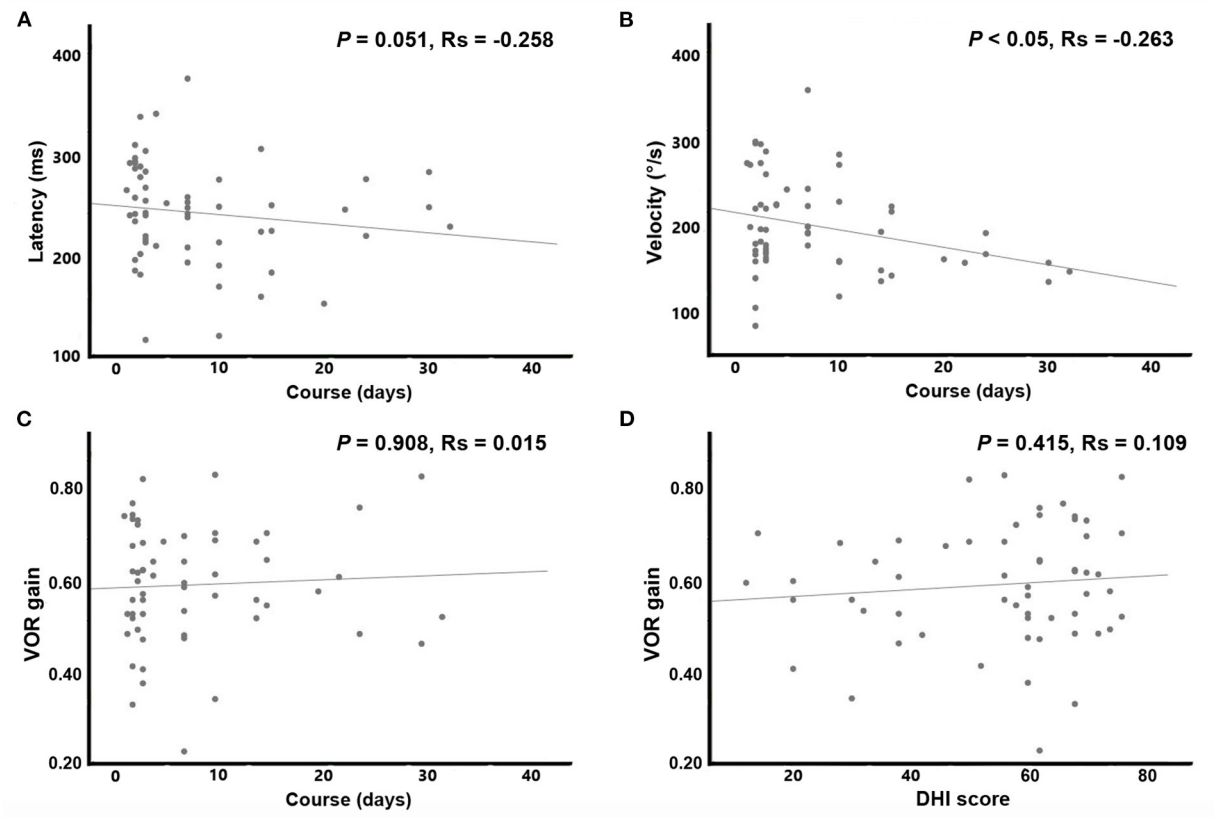

FIGURE 3
Scatterplots and results of Spearman correlation. With a longer disease course, the velocity of overt saccade was smaller ($p < 0.05$, Rs = −0.263) in patients with VN. **(A)** Abscissa: disease course (days); ordinate: latency of overt saccades (ms). **(B)** Abscissa: disease course (days); ordinate: velocity of overt saccades (°/s). **(C)** Abscissa: disease course (days); ordinate: VOR gain. **(D)** Abscissa: DHI score (points); ordinate: VOR gain.

between the EV and the SV groups, which might facilitate vestibular recovery and impact the manifestations. However, neither the incidence of overt saccades nor the parameters of covert saccades showed a significant difference between the two subgroups yet. Further investigation of larger samples might provide a better understanding of the different patterns of saccades in VN patients with episodic vertigo.

To date, diagnosis of VN remains to be exclusively based on symptomatology, and no supplementary testing can be used as a gold standard. Therefore, even with varied auxiliary results for reference, we still could not totally rule out the possibilities of alternative episodic vestibular syndromes in the enrolled patients with EV, such as a first manifestation of vestibular migraine or Meniere disease, not even a mild form of ischemic disease. Some supporting foundation would be that all patients exhibited a normal cranial MRI, and none of them had another episode during the one-year follow-up. Meanwhile, to make the VN diagnosis as accurate as possible, patients with auditory symptoms or a history of diabetes, migraine or anxiety were also excluded in this study. However, a long term follow-up is still warranted to fully exclude the possibility of other diseases.

This study has a few limitations. Firstly, the interference of personal emotions with the results was unavoidable. For example, in patients with severe vertigo and higher DHI score, the duration of remission period may have been subjectively shortened. To avoid the statistical bias, we used standard tabulated questionnaires, checking with families and telephone follow-ups to mutually verify the reliability of symptomatology data. Secondly, this study contained many variables whereas the sample size was only 58, a much smaller proportion of which exhibit of episodic vertigo. It is inappropriate to operate Logistic regression fitting the factors contributing to episodic vertigo, thus making the findings of this study unstable. Further prospective studies with a larger sample size would be established to vertify the value of parameters of SN and DHI score in VN diagnosis with episodic vertigo.

Conclusion

Our findings support the following conclusion: (1) some patients with VN may have episodic vertigo and instability;

(2) non-sustained manifestations in VN patients overlap with other vestibular disorders and stroke-related vertigo, which add an additional layer of complexity to the differential diagnosis of new onset episodic vertigo; (3) our retrospective analysis of the clinical characteristics and vHIT parameters reveals the atypical features and potential pathophysiological mechanism of episodic syndromes in VN; and (4) VOR gain and saccades measured by vHIT promise to be reliable indicators for vestibular rehabilitation process.

Data availability statement

The original contributions presented in the study are included in the article/supplementary material, further inquiries can be directed to the corresponding authors.

Ethics statement

The studies involving human participants were reviewed and approved by the Ethics Committee of the Affiliated Brain Hospital of Nanjing Medical University. Written informed consent to participate in this study was provided by the participants' legal guardian/next of kin.

Author contributions

LT conceived the content, wrote the preliminary version of the manuscript, and interpreted the data. WJ contributed to the patients' follow-ups, conceptualization of the content, and co-writing the academic content related to neurology. XW revised the article and approved the final manuscript before submission. All authors contributed to the article and approved the submitted version.

Acknowledgments

The authors would like to express their appreciation to Dr. Li Zhang, Feng Li, and Xiaobing Song of the Affiliated Brain Hospital of Nanjing Medical University, for screening patients and operating the vestibular function tests. The authors also thank Prof. Ronggen Shi from the School of Foreign Languages, Nanjing Medical University, for proofreading English in our manuscript.

Conflict of interest

The authors declare that the research was conducted in the absence of any commercial or financial relationships that could be construed as a potential conflict of interest.

Publisher's note

All claims expressed in this article are solely those of the authors and do not necessarily represent those of their affiliated organizations, or those of the publisher, the editors and the reviewers. Any product that may be evaluated in this article, or claim that may be made by its manufacturer, is not guaranteed or endorsed by the publisher.

References

1. Greco A, Macri GF, Gallo A, Fusconi M, De Virgilio A, Pagliuca G, et al. Is vestibular neuritis an immune related vestibular neuropathy inducing vertigo? *J Immunol Res.* (2014) 2014:459048. doi: 10.1155/2014/459048

2. Bartual-Pastor J. Vestibular neuritis: etiopathogenesis. *Rev Laryngol Otol Rhinol (Bord).* (2005) 126:279–81.

3. Silvoniemi P. Vestibular neuronitis. An otoneurological evaluation. *Acta Otolaryngol Suppl.* (1988) 453:1–72. doi: 10.3109/00016488809098974

4. Hart CW. Vestibular paralysis of sudden onset and probably viral etiology. *Ann Otol Rhinol Laryngol.* (1965) 74:33–47. doi: 10.1177/000348946507400103

5. Kassner SS, Schottler S, Bonaterra GA, Stern-Straeter J, Hormann K, Kinscherf R, et al. Proinflammatory activation of peripheral blood mononuclear cells in patients with vestibular neuritis. *Audiol Neurootol.* (2011) 16:242–7. doi: 10.1159/000320839

6. Jeong SH, Kim HJ, Kim JS. Vestibular neuritis. *Semin Neurol.* (2013) 33:185–94. doi: 10.1055/s-0033-1354598

7. Le TN, Westerberg BD, Lea J. Vestibular neuritis: recent advances in etiology, diagnostic evaluation, and treatment. *Adv Otorhinolaryngol.* (2019) 82:87–92. doi: 10.1159/000490275

8. Karlberg ML, Magnusson M. Treatment of acute vestibular neuronitis with glucocorticoids. *Otol Neurotol.* (2011) 32:1140–3. doi: 10.1097/MAO.0b013e3182267e24

9. Strupp M, Bisdorff A, Furman J, Hornibrook J, Jahn K, Maire R, et al. Acute unilateral vestibulopathy/vestibular neuritis: Diagnostic criteria. *J Vestib Res.* (2022). pp. 1–18. doi: 10.3233/VES-220201 [E pub ahead of print].

10. Ahn SH, Shin JE, Kim CH. Final diagnosis of patients with clinically suspected vestibular neuritis showing normal caloric response. *J Clin Neurosci.* (2017) 41:107–10. doi: 10.1016/j.jocn.2017.02.064

11. Kattah JC. Use of HINTS in the acute vestibular syndrome. An overview. *Stroke Vasc Neurol.* (2018) 3:190–6. doi: 10.1136/svn-2018-000160

12. Thomas JO, Sharobeam A, Venkat A, Blair C, Ozalp N, Calic Z, et al. Video head impulse testing to differentiate vestibular neuritis from posterior circulation stroke in the emergency department: a prospective observational study. *BMJ Neurol Open.* (2022) 4:e000284. doi: 10.1136/bmjno-2022-000284

13. Dmitriew C, Regis A, Bodunde O, Lepage R, Turgeon Z, McIsaac S, et al. Diagnostic accuracy of the HINTS exam in an emergency department: a retrospective chart review. *Acad Emerg Med.* (2021) 28:387–93. doi: 10.1111/acem.14171

14. Newman-Toker DE, Kerber KA, Hsieh YH, Pula JH, Omron R, Saber Tehrani AS, et al. HINTS outperforms ABCD2 to screen for stroke in acute continuous vertigo and dizziness. *Acad Emerg Med.* (2013) 20:986–96. doi: 10.1111/acem.12223

15. Alhabib SF, Saliba I. Video head impulse test: a review of the literature. *Eur Arch Otorhinolaryngol.* (2017) 274:1215–22. doi: 10.1007/s00405-016-4157-4

16. Fetter M. Vestibulo-ocular reflex. *Dev Ophthalmol.* (2007) 40:35–51. doi: 10.1159/000100348

17. Weber KP, MacDougall HG, Halmagyi GM, Curthoys IS. Impulsive testing of semicircular-canal function using video-oculography. *Ann N Y Acad Sci.* (2009) 1164:486–91. doi: 10.1111/j.1749-6632.2008.03730.x

18. Redondo-Martinez J, Becares-Martinez C, Orts-Alborch M, Garcia-Callejo FJ, Perez-Carbonell T, Marco-Algarra J. Relationship between video head impulse test (vHIT) and caloric test in patients with vestibular neuritis. *Acta Otorrinolaringol Esp.* (2016) 67:156–61. doi: 10.1016/j.otoeng.2016.04.012

19. Wang H, Li Z, Zhang S, He J, Yu D. Horizontal nystagmus is gravity-dependent in patients with vestibular neuritis. *Am J Otolaryngol.* (2021) 42:102967. doi: 10.1016/j.amjoto.2021.102967

20. Newman-Toker DE, Curthoys IS, Halmagyi GM. Diagnosing stroke in acute vertigo: the HINTS family of eye movement tests and the future of the "Eye ECG". *Semin Neurol.* (2015) 35:506–21. doi: 10.1055/s-0035-1564298

21. Kattah JC, Talkad AV, Wang DZ, Hsieh YH, Newman-Toker DE, HINTS. to diagnose stroke in the acute vestibular syndrome: three-step bedside oculomotor examination more sensitive than early MRI diffusion-weighted imaging. *Stroke.* (2009) 40:3504–10. doi: 10.1161/STROKEAHA.109.551234

22. Safran AB, Vibert D, Issoua D, Hausler R. Skew deviation after vestibular neuritis. *Am J Ophthalmol.* (1994) 118:238–45. doi: 10.1016/S0002-9394(14)72904-6

23. Shepard NT, Jacobson GP. The caloric irrigation test. *Handb Clin Neurol.* (2016) 137:119–31. doi: 10.1016/B978-0-444-63437-5.00009-1

24. Hwang K, Kim BG, Lee JD, Lee ES, Lee TK, Sung KB. The extent of vestibular impairment is important in recovery of canal paresis of patients with vestibular neuritis. *Auris Nasus Larynx.* (2019) 46:24–6. doi: 10.1016/j.anl.2018.05.009

25. Magliulo G, Gagliardi S, Ciniglio Appiani M, Iannella G, Re M. Vestibular neurolabyrinthitis: a follow-up study with cervical and ocular vestibular evoked myogenic potentials and the video head impulse test. *Ann Otol Rhinol Laryngol.* (2014) 123:162–73. doi: 10.1177/0003489414522974

26. Zellhuber S, Mahringer A, Rambold HA. Relation of video-head-impulse test and caloric irrigation: a study on the recovery in unilateral vestibular neuritis. *Eur Arch Otorhinolaryngol.* (2014) 271:2375–83. doi: 10.1007/s00405-013-2723-6

27. Blatt PJ, Schubert MC, Roach KE, Tusa RJ. The reliability of the Vestibular Autorotation Test (VAT) in patients with dizziness. *J Neurol Phys Ther.* (2008) 32:70–9. doi: 10.1097/NPT.0b013e3181733709

28. Lee H, Kim BK, Park HJ, Koo JW, Kim JS. Prodromal dizziness in vestibular neuritis: frequency and clinical implication. *J Neurol Neurosurg Psychiatry.* (2009) 80:355–6. doi: 10.1136/jnnp.2008.155978

29. Kim JS. When the room is spinning: experience of vestibular neuritis by a neurotologist. *Front Neurol.* (2020) 11:157. doi: 10.3389/fneur.2020.00157

30. Horak FB, Jones-Rycewicz C, Black FO, Shumway-Cook A. Effects of vestibular rehabilitation on dizziness and imbalance. *Otolaryngol Head Neck Surg.* (1992) 106:175–80. doi: 10.1177/019459989210600220

31. Weber KP, Aw ST, Todd MJ, McGarvie LA, Curthoys IS, Halmagyi GM. Horizontal head impulse test detects gentamicin vestibulotoxicity. *Neurology.* (2009) 72:1417–24. doi: 10.1212/WNL.0b013e3181a18652

32. Yang CJ, Lee JY, Kang BC, Lee HS, Yoo MH, Park HJ. Quantitative analysis of gains and catch-up saccades of video-head-impulse testing by age in normal subjects. *Clin Otolaryngol.* (2016) 41:532–8. doi: 10.1111/coa.12558

33. Sabour S. Diagnostic Value of video head impulse test in vestibular neuritis: methodological issues. *Otolaryngol Head Neck Surg.* (2018) 159:400. doi: 10.1177/0194599818779792

34. MacDougall HG, Weber KP, McGarvie LA, Halmagyi GM, Curthoys IS. The video head impulse test: diagnostic accuracy in peripheral vestibulopathy. *Neurology.* (2009) 73:1134–41. doi: 10.1212/WNL.0b013e3181bacf85

35. Ulmer E, Bernard-Demanze L, Lacour M. Statistical study of normal canal deficit variation range. Measurement using the Head Impulse Test video system. *Eur Ann Otorhinolaryngol Head Neck Dis.* (2011) 128:278–82. doi: 10.1016/j.anorl.2011.05.005

36. Fu W, He F, Zhao R, Wei D, Bai Y, Wang X, et al. Effects of Hand Positions During Video Head-Impulse Test (vHIT) in patients with unilateral vestibular neuritis. *Front Neurol.* (2018) 9:531. doi: 10.3389/fneur.2018.00531

37. Fu W, He F, Wei D, Bai Y, Shi Y, Wang X, et al. Recovery pattern of high-frequency acceleration vestibulo-ocular reflex in unilateral vestibular neuritis: a preliminary study. *Front Neurol.* (2019) 10:85. doi: 10.3389/fneur.2019.00085

38. Palla A, Straumann D. Recovery of the high-acceleration vestibulo-ocular reflex after vestibular neuritis. *J Assoc Res Otolaryngol.* (2004) 5:427–35. doi: 10.1007/s10162-004-4035-4

39. Roberts HN, McGuigan S, Infeld B, Sultana RV, Gerraty RP. A video-oculographic study of acute vestibular syndromes. *Acta Neurol Scand.* (2016) 134:258–64. doi: 10.1111/ane.12536

40. Eggers SDZ, Bisdorff A, von Brevern M, Zee DS, Kim JS, Perez-Fernandez N, et al. Classification of vestibular signs and examination techniques: Nystagmus and nystagmus-like movements. *J Vestib Res.* (2019) 29:57–87. doi: 10.3233/VES-190658

41. Choi KD, Oh SY, Kim HJ, Koo JW, Cho BM, Kim JS. Recovery of vestibular imbalances after vestibular neuritis. *Laryngoscope.* (2007) 117:1307–12. doi: 10.1097/MLG.0b013e31805c08ac

42. Balaban CD, RG J. Background and history of the interface between anxiety and vertigo. *J Anxiety Disord.* (2001) 15:27–51. doi: 10.1016/S0887-6185(00)00041-4

43. Huppert D, Wuehr M, Brandt T. Acrophobia and visual height intolerance: advances in epidemiology and mechanisms. *J Neurol.* (2020) 267:231–40. doi: 10.1007/s00415-020-09805-4

44. Neupane AK, Kapasi A, Patel N. Psychometric features of dizziness handicap inventory (DHI): development and standardization in Gujarati language. *Int Tinnitus J.* (2019) 23:86–90. doi: 10.5935/0946-5448.20190015

45. Jacob RG, Furman JM. Psychiatric consequences of vestibular dysfunction. *Curr Opin Neurol.* (2001) 14:41–6. doi: 10.1097/00019052-200102000-00007

46. Cousins S, Kaski D, Cutfield N, Arshad Q, Ahmad H, Gresty MA, et al. Predictors of clinical recovery from vestibular neuritis: a prospective study. *Ann Clin Transl Neurol.* (2017) 4:340–6. doi: 10.1002/acn3.386

47. Bronstein AM, Dieterich M. Long-term clinical outcome in vestibular neuritis. *Curr Opin Neurol.* (2019) 32:174–80. doi: 10.1097/WCO.0000000000000652

48. Macdougall HG, Curthoys IS. Plasticity during vestibular compensation: the role of saccades. *Front Neurol.* (2012) 3:21. doi: 10.3389/fneur.2012.00021

49. Lacour M. Restoration of vestibular function: basic aspects and practical advances for rehabilitation. *Curr Med Res Opin.* (2006) 22:1651–9. doi: 10.1185/030079906X115694

frontiers | Frontiers in Neurology

TYPE Original Research
PUBLISHED 14 October 2022
DOI 10.3389/fneur.2022.1036214

Check for updates

OPEN ACCESS

EDITED BY
Sulin Zhang,
Huazhong University of Science and Technology, China

REVIEWED BY
Hubertus Axer,
Jena University Hospital, Germany
Alexandre Bisdorff,
Hospital Center Emile Mayrisch, Luxembourg
Tino Prell,
University Hospital in Halle, Germany

*CORRESPONDENCE
Tzu-Pu Chang
neurochang0617@gmail.com

SPECIALTY SECTION
This article was submitted to Neuro-Otology, a section of the journal Frontiers in Neurology

RECEIVED 04 September 2022
ACCEPTED 27 September 2022
PUBLISHED 14 October 2022

CITATION
Chen CC, Lee TY, Lee HH, Kuo YH, Bery AK and Chang TP (2022) Vestibular paroxysmia: Long-term clinical outcome after treatment. *Front. Neurol.* 13:1036214. doi: 10.3389/fneur.2022.1036214

COPYRIGHT
© 2022 Chen, Lee, Lee, Kuo, Bery and Chang. This is an open-access article distributed under the terms of the Creative Commons Attribution License (CC BY). The use, distribution or reproduction in other forums is permitted, provided the original author(s) and the copyright owner(s) are credited and that the original publication in this journal is cited, in accordance with accepted academic practice. No use, distribution or reproduction is permitted which does not comply with these terms.

Vestibular paroxysmia: Long-term clinical outcome after treatment

Chih-Chung Chen[1,2,3], Ting-Yi Lee[1,2,3], Hsun-Hua Lee[1,2,3], Yu-Hung Kuo[4], Anand K. Bery[5] and Tzu-Pu Chang[6,7]*

[1]Dizziness and Balance Disorder Center, Taipei Medical University–Shuang Ho Hospital, New Taipei City, Taiwan, [2]Taipei Neuroscience Institute, Taipei Medical University, New Taipei City, Taiwan, [3]Department of Neurology, School of Medicine, College of Medicine, Taipei Medical University, Taipei, Taiwan, [4]Department of Research, Taichung Tzu Chi Hospital, Buddhist Tzu Chi Medical Foundation, Taichung, Taiwan, [5]Division of Neurology, Department of Medicine, University of Ottawa, Ottawa, ON, Canada, [6]Department of Neurology, Neuro-Medical Scientific Center, Taichung Tzu Chi Hospital, Buddhist Tzu Chi Medical Foundation, Taichung, Taiwan, [7]Department of Neurology, School of Medicine, Tzu Chi University, Hualien, Taiwan

Objective: To study the long-term treatment outcome of vestibular paroxysmia (VP).

Study design: Retrospective study.

Setting: Tertiary referral hospital.

Methods: We analyzed records of 29 consecutive patients who were diagnosed with VP and who were treated with VP-specific anticonvulsants for at least 3 months. Patients were followed for a minimum of 6 months. We recorded and assessed starting and target dosage of medications, time to achieve adequate therapeutic response, adverse effects, and the rates of short-term and long-term remission without medication.

Results: All 29 patients were started on oxcarbazepine as first-line treatment, and 93.1% and 100% of patients reported good-to-excellent therapeutic response within 2 and 4 weeks, respectively. Three patients switched to other anticonvulsants at 3 months. At long-term follow-up (8–56 months), most (84.6%) oxcarbazepine-treated patients maintained good therapeutic response at doses between 300 and 600 mg/day. Eleven (37.9%) patients experienced complete remission without medication for more than 1 month, of which six (20.7%) had long-term remission off medication for more than 12 months. Nineteen (65.5%) patients had neurovascular compression (NVC) of vestibulocochlear nerve on MRI, but its presence or absence did not predict treatment response or remission.

Conclusion: Low-dose oxcarbazepine monotherapy for VP is effective over the long term and is generally well-tolerated. About 20% of patients with VP in our study had long-term remission off medication.

KEYWORDS

dizziness, neurovascular compression, trigeminal neuralgia, typewriter tinnitus, vertigo, vestibular paroxysmia

Introduction

Vestibular paroxysmia (VP) is a debilitating clinical condition characterized by brief episodes of spontaneous or positional vertigo. Similar to trigeminal neuralgia (TN), VP is felt to be caused by neurovascular compression (NVC) of the vestibular nerve near the root entry zone (1). Vascular compression leads to focal demyelination and subsequent ectopic/ephaptic discharges of the affected cranial nerves (CN5 in TN; CN8 in VP). As they share the same presumed pathophysiology, TN and VP characteristically show significant responses to carbamazepine or oxcarbazepine.

The consensus paper on VP published by the Classification Committee for International Classification of Vestibular Disorders (ICVD) in 2016 has been widely adopted as a gold standard of diagnosis (Table 1) (2). The actual incidence of VP is unknown, but one study found it represented 3.9% of vestibular diagnoses at a tertiary outpatient clinic (3). Although it is a treatable disorder, it is easy to overlook VP because it can be difficult to distinguish from other causes of episodic dizziness on history and physical exam alone.

Despite significant therapeutic response to carbamazepine/oxcarbazepine, detailed outcome after treatment, especially long-term treatment, remains unknown. Clinicians intuitively suppose that most patients need life-long medical control unless undergoing microvascular decompression surgery, which is thought to be the only means of true "cure." In our clinical experience, however, after a period of medical control we have seen some patients discontinue medication and remain symptom-free. If it holds true that some patients of VP have short-term or long-term remission, discontinuation of carbamazepine/oxcarbazepine may be a valuable option for patients who have been symptom-free for a period (e.g., 6 months). In addition, if medical management effectively controls symptoms over the long term, surgical intervention may not be the exclusive choice for cure. It has been demonstrated that various periods of complete remission is a characteristic of TN (4, 5). It is worth investigating whether VP has a similar natural history.

To answer these questions, we reviewed consecutive patients diagnosed with VP and followed them longitudinally at our center, with particular emphasis on their presenting clinical features, therapeutic response, and most importantly, long-term outcomes.

TABLE 1 ICVD diagnostic criteria for definite vestibular paroxysmia (2).

(A)	At least 10 attacks of spontaneous spinning or non-spinning vertigo
(B)	Duration <1 min
(C)	Stereotyped phenomenology in a particular patient
(D)	Response to treatment with carbamazepine/oxcarbazepine
(E)	Not better accounted for by another diagnosis

ICVD, International Classification of Vestibular Disorders.

Materials and methods

Dizziness registry system and ethics

The data from this study come from a well-curated institutional registry on all patients with dizziness (The Dizziness Registry System) based out of the Dizziness and Balance Disorder Center at Taipei Medical University, Shuang Ho Hospital in Taipei, Taiwan. All patients who have received medical services at the center since its founding in 2017 were included and their diagnoses were recorded according to International Classification of Diseases, 9th Edition, Clinical Modification (ICD-9-CM) or International Classification of Diseases, 10th Edition (ICD-10). A well-trained case manager constantly updates data entries of registered patients by chart review and telephone interview. There are ongoing monthly team conferences to inspect and analyze the data. The study protocol was approved by our institution's Joint Institutional Review Board (N202108060). The board granted a waiver for written informed consent because of the retrospective nature of the study.

Patients

We retrospectively reviewed clinical information for all patients in our registry diagnosed with VP between 2017 and 2020. In order to investigate the long-term outcome and remission after medical treatment, we included the patients who fulfilled all of the following: (i) met ICVD criteria for "definite VP," (ii) had received VP-specific anticonvulsants at least 3 months, (iii) had been continuously followed up for at least 6 months, and (iv) were not taking other anti-vertigo medications. In keeping with previous reports, carbamazepine, oxcarbazepine, gabapentin, pregabalin, lacosamide, and lamotrigine were all accepted as VP-specific anticonvulsants for the purposes of study enrollment (6–8). Figure 1 shows the flowchart for cohort derivation.

Follow-up

All included patients were followed until July 31, 2021. At the conclusion of the study, records were reviewed and patients were classified into one of two groups: (i) those who remained on VP-specific anticonvulsants, or (ii) those who had discontinued said medications. Through chart review and telephone interview, we collected detailed information about initial symptoms, neurologic and neuro-otologic signs,

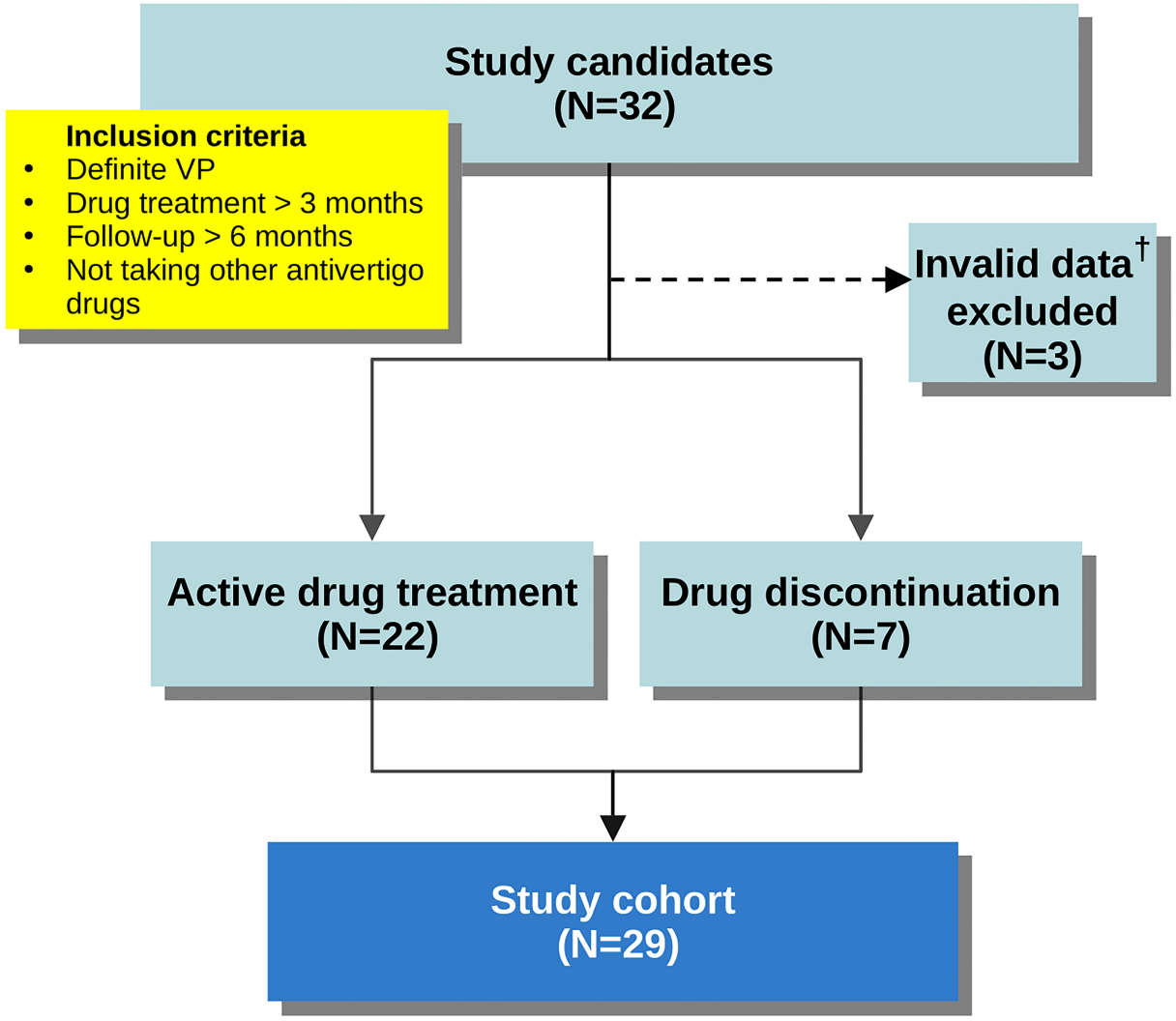

FIGURE 1
Flowchart demonstrating cohort derivation. †Patient records that had not been updated in the last 3 months before study enrollment.

medications, dosage, therapeutic response, and neuroimaging results. For the patients who had discontinued VP-specific medications, detailed information about the symptom-free duration, time of recurrence, and current use of non-specific vestibular suppressant medications were obtained. Patient records that had not been updated in the last 3 months were regarded as invalid and were excluded from this analysis.

Treatment outcome

Since VP is a paroxysmal disorder, we defined therapeutic response as reduction in frequency of attacks. Change in attack frequency after treatment was dichotomized as follows: poor response (0–20% reduction), modest response (20–50% reduction), good response (50–80% reduction), and excellent response (80–100% reduction). In addition to vestibular attacks, episodes of concomitant paroxysmal cranial nerve disorders, including typewriter tinnitus, hemifacial spasm (HFS), TN, glossopharyngeal neuralgia, and inferior oblique myokymia, were also counted as attacks (9). "Stable dosage" was defined as the minimum dosage of the medication which could maintain "good" or "excellent" therapeutic response for at least 3 months. While there is no authoritative definition of remission for VP, we adopted the outcome measures used by a prospective study on TN (9). Short-term remission was defined as having continuous symptom-free periods, without use of anti-vertigo medications, for at least 1 month. Long-term remission was defined as continuous symptom-free periods of at least 12 months without medication.

TABLE 2 Summary of the study cohort ($N = 29$).

Age		
	Mean ± SD	64.7 ± 10.2
	Range	44–79
Sex (*n*)		
	Male	19
	Female	10
Duration of symptoms prior to index visit (months)		
	Mean ± SD	24 ± 26
	Range	1–108
Concomitantparoxysmal cranial nerve disorders (*n*)		
	Typewriter tinnitus	13
	Hemifacial spasm	2
	Trigeminal neuralgia	2
Medication (*n*)		
	Oxcarbazepine	26
	Pregabalin	2
	Gabapentin	1
Treatment duration (months)		
	Mean ± SD	23 ± 15
	Range	4–56
Follow-up duration (months)		
	Mean ± SD	30 ± 14
	Range	8–56

Statistical analysis

We recorded and analyzed the starting dosage of medications, therapeutic period of achieving good or excellent response for vestibular symptoms, stable dosage, durations of treatment, adverse effects, therapeutic responses for concomitant NVC disorders, and durations of remissions. The rates of short-term and long-term remissions without medication were calculated. We reported descriptive statistics and the cumulative remission rate after VP medical treatment. One-way ANOVA was used to compare the stable dosage of oxcarbazepine between the patients with and without NVC. Univariate logistic regression was used to determine if the duration of VP, age, the NVC in MRI, the concomitant paroxysmal cranial nerve disorders, the stable drug dosage or the duration of treatment can predict remission. Odds ratios and 95% confidence intervals (CI) were calculated. The statistical analysis was performed using SPSS v23 (Armonk, NY).

Results

Characteristics of patients

After excluding three invalid entries, 29 patients met study inclusion. Twenty-two (75.9%) patients were on active treatment at the end of follow-up. Seven (24.1%) patients were not on active treatment at the end of follow-up. The cohort comprised 19 males and 10 females, aged 44–79 and the follow-up periods ranged from 8 to 56 months (detailed information in Supplementary Table 1). The duration of symptoms before diagnosis of VP ranged from 1 month to 9 years. Fourteen patients had concomitant paroxysmal cranial nerve disorders—typewriter tinnitus in 13 (44.8%), HFS in 2 (6.9%), and TN in 2 (6.9%). Nystagmus was recorded in eight patients (27.6%), including ictal spontaneous nystagmus in 1 (3.4%), interictal spontaneous nystagmus in 1 (3.4%), head-shaking nystagmus in 3 (10.3%), hyperventilation-induced nystagmus in 3 (10.3%), and positional nystagmus in 3 (10.3%). MRI showed NVC in 19 (65.5%) patients, and 4 patients (13.8%) had prominent nerve distortion. Nine of the 14 patients with concomitant paroxysmal cranial nerve disorders had NVC ipsilateral to the lesion side (7/13 in typewriter tinnitus, 1/2 in HFS, and 1/2 in TN). The duration of treatment ranged from 4 to 56 months. Patient demographics, presenting symptoms, and treatment details of the study cohort are summarized in Table 2.

Therapeutic response for vestibular symptoms

All 29 patients were started on oxcarbazepine as first-line treatment, at a starting dosage of 300–600 mg/day. At 1-month follow-up, all patients achieved "good" or "excellent" therapeutic response (see definitions above). Specifically, 27 (93.1%) patients reported good-to-excellent therapeutic response within 2 weeks. At 3-month follow-up, 26 patients (89.7%) maintained good-to-excellent responses on oxcarbazepine while the other three patients (10.3%) switched to other anticonvulsants despite the initial good response of oxcarbazepine. Two of them switched to pregabalin due to intolerable side effects of oxcarbazepine (weakness and hyponatremia). One switched to gabapentin because the therapeutic effect of oxcarbazepine diminished.

At long-term follow-up, the same 26 patients continued on oxcarbazepine monotherapy and had satisfactory control. Among them, 15 patients remained at a stable dosage of 300 mg/day, one at 450 mg/day, six at 600 mg/day, two at 900 mg/day, and two at 1,200 mg/day. Most (22/26, 84.6%) of the patients had optimal response at doses between 300 and 600 mg/day. Two patients who had concomitant HFS required higher dosages (900–1,200 mg/day) to relieve their dizziness (see Table 3 for details on therapeutic response). The stable dosages were not significantly different between the patients with NVC and without NVC (mean dosage 485 vs. 500 mg, $p = 0.90$, One-way ANOVA).

TABLE 3 Oxcarbazepine regimen and efficacy in 26 VP patients.

No.	Age	Sex	Concomitant cranial nerve disorders	Duration of follow-up (months)	Therapeutic response for dizziness	Weeks to optimal response	Stable dosage (mg/d)	Therapeutic response for concomitant cranial nerve disorders
1	54	M	–	14	Excellent	1	300	N/A
2	65	M	Tinnitus	42	Excellent	1	300	Modest
3	71	F	Tinnitus	44	Excellent	1	600	Modest
4	76	M	–	50	Excellent	1	300	N/A
5	73	M	–	15	Excellent	4	300	N/A
6	57	M	Tinnitus	10	Excellent	2	900	Modest
7	69	M	Tinnitus	25	Excellent	2	300	Good
8	48	M	–	22	Excellent	2	300	N/A
9	57	F	Tinnitus	14	Excellent	2	450	Good
10	66	M	–	56	Excellent	1	600	N/A
12	51	M	HFS	38	Excellent	1	900	Poor
13	69	M	–	42	Excellent	2	300	N/A
14	74	M	–	33	Excellent	1	300	N/A
15	73	F	Tinnitus	14	Excellent	1	600	Excellent
16	75	M	–	46	Excellent	2	300	N/A
17	79	F	Tinnitus, HFS, TN	8	Good	4	1,200	Poor for tinnitus and HFS; excellent for TN
18	66	F	–	16	Good	2	600	N/A
21	79	F	–	39	Excellent	2	300	N/A
22	63	F	Tinnitus	8	Excellent	1	600	Good
23	64	F	–	52	Excellent	2	300	N/A
24	59	F	Tinnitus	48	Excellent	1	300	Excellent
25	55	M	–	35	Excellent	1	300	N/A
26	67	M	Tinnitus, TN	36	Excellent	1	300	Excellent for both
27	76	M	–	34	Excellent	2	600	N/A
28	57	M	Tinnitus	42	Excellent	1	1,200	Modest
29	72	M	Tinnitus	23	Excellent	2	300	Good

HFS, hemifacial spasm; TN, trigeminal neuralgia; VP, vestibular paroxysmia.

Therapeutic response for concomitant typewriter tinnitus and other paroxysmal cranial nerve disorders

Of the patients with concomitant typewriter tinnitus, 12 patients were treated with oxcarbazepine (Table 3) and one was treated with gabapentin. Therapeutic response for tinnitus at the stable dosages for dizziness were excellent in three patients (23.1%), good in 5 (38.5%), modest in 4 (30.8%) and poor in 1 (7.7%). The therapeutic responses for TN ($n = 2$) were both "excellent" while the responses for HFS ($n = 2$) were both "poor." An optimal therapeutic dose range for these poorly-responsive tinnitus and HFS symptoms was not clear because clinicians targeted at the most bothersome vestibular symptoms of these patients and did not necessarily up-titrate the dosages to treat other concomitant paroxysmal cranial nerve disorders.

Remission

Overall, 11 of 29 patients (37.9%) experienced various periods of complete remission without medication, including 6 (20.7%) with long-term remission and 4 (13.8%) who experienced short-term remission but subsequent relapse (Figure 2). Another patient (3.4%) had been in remission off medication at 6 months (which coincided with the end of the study, so we cannot for sure say the remission was "long term"). Regarding the four who achieved short-term remission, these patients essentially relapsed within 4–8 months and

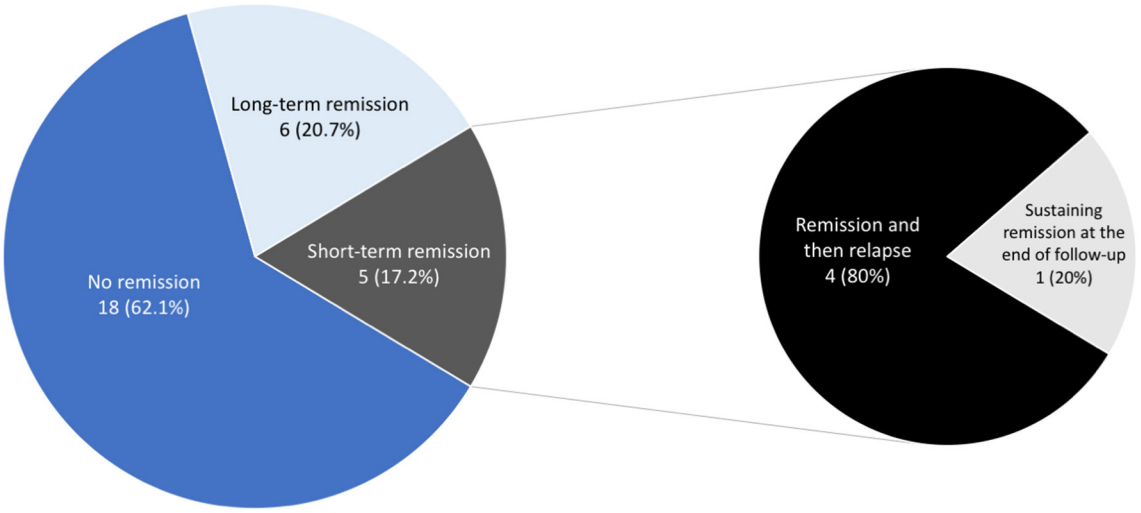

FIGURE 2
Short-term and long-term remission off medication.

TABLE 4 Univariate logistic regression analysis for different variables for predicting remission.

Variables	OR for remission	95% CI
Duration of VP	0.98	0.95–1.02
Age at diagnosis	0.95	0.87–1.05
NVC on MRI	3.94	0.63–24.73
Concomitant paroxysmal cranial nerve disorders	2.63	0.53–13.07
Duration of treatment	0.96	0.91–1.01

NVC, neurovascular compression; VP, vestibular paroxysmia.

had to restart medical treatment. The six patients with long-term remission had been symptom-free off medication for at least 20–43 months, as confirmed by follow-up telephone interviews. The duration of VP, the age at diagnosis, the presence of NVC on MRI, the presence of concomitant paroxysmal cranial nerve disorders, and the duration of treatment did not predict short-term or long-term remission (Table 4). Since the duration of follow-up varies in each patient, we demonstrate the cumulative remission rate considering censored data in Figure 3.

Discussion

There are two important findings of this study in long-term outcome (>6 months) after medical treatment for VP. First, we found that complete remission off anticonvulsants occurs in about 40% of VP patients, and about 20% of these patients remain symptom-free for more than 1 year after discontinuing their medication. To our knowledge, this phenomenon has not been well-documented in the literature. Second, most patients (93.1%) report good-to-excellent therapeutic effect within 2 weeks of oxcarbazepine treatment, and most (84.6%) remain well-controlled at a low dosage of oxcarbazepine (i.e., 300–600 mg/day) in long-term follow-up.

The underlying pathophysiology of VP is assumed to be microvascular compression of the eighth cranial nerve. We were somewhat surprised to see such a high rate of remission (37.9%) because one might not expect medical treatment (sodium channel blockade) to physically relieve NVC or restore myelination. However, a similar finding has been shown in another study with 73 definite VP patients, of which 56% became attack-free after discontinuing carbamazepine or oxcarbazepine (10). In clinical practice the possibility of remission in some TN patients has been suspected for years (4). A large prospective study of TN showed that 63% of cases experienced remission for at least 1 month. Pain-free periods of several years were not uncommon (11). Over time, partial remyelination, or normalization of membrane-channel activation may reduce nerve excitability, bring the triggering level below threshold, and result in remission of TN (5). The same mechanism may, at least partially, explain our finding in the present study on VP. Moreover, some of our patients did not demonstrate evident NVC on MRI, which is similar to the condition in idiopathic TN. Positive therapeutic response of anticonvulsants in VP supports the pathomechanism of ectopic/ephaptic discharges, whether NVC is present or not. The role of NVC in VP warrants further clarification.

In our study, response to VP-specific medication was almost stable and long-lasting. This suggests only very selected patients

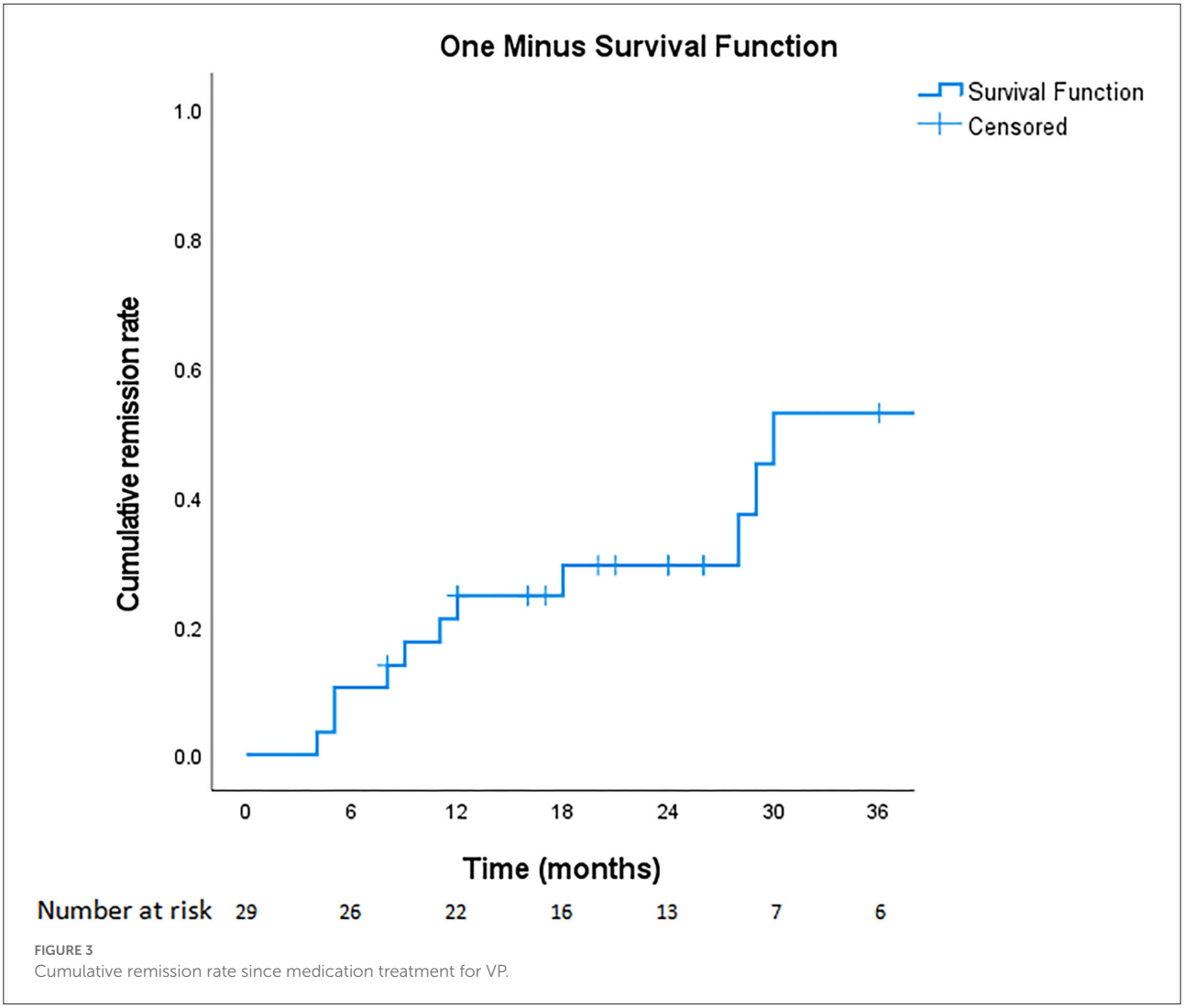

FIGURE 3
Cumulative remission rate since medication treatment for VP.

should be considered for microvascular decompression surgery. Moreover, given the number of our patients with long periods of remission of medication, this study hints at the possibility that a drug taper can be attempted after patients have achieved an initial satisfactory response. Though some patients will still require continuation at the lowest effective dose, a large enough proportion of patients achieved remission in our study that tapering should be considered. More work is needed to confirm these observational findings.

Although the ICVD criteria include a positive response of sodium channel blockers to support the diagnosis of definite VP, studies about the long-term efficacy of oxcarbazepine are still limited (12, 13). Hufner et al. first demonstrated the effectiveness of oxcarbazepine in five cases of VP in 2008 (12). A retrospective analysis of 196 cases of VP in 2016 only looked at short-term (12 week) treatment effect of adjuvant betahistine (14). A randomized, cross-over trial showed a significant benefit of oxcarbazepine over placebo, but the high dropout rate in the trial resulted in only using data of 18 patients for analysis (15). More recently, there were two studies investigating the treatment outcome of VP. One study included 63 patients with carbamazepine but only 10 patients with oxcarbazepine. Most of them had good treatment responses and outcomes (10). The other study concluded an unfavorable outcome, but there were only 12 patients treated with carbamazepine and none with oxcarbazepine (16). When compared with these previous studies, our study is the largest case series of long-term oxcarbazepine monotherapy for VP in the real world.

In our study, most patients (93.1%) reported good-to-excellent improvement within the first 2 weeks of medical therapy. This finding also has diagnostic value. If a patient fails to show improvement on oxcarbazepine in 2 weeks, VP may not be the correct diagnosis. We also found that most patients (84.6%) obtained satisfactory results at a stable dosage of oxcarbazepine 300–600 mg/day while only four patients (15.4%; two with concomitant HFS) needed a dosage higher than 600 mg/day. As a result, one should expect to see significant improvement in most patients at a dosage of oxcarbazepine 600 mg/day. Patients

who fail to show any improvement at this dosage should be considered to have other etiologies of dizziness. Our proposed dosing plan is listed in Supplementary Table 2.

Besides, our study illustrated the treatment results of anticonvulsants on concomitant typewriter tinnitus. In a literature review of combined VP and typewriter tinnitus, only 5 of 21 (23.8%) cases were able to achieve complete remission of tinnitus by drug therapy alone (17). In our cohort, only 8 of the 13 (61.5%) patients reported good or excellent responses in tinnitus, despite all of them having good-to-excellent responses in terms of dizziness symptoms. Both studies suggested that the control of auditory symptoms was suboptimal at stable dosages required for control of vestibular symptoms. We speculate that the dosage required to relieve auditory symptoms is higher than that required to relieve vestibular symptoms. The differential drug response between these two symptoms may result from the difference in nerve sizes and nuclei reorganization (18). Accordingly, our findings suggest a higher dosage of oxcarbazepine or an add-on anticonvulsant may be necessary to fully relieve the tinnitus.

Interestingly, our study revealed that only 65.5% of VP patients had the evidence of NVC in MRI, which was lower than the previous reports (12, 13, 19, 20). To our knowledge, NVC being the cause of VP is still debated given that up to 25% of healthy people have NVC (21). In our study, the patients with NVC did not show different therapeutic response or remission rate when compared to those without NVC. More importantly, in the 13 patients with combined VP and typewriter tinnitus, only seven had the NVC which were ipsilateral to the side of tinnitus. Therefore, our study findings do not fully support the theory of NVC. In our opinion, when the clinical presentations are compatible with VP, the patients should be treated with VP medication first even though their MRI findings are negative.

Some limitations of this study should be addressed here. Firstly, this was a retrospective study. Two factors may have unduly influenced our remission rate: (i) duration of follow-up differed among patients, and (ii) and some patients were more hesitant than others to discontinue medications for fear of relapse—even though they remained symptom-free on medication. In addition, to meet diagnostic criteria for VP, all patients in this study had to already show positive therapeutic response to carbamazepine or oxcarbazepine (i.e., positive drug response is part of the diagnostic criteria for VP). Therefore, we did not include the patients who potentially had NVC-induced vertigo but were resistant to these two medications. Additionally, metrics on dizziness frequency were self-reported and thus subject to recall bias. We also did not use formal scales for assessing the severity of dizziness, such as the Dizziness Handicap Inventory. Lastly, none of our patients received carbamazepine so we did not compare the efficacy of carbamazepine and oxcarbazepine.

Conclusion

Vestibular paroxysmia is a debilitating but treatable condition. In this study, medical treatment for VP remains remarkably effective even when patients are followed longitudinally. Moreover, a significant number of patients see complete remission off medication, supporting the notion that medication taper can be considered in select cases. Given the long-term stable response to medication, surgical microvascular decompression should be reserved only for truly refractory cases. In the future, a randomized controlled trial is needed for further confirming the long-term efficacy and outcome of drug treatment for VP.

Data availability statement

The original contributions presented in the study are included in the article/Supplementary material, further inquiries can be directed to the corresponding author/s.

Ethics statement

The studies involving human participants were reviewed and approved by Taipei Medical University Joint Institutional Review Board (N202108060). Written informed consent for participation was not required for this study in accordance with the national legislation and the institutional requirements.

Author contributions

C-CC designed the study, collected, analyzed, and interpreted the data, drafted the manuscript, and approved the final manuscript. T-YL and H-HL collected the data and designed the tables, and approved the final manuscript. Y-HK performed statistics and analyzed the results. AB revised the manuscript and approved the final manuscript. T-PC designed the study, interpreted the data, revised the manuscript, and approved the final manuscript. All authors contributed to the article and approved the submitted version.

Funding

This research was supported by Taipei Medical University (TMU106-AE1-B07).

Acknowledgments

We would like to thank Ms. Jia-Min Kang for maintaining the Dizziness Registry System and performing telephone interviews.

Conflict of interest

The authors declare that the research was conducted in the absence of any commercial or financial relationships that could be construed as a potential conflict of interest.

Publisher's note

All claims expressed in this article are solely those of the authors and do not necessarily represent those of their affiliated organizations, or those of the publisher, the editors and the reviewers. Any product that may be evaluated in this article, or claim that may be made by its manufacturer, is not guaranteed or endorsed by the publisher.

Supplementary material

The Supplementary Material for this article can be found online at: https://www.frontiersin.org/articles/10.3389/fneur.2022.1036214/full#supplementary-material

References

1. Brandt T, Dieterich M. Vestibular paroxysmia: vascular compression of the eighth nerve? *Lancet.* (1994) 343:798–9. doi: 10.1016/S0140-6736(94)91879-1

2. Strupp M, Lopez-Escamez JA, Kim JS, Straumann D, Jen JC, Carey J, et al. Vestibular paroxysmia: diagnostic criteria. *J Vestib Res.* (2016) 26:409–15. doi: 10.3233/VES-160589

3. Strupp M, Mandalà M, López-Escámez JA. Peripheral vestibular disorders: an update. *Curr Opin Neurol.* (2019) 32:165–73. doi: 10.1097/WCO.0000000000000649

4. Rushton JG, Macdonald HN. Trigeminal neuralgia; special considerations of nonsurgical treatment. *J Am Med Assoc.* (1957) 165:437–40. doi: 10.1001/jama.1957.02980230007002

5. Devor M, Amir R, Rappaport ZH. Pathophysiology of trigeminal neuralgia: the ignition hypothesis. *Clin J Pain.* (2002) 18:4–13. doi: 10.1097/00002508-200201000-00002

6. Strupp M, Elger C, Goldschagg N. Treatment of vestibular paroxysmia with lacosamide. *Neurol Clin Pract.* (2019) 9:539–41. doi: 10.1212/CPJ.0000000000000610

7. Zwergal A, Strupp M, Brandt T. Advances in pharmacotherapy of vestibular and ocular motor disorders. *Expert Opin Pharmacother.* (2019) 20:1267–76. doi: 10.1080/14656566.2019.1610386

8. Chang TP, Wu YC, Hsu YC. Vestibular paroxysmia associated with paroxysmal pulsatile tinnitus: a case report and review of the literature. *Acta Neurol Taiwan.* (2013) 22:72–5.

9. Haller S, Etienne L, Kövari E, Varoquaux AD, Urbach H, Becker M. Imaging of neurovascular compression syndromes: trigeminal neuralgia, hemifacial spasm, vestibular paroxysmia, and glossopharyngeal neuralgia. *AJNR Am J Neuroradiol.* (2016) 37:1384–92. doi: 10.3174/ajnr.A4683

10. Steinmetz K, Becker-Bense S, Strobl R, Grill E, Seelos K, Huppert D. Vestibular paroxysmia: clinical characteristics and long-term course. *J Neurol.* (2022). doi: 10.1007/s00415-022-11151-6. [Epub ahead of print].

11. Maarbjerg S, Gozalov A, Olesen J, Bendtsen L. Trigeminal neuralgia–a prospective systematic study of clinical characteristics in 158 patients. *Headache.* (2014) 54:1574–82. doi: 10.1111/head.12441

12. Hüfner K, Barresi D, Glaser M, Linn J, Adrion C, Mansmann U, et al. Vestibular paroxysmia: diagnostic features and medical treatment. *Neurology.* (2008) 71:1006–14. doi: 10.1212/01.wnl.0000326594.91291.f8

13. Best C, Gawehn J, Krämer HH, Thömke F, Ibis T, Müller-Forell W, et al. MRI and neurophysiology in vestibular paroxysmia: contradiction and correlation. *J Neurol Neurosurg Psychiatr.* (2013) 84:1349–56. doi: 10.1136/jnnp-2013-305513

14. Yi C, Wenping X, Hui X, Xin H, Xiue L, Jun Z, et al. Efficacy and acceptability of oxcarbazepine vs. carbamazepine with betahistine mesilate tablets in treating vestibular paroxysmia: a retrospective review. *Postgrad Med.* (2016) 128:492–5. doi: 10.1080/00325481.2016.1173515

15. Bayer O, Brémová T, Strupp M, Hüfner K. A randomized double-blind, placebo-controlled, cross-over trial (Vestparoxy) of the treatment of vestibular paroxysmia with oxcarbazepine. *J Neurol.* (2017) 265:291–8. doi: 10.1007/s00415-017-8682-x

16. Hanskamp LAJ, Schermer TR, van Leeuwen RB. Long-term prognosis of vertigo attacks and health-related quality of life limitations in patients with vestibular paroxysmia. *Otol Neurotol.* (2022) 43:e475–81. doi: 10.1097/MAO.0000000000003465

17. Koo YJ, Kim HJ, Choi JY, Kim JS. Vestibular paroxysmia associated with typewriter tinnitus: a case report and literature review. *J Neurol.* (2021) 268:2267–72. doi: 10.1007/s00415-021-10525-6

18. Schwaber MK, Whetsell WO. Cochleovestibular nerve compression syndrome. II. Vestibular nerve histopathology and theory of pathophysiology. *Laryngoscope.* (1992) 102:1030–6. doi: 10.1288/00005537-199209000-00013

19. Sivarasan N, Touska P, Murdin L, Connor S. MRI findings in vestibular paroxysmia - an observational study. *J Vestib Res.* (2019) 29:137–45. doi: 10.3233/VES-180661

20. Ihtijarevic B, Van Ombergen A, Celis L, Maes LK, Wuyts FL, Van de Heyning PH, et al. Symptoms and signs in 22 patients with vestibular paroxysmia. *Clin Otolaryngol.* (2019) 44:682–7. doi: 10.1111/coa.13356

21. Makins AE, Nikolopoulos TP, Ludman C, O'Donoghue GM. Is there a correlation between vascular loops and unilateral auditory symptoms? *Laryngoscope.* (1998) 108(11 Pt 1):1739–42. doi: 10.1097/00005537-199811000-00027

frontiers | Frontiers in Neurology

TYPE Original Research
PUBLISHED 02 November 2022
DOI 10.3389/fneur.2022.1017608

Check for updates

OPEN ACCESS

EDITED BY
Sulin Zhang,
Huazhong University of Science and Technology, China

REVIEWED BY
Francesco Gazia,
University of Messina, Italy
Tongxiang Diao,
Peking University People's Hospital, China

*CORRESPONDENCE
Maoli Duan
maoli.duan@ki.se
Jun Yang
yangjun@xinhuamed.com.cn
Yulian Jin
jinyulian8548@xinhuamed.com.cn

SPECIALTY SECTION
This article was submitted to Neuro-Otology, a section of the journal Frontiers in Neurology

RECEIVED 12 August 2022
ACCEPTED 09 September 2022
PUBLISHED 02 November 2022

CITATION
Liang M, Wu H, Chen J, Zhang Q, Li S, Zheng G, He J, Chen X, Duan M, Yang J and Jin Y (2022) Vestibular evoked myogenic potential may predict the hearing recovery in patients with unilateral idiopathic sudden sensorineural hearing loss. *Front. Neurol.* 13:1017608. doi: 10.3389/fneur.2022.1017608

COPYRIGHT
© 2022 Liang, Wu, Chen, Zhang, Li, Zheng, He, Chen, Duan, Yang and Jin. This is an open-access article distributed under the terms of the Creative Commons Attribution License (CC BY). The use, distribution or reproduction in other forums is permitted, provided the original author(s) and the copyright owner(s) are credited and that the original publication in this journal is cited, in accordance with accepted academic practice. No use, distribution or reproduction is permitted which does not comply with these terms.

Vestibular evoked myogenic potential may predict the hearing recovery in patients with unilateral idiopathic sudden sensorineural hearing loss

Min Liang[1,2,3], Hui Wu[1,2,3], Jianyong Chen[1,2,3], Qin Zhang[1,2,3], Shuna Li[1,2,3], Guiliang Zheng[1,2,3], Jingchun He[1,2,3], Xiangping Chen[1,2,3], Maoli Duan[4,5]*, Jun Yang[1,2,3]* and Yulian Jin[1,2,3]*

[1]Department of Otolaryngology-Head and Neck Surgery, Xinhua Hospital, Shanghai Jiaotong University School of Medicine, Shanghai, China, [2]Ear Institute, Shanghai Jiao Tong University School of Medicine, Shanghai, China, [3]Shanghai Key Laboratory of Translational Medicine on Ear and Nose Disease, Shanghai, China, [4]Department of Otolaryngology-Head and Neck Surgery, Karolinska University Hospital, Karolinska Institute, Stockholm, Sweden, [5]Department of Clinical Science, Intervention and Technology, Karolinska Institute, Stockholm, Sweden

Objective: This study investigates the association between vestibular function and prognosis in patients with unilateral idiopathic sudden sensorineural hearing loss (UISSNHL).

Design: A retrospective analysis of 64 patients with UISSNHL was performed. Pure tone audiometry and vestibular function tests for otoliths and semicircular canals were performed to assess the influence of vestibular functional status on the outcome of patients with UISSNHL.

Results: Patients with abnormal cervical vestibular evoked myogenic potential (cVEMP) or ocular vestibular evoked myogenic potential (oVEMP) responded less favorably to treatment. In the ineffective group, cVEMP was normal in four patients (6.3%) and oVEMPs in three (4.7%). Meanwhile, cVEMP was abnormal in 32 patients (50.0%) and oVEMP in 33 (51.6%). Better hearing recovery occurred in those with normal cVEMP (33.76 ± 15.07 dB HL improvement) or oVEMP (32.55 ± 19.56 dB HL improvement), but this was not the case in those with normal caloric tests. Patients with abnormalities in both cVEMP and oVEMP were less responsive to treatment and had worse hearing recovery than those with normal results in only one of the two tests.

Conclusion: Abnormal oVEMP and/or cVEMP results indicate poor auditory outcomes in patients with UISSNHL. Patients with impaired otolith organ function are likely to have a larger and more severe pathological change in their inner ear.

KEYWORDS

unilateral idiopathic sudden sensorineural hearing loss, vestibular function, vestibular evoked myogenic potential, caloric test, otolith organ, sacculus, utriculus

Introduction

Sudden sensorineural hearing loss (SSNHL) is a serious, rapid-onset inner ear disease without known etiology. It is defined as a sensorineural hearing loss of at least 30 dB over at least three connected/consecutive frequencies (1, 2) occurring within 72 h (3). Various postulated etiological theories have been proposed in the literature, including viral infection, vascular embolism, and metabolic abnormalities (4–7). Nearly 40%−55% of patients with SSNHL show vestibular symptoms such as dizziness and instability, which can be delayed or occur at the same time with sudden hearing loss (8–10). This suggests that cochlear impairment and vestibular dysfunction can accompany each other (8, 9, 11–13).

The cochlear and vestibular embryos are homologous. The otic vesicles are derived from the otic placodes situated on either side of the embryonic hindbrain and differentiate into superior vestibular and inferior cochlear parts (14, 15). As a disease of unknown etiology, SSNHL can cause damage to both cochlear and vestibular organs, which share a common origin in terms of cochlear and vestibular arteries (16). A poor prognosis was reported in SSNHL patients with vertigo (3, 4, 17–20). However, the underlying vertigo assessment of peripheral vestibular organs has not yet been well described.

Various vestibular function tests may assist in mapping the affected area of vestibulopathy and provide information that improves the prediction of hearing outcomes. Vestibular evoked myogenic potential (VEMP), including cervical vestibular evoked myogenic potential (cVEMP) and ocular vestibular evoked myogenic potential (oVEMP), is recorded on the surface of the skeletal muscle under tension evoked by strong acoustic stimulation on vestibular terminal sensors. They reflect the functions of the sacculus and utriculus, respectively. The caloric test is clinically used to examine the horizontal semicircular canal and the supra-vestibular nerve pathways. When combined with audiometric tests, the vestibular function test battery, including cVEMP, oVEMP, and caloric test, can provide a more accurate and comprehensive assessment of the cochlear and vestibular system to check the function of almost the entire inner ear (cochlea, sacculus, utriculus, and horizontal semicircular canal).

To date, the involvement of vestibular organs in SSNHL remains controversial. Moreover, it is still unknown whether detecting normal or abnormal VEMP responses is useful in determining a patient's prognosis. This study aims to analyze the relationship between the aforementioned vestibular function as part of a complete neurotological evaluation and auditory outcome in patients with UISSNHL and to determine the possible predictive significance of vestibular function in the participating patients.

Materials and methods

Patients

In total, 64 patients with UISSNHL were recruited from the Department of Otolaryngology-Head and Neck Surgery, Xinhua Hospital, affiliated with the Shanghai Jiaotong University School of Medicine, from May 2017 to July 2021. This included 38 men and 26 women aged between 18 and 87 years (average of 53.75 ± 17.00 years), with moderate deafness in four ears, moderate to severe deafness in 15 ears, severe deafness in six ears, profound deafness in 13 ears, and total deafness in 26 ears. Of the patients, 28 had hearing loss in the left ear and 36 in the right ear. Vertigo, dizziness, or unsteadiness appeared in 35 patients. The diagnosis of UISSNHL followed the American Academy of Otolaryngology-Head and Neck Surgery Foundation's (AAOHNSF) "Clinical Practice Guideline: Sudden Hearing Loss" (2). All human procedures were approved by the institutional review board in Xinhua Hospital, affiliated with the Shanghai Jiaotong University School of Medicine. All participants provided verbal informed consent.

The inclusion criteria were as follows: ① age ≥ 18 years; ② an unknown cause; ③ moderate to total hearing loss; ④ initiation of treatment within 30 days after onset; and ⑤ those who underwent all the following vestibular function tests: cVEMP, oVEMP, and the caloric test before treatment. The treatment protocol included administering steroids *via* intravenous and intratympanic injection and concurrent hyperbaric oxygen therapy for 10 consecutive days.

The exclusion criteria were defined as follows: central nervous system diseases, external and middle ear diseases, any cochlear and retrocochlear lesions observed on MR imaging, and hypertension or diabetes.

Audiometry and hearing outcomes

Repeated pure-tone audiometry (PTA) was carried out before and after the 10-day treatment. PTA was measured using the clinical diagnostic audiometry system MADSEN Astera (GN Otometrics, Denmark). The average threshold was calculated based on the corresponding impaired frequency.

Hearing outcome was classified as complete recovery (hearing improvement to normal range), remarkable recovery (hearing improvement >30 dB HL), mild recovery (15 dB HL ≤ hearing improvement ≤ 30 dB HL), and no recovery (hearing improvement < 15 dB HL). Patients were tested in a standard soundproof room after removing cerumen in the external auditory canal. If no response occurred for a certain frequency, which exceeded the maximum output of the instrument (120 dB HL), 120 dB HL was used as the estimated hearing threshold.

Vestibular evoked myogenic potential

The recording device for both cVEMP and oVEMP was the audiometry system ICS Chartr EP 200 (GN Otometrics, Denmark).

Cervical vestibular evoked myogenic potential

A reference electrode was placed between the clavicle joints, and a ground electrode was placed between the forehead and the eyebrows. The left and right recording electrodes were placed in the middle of the left and right sternocleidomastoid muscles. The electrode impedance was <5 KΩ. The air-conducted sound was presented with 500-Hz short tone bursts (1 ms rise/fall time, 2 ms plateau time, 5 Hz stimulus frequency, and 50 times superimposition). The starting stimulus intensity was 100 dB nHL, which decreased by 5 dB nHL each time until the meaningful VEMP wave was undetectable. During the test, the subject was instructed to slightly raise his or her head by 30° to activate the sternocleidomastoid muscles.

Ocular vestibular evoked myogenic potential

The recording parameters were similar to those in the cVEMP. The reference electrode was placed in the mandible, the ground electrode was placed between the forehead and the eyebrows, and the recording electrode was placed 1 cm below the center of the contralateral eyelid. During the test, the subject was positioned supine and stared upward (∼25°-30° above the horizontal plane), trying to blink as rarely as possible to activate the inferior oblique muscles.

Recording indicators included the threshold, an initial positive peak P13(N10), a subsequent negative peak N23(P15), and P13–N23(N10–P15). The threshold value is the minimum sound stimulus intensity that elicits the typical VEMP waveform. The P13(N10) latency is the time from initiating the stimulation to the generation of the P13(N10) wave (typically 13 ms). The N23(P15) latency is the time from initiating the stimulation to the generation of the N23(P15) wave (typically 23 ms). The wave interval is the duration (ms) between the apex of the N23(P15) wave and the P13(N10) wave. The amplitude is the vertical distance (μV) from the apex of the N23(P15) wave to the apex of the P13(N10) wave. The amplitude asymmetry ratio (AR) is the ratio of the absolute value of the difference between the two sides and the sum of the two sides. An increase in AR often indicates damage to one side of the otolith organ and the superior/inferior vestibular nerve pathway. We defined the abnormal result of VEMP as (1) the absence of a meaningful waveform, (2) delayed response, whereby the threshold shift was out of the range, or (3) AR $>$ 29%.

Caloric test

The integrity of the external auditory canal and the tympanic membrane was checked to assess the middle ear condition before the tests were conducted. The subject was positioned supine with the head flexed at 30°. The test was performed using cold (24°) or warm (50°) air irrigation (30–60s). The nystagmus was observed for 60 s after perfusion. The canal paresis (CP) value represents the ratio of the absolute value of the difference and the total value of the left and right responses to stimulation, reflecting whether the reaction of bilateral semicircular canals was symmetrical. The directional preponderance (DP) was used to quantify the difference between the caloric responses of the two ears to judge which nystagmus direction was stronger. The abnormal caloric result was defined as an absolute value of CP% greater than 25% and/or an absolute value of DP greater than 30%.

Statistical analysis

SPSS Statistics 26.0 was used for statistical analysis. Descriptive data were presented as mean and standard deviation values. The mean values were compared by an independent-sample t-test or a Kruskal–Wallis test after analyzing the normality of values using a Kolmogorov–Smirnov test (K–S test). Categorical data were expressed as number and percentage values and were compared using Pearson's χ^2. A difference was regarded as significant if $P < 0.05$.

Results

Before treatment, 64 patients underwent three vestibular function tests, namely, cVEMP, oVEMP, and caloric test. Only two patients had all normal results, whereas 24 patients had all abnormal results. The mean delay of treatment, defined as the period from disease onset to commencement of therapy, was 6.22 ± 5.36 days. The cVEMP and oVEMP results of typical cases are shown in Figures 1A,B.

The therapeutic efficacy was divided into two groups, namely, effective and ineffective. The effective group comprised patients with an auditory outcome showing either complete recovery, remarkable recovery, or mild recovery. In the effective group, the normal rate of cVEMP was 28.1%, and the abnormal rate was 15.6%. The normal rate of oVEMP was 17.2%, and the abnormal rate was 26.6%. In the ineffective group, the normal rate of cVEMP was 6.3%, and the abnormal rate was 50.0%. The normal rate of oVEMP was 4.7%, and the abnormal rate

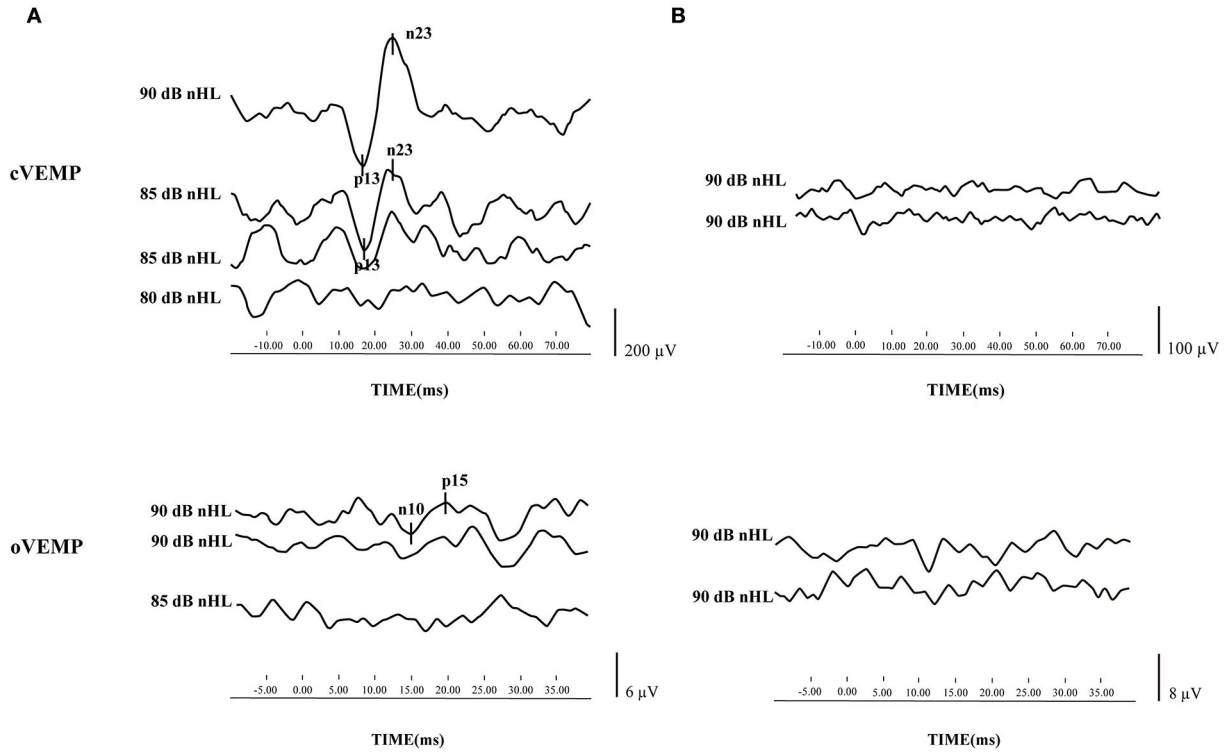

FIGURE 1
Cervical vestibular evoked myogenic potential (cVEMP) and ocular vestibular evoked myogenic potential (oVEMP) results of typical cases. **(A)** cVEMP and oVEMP were elicited from one patient with sudden sensorineural hearing loss (SSNHL) in the left ear. **(B)** cVEMP and oVEMP waveforms were absent from one patient with SSNHL in the left ear.

was 51.6%. The result of VEMP had a significant effect on the auditory outcome ($P = 2.9 \times 10^{-5}$, $P = 0.008$). However, the normal rate of the caloric test was 18.6%, and the abnormal rate was 37.5% in patients in the ineffective group. The caloric test results did not impact the auditory outcome in patients with UISSNHL ($P = 0.287$, Table 1).

We further investigated the contribution of vestibular function to the prognosis of patients with UISSNHL (Table 2). A better hearing improvement was observed in patients with normal cVEMP and/or oVEMP. Impaired hearing in patients with normal cVEMP improved by 33.76 ± 15.07 dB HL ($P = 3.36 \times 10^{-6}$), while those with abnormal cVEMP improved by 11.37 ± 17.42 dB HL. The impaired hearing in patients with normal oVEMP improved by 32.55 ± 19.56 dB HL ($P = 0.001$). However, only 15.29 ± 18.19 dB HL increased in patients with abnormal oVEMP. The caloric test results did not affect hearing improvement in patients with UISSNHL ($P = 0.728$).

Finally, we investigated the impact of VEMP results on the efficacy of patients with UISSNHL (Table 3). Of the 64 patients with UISSNHL who underwent both cVEMP and oVEMP examinations, 30 with both abnormal cVEMP and oVEMP had no response to treatment, while five with only one abnormality had no recovery from hearing impairments. Thus, the therapeutic efficacy was worse in patients with both abnormal cVEMP and oVEMP ($P = 2.16 \times 10^{-4}$, $P = 0.01$). Impaired hearing of patients with both normal cVEMP and oVEMP results improved by 39.24 ± 13.54 dB HL, and only one patient with both normal examinations failed to respond to treatment. Patients with either abnormal cVEMP or abnormal oVEMP results improved by 25.85 ± 17.71 dB HL. Patients with abnormal cVEMP and oVEMP results only improved by 10.90 ± 16.77 dB HL (Table 4). As a result, UISSNHL patients with both abnormal VEMP results had poorer hearing improvement.

Discussion

In this study, of 10 patients with normal cVEMP and oVEMP, only one failed to respond to treatment. Therefore, patients with normal cVEMP and oVEMP had better therapeutic efficacy overall. Of the 36 patients who failed to respond to treatment, 32 had abnormal oVEMP and 33 had abnormal cVEMP. Furthermore, patients with abnormalities in both cVEMP and oVEMP had a poorer auditory outcome and an effective rate than those with only one VEMP abnormality. Those with abnormal VEMP (cVEMP and/or oVEMP) also had

TABLE 1 Comparison of auditory outcome in terms of vestibular function in patients with UISSNHL.

Auditory outcome	cVEMP (*n*)		oVEMP (*n*)		Caloric test (*n*)	
	Normal	Abnormal	Normal	Abnormal	Normal	Abnormal
Ineffective	4 (6.3%)	32 (50.0%)	3 (4.7%)	33 (51.6%)	12 (18.6%)	24 (37.5%)
Total effective	18 (28.1%)	10 (15.6%)	11 (17.2%)	17 (26.6%)	13 (20.3%)	15 (24.3%)
	$P = 2.9 \times 10^{-5}$		$P = 0.008$		$P = 0.287$	

TABLE 2 Relationship between vestibular function and hearing improvement.

	cVEMP		Caloric test		oVEMP	
	Normal	Abnormal	Normal	Abnormal	Normal	Abnormal
Hearing improvement (dB HL)	33.76 ± 15.07	11.37 ± 17.42	32.55 ± 19.56	15.29 ± 18.19	20.03 ± 19.54	18.44 ± 20.03
	$P = 3.36 \times 10^{-6}$		$P = 0.001$		$P = 0.728$	

TABLE 3 Relationship between VEMP results and patients with hearing recovery.

	Ineffective	Effective
cVEMP and oVEMP both normal	1/10 (10.0%)*	9/10 (90.0%)
cVEMP or oVEMP abnormal	5/16 (31.3%)*	11/16 (68.8%)
cVEMP and oVEMP both abnormal	30/38 (78.9%)	8/38 (21.1%)

*Compared with cVEMP and oVEMP both abnormal group, $P = 2.28 \times 10^{-4}$, $P = 0.002$.

TABLE 4 Relationship between VEMP result and hearing improvement.

	Hearing improvement (dB HL)	*P*
cVEMP and oVEMP both normal	39.24 ± 13.54*	4.75×10^{-8}
cVEMP or oVEMP abnormal	25.85 ± 17.71*	
cVEMP and oVEMP both abnormal	10.90 ± 16.77	

*Compared with cVEMP and oVEMP both abnormal group, $P = 2.16 \times 10^{-4}$, $P = 0.01$.

a relatively poorer prognosis. These results suggest that impaired function occurs in the vestibular system, most likely in the otolith organ apart from the cochlea in patients with UISSNHL. The results of cVEMP and oVEMP significantly impact the auditory outcome. One abnormality was frequently followed by another in these two tests, attributable to their high degree of consistency.

In patients with UISSNHL, the proportion of vestibular dysfunction is very high, making it crucial to conduct a vestibular evaluation in these patients (21). It has been reported that SSNHL patients with vertigo were more susceptible to a more pronounced hearing loss and had a poorer auditory outcome; hence, vertigo is likely to be a predictor of hearing improvement (3, 22, 23). In this study, 54.7% (35/64) of patients complained of vertigo, with 97.1% (34/35) of cases having vestibular dysfunction, confirming that the incidence of vestibular dysfunction is extremely high in patients with UISSNHL. However, it is worth noting that in 29 patients with UISSNHL who did not have vertigo, 96.6% (28/29) of them were accompanied by vestibular function decline, and 72.4% (21/29) of them were ineffective after treatment. Therefore, vestibular dysfunction can probably appear even in those without vertigo, and it is inappropriate to estimate whether the vestibule is involved and whether the hearing prognosis is based on symptoms of vertigo alone. Korres et al. (24) proposed that vertigo alone had no value in predicting the prognosis. You et al. (25) suggested that whether SSNHL is accompanied by vertigo or not is unrelated to the extent of inner ear damage, i.e., it is inaccurate to indicate the definite lesion site of the inner ear in patients with SSNHL.

One study in India found that 61.5% of SSNHL patients with hearing loss exceeding 90 dB HL could not elicit VEMP and sacculus damage, and the degree of hearing loss did not affect whether patients were accompanied by vertigo (26). Another study also found a better prognosis in severe and profound SSNHL patients with normal VEMP. However, the worse the vestibular function, the poorer the prognosis in patients with profound SSNHL with vertigo (24, 27). Vestibular dysfunction often indicates that patients with SSNHL have a more extensive and severe inner ear injury, while the involvement of the otolith organs suggests a relatively poorer prognosis (28). Hong et al. (29) reported that in SSNHL patients without vertigo, the abnormal rate of VEMP was higher in patients with profound high-frequency hearing loss and was positively correlated with the degree and type of hearing loss. The degree of inner ear impairment is negatively correlated with the possibility of early recovery. In this study, of 29 UISSNHL patients without vertigo, only 10 cases (34.5%) were normal in cVEMP tests, and seven cases (24.1%) were normal in oVEMP tests. This suggests that

the occurrence and degree of vestibular dysfunction are not entirely related to the presence or absence of vertigo or the degree of hearing impairment.

The sacculus was more susceptible to injury than the horizontal semicircular canal in patients with SSNHL (30). This is consistent with the results of this study, which found a larger number of UISSNHL patients with abnormal cVEMP compared with those with an abnormal caloric test. Ciodaro et al. (31) investigated VEMP results in 40 patients with moderate to profound sensorineural hearing loss (MPSHL) and 30 healthy adults and found that cVEMPs were induced in 71.5% of ears in patients with MPSHL. The response rate in healthy adults was 100%, showing a high incidence of damage to the labyrinthine organs. Fujimoto et al. (4) classified SSNHL patients with vertigo based on their patterns of vestibular dysfunction and found that most of them belonged to the cochlear type, cochlear-sacculus type, and cochlear-sacculus-utriculus-semicircular canal type. Only a few patients were classified as the cochlear-utriculus type, cochlea-utriculus-horizontal semicircular canal type, and cochlea-horizontal semicircular canal type, suggesting that vestibular dysfunction in patients with SSNHL affects the vestibular organs close to the cochlea in the first place. Atrophic changes in the sacculus were observed in the vestibular organs in patients with SSNHL (5, 6, 32–34). Histopathological studies of temporal bones also reported that vestibular hair cell reduction in patients with SSNHL often occurred in the sacculus rather than in the semicircular canal (6).

The abnormal rate of the caloric test in patients with SSNHL was found to be lower than that in patients with vestibular neuritis (35). The sacculus or inferior vestibular nerve was more likely involved in SSNHL patients with vertigo, and the injury was closer to the terminal nerve, which was in a low-frequency range. Compared with the sacculus, the horizontal semicircular canal is farther away from the cochlea, making it less involved than the sacculus. However, the semicircular canal function of some patients may have been restored or compensated during the examination, and other clinical examinations are needed to evaluate the vestibular function (36). This study found that the results of the caloric test did not affect the auditory outcome of patients with UISSNHL. Of 39 patients with abnormal caloric tests, 61.5% (24/39) failed to respond to treatment. However, we noticed a considerable number of patients with abnormal caloric test outcomes in this study, and their prognosis was poor. The caloric test can evaluate the function of the bilateral horizontal semicircular canals with high sensitivity. Compared with the normal caloric test, the average hearing threshold of patients with an abnormal caloric test was higher (4). Some authors concluded that the caloric test and VEMP are predictors of early recovery of SSNHL (24). The abnormality rate of the caloric test was higher in patients with profound SSNHL. Therefore, based on these results, the cochlea, otolith organ, and semicircular canals in such patients are more likely to be affected simultaneously (24). However, the caloric test can only reflect the function of the horizontal semicircular canal, which is limited to evaluating the function of the vestibular ocular reflex (VOR) in the low-frequency range (<0.01 Hz) (37), causing poor reproducibility and intolerance in a specific group of patients.

In summary, for the first time, we combined three vestibular function tests to analyze relatively large samples and explored their influence on the auditory outcome to comprehensively predict the prognosis in patients with UISSNHL. The limitation of this study is that it included a higher proportion of older patients. They can lose the VEMP reflex, which may limit an accurate conclusion. Our results demonstrated that the prognosis of patients with abnormal cVEMP and oVEMP was poor. Generally, cVEMP and/or oVEMP are potentially valuable in predicting the outcome in patients with UISSNHL.

Data availability statement

The raw data supporting the conclusions of this article will be made available by the authors, without undue reservation.

Ethics statement

Written informed consent was obtained from the individual(s) for the publication of any potentially identifiable images or data included in this article.

Author contributions

ML: data collection, writing—original draft, and funding acquisition. HW: data analysis. JC and QZ: software and validation. SL: methodology. GZ: writing—review and editing and funding acquisition. JH: visualization and funding acquisition. XC: supervision and project administration. JY: design and writing—review and editing. MD: critical revision. YJ: statistical analysis and supervision. All authors contributed to the article and approved the submitted version.

Funding

This study was supported by the National Natural Science Foundation of China (Grant Nos. 81800903, 81970881, and 82071069).

Conflict of interest

The authors declare that the research was conducted in the absence of any commercial or financial relationships that could be construed as a potential conflict of interest.

Publisher's note

All claims expressed in this article are solely those of the authors and do not necessarily represent those of their affiliated organizations, or those of the publisher, the editors and the reviewers. Any product that may be evaluated in this article, or claim that may be made by its manufacturer, is not guaranteed or endorsed by the publisher.

References

1. Wilson WR, Byl FM, Laird N. The efficacy of steroids in the treatment of idiopathic sudden hearing loss: a double-blind clinical study. *Arch Otolaryngol.* (1980) 106:772–6. doi: 10.1001/archotol.1980.00790360050013

2. Stachler RJ, Chandrasekhar SS, Archer SM, Rosenfeld RM, Schwartz SR, Barrs DM, et al. Clinical practice guideline: Sudden hearing loss. *Otolaryngol Head Neck Surg.* (2012) 146(SUPPL.3):S1–35. doi: 10.1177/0194599812436449

3. Chinese Journal of Otorhinolaryngology Head and Neck Surgery So, Otorhinolaryngology Head and Neck Surgery CMA. Guideline of diagnosis and treatment of sudden deafness (2015). *Zhonghua Er Bi Yan Hou Tou JingWai Ke Za Zhi*. (2015) 50:443–7. doi: 10.3760/cma.j.issn.1673-0860.2015.06.002

4. Fujimoto C, Egami N, Kinoshita M, Sugasawa K, Yamasoba T, Iwasaki S. Involvement of vestibular organs in idiopathic sudden hearing loss with vertigo: an analysis using oVEMP and cVEMP testing. *Clin Neurophysiol.* (2015) 126:1033–8. doi: 10.1016/j.clinph.2014.07.028

5. Schuknecht HF, Donovan ED. The pathology of idiopathic sudden sensorineural hearing loss. *Arch Otorhinolaryngol.* (1986) 243:1–15. doi: 10.1007/BF00457899

6. Gussen R. Sudden deafnfess of vascular origin: a human temporal bone study. *Ann Otol Rhinol Laryngol.* (1976) 85:94–100. doi: 10.1177/000348947608500117

7. Lu YY, Jin Z, Tong BS, Yang JM, Liu YH, Duan M. A clinical study of microcirculatory disturbance in Chinese patients with sudden deafness. *Acta Otolaryngol.* (2008) 128:1168–72. doi: 10.1080/00016480801901626

8. Nakashima T, Yanagita N. Outcome of sudden deafness with and without vertigo. *Laryngoscope.* (1993) 103:1145–9. doi: 10.1288/00005537-199310000-00012

9. Shaia FT, Sheehy JL. Sudden sensori-neural hearing impairment: a report of 1,220 cases. *Laryngoscope.* (1976) 86:389–98. doi: 10.1288/00005537-197603000-00008

10. Zhang X, Xu X, Ma W, Zhang Q, Tong B, Yu H, et al. A clinical study of sudden deafness. *Acta Otolaryngol.* (2015) 135:1030–5. doi: 10.3109/00016489.2015.1060629

11. Mattox DE, Simmons FB. Natural history of sudden sensorineural hearing loss. *Ann Otol Rhinol Laryngol.* (1977) 86:463–80. doi: 10.1177/000348947708600406

12. Wilson WR, Laird N, Kavesh DA. Electronystagmographic findings in idiopathic sudden hearing loss. *Am J Otolaryngol.* (1982) 3:279–85. doi: 10.1016/S0196-0709(82)80067-7

13. Oiticica J, Bittar RS, Castro CC, Grasel S, Pereira LV, Bastos SL, et al. Contribution of audiovestibular tests to the topographic diagnosis of sudden deafness. *Int Arch Otorhinolaryngol.* (2013) 17:305–14. doi: 10.7162/S1809-97772013000300011

14. Jeffery N, Spoor F. Prenatal growth and development of the modern human labyrinth. *J Anat.* (2004) 204:71–92. doi: 10.1111/j.1469-7580.2004.00250.x

15. Lim R, Brichta AM. Anatomical and physiological development of the human inner ear. *Hear Res.* (2016) 338:9–21. doi: 10.1016/j.heares.2016.02.004

16. Lyon MJ, Payman RN. Comparison of the vascular innervation of the rat cochlea and vestibular system. *Hear Res.* (2000) 141:189–98. doi: 10.1016/S0378-5955(00)00004-6

17. Tiong TS. Prognostic indicators of management of sudden sensorineural hearing loss in an Asian hospital. *Singapore Med J.* (2007) 48:45–9.

18. Wang Y, Wang L, Jing Y, Yu L, Ye F. Association between hearing characteristics/prognosis and vestibular function in sudden sensorineural hearing loss with vertigo. *Front Neurol.* (2020) 11:579757. doi: 10.3389/fneur.2020.579757

19. Huy PT, Sauvaget E. Idiopathic sudden sensorineural hearing loss is not an otologic emergency. *Otol Neurotol.* (2005) 26:896–902. doi: 10.1097/01.mao.0000185071.35328.6d

20. Ben-David J, Luntz M, Podoshin L, Sabo E, Fradis M. Vertigo as a prognostic sign in sudden sensorineural hearing loss. *Int Tinnitus J.* (2002) 8:127–8.

21. Sokolov M, Gordon KA, Polonenko M, Blaser SI, Papsin BC, Cushing SL. Vestibular and balance function is often impaired in children with profound unilateral sensorineural hearing loss. *Hear Res.* (2019) 372:52–61. doi: 10.1016/j.heares.2018.03.032

22. Arbusow V, Schulz P, Strupp M, Dieterich M, Von Reinhardstoettner A, Rauch E, et al. Distribution of herpes simplex virus type 1 in human geniculate and vestibular ganglia: Implications for vestibular neuritis. *Ann Neurol.* (1999) 46:416–9. doi: 10.1002/1531-8249(199909)46:3<416::aid-ana20>3.0.co;2-w.

23. Xie W, Dai Q, Liu J, Liu Y, Hellström S, Duan M. Analysis of clinical and laboratory findings of idiopathic sudden sensorineural hearing loss. *Sci Rep.* (2020) 10:6057. doi: 10.1038/s41598-020-63046-z

24. Korres S, Stamatiou GA, Gkoritsa E, Riga M, Xenelis J. Prognosis of patients with idiopathic sudden hearing loss: role of vestibular assessment. *J Laryngol Otol.* (2011) 125:251–7. doi: 10.1017/S0022215110002082

25. You TZ, Wang SJ, Young YH. Registering grades of sudden deafness to predict the hearing outcome via an inner-ear test battery. *Int J Audiol.* (2014) 53:153–8. doi: 10.3109/14992027.2013.851798

26. Khan F, Balraj A, Lepcha A. Vestibular evoked myogenic potential in sudden sensorineural hearing loss. *Ind J Otol.* (2013) 19:55–8. doi: 10.4103/0971-7749.113504

27. Wang CT, Huang TW, Kuo SW, Cheng PW. Correlation between audiovestibular function tests and hearing outcomes in severe to profound sudden sensorineural hearing loss. *Ear Hear.* (2009) 30:110–4. doi: 10.1097/AUD.0b013e318192655e

28. Park HM, Jung SW, Rhee CK. Vestibular diagnosis as prognostic indicator in sudden hearing loss with vertigo. *Acta Otolaryngol.* (2001) 545:80–3. doi: 10.1080/713792589

29. Hong SM, Byun JY, Park CH, Lee JH, Park MS, Cha CI. Saccular damage in patients with idiopathic sudden sensorineural hearing loss without vertigo. *Otolaryngol Head Neck Surg.* (2008) 139:541–5. doi: 10.1016/j.otohns.2008.07.003

30. Iwasaki S, Takai Y, Ozeki H, Ito K, Karino S, Murofushi T. Extent of lesions in idiopathic sudden hearing loss with vertigo: study using click and galvanic vestibular evoked myogenic potentials. *Arch Otolaryngol Head Neck Surg.* (2005) 131:857–62. doi: 10.1001/archotol.131.10.857

31. Ciodaro F, Freni F, Alberti G, Forelli M, Gazia F, Bruno R, et al. Application of cervical vestibular-evoked myogenic potentials in adults with moderate to profound sensorineural hearing loss: a preliminary study. *Int Arch Otorhinolaryngol.* (2020) 24:e5–10. doi: 10.1055/s-0039-1697988

32. Inagaki T, Cureoglu S, Morita N, Terao K, Sato T, Suzuki M, et al. Vestibular system changes in sudden deafness with and without vertigo: a human temporal bone study. *Otol Neurotol.* (2012) 33:1151–5. doi: 10.1097/MAO.0b013e3182635440

33. Ishii T, Toriyama M. Sudden deafness with severe loss of cochlear neurons. *Ann Otol Rhinol Laryngol.* (1977) 86:541–7. doi: 10.1177/000348947708600414

34. Yood TH, Paparella MM, Schacern PA, Alleva M. Histopathology of sudden hearing loss. *Laryngoscope.* (1990) 100:707–15. doi: 10.1288/00005537-199007000-00006

35. Li J, Liu X, Liu C, Liu S, Zhang S, Wu Z. Study on difference of vestibular damage of sudden deafness and vestibular neuritis. *Chin Arch Otolaryngol Head Neck Surg.* (2017) 24:25–7. doi: 10.16066/j.1672-7002.2017.01.005

36. Bartolomeo M, Biboulet R, Pierre G, Mondain M, Uziel A, Venail F. Value of the video head impulse test in assessing vestibular deficits following vestibular neuritis. *Eur Arch Otorhinolaryngol Surg.* (2014) 271:681–8. doi: 10.1007/s00405-013-2451-y

37. Strupp M, Feil K, Dieterich M, Brandt T. Chapter 17 - Bilateral vestibulopathy. In: Furman JM, Lempert T, editors. *Handbook of Clinical Neurology*, Vol. 137. Amsterdam: Elsevier (2016), p. 235–40. doi: 10.1016/B978-0-444-63437-5.00017-0

frontiers | Frontiers in Neurology

TYPE Original Research
PUBLISHED 03 November 2022
DOI 10.3389/fneur.2022.1024743

Check for updates

OPEN ACCESS

EDITED BY
Lisheng Yu,
Peking University People's Hospital, China

REVIEWED BY
Furong Ma,
Peking University Third Hospital, China
Zhaohui Hou,
Chinese PLA General Hospital, China

*CORRESPONDENCE
Junbo Zhang
zhangjunbo354@163.com
Zhen Zhong
1341466115@qq.com

†These authors have contributed equally to this work

SPECIALTY SECTION
This article was submitted to Neuro-Otology, a section of the journal Frontiers in Neurology

RECEIVED 22 August 2022
ACCEPTED 14 October 2022
PUBLISHED 03 November 2022

CITATION
Zhen Z, Zhao T, Wang Q, Zhang J and Zhong Z (2022) Laryngopharyngeal reflux as a potential cause of Eustachian tube dysfunction in patients with otitis media with effusion. *Front. Neurol.* 13:1024743. doi: 10.3389/fneur.2022.1024743

COPYRIGHT
© 2022 Zhen, Zhao, Wang, Zhang and Zhong. This is an open-access article distributed under the terms of the Creative Commons Attribution License (CC BY). The use, distribution or reproduction in other forums is permitted, provided the original author(s) and the copyright owner(s) are credited and that the original publication in this journal is cited, in accordance with accepted academic practice. No use, distribution or reproduction is permitted which does not comply with these terms.

Laryngopharyngeal reflux as a potential cause of Eustachian tube dysfunction in patients with otitis media with effusion

Zhen Zhen[1†], Tingting Zhao[2†], Quangui Wang[1†], Junbo Zhang[1*] and Zhen Zhong[1*]

[1]Department of Otolaryngology, Head and Neck Surgery, Peking University First Hospital, Beijing, China, [2]Department of Head and Neck Surgery, National Cancer Center/National Clinical Research Center for Cancer/Cancer Hospital and Shenzhen Hospital, Chinese Academy of Medical Sciences and Peking Union Medical College, Shenzhen, China

Objective: To explore the association between laryngopharyngeal reflux disease (LPRD)-related symptoms and the Eustachian tube (ET) function in adult patients with otitis media with effusion (OME).

Materials and methods: A total of 105 adult patients with OME were retrospectively studied. All these patients had undergone tubomanometry (TMM) test for the affected ears before treatments. The LPRD-related symptoms were all assessed by the Reflux Symptom Index (RSI) scale.

Results: Among the 105 included patients, the numbers of subjects with only one and both two ears affected were 65 (57.1%) and 40 (42.9%), respectively. Therefore, a total of 145 affected ears were studied. For these affected ears, a linear regression analysis that included sex, age, BMI, smoking history, drinking history, RSI value, and the condition of the contralateral ear suggested that only RSI value was significantly associated with TMM value ($P < 0.001$), with the correlation coefficient of −0.112. Among the 9 symptoms in RSI scale, affected ears with the following symptoms (vs. affected ears without) showed significantly lower TMM values: excess throat mucus or postnasal drip, difficulty swallowing food, liquids, or pills, and sensations of something stuck in your throat or a lump in your throat (all $P < 0.05$).

Conclusion: LPRD may disrupt ET function in adult OME patients. A higher RSI score is independently predictive for a bad ET patency in such patients and is indicative for an additional anti-reflux therapy.

KEYWORDS

laryngopharyngeal reflux, Eustachian tube, otitis media with effusion, tubomanometry (TMM), Reflux Symptom Index (RSI)

Introduction

Otitis media with effusion (OME) is a non-suppurative disease characterized by the presence of fluid in the middle ear cavity without acute infection. Its main symptoms include hearing loss, ear fullness, earache, and tinnitus. Although there is a certain chance of self-healing, there are still a great number of such patients who need treatments. When treated inappropriately, this disease may cause long-term complications such as adhesive otitis media, cholesteatoma, tympanosclerosis, and ossicular necrosis (1).

Currently, there are not standard criteria for treating adult OME. Conservative treatments including medication or the combination of medication and Eustachian tube (ET) auto-inflation are usually preferred for newly diagnosed patients (2, 3), with advantages of non-invasiveness and good compliance. However, conservative treatments are usually less effective for those with bad ET patency (4, 5). Therefore, exploring factors related to ET function are important for a precise treatment for this disease.

Laryngopharyngeal reflux disease (LPRD) refers to an inflammatory condition of the upper aerodigestive tract tissues related to gastric or duodenal content reflux (6, 7). This disease could be associated with laryngological, rhinological, and ontological conditions (8–10). Animal experiments have confirmed the role of such reflux in disrupting the ET patency through decreased ciliary clearance, mucosal hyperemia, and edema (11). However, few clinical researches are available with respect to the effects of LPRD on ET function.

The present study aimed to investigate the correlation between LPRD and ET function assessed by tubomanometry (TMM) in adult OME patients. The occurrence and severity of LPRD were assessed by Reflux Symptom Index (RSI), a widely used subjective scale proposed by Belafsky et al. (12). These results may be important reference for the indication of anti-reflux therapy in OME patients.

Materials and methods

Study population

Between Jan 2019 and Jan 2020, a total of 105 newly diagnosed OME patients in our database who met the following criteria were retrospectively studied: (1) age ≥18 years; (2) typical primary complaints included ear fullness and (or) hearing loss of more than 2 weeks; (3) conductive hearing loss on pure tone test and type B or C results from the tympanometry test; (4) an intact tympanic membrane and no nasopharyngeal neoplasms or adenoidal hyperplasia according to endoscopy examination; (5) no upper respiratory allergy or infection during the course of treatments; and (6) complete RSI assessment data. The baseline information of all studied patients including age, sex, body mass index (BMI), smoking history, drinking history, and RSI value are shown in Table 1. This study protocol was approved by the ethics committee of Peking University First Hospital.

TABLE 1 The baseline information of the 105 newly diagnosed OME patients.

	Numbers/ Mean ± SD	Percentage (%)/range
Age (years)	49.9 ± 15.3	18–87
Sex		
Male	47	44.8
Female	58	55.2
BMI (kg/m^2)	24.4 ± 3.6	14.9–33.2
Smoking history		
Yes	21	20
No	84	80
Drinking history		
Yes	11	10.5
No	94	89.5
RSI value	5.1 ± 5.8	0-30

TMM

The TMM (Spiggle and Theis, Overath, Germany) was performed for all affected ears in our patients as described previously (13). The patients took a sitting position with the pressure receptor probe set in the ear canal. After the patients held a small amount of water in the mouth, a nasal adapter was set into both nostrils. The patients were then told to tightly close the teeth and swallow. The pressure receptor probe records the pressure changes transmitted through the movements of the tympanic membrane. The pressure changed in the nasopharynx and external auditory canal also could be recorded; the data were saved on a computer, and figures measure the pressure changes in the nasopharynx and ear canal in millibars (mbar) against time in seconds. 30, 40, and 50 mbar were used as three initial nasal cavity pressures in the test. The functional state of the ET was evaluated using the opening latency index (R value) by R = (P1 – C1)/(C2 – C1). P1 is the start of the movement of the eardrum after pressure application, C1 is the start of the pressure increase in the nasopharynx, and C2 is the maximum pressure increase in the nasopharynx. P1 – C1 represents the latency of tubal opening, and C2 – C1 represents the time of increased pressure in the nasopharynx. The R value quantifies the ET patency: an R value ≤1 indicates satisfactory ET function and is weighted as two points, indicating that the tube opening occurs before C2; an *R* value >1 suggests a delayed opening or restricted ET function and is weighed as 1 point, indicating that the tube

TABLE 2 The TMM value distribution of all 145 affected ears and corresponding RSI values.

TMM	No. of ears	RSI value	*P*-value
0	20	7.1 ± 7.3	0.007
1	8	11.4 ± 9.5	
2	16	6.1 ± 5.9	
3	15	5.2 ± 4.2	
4	12	4.8 ± 4.7	
5	19	5.0 ± 5.6	
6	55	3.4 ± 4.3	

opening occurs after C2; while a negative or non-measurable R value indicates that the ET has not opened or is occluded and is weighted as 0 point. The TMM values are calculated as the sum of all points at 30, 40, and 50 mbar; hence, the theoretical range of TMM should be 0–6 (13).

RSI assessment

RSI is a 9-item patient questionnaire scoring system used to assess severity of reflux symptoms. Each item of RSI was scored from 0 (no symptom) to 5 (the most serious symptom), and the total score can be between 0 and 45 points. The questionnaire was distributed on site by one designated researcher to all the OME patients and was collected after they had completed it.

Statistical analysis

The statistical analysis in current study was all performed with SPSS software version 20.0 (IBM, Armonk, NY). Continuous variables were all displayed as mean ± standard deviation. The unpaired Student *t*-test and one-way ANOVA were used to compare continuous variables between different groups. The linear regression analysis was used to identify significant associations. For all analyses, a *P*-value <0.05 was considered to be statistically significant.

Results

Among the 105 included patients, the numbers of subjects with only one and both two ears affected were 65 (57.1%) and 40 (42.9%), respectively. Therefore, a total of 145 affected ears were studied. The overall TMM value of these ears was 3.9 ± 2.2, with a range of 0–6. The RSI score according to different TMM values was shown in Table 2, suggesting a decrease tend of RSI with an increase of TMM value ($P = 0.007$).

A linear regression analysis including sex, age, BMI, smoking history, drinking history, RSI value, and the condition of the contralateral ear suggested that only RSI value was significantly associated with TMM value ($P < 0.001$). The coefficient of this correlation was −0.112 (SE 0.03) and the R^2 of this model was 0.087 (adjusted R^2 0.081, SE of the estimate 2.123).

The TMM value was also compared according to different items of RSI scale. As shown in Table 3, affected ears with the following symptoms (vs. affected ears without) showed significantly lower TMM values: excess throat mucus or postnasal drip, difficulty swallowing food, liquids, or pills, and sensations of something stuck in your throat or a lump in your throat (all $P < 0.05$).

Discussion

ET is a potential ventilation passage connecting the middle ear cavity to the nasopharynx with the primary function of adjusting middle ear pressure (14). ET dysfunction plays an important role in the pathogenesis and progression of OME (15, 16). Currently, there have been several studies that had explored the relationship between OME and LPRD (17, 18), with some ones had directly detected pepsin/pepsinogen in middle ear secretions (19–21). However, the effect of LPRD on ET function in OME patients is not clear. This is mainly due to the lack of accurate methods in evaluating the ET patency in the past. The TMM method introduced by Schroder et al. is a relatively new semi-objective method for evaluating ET patency (13). Using this method, we investigated the potential effect of LPRD on ET function among OME patients.

The most important finding of present study was that a high RSI score was independently predictive for a low TMM value, suggesting an important role of LPRD in damaging ET function of OME patients. This not only further proved that LPRD can be involved in the occurrence and progression of OME by affecting ET function, but also suggested that the simple RSI score could be used as a reference for anti-reflux therapy in adult OME patients. As the ET dysfunction evaluated by TMM method had been proved to be associated with ineffective conservative treatments (4, 5), the clinical research conducted by Pang et al. had proved the potential advantages of acid-suppressive drugs in OME patients with abnormal RSI results (22). Our results further suggested that the mechanism may be attributed to the prevention of LPRD in disrupting ET patency. Therefore, an additional anti-reflux therapy should be suggested for OME patients with abnormal RSI scores.

In current study, we also explored what symptoms included in RSI scale are more likely to be associated with a lower TMM value and found them to be excess throat mucus or postnasal drip, difficulty swallowing food, liquids, or

TABLE 3 The comparison of TMM value between ears with different RSI symptoms.

Items of RSI scale	No. of ears	TMM value	*P*
Hoarseness or problem with your voice			0.236
Yes	32	3.4 ± 2.2	
No	113	4.0 ± 2.2	
Clearing your throat			0.066
Yes	59	3.4 ± 2.3	
No	86	4.1 ± 2.2	
Excess throat mucus or postnasal drip			0.015
Yes	71	3.4 ± 2.3	
No	74	4.3 ± 2.1	
Difficulty swallowing food, liquids, or pills			0.006
Yes	12	2.2 ± 2.1	
No	133	4.0 ± 2.2	
Coughing after you ate or after lying down			0.109
Yes	27	3.2 ± 2.5	
No	118	4.0 ± 2.1	
Breathing difficulties or choking episodes			0.367
Yes	22	3.5 ± 2.2	
No	123	3.9 ± 2.2	
Troublesome or annoying cough			0.061
Yes	36	3.3 ± 2.3	
No	109	4.1 ± 2.1	
Sensations of something stuck in your throat or a lump in your throat			0.030
Yes	62	3.4 ± 2.1	
No	83	4.2 ± 2.2	
Heart burn, chest pain, indigestion, or stomach acid coming up			0.175
Yes	39	3.4 ± 2.3	
No	106	4.0 ± 2.2	

pills, and sensations of something stuck in your throat or a lump in your throat. As a result, OME patients with such reflux symptoms may benefit more from an additional anti-reflux therapy.

The study had some limitations that need to be addressed. First, there was no further confirmatory research that could explore the effect of anti-reflux therapies in improving ET function. This is important and has been added into our future research plans. Second, the RSI scale is not an objective method in evaluating LPRD and its accuracy can be easily affected by some subjective factors. Some other objective evaluations of LPRD which were not collected may be more useful in predicting TMM values, such as salivary pepsin value or pH test results. However, there were some studies that had proved the close relationship between RSI with the diagnostic gold standards of LPRD (dynamic multi-probe esophageal impedance and PH value monitoring) (23, 24). At last, we did not detect the mechanism by which LPRD affects ET function. We hypothesized that local fluid mechanic and micro-environment changes brought by reflux may be the main reasons, which need further researches.

Conclusions

In summary, the current study suggested that LPRD may disrupt ET function in OME patients. A higher RSI score is independently predictive for a bad ET patency in such patients and is indicative for an additional anti-reflux therapy.

Data availability statement

The raw data supporting the conclusions of this article will be made available by the authors, without undue reservation.

Ethics statement

The studies involving human participants were reviewed and approved by the Ethics Committee of Peking University First Hospital. Written informed consent for participation was not required for this study in accordance with the national legislation and the institutional requirements.

Author contributions

JZ and ZZho designed the study and revised the manuscript. ZZhe, TZ, and QW participated in the material preparation, data collection, data analysis, and drafting of the manuscript. All authors commented on previous versions of the manuscript, read, and approved the final manuscript.

Funding

This study was supported by Natural Science Foundation of Beijing Municipality (7204315), Youth clinical research project of Peking University First Hospital (2019CR30), and Capital Foundation of Medical Development (2022-2-4078).

Conflict of interest

The authors declare that the research was conducted in the absence of any commercial or financial relationships that could be construed as a potential conflict of interest.

Publisher's note

All claims expressed in this article are solely those of the authors and do not necessarily represent those of their affiliated organizations, or those of the publisher, the editors and the reviewers. Any product that may be evaluated in this article, or claim that may be made by its manufacturer, is not guaranteed or endorsed by the publisher.

References

1. Paksoy M, Altin G, Eken M, Hardal U. Effectiveness of intratympanic dexamethasone in otitis media with effusion resistant to conventional therapy. *Indian J Otolaryngol Head Neck Surg.* (2013) 65:461–7. doi: 10.1007/s12070-011-0281-z

2. Schilder AG, Marom T, Bhutta MF, Casselbrant ML, Coates H, Gisselsson-Solen M, et al. Panel 7: Otitis Media: Treatment and Complications. *Otolaryngol Head Neck Surg.* (2017) 156:S88–S105. doi: 10.1177/0194599816633697

3. Perera R, Glasziou PP, Heneghan CJ, McLellan J, Williamson I. (2013). Autoinflation for hearing loss associated with otitis media with effusion. *Cochrane Database Syst Rev.* (2013) 5:CD006285. doi: 10.1002/14651858.CD006285.pub2

4. Zhong Z, Zhang J, Ren L, Liu Y, Zhen Z, Xiao S, et al. Predictors of Conservative Treatment Outcomes for Adult Otitis Media with Effusion. *J Int Adv Otol.* (2020) 16:248–52. doi: 10.5152/iao.2020.8091

5. Zhang J, Zhong Z, Xiao S, Liu Y, Zhen Z, Ren L, et al. Tubomanometry value as an associated factor for medication outcomes in adult acute otitis media with effusion. *Eur Arch Otorhinolaryngol.* (2018) 275:53–7. doi: 10.1007/s00405-017-4772-8

6. Lechien JR, Akst LM, Hamdan AL, Schindler A, Karkos PD, Barillari MR, et al. Evaluation and Management of Laryngopharyngeal Reflux Disease: State of the Art Review. *Otolaryngol Head Neck Surg.* (2019) 160:762–82. doi: 10.1177/0194599819827488

7. Lechien JR, Saussez S, Muls V, Barillari MR, Chiesa-Estomba CM, Hans S, et al. Laryngopharyngeal reflux: a state-of-the-art algorithm management for primary care physicians. *J Clin Med.* (2020) 9:3618. doi: 10.3390/jcm9113618

8. Lechien JR, Akst LM, Saussez S, Crevier-Buchman L, Hans S, Barillari MR, et al. Involvement of laryngopharyngeal reflux in select nonfunctional laryngeal diseases: a systematic review. *Otolaryngol Head Neck Surg.* (2021) 164:37–48. doi: 10.1177/0194599820933209

9. Ozmen S, Yucel OT, Sinici I, Ozmen OA, Suslu AE, Ogretmenoglu O, et al. Nasal pepsin assay and pH monitoring in chronic rhinosinusitis. *Laryngoscope.* (2008) 118:890–4. doi: 10.1097/MLG.0b013e318165e324

10. Poelmans J, Tack J, Feenstra L. Chronic middle ear disease and gastroesophageal reflux disease: a causal relation? *Otol Neurotol.* (2001) 22:447–50. doi: 10.1097/00129492-200107000-00005

11. Lou Z, Xue C, Kang J, Gong T, Scholp A, Jiang JJ, et al. Establishment of a novel and effective reflux laryngitis model in rabbits: a preliminary study. *Eur Arch Otorhinolaryngol.* (2019) 276:175–83. doi: 10.1007/s00405-018-5234-7

12. Belafsky PC, Postma GN, Koufman JA. Validity and reliability of the reflux symptom index (RSI). *J Voice.* (2002) 16:274–7. doi: 10.1016/S0892-1997(02)00097-8

13. Schroder S, Lehmann M, Sauzet O, Ebmeyer J, Sudhoff H. A novel diagnostic tool for chronic obstructive eustachian tube dysfunction-the eustachian tube score. *Laryngoscope.* (2015) 125:703–8. doi: 10.1002/lary.24922

14. Bluestone CD, Doyle WJ. Anatomy and physiology of eustachian tube and middle ear related to otitis media. *J Allergy Clin Immunol.* (1988) 81:997–1003. doi: 10.1016/0091-6749(88)90168-6

15. Doyle WJ. Functional eustachian tube obstruction and otitis media in a primate model. *A review Acta Otolaryngol Suppl.* (1984) 414:52–7. doi: 10.3109/00016488409122882

16. Mills R, Hathorn I. Aetiology and pathology of otitis media with effusion in adult life. *J Laryngol Otol.* (2016) 130:418–24. doi: 10.1017/S0022215116000943

17. Sone M, Kato T, Nakashima T. Current concepts of otitis media in adults as a reflux-related disease. *Otol Neurotol.* (2013) 34:1013–7. doi: 10.1097/MAO.0b013e318299aa52

18. Lechien JR, Hans S, Simon F, Horoi M, Calvo-Henriquez C, Chiesa-Estomba CM, et al. Association between laryngopharyngeal reflux and media otitis: a systematic review. *Otol Neurotol.* (2021) 42:e801–14. doi: 10.1097/MAO.0000000000003123

19. Al-Saab F, Manoukian JJ, Al-Sabah B, Almot S, Nguyen LH, Tewfik TL, et al. Linking laryngopharyngeal reflux to otitis media with effusion: pepsinogen study of adenoid tissue and middle ear fluid. *J Otolaryngol Head Neck Surg.* (2008) 37:565–71.

20. Dogru M, Kuran G, Haytoglu S, Dengiz R, Arikan OK. Role of laryngopharyngeal reflux in the pathogenesis of otitis media with effusion. *J Int Adv Otol.* (2015) 11:66–71. doi: 10.5152/iao.2015.642

21. O'Reilly RC, He Z, Bloedon E, Papsin B, Lundy L, Bolling L, et al. The role of extraesophageal reflux in otitis media in infants and children. *Laryngoscope.* (2008) 118:1–9. doi: 10.1097/MLG.0b013e31817924a3

22. Pang K, Di Y, Li G, Li J, Li X, Sun L, et al. Can reflux symptom index and reflux finding score be used to guide the treatment of secretory otitis media in adults? *ORL J Otorhinolaryngol Relat Spec.* (2020) 82:130–8. doi: 10.1159/000505929

23. Cumpston EC, Blumin JH, Bock JM. Dual pH with multichannel intraluminal impedance testing in the evaluation of subjective laryngopharyngeal reflux symptoms. *Otolaryngol Head Neck Surg.* (2016) 155:1014–20. doi: 10.1177/0194599816665819

24. Plocek A, Gebora-Kowalska B, Bialek J, Fendler W, Toporowska-Kowalska E. Esophageal impedance-pH monitoring and pharyngeal ph monitoring in the diagnosis of extraesophageal reflux in children. *Gastroenterol Res Pract.* (2019) 2019:6271910. doi: 10.1155/2019/6271910

frontiers | Frontiers in Neurology

TYPE Original Research
PUBLISHED 03 November 2022
DOI 10.3389/fneur.2022.1016577

Check for updates

OPEN ACCESS

EDITED BY
Lisheng Yu,
Peking University People's Hospital, China

REVIEWED BY
Tzu-Pu Chang,
Tzu Chi University, Taiwan
Qing Zhang,
Shanghai Jiaotong University School of Medicine, China

*CORRESPONDENCE
Tadao Yoshida
tadaoy@med.nagoya-u.ac.jp
Shinji Naganawa
naganawa@med.nagoya-u.ac.jp

SPECIALTY SECTION
This article was submitted to Neuro-Otology, a section of the journal Frontiers in Neurology

RECEIVED 11 August 2022
ACCEPTED 26 September 2022
PUBLISHED 03 November 2022

CITATION
Yoshida T, Naganawa S, Kobayashi M, Sugimoto S, Katayama N, Nakashima T, Kato Y, Ichikawa K, Yamaguchi H, Nishida K and Sone M (2022) ^{17}O-labeled water distribution in the human inner ear: Insights into lymphatic dynamics and vestibular function. *Front. Neurol.* 13:1016577. doi: 10.3389/fneur.2022.1016577

COPYRIGHT
© 2022 Yoshida, Naganawa, Kobayashi, Sugimoto, Katayama, Nakashima, Kato, Ichikawa, Yamaguchi, Nishida and Sone. This is an open-access article distributed under the terms of the Creative Commons Attribution License (CC BY). The use, distribution or reproduction in other forums is permitted, provided the original author(s) and the copyright owner(s) are credited and that the original publication in this journal is cited, in accordance with accepted academic practice. No use, distribution or reproduction is permitted which does not comply with these terms.

^{17}O-labeled water distribution in the human inner ear: Insights into lymphatic dynamics and vestibular function

Tadao Yoshida[1]*, Shinji Naganawa[2]*, Masumi Kobayashi[1], Satofumi Sugimoto[1], Naomi Katayama[3], Tsutomu Nakashima[4], Yutaka Kato[5], Kazushige Ichikawa[5], Hiroshi Yamaguchi[6], Kazuki Nishida[7] and Michihiko Sone[1]

[1]Department of Otorhinolaryngology, Nagoya University Graduate School of Medicine, Nagoya, Japan, [2]Department of Radiology, Nagoya University Graduate School of Medicine, Nagoya, Japan, [3]Department of Health and Nutrition, Faculty of Health and Sciences, Nagoya Women's University, Nagoya, Japan, [4]Department of Rehabilitation, Ichinomiya Medical Treatment and Habilitation Center, Ichinomiya, Japan, [5]Department of Radiological Technology, Nagoya University Hospital, Nagoya, Japan, [6]Medical Branch of Radioisotope Research Center, Nagoya University, Nagoya, Japan, [7]Department of Biostatistics Section, Center for Advanced Medicine and Clinical Research, Nagoya University Graduate School of Medicine, Nagoya, Japan

We evaluated the inner ear distribution of ^{17}O-labeled saline administered to the human tympanic cavity. Magnetic resonance imaging was performed after intratympanic administration in five healthy volunteers and one patient with cochlear endolymphatic hydrops. In all volunteers, ^{17}O-labeled water permeated the cochlear basal turn and vestibule at 30 min and disappeared gradually within 2–4 h. All participants experienced positional vertigo lasting a few hours to a few days. Visualization of ^{17}O-labeled water distribution in the endolymphatic space of the posterior ampulla showed indistinct separation of endolymph and perilymph in the cochlea and most of the vestibule in all participants. Intralabyrinthine distribution of ^{17}O-labeled water differed from that in previous reports of intratympanically administered gadolinium-based contrast agent. ^{17}O-labeled water in the endolymphatic space may cause heavier endolymph and positional vertigo. These results of this study may add new insights for investigating the distribution and the effects of molecules in the inner ear after the intratympanic administration in living humans.

KEYWORDS
^{17}O-labeled water, MRI, perilymph, endolymph, vertigo

Introduction

^{17}O has a low natural abundance of 0.038% and is the only stable isotope of oxygen that produces signal changes in proton magnetic resonance imaging (MRI) (1–3). Because of its low natural abundance, enrichment is required for the detection of ^{17}O (2). The direct detection method of ^{17}O uses the Larmor frequency of the ^{17}O nucleus in humans and animals (4–6), and requires specific hardware. In the indirect detection

method, the proton of water molecules labeled with ^{17}O can be viewed as a signal change because of T2 shortening (1, 3, 7). Given that ^{17}O-labeled water is a water molecule, it can be safely administered without inducing an allergic reaction in living organisms or risk in patients with renal failure. The safety of intravenous and intrathecal administration of ^{17}O-labeled water has been reported in humans (3, 8).

^{15}O-positron emission tomography (PET) is considered to be the gold standard for the quantitative analysis of cerebral blood flow and oxygen metabolism. However, ^{15}O has a short half-life of 122 s, requires a cyclotron for quantification, and involves radiation exposure (9). The spatial resolution of PET is insufficient for the analysis of tiny structures such as the inner ear. One significant advantage of ^{17}O is that it has no half-life as a nuclide, which allows for extended time tracer analysis, and no radiation exposure.

The first visualization of endolymphatic hydrops in a patient with Ménière's disease was achieved using three-dimensional (3-D) fluid-attenuated inversion recovery images at 3 T 24 h after intratympanic administration of a gadolinium-based contrast agent (GBCA), and this method has been used by many researchers since then (10–13). The preferential distribution of GBCA in the perilymph allows endolymphatic hydrops to be imaged (14, 15). Water has a minimal molecular weight (18 for regular water, 19 for ^{17}O-labeled water) compared with GBCA (500–800 depending on the type of agent).

In this study, we hypothesized that ^{17}O-labeled water administered into the tympanic cavity would penetrate the perilymph through the round window faster than GBCA. The purpose of this study was to evaluate the permeability and distribution of intratympanically administered ^{17}O-labeled water in healthy people without auditory vestibular symptoms and in a patient with endolymphatic hydrops.

Methods

Participants

Volunteers with no previous auditory or vestibular symptoms were recruited between November 2021 and December 2021. Eligible participants had to be at least 20 years of age; four male volunteers and one female volunteer (mean age: 34 years; age range: 30–42 years) were included. A male patient aged in his 40 s with endolymphatic hydrops in the cochlea noted by previous gadolinium-contrast MRI was also included. The patient had a previous history of acute low-tone sensorineural hearing loss but had no history of vertigo and was currently asymptomatic. The study was approved by the institutional review board of the study institution (No. 2021-0309), and written informed consent was obtained from all participants before enrolment.

^{17}O-labeled saline (10 mol% $H_2^{17}O$; Taiyo Nippon Sanso Corp., Tokyo, Japan) was injected intratympanically using a 23-G needle and 1-mL syringe into the left ear of the five volunteers and into the right ear of the patient with endolymphatic hydrops. Each participant was placed in the supine position with their head turned ∼30° away from the sagittal line toward the non-injected side ear. The solution was warmed to body temperature before injection. ^{17}O-labeled saline was injected until a backflow of fluid into the external ear was observed through a microscope, and the injected volume was 0.6–0.8 mL per participant. After the injection, the participants remained in the supine position for 30 min with the head turned ∼60° away from the sagittal line toward the non-injected side ear. This water tracer was made under good manufacturing practice standards for intravenous injection in human participants. In a previous study, 1 mL/kg of 20 mol% $H_2^{17}O$ was administered intravenously at a rate of 3 mL/s to 14 volunteers without any adverse effects (3). To our knowledge, the present study is the first to apply this tracer intratympanically in humans.

MRI

The estimated GBCA concentration in perilymph 24 h after intratympanic administration of GBCA is ∼1/625 of that of the administered solution (15). The molecular weight of gadoteridol used for intratympanic administration is 558.7, and that of ^{17}O-labeled water is only 19. Therefore, <625 times dilution is expected for ^{17}O-labeled water compared with GBCA in the perilymph after intratympanic administration.

Phantom experiments and sequence optimization in human volunteers

In a pilot study, we performed phantom experiments to optimize the pulse sequence parameters for the scan after intratympanic administration of ^{17}O-labeled saline. ^{17}O-labeled water shortens the T2 time as an indirect effect in proton MRI (3). We prepared test tubes with various dilutions of 10 mol% ^{17}O-labeled saline (Taiyo-Nissan Co. Ltd, Tokyo, Japan) as follows: original solution; dilutions of 2, 4, 8, 16, 32, 64, 128, 192, 256, 512, 1,024, 2,048, 4,096, 8,192, and 16,384 times; and normal saline. To visualize low concentrations of ^{17}O-labeled water using T2-weighted images in the human inner ear with fine anatomy, we used hT2W MR cisternography and 3-D turbo spin–echo (SPACE: sampling perfection with application-optimized contrasts using different flip angle evolution) with TEs of 500–5,600 ms (16). In the phantom experiments, we

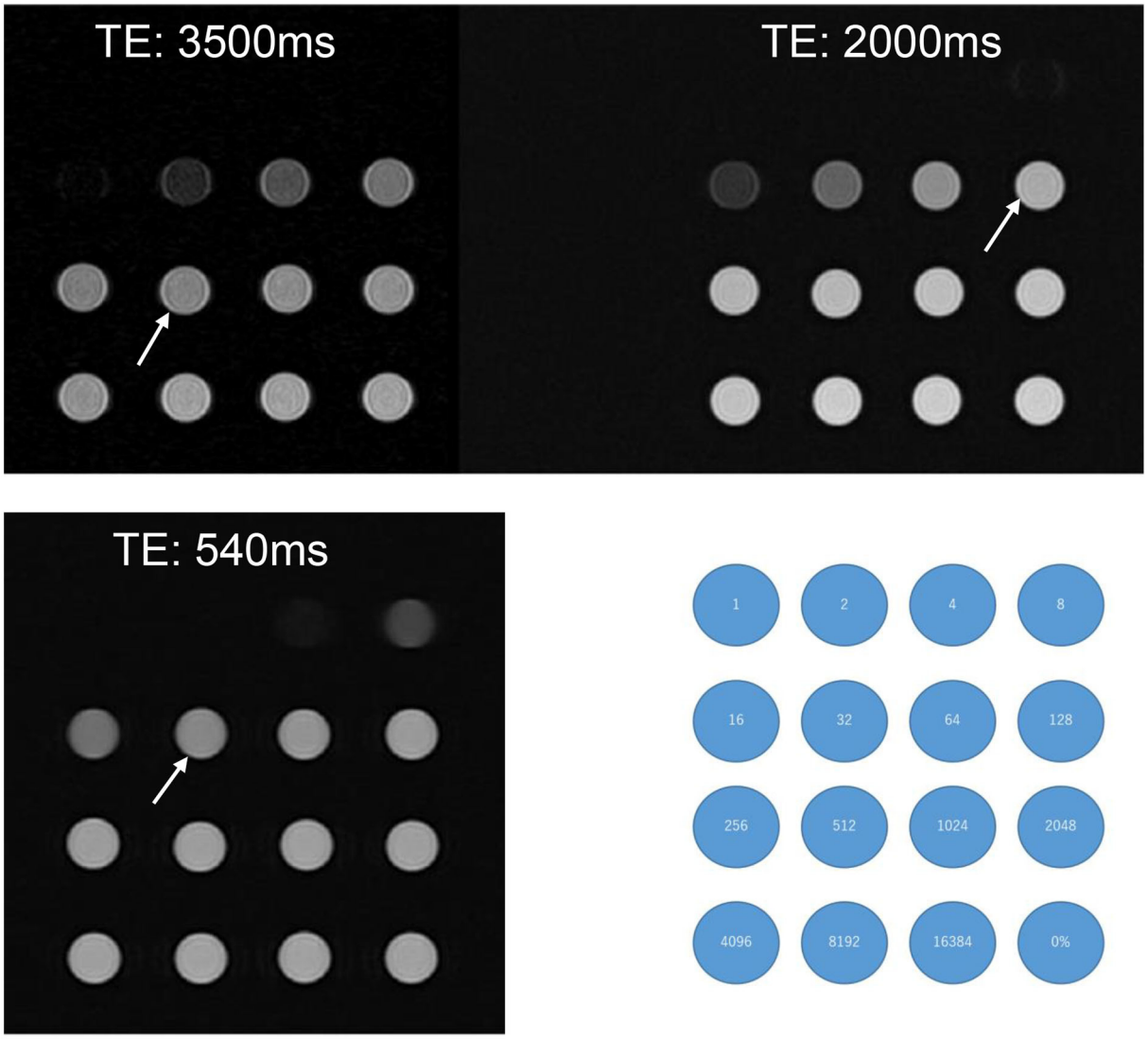

FIGURE 1
A phantom experiment with test tubes of various ^{17}O-saline concentrations. 10 mol% ^{17}O-saline was diluted with normal saline. Numbers in the blue circles indicate the dilutions. The right lower corner tube (0%) indicates the tube filled with normal saline. Compared with normal saline, the slight signal decrease for ^{17}O-saline was barely recognizable for the 512 times dilution for a TE of 3,500 ms (arrow), 128 times dilution for a TE of 2,000 ms (arrow), and 32 times dilution for a TE of 540 ms (arrow). Even at a TE of 540 ms, dilutions of <8 did not produce a visible signal.

could differentiate the 512 times dilution and normal saline using a TE of 3,500 ms (Figure 1). With an increasing TE, the signal–intensity ratio (SIR) (normal saline/512-times diluted ^{17}O-labeled water) increased to 1.00 at a TE of 500 ms, 1.06 at a TE of 2,000 ms, 1.10 at a TE of 3,000 ms, and 1.12 at a TE of 3,500 ms. However, with an increasing TE, the image noise increased. We needed to identify the maximum TE value to visualize the fine inner ear anatomy with a reasonable scan time in humans.

Before the administration of ^{17}O-labeled saline, we scanned three volunteers. The maximum TE to visualize the inner ear anatomy steadily in a reasonable scan time of 6 min was 3,200 ms (Figure 2). We could not predict the exact dilution ratio of ^{17}O-labeled water saline in the perilymph nor how fast the ^{17}O-labeled water or saline would permeate and distribute within the labyrinth. We decided to use three TEs to accommodate the various concentrations, 540, 2,000, and 3,200 ms, and to obtain images at multiple times. Using multiple TEs and images with various sensitivity to low concentrations of ^{17}O-labeled water allowed us to perform image processing of the different TEs and to produce easily recognized images for the visualization of the ^{17}O-labeled water distribution. All MRI scans were performed using a 3 T unit (Skyra, Siemens Healthineers, Erlangen, Germany) using a 32-channel

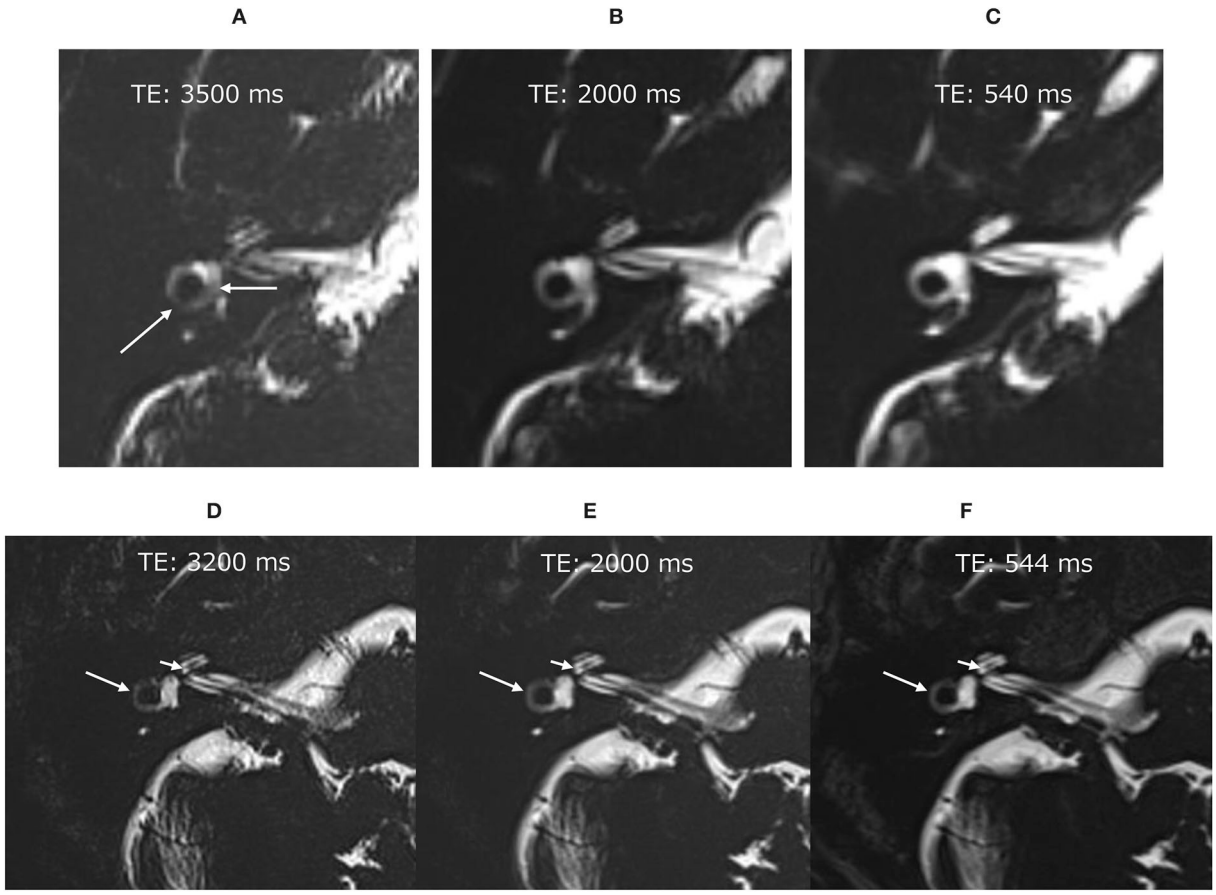

FIGURE 2
Pilot scans in volunteers without administration of the ^{17}O-labeled water tracer. In the image with an echo time (TE) of 3,500 ms **(A)**, the vestibular signal was not uniform, and the lateral semicircular canal was not continuous (arrows). Note that these structures were visualized clearly in the images with a TE of 2,000 ms **(B)** and TE of 540 ms **(C)**. Pilot scans in another volunteer without ^{17}O-labeled water tracer administration. Although the image with a TE of 3,200 ms was slightly noisy **(D)**, the anatomy of the labyrinth could be seen clearly. The signal for the vestibule was more uniform in the image with a TE of 3,200 ms **(D)** than in that with a TE of 3,500 ms **(A)**. For example, the osseous spiral lamina of the cochlea (short arrow) and the lateral semicircular canal (arrow) could be identified in all images of this volunteer **(D–F)**.

array head coil. Details of the scan parameters are shown in Table 1.

MRI scanning

MRI was performed 30 min, 2 h, 4 h, and 24 h after the intratympanic administration of ^{17}O-labeled saline in all volunteers. All volunteers underwent hT2W MR cisternography with three different TEs (544, 2,000, and 3,200 ms) for 3 min for a TE of 544 ms and for 6 min for the other TEs. The first scan was followed by an additional imaging using a TE of 3,200 ms 15 min after the start of the first phase in three volunteers. In the male patient with endolymphatic hydrops in the cochlea, the 6 min scan for a TE of 3,200 ms was performed five times and a subsequent 3 min scan for a TE of 540 ms was obtained.

Evaluation of ^{17}O-labeled water contrast effects

The contrast effects on the cochlear and vestibular fluid were evaluated semiquantitatively, as reported previously in patients with sudden deafness or Ménière's disease (17, 18). The SIR was measured three times, and the average SIR value was calculated. The signal intensities of each inner ear were quantified as follows. The measurement sites were the basal and apical–middle turns of the cochlea, vestibular cavity, and ampulla of the posterior semicircular canal.

For the basal turn region of interest (ROI), the slice was selected at least three slices below the center slice on which the cochlear modiolus appeared largest. For the apical–middle turn ROI, the slice was selected at the center slice on which the cochlear modiolus appeared largest. The ROI for the vestibule

10.3389/fneur.2022.1016577

TABLE 1 Scan paremeters for 3 kinds of MR cisternography.

Sequence name	Type	Repetition time (ms)	Echo time (ms)	Flip angle (degree)	Section thickness/re (mm) construction step (mm)	Pixel size (mm)	Number of slices	Echo spacing (ms)	Echo train length	Echo train duration (ms)	Phase partial fourier (%)	Field of view (mm)	Matrix size	Number of excitations	GRAPPA	Bandwidth (Hz/pixel)	Slice oversampling (%)	Scan time (min:s)
MR cisternography 1	3D T2 SPACE	15,000	3,200	90/constant160	2.0/1.0	0.5×0.5	80	7.23	599	4,345	77	165 × 196	324 × 384	1.4	3	434	100	6:00
MR cisternography 2	3D T2 SPACE	15,000	2,000	90/constant160	2.0/1.0	0.5×0.5	80	7.23	599	4,157	96	165 × 196	324 × 384	1.4	3	434	100	6:00
MR cisternography 3	3D T2 SPACE	4,000	540	90/constant130	2.0/1.0	0.5×0.5	80	6.11	272	1,369	82	165 × 196	324 × 384	1.4	3	434	100	3:28

SPACE, Sampling perfection with application-optimized contrasts using different flip angle evolutions.
GRAPPA, GeneRalized autocalibrating partial parallel acquisition.
All three sequences utilize a restore magnetization pulse and slab selective excitation pulse.
3D slab is set in an axial orientation.

was drawn on the lowest slice on which the lateral semicircular canal ring was visualized at more than 240° and excluded the semicircular canal and ampulla when the ROI for the vestibule was drawn on MR images with a TE of 540 ms. For the ampulla of the posterior semicircular canal ROI, one slice below the slice on which the vestibule was assessed was selected.

For quantitative evaluation, the SIR between the signals of the injected left side and the non-injected right side was measured on MR images with a TE of 3,200 ms. The ROIs were drawn manually on the MR images with a TE of 540 ms, and were copied and pasted onto MR images with a TE of 3,200 ms and onto MR images taken during another time phase (Figure 3). If motion was detected between the scans, fine adjustments were made manually. Using the signal value of the ROI for the right side as a control, each SIR was calculated as the signal intensity of the ROI in the left side divided by that in the right ear. The ROIs were placed using a PACS viewer (Rapideye Core, Canon Medical Systems, Tochigi, Japan) by a single observer with 15 years of experience in the evaluation of inner ear MRI.

Evaluation of positional nystagmus

Nystagmus was evaluated by VOG using a yVOG glass device (Daiichi Medical Company, Tokyo, Japan). VOG evaluates all the three dimensions of eye movements, namely, the horizontal, vertical, and torsional components. Spontaneous nystagmus in the dark was recorded in the left inferior, supine, and right inferior head positions.

Results

All volunteers received intratympanic administration of ^{17}O-labeled saline to their left ear and completed the study protocol. The volunteers had no symptoms of positional vertigo during the 30-min rest period after administration of ^{17}O-labeled saline and before the start of the MRI study. However, all volunteers experienced positional vertigo after 30 min following the intratympanic administration of ^{17}O-labeled saline lasting 40 min to 6 h. The duration of vertigo for each volunteer was as follows: volunteer #1 for 6 h, volunteer #2 for 4 h, volunteer #3 for 3.5 h, volunteer #4 for 5.5 h, and volunteer #5 for 40 min. We could not record the nystagmus of the volunteers, but observation under Frenzel goggles revealed a horizontal rotatory direction-changing positional geotropic nystagmus. Vertigo and nystagmus lessened when the head position was returned to rest with the injected side up. After the vertigo symptoms disappeared, there were no complaints of auditory vestibular symptoms, and all volunteers returned to their pretreatment state.

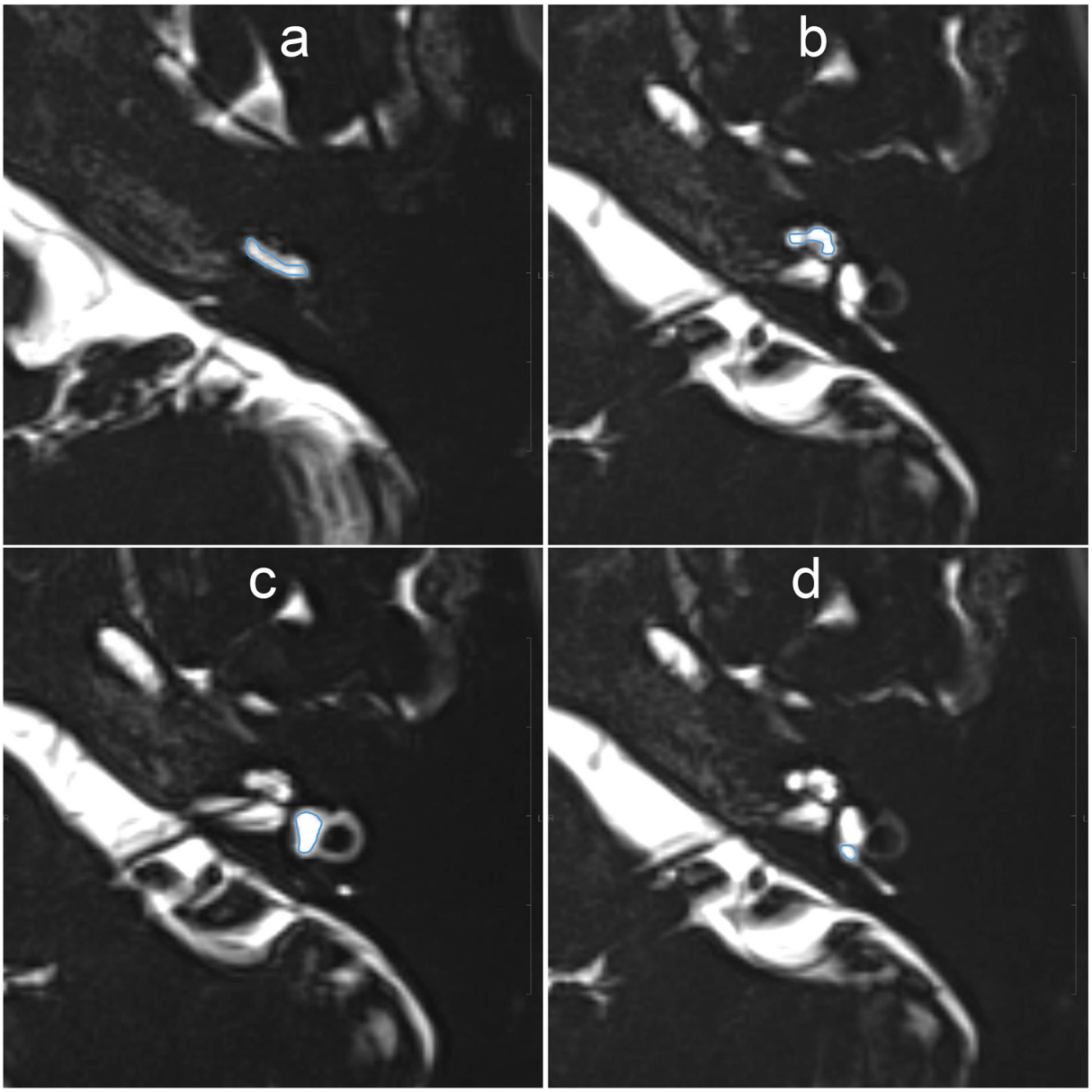

FIGURE 3
Example images for setting of the region of interest (ROI) on MR images with an echo time (TE) of 540 ms. The scala tympani of the basal turn of the cochlea **(a)**, whole apical–middle turn **(b)**, vestibule **(c)**, and the ampulla of the posterior semicircular canal **(d)** appeared contoured. The ROIs were then copied onto the other TE images. Each signal–intensity ratio was calculated using the signal value of the contralateral inner ear as a control.

In the male patient with endolymphatic hydrops in the right cochlea, ^{17}O-labeled saline was administered intratympanically to the right ear. This patient also experienced vertigo symptoms and nystagmus, and video oculography (VOG) showed horizontal rotatory direction-changing positional geotropic nystagmus (Figure 4). His vertigo lasted for 6.5 h and was followed by several days of dizziness and nystagmus. In the horizontal component, the rapid phase of nystagmus in the left lower head position (injection side up) was leftward, and the frequency was low. By contrast, in the right lower head position (injection side down), the rapid phase changed to the rightward and increased frequency. Although the waveform in the supine position could not be obtained because of errors at 270 min after injection, we confirmed that the leftward nystagmus in the supine position changed to the rightward direction after 390 min in the later scan. The torsional component was clockwise in the right lower head position and counterclockwise in the left head lower position. The vertical component was always upward. The

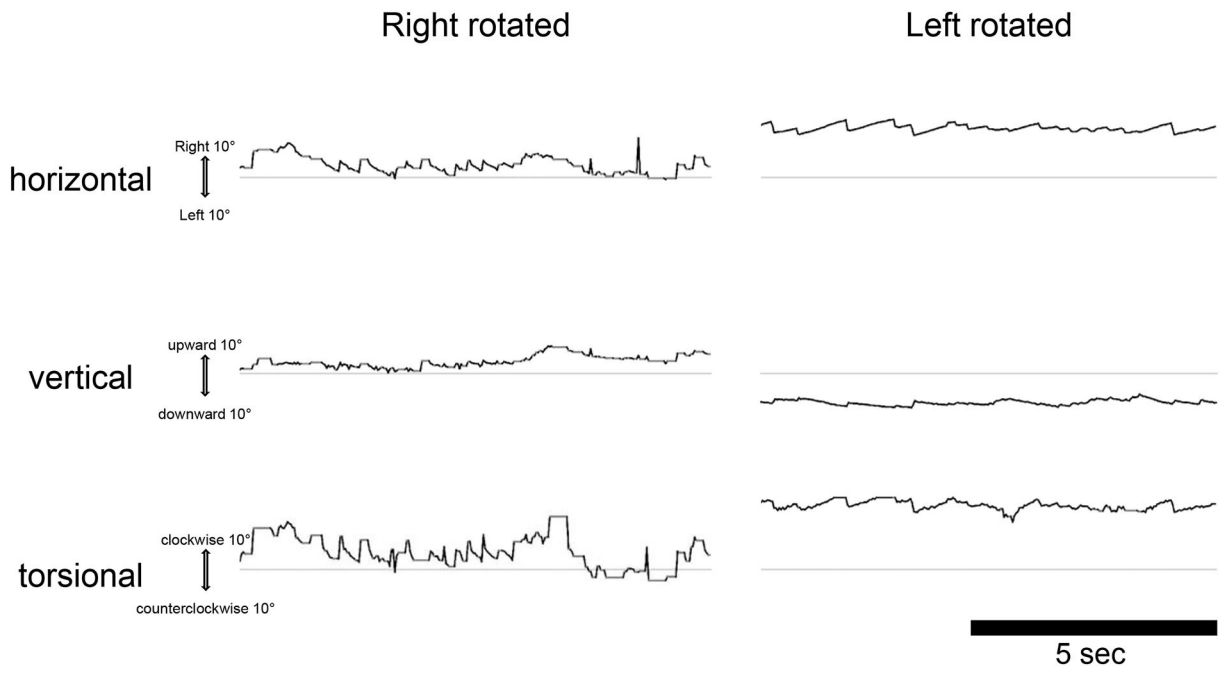

FIGURE 4
Video oculography findings in the dark 270 min after injection of ^{17}O-labeled water in the right (affected) tympanic space in a patient with cochlear endolymphatic hydrops. The eye movements are displayed from top to bottom, as horizontal, vertical, and torsional as indicated. The upward direction of each trace indicates right, up, and clockwise (from the subject view). The ordinate and abscissa indicate the eye position in degrees and time in seconds, respectively. The average slow phase speed of nystagmus was 4°/s to the right, 2°/s down, and 6°/s clockwise for the left rotated, and 8°/s to the left, 3°/s down, and 19°/s counterclockwise for the right rotated.

nystagmus showed no latency and no fatigue phenomenon. The amplitude and frequency of the nystagmus decreased gradually with time. The position of the vestibule with the head position is shown in Figure 5.

MRI findings after ^{17}O-labeled water injection into the inner ear

In all participants, ^{17}O-labeled water was found to be distributed in the inner ear on the injected side (Figures 6–9). That is, there was a decrease in signal in the inner ear on the injected side on T2-weighted MR images. In the image with an echo time (TE) of 3,200 ms, the whole vestibular signal decreased because of the high sensitivity to the T2-shortening effect of ^{17}O-labeled saline (Figure 6A). The basal turn and anterior part of the second turn of the cochlea also showed decreased signals in the scala tympani, scala vestibuli, and scala media. The image for a TE of 2,000 ms (Figure 6B) showed the anatomy of the labyrinth and the contrast between the areas with rich and poor ^{17}O-labeled water distribution. The image for a TE of 540 ms (Figure 6C) showed a nearly unrecognizable T2-shortening effect after administration of ^{17}O-labeled water.

The images with shorter TE provided details on the anatomy of the labyrinth. Serially acquired images provided information about the time course of the spatial distribution of ^{17}O-labeled water (Figures 7, 8). The separation between the endolymph and perilymph was not distinct in the cochlea and vestibule (Figures 6–9), and we could not identify the shape of the saccule and utricle. The distribution of ^{17}O-labeled water to the posterior ampulla could be visualized in the longest TE images (Figures 6, 7, 9). In the patient, repeated scans for the longest TE images showed that ^{17}O-labeled water distributed gradually to the posterior ampulla (Figure 9).

Time course of the signal–intensity ratio

The lowest SIR values were observed in the images obtained 30 min after the administration of ^{17}O-labeled saline. In the volunteers, we obtained MR images at later times. After 2 h, the signal in the basal turn of the cochlea and the whole vestibular cavity had recovered slightly, and further signal recovery was observed after 4 h when the left–right difference disappeared almost completely. SIR values differed between the volunteers. At 30 min after intratympanic administration, the basal turn of the cochlea showed the lowest signal, followed by the vestibular

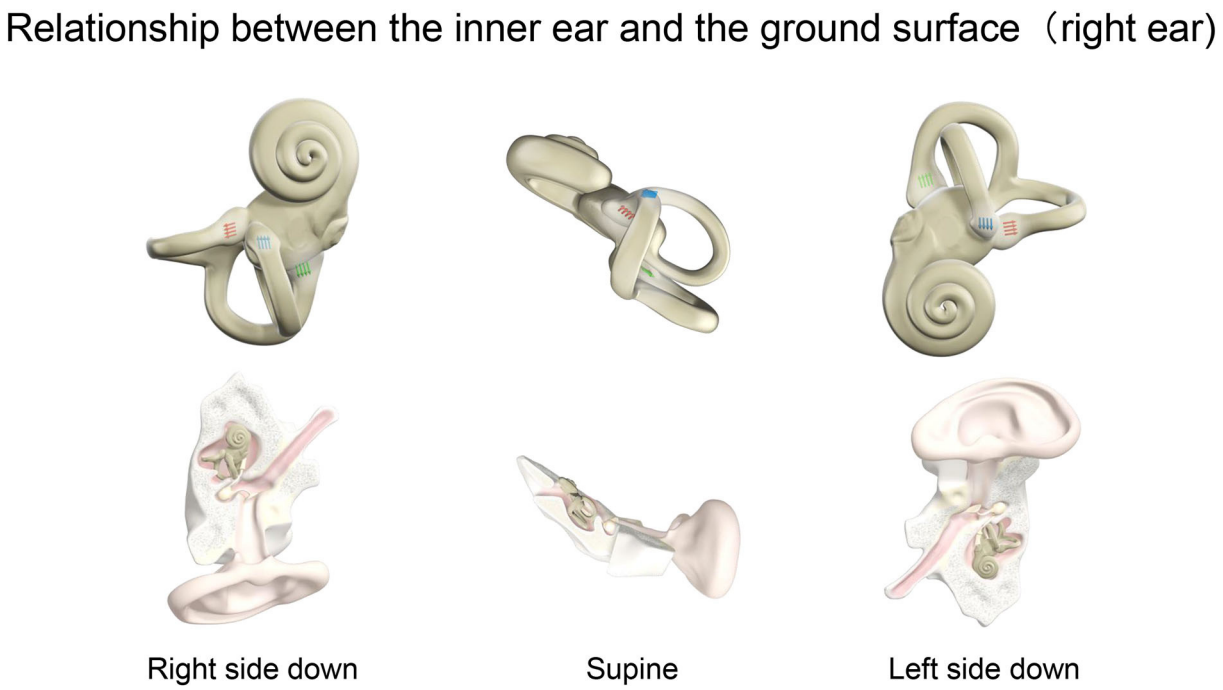

FIGURE 5
Relationship between the inner ear and the ground surface (right ear). The positional relationship of the inner ear for right ear side down, supine, and left ear side down in a person lying on the MRI bed. The right inner ear is viewed in the horizontal plane. The ampulla is shown for the three semicircular canals. Blue, red, and green arrows indicate the ampulla in the horizontal, anterior, and posterior semicircular canal, respectively. The direction of the arrows shows the stimulus direction of endolymph movement. In the horizontal canal, ampullopetal flow toward the ampulla causes a stronger stimulus. By contrast, ampullofugal flow leaving the ampulla causes a stronger stimulus in the anterior and posterior canals. Nystagmus, a fast component of eye movement, moves in the opposite direction to the arrows of the three semicircular canals combined.

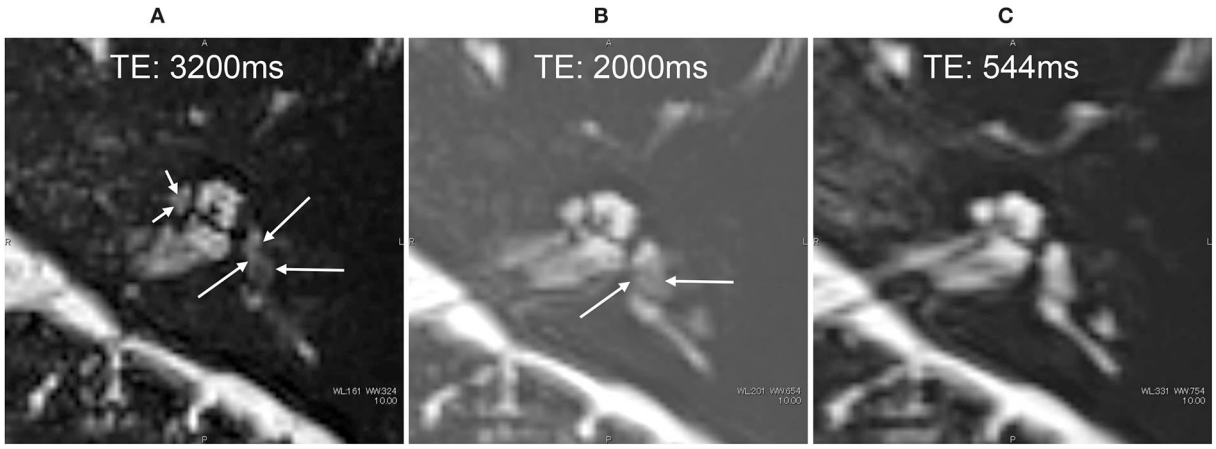

FIGURE 6
MR cisternography of the left ear in a 34-year-old male volunteer at the start of the scan. The MR scan was initiated 30 min after the intratympanic administration of ^{17}O-labeled saline **(A–C)**. Images were obtained serially in the order of **(A–C)**. In the image with an echo time (TE) of 3,200 ms **(A)**, the signal of the whole vestibule (arrows) decreased because of the highest sensitivity to the T2-shortening effect of ^{17}O-labeled saline. The anterior part of the cochlea also showed a decreased signal (short arrows). In the image with a TE of 2,000 ms **(B)**, the anatomy of the labyrinth and the contrast between the area with rich ^{17}O-labeled water distribution (arrows) and that with poor ^{17}O-labeled water distribution can be seen. In the image with a TE of 544 ms **(C)**, the T2-shortening effect of ^{17}O-labeled water was almost unrecognizable, and the anatomy of the labyrinth could be seen.

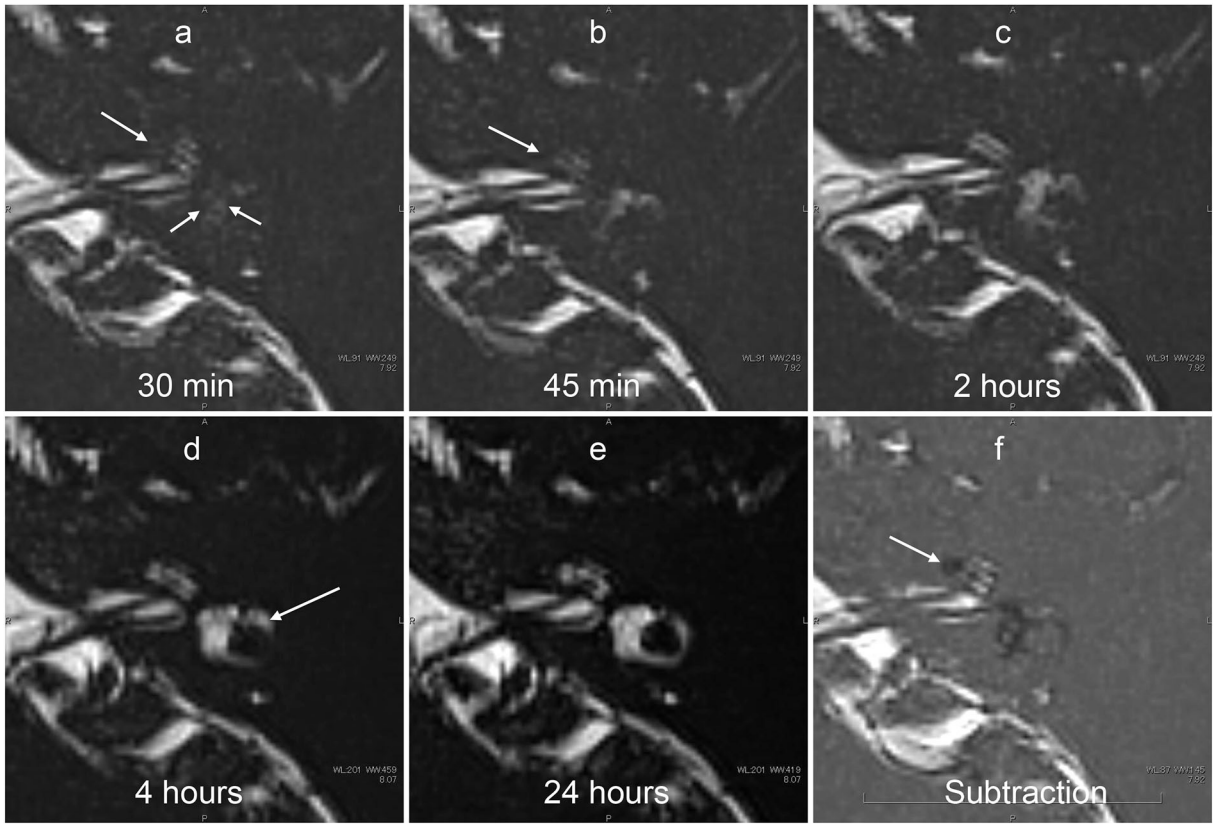

FIGURE 7
Serial MR cisternography (TE: 3,200 ms) of the left ear in a 34-year-old male volunteer (different volunteer from that shown in Figure 3) at 30 min **(a)**, 45 min **(b)**, 2 h **(c)**, 4 h **(d)**, and 24 h **(e)** after intratympanic administration of ^{17}O-labeled saline. The subtraction image is also shown **(f)**. This subtraction image was generated as the value for **(b)** minus the value for a TE of 540 s × 0.18. The MR scan was initiated ∼30 min after the intratympanic administration of ^{17}O-labeled saline to the left middle ear. The images at the level of the cochlear nerve are shown. The signal decrease in the vestibule (short arrows in **a**) and in the anterior part of the basal cochlear turn (arrows in **a,b**) was most prominent in the image obtained at 30 min. At 45 min **(c)**, some parts of the cochlear (arrow) and the vestibular signal began to recover. At 2 h, the vestibular signal and the signal in the basal turn of the cochlea recovered further **(c)**. At 4 h, the signal for the lateral semicircular canal had recovered (arrows in **d**). At 24 h **(e)**, the signal for the left labyrinthine fluid had recovered to a level similar to that for the contralateral side (not shown). In the subtraction image **(f)**, an area with a rich distribution of ^{17}O-labeled water was seen as a lower signal area (arrow). This subtraction image provided an overview of the distribution of ^{17}O-labeled water and the anatomy of the labyrinth simultaneously in a single image.

space (Figure 10A). The apical–middle turn tended to have a slightly lower signal at 2 h than at 30 min, but this difference was not obvious (Figure 10B). The average SIR was higher for the ampulla of the posterior semicircular canal than that for the vestibular space but was lowest in both locations at 30 min after injection (Figures 10C,D). 24 h after injection, the SIR did not differ between the left and right sides of the inner ear at all measurement sites in all volunteers. Volunteers #1 and #4, whose dizziness persisted for more than 5 h, tended to have vestibular SIR values <0.4 at 30 min after the injection, and these values were lower than in the other volunteers. After 45 min from the injection of ^{17}O-labeled saline, the patient with endolymphatic hydrops had severe vertigo symptoms, making it challenging to perform imaging. The SIR at 30 min after intratympanic administration of ^{17}O-labeled saline was 0.2 in the basal turn of the cochlea, 0.8 in the apical-middle turn, 0.1 in the vestibular space, and 0.6 in the ampulla of the posterior semicircular canal, which was comparable to those in volunteers where the signal decrease was most evident.

Discussion

This report is the first study in humans to show that intratympanic administration of ^{17}O-labeled saline can produce contrast that can be examined using proton MRI of the inner ear. Intratympanic or intravenous GBCA administration is used as a contrast method for the separate visualization of endolymph and perilymph in the inner ear (10, 13, 19). Intratympanically administered GBCA distributes mainly into the perilymphatic fluid space and not into the endolymphatic space (11, 14). In the presence of endolymphatic hydrops, the endolymphatic

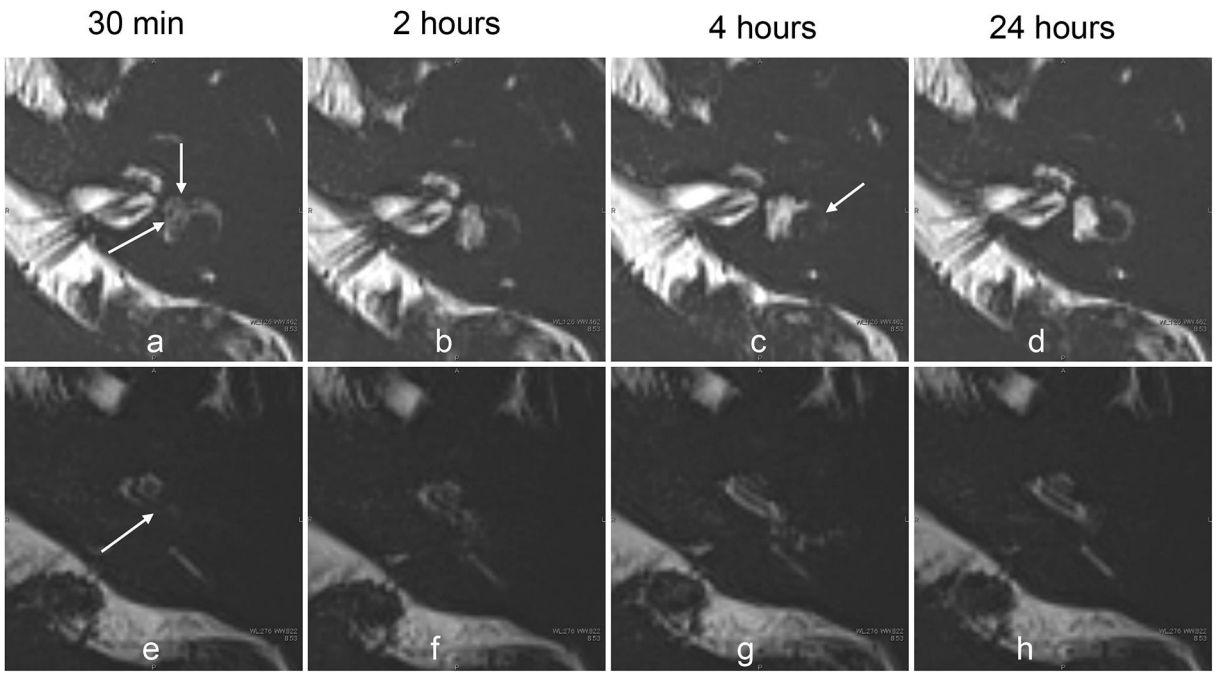

FIGURE 8
Serial MR cisternography (TE: 3,200 ms) of the left ear in a 33-year-old female volunteer at 30 min, and 2, 4, and 24 h after the intratympanic administration of ^{17}O-labeled saline **(a–c)**. The MR scan was initiated ~30 min after the intratympanic administration of ^{17}O-labeled saline into the left middle ear. The upper row **(a–d)** shows the images at the level of the cochlear nerve. The lower row **(e–h)** shows the images at the level of the cochlear aqueduct. The signal decreases in the vestibule (arrows, **a**) and in the basal turn of the cochlea (arrows, **e**) were most prominent in the image obtained at 30 min. The extent of the signal decrease in the vestibule in this volunteer is less than that for the volunteer whose images are shown in Figure 4. At 2 h, the vestibular signal and the signal in the basal turn of the cochlea began to recover **(b,f)**. At 4 h, the signal for the lateral semicircular canal decreased (arrows, **c**), and the signal for the cochlear basal turn recovered **(g)**. At 24 h **(d,h)**, the signal for the left labyrinthine fluid recovered to the level seen in the contralateral side (not shown).

space is seen as an enlarged low-signal area separated from the high-signal area of the perilymphatic space with GBCA distribution. However, GBCA is not suitable for use in patients with asthma, allergies, or renal insufficiency. If endolymphatic hydrops can be identified without the use of conventional gadolinium contrast agents, ^{17}O-labeled saline enhancement allows examining patients with asthma, renal dysfunction, and allergy to contrast agents.

^{17}O-labeled water has an indirect effect by shortening the T2 value in proton MRI. The R_2 value is estimated as 3.33 s^{-1} 8. To detect low-concentration ^{17}O-labeled water, a T2-weighted pulse sequence is required. In a previous study, a steady-state sequence was used in the evaluation of the brain parenchyma3. In the present study, we focused on the signal change for the inner ear lymph fluid, which has a very long T2 value. To detect the subtle shortening of T2 for the fluid with a high spatial resolution in a reasonable scan time, we used MR cisternography and a 3-D-turbo spin–echo sequence with an extremely long TE (3,200 ms). This kind of ultra-heavily T2-weighted (hT2W) imaging has not been used in clinical settings.

Systemic administration of 20% ^{17}O-labeled water at a dose of 1 mL/kg caused no side effects in 14 participants in one study (3). Intrathecal administration of 10 mL of 10% ^{17}O-labeled water caused no adverse effects in four patients in another study (8). ^{17}O-labeled water is a safe but expensive tracer (several hundred US dollars per mL), and the routine use of large amounts of this tracer is not practical. Local administration of a small amount of this tracer might be practical, although the transitional positional vertigo following the intratympanic administration of this tracer should be explained in advance, and patients should be monitored closely. One has to explore the threshold level of the ^{17}O-labeled saline concentration that does not produce vertigo. We need to set up an imaging protocol to identify low concentrations of ^{17}O-labeled saline.

Analysis of the time course of the SIR showed that the lowest values, which represent the highest concentration of ^{17}O-labeled water in the inner ear, occurred 30 min after intratympanic administration. We waited 30 min after intratympanic administration of ^{17}O-labeled saline before the start of the initial MRI scan in the present study. The ^{17}O-labeled saline penetrated both the perilymph and the endolymph in the cochlea and the vestibule. In the patient who underwent serial scans with a TE 3,200 ms, we could see the gradual filling of the posterior ampulla by ^{17}O-labeled saline. In the present study, we have visually shown that the water in the perilymph reaches the endolymph in a short time. In addition,

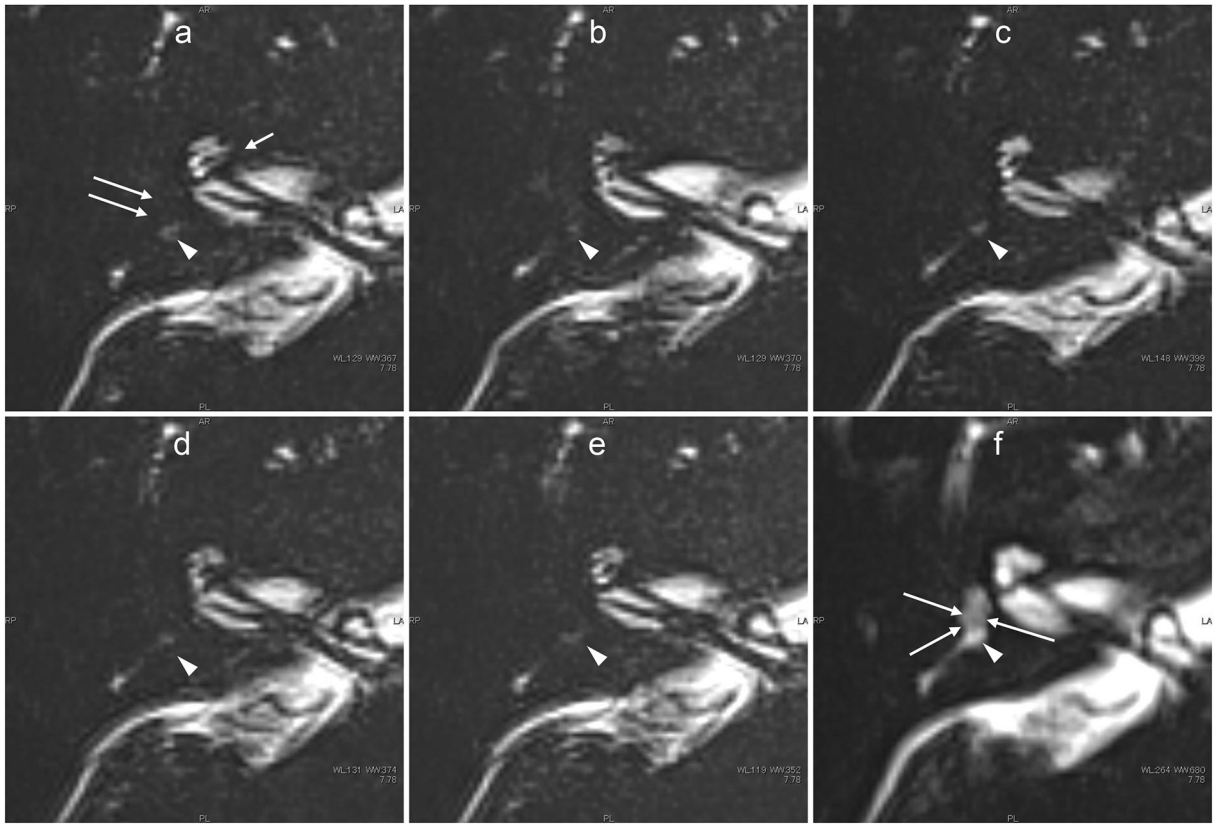

FIGURE 9
Images obtained from the male patient aged in his 40's with a history of acute low-tone sensorineural hearing loss 3 years previously but no history of vertigo who was currently asymptomatic. 3 years earlier, the patient had been shown to have cochlear endolymphatic hydrops by previous contrast-enhanced MR imaging using an intravenous gadolinium-based contrast agent. In this patient, five ultra-heavily T2-weighted images (6 min scan with a TE of 3,200 ms) were obtained serially **(a–e)**, and a 3 min scan image with a TE of 540 ms was obtained as a less sensitive scan to delineate the labyrinthine anatomy **(f)**. From the initial scan obtained ~30 min after intratympanic administration of ^{17}O-labeled water **(a)**, the signals for the vestibular signal (arrows) and anterior part of the basal turn in the cochlea (short arrow) were almost completely lost because of the distribution of ^{17}O-labeled water. Note that most of the vestibule showed a slightly decreased signal even in the less sensitive image with a TE of 540 ms (arrows, **f**). The concentration of intralabyrinthine ^{17}O-labeled water was higher in this patient than in the volunteers. The signal for the posterior ampulla (arrowheads in **a**–**f**) decreased gradually from the initial phase **(a)** to the third phase **(c)**. From the third phase **(c)** to the fifth phase **(e)**, almost no signal was observed in the posterior ampulla.

vertigo was prolonged in cases with a good distribution of ^{17}O-labeled water and significant MRI signal reduction. These are the major discoveries of this study that have not been reported. The brain's delayed water dynamics or impaired glymphatic function is now intensively investigated as the cause of neurodegenerative diseases, including Alzheimer's disease and idiopathic normal pressure hydrocephalus (20–26). Impaired glymphatic system function (i.e., impaired waste clearance function) results in the deposition of amyloid beta and tau protein in the brain of patients with Alzheimer's disease. The ocular glymphatic system is also a hot topic in ophthalmology for the pathogenesis of neurodegeneration in glaucoma (20–24). The similarity of amyloid beta and tau protein deposition between Alzheimer's disease and glaucoma has been reported. The link between these diseases is also suggested based on the same glymphatic background (27, 28). Further research of the water dynamics using ^{17}O-labeled water in the inner ear might open the door to reveal the mystery of the neurodegeneration in Ménière's disease.

The timing of 30 min after intratympanic administration of ^{17}O-labeled saline was not optimal for discriminating endolymph from perilymph. Had we obtained much earlier images after intratympanic administration, we might have been able to visualize the signal difference between the endolymph and perilymph in the cochlea and vestibule. Obtaining MR images at earlier times would require intratympanic administration with the patient or participant already on the MR scanner table.

An animal study of the permeability of the endolymph–perilymph barrier using tritiated water reported that the permeability is 130 times higher for water than for K^+ (29). A study in rats using tracers reported the following findings:

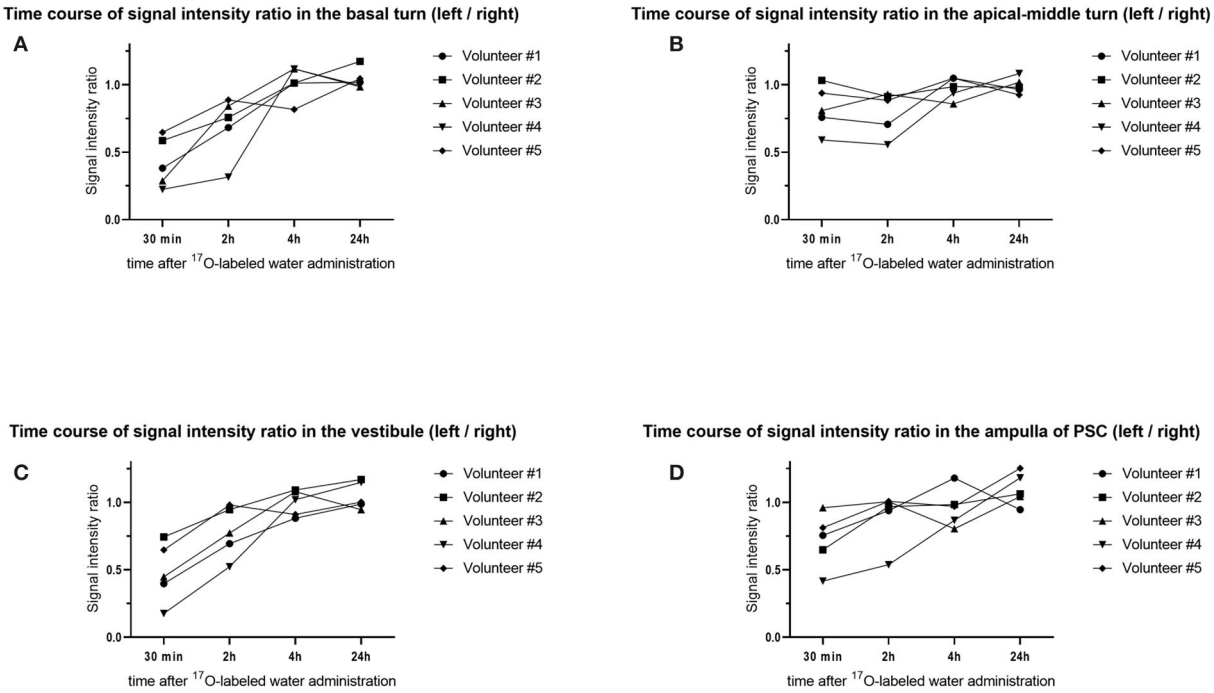

FIGURE 10
Time course of the signal–intensity ratio (SIR) in the five volunteers. The vertical axis shows the SIR and the horizontal axis shows the time elapsed since injection of the ^{17}O-labeled water. Using the signal value for the right side as a control, each SIR was calculated as the signal intensity of the region of interest/signal intensity of the right ear. Time course of the SIR in **(A)** the basal turn of the cochlea, **(B)** the apical–middle turn of the cochlea, **(C)** the vestibule, and **(D)** the ampulla of the posterior semicircular canal (PSC). Note that the distribution of ^{17}O-labeled water in the basal turn of the cochlea and vestibule at 30 min is obvious but is not obvious in the apical–middle turn. For the ampulla of the PSC, the distribution of ^{17}O-labeled water at 30 min was seen in four volunteers.

a rapid turnover of water in the endolymph, perilymph, and cerebrospinal fluid because $^{3}H_2O$ equilibrated with plasma within a few min; slow entry of ^{42}K and ^{36}Cl into the perilymph because ^{36}Cl equilibrated with the plasma after 2 h and ^{42}K did not at 6 h; and an extremely slow entry of ^{42}K and ^{36}Cl into the endolymph because no equilibrium with plasma was obtained within the 5 h of the experiments (30).

Although evaluation of water permeability through the human endolymph–perilymph barrier has not been reported, this permeability is considered to be very high, as reported in animal experiments. In our study, the earliest sites of the distribution of ^{17}O-labeled water were in the basal turn of the cochlea and the vestibular space, as also seen with intratympanic GBCA administration. This probably reflects the existence of a pathway for water administered into the tympanic cavity to enter the perilymph through the round window and the periphery of the stapes. However, 2 h after the injection, the signal tended to recover, which suggests that the decrease in concentration reflected the production and absorption of perilymph and endolymph or the diffusion of ^{17}O-labeled water.

It is well-known that positional vertigo is caused by endolymphatic flow in the semicircular canal. In clinical settings, the procedure of tympanic space lavage with saline does not induce prolonged dizziness. No adverse effects of dizziness were reported in a case–control study involving intratympanic administration of saline (31). ^{17}O-labeled water diffused into the inner ear may have caused endolymphatic flow in the semicircular canal with a change in the head position. Money and Myles examined the response to ingestion of 100–200 g deuterium oxide, which caused vigorous lateral positional nystagmus lasting some hours in humans accompanied by a directional characteristic opposite to that of postural alcohol nystagmus (32).

Deuterium oxide ("heavy water") has a molecular weight of 20.030, as compared with 18.016 for water, and is thought to diffuse earlier into the cupula than the endolymph. If a sufficiently large specific gravity differential is maintained between the two, the cupula may act inappropriately as a gravity transducer. Koizuka et al. (33) demonstrated that both ethyl alcohol and heavy water affect the long-time constant of the vestibulo-ocular reflex and apogeotropic-type positional nystagmus lasted ∼4 h in rabbits. These findings suggest that ethyl alcohol and heavy water directly alter the dynamics of the cupula–endolymph system in the vestibular end organs. The semicircular canal may be responsible for ethyl alcohol- or heavy water-induced positional nystagmus.

In the present study, the duration of vertigo was several hours, which was similar to that reported in previous animal studies using heavy water (32, 33). The VOG results showed no latency or attenuation in the nystagmus, suggesting a so-called light cupula (heavy endolymph) rather than canalolithiasis (34). The water component of the endolymph around the cupula is replaced by ^{17}O-labeled water, which may make the cupula lighter. In the current study, increased endolymph density in the vestibule induced a light cupula phenomenon in the lateral and posterior semicircular canal according to the anatomical and gravitational situations and elicited persistent irritative nystagmus. Clinical light cupula syndrome was first proposed in 2004 (35), and various reports have been identified in the literature. In the present study, in which ^{17}O-labeled water, a type of heavy water, was administered intratympanically, it can serve as a reproducible model of positional nystagmus in clinical light cupula syndrome.

The formula to convert the signal intensity to of ^{17}O concentration has been reported (8). The concentration of ^{17}O-labeled water can be estimated from the echo time (in s), signal intensity before and after administration, natural abundance ratio of ^{17}O (0.038%), and R_2 of ^{17}O 3.33 s^{-1}. Using MRI, we estimated that the concentration of ^{17}O-labeled water administered intratympanically was diluted by 32–64 times in the vestibule in the patient whose concentration of ^{17}O-labeled water was the highest of all the participants in the present study. The molecular weight of ^{17}O-labeled water is 19 compared with 18 for normal water, and the specific gravity is slightly higher for ^{17}O-labeled water. Therefore, the increase in the water density in the vestibule may have been 0.08–0.16% in this study. This percentage increase or decrease in the water density is caused by a 2–4°C decrease or increase in body temperature, respectively. The protein concentration in the endolymph is 20–30 mg/dL in healthy people and 182–348 mg/dL in people with Ménière's disease (36). Therefore, an increase in the endolymphatic protein concentration of 80–160 mg/dL corresponds to a 0.08–0.16% elevation in endolymph density. Our results suggest that the change in endolymph density can elicit caloric nystagmus and vertigo in people with Ménière's disease (i.e., the buoyancy theory).

Our study has some limitations. The number of participants was small because of the vertigo experienced after intratympanic administration of ^{17}O-labeled water. This made statistical analysis difficult. Another limitation is individual variation in the round window permeability. A study of intratympanic GBCA administration found that round window permeability was absent in 5% of ears and poor in 13% of ears (37). In this study, the concentration of ^{17}O-labeled water in the inner ear, or SIR, varied between volunteers. The distribution of ^{17}O-labeled water to the inner ear was very rapid. It was clear that the contrast findings of the inner ear changed within a small timeframe after intratympanic injection. The temporal resolution can be improved by focusing on obtaining single types of echo time images (i.e., 3,200 ms), as we did in the patient.

Another limitation is that we did not perform a control study involving intratympanic administration of normal saline (^{16}O-labeled saline) to confirm that the symptoms shown in the present study were caused by ^{17}O-labeled saline. We also did not perform a contrast-enhanced study using GBCA in volunteers to visualize the individual anatomy of endolymphatic space.

Conclusion

The inner ear water dynamics *in vivo* have not been clarified until now, and this study has revealed a part of it. In the future, elucidating the water dynamics in patients with endolymphatic hydrops, such as those with Ménière's disease, may help to elucidate the mechanism responsible for endolymphatic hydrops formation and vertigo attacks.

Data availability statement

The original contributions presented in the study are included in the article/supplementary material, further inquiries can be directed to the corresponding author/s.

Ethics statement

The studies involving human participants were reviewed and approved by the Nagoya University Clinical Research Review Board, Nagoya, Japan. The patients/participants provided their written informed consent to participate in this study.

Author contributions

TY and SN designed the study. SN, MS, and TN coordinated and directed the project. TY, MK, and SS collected the clinical and imaging data. TY and SN wrote the report. SN, MS, and TN provided scientific direction. SN performed the image analysis. TY, SN, and KN performed the data analysis. All authors contributed to the article and approved the submitted version.

Funding

This research was partially supported by Nagoya University Hospital Funding for Clinical Development.

Conflict of interest

The authors declare that the research was conducted in the absence of any commercial or financial relationships that could be construed as a potential conflict of interest.

Publisher's note

All claims expressed in this article are solely those of the authors and do not necessarily represent those of their affiliated organizations, or those of the publisher, the editors and the reviewers. Any product that may be evaluated in this article, or claim that may be made by its manufacturer, is not guaranteed or endorsed by the publisher.

References

1. Zhu XH, Zhang N, Zhang Y, Zhang X, Ugurbil K, Chen W. In vivo 17O NMR approaches for brain study at high field. *NMR Biomed.* (2005) 18:83–103. doi: 10.1002/nbm.930

2. Kudo K, Harada T, Kameda H, Uwano I, Yamashita F, Higuchi S, et al. Indirect MRI of (17) o-labeled water using steady-state sequences: Signal simulation and preclinical experiment. *J Magn Reson Imag.* (2018) 47:1373–9. doi: 10.1002/jmri.25848

3. Kudo K, Harada T, Kameda H, Uwano I, Yamashita F, Higuchi S, et al. Indirect proton MR imaging and kinetic analysis of 17O-labeled water tracer in the brain. *Magn Reson Med Sci.* (2018) 17:223–30. doi: 10.2463/mrms.mp.2017-0094

4. Atkinson IC, Thulborn KR. Feasibility of mapping the tissue mass corrected bioscale of cerebral metabolic rate of oxygen consumption using 17-oxygen and 23-sodium MR imaging in a human brain at 94 T. *Neuroimage.* (2010) 51:723–33. doi: 10.1016/j.neuroimage.2010.02.056

5. Cui W, Zhu X-H, Vollmers ML, Colonna ET, Adriany G, Tramm B, et al. Non-invasive measurement of cerebral oxygen metabolism in the mouse brain by ultra-high field (17)O MR spectroscopy. *J Cereb Blood Flow Metab.* (2013) 33:1846–9. doi: 10.1038/jcbfm.2013.172

6. Hoffmann SH, Radbruch A, Bock M, Semmler W, Nagel AM. Direct (17)O MRI with partial volume correction: first experiences in a glioblastoma patient. *MAGMA.* (2014) 27:579–87. doi: 10.1007/s10334-014-0441-8

7. Hopkins AL, Lust WD, Haacke EM, Wielopolski P, Barr RG, Bratton CB. The stability of proton T2 effects of oxygen-17 water in experimental cerebral ischemia. *Magn Reson Med.* (1991) 22:167–74. doi: 10.1002/mrm.1910220118

8. Sugimori H, Kameda H, Harada T, Ishizaka K, Kajiyama M, Kimura T, et al. Quantitative magnetic resonance imaging for evaluating of the cerebrospinal fluid kinetics with 17O-labeled water tracer: a preliminary report. *Magn Reson Imaging.* (2022) 87:77–85. doi: 10.1016/j.mri.2021.12.005

9. Leung K. "*17O-Labeled water.*," *Molecular Imaging and Contrast Agent Database (MICAD).* Bethesda, MD: National Center for Biotechnology Information (US) (2010).

10. Nakashima T, Naganawa S, Sugiura M, Teranishi M, Sone M, Hayashi H, et al. Visualization of endolymphatic hydrops in patients with Meniere's disease. *Laryngoscope.* (2007) 117:415–20. doi: 10.1097/MLG.0b013e31802c300c

11. Pyykkö I, Zou J, Gürkov R, Naganawa S, Nakashima T. Imaging of temporal bone. *Adv Otorhinolaryngol.* (2019) 82:12–31. doi: 10.1159/000490268

12. Zou J, Poe D, Bjelke B, Pyykko I. Visualization of inner ear disorders with MRI in vivo: from animal models to human application. *Acta Otolaryngol Suppl.* (2009) 5:22–31. doi: 10.1080/00016480902729850

13. Naganawa S, Satake H, Kawamura M, Fukatsu H, Sone M, Nakashima T. Separate visualization of endolymphatic space, perilymphatic space and bone by a single pulse sequence; 3D-inversion recovery imaging utilizing real reconstruction after intratympanic Gd-DTPA administration at 3 Tesla. *Eur Radiol.* (2008) 18:920–4. doi: 10.1007/s00330-008-0854-8

14. Nakashima T, Pyykkö I, Arroll MA, Casselbrant ML, Foster CA, Manzoor NF, et al. Meniere's disease. *Nat Rev Dis Primers.* (2016) 2:16028. doi: 10.1038/nrdp.2016.28

15. Naganawa S, Nakashima T. Visualization of endolymphatic hydrops with MR imaging in patients with Ménière's disease and related pathologies: current status of its methods and clinical significance. *Jpn J Radiol.* (2014) 32:191–204. doi: 10.1007/s11604-014-0290-4

16. Mugler JP III. Optimized three-dimensional fast-spin-echo MRI. *J Magn Reson Imaging.* (2014) 39:745–67. doi: 10.1002/jmri.24542

17. Morimoto K, Yoshida T, Kobayashi M, Sugimoto S, Nishio N, Teranishi M, et al. Significance of high signal intensity in the endolymphatic duct on magnetic resonance imaging in ears with otological disorders. *Acta Otolaryngol.* (2020) 140:818–22. doi: 10.1080/00016489.2020.1781927

18. Yoshida T, Kobayashi M, Sugimoto S, Teranishi M, Naganawa S, Sone M. Evaluation of the blood-perilymph barrier in ears with endolymphatic hydrops. *Acta Otolaryngol.* (2021) 141:736–41. doi: 10.1080/00016489.2021.1957500

19. Gürkov R, Flatz W, Louza J, Strupp M, Ertl-Wagner B, Krause E. Herniation of the membranous labyrinth into the horizontal semicircular canal is correlated with impaired caloric response in Ménière's disease. *Otol Neurotol.* (2012) 33:1375–9. doi: 10.1097/MAO.0b013e318268d087

20. Lohela TJ, Lilius TO, Nedergaard M. The glymphatic system: implications for drugs for central nervous system diseases. *Nat Rev Drug Discov.* (2022) 3:9 doi: 10.1038/s41573-022-00500-9

21. Wostyn P. Do normal-tension and high-tension glaucoma result from brain and ocular glymphatic system disturbances, respectively? *Eye.* (2021) 35:2905–6. doi: 10.1038/s41433-020-01219-w

22. Nakashima T, Sone M, Teranishi M, Yoshida T, Terasaki H, Kondo M, et al. perspective from magnetic resonance imaging findings of the inner ear: relationships among cerebrospinal, ocular and inner ear fluids. *Auris Nasus Larynx.* (2012) 39:345–55. doi: 10.1016/j.anl.2011.05.005

23. Taoka T, Naganawa S. Imaging for central nervous system (CNS) interstitial fluidopathy: disorders with impaired interstitial fluid dynamics. *Jpn J Radiol.* (2021) 39:1–14. doi: 10.1007/s11604-020-01017-0

24. Taoka T, Naganawa S. Glymphatic imaging using MRI. *J Magn Reson Imaging.* (2020) 51:11–24. doi: 10.1002/jmri.26892

25. Rasmussen MK, Mestre H, Nedergaard M. The glymphatic pathway in neurological disorders. *Lancet Neurol.* (2018) 17:1016–24. doi: 10.1016/S1474-4422(18)30318-1

26. Bae YJ, Choi BS, Kim J-M, Choi J-H, Cho SJ, Kim JH. Altered glymphatic system in idiopathic normal pressure hydrocephalus. *Parkinsonism Relat Disord.* (2021) 82:56–60. doi: 10.1016/j.parkreldis.2020.11.009

27. Sen S, Saxena R, Tripathi M, Vibha D, Dhiman R. Neurodegeneration in Alzheimer's disease and glaucoma: overlaps and missing links. *Eye.* (2020) 34:1546–53. doi: 10.1038/s41433-020-0836-x

28. Wostyn P, De Groot V, Van Dam D, Audenaert K, Killer HE, De Deyn PP. Age-related macular degeneration, glaucoma and Alzheimer's disease: amyloidogenic diseases with the same glymphatic background? *Cell Mol Life Sci.* (2016) 73:4299–301. doi: 10.1007/s00018-016-2348-1

29. Konishi T, Hamrick PE, Mori H. Water permeability of the endolymph-perilymph barrier in the guinea pig cochlea. *Hear Res.* (1984) 15:51–8. doi: 10.1016/0378-5955(84)90224-7

30. Sterkers O, Saumon G, Tran Ba Huy P, Amiel CK. Cl, and H2O entry in endolymph, perilymph, and cerebrospinal fluid of the rat. *Am J Physiol.* (1982) 243:F173–80. doi: 10.1152/ajprenal.1982.243.2.F173

31. Araújo MFS, Oliveira CA, Bahmad FM Jr. Intratympanic dexamethasone injections as a treatment for severe, disabling tinnitus: does it work? *Arch Otolaryngol Head Neck Surg.* (2005) 131:113–7. doi: 10.1001/archotol.131.2.113

32. Money KE, Myles WS. Heavy water nystagmus and effects of alcohol. *Nature.* (1974) 247:404–5. doi: 10.1038/247404a0

33. Koizuka I, Takeda N, Kubo T, Matsunaga T, Cha CI. Effects of ethyl alcohol and heavy-water administration on vestibulo-ocular reflex in

rabbits. *ORL J Otorhinolaryngol Relat Spec.* (1989) 51:151–5. doi: 10.1159/000276050

34. Imai T, Matsuda K, Takeda N, Uno A, Kitahara T, Horii A, et al. Light cupula: the pathophysiological basis of persistent geotropic positional nystagmus. *BMJ Open.* (2015) 5:e006607. doi: 10.1136/bmjopen-2014-006607

35. Hiruma K, Numata T. Positional nystagmus showing neutral points. *ORL J Otorhinolaryngol Relat Spec.* (2004) 66:46–50. doi: 10.1159/000077234

36. Silverstein H, Schuknecht HF. Biochemical studies of inner ear fluid in man. Changes in otosclerosis, Meniere's disease, and acoustic neuroma. *Arch Otolaryngol.* (1966) 84:395–402. doi: 10.1001/archotol.1966.00760030397003

37. Yoshioka M, Naganawa S, Sone M, Nakata S, Teranishi M, Nakashima T. Individual differences in the permeability of the round window: evaluating the movement of intratympanic gadolinium into the inner ear. *Otol Neurotol.* (2009) 30:645–8. doi: 10.1097/MAO.0b013e31819bda66

frontiers | Frontiers in Neurology

TYPE Original Research
PUBLISHED 08 November 2022
DOI 10.3389/fneur.2022.1007992

Check for updates

OPEN ACCESS

EDITED BY
Jian-hua Zhuang,
Shanghai Changzheng Hospital, China

REVIEWED BY
Erika Celis-Aguilar,
Autonomous University of Sinaloa, Mexico
Lisheng Yu,
Peking University People's Hospital, China

*CORRESPONDENCE
Jijun Song
songjijun68@163.com

SPECIALTY SECTION
This article was submitted to Neuro-Otology, a section of the journal Frontiers in Neurology

RECEIVED 31 July 2022
ACCEPTED 17 October 2022
PUBLISHED 08 November 2022

CITATION
Zhao C, Yang Q and Song J (2022) Dynamic changes of otolith organ function before and after repositioning in patients with benign paroxysmal positional vertigo detected by virtual reality auxiliary technology: A cohort study. *Front. Neurol.* 13:1007992. doi: 10.3389/fneur.2022.1007992

COPYRIGHT
© 2022 Zhao, Yang and Song. This is an open-access article distributed under the terms of the Creative Commons Attribution License (CC BY). The use, distribution or reproduction in other forums is permitted, provided the original author(s) and the copyright owner(s) are credited and that the original publication in this journal is cited, in accordance with accepted academic practice. No use, distribution or reproduction is permitted which does not comply with these terms.

Dynamic changes of otolith organ function before and after repositioning in patients with benign paroxysmal positional vertigo detected by virtual reality auxiliary technology: A cohort study

Chunjie Zhao, Qingjun Yang and Jijun Song*

Department of Otolaryngology, Head and Neck Surgery, Zhou Kou Central Hospital, Zhoukou City, China

Objectives: To dynamically investigate otolith function in patients with benign paroxysmal positional vertigo (BPPV) before, after, and 1 month after repositioning, and explore the possible compensation mechanisms.

Methods: Thirty-six patients confirmed with BPPV (canal lithiasis) treated in our hospital between August 2020 and March 2021, as well as 36 health controls matched for age and gender (normal control group, NC group) were enrolled. For NC group, the virtual reality (VR) auxiliary static subjective visual vertical (SVV), subjective visual horizontal (SVH), and SVV of dynamic unilateral centrifugation (DUC), were measured at inclusion. For the BPPV group, visual analog scale (VAS) was used to assess the vertigo degree, while static SVV, SVH, and DUC were performed before, after, and 1 month after repositioning. First, we compare the deviations of SVV0/SVH0° when the subject's head is in the positive position, and SVV of DUC between BPPV and NC groups before repositioning, after which we compared the deviations in SVV45, SVV90, SVH45, SVH90°, and SVV of DUC between the affected and unaffected sides before repositioning. Finally, paired *t*-test was used to compare the VAS score, deviations in static SVV0, SVV45, SVV90, SVH0, SVH45, and SVH90°, and deviations in SVV of DUC before, after, and 1 month after repositioning. (Here, 0, 45, and 90° refer to the angle which the center axis of head deviates from the gravity line.)

Results: SVV0 SVH0°, and SVV of DUC at 120 and 180°/s 0 significantly differed between BPPV and NC group before repositioning. The deviations in SVV45, SVV90, SVH45, SVH90°, and SVV of DUC at 120°/s-2 and 180°/s-4.5 did not significantly differ between bilateral sides in BPPV patients before repositioning. The deviation in SVH90° was significantly lower after repositioning than before. The deviation in SVH45° was significantly higher 1 month after repositioning than before. The deviation angle of SVV of DUC at 180°/s-0 was significantly lower after repositioning than before. The vertigo VAS score of patient with BPPV continued to decrease after repositioning.

Conclusion: Before repositioning, the otolithic organ function of BPPV patients was obviously impaired, with no significant difference between the healthy and affected ear. After repositioning, there was a transient recovery of otolithic organ dysfunction followed by a sustained decline to similar levels to before repositioning.

KEYWORDS

BPPV, otolith organ function, virtual reality auxiliary, subjective visual vertical, subjective visual horizontal, dynamic unilateral centrifugation, dynamic change

Introduction

Benign paroxysmal positional vertigo (BPPV) is a peripheral vestibular disorder with repeated transient vertigo and typical nystagmus that is induced by changes in head position relative to the direction of gravidity. BPPV accounts for 20–30% of vestibular vertigos. It has a very high prevalence in individuals who are 40–59 years old, while the male-to-female rate is approximately 1:1.5–1:2.0 (1). The pathogenesis of BPPV remains unclear; however, the most acknowledged theories include canalolithiasis and cupulolithiasis (2), while the dislodgment of otolith particles from otolith organ (*utricular maculae*), the peripheral vestibular receptor, has been considered as the major pathogenesis. Specific particle repositioning maneuvers could rapidly alleviate nystagmus and vertigo in most patients (3–5). Yet, studies have shown that the recurrence rate of BPPV is as high as 37–67.3%. In addition, the recurrence could influence both the affected and unaffected side, while approximately 56% of the recurrences occur within 1 year after repositioning (6, 7). Only very few studies have investigated the functions of otolith organ after repositioning in BPPV patients.

Utriculus (otolith organ) mainly senses linear acceleration and gravity (8) and is the potential pathogenic site of BPPV. Currently, the methods that indirectly assess the functions of utriculus include vestibular evoked myogenic potentials (VEMPs), subjective visual vertical (SVV), and subjective visual horizontal (SVH). SVV and SVH refer to the perception of humans to gravitational vertical and gravitational horizontal lines in a dark environment, respectively, which serves to rule out the influences of visual references. SVV and SVH are rapid and convenient methods for assessing the functions of utriculus, and the preset angle could reflect the asymmetry and balancing of static tensions of bilateral utriculus (9–12). Currently, a simple device called "bucket test" is generally used for the examination at the midline of the head of 0° in the static state and the dynamic examinations during off-axis rotations (13). Yet, few studies reported using virtual reality (VR) glasses to assist the examination of dynamic and static SVV and SVH. In addition, some scholars have found that dynamic SVV examination is more sensitive than static examination (14, 15), that is, SVV is examined simultaneously with centrifugal acceleration stimulation of otolith, namely dynamic unilateral centrifugation (DUC). The vestibular otolith organs are symmetrical organs located in the temporal bones on both sides of the cranial sagittal plane. When the center of the head is 3.87 cm away from the rotation axis to the left or right, the utricle on one side is located at the rotation axis, and the other side is deviated from the rotation axis by 7.74 cm. When the distance between the center of the head and the axis of rotation exceeds this distance, the utricles on both sides will be stimulated, but the stimulation amount is different. Off-axis rotation SVV can be detected when the person deviates from the axis and rotates around the axis, also known as off-axis rotation, or unilateral centrifugal force detection. During the detection, the tested ear is 7–8 cm away from the axis, and the contralateral ear is located at the axis and rotates at a constant speed at a certain speed. The vestibular eye movement response of the horizontal semicircular canal disappeared during constant rotation, centrifugal force was generated by off-axis rotation, or linear acceleration stimulated the utricle located off-axis. Unlike the rotation around the axis (bilateral centrifugal force), only the detection ear (located off the axis) is affected by the gravitational inertia force (GIF) formed by the unilateral centrifugal force. People with normal vestibular function are affected by unilateral centrifugal force, and the SVV skew values on both sides are symmetrical. When left ear is off-axis, namely left utricle is stimulated, SVV tilts to the right. When right ear is off-axis, namely right utricle is stimulated, SVV is left tilt (36).

A series of studies have also been conducted on DUC before. Gonzalez Set the translation time of UC-SVV rotation axis as 5, 10, 15, At 20, 25, and 30 s, 43 young healthy volunteers were randomly divided into groups for peak The UC-SVV test at a speed of 300° / s found that the rotation axis Short translation time will lead to greater variation in test results (16). Clarke, etc. It is considered that the GIA can be operated only when the rotation peak speed reaches 300 −400° / s. The unilateral elliptic sac produces marked excitation. The rotation axis peaks at 300° / s Speed translation of 3.5 cm centrifugal rotation will yield 0.192 g (1.9 m/s) the angular deflection can reach 11.3° (17). Chen Taisheng et al. performed UC-SVV with a rotation

speed of 60°/s and a displacement of 3.85 cm in the normal population. After repeated examination, the average value was taken, and the results were in line with normal distribution (18).

Therefore, this study compared the SVV and SVH at different preset angles of the head, as well as the changes in SVV of dynamic unilateral centrifugation (DUC in patients with unilateral idiopathic BPPV). We also explored the dynamic changes in the function of the otolith organ before and after repositioning in canal BPPV patients. Our findings provide theoretical evidence for clinical diagnosis and treatment of BPPV, as well as investigations of possible pathogenic and compensatory mechanisms of BPPV.

Subjects and methods

Subjects

A total of 36 patients with unilateral idiopathic canal BPPV who were treated in the Otolaryngology Department of Zhoukou Central Hospital between August 2020 and March 2021 were included in this study. The inclusion criteria were as follows (19): (1) with the chief complaint of head position change induced transient vertigo, lasting <1 min; (2) Dix-Hallpike test or roll test could induce vertigo and typical nystagmus, characterized by latent, transient, fatigability, and convertibility; (3) the type of nystagmus was in agreement with the presentations of affected semicircular canal; and (4) informed consents were obtained from the patients or the families. The exclusion criteria were: (1) with a previous history of vestibular diseases or ear diseases; (2) with a history of any type of dizziness or vertigo before; (3) cranial MRI examination showed disorders of the central nervous system (CNS); (4) could not cooperate during the examinations or participate in follow up due to other severe diseases or cognition impairment.

Thirty-six concurrent healthy adults matched for age and gender were enrolled as the controls (NC group). The inclusion were: (1) with no history of dizziness or vertigo, equilibrium disorder, hearing disorder, or otitis media; with no nervous system or skeletal system diseases; with no closure or open cranial trauma history; (2) with good neck movement ability; (3) with normal visual acuity or the corrected visual acuity of ≥1.0; (4) could understand and cooperate in the examinations, and those who signed informed consents. The exclusion criteria were as follows: (1) with a history of dizziness or vertigo; (2) with hearing disorders; (3) with eye diseases; (4) could not understand the study or could not cooperate in the study.

Epidemiology, clinical characteristics, and VAS score of vertigo

Clinical data including age, gender, side of the disease, site of disease, time from disease onset to diagnosis, pure tone audiometry (PTA) results; accompaniment of chronic diseases (such as hypertension, diabetes, and hyperlipidemia) before the treatment were collected for all the subjects. Visual Analog Scale (VAS) was used to assess the severity of vertigo symptoms (0–10), which was performed for the included BPPV patients before, after, and 1 month after repositioning.

SVV, SVH, and dynamic unilateral centrifugation

Static SVV and SVH, as well as DUC were performed before, after, and 1 month after repositioning for all BPPV patients, while for healthy controls, they were performed only at the time of inclusion.

Epley maneuver was performed for patients with posterior semicircular canal BPPV, and the Barbecue maneuver was performed for patients with horizontal semicircular canal BPPV. Dix-Hallpike test was performed again for all the patients 30 min after repositioning, and the disappearance of nystagmus and vertigo indicated the success of the repositioning maneuver.

VR auxiliary technology was used for the examination of static SVV and SVH, as well as SVV of DUC at 120 and 180°/s for all the subjects. All the tests were performed by experienced laboratory physicians engaged in clinical practices for at least 5 years. For the examinations of SVV and SVH, the subjects were asked to wear VR glasses (Yougeng ZT-VNG-I), after which the examinations were performed at the following fixed angles of head: midline position (0°), left tilted for 45°, left tilted for 90°, right tilted for 45°, and right tilted for 90°. Two pre-examinations were firstly performed to familiarize patients with the examination procedures, after which five measurements were acquired at each head position, and the mean values were calculated. For the one-sided centrifugation experiment, the subjects were asked to sit in a high-frequency, high-speed rotating chair (Yougeng ZT-VNG-I). The rotation was started from the central vertical axis, and the speed was gradually increased to 120 or 180°/s and then maintained at a constant speed. The rotation was stopped when the stimulation of bilateral semicircular canals appeared, and the SVV deviation was recorded. Afterward, rotations at the constant speeds of 120 and 180°/s were performed, and the present angles of left/right SVV at different rotation speeds were measured when the vertical axis horizontally deviated to left/right for 3.9 cm from the central.

Ethics statement

The Zhou Kou Central Hospital Ethical permission committee approved study (AF-HEC-006-02.0) and all subjects provided their informed consents.

TABLE 1 Epidemiological and clinical data of the 36 BPPV patients.

	x ± σ/percentage
Age (year)	46.75 ± 10.327
Sex (female)	23/36
Lateral (left)	10/36
Onset to therapy	8.94 ± 8.672
Horizontal semicircular canal	8/36
Posterior semicircular canal	28/36
Effect of otolith reduction treatment (well)	32/36

Statistical analysis

SPSS25.0 software (IBM, Armonk, NY, USA) was used for all statistical analyses. Consecutive data were described by means and standard deviations. The *t*-test was used for the comparison of consecutive data between different groups, and the chi-square test was used for the comparison of qualitative data between different groups. The dynamic changes in static SVV and SVH at different head positions, SVV of DUC (120 and 180°/s), and dynamic changes of VAS scores of vertigo in BPPV patients were analyzed by paired *t*-test. $P < 0.05$ was considered statistically significant.

Results

Epidemiological and clinical characteristics

A total of 36 BPPV patients, 13 males and 23 females, with a mean age of 46.75 ± 10.327 years (23–63 years), were included in this study. The time from disease onset to diagnosis of these patients was 8.94 ± 8.672 d (2–30 d). Among them, 10 were with the disease on the left side and 26 on the right side, respectively. Eight patients were with the disease in the horizontal semicircular canal, and 28 patients were with the disease in the posterior semicircular canal. The effect of repositioning was good in 32 patients and suboptimal in four patients (Table 1).

Comparison of otolith organ functions in BPPV patients before and after repositioning

An Independent *t*-test was used to analyze whether the deviations of SVH0, SVV0°, and SVV of DUC at 120 and 180°/s 0 were significantly different between the BPPV group and the age and gender-matched NC group. We found that compared with the NC group, the deviations in SVH0, SVV0°, and SVV of DUC at 120 and 180°/s 0 were significantly higher in the BPPV group, indicating the presence of otolith organ dysfunction in the BPPV group (Table 2).

TABLE 2 Comparison of deviations in SVH, SVV, and DUC-120°/s 0 and 180°/s 0 SVV between the BPPV and NC group before repositioning.

	BPPV ($n = 36$)	NC ($n = 36$)	p
SVH0° (°) x ±σ	1.854 ± 1.815	0.993 ± 0.792	0.012*
SVV0° (°) x ±σ	2.709 ± 1.979	1.541 ± 1.661	0.008*
DUC at 120°/s 0	2.527 ± 2.099	1.677 ± 0.960	0.032*
DUC at 180°/s 0	3.622 ± 2.676	1.677 ± 1.656	0.000*
Sex (female)	23/36 (63.89%)	22/36 (61.11%)	0.808
Age (year)	46.75 ± 10.327	47.33 ± 10.312	0.811

*$p < 0.05$.

TABLE 3 Comparison of deviations of SVV45°, SVV90°, SVH45°, SVH90°, and DUC-120°/s-2, DUC-180°/s-4.5 SVV between the affected and unaffected sides in BPPV patients before repositioning.

	Affected side	Healthy side	p
SVV45° (°)	5.171 ± 4.1408	6.006 ± 4.800	0.432
SVV90 (°)	6.972 ± 7.064	6.947 ± 5.204	0.978
SVH45° (°)	5.661 ± 4.911	7.213 ± 5.600	0.215
SVH90° (°)	6.456 ± 6.097	5.306 ± 5.722	0.412
DUC at 120°/s-2	3.163 ± 2.484	2.982 ± 2.588	0.763
DUC at 180°/s-4.5	3.788 ± 3.468	4.182 ± 2.718	0.593

Comparison of otolith organ functions between the affected and unaffected sides

An independent *t*-test was used to investigate whether the deviations in SVV45°, SVV90, SVH45°, SVH90°, and SVV of DUC at 120°/s-2 and 120°/s-4.5 in BPPV patients were significantly different between the affected and unaffected sides before repositioning. The findings showed that the deviations in S VV45, SVV90, SVH45°, SVH90°, and SVV of DUC at 120°/s-2 and 120°/s-4.5 did not significantly differ between the two sides in BPPV patients, indicating that the otolith organ functions were not significantly different between the affected and unaffected sides in BPPV patients (Table 3).

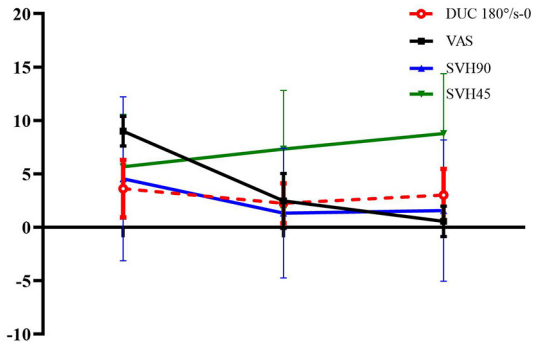

FIGURE 1
Dynamic changes of otolith organ functions in BPPV patients.

Dynamic changes of otolith organ functions before and after repositioning in BPPV patients

Paired *t*-test was used to compare the deviations in SVV0°, SVH0°, and SVV of DUC 120°/s-0 and 180°/s-0 of BPPV patients, as well as deviations in SVV45°, SVV90, SVH45°, SVH90°, SVV of DUC at 120°/s-2 and 180°/s-4.5, and VAS score of the affected side among different time points, i.e., before, after, and 1 month after repositioning. The findings showed that compared with before repositioning, the deviation in SVH90° and SVV of DUC at 180°/s-2 were significantly lower immediately after repositioning, and the VAS score was also significantly reduced. Compared with before repositioning, the deviation in SVH45° significantly increased, while VAS score significantly decreased 1 month after repositioning (Figure 1). These findings indicated that the otolith organ functions could be transiently restored immediately after repositioning in BPPV patients, and the vertigo degree also decreased continuously thereafter, while the otolith organ functions continued to reduce until reaching similar levels as those before repositioning (Table 4).

Discussion

In this study, the changes in SVV, SVH, and SVV of DUC at different head positions were compared between patients with unilateral idiopathic canal BPPV and healthy controls. The findings showed that the SVV0, SVH0°, and SVV of DUC at 120°/s 0 and 180°/s 0 significantly differed between BPPV patients and healthy controls before repositioning. The deviations in SVV45°, SVV90, SVH45°, SVH90°, and DUC at 120°/s-2 and 180°/s-4.5 were not significantly different between the two sides in BPPV patients before repositioning. The deviation in SVH90° was significantly lower after repositioning compared with the preset angle before repositioning. The deviation in SVH45° was significantly higher 1 month after repositioning compared with the preset angle before repositioning. The deviation in SVV of one-sided centrifugation experiments at 180°/s 0 was significantly lower after repositioning than before repositioning. However, the deviation in SVV of DUCC at 180°/s 0 increased; yet, statistical significance was not reached at 1 month after repositioning, compared with immediately after repositioning, and was not significantly lower than before repositioning.

Otolith organ dysfunction was present in BPPV patients before repositioning

BPPV is the most common cause of peripheral vestibular vertigo (1, 19). The dislodgment of otoconia from the utriculus into a semicircular canal in BPPV patients is considered the most common cause of semicircular canal-canal BPPV (20). Various autopsy studies have shown that patients with BPPV are generally accompanied by injuries of utricular maculae (21). The findings of this study showed that the deviations in SVV0°, SVH0°, and SVV of DUC (120°/s-0/2 and 180°/s-0/4.5) before repositioning significantly differed between BPPV patients and healthy controls matched for age and gender, indicating the presence of otolith organ dysfunction in BPPV patients. Consistent with our findings, a study performed by Munetaka Ushio et al. in 2007 revealed that canal-BPPV patients were accompanied by otolith organ dysfunction, and ∼82.1% (23/82) p-BPPV (posterior semicircular canal-BPPV) patients were with the deviation of SVH toward the unaffected side (22).

The otolith organ functions were not significantly different between the bilateral sides in BPPV patients

The results of this study showed that the deviations of SVV45°, SVV90, SVH45°, SVH90°, and SVV of DUC at 120°/s-2 and 180°/s-4.5 did not significantly differ between the affected and unaffected sides in BPPV patients before repositioning, indicating that BPPV could be the result of metabolic dysfunctions of bilateral otolith organs, which were in agreement with the findings of previous studies (23, 24). In 2015, Kim et al. (25) investigated o-VEMP and c-VEMP in 112 BPPV patients and 50 healthy controls to explore the functions of utriculus and saccule in the acute phase and resolved phase, demonstrating that the percentages of patients with abnormal cVEMP and oVEMP did not significantly differ in BPPV patients (25). Therefore, we speculated that the occurrence of BPPV was associated with the diseases of bilateral utricular maculae (26–29). The pathogenesis of otoconia dislodgment still remains unclear. Several studies have suggested that degenerative diseases could lead to the decrease of a gelatinous layer of the otolithic membrane, which in

TABLE 4 Changes of deviations of SVV0°, SVV45°, SVV90°, SVH0°, SVH45°, SVH90°, and DUC-120°/s-0/2 and 180°/s-0/4.5 SVV before, after, and 1 month after repositioning.

	Before x ± σ	After x ± σ	p	Before x ± σ	1 month later x ± σ	*p*
SVH0°	1.854 ± 1.815	1.657 ± 1.159	0.593	1.854 ± 1.815	2.288 ± 2.297	0.275
SVH45°	5.661 ± 4.911	7.330 ± 5.487	0.111	5.661 ± 4.911	8.767 ± 5.609	0.006*
SVH90°	6.456 ± 6.097	3.961 ± 4.749	0.029*	6.456 ± 6.097	4.770 ± 4.643	0.102
SVV0°	2.709 ± 1.979	2.341 ± 1.910	0.312	2.709 ± 1.979	2.666 ± 1.658	0.904
SVV45°	5.171± ± 4.141	6.991 ± 6.593	0.144	5.171 ± 4.141	5.855 ± 5.171	0.495
SVV90	6.972 ± 7.064	7.685 ± 6.586	0.485	6.972 ± 7.064	7.708 ± 6.706	0.536
120°/s-0	2.527 ± 2.099	2.239 ± 1.751	0.481	2.527 ± 2.099	2.116 ± 2.989	0.522
120°/s-2	3.163 ± 2.484	2.605 ± 2.036	0.236	2.527 ± 2.099	3.385 ± 2.762	0.123
180°/s-0	3.622 ± 2.676	2.251 ± 1.860	0.008*	3.622 ± 2.676	3.024 ± 2.453	0.321
180°/s-4.5	3.788 ± 3.468	3.072 ± 2.435	0.164	3.788 ± 3.468	3.543 ± 2.525	0.714
VAS	9.00 ± 1.394	2.47 ± 2.569	0.000	9.00 ± 1.394	0.56 ± 1.423	0.000

*$p < 0.05$.

turn induces the spontaneous dislodgment of the otoconia from the utricular or saccular maculae (30, 31). In addition, the anatomical study, as well as quantitative and qualitative investigations performed by Richard et al. in 5 samples of the temporal bone (TB) from BPPV patients revealed the following: (1) all the 5TBs showed ∼50% loss of ganglion cells in the superior vestibular division; (2) three TBs showed 50% loss of neurons in the inferior vestibular division, and the other two TBs with abnormal saccular ganglion cells showed 30% loss of neurons in the inferior vestibular division. Therefore, the investigators speculated that the occurrence of BPPV could be associated with the loss or reduction of bilateral otolith organs in semicircular canal (27), which could also explain why the recurrence of unilateral BPPV can affect the contralateral or even bilateral ears of patients (6).

Dynamic otolith organ functions changes in BPPV patients

Our results demonstrated that the deviations of SVH90° and SVV of DUC at 180°/s-0 were significantly lower immediately after repositioning than before repositioning. According to the current understanding, vertigo induced by head movement in BPPV could be explained by the migration of calcium carbonate granules induced by the fractionation of otoconia in utricular maculae (32). Therefore, the rationale for canalith repositioning is promoting the otoconia to restore the positions in the utriculus through a series of procedures that change the positions of the head and body (19, 33). Consistent with the findings of this study, Maristela Mian Ferreira investigated the SVV deviation degree in 20 BPPV patients before and after repositioning by the "bucket test" in 2017 and found that the SVV deviation was significantly lower immediately after repositioning than before repositioning (34).

Our results demonstrated that although the VAS scores of vertigo continuously decreased after repositioning in BPPV patients, the deviation angles of SVH90° and SVV of DUC at 180°/s-0 gradually increased, coming close to the levels before repositioning. In addition, the SVH45° deviation degree significantly increased 1 month after repositioning than before repositioning. Our findings were in agreement with that of Kim et al. (25) published in 2015. In their study, they re-examined the VEMP 2 months after repositioning in 59 out of the 102 BPPV patients who were initially included in the study. Their findings showed that the VEMP of the affected and unaffected ears did not significantly differ at 2 months after repositioning compared with the levels before repositioning, which indicated that in contrast to other peripheral vestibular diseases (such as vestibular neuritis) where the damaged VEMP could be restored, otolith organ dysfunction could be persistent in BPPV patients after repositioning. This could be because with the process of aging, the decrease in a gelatinous layer of the otolithic membrane could more easily induce the spontaneous dislodgment of the otoconia from bilateral saccular maculae (26). However, although the dislodged otoconia debris could influence the deviation degree of SVV/SVH, i.e., the functions of otolith organs, it cannot induce the BPPV-related symptoms. Consistent with these findings, it is widely acknowledged that reduction in bone mass, osteoporosis, and vitamin D deficiency could induce the occurrence of BPPV through the disorders related to calcium metabolism in vestibular organs (35). Therefore, we speculated that with the increase in age and emergence of disorders related to calcium metabolism, the occurrence of vestibular degeneration could induce the dysfunction in bilateral otolith organs, which is also observed in patients with unilateral BPPV. The accumulation of debris dislodged from utricular maculae could induce the BPPV-related symptoms to a certain degree.

Limitations

First, this study mainly focused on the dynamic changes in the function of otolith organs in BPPV patients before and after repositioning, without paying attention to the function of otolith organs and residual vertigo, which we plan to further investigate in our future studies. Secondly, dynamic and static SVV/SVH could be used for indirect assessment of the function of otolith organs, where procedures are simple and not influenced by the ages and muscle strength of patients and are therefore worthy of promotion in clinical practices. However, only very few studies investigated SVV/SVH by VR auxiliary technology in clinical practices, and the reference ranges need to be further standardized in more studies. Finally, the sample size in the present study was relatively small, which could lead to certain biases in statistical analysis. In our future clinical studies, we plan to include more patients and use multiple methods to assess the functions of otolith organs, thus further improving the findings of the present study.

Conclusion

Before repositioning, the otolithic organ function of BPPV patients was obviously impaired, with no significant difference between the healthy and affected ear. After repositioning, there was a transient recovery of otolithic organ dysfunction followed by a sustained decline to similar levels to before repositioning.

Data availability statement

The raw data supporting the conclusions of this article will be made available by the authors, without undue reservation.

Ethics statement

The studies involving human participants were reviewed and approved by the Zhou Kou Central Hospital Ethical permission committee. The patients/participants provided their written informed consent to participate in this study.

Author contributions

JS, CZ, and QY contributed to the study conception and design. CZ and JS contributed to the analysis and interpretation of data. CZ and QY wrote the first draft of the manuscript. JS made critical revision for important intellectual content. All authors contributed to the material preparation, data collection, read, and approved the final manuscript.

Conflict of interest

The authors declare that the research was conducted in the absence of any commercial or financial relationships that could be construed as a potential conflict of interest.

Publisher's note

All claims expressed in this article are solely those of the authors and do not necessarily represent those of their affiliated organizations, or those of the publisher, the editors and the reviewers. Any product that may be evaluated in this article, or claim that may be made by its manufacturer, is not guaranteed or endorsed by the publisher.

References

1. von Brevern M, Radtke A, Lezius F, Feldmann M, Ziese T, Lempert T, et al. Epidemiology of benign paroxysmal positional vertigo: a population based study. *J Neurol Neurosurg Psychiatry.* (2007) 78:710–5. doi: 10.1136/jnnp.2006.100420

2. Schuknecht HF. Cupulolithiasis. *Arch Otolaryngol.* (1969) 90:765–78. doi: 10.1001/archotol.1969.00770030767020

3. Fife TD, Iverson DJ, Lempert T, Furman JM, Baloh RW, Tusa RJ, et al. Practice parameter: therapies for benign paroxysmal positional vertigo (an evidence-based review): report of the quality standards subcommittee of the American academy of neurology. *Neurology.* (2008) 70:2067–74. doi: 10.1212/01.wnl.0000313378.77444.ac

4. Helminski JO, Zee DS, Janssen I, Hain TC. Effectiveness of particle repositioning maneuvers in the treatment of benign paroxysmal positional vertigo: a systematic review. *Phys Ther.* (2010) 90:663–78. doi: 10.2522/ptj.20090071

5. Kerber KA, Burke JF, Skolarus LE, Meurer WJ, Callaghan BC, Brown DL, et al. Use of BPPV processes in emergency department dizziness presentations: a population-based study. *Otolaryngol Head Neck Surg.* (2013) 148:425–30. doi: 10.1177/0194599812471633

6. Luryi AL, Lawrence J, Bojrab DI, LaRouere M, Babu S, Zappia J, et al. Recurrence in benign paroxysmal positional vertigo: a large, single-institution study. *Otol Neurotol.* (2018) 39:622–7. doi: 10.1097/MAO.0000000000001800

7. Teggi R, Guidetti R, Gatti O, Guidetti G. Recurrence of benign paroxysmal positional vertigo: experience in 3042 patients. *Acta Otorhinolaryngol Ital.* (2021) 41:461–6. doi: 10.14639/0392-100X-N1233

8. Ji L, Zhai S. Aging and the peripheral vestibular system. *J Otol.* (2018) 13:138–40. doi: 10.1016/j.joto.2018.11.006

9. Clarke AH, Schönfeld U, Helling K. Unilateral examination of utricle and saccule function. *J Vestib Res.* (2003) 13:215–25. doi: 10.3233/VES-2003-134-606

10. Pagarkar W, Bamiou DE, Ridout D, Luxon LM. Subjective visual vertical and horizontal: effect of the preset angle. *Arch Otolaryngol Head Neck Surg.* (2008) 134:394–401. doi: 10.1001/archotol.134.4.394

11. Byun JY, Hong SM, Yeo SG, Kim SH, Kim SW, Park MS, et al. Role of subjective visual vertical test during eccentric rotation in the recovery phase of vestibular neuritis. *Auris Nasus Larynx.* (2010) 37:565–9. doi: 10.1016/j.anl.2010.02.004

12. Schönfeld U, Helling K, Clarke AH. Evidence of unilateral isolated utricular hypofunction. *Acta Otolaryngol.* (2010) 130:702–7. doi: 10.3109/00016480903397686

13. Michelson PL, McCaslin DL, Jacobson GP, Petrak M, English L, Hatton K, et al. Assessment of subjective visual vertical (SVV) Using the "bucket test" and the virtual SVV system. *Am J Audiol.* (2018) 27:249–59. doi: 10.1044/2018_AJA-17-0019

14. Böhmer A, Mast F. Chronic unilateral loss of otolith function revealed by the subjective visual vertical during off center yaw rotation. *J Vestib Res.* (1999) 9:413–22. doi: 10.3233/VES-1999-9603

15. Karlberg M, Aw ST, Halmagyi GM, Black RA. Vibration-induced shift of the subjective visual horizontal: a sign of unilateral vestibular deficit. *Arch Otolaryngol Head Neck Surg.* (2002) 128:21–7. doi: 10.1001/archotol.128.1.21

16. González JE, King JE, Kiderman A. Subjective visual vertical (SVV) patterns obtained using different translation times during unilateral centrifugation (UC) testing. *J Am Acad Audiol.* (2014) 25:253–60. doi: 10.3766/jaaa.25.3.4

17. Clarke AH, Engelhorn A. Unilateral testing of utricular function. *Exp Brain Res.* (1998) 121:457–64. doi: 10.1007/s002210050481

18. Chen TS, Han X, Liu Q, Li SS, Wen C, Wang W, et al. A pilot study of the unilateral centrifugation subjective visual vertical in healthy young people. *Zhonghua Er Bi Yan Hou Tou Jing Wai Ke Za Zhi.* (2018) 53:811–4. doi: 10.3760/cma.j.issn.1673-0860.2018.11.003

19. Bhattacharyya N, Baugh RF, Orvidas L, Barrs D, Bronston LJ, Cass S, et al. Clinical practice guideline: benign paroxysmal positional vertigo. *Otolaryngol Head Neck Surg.* (2008) 139(5 Suppl 4):S47–81. doi: 10.1016/j.otohns.2008.08.022

20. Instrum RS, Parnes LS. Benign paroxysmal positional vertigo. *Adv Otorhinolaryngol.* (2019) 82:67–76. doi: 10.1159/000490273

21. Walther LE, Wenzel A, Buder J, Bloching MB, Kniep R, Blödow A, et al. Detection of human utricular otoconia degeneration in vital specimen and implications for benign paroxysmal positional vertigo. *Eur Arch Otorhinolaryngol.* (2014) 271:3133–8. doi: 10.1007/s00405-013-2784-6

22. Ushio M, Murofushi T, Iwasaki S. Subjective visual horizontal in patients with posterior canal benign paroxysmal positional vertigo. *Acta Otolaryngol.* (2007) 127:836–8. doi: 10.1080/00016480601053115

23. Korres S, Gkoritsa E, Giannakakou-Razelou D, Yiotakis I, Riga M, Nikolpoulos TP, et al. Vestibular evoked myogenic potentials in patients with BPPV. *Med Sci Monit.* (2011) 17:Cr42–47. doi: 10.12659/MSM.881328

24. Nakahara H, Yoshimura E, Tsuda Y, Murofushi T. Damaged utricular function clarified by oVEMP in patients with benign paroxysmal positional vertigo. *Acta Otolaryngol.* (2013) 133:144–9. doi: 10.3109/00016489.2012.720030

25. Kim EJ, Oh SY, Kim JS, Yang TH, Yang SY. Persistent otolith dysfunction even after successful repositioning in benign paroxysmal positional vertigo. *J Neurol Sci.* (2015) 358:287–93. doi: 10.1016/j.jns.2015.09.012

26. Welling DB, Parnes LS, O'Brien B, Bakaletz LO, Brackmann DE, Hinojosa R, et al. Particulate matter in the posterior semicircular canal. *Laryngoscope.* (1997) 107:90–4. doi: 10.1097/00005537-199701000-00018

27. Gacek RR. Pathology of benign paroxysmal positional vertigo revisited. *Ann Otol Rhinol Laryngol.* (2003) 112:574–82. doi: 10.1177/000348940311200702

28. Hong SM, Park DC, Yeo SG, Cha CI. Vestibular evoked myogenic potentials in patients with benign paroxysmal positional vertigo involving each semicircular canal. *Am J Otolaryngol.* (2007) 29:184–7. doi: 10.1016/j.amjoto.2007.07.004

29. Longo G, Onofri M, Pellicciari T, Quaranta N. Benign paroxysmal positional vertigo: is vestibular evoked myogenic potential testing useful? *Acta Otolaryngol.* (2012) 132:39–43. doi: 10.3109/00016489.2011.619570

30. Kim JS, Oh SY, Lee SH, Kang JH, Kim DU, Jeong SH, et al. Randomized clinical trial for geotropic horizontal canal benign paroxysmal positional vertigo. *Neurology.* (2012) 79:700–7. doi: 10.1212/WNL.0b013e3182648b8b

31. Lee JD, Park MK, Lee BD, Lee TK, Sung KB, Park JY, et al. Abnormality of cervical vestibular-evoked myogenic potentials and ocular vestibular-evoked myogenic potentials in patients with recurrent benign paroxysmal postitional vertigo. *Acta Otolaryngol.* (2013) 133:150–3. doi: 10.3109/00016489.2012.723823

32. Strupp M, Brandt T. Diagnosis and treatment of vertigo and dizziness. *Dtsch Arztebl Int.* (2008) 105:173–80. doi: 10.3238/arztebl.2008.0173

33. Hilton MP, Pinder DK. The Epley (canalith repositioning) manoeuvre for benign paroxysmal positional vertigo. *Cochrane Database Syst Rev.* (2014) 12:Cd003162. doi: 10.1002/14651858.CD003162.pub3

34. Ferreira MM, Ganança MM, Caovilla HH. Subjective visual vertical after treatment of benign paroxysmal positional vertigo. *Braz J Otorhinolaryngol.* (2016) 83:659–64. doi: 10.1016/j.bjorl.2016.08.014

35. Jeong SH, Kim JS, Shin JW, Kim S, Lee H, Lee AY, et al. Decreased serum vitamin D in idiopathic benign paroxysmal positional vertigo. *J Neurol.* (2013) 260:832–8. doi: 10.1007/s00415-012-6712-2

36. Curthoys IS, Dai MJ, Halmagyi GM. Human otolithic function before and after unilateral vestibular neurectomy. *J Vestib Res.* (1990–1991) 1:199–209.

frontiers | Frontiers in Neurology

TYPE Original Research
PUBLISHED 17 November 2022
DOI 10.3389/fneur.2022.1049806

Check for updates

OPEN ACCESS

EDITED BY
Jian-hua Zhuang,
Shanghai Changzheng Hospital, China

REVIEWED BY
Jun Wang,
Huazhong University of Science and Technology, China
Virginia L. Flanagin,
Ludwig Maximilian University of Munich, Germany

*CORRESPONDENCE
Yuhe Liu
liuyuhefeng@163.com

SPECIALTY SECTION
This article was submitted to Neuro-Otology, a section of the journal Frontiers in Neurology

RECEIVED 21 September 2022
ACCEPTED 01 November 2022
PUBLISHED 17 November 2022

CITATION
Zhang X, Huang Y, Xia Y, Yang X, Zhang Y, Wei C, Ying H and Liu Y (2022) Vestibular dysfunction is an important contributor to the aging of visuospatial ability in older adults–Data from a computerized test system. *Front. Neurol.* 13:1049806. doi: 10.3389/fneur.2022.1049806

COPYRIGHT
© 2022 Zhang, Huang, Xia, Yang, Zhang, Wei, Ying and Liu. This is an open-access article distributed under the terms of the Creative Commons Attribution License (CC BY). The use, distribution or reproduction in other forums is permitted, provided the original author(s) and the copyright owner(s) are credited and that the original publication in this journal is cited, in accordance with accepted academic practice. No use, distribution or reproduction is permitted which does not comply with these terms.

Vestibular dysfunction is an important contributor to the aging of visuospatial ability in older adults–Data from a computerized test system

Xuehao Zhang[1], Yan Huang[1], Yuqi Xia[2], Xiaotong Yang[1], Yanmei Zhang[2], Chaogang Wei[2], Hang Ying[1] and Yuhe Liu[3]*

[1]School of Medical Technology and Information Engineering, Zhejiang Chinese Medical University, Hangzhou, China, [2]Department of Otolaryngology, Head and Neck Surgery, Peking University First Hospital, Beijing, China, [3]Department of Otolaryngology, Head and Neck Surgery, Beijing Friendship Hospital, Capital Medical University, Beijing, China

Background: A convergence of research supports a key role of the vestibular system in visuospatial ability. However, visuospatial ability may decline with age. This work aims to elucidate the important contribution of vestibular function to visuospatial ability in old adults through a computerized test system.

Methods: Patients with a clinical history of recurrent vertigo and at least failed one vestibular test were included in this cross-sectional study. Healthy controls of three age groups: older, middle-aged, and young adults were also involved. Visuospatial cognitive outcomes including spatial memory, spatial navigation, and mental rotation of all the groups were recorded. Comparing the performance of the visuospatial abilities between patients and age-matched controls as well as within the controls.

Results: A total of 158 individuals were enrolled. Results showed that patients performed worse than the age-matched controls, with the differences in the forward span ($p < 0.001$), the time of the maze 8 × 8 ($p = 0.009$), and the time of the maze 12 × 12 ($p = 0.032$) being significant. For the differences in visuospatial cognitive outcomes within the controls, the younger group had a significantly better performance than the other groups. The older group and the middle-aged group had comparable performances during all the tests.

Conclusions: Older patients with vestibular dysfunction had more difficulties during visuospatial tasks than age-matched controls, especially in spatial memory and spatial navigation. Within the controls, younger adults did much better than other age groups, while older adults behaved similarly to middle-aged adults. It is a valuable attempt to computerize the administration of tests for visuospatial ability.

KEYWORDS

vestibular dysfunction, recurrent vertigo, aging, visuospatial ability, computerized test system

Introduction

A growing body of research suggests that the vestibular system is involved in both reflexes at the brainstem level and in complex cognitive processes (1, 2). This seems plausible since, compared to other sensory information, the perception of vestibular input is more dependent on the individual's own continuous and dynamic mental activity (3). Anatomical evidence indicates that vestibular information is further transmitted to the cerebral cortex *via* the vestibular nucleus to form complex, conscious mental representations, enabling individuals to perceive their position and state in the real-time environment and to complete real-life orientation and navigation (4–7).

Researchers have carried out valuable explorations in vestibular-related cognitive domains. Wherein, visuospatial ability is more closely related to the vestibular system. It refers to the ability to understand and organize information about the environment in two- and three-dimensional space, which includes a variety of skills such as spatial memory, spatial navigation, and mental rotation (8). A study has found that compared to controls, patients with bilateral vestibulopathy (BVP) show poorer spatial learning ability and more severe spatial anxiety in the virtual Morris Water Task (VMWT)—a computerized version of the Morris Water Maze (MWT), which is used for assessing visuospatial ability of rats (9). Additional studies have shown that BVP patients have difficulty completing mental rotation tasks (10, 11). In addition, vestibular stimuli (e.g., the rotary chair test) have been shown to be able to affect individuals' ability to perform mental rotation tasks (12–14). Some studies have shown that even unilateral vestibular dysfunction may also lead to a decline of visuospatial ability (15–17).

Numerous neuroimaging studies have further established the physiological basis for the connection between the vestibular system and cognition (3, 18). A wider vestibular network in the brain has been identified. Vestibular information forms extensive vestibular-cortical projection areas in the cerebral cortex *via* the thalamus, including frontal regions that are highly relevant to cognitive function (19). A functional near-infrared imaging study found lower activation of the prefrontal cortex in patients with visual vertigo (VV) than in controls during dual-task performance (20). Most of these projection areas play an important role in spatial cognitive tasks. Among them, the hippocampus is considered to be a cardinal structure involved in vestibular-related cognitive functions. The vestibular input related to the environment (e.g., spatial memory, head movements, spatial learning, etc.) is transmitted to the hippocampal-entorhinal cortex through different pathways, then further affects the firing activity of Grid cells, Place cells and HD cells in the hippocampus (21). It was found that the hippocampal volume atrophy seen in patients with bilateral vestibular dysfunction was closely related to spatial memory and spatial navigation deficits (22–24). In addition to the anatomical link, it has been theorized that patients with vestibular dysfunction may need to compensate for visual acuity, balance, and orientation to maintain normal movement, thereby increasing the cognitive load (25).

However, at present, the findings of vestibular-related cognitive abilities are difficult to converge, probably for the following reasons: (1) Existing assessment dimensions are relatively broad, with visuospatial ability accounting for a small proportion, which may be insufficient to reflect the impact of vestibular function; (2) Various types of tools for assessing visuospatial ability make the results of different studies incomparable; (3) Confounding factors, such as hearing status, anxiety and depression, are not strictly controlled, which may also affect the conclusions.

Visuospatial abilities also decline with age. A study found that spatial orientation and navigation abilities decline with age (26). Older populations performed worse than younger populations in the spatial memory task of recalling and replicating visual sequences (27, 28). An interesting study (29), which used a mobile device-based video game program to collect the largest spatial navigation dataset to date, assessed the spatial navigation abilities of a normal population in a virtual environment. The results showed a linear age-related decline in navigation abilities between the ages of 19 and 60. Given the connection between vestibular function, aging, and visuospatial ability, it is necessary to distinguish whether the decline in visuospatial ability regarding older patients with vestibular dysfunction is more due to aging or to vestibular dysfunction.

This study specifically aims to clarify that the vestibular dysfunction is an important factor affecting visuospatial ability in addition to age and whether it is reflected differently in each sub-dimension. Also, to further represent the effect of aging, we included healthy controls of three age groups: older, middle-aged, and young adults. The impact of vestibular function on visuospatial ability was investigated by comparing the performance of patients with age-matched controls and the effect of aging was investigated by comparing the performance within the control group. Moreover, in this study, we developed a computerized Visuospatial Cognition Assessment System (VCAS), which aims to comprehensively assess the visuospatial ability of participants. The mobile terminal presentation of VCAS will give participants a better human-computer interaction experience. It is noted that such computerized assessment has been shown to have similar results to that performed in the real world (30).

Materials and methods

Participants

We recruited patients over 60 years old from the outpatient clinic for otolaryngology head and neck surgery at the Peking University First Hospital from December 2021 to May 2022. Patients underwent the appropriate vestibular function tests purely for clinical purposes, including: air-conducted cervical vestibular-evoked myogenic potentials (c-VEMP), video head impulse tests (v-HIT), posturography, videonystagmography (VNG) with bithermal caloric tests. All tests were performed by the same clinical technician. Among them, c-VEMP evaluates saccular function, recording from the sternocleidomastoid (SCM) muscles ipsilateral to the stimulated ear in response to a short pure tone (100 dB SPL) delivered monaurally through insert headphones. Take a 10 dB step until no recognizable P1 and N1 waves (first positive and negative wave with latency ranging from 13 to 23 ms) can be seen. The lower frequencies function of the lateral semi-circular canals was evaluated by v-HIT and bithermal caloric tests. During the v-HIT test, subjects were 1.2 m away from the visual target. Vestibulo-ocular reflex (VOR) gain is defined as the ratio of the angular velocity of eye movement to the angular velocity of head movement. Caloric irrigation was conducted by using cold air at 24°C and hot air at 50°C. Each irrigation was performed after the evoked nystagmus had completely disappeared. Patients who met the following criteria were included in the group of older vertigo patients (OVP).

Inclusion criteria for clinical patients were:

(1) Had a clinical history of recurrent vertigo.

(2) Failed at least one of the following vestibular function tests:

- no recognizable P1 and N1 waves can be seen in either test ear at 100 dB SPL and/or bilateral asymmetry ratio (AR) of amplitude $\geq$ 1.6, measured by the c-VEMP.
- horizontal angular VOR gain $<$ 0.8 ($<$ 0.7 for vertical direction) with saccade wave, measured by the v-HIT.
- vertigo and characteristic positional nystagmus (torsional nystagmus in the Dix-Hallpike test, horizontal nystagmus in the Roll test) during the posturography.
- reduced caloric response (sum of bithermal, 24 and 50°C maximum peak slow phase velocity (SPV) on each side $<$ 12°/s), and/or unilateral weakness (UW) $\geq$ 25%.

(3) Subjects might suffer from a post-lingual hearing loss.

To better illustrate the effect of age on visuospatial ability, three types of control participants were recruited, including a young group (YC; 18–44 years old), a middle-aged group (MAC; 45–59 years old), and an older group (OC; 60 years old and above). Some of them were recruited from society, and some were from the examiner's friends and hospital staff. The inclusion criteria for the control group were: (1) 18 years of age and above; (2) had no history of benign paroxysmal positional vertigo (BPPV), meniere disease (MD), vestibular neuritis (VN), vestibular migraine (VM), and other diseases that may cause vertigo.

In addition, audiometric data were also available from subjects using a clinical audiometer (AD229e, Interacoustics, Denmark), TDH39 headphones, and testing in a standard soundproof booth ($<$ 30 dB A). Hearing status was indexed by the averaged pure tone hearing threshold (PTA) of the four frequencies (0.5/1/2/4 kHz) of the better ear.

Basic information for all subjects, including gender, age, and education, was collected before the test. For both patients and controls, individuals were excluded if they: (1) had hearing loss that affects daily communication; (2) had visual impairment; (3) had middle ear disease or long-term noise exposure; (4) had a history of psychiatric and/or neurological disorders such as anxiety and depression; (5) had years of education $<$ 6 years; (6) had dementia disease, such as Alzheimer's Disease (AD).

Visuospatial ability assessment

We used the Lenovo TB-J606F tablet with a resolution of 2,000 $\times$ 1,200 and a screen size of 11 inches to run the VCAS, which includes four modules: the "Weeding Test," "Maze Test," "Three-dimensional Driving (3D Driving)," and "Card Rotation Test." Subjects were seated next to the experimenter with the tablet in front of them and completed tasks by touching the screen. Before any formal test, the subject is first directed through the "training mode" designed for each test to make sure that they have familiar with the processes. To avoid learning effects, the items in the training mode are different from those in the formal test. It takes approximately 40 min to complete all the tests. For patients, visuospatial assessment was performed before vestibular function tests. All test results will be stored in the Tencent Cloud storage bucket and displayed on the "Result Query" page allowing further analysis.

Weeding test

We designed the "weeding test" inspired by the traditional Corsi Block Tapping paradigm and the work of Claessen et al. (31) and Lacroix et al. (32), which evaluates visuospatial attention and working memory processes. There are two sub-tests in the task: a forward and a backward condition. During the test, 9 squares symbolizing the "grass" were shown on the screen with a flashing time of 500 ms and an inter-block interval of 1 s. The relative block positions were the same as the traditional paradigm. Subjects have to memorize the sequence and click on the corresponding "grass" (i.e., weeding). In the forward condition, subjects need to reproduce the block sequence in

the same serial order as indicated by the system, while in the backward condition, they repeat it in reverse order. Two trials per sequence length, ranging from two to nine blocks (for backwards, ranging from two to eight blocks). As long as the subject reproduce the block sequence completely correct in either of the two trials, one can enter the next sequence, and the game is over if the subject fails twice. The system automatically registered performance in terms of the span (forward/backward) which is used to evaluate the spatial working memory and the velocity (forward/backward), which is used to reflect the subject's click speed during the working memory process. The velocity was defined as the ratio of the total number of blocks clicked by the subject to the time spent in the test. The diagram is shown in Figure 1A.

Maze test

Inspired by Lacroix et al. (32), we designed the "maze test" to assess spatial navigation and executive function. The map was randomly generated through math algorithm, which can be divided into numerous small squares (map "8 × 8," i.e., this map can be divided into 64 small squares). The complexity of the map depends on the number of squares. Users can create different mazes for specific purposes by entering specific numbers in the input box at the top right of the screen and clicking the button "Create a maze." According to the results of pre-experiment in a normal population, we included three maps of different difficulty levels (8 × 8, 10 × 10, and 12 × 12) here. At the subject level, the degree of difficulty is controlled by the number of corners. The calf in the lower left corner of the screen is the "starting point" and the straw in the upper right corner is the "destination." Subjects have to move the calf to the "destination" by clicking the control panel in the lower right corner of the screen. There is only one correct route. All the subjects were instructed to get out of the maze as quickly as possible. The system automatically registered performance in terms of the time subjects took and the steps they moved for each maze. The diagram is shown in Figure 1B.

Three-dimensional driving

Spatial memory and spatial navigation are often interdependent in real life. Inspired by Coutrot et al. (29), we designed "3D driving" to assess spatial memory and spatial navigation in a comprehensive manner. When the test begins, a two-dimensional map with all the intersections will be displayed in the center of the screen for 5 s. The subjects need to keep the map in mind and "drive" the car to the destination in a virtual three-dimensional scene according to the memorized route. Taking into account the limited operation ability of older people, we designed the autopilot mode to make the car move automatically and stop at each intersection. Only if the subjects click the buttons for direction selection ("turn left," "forward," and "turn right") that appear on the screen correctly, the car will continue to drive. If the wrong selection was made, one will be prompted to re-select. To avoid learning effects, subjects have to complete three times (maps with different routes only) and the final results are averaged. The program automatically registered performance in terms of the thinking time and the number of errors at intersection. The diagram is shown in Figures 1C,D.

Card rotation test

The "card rotation test" is inspired by traditional mental rotation paradigm and the work of Lacroix et al. (32) and Henn et al. (33). There are 8 questions in total. Each question takes a 2D or 3D figure as an example, and at the bottom of the screen are four figures with the same size and color but different rotation angles from the example. We used letters and numbers as 2D-object and blocks with numbers as 3D-object. Subjects were required to mentally switch to determine the option that was exactly the same or completely different from the example and click the corresponding button. There is only one correct answer. The same difficulty level included 2 questions. A correct answer is scored as 1 point, and an incorrect answer is scored as 0. The program automatically registered the performance in terms of the final score and the time spent on the subject. The diagram is shown in Figures 1E,F.

Statistical analysis

All statistical analyses were performed with SPSS 25 (IBM; Armonk, NY, United States). The normality of distributions was evaluated using Shapiro-Wilk tests. Demographic data were analyzed with parametric analysis of variance (one-way ANOVA) for continuous data and chi-squared test for categorical data. We performed a multivariate ANOVA (for the weeding test and maze test) or multifactorial ANOVA (for the 3D driving test and card rotation test) followed by a *post-hoc* test (LSD) to compare the performance of different groups on each test of the VCAS. Each index was used as the dependent variable. Group, education, and gender were used as fixed factors, and only the factors with main effects were tested for interaction effects. For data do not meet the normal distribution, a ln logarithmic transformation is performed before ANOVA. To compare differences between subjects in the weeding test, two-way analyses of variance (ANOVAs) for repeated measures were performed on the span with 4*group (OVP, OC, MAC, YC) as a between-subject factor and 2*recall order (forward, backward) as a within-subject factor. The effect sizes are reported in terms of partial η^2. An alpha level of 0.05 was used.

FIGURE 1
Visuospatial Cognition Assessment System (VCAS). **(A)** Diagram of weeding test. **(B)** Diagram of maze test, take map 8 × 8 as an example. **(C)** The map of three-dimensional driving (3D driving), and **(D)** The diagram of 3D driving, take one map as an example. **(E)** 2D-object of card rotation test, and **(F)** 3D-object of card rotation test.

Results

Demographic and clinical characteristics

A total of 184 subjects participated in the study. Of these, 67 were clinical patients, and 117 were controls. According to the inclusion and exclusion criteria, 24 patients were excluded, including 15 with incomplete basic information, and 9 had normal vestibular test results (1 with a right ear perforation). Two controls with cataract were also excluded. Finally, 158 subjects (63.92% females) were included, including 43 patients (OVP; mean age: 66.14 years, SD: 4.5), 32 older controls (OC; mean age: 66.06 years, SD: 5.95), 38 middle-aged controls (MAC; mean age: 50.87 years, SD: 4.10), and 45 young controls (YC; mean age: 34.02 years, SD: 6.52). According to education, subjects were divided into primary education; secondary education, which includes middle school, high school, and technical secondary school; and higher education, which includes junior college, university, and postgraduate.

Age differences between the groups were statistically significant ($p < 0.001$). *Post-hoc* analyses indicated comparable ages between the OVP and the OC group. Gender differences were not statistically significant ($p = 0.190$). Education differences were statistically significant ($p < 0.001$). *Post-hoc* analyses showed no statistically significant difference between the OVP group and the OC group. Audiometric data was available in 116 of 158 subjects. The difference between the groups was statistically significant ($p < 0.001$). *Post-hoc* analyses showed that it was comparable between the OVP and the OC group as well as between the MAC and the YC group. Since the hearing thresholds of the OVP and OC groups were almost close to the normal range (≤ 25 dB HL), the hearing

TABLE 1 Demographic, and hearing performance of all groups.

	OVP ($N = 43$)	OC ($N = 32$)	MAC ($N = 38$)	YC ($N = 45$)	*P*-value
Age (mean, SD)	66.14 (4.50)[a]	66.06 (5.95)[a]	50.87 (4.10)[b]	34.02 (6.52)[c]	**<0.001**
Sex (n, %)					0.19
Male	17 (39.50)	16 (50.00)	11 (28.90)	13 (28.90)	
Female	26 (60.50)	16 (50.00)	27 (71.10)	32 (71.10)	
Education (n, %)					**<0.001**
Primary education	2 (4.70)[a]	1 (3.10)[a]	7 (18.40)[a]	1 (2.20)[a]	
Secondary Education	29 (67.40)[a]	16 (50.00)[a]	15 (39.50)[a]	3 (6.70)[b]	
Higher Education	12 (27.90)[a]	15 (46.90)[a]	16 (42.10)[a]	41 (91.10)[b]	
Hearing performance of the better ear (mean, SD in dB)	28.9 (13.76)[a]	28.13 (14.97)[a]	16.2 (8.98)[b]	10.55 (7.48)[b]	**<0.001**

OVP, Older vertigo patients; OC, Older controls; MAC, Middle-aged controls; YC, Young controls. [a–c]Intergroup Comparison. Statistically significant results are bolded.

performance of the subjects was not further examined in this study. Demographic and hearing performance are presented in Table 1. Results of the vestibular function tests and hearing results of patients are shown in Supplementary Table S1.

Visuospatial cognitive outcomes between the OVP and OC group

For the weeding test, results displayed in Figure 2 and Table 2 show that only the factor group had a significant main effect on the span ($F_{FW} = 7.062$, $p < 0.001$, $\eta^2_p = 0.135$; $F_{BW} = 3.406$, $p = 0.020$, $\eta^2_p = 0.070$). *Post-hoc* analyses showed that the forward span was significantly shorter in the OVP group than in other groups ($p < 0.001$). For the backward span, there was no statistically significant difference between the OVP and OC groups ($p = 0.057$), but the OVP group performed significantly worse than the MAC group ($p = 0.046$) and the YC group ($p < 0.001$). Regarding the velocity, there was a main effect of group on backward condition ($F_{FW} = 1.343$, $p = 0.263$, $\eta^2_p = 0.029$; $F_{BW} = 2.709$, $p = 0.048$, $\eta^2_p = 0.057$), and a significant main effect of education on both forward and backward conditions ($F_{FW} = 5.633$, $p = 0.004$, $\eta^2_p = 0.078$; $F_{BW} = 5.063$, $p = 0.008$, $\eta^2_p = 0.070$). *Post-hoc* analyses showed the differences between the OVP and OC groups were nonsignificant in both conditions (FW, $p = 0.654$; BW, $p = 0.527$). Between the OVP and MAC groups, only the difference in the backward condition was significant ($p = 0.043$). Additionally, the OVP group performed significantly worse than the YC group in both conditions ($p < 0.001$). People with higher education levels had a faster click rate (FW, $p = 0.004$; BW, $p = 0.008$). The interaction between group and education was nonsignificant ($F_{FW} = 0.817$, $p = 0.558$, $\eta^2_p = 0.055$; $F_{BW} = 1.008$, $p = 0.422$, $\eta^2_p = 0.057$).

Results of the two-factor repeated measures ANOVA revealed significant within-subjects effects (Figure 3). The forward span was significantly longer than the backward span ($F = 21.159$, $p < 0.001$, $\eta^2_p = 0.121$). There was no interaction effect between group and recall order ($F = 1.773$, $p = 0.155$, $\eta^2_p = 0.034$). That is, the difference between different recall orders did not change with the group. A paired *t*-test applied to the OVP group individually revealed no significant difference between the different recall orders ($t = 0.461$, $p = 0.648$).

Data in the maze test was transformed by the ln function before ANOVA. Results are shown in Figure 4 and Table 3. In all mazes, group had a significant effect on time [$F_{(8\times8)} = 5.995$, $p = 0.001$, $\eta^2_p = 0.130$; $F_{(10\times10)} = 7.666$, $p < 0.001$, $\eta^2_p = 0.161$; $F_{(12\times12)} = 9.690$, $p < 0.001$, $\eta^2_p = 0.195$]. *Post-hoc* analyses showed that the OVP group took significantly longer time than the OC group in different mazes except the maze 10 × 10 (8 × 8, $p = 0.009$; 10 × 10, $p = 0.953$; 12 × 12, $p = 0.032$). Gender had a main effect on the time for maze 10 × 10 and maze 12 × 12 [$F_{(10\times10)} = 5.476$, $p = 0.021$, $\eta^2_p = 0.044$; $F_{(12\times12)} = 12.264$, $p = 0.001$, $\eta^2_p = 0.093$] expect the maze 8 × 8 [$F_{(8\times8)} = 2.662$, $p = 0.105$, $\eta^2_p = 0.022$]. There was no interaction effect between group and gender in all mazes [$F_{(8\times8)} = 0.004$, $p = 1.000$, $\eta^2_p < 0.001$; $F_{(10\times10)} = 0.104$, $p = 0.957$, $\eta^2_p = 0.003$; $F_{(12\times12)} = 0.212$, $p = 0.888$, $\eta^2_p = 0.005$]. Regarding the steps of the maze, no factors included in the analysis had main effect.

Results of the 3D driving test are shown in Figure 5 and Table 4. There was a main effect of group and gender on thinking time ($F_{group} = 5.177$, $p = 0.003$, $\eta^2_p = 0.195$; $F_{gender} = 5.472$, $p = 0.022$, $\eta^2_p = 0.079$). And there was no interaction effect between these two factors ($F = 0.581$, $p = 0.630$, $\eta^2_p = 0.027$). *Post-hoc* analyses showed that the OVP group took longer time to think than the OC group, while the difference between the groups was nonsignificant ($p = 0.774$). Regarding the number of errors, there was only a main effect of group ($F = 4.514$, $p = 0.006$, $\eta^2_p = 0.151$). *Post-hoc* analyses showed that the OVP group made a few more errors than the OC group, but the difference was nonsignificant ($p = 0.399$).

Results of the card rotation test are shown in Figure 6 and Table 5. There was no main effect of group on both score ($F = 0.434$, $p = 0.729$, $\eta^2_p = 0.021$) and time ($F = 0.157$, $p = 0.925$, $\eta^2_p = 0.008$). However, the OVP group indeed scored lower

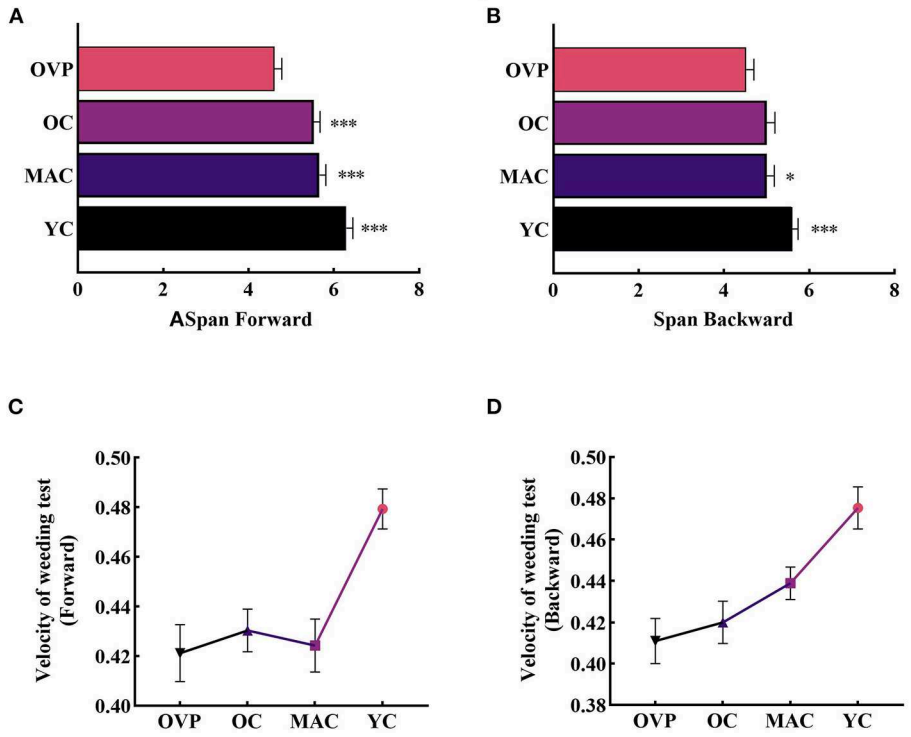

FIGURE 2
Span and Velocity of Weeding test between groups. **(A)** Span in the forward condition. **(B)** Span in the backward condition. **(C)** Velocity in the forward condition. OVP group only performed worse than YC group ($p < 0.001$). **(D)** Velocity in the backward condition. Older vertigo patients (OVP) performed worse than middle-aged controls (MAC) ($p < 0.05$) and young controls (YC) ($p < 0.001$). *Post-hoc* multiple comparisons between groups using OVP group as reference, significantly differences were indicated by the asterisk. OVP, Older vertigo patients; OC, Older controls; MAC, Middle-aged controls; YC, Young controls. *$p < 0.05$; ***$p < 0.001$. Error bars indicate the SEM.

TABLE 2 Comparison of weeding test indexes between groups.

	Span		Velocity	
	FW Mean (SD)	BW Mean (SD)	FW Mean (SD)	BW Mean (SD)
OVP	4.62 (1.15)	4.52 (1.15)	0.42 (0.07)	0.41 (0.07)
OC	5.53 (0.80)	5.00 (1.11)	0.43 (0.05)	0.42 (0.06)
MAC	5.66 (0.94)	5.00 (1.12)	0.42 (0.07)	0.44 (0.05)
YC	6.29 (1.04)	5.60 (0.91)	0.48 (0.05)	0.47 (0.07)
***P*-value**	**<0.001**	**0.021**	0.263	**0.048**
Primary education	4.91 (1.45)	4.91 (1.14)	0.38 (0.08)	0.42 (0.07)
Secondary education	5.08 (1.00)	4.69 (1.10)	0.42 (0.06)	0.41 (0.06)
Higher education	5.95 (1.11)	5.32 (1.10)	0.46 (0.06)	0.46 (0.06)
***P*-value**	0.064	0.807	**0.004**	**0.008**

FW, forward; BW, backward; OVP, Older vertigo patients; OC, Older controls; MAC, Middle-aged controls; YC, Young controls. Statistically significant results are bolded.

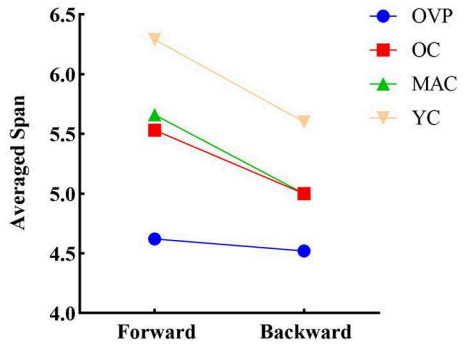

FIGURE 3
Differences in recall order of span for individual level. The forward span is significantly longer than the backward span ($p < 0.001$). Paired *t*-test revealed that the difference between recall order in OVP group was not statistically significant ($p = 0.648$). OVP, Older vertigo patients; OC, Older controls; MAC, Middle-aged controls; YC, Young controls.

and took more time than the OC group, although the difference between the groups was nonsignificant ($p = 0.400$), while the difference in time between the groups was nearly statistically significant ($p = 0.056$). The results showed that only education had a main effect on the score ($F = 3.190$, $p = 0.048$, $\eta^2_p = 0.093$). *Post-hoc* analyses showed that subjects with higher education scored a little higher than the other two groups.

Effects of aging on visuospatial cognitive outcomes in controls

For all the test metrics, we observed a stepwise increase in the performance between young controls, middle-aged controls, and older controls, although there were no significant differences between the OC group and the MAC group (Supplementary Figure S1). The YC group performed significantly better than the other groups separately in the

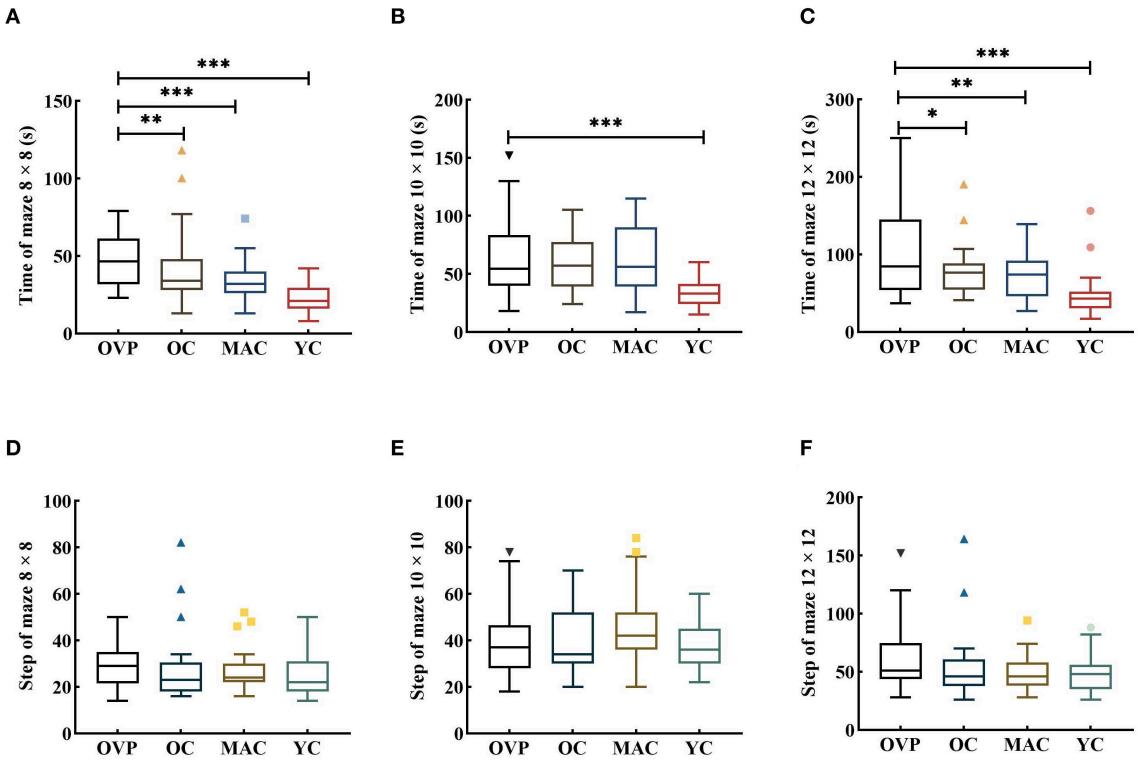

FIGURE 4
Time and Step of Maze test between groups. All the figures were Boxplot. The top and bottom lines of a column represented the maximum and minimum values of the data, respectively. The top and bottom lines of the box represented the third quartile and the first quartile, respectively, and the line in the middle of the box represents the median of the data. Colored symbols represented outliers. **(A–C)** Time of each group in different maps; **(D–F)** Step of each group in different maps. *Post-hoc* multiple comparisons between groups using OVP group as reference, significantly differences were indicated by the asterisk. OVP, Older vertigo patients; OC, Older controls; MAC, Middle-aged controls; YC, Young controls. *$p < 0.05$; **$p < 0.01$; ***$p < 0.001$.

TABLE 3 Comparison of maze test indexes between groups.

	Map 8 × 8		Map 10 × 10		Map 12 × 12	
	Time (s) Median (IQR)	Step Median (IQR)	Time (s) Median (IQR)	Step Median (IQR)	Time (s) Median (IQR)	Step Median (IQR)
OVP	46.50 (29.50)	29.00 (13.50)	54.50 (43.75)	37.00 (18.50)	84.50 (91.25)	51.00 (31.00)
OC	34.00 (23.00)	23.00 (12.50)	57.00 (38.50)	34.00 (22.00)	76.50 (34.00)	46.00 (23.00)
MAC	32.00 (14.00)	24.00 (8.00)	56.00 (51.00)	42.00 (16.00)	74.00 (46.00)	46.00 (20.00)
YC	21.00 (13.50)	22.00 (13.00)	33.00 (17.50)	36.00 (15.00)	43.00 (21.50)	48.00 (21.00)
***P*-value**	**0.001**	0.104	**<0.001**	0.104	**<0.001**	0.176
Male	29.00 (15.25)	23.00 (10.50)	40.50 (29.50)	37.00 (16.50)	58.00 (38.00)	48.00 (20.50)
Female	32.50 (25.50)	26.00 (12.50)	48.00 (38.50)	38.00 (18.00)	63.00(47.75)	49.00 (24.00)
***P*-value**	0.105	0.271	**0.021**	0.271	**0.001**	0.152

OVP, Older vertigo patients; OC, Older controls; MAC, Middle-aged controls; YC, Young controls. IQR, interquartile range. Statistically significant results are bolded.

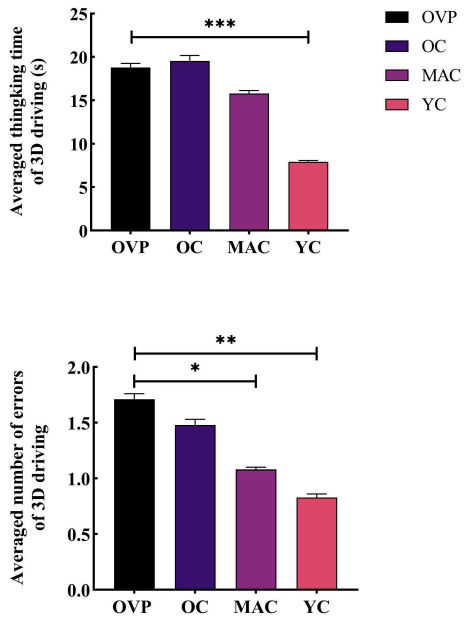

FIGURE 5
Time and errors of 3D driving test between groups. **(A)** Averaged thinking time of 3D driving. **(B)** Number of Errors of 3D driving. *Post-hoc* multiple comparisons between groups using OVP group as reference, significantly differences were indicated by the asterisk. OVP, Older vertigo patients; OC, Older controls; MAC, Middle-aged controls; YC, Young controls. *$p < 0.05$; **$p < 0.01$; ***$p < 0.001$. Error bars indicate the SEM.

TABLE 4 Comparison of 3D driving test indexes between groups.

	Map	
	Thinking time (s) Mean (SD)	Errors Mean (SD)
OVP	18.78 (7.36)	1.71 (1.02)
OC	19.56 (11.84)	1.48 (1.10)
MAC	15.81 (8.59)	1.08 (0.68)
YC	7.92 (3.45)	0.83 (0.79)
***P*-value**	**0.003**	**0.006**
Male	12.24 (7.49)	1.03 (0.87)
Female	16.59 (9.91)	1.34 (0.96)
***P*-value**	**0.022**	0.156

OVP, Older vertigo patients; OC, Older controls; MAC, Middle-aged controls; YC, Young controls. Statistically significant results are bolded.

span of the weeding test (FW: $p = 0.001$, $p = 0.004$; BW: $p = 0.015$, $p = 0.011$), the velocity of the weeding test (FW: $p = 0.001$, $p < 0.001$; BW: $p < 0.001$, $p = 0.017$), the time of the maze test (8 × 8: $p < 0.001$, $p < 0.001$; 10 × 10: $p < 0.001$, $p < 0.001$; 12 × 12: $p < 0.001$, $p < 0.001$) and the thinking time of the 3D driving ($p < 0.001$; $p = 0.001$). For the number of errors in the 3D driving, only the OC group had significantly more errors than the YC group ($p = 0.014$). In the card rotation test, although there was no main effect of group on both score and time ($F_{score} = 0.434$, $p = 0.729$, $\eta^2_p = 0.021$; $F_{time} = 0.157$, $p = 0.925$, $\eta^2_p = 0.008$), *post-hoc* analyses revealed that the YC group scored significantly higher than the OC group ($p = 0.005$) and the MAC group ($p = 0.006$), but the differences in time between all the control groups were nonsignificant.

Discussion

In the present study, we assessed visuospatial ability through a portable computerized Visuospatial Cognition Assessment System (VCAS). We found that patients performed worse than the age-matched controls, but the differences of their performance on the 3D driving and card rotation tests were not statistically significant. Also, considering the importance of aging, we further divided the controls into different age groups and found that the older and middle-aged groups

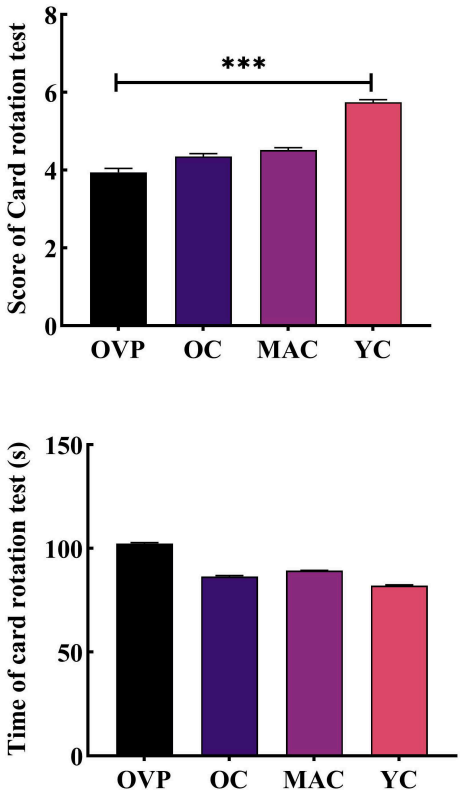

FIGURE 6
Score and time of Card rotation test between groups. **(A)** Score of card rotation test. **(B)** Time of card rotation test. *Post-hoc* multiple comparisons between groups using OVP group as reference, significantly differences were indicated by the asterisk. OVP, Older vertigo patients; OC, Older controls; MAC, Middle-aged controls; YC, Young controls. ***$p < 0.001$. Error bars indicate the SEM.

had comparable performance on all tasks, but both groups performed worse than the younger group on each task. Results suggest that: (1) Vestibular dysfunction is a risk factor for the decline in visuospatial ability, validating the link between the vestibular system and visuospatial ability; (2) Visuospatial ability declines with natural aging and may subsequently stabilize gradually; and (3) Assessing vestibular-related cognitive ability in a computerized way may be of great value in the future.

Contribution of vestibular function on visuospatial cognitive outcomes

Spatial memory stores and manages information about the environment (e.g., location and relative position). We designed a computerized version of the Corsi block tapping task (CBT) (31) to evaluate visuospatial working memory (VSWM). Results found that the OVP group had a significantly shorter span than the age-matched controls in the forward condition. This is in line with previous work that short-term spatial memory was impaired in patients with chronic vestibular dysfunction during computerized CBT, with 4.11 ± 1.07 and 5.29 ± 0.77 for the forward span of older patients and controls, respectively (34). Unfortunately, they didn't talk about the backward condition. Our results showed that the OVP group indeed performed worse than the OC group in the backward condition, but the difference was not statistically significant, which may be due to the backward condition being more difficult and affecting the performance of controls. Regarding the differences between the forward and backward conditions, some studies argue that the backward condition, in which participants need to recall in the opposite order, increases the burden on cognition and is therefore more strenuous (27). However, similar results have been found between these two conditions (31), and one study even found that subjects performed better on the backward condition (35). In the present study, the forward span was significantly larger than the backward condition for controls, supporting the very first perspective. However, difference of the performance in the OVP group was nonsignificant, this may be due to the patients' poorer performance in the forward condition. There is still no consensus on whether these two conditions indeed tap into different cognitive processes. Future work is needed to further explore this issue.

For spatial navigation ability, results found that the OVP group took significantly longer time than the OC group. We did not observe a significant difference in steps between the two groups. It should be noted that during the test, we observed that more subjects in the OVP group took the wrong route and then retraced it to the correct one, which may lead to a significant increase in the time and steps. This can also be reflected on the larger interquartile range (IQR) of the OVP group. Our results confirm and extend prior reports regarding poorer performance in spatial orientation and spatial navigation in patients with vestibular dysfunction (9).

TABLE 5 Comparison of card rotation test indexes between groups.

	Card rotation test	
	Score Mean (SD)	Score Mean (SD)
OVP	3.94 (1.71)	102.29 (35.88)
OC	4.35 (1.27)	86.41 (34.47)
MAC	4.52 (1.39)	89.25 (28.07)
YC	5.74 (1.41)	82.11 (25.74)
***P*-value**	0.729	0.925
Primary education	4.25 (1.26)	80.00 (30.36)
Secondary education	4.00 (1.35)	96.35 (32.08)
Higher education	5.35 (1.51)	84.03 (29.59)
***P*-value**	**0.048**	0.807

OVP, Older vertigo patients; OC, Older controls; MAC, Middle-aged controls; YC, Young controls. Statistically significant results are bolded.

During the 3D driving test, although there were no statistically significant differences, the OVP group indeed made more errors than the OC group, suggesting that patients may have had some difficulties, such as poorer memory of routes or being more susceptible to getting confused. However, this did not seem to affect their ability to make the correct choice they thought. It is also to be noted that there were only three intersections in the map, which may have weakened the differences between groups.

As to mental rotation ability, we also did not find statistically significant differences between groups, although the OVP group still had a lower score and took longer time. This may be due to the highly diverse in terms of the type of vestibular diagnosis among patients, which was not sufficient to reflect the differences with controls in this task. Currently,the research on mental rotation ability is still controversial. Some studies have found that, BVP patients and patients with VN or BPPV may exhibit significant impairment in mental rotation task (10, 16). However, Nair et al. (36) found no significant differences in overall performance between BPPV patients and controls in a mental rotation task of 3D objects. More studies with large samples will be helpful for this issue in the future.

Effect of aging on visuospatial ability in normal controls

With age, spatial orientation and navigational abilities may deteriorate (26). Collectively, in our study, the YC group had a better performance than other groups which is consistent with previous studies. However, the OC group and the MAC group had comparable performances during all the tests. We infer that visuospatial ability decreases with age and may gradually stabilize thereafter. It is intriguing that in the study by Coutrot et al. (29), there is an "inflection point" where performance on the navigation task improved for those over 75 years of age, and the authors explain that this could be a selective bias that these people may have extraordinary cognitive abilities.

The solid influence of aging on visuospatial abilities can be explained in terms of fluid intelligence (FUI), which refers to the ability to transfer and reason independently of prior experience and knowledge, and is more susceptible to aging than crystal intelligence, which relies on inherent experience accumulation (37). In addition, vestibular loss associated with normal aging may also mediate age-induced decline in cognition (38, 39). Therefore, it is not yet able to fully exclude the effects of age-related vestibular loss in this study. In the future, multicenter studies focusing on the effect of aging on visuospatial ability with larger sample size and finer age group delineation can help further clarify this issue.

Computerized of test system

Previous studies have used a variety of instruments to assess visuospatial ability such as comprehensive scales or single-dimensional neuropsychological tests. Most of the tools are paper and pencil tests, which have some shortcomings: (1) It is difficult to control the experimental conditions accurately and is inconvenient for the management of test data. (2) The test conditions are mostly static, with little sense of dynamics. (3) Concentrate primarily on one dimension of visuospatial abilities. Furthermore, although some paradigms already have a computerized version, such as the computerized CBT (27, 31, 40), most of them are limited to the PC, which is inconvenient to carry for bedside evaluation. Therefore, we hope to develop an effective and convenient tablet-based test battery to provide a more dynamic and three-dimensional test condition and mainly focus on evaluating visuospatial ability, including spatial memory, spatial navigation, and mental rotation.

Our test system has specific advantages like other computerized task, such as precise control of the presentation interval and automatic recording of test metrics. However, we should be aware that there are still some potential issues. Firstly, it should be noted that there are possible differences between computerized versions and traditional test paradigms. For example, during the CBT, Popp et al. found a statistically significant difference between BVD patients and controls in the backward condition using a traditional tapping paradigm (41), which is different from the results we observed. One study has proposed that the hand movements of the experimenter in the traditional paradigm induce a motor-priming effect (31). The motor stimulus pre-presented will have either a positive or negative effect on the observer's motor processing, which indicates that the mental processes involved in the two modalities may differ and may limit the generalization of the results. Collectively, at least in the forward condition, there is an effect of vestibular dysfunction on spatial memory, and the use of the backward condition as a representative of spatial memory should clearly be reconsidered, especially in such computerized version. A larger number of subgroups using different modalities of CBT will be helpful to systematically investigate this issue.

Secondly, it has also been proposed that subjects do not rely on vestibular input from actual movement when completing such computerized task and only need to remain seated during the test, and attentional resources can be directed exclusively to the spatial memory task (42). Therefore, a purely static test setup may not be sufficient to capture the degree of impairment in real-life in patients with vestibular dysfunction. However, Kalová et al. (30) found that the results of a navigation test using a computerized version were similar to navigation performed in the real world, supporting the use of a computerized test modality to assess cognitive function.

In addition, the impact of subjects' familiarity and operation ability with electronic devices should be carefully considered when applying such computerized versions of the test, especially for older adults. To sum, although a computerized test system has been proven to have certain practical advantages, it is more sensible to be careful when quantitatively comparing visuospatial ability in virtual and real-world environments. Computerized versions of neuropsychological tasks should be carefully evaluated through a large-sample research design with normative data established for different age groups as well. And we believe that combine tablet-based test system and VR technology may improve our assessment tools more portable and effective in the future.

Limitations

Of note, there are several limitations of the study. First, the cross-sectional design limits the causality of conclusions that can be drawn from it. Future work is needed to further explore such scenarios by developing longitudinal cohort studies; Secondly, the sample size of the subgroups in this study was small, which makes it difficult to further investigate the disease-specific effect within the OVP group and demonstrate a more refined trend in visuospatial abilities of controls; Finally, although the computerized version has certain advantages, it still lacks the input of dynamic vestibular information, which may not be sufficient to reflect the cognitive symptoms of patients.

Conclusions

Vestibular cognition is a valuable area for clinical work. The current study presents evidence from a computerized Visuospatial Cognition Assessment System (VCAS) showing the close association between the vestibular system and visuospatial ability. Older adults with vestibular dysfunction have more difficulties during all tasks, especially spatial memory and spatial navigation. Visuospatial ability decreases with age and may gradually tend to be stable thereafter. Furthermore, computerizing the assessment of visuospatial ability is a valuable endeavor, but its effectiveness still should be treated with caution.

Data availability statement

The raw data supporting the conclusions of this article will be made available by the authors, without undue reservation.

Ethics statement

The studies involving human participants were reviewed and approved by the Ethical Committee of Peking University and the Peking University First Hospital (Approval No. 2021-390). The patients/participants provided their written informed consent to participate in this study.

Author contributions

XZ designed and conceptualized the study, collected, analyzed, interpreted the data, designed, and drafted the manuscript. YL made a substantial contribution to the design and conception of this work and revised the manuscript critically for important intellectual content. YH participated in the collection and interpretation of the data and revising the manuscript. YX provided suggestions for experimental design, and revised the manuscript. XY participated in figure drawing. YZ, CW, and HY provided suggestions for experimental design. All authors contributed to the article and approved the submitted version.

Funding

This research was supported by the Capital Clinical Special Application Research Project (Grant No. Z151100004015137).

Conflict of interest

The authors declare that the research was conducted in the absence of any commercial or financial relationships that could be construed as a potential conflict of interest.

Publisher's note

All claims expressed in this article are solely those of the authors and do not necessarily represent those of their affiliated organizations, or those of the publisher, the editors and the reviewers. Any product that may be evaluated in this article, or claim that may be made by its manufacturer, is not guaranteed or endorsed by the publisher.

Supplementary material

The Supplementary Material for this article can be found online at: https://www.frontiersin.org/articles/10.3389/fneur.2022.1049806/full#supplementary-material

References

1. Besnard S, Lopez C, Brandt T, Denise P, Smith PF. Editorial: the vestibular system in cognitive and memory processes in mammalians. *Front Integr Neurosci.* (2015) 9:55. doi: 10.3389/fnint.2015.00055

2. Smith PF. The vestibular system and cognition. *Curr Opin Neurol.* (2017) 30:84–9. doi: 10.1097/WCO.0000000000000403

3. Ferre ER, Haggard P. Vestibular cognition: state-of-the-art and future directions. *Cogn Neuropsychol.* (2020) 37:413–20. doi: 10.1080/02643294.2020.1736018

4. Lopez C. Making sense of the body: the role of vestibular signals. *Multisens Res.* (2015) 28:525–57. doi: 10.1163/22134808-00002490

5. Lopez C. The vestibular system: balancing more than just the body. *Curr Opin Neurol.* (2016) 29:74–83. doi: 10.1097/WCO.0000000000000286

6. Mast FW, Preuss N, Hartmann M, Grabherr L. Spatial cognition, body representation and affective processes: the role of vestibular information beyond ocular reflexes and control of posture. *Front Integr Neurosci.* (2014) 8:44. doi: 10.3389/fnint.2014.00044

7. Moser EI, Moser MB, McNaughton BL. Spatial representation in the hippocampal formation: a history. *Nat Neurosci.* (2017) 20:1448–64. doi: 10.1038/nn.4653

8. Pinker S. Visual cognition: an introduction. *Cognition.* (1984) 18:1–63. doi: 10.1016/0010-0277(84)90021-0

9. Kremmyda O, Hufner K, Flanagin VL, Hamilton DA, Linn J, Strupp M, et al. Beyond dizziness: virtual navigation, spatial anxiety and hippocampal volume in bilateral vestibulopathy. *Front Hum Neurosci.* (2016) 10:139. doi: 10.3389/fnhum.2016.00139

10. Grabherr L, Cuffel C, Guyot JP, Mast FW. Mental transformation abilities in patients with unilateral and bilateral vestibular loss. *Exp Brain Res.* (2011) 209:205–14. doi: 10.1007/s00221-011-2535-0

11. Wallwork SB, Butler DS, Moseley GL. Dizzy people perform no worse at a motor imagery task requiring whole body mental rotation; a case-control comparison. *Front Hum Neurosci.* (2013) 7:258. doi: 10.3389/fnhum.2013.00258

12. Mast FW, Merfeld DM, Kosslyn SM. Visual mental imagery during caloric vestibular stimulation. *Neuropsychologia.* (2006) 44:101–9. doi: 10.1016/j.neuropsychologia.2005.04.005

13. Lenggenhager B, Lopez C, Blanke O. Influence of galvanic vestibular stimulation on egocentric and object-based mental transformations. *Exp Brain Res.* (2008) 184:211–21. doi: 10.1007/s00221-007-1095-9

14. Dilda V, MacDougall HG, Curthoys IS, Moore ST. Effects of galvanic vestibular stimulation on cognitive function. *Exp Brain Res.* (2012) 216:275–85. doi: 10.1007/s00221-011-2929-z

15. Brandt T, Zwergal A, Glasauer S. 3-D spatial memory and navigation: functions and disorders. *Curr Opin Neurol.* (2017) 30:90–7. doi: 10.1097/WCO.0000000000000415

16. Candidi M, Micarelli A, Viziano A, Aglioti SM, Minio-Paluello I, Alessandrini M. Impaired mental rotation in benign paroxysmal positional vertigo and acute vestibular neuritis. *Front Hum Neurosci.* (2013) 7:783. doi: 10.3389/fnhum.2013.00783

17. Péruch P, Lopez C, Redon-Zouiteni C, Escoffier G, Zeitoun A, Sanjuan M, et al. Vestibular information is necessary for maintaining metric properties of representational space: evidence from mental imagery. *Neuropsychologia.* (2011) 49:3136–44. doi: 10.1016/j.neuropsychologia.2011.07.026

18. Smith JL, Trofimova A, Ahluwalia V, Casado Garrido JJ, Hurtado J, Frank R, et al. The "vestibular neuromatrix": a proposed, expanded vestibular network from graph theory in post-concussive vestibular dysfunction. *Hum Brain Mapp.* (2022) 43:1501–18. doi: 10.1002/hbm.25737

19. Shinder ME, Taube JS. Differentiating ascending vestibular pathways to the cortex involved in spatial cognition. *J Vestib Res.* (2010) 20:3–23. doi: 10.3233/VES-2010-0344

20. Hoppes CW, Huppert TJ, Whitney SL, Dunlap PM, DiSalvio NL, Alshebber KM, et al. Changes in cortical activation during dual-task walking in individuals with and without visual vertigo. *J Neurol Phys Ther.* (2020) 44:156–63. doi: 10.1097/NPT.0000000000000310

21. Hitier M, Besnard S, Smith PF. Vestibular pathways involved in cognition. *Front Integr Neurosci.* (2014) 8:59. doi: 10.3389/fnint.2014.00059

22. Brandt T, Schautzer F, Hamilton DA, Bruning R, Markowitsch HJ, Kalla R, et al. Vestibular loss causes hippocampal atrophy and impaired spatial memory in humans. *Brain.* (2005) 128(Pt 11):2732–41. doi: 10.1093/brain/awh617

23. Balabhadrapatruni S, Zheng Y, Napper R, Smith PF. Basal dendritic length is reduced in the rat hippocampus following bilateral vestibular deafferentation. *Neurobiol Learn Mem.* (2016) 131:56–60. doi: 10.1016/j.nlm.2016.03.009

24. Besnard S, Machado ML, Vignaux G, Boulouard M, Coquerel A, Bouet V, et al. Influence of vestibular input on spatial and nonspatial memory and on hippocampal Nmda receptors. *Hippocampus.* (2012) 22:814–26. doi: 10.1002/hipo.20942

25. Kingma H, van de Berg R. Anatomy, physiology, and physics of the peripheral vestibular system. *Handb Clin Neurol.* (2016) 137:1–16. doi: 10.1016/B978-0-444-63437-5.00001-7

26. Lester AW, Moffat SD, Wiener JM, Barnes CA, Wolbers T. The aging navigational system. *Neuron.* (2017) 95:1019–35. doi: 10.1016/j.neuron.2017.06.037

27. Brunetti R, Del Gatto C, Delogu F. Ecorsi: implementation and testing of the corsi block-tapping task for digital tablets. *Front Psychol.* (2014) 5:939. doi: 10.3389/fpsyg.2014.00939

28. Previc FH, Krueger WW, Ross RA, Roman MA, Siegel G. The relationship between vestibular function and topographical memory in older adults. *Front Integr Neurosci.* (2014) 8:46. doi: 10.3389/fnint.2014.00046

29. Coutrot A, Silva R, Manley E, de Cothi W, Sami S, Bohbot VD, et al. Global determinants of navigation ability. *Curr Biol.* (2018) 28:2861–6 e4. doi: 10.1016/j.cub.2018.06.009

30. Kalová E, Vlcek K, Jarolímová E, Bures J. Allothetic orientation and sequential ordering of places is impaired in early stages of alzheimer's disease: corresponding results in real space tests and computer tests. *Behav Brain Res.* (2005) 159:175–86. doi: 10.1016/j.bbr.2004.10.016

31. Claessen MH, van der Ham IJ, van Zandvoort MJ. Computerization of the standard corsi block-tapping task affects its underlying cognitive concepts: a pilot study. *Appl Neuropsychol Adult.* (2015) 22:180–8. doi: 10.1080/23279095.2014.892488

32. Lacroix E, Cornet S, Deggouj N, Edwards MG. The visuo-spatial abilities diagnosis (Vsad) test: evaluating the potential cognitive difficulties of children with vestibular impairment through a new tablet-based computerized test battery. *Behav Res Methods.* (2021) 53:1910–22. doi: 10.3758/s13428-020-01432-1

33. Henn P, Gallagher AG, Nugent E, Seymour NE, Haluck RS, Hseino H, et al. Visual spatial ability for surgical trainees: implications for learning endoscopic, laparoscopic surgery and other image-guided procedures. *Surg Endosc.* (2018) 32:3634–9. doi: 10.1007/s00464-018-6094-3

34. Guidetti G, Guidetti R, Manfredi M, Manfredi M. Vestibular pathology and spatial working memory. *Acta Otorhinolaryngol Ital.* (2020) 40:72–8. doi: 10.14639/0392-100X-2189

35. Cornoldi C, Mammarella IC. A comparison of backward and forward spatial spans. *Q J Exp Psychol (Hove).* (2008) 61:674–82. doi: 10.1080/17470210701774200

36. Nair MA, Mulavara AP, Bloomberg JJ, Sangi-Haghpeykar H, Cohen HS. Visual dependence and spatial orientation in benign paroxysmal positional vertigo. *J Vestib Res.* (2018) 27:279–86. doi: 10.3233/VES-170623

37. Bajpai S, Upadhayay AD, Banerjee J, Chakrawarthy A, Chatterjee P, Lee J, et al. Discrepancy in fluid and crystallized intelligence: an early cognitive marker of dementia from the lasi-dad cohort. *Dement Geriatr Cogn Dis Extra.* (2022) 12:51–9. doi: 10.1159/000520879

38. Xie Y, Bigelow RT, Frankenthaler SF, Studenski SA, Moffat SD, Agrawal Y. Vestibular loss in older adults is associated with impaired spatial navigation: data from the triangle completion task. *Front Neurol.* (2017) 8:173. doi: 10.3389/fneur.2017.00173

39. Coto J, Alvarez CL, Cejas I, Colbert BM, Levin BE, Huppert J, et al. Peripheral vestibular system: age-related vestibular loss and associated deficits. *J Otol.* (2021) 16:258–65. doi: 10.1016/j.joto.2021.06.001

40. Siddi S, Preti A, Lara E, Brebion G, Vila R, Iglesias M, et al. Comparison of the touch-screen and traditional versions of the corsi block-tapping test in patients with psychosis and healthy controls. *BMC Psychiatry.* (2020) 20:329. doi: 10.1186/s12888-020-02716-8

41. Popp P, Wulff M, Finke K, Ruhl M, Brandt T, Dieterich M. Cognitive deficits in patients with a chronic vestibular failure. *J Neurol.* (2017) 264:554–63. doi: 10.1007/s00415-016-8386-7

42. Dobbels B, Mertens G, Gilles A, Moyaert J, van de Berg R, Fransen E, et al. The virtual morris water task in 64 patients with bilateral vestibulopathy and the impact of hearing status. *Front Neurol.* (2020) 11:710. doi: 10.3389/fneur.2020.00710

frontiers | Frontiers in Neurology

TYPE Correction
PUBLISHED 30 March 2023
DOI 10.3389/fneur.2023.1166687

Check for updates

OPEN ACCESS

EDITED AND REVIEWED BY
Jian-hua Zhuang,
Shanghai Changzheng Hospital, China

*CORRESPONDENCE
Yuhe Liu
✉ liuyuhefeng@163.com

SPECIALTY SECTION
This article was submitted to Neuro-Otology, a section of the journal Frontiers in Neurology

RECEIVED 15 February 2023
ACCEPTED 13 March 2023
PUBLISHED 30 March 2023

CITATION
Zhang X, Huang Y, Xia Y, Yang X, Zhang Y, Wei C, Ying H and Liu Y (2023) Corrigendum: Vestibular dysfunction is an important contributor to the aging of visuospatial ability in older adults–Data from a computerized test system. *Front. Neurol.* 14:1166687. doi: 10.3389/fneur.2023.1166687

COPYRIGHT
© 2023 Zhang, Huang, Xia, Yang, Zhang, Wei, Ying and Liu. This is an open-access article distributed under the terms of the Creative Commons Attribution License (CC BY). The use, distribution or reproduction in other forums is permitted, provided the original author(s) and the copyright owner(s) are credited and that the original publication in this journal is cited, in accordance with accepted academic practice. No use, distribution or reproduction is permitted which does not comply with these terms.

Corrigendum: Vestibular dysfunction is an important contributor to the aging of visuospatial ability in older adults–Data from a computerized test system

Xuehao Zhang[1], Yan Huang[1], Yuqi Xia[2], Xiaotong Yang[1], Yanmei Zhang[2], Chaogang Wei[2], Hang Ying[1] and Yuhe Liu[3]*

[1]School of Medical Technology and Information Engineering, Zhejiang Chinese Medical University, Hangzhou, China, [2]Department of Otolaryngology, Head and Neck Surgery, Peking University First Hospital, Beijing, China, [3]Department of Otolaryngology, Head and Neck Surgery, Beijing Friendship Hospital, Capital Medical University, Beijing, China

KEYWORDS

vestibular dysfunction, recurrent vertigo, aging, visuospatial ability, computerized test system

A corrigendum on
Vestibular dysfunction is an important contributor to the aging of visuospatial ability in older adults–Data from a computerized test system

by Zhang, X., Huang, Y., Xia, Y., Yang, X., Zhang, Y., Wei, C., Ying, H., and Liu, Y. (2022). *Front. Neurol.* 13:1049806. doi: 10.3389/fneur.2022.1049806

In the published article, there was an error in Materials and methods. Participants, paragraph 4. The stated inclusion criteria was not strict enough and previously stated "vertigo and characteristic positional nystagmus (torsional nystagmus in the Dix-Hallpike test, horizontal nystagmus in the Roll test) during the posturography, with the nystagmus lasting no more than 1 min." This should have been "vertigo and characteristic positional nystagmus (torsional nystagmus in the Dix-Hallpike test, horizontal nystagmus in the Roll test) during the posturography." The corrected paragraph appears below:

(2) Failed at least one of the following vestibular function tests:

- no recognizable P1 and N1 waves can be seen in either test ear at 100 dB SPL and/or bilateral asymmetry ratio (AR) of amplitude $\geq$1.6, measured by the c-VEMP.
- horizontal angular VOR gain $<$ 0.8 ($<$ 0.7 for vertical direction) with saccade wave, measured by the v-HIT.
- vertigo and characteristic positional nystagmus (torsional nystagmus in the Dix-Hallpike test, horizontal nystagmus in the Roll test) during the posturography.
- reduced caloric response (sum of bithermal, 24 and 50°C maximum peak slow phase velocity (SPV) on each side $<$ 12°/s), and/or unilateral weakness (UW) $\geq$25%.

In the published article, the reference "Guidetti G, Guidetti R, Manfredi M, Manfredi M. Vestibular pathology and spatial working memory. *Acta Otorhinolaryngol Ital*. (2020) 40:72–8. doi: 10.14639/0392-100X-2189," was not cited in the article. The citation has now been inserted as reference (34) in Discussion, Contribution of vestibular function on visuospatial cognitive outcomes, paragraph 1 and should read:

This is in line with previous work that short-term spatial memory was impaired in patients with chronic vestibular dysfunction during computerized CBT, with 4.11 ± 1.07 and 5.29 ± 0.77 for the forward span of older patients and controls, respectively (34).

In the published article, there was also an error in Supplementary Table 1 as published. In the table "Hearing performance of the better ear" should have been "Hearing performance of the better ear (*n*, %)". Supplementary Table 1 has been updated in the Supplementary material of the published article.

The authors apologize for these errors and state that this does not change the scientific conclusions of the article in any way. The original article has been updated.

Publisher's note

All claims expressed in this article are solely those of the authors and do not necessarily represent those of their affiliated organizations, or those of the publisher, the editors and the reviewers. Any product that may be evaluated in this article, or claim that may be made by its manufacturer, is not guaranteed or endorsed by the publisher.

frontiers | Frontiers in Neurology

TYPE Original Research
PUBLISHED 30 November 2022
DOI 10.3389/fneur.2022.1050282

Check for updates

OPEN ACCESS

EDITED BY
Sulin Zhang,
Huazhong University of Science and Technology, China

REVIEWED BY
Chen Taisheng,
Key Laboratory of Auditory Speech and Balance Medicine, China
Jin Zhang,
Shaanxi Provincial People's Hospital, China

*CORRESPONDENCE
Yulian Jin
jinyulian8548@xinhuamed.com.cn
Jun Yang
yangjun@xinhuamed.com.cn
Qing Zhang
zhangqing03@xinhuamed.com.cn

†These authors have contributed equally to this work and share first authorship

SPECIALTY SECTION
This article was submitted to Neuro-Otology, a section of the journal Frontiers in Neurology

RECEIVED 21 September 2022
ACCEPTED 14 November 2022
PUBLISHED 30 November 2022

CITATION
Zhang Q, Wu Q, Chen J, Wang X, Zhang Y, Liu S, Wang L, Shen J, Shen M, Tang X, Mei L, Chen X, Jin Y, Yang J and Zhang Q (2022) Characteristics of vestibular migraine, probable vestibular migraine, and recurrent vertigo of childhood in caloric and video head impulse tests. *Front. Neurol.* 13:1050282. doi: 10.3389/fneur.2022.1050282

COPYRIGHT
© 2022 Zhang, Wu, Chen, Wang, Zhang, Liu, Wang, Shen, Shen, Tang, Mei, Chen, Jin, Yang and Zhang. This is an open-access article distributed under the terms of the Creative Commons Attribution License (CC BY). The use, distribution or reproduction in other forums is permitted, provided the original author(s) and the copyright owner(s) are credited and that the original publication in this journal is cited, in accordance with accepted academic practice. No use, distribution or reproduction is permitted which does not comply with these terms.

Characteristics of vestibular migraine, probable vestibular migraine, and recurrent vertigo of childhood in caloric and video head impulse tests

Qin Zhang[1,2,3†], Qiong Wu[1,2,3†], Jianyong Chen[1,2,3†], Xueyan Wang[4], Yuzhong Zhang[5], Shuyun Liu[6], Lu Wang[1,2,3], Jiali Shen[1,2,3], Min Shen[1,2,3], Xinyi Tang[1,2,3], Ling Mei[1,2,3], Xiangping Chen[1,2,3], Yulian Jin[1,2,3*], Jun Yang[1,2,3*] and Qing Zhang[1,2,3*]

[1]Department of Otolaryngology Head and Neck Surgery, Xinhua Hospital, Shanghai Jiaotong University School of Medicine, Shanghai, China, [2]Ear Institute, Shanghai Jiaotong University School of Medicine, Shanghai, China, [3]Shanghai Key Laboratory of Translational Medicine in Ear and Nose Diseases, Shanghai, China, [4]Department of Otolaryngology Head and Neck Surgery, Affiliated Hospital of Yanbian University, Yanji, Jilin, China, [5]Department of Otolaryngology Head and Neck Surgery, Second Affiliated Hospital of Xi'an Jiaotong University, Xi'an, Shanxi, China, [6]Department of Otolaryngology Head and Neck Surgery, The Affiliated Hospital of Southwest Medical University, Luzhou, Sichuan, China

Objective: Vertigo is very common in children, but the specific diagnosis and characteristics are not clear. The main objective of this study was to analyze the characteristics of caloric test (CT) and video head impulse test (vHIT) in vestibular migraine of childhood (VMC), probable vestibular migraine of childhood (PVMC), and recurrent vertigo of childhood (RVC), which can provide a reference value for their clinical diagnosis.

Methods: We selected VMC, PVMC and RVC patients under 18 years of age from the outpatient Department of Otolaryngology–Head and Neck Surgery between May 2021 and August 2022. All patients underwent vestibular function examinations, including eye movement recording CT and vHIT. CT results depended on whether both canal paresis and directional preponderance were under normal limits, and vHIT results depended on the gain values of vestibulo-ocular reflex. The results of both tests were analyzed according to the disease type.

Results: Among the 81 pediatric vertigo patients aged 5–17 years, 44 were females and 37 were males. According to the type of vertigo, 29 patients (25.80%) were diagnosed with VMC, 11 (13.58%) with PVMC, and 41 (50.62%) with RVC. The abnormal rates of the CT in VMC, PVMC, and RVC patients were 24.14%, 36.36%, and 17.07%, respectively. There was no significant difference in the abnormal rates among the three groups ($P > 0.05$). None of the patients showed abnormal vHIT results (all abnormal rates 0.00%). The abnormal CT rates were significantly higher than those of abnormal vHIT rates ($P < 0.05$).

Conclusions: VMC, PVMC, and RVC are more likely to be diagnosed by symptoms, as neither CT nor vHIT are specific to any conditions. Due to different clinical presentations of vertigo in pediatric patients, it is critical to further clarify the diagnosis with medical history and clinical characteristics.

KEYWORDS

caloric test, child, symptoms, vestibular migraine, vertigo, video head impulse test

Introduction

The prevalence of vertigo and dizziness in pediatric patients ranges from 0.4 to 15% (1). In 2021, the Committee for the Classification of Vestibular Disorders of the Bárány Society (ICVD) and the Migraine Classification subgroup of the International Headache Society proposed the diagnostic criteria for vestibular migraine and recurrent vertigo occurring in childhood. For the first time, the new consensus reclassified and formulated the diagnostic criteria for children's vestibular migraine and recurrent vertigo, and defined three disorders: "vestibular migraine of childhood" (VMC), "probable vestibular migraine of childhood" (PVMC), and "recurrent vertigo of childhood" (RVC) (2).

As most children cannot describe their symptoms precisely, it is difficult to distinguish these types of vestibular disorders accurately. The correct diagnostic evaluation of vertigo in children includes not only a detailed medical history and careful physical examination, but also further vestibular tests based on clinical indications (3). The caloric test (CT) and video head impulse test (vHIT) are the most accepted methods for evaluating peripheral vestibular function (4, 5). The CT is a traditional tool to reflect the function of the left and right horizontal semicircular canals (HSCs) and evaluate the status of vestibular function at ultralow frequencies by detecting the vestibulo-ocular reflex (VOR) function in HSCs (6). A new tool, vHIT, comprehensively assesses the function of the three pairs of semicircular canals (HSCs, posterior semicircular canals [PSCs], and anterior semicircular canals [ASC]) at physiological frequencies (7–10). The vHIT and CT are useful in determining the side and severity of affliction in patients with unilateral lesions. However, the two tests might occasionally produce dissociated results in cases of peripheral vestibular disorders (11), such as vestibular neuritis (12, 13) and Meniere's disease (14–16).

Therefore, it remains unclear whether the results of CT and vHIT are dissociated in pediatric patients with vertigo. Thus, in order to improve the accuracy of clinical diagnosis, this article aimed to compare the characteristics of the CT and vHIT in patients with VMC, PVMC, and RVC, and explored the site and possible pathogenesis of vestibular disorders.

Methods

Research participants

The study retrospectively reviewed 29 patients (age 10.90 ± 2.94 years) diagnosed as having VMC, 11 patients (age 11.45 ± 3.01 years) diagnosed as having PVMC, and 41 patients (age 9.51 ± 2.61 years) diagnosed as having RVC. Patients were treated in the Diagnosis and Treatment Center of Hearing Impairment and Vertigo, Xinhua Hospital, Shanghai Jiaotong University School of Medicine, Shanghai, China, from May 2021 to August 2022. The vestibular function of all patients was examined by videonystagmography (VNG) examination and vHIT. The specific parameters and response rates of the CT and vHIT results were compared and analyzed among the three groups.

Eligibility criteria

Patients diagnosed with VMC, PVMC, and RVC were selected according to the diagnostic criteria of the Bárány Society and International Headache Society (2).

We included patients whose medical history data were complete and who could be clearly diagnosed; who were able to cooperate with all the tests; and who had not taken vestibular inhibitors and other drugs within the past 48 h.

We excluded patients with intracranial lesions, hereditary neurological diseases, metabolic diseases, or other systemic diseases; ophthalmic diseases; other peripheral vestibular vertigo diseases, such as Meniere's disease; or external and middle ear diseases.

VNG examination

The participants underwent VNG (VO425, Interacoustics, Middelfart, Denmark), including the spontaneous nystagmus

TABLE 1 Baseline data of the three groups.

Characteristics	VMC	PVMC	RVC	Total
Number of patients, *n* (%)	29 (35.80%)	11 (13.58%)	41 (50.62%)	81 (100.00%)
Sex (Male/Female)	14/15	4/7	19/22	37/44
Age (Mean ± SD), years	10.90 ± 2.94	11.45 ± 3.01	9.51 ± 2.61	10.27 ± 2.86

VMC, vestibular migraine of childhood; PVMC, probable vestibular migraine of childhood; RVC, recurrent vertigo of childhood.

TABLE 2 Comparison of abnormal VNG rates.

Test	VMC	PVMC	RVC	χ^2	*P*
VNG, *n* (%)	2 (7.69%)	0 (0.00%)	0 (0.00%)	3.138	0.222
Spontaneous nystagmus, *n* (%)	18 (64.28%)	1 (9.09%)	25 (61.00%)	10.934	0.004
Positional nystagmus, *n* (%)	20 (69.00%)	5 (45.45%)	30 (73.17%)	3.080	0.247
CT, *n* (%)	7 (24.14%)	4 (36.36%)	7 (17.07%)	1.963	0.374

Fisher's exact test was conducted when the chi-square test conditions were not met.
VMC, vestibular migraine of childhood; PVMC, probable vestibular migraine of childhood; RVC, recurrent vertigo of childhood; VNG, videonystagmography; CT, caloric test; χ^2, chi-square value/Fisher's exact test value; *P*, *P*-value.

test, gaze test, random saccade test, smooth pursuit tracking test, optokinetic nystagmus test, positional nystagmus test, and CT.

Eye movement recording

The patients wore Frenzel glasses and sat upright with their eyes in the horizontal plane and looked at the target without moving their head. After calibration, tests were performed in the order listed as follows: (1) Spontaneous nystagmus test: the patient was asked to look forward in a dark room without any stimulation for at least 60 s, and the presence of nystagmus was assessed. (2) Gaze test: the patient was asked to focus on the visual target at the center and four eccentric positions for at least 20 s; the absence of nystagmus and the ability to maintain gaze were regarded as normal outcomes. (3) Random saccade test: the patient was asked to track a target that moved randomly within the range of 5–30° in the horizontal direction, with a time interval of 2 s; delay time, peak velocity, and accuracy were calculated by the computer, and saccadic hypometria, saccadic hypermetria, saccadic disorder, and saccadic slowing were considered as abnormal outcomes. (4) Smooth pursuit tracking test was performed by asking the patient to track the visual target moving in the horizontal plane at 0.1–0.5 Hz; eye movement curves were recorded at the same time, and the smooth sine curve with the eye movement curve basically consistent with the visual target curve was considered a normal result. Another parameter evaluated was gain, which was the ratio of eye movement velocity to visual target velocity; it was calculated by the computer, and the normal value was generally not <0.6. (5) Optokinetic nystagmus test: the patient was required to count a series of targets that continued moving at a constant speed of 20 and 40°/s; the direction of nystagmus was opposite to the direction of target movement, and the amplitude and bidirectional amplitude of nystagmus were basically symmetrical. (6) Positional nystagmus test was recorded in the CT position for 40 s, and the presence of nystagmus was assessed.

CT and analysis

CT was performed in a dark room using an Air Fix air irrigator (Interacoustics, Middelfart, Denmark) with an airflow of 8 L/min at 50 and 24°C. The patients were placed in the supine position with the head raised at 30° to maintain the horizontal canal in a vertical position. The external auditory canal was irrigated with warm air at 50°C and with cool air at 24°C for caloric testing, respectively. The interval between successive irrigations was 5 min. The sequence used to irrigate the ear canal was right warm (RW), followed by left warm (LW), right cool (RC), and left cool (LC).

The peak caloric response for each irrigation was calculated by averaging the slow-phase velocity (SPV) of a few nystagmus beats that had the highest velocities, which were represented by the symbols RW, LW, RC, and LC. The difference between the caloric responses from the right and left ears was quantified by the percentage of canal paresis (CP), and the CP was calculated as [(RW + RC) – (LW + LC)] / (RW + RC + LW + LC) × 100%. Which can be considered as the caloric weakness when the CP-value is over 25%. Another parameter that was evaluated was directional preponderance (DP). DP was calculated as [(RW + LC) – (LW + RC)] / (RW + RC + LW + LC) × 100%, and which can be considered as the caloric weakness when the DP-value is over 30% (17).

vHIT and analysis

vHIT was performed using a video oculography device (EyeSeeCam, Interacoustics). The patients were instructed to maintain a sitting position and fixate their gaze on an earth-fixed target in front of both eyes. The target height was flush with the sight line of the patients, and the distance between the patients and target was 1.5 m. The participants were given a video-head impulse tester, which was a special spectacle frame with a built-in camera that tracked pupil movements. The camera of the tester was fixed to the upper-left side of the spectacle frame. For calibration, the patients were asked to keep their heads still and gaze at the alternating laser spot on either side of the target. The patients then provided a slow sinusoidal motion of the head while they kept their gaze fixed on the target.

We conducted a formal test after correct calibration according to the software requirements. An experienced laboratory technician delivered at least 20 brief, abrupt, and unpredictable head impulses per side (10–20° angle, duration 150–200 ms, horizontal semicircular canal impulse peak velocity of 150–300°/s, vertical semicircular canal impulse peak velocity of 100–300°/s). The patients were required to keep gazing at a fixed target in front of them during the head-shaking process.

The reduction in VOR gain was defined as semicircular canals dysfunction. The VOR gain value was automatically calculated as the ratio of eye velocity (°/s) to head velocity (°/s), using the device software. vHIT results were considered abnormal when the VOR value of the HSCs at 60 ms was < 0.8 or the VOR value of the vertical semicircular canals (PSC and ASC) was < 0.7 (18). The normal rate was calculated as normal/total $\times$ 100.

Statistical analysis

All data were analyzed using SPSS v. 26 software (IBM Corp., NY, US). The chi-squared test was used to analysis the response rate of the VNG and vHIT and the abnormality rate of each parameter. Continuous data are presented as the mean ± standard deviation. In the multiple comparisons of parameters, the analysis of variance was adopted when the variance was homogeneous; and the H test was used when the variance was not homogeneous. Graphs were produced using R version 4.2.1 (https://www.r-project.org). It is considered statistical significance when $P < 0.05$.

Results

Patient characteristics

All of the inclusive 81 children with vertigo were tested for vestibular function examination. The study population was composed of 37 males and 44 females, with a mean age of 10.27 ± 2.86 years (ranging from 5 to 17 years). According to the type of vertigo, 29 patients (25.80%, 14 males and 15 females) were diagnosed with VMC, 11 patients (13.58%, 4 males and 7 females) were diagnosed with PVMC, and 41 patients (50.62%, 19 males and 22 females) were diagnosed with RVC. The baseline characteristics of patients were generalized in Table 1.

Comparison of eye movement recording results among the VMC, PVMC, and RVC groups

We calculated the abnormal and normal rates in the total gaze test, random saccade test, smooth pursuit tracking test, and optokinetic nystagmus test as VNG examination response rates among the VMC, PVMC, and RVC groups. During the tests, 3 subjects did not cooperate well with the VNG examination, and at the same time, 1 pediatric patient failed to complete the spontaneous nystagmus test. Almost all of the patients presented with normal results in the VNG examination, while only two (7.69%) patients with VMC showed abnormal VNG results. No statistically significant differences were obtained among the VMC, PVMC, and RVC groups in the VNG examination results ($\chi 2 = 3.138$, $P = 0.222$; Table 2). Although the majority of participants displayed normal results in the gaze test, random saccade test, smooth pursuit tracking test, and optokinetic nystagmus test, the incidence of positional and spontaneous nystagmus was still high. Eighteen (64.28%) patients with VMC, one (9.09%) with PVMC, and 25 (61.00%) with RVC demonstrated positive results for spontaneous nystagmus. The abnormal rate of spontaneous nystagmus in children with PVMC was lower than that in children with VMC and RVC, and the difference among the three groups was statistically significant ($\chi 2 = 10.934$, $P = 0.004$) (Figure 1A). Twenty (69.00%) patients with VMC, five (45.45%) with PVMC, and 30 (73.17%) with RVC presented with positional nystagmus in the CT. No statistical difference was calculated in the incidence of positional nystagmus among the three groups ($\chi 2 = 3.080$, $P = 0.247$; Table 2). The findings of the normal rates for the VNG examination, spontaneous nystagmus test, and positional nystagmus test are intuitively exhibited in Figure 1B.

Comparison of CT results among the VMC, PVMC, and RVC groups

Among the VMC, PVMC, and RVC groups, the response rate (normal and abnormal) and the specific parameters (CP and DP) of CT were compared. Seven (24.14%) patients with VMC, four (36.36%) with PVMC, and seven (17.07%) with RVC presented with abnormal reactions in the CT. However, there was no statistically significant difference in the abnormal rate of the CT among the three groups ($\chi^2 = 1.963$, $P =$

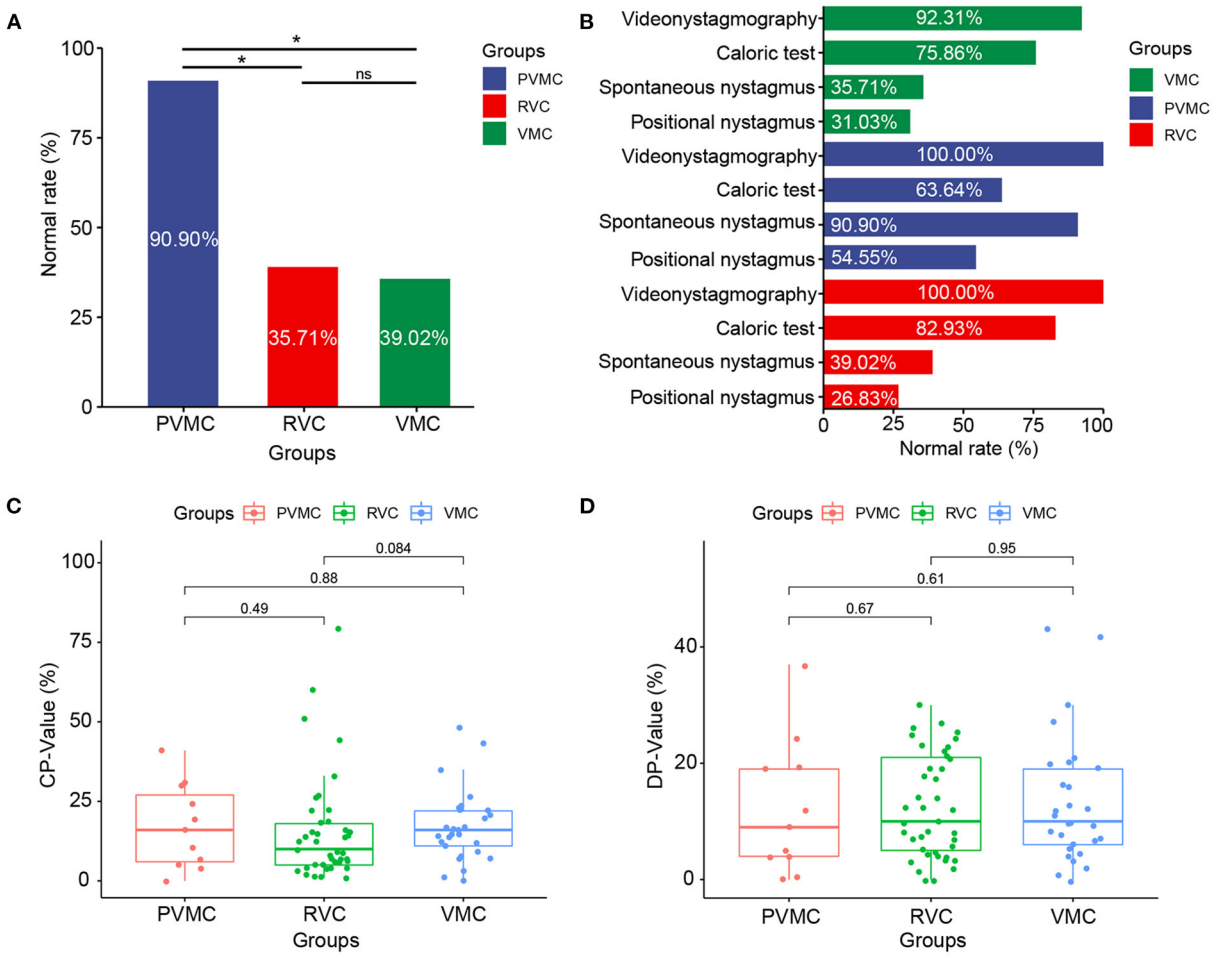

FIGURE 1
Characteristics of the VNG results. **(A)** Normal rate of spontaneous nystagmus results in patients with VMC, PVMC, and RVC. **(B)** Normal rate of videonystagmography, caloric test, positional nystagmus, spontaneous nystagmus results in patients with VMC, PVMC, and RVC. **(C)** Results of CP-value in caloric tests among the three groups, and **(D)** Results of DP-value in caloric tests among the three groups. *$P \leq 0.05$; ns, $P > 0.05$. VMC, vestibular migraine of childhood; PVMC, probable vestibular migraine of childhood; RVC, recurrent vertigo of childhood; CP, canal paresis; DP, directional preponderance.

0.374) (Table 2). Through comparison of specific parameters, we calculated that the CP-values of the CT were 17.28 ± 11.08 in the VMC group, 17.00 ± 13.21 in the PVMC group and 15.54 ± 16.69 in the RVC group. The DP-values of CT were 13.31 ± 11.04 in the VMC group, 12.09 ± 11.58 in the PVMC group, and 12.41 ± 8.80 in the RVC group. Table 3 presents the specific statistical results; no statistical differences were observed among the VMV, PVMC, and RVC groups in either CP-values ($F = 0.135$, $P = 0.874$) or DP-values ($F = 0.090$, $P = 0.914$) (Figures 1C,D).

Comparison of vHIT results among the VMC, PVMC, and RVC groups

The instantaneous and regression VOR gain values of the three pairs of semicircular canals are compared in Table 4 and Figure 2. We calculated the instantaneous and regression VOR gain values in the HSCs, including the left HSC (LH) and right HSC (RH), and the regression VOR gain values in the vertical semicircular canals, including the left ASC (LA), right ASC (RA), left PSC (LP), and right PSC (RP). None of the pediatric patients showed an abnormal reaction in the vHIT. There was no statistically significant difference in the vHIT results among the pediatric patients with vertigo ($P > 0.05$).

Comparison of CT and vHIT results among the VMC, PVMC, and RVC groups

We compared and analyzed the results of the CT and vHIT among patients with VMC, PVMC, and RVC. As shown, the abnormality rate in the vHIT among all patients

TABLE 3 Characteristics of nystagmus induced by caloric tests.

Parameters	VMC	PVMC	RVC	F	P
CP (Mean ± SD)	17.28 ± 11.08	17.00 ± 13.21	15.54 ± 16.69	0.135	0.874
DP (Mean ± SD)	13.31 ± 11.04	12.09 ± 11.58	12.41 ± 8.80	0.090	0.914

VMC, vestibular migraine of childhood; PVMC, probable vestibular migraine of childhood; RVC, recurrent vertigo of childhood; CP, canal paresis; DP, directional preponderance; SD, standard deviation.

TABLE 4 Characteristics of VOR gains induced by vHIT.

Test	VMC	PVMC	RVC	F	*P*
RH–Instantaneous (Mean ± SD)	1.10 ± 0.11	1.15 ± 0.90	1.09 ± 0.09	1.949	0.149
RH–Regression (Mean ± SD)	1.12 ± 0.09	1.15 ± 0.71	1.12 ± 0.07	1.041	0.358
LH–Instantaneous (Mean ± SD)	1.12 ± 0.08	1.15 ± 0.11	1.09 ± 0.08	2.692	0.074
LH–Regression (Mean ± SD)	1.12 ± 0.07	1.15 ± 0.10	1.10 ± 0.07	2.135	0.125
RA–Regression (Mean ± SD)	1.17 ± 0.30	1.09 ± 0.17	1.14 ± 1.45	0.172	0.842
LA–Regression (Mean ± SD)	1.50 ± 0.22	1.49 ± 0.19	1.40 ± 0.20	2.118	0.127
RP–Regression (Mean ± SD)	1.58 ± 0.27	1.57 ± 0.15	1.52 ± 0.20	0.602	0.550
LP–Regression (Mean ± SD)	1.20 ± 0.17	1.15 ± 0.11	1.20 ± 0.16	0.430	0.652

VMC, vestibular migraine of childhood; PVMC, probable vestibular migraine of childhood; RVC, recurrent vertigo of childhood; VOR, Vestibulo-ocular reflex; RH, right horizontal semi-circular canal; LH, left horizontal semi-circular canal; RA, right anterior semi-circular canal; LA, left anterior semi-circular canal; RP, right posterior semi-circular canal; LP, left posterior semi-circular canal.

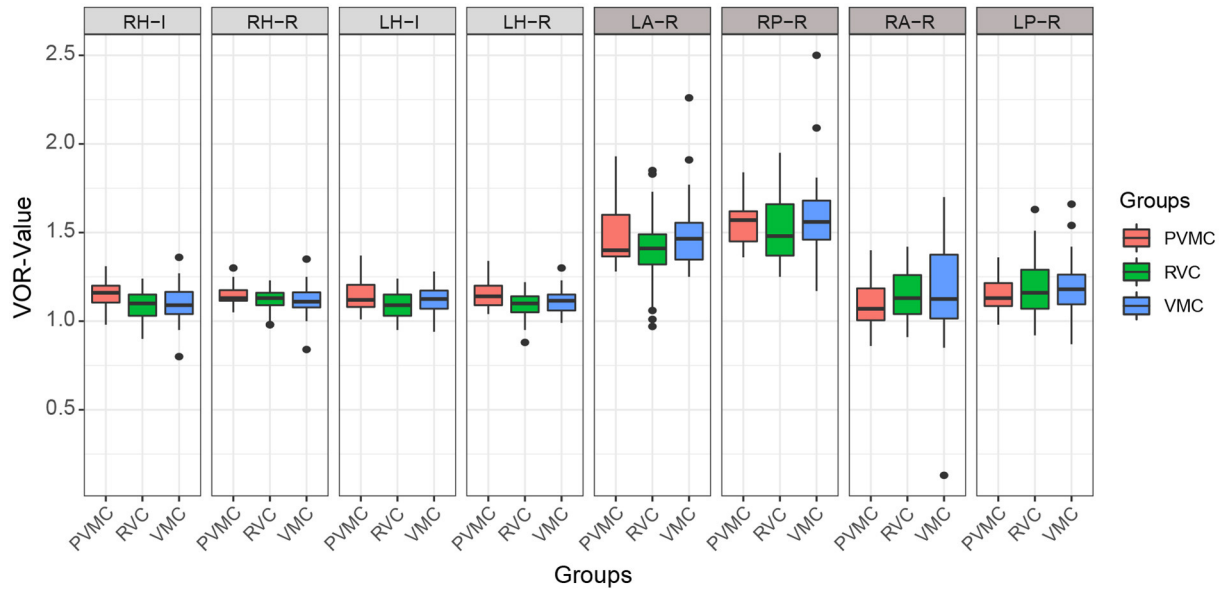

FIGURE 2
Characteristics of vHIT results. Results of instantaneous and regression VOR gain of each semicircular canals. The center line of the box represents the average VOR gain. RH-I, Instantaneous VOR gains in the right horizontal semi-circular canal; RH-R, Regression VOR gains in the right horizontal semi-circular canal; LH-I, Instantaneous VOR gains in the left horizontal semi-circular canal; LH-R, Regression VOR gains in the left horizontal semi-circular canal; LA-R, Regression VOR gains in the left anterior semi-circular canal; RP-R, Regression VOR gains in the right posterior semi-circular canal; RA-R, Regression VOR gains in the right anterior semi-circular canal; LP-R, Regression VOR gains in the left posterior semi-circular canal.

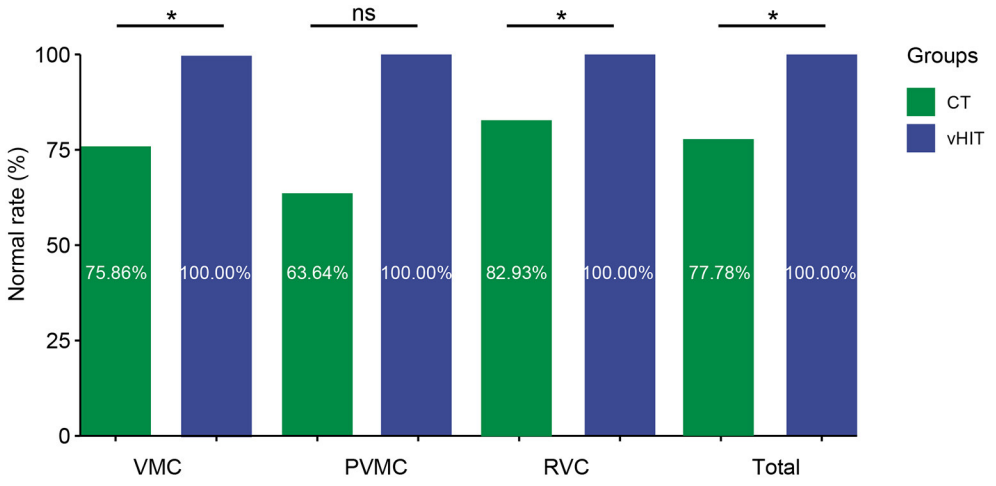

FIGURE 3
Comparison of normal result rates between CT and vHIT. Comparison of normal result rates between caloric test and vHIT in patients with VMC, PVMC, RVC. *$P \leq 0.05$; ns, $P > 0.05$.

TABLE 5 Comparison of abnormal result rates between CT and vHIT.

Group	CT	vHIT	χ^2	*P*
VMC	7 (24.14%)	0 (0.00%)	Fisher	0.010
PVMC	4 (36.36%)	0 (0.00%)	Fisher	0.090
RVC	7 (17.07%)	0 (0.00%)	5.623	0.018
Total	18 (22.22%)	0 (0.00%)	20.250	<0.001

Fisher's exact test was conducted when the chi-square test conditions were not met.
VMC, vestibular migraine of childhood; PVMC, probable vestibular migraine of childhood; RVC, recurrent vertigo of childhood; CT, caloric test; vHIT, video head impulse test.

(0.00%) was lower than that in the CT (22.22%) ($P < 0.001$) (Figure 3 and Table 5). The differences between the results of the CT and vHIT in patients with VMC ($P = 0.01$) and RVC ($P = 0.018$) were both statistically significant, whereas no statistical difference was observed in patients with PVMC ($P = 0.09$).

Discussion

As a special group, vertigo in children has challenged clinicians over the years. The diagnosis of vertigo in pediatric patients is difficult, due to the inability of children to describe their symptoms and lack of cooperation with vestibular function examinations. Short-lived manifestations due to rapid compensation make the condition difficult to detect for the parents (19). The most common causes of vertigo and dizziness in childhood are vestibular migraine and benign paroxysmal vertigo, although the frequencies vary among studies (20–22). A consensus on the diagnostic criteria for vestibular migraine and recurrent vertigo in children was proposed in 2021 by the Committee of the International Classification of Vestibular Diseases (ICVD) of the Bárány Society and the Migraine Classification subgroup of the International Headache Society. Their consensus statement updated the diagnostic term benign paroxysmal vertigo to vestibular migraine and recurrent vertigo in children, and reclassified and established the diagnostic criteria for vestibular migraine and recurrent vertigo in children.

The audio vestibular system in humans is anatomically developed and functionally responsive at birth (23). However, only few reports have systematically reported findings on the vestibular function in pediatric patients with vertigo. With the progress and development of medicine, innovation in testing technology makes it possible to evaluate the vestibular function of infants and children with vertigo. CT and vHIT are common diagnostic tools used to evaluate semicircular canal function in order to identify and diagnose vertigo in suspected pediatric patients (24, 25). Thus, we sought to analyze the characteristics of the CT and vHIT in VMC, PVMC, and RVC, with a view to provide a reference for their clinical treatment and diagnosis.

Comparison of eye movement recording among the VMC, PVMC, and RVC groups

The occurrence of nystagmus is closely related to vertigo. It refers to the patient's inability to continuously focus on the target; the eye moves slowly to one side and deviates from the target, followed by rapid corrective rebound, which can be physiological or pathological. There are three main types of pathological nystagmus: spontaneous nystagmus, staring nystagmus, and positional nystagmus, which are common in

peripheral and central vestibular system lesions. In our study, we found that the three groups of patients had spontaneous nystagmus and positional nystagmus of different frequencies.

Spontaneous nystagmus refers to a continuous, involuntary, rhythmic back and forth movement of the eyeball without inducing factors, which can occur in vestibular peripheral lesions, central lesions, and some eye diseases. It is reported that the frequency of spontaneous nystagmus in children with vertigo is ∼17–75% (26–31), which is similar to our research results. We found that the incidence of spontaneous nystagmus in the PVMC group was significantly lower than that in the other two groups ($P < 0.05$). However, this may be due to the fact that there were fewer cases in the PVMC group, and the statistical results were not accurate. It was also possible that a patient with PVMC was a possible patient of vestibular migraine, and the clinical symptoms were not obvious, similar to a transitional disease; thus, the extraction rate of nystagmus was not high.

Positional nystagmus refers to the nystagmus that occurs when the head is placed in one or several specific positions, but it does not occur in other positions. It is also accompanied by vertigo, which is called positional vertigo. The mechanism of positional nystagmus is unknown. It is generally believed that it is caused by otolith lesions, but there may also be semicircular canal, vestibular nerve, cerebellum, brain stem, brain, and other lesions. Previous studies found positional nystagmus in only 20% of children with vertigo (32, 33). In our case, we found that the extraction rate of positional nystagmus was significantly high: 69.00% in the VMC group, 45.45% in the PVMC group, and 73.17% in the RVC group. The reason for the high frequency of positional nystagmus may be because the patients we included were children with vertigo who were selected according to the latest diagnostic criteria for children's vestibular migraine and recurrent vertigo, and they had a higher degree of cooperation with the vestibular function test, while previous research focused on vestibular diseases in children, which was more extensive.

Comparison of CT results among the VMC, PVMC, and RVC groups

The CT belongs to the ultra-low frequency testing method (0.002–0.004 Hz), which mainly detects the function of the supravestibular nerve and horizontal semicircular canals. It can stimulate the horizontal semicircular canal on both sides and is the gold standard for evaluating vestibular function (6). We found no statistically significantly abnormal CT rates among patients with VMC (24.14%), PVMC (36.36%), and RVC (17.07%). Langhagen et al. (34) found that the rate of abnormal CT findings was 21.0 and 25.0%, respectively, in the RVC and VMC patients, and Marcelli et al. (35) conducted a CT on pediatric patients with vestibular migraine and reported an abnormal rate of 33.0%. These findings are similar to our research results, indicating that children with vertigo may have damaged to a certain extent the function of the low-frequency horizontal semicircular canals.

Comparison of vHIT results among the VMC, PVMC, and RVC groups

The vHIT has been shown to be effective for diagnosing VOR deficits resulting from peripheral vestibular impairment, and allows rapid evaluation of the high-frequency (2–5 Hz) function of the three pairs of semicircular canals (36, 37). Our statistical results showed that none of the pediatric patients had an abnormal reaction to vHIT. Similar results also appeared in the study of Salmito et al. (38), who found that the vestibular function of patients with vestibular migraine was generally normal in the non-acute phase. Additionally, Chen et al. (39) studied 36 RVC patients, and found no statistically significant difference in the abnormal rate of vHIT between the normal control group and the RVC group. This may be because, in daily life, pediatric patients with vertigo receive more high-frequency stimulation to the vestibule, and high-frequency vestibular function is prone to compensation, which leads to a low rate of abnormal vHIT results. Therefore, the vHIT may be used as the main assessment method for the early or decompensated stage of vertigo in pediatric patients. Undoubtedly, the vHIT plays an important role during bedside physical examinations of patients with acute dizziness.

Comparison of the vHIT and CT results among the VMC, PVMC, and RVC groups

Before the widespread application of vHIT to evaluate vestibular function, the CT was considered as the gold standard of unilateral horizontal semicircular canal dysfunction. However, currently, we can detect abnormalities for any semicircular canal and clearly view overt and covert saccades by vHIT. However, these two tests might occasionally produce conflicting results. Many investigations have verified the dissociation between the outcomes of the two tests, and it is common to obtain a normal result in one of the two tests, while an abnormal result in the other, particularly in peripheral vestibular disorders, such as Meniere's disease (14–16) and vestibular neuritis (12, 13). In our study, we found that 22.2% of pediatric patients showed abnormal CT results, while no abnormal vHIT results were found, which may indicate that the CT was ultimately more sensitive for

diagnosing vestibular diseases. Moreover, although both tests estimate the function of horizontal semicircular canals, they have noteworthy limitations and differences. As in cochlear disease, the involvement of the semicircular canals can lead to specific frequency dysfunctions. Due to the limitation of external auditory canal and eardrum, non-physiological stimulation (~0.003 Hz) is required during the CT. Further, CT can only assess the low frequency functional state of the horizontal semicircular canals, whereas vHIT can assess the function of vestibular system under high-frequency (2–5 Hz) stimulation that cannot be determined by CT. The subjects received physiological stimulation similar to head rotation, which will not cause obvious discomfort during the examination. The vHIT may be a useful addition to the existing vestibular function test, however, it does not appear to be an alternative. These tests evaluate different segments and frequency of the semicircular canals, and consequently, it has been proven that the combination of CT and vHIT can more systematically evaluate vestibular function (40–45).

Limitations

The article detailedly studied the differences between eye movement recording, CT and vHIT-test results among patients with VMC, PVMC, and RVC. It was preliminarily concluded that CT can detect vestibular function more sensitively than vHIT in children with vertigo. Additionally, through the examination of nystagmus, we obtained a better understanding of vertigo in children. Nonetheless, the sample size of the study is still insufficient. In the future, we can analyze the specific characteristics of different nystagmus, and preliminarily identify that nystagmus is caused by peripheral or central diseases. And, future studies need to expand the sample size for prospective verification and include other vestibular function tests to comprehensively assess the characteristics of vertigo in children.

Conclusion

Comprehensive ontological and neurological examinations, including history, physical examination, audiological assessment, vestibular function test, and imaging studies, are required for the proper diagnosis of vertigo in children. The CT and vHIT showed no specific diagnostic value in our patients with VMC, PVMC, and RVC. Therefore, history taking is of the utmost importance, not only in regard to the various symptoms or observations, but also in regard to the sequencing of symptoms and their progression or lessening over time, as RVC, VMC, and PVMC are more likely to be diagnosed based on symptoms.

Data availability statement

The original contributions presented in the study are included in the article/supplementary material, further inquiries can be directed to the corresponding authors.

Ethics statement

Written informed consent was obtained from the minor(s)' legal guardian/next of kin for the publication of any potentially identifiable images or data included in this article.

Author contributions

QinZ and QW designed the study, collected patients, statistical analyses, and drafted the manuscript. JC, XW, and YZ assisted in drafting the protocol, conducting data collection and processing, and editing the manuscript. SL, LM, JS, and MS performed data extraction. XT, LM, and XC prepared figures and revised the manuscript. QingZ, YJ, and JY critically evaluated the manuscript. All authors reviewed and approved the final version of the manuscript. All authors contributed to the article and approved the submitted version.

Funding

This research was funded by the National Natural Science Foundation of China (Grant Nos. 82171137, 81970891, and 81860189), the Clinical Research Plan of SHDC (SHDC2022CRD013), the Key International Cooperation Project of Shaanxi Province (Grant No. 2020KWZ-019), and the Science and Technology Project of Shanghai Science and Technology Commission (Grant No. 21S31900600).

Acknowledgments

We would like to thank the National Natural Science Foundation of China for supporting this work.

Conflict of interest

The authors declare that the research was conducted in the absence of any commercial or financial relationships that could be construed as a potential conflict of interest.

Publisher's note

All claims expressed in this article are solely those of the authors and do not necessarily represent those of their affiliated

organizations, or those of the publisher, the editors and the reviewers. Any product that may be evaluated in this article, or claim that may be made by its manufacturer, is not guaranteed or endorsed by the publisher.

References

1. Fancello V, Palma S, Monzani D, Pelucchi S, Genovese E, Ciorba A. Vertigo and dizziness in children: an update. *Children*. (2021) 8:1025. doi: 10.3390/children8111025

2. van de Berg R, Widdershoven J, Bisdorff A, Evers S, Wiener-Vacher S, Cushing SL. et al. Vestibular migraine of childhood and recurrent vertigo of childhood: diagnostic criteria consensus document of the committee for the classification of vestibular disorders of the Bárány society and the international headache society. *J Vestib Res*. (2021) 31:1–9. doi: 10.3233/VES-200003

3. Gruber M, Cohen-Kerem R, Kaminer M, Shupak A. Vertigo in children and adolescents: characteristics and outcome. *Sci World J*. (2012) 2012:109624. doi: 10.1100/2012/109624

4. Waissbluth S, Sepúlveda V. Dissociation between caloric and video head impulse tests in dizziness clinics. *Audiol Res*. (2022) 12:423–32. doi: 10.3390/audiolres12040043

5. Li X, Ling X, Li Z, Song N, Ba X, Yang B. et al. Clinical characteristics of patients with dizziness/vertigo showing a dissociation between caloric and video head impulse test results. *Ear Nose Throat J*. (2022) 11:1455613221113790. doi: 10.1177/01455613221113790

6. Perez N, Rama-Lopez J. Head-impulse and caloric tests in patients with dizziness. *Otol Neurotol*. (2003) 24:913–7. doi: 10.1097/00129492-200311000-00016

7. Zhang Q, Zhang Q, Wu Q, Jin Y, Chen X, Shen M. et al. Gain characteristics of three pairs of semicircular canals in video head impulse paradigm test and suppression head impulse paradigm test in healthy young Chinese population. *Lin Chung Er Bi Yan Hou Tou Jing Wai Ke Za Zhi*. (2022) 36:659–64.

8. Halmagyi GM, Curthoys IS. A clinical sign of canal paresis. *Arch Neurol*. (1988) 45:737–9. doi: 10.1001/archneur.1988.00520310043015

9. Abdulrahim R, Bhandary BSK, Rajeshwary A, Goutham MK, Bhat V. et al. The role of video head impulse test (Vhit) in diagnosing benign paroxysmal positional vertigo (BPPV). *Indian J Otolaryngol Head Neck Surg*. (2022) 74:506–10. doi: 10.1007/s12070-020-02351-5

10. Koç A, Akkiliç EC. Evaluation of video head impulse test during vertiginous attack in vestibular migraine. *Acta Otorhinolaryngol Ital*. (2022) 42:281–6. doi: 10.14639/0392-100X-N1951

11. Mezzalira R, Bittar RSM, do Carmo Bilécki-Stipsky MM, Brugnera C, Grasel SS. Sensitivity of caloric test and video head impulse as screening test for chronic vestibular complaints. *Clinics*. (2017) 72:469–73. doi: 10.6061/clinics/2017(08)03

12. Strupp M, Dlugaiczyk J, Ertl-Wagner BB, Rujescu D, Westhofen M, Dieterich M. Vestibular disorders. *Dtsch Arztebl Int*. (2020) 117:300–10. doi: 10.3238/arztebl.2020.0300

13. Pogson JM, Taylor RL, Young AS, McGarvie LA, Flanagan S, Halmagyi GM. et al. Vertigo with sudden hearing loss: audio-vestibular characteristics. *J Neurol*. (2016) 263:2086–96. doi: 10.1007/s00415-016-8214-0

14. Lopez-Escamez JA, Carey J, Chung WH, Goebel JA, Magnusson M, Mandalà M. et al. Diagnostic criteria for Menière's disease. *J Vestib Res*. (2015) 25:1–7. doi: 10.3233/VES-150549

15. Hannigan IP, Welgampola MS, Watson SRD. Dissociation of caloric and head impulse tests: a marker of Meniere's disease. *J Neurol*. (2021) 268:431–9. doi: 10.1007/s00415-019-09431-9

16. Lee JY, Kwon E, Kim HJ, Choi JY, Oh HJ, Koo JW. et al. Dissociated results between caloric and video head impulse tests in dizziness: prevalence, pattern, lesion location, and etiology. *J Clin Neurol*. (2020) 16:277–84. doi: 10.3988/jcn.2020.16.2.277

17. Shepard NT, Jacobson GP. The caloric irrigation test. *Handb Clin Neurol*. (2016) 137:119–31. doi: 10.1016/B978-0-444-63437-5.00009-1

18. McGarvie LA, MacDougall HG, Halmagyi GM, Burgess AM, Weber KP, Curthoys IS. The video head impulse test (vHIT) of semicircular canal function - age-dependent normative values of VOR gain in healthy subjects. *Front Neurol*. (2015) 6:154. doi: 10.3389/fneur.2015.00154

19. Casani AP, Dallan I, Navari E, Sellari Franceschini S, Cerchiai N. Vertigo in childhood: proposal for a diagnostic algorithm based upon clinical experience. *Acta Otorhinolaryngol Ital*. (2015) 35:180–5.

20. Devaraja, K. Vertigo in children; a narrative review of the various causes and their management. *Int J Pediatr Otorhinolaryngol*. (2018) 111:32–8. doi: 10.1016/j.ijporl.2018.05.028

21. Russell G, Abu-Arafeh I. Paroxysmal vertigo in children–an epidemiological study. *Int J Pediatr Otorhinolaryngol*. (1999) 49, S105–107. doi: 10.1016/S0165-5876(99)00143-3

22. Lanzi G, Balottin U, Borgatti R. A prospective study of juvenile migraine with aura. *Headache*. (1994) 34:275–8. doi: 10.1111/j.1526-4610.1994.hed3405275.x

23. Ornitz EM, Atwell CW, Walter DO, Hartmann EE, Kaplan AR. The maturation of vestibular nystagmus in infancy and childhood. *Acta Otolaryngol*. (1979) 88:244–56. doi: 10.3109/00016487909137166

24. Fife TD, Tusa RJ, Furman JM, Zee DS, Frohman E, Baloh RW. et al. Assessment: vestibular testing techniques in adults and children: report of the therapeutics and technology assessment subcommittee of the american academy of neurology. *Neurology*. (2000) 55:1431–41. doi: 10.1212/WNL.55.10.1431

25. Hamilton SS, Zhou G, Brodsky JR. Video head impulse testing (vHIT) in the pediatric population. *Int J Pediatr Otorhinolaryngol*. (2015) 79:1283–7. doi: 10.1016/j.ijporl.2015.05.033

26. Basser Lsbenign Paroxysmal Vertigo of Childhood. A variety of vestibular neuronitis. *Brain*. (1964) 87:141–52. doi: 10.1093/brain/87.1.141

27. Koenigsberger MR, Chutorian AM, Gold AP, Schvey MS. Benign paroxysmal vertigo of childhood. *Neurology*. (1968) 18:301–2.

28. Dunn DW, Snyder CH. Benign paroxysmal vertigo of childhood. *Am J Dis Child*. (1976) 130:1099–100. doi: 10.1001/archpedi.1976.02120110061008

29. Koehler B. Benign paroxysmal vertigo of childhood: a migraine equivalent. *Eur J Pediatr*. (1980) 134:149–51. doi: 10.1007/BF01846035

30. Mierzwiński J, Polak M, Dalke K, Burduk P, Kazmierczak H, Modrzyński M. Benign paroxysmal vertigo of childhood. *Otolaryngol Pol*. (2007) 61:307–10. doi: 10.1016/S0030-6657(07)70431-6

31. Kostić M, Trotić R, Jankes KR, Leventić M. Benign paroxysmal vertigo in childhood. *Coll Antropol*. (2012) 36:1033–6.

32. Gedik-Soyuyuce O, Gence-Gumus Z, Ozdilek A, Ada M, Korkut N. Vestibular disorders in children: A retrospective analysis of vestibular function test findings. *Int J Pediatr Otorhinolaryngol*. (2021) 146:110751. doi: 10.1016/j.ijporl.2021.110751

33. Marcelli V, Russo A, Cristiano E, Tessitore A. Benign paroxysmal vertigo of childhood: A 10-year observational follow-up. *Cephalalgia*. (2015) 35:538–44. doi: 10.1177/0333102414547781

34. Langhagen T, Lehrer N, Borggraefe I, Heinen F, Jahn K. Vestibular migraine in children and adolescents: clinical findings and laboratory tests. *Front Neurol*. (2014) 5:292. doi: 10.3389/fneur.2014.00292

35. Marcelli V, Furia T, Marciano E. Vestibular pathways involvement in children with migraine: a neuro-otological study. *Headache*. (2010) 50:71–6. doi: 10.1111/j.1526-4610.2009.01454.x

36. Schmid-Priscoveanu A, Böhmer A, Obzina H, Straumann D. Caloric and search-coil head-impulse testing in patients after vestibular neuritis. *J Assoc Res Otolaryngol*. (2001) 2:72–8. doi: 10.1007/s101620010060

37. Aw ST, Fetter M, Cremer PD, Karlberg M, Halmagyi GM. Individual semicircular canal function in superior and inferior vestibular neuritis. *Neurology*. (2001) 57:768–74. doi: 10.1212/WNL.57.5.768

38. Salmito MC, Ganança FF. Video head impulse test in vestibular migraine. *Braz J Otorhinolaryngol*. (2021) 87:671–7. doi: 10.1016/j.bjorl.2019.12.009

39. Chen JY, Yang J, Zhang Q, Wang W, Ma XB, Mei L. et al. An analysis of the results of video head impulse test in benign paroxysmal vertigo of childhood. *Lin Chung Er Bi Yan Hou Tou Jing Wai Ke Za Zhi*. (2019) 33:232–6.

40. Alhabib SF, Saliba I. Video head impulse test: a review of the literature. *Eur Arch Otorhinolaryngol*. (2017) 274:1215–22. doi: 10.1007/s00405-016-4157-4

41. McCaslin DL, Rivas A, Jacobson GP, Bennett ML. The dissociation of video head impulse test (vHIT) and bithermal caloric test results provide topological localization of vestibular system impairment in patients with "definite" *Ménière's disease*. *Am J Audiol*. (2015) 24:1–10. doi: 10.1044/2014_AJA-14-0040

42. Bell SL, Barker F, Heselton H, MacKenzie E, Dewhurst D, Sanderson A. A study of the relationship between the video head impulse test and air calorics. *Eur Arch Otorhinolaryngol*. (2015) 272:1287–94. doi: 10.1007/s00405-014-3397-4

43. Zellhuber S, Mahringer A, Rambold HA. Relation of video-head-impulse test and caloric irrigation: a study on the recovery in unilateral vestibular neuritis. *Eur Arch Otorhinolaryngol*. (2014) 271:2375–83. doi: 10.1007/s00405-013-2723-6

44. McCaslin DL, Jacobson GP, Bennett ML, Gruenwald JM, Green AP. Predictive properties of the video head impulse test: measures of caloric symmetry and self-report dizziness handicap. *Ear Hear*. (2014) 35:e185–91. doi: 10.1097/AUD.0000000000000047

45. Mahringer A, Rambold HA. Caloric test and video-head-impulse: a study of vertigo/dizziness patients in a community hospital. *Eur Arch Otorhinolaryngol*. (2014) 271:463–72. doi: 10.1007/s00405-013-2376-5

frontiers | Frontiers in Neurology

TYPE Review
PUBLISHED 02 December 2022
DOI 10.3389/fneur.2022.1056724

Check for updates

OPEN ACCESS

EDITED BY
Lisheng Yu,
Peking University People's Hospital, China

REVIEWED BY
Qing Sun,
PLA General Hospital, China
Maoli Duan,
Karolinska Institutet (KI), Sweden

*CORRESPONDENCE
Haibo Wang
whboto11@163.com
Daogong Zhang
zhangdaogong1978@163.com

†These authors share first authorship

SPECIALTY SECTION
This article was submitted to Neuro-Otology, a section of the journal Frontiers in Neurology

RECEIVED 29 September 2022
ACCEPTED 18 November 2022
PUBLISHED 02 December 2022

CITATION
Lyu Y, Guo J, Li X, Jian H, Li Y, Wang J, Fan Z, Wang H and Zhang D (2022) Long-term efficacy of dexamethasone treatment *via* tympanic antrum catheterization for intractable Meniere's disease. *Front. Neurol.* 13:1056724. doi: 10.3389/fneur.2022.1056724

COPYRIGHT
© 2022 Lyu, Guo, Li, Jian, Li, Wang, Fan, Wang and Zhang. This is an open-access article distributed under the terms of the Creative Commons Attribution License (CC BY). The use, distribution or reproduction in other forums is permitted, provided the original author(s) and the copyright owner(s) are credited and that the original publication in this journal is cited, in accordance with accepted academic practice. No use, distribution or reproduction is permitted which does not comply with these terms.

Long-term efficacy of dexamethasone treatment *via* tympanic antrum catheterization for intractable Meniere's disease

Yafeng Lyu[1,2,3†], Jia Guo[1,2,3†], Xiaofei Li[1,2,3], Huirong Jian[1,2,3], Yawei Li[1,2,3], Jing Wang[1,2,3], Zhaomin Fan[1,2,3], Haibo Wang[1,2,3*] and Daogong Zhang[1,2,3*]

[1]Department of Otolaryngology-Head and Neck Surgery, Shandong Provincial ENT Hospital, Shandong University, Jinan, China, [2]Shandong Provincial Vertigo and Dizziness Medical Center, Jinan, China, [3]Laboratory of Vertigo Disease, Shandong Institute of Otorhinolaryngology, Jinan, China

Objective: To explore the long-term efficacy and safety of dexamethasone treatment *via* tympanic antrum catheterization (TAC) in intractable Meniere's disease (MD).

Methods: In this retrospective analysis, 60 unilateral intractable MD patients treated with TAC in our hospital from January 2020 to August 2020 were followed for 2 years. Fifty patients who underwent endolymphatic sac decompression (ESD) and 50 patients who accepted intratympanic steroids (ITS) were established as the control groups. Vertigo control, hearing level, tinnitus, aural fullness and functional level were assessed during the study.

Results: The effective vertigo control rate of intractable MD patients with TAC treatment was 76.7% (46/60) after 2 years follow-up, with a complete control rate of 58.3% (35/60) and a substantial control rate of 18.3% (11/60). The vertigo control rate of TAC was comparable to that of ESD ($\chi^2 = 0.313$, $p > 0.05$), and significantly higher than that of ITS ($\chi^2 = 4.380$, $p < 0.05$). The hearing loss rate of these patients was 10.8% (4/37), which was not significantly different from the control groups ($\chi^2 = 2.452$, $p > 0.05$). The tinnitus improvement rate of patients with TAC was 56.7% (34/60), which was significantly higher than that of patients with ESD (χ^2 =11.962, $p < 0.001$) and ITS (χ^2 =15.278, $p < 0.001$). The aural fullness improvement rate in the TAC group was 56.7% (34/60), which was significantly higher than that in the ESD ($\chi^2 = 11.962$, $p < 0.001$) and ITS groups ($\chi^2 = 5.635$, $p < 0.05$). The functional level improvement rate in the TAC group was 71.7% (43/60), which was much higher than that in the ITS group ($\chi^2 = 17.256$, $p < 0.001$), but there was no significant difference between TAC and ESD ($\chi^2 = 0.410$, $p > 0.05$). No patients had complications or adverse reactions following TAC treatment.

Conclusion: Dexamethasone treatment *via* TAC can effectively control vertigo attacks and improve related symptoms of intractable MD patients, providing valuable new insights into the treatment of MD.

KEYWORDS

vestibular plugging, otolith dysfunction, Meniere's disease, drop attack, semicircular canal plugging

Introduction

Meniere's disease (MD) is an inner ear disease with idiopathic endolymphatic hydrops, characterized by intermittent vertigo attacks, sensorineural hearing loss, tinnitus, and/or aural fullness. Its prevalence varies from 0.513 to 3.5%, and MD is most commonly seen in adults aged 40–60 years, with a female predominance (1). Most patients have unilateral onset of MD, but ∼25–45% of patients progress to bilateral MD as the disease progresses (2). Devastating vertigo attacks, progressive hearing loss, and the resulting psychosomatic problems such as anxiety and depression make MD a disabling disease that seriously affects patients' daily living, social life, and work.

Since the definitive etiology and pathogenesis are still unknown, there is no cure for MD. At present, treatment is mainly based on symptomatic measures to reduce vertigo attacks preserve hearing and improve vestibular function (3). Steroid hormones, diuretics, betahistine, and other medical treatments for MD can relieve ∼80% of patients with vertigo (1). Surgical procedures were considered when medical treatment failed. Endolymphatic sac decompression (ESD) is the most commonly used non-destructive procedure for intractable MD. A recent study reported the vertigo control rate among different endolymphatic sac surgery is 70–88.6%, only in favor of MD patients at early or middle stages (4). Despite the high rate of vertigo control, post-operative complications such as cerebrospinal fluid leakage, total deafness and intracranial infection may occur following vestibular neurectomy (5). As a completely destructive surgery, labyrinthectomy is only recommended for patients with severe to profound sensorineural hearing loss. As a last resort, labyrinthectomy is only recommended for patients with total deafness due to complete destruction of inner ear function (6). Additionally, the vertigo control rate of triple semicircular canal plugging reported in our previous study (7) was excellent at 98.7%, although 26.3% of the patients had hearing loss.

Intratympanic drug delivery is an alternative approach to MD (8). Intratympanic gentamicin (ITG), is known as chemical labyrinthectomy, with a vertigo control rate up 96.8% but accompanied by 0–75% hearing impairment (9, 10). Growing evidence has indicated intratympanic steroids (ITS) provide an effective alternative to ITG in symptom control, especially multi-session ITS (11, 12). However, repeated injections *via* tympanic puncture can cause burning and painful sensation (8). Moreover, the rapid loss of fluids through the Eustachian tube results in low drug absorption, unstable effects, and individual differences (13, 14). Therefore, we conceived a new type of topical medication, tympanic antrum catheterization (TAC), to treat intractable MD. Repeated intra-aural drug infusion through post-auricular placement effectively controlled vertigo attacks and showed a positive effect in preventing hearing loss and improving related symptoms.

The aim of this study was to evaluate the long-term efficacy of TAC and to compare it with ESD and ITS to determine its therapeutic value for intractable MD.

Materials and methods

Patients

This study retrospectively analyzed 60 patients (27 men, 34 women; aged 51.8 ± 12.4 years, with a disease duration of 50.2 ± 76.1 months) who accepted TAC treatment in the vertigo department of our hospital from January 2020 to August 2020. Fifty patients who underwent ESD (22 men, 28 women; aged 55.2 ± 11.0 years, with a disease duration of 57.8 ± 47.1 months) and 50 patients who underwent ITS (23 men, 27 women; aged 52.7 ± 13.2 years, with a disease duration of 43.1 ± 59.0 months) in the same period were allocated to the control groups. These patients were clinically diagnosed with definite MD based on the criterion of the Barany society (15). All patients continued to experience recurrent vertigo (at least 2 attacks per month, each attack lasting more than 20 min), even after at least 6 months of medical treatment (betahistine 12 mg tid and hydrochlorothiazide 25 mg bid).

Referring to previous study (16), other vestibular disorders or vertigo diseases were excluded by a series of examinations including auditory examination, vestibular function examinations and magnetic resonance imaging. All patients were followed up for 2 years. The evaluation of therapeutic effects consisted of vertigo control, hearing level,

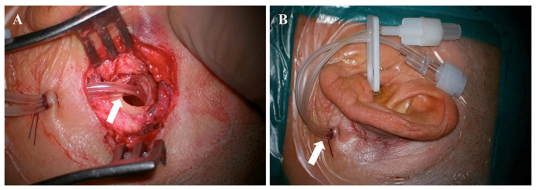

FIGURE 1
Intraoperative **(A)** and postoperative **(B)** pictures of tympanic antrum catheterization (arrows).

as well as the improvement of tinnitus, aural fullness, and functional level.

This study was approved by the Ethics Committee of Shandong Provincial ENT Hospital, and informed consents were obtained from all patients.

Dexamethasone treatment *via* TAC

TAC was performed using a post-auricular approach under local anesthesia. An incision ∼3 cm in length was made on the upper part of the retroauricular sulcus. After exposing the mastoid cortex, an electric drill was used to make a bone window of about 1.5–2 cm in diameter directly to the tympanic antrum. Two catheters (part of the infusion set, 3 mm in diameter) were placed in the tympanic antrum, tunneled subcutaneously and secured with 3–0 silk suture (Figure 1A). One catheter was for drug delivery and the other for regulation of the middle ear pressure during drug delivery. The incision was closed, and the external openings of the catheters were sealed and fixed in the preauricular region (Figure 1B). Dexamethasone sodium phosphate (Xinhua Pharmaceutical Co., LTD., Zibo, Shandong, China) 5 mg (1 ml) was administered through the catheter once a day for a total of 7 days. Patients were instructed to stay still in bed without talking or swallowing for at least half an hour after every injection.

Surgical procedure of ESD

ESD was performed using a post-auricular approach under general anesthesia. An incision was made ∼1 cm behind the retroauricular sulcus and was ∼7 cm in length. After a standard mastoidectomy, anatomic landmarks, including the sigmoid sinus, horizontal semicircular canal, and middle cranial fossa meninges, were recognized. The endolymphatic sac was located between the sigmoid sinus and posterior semicircular canal and was usually below the plane of the horizontal semicircular canal. A grinding drill was used to remove the bone and fully expose the endolymphatic sac. Finally, the incision was closed, and the surgery was completed.

Intratympanic steroid

Intratympanic injections were administered under surface anesthesia. About 0.4–0.6 ml dexamethasone sodium phosphate (Xinhua Pharmaceutical Co., LTD., Zibo, Shandong, China) diluted with normal saline (4:1 in volume) was injected into the tympanic cavity through the anterior inferior part of the tympanic membrane. The patients were instructed to stay still in bed without talking or swallowing for at least half an hour after each injection. Three injections during a period of 1 week (the 1st, 4th, and 7th day) were administered to each patient.

Evaluation of vertigo

According to the 1995 criteria set by American Academy of Otolaryngology-Head and Neck Surgery (AAO-HNS) (17), a definitive spell of vertigo lasting more than 20 min was regarded as a Meniere's vertigo attack. The numerical value of the formula (the average number of vertigo attacks per month from 18 to 24 months after therapy× 100 /the average number of vertigo attacks per month for the 6 months before therapy) divided vertigo control into six scales: A (0), B (1–40), C (41–80), D (81–120), E (>120), and F (secondary treatment). Scale A (complete control) and B (substantial control) were regarded as effective vertigo control.

In addition, the dizziness handicap inventory (DHI, 0–100 scale) was used to evaluate the physical, emotional and functional effects of this disorder (18). The vertigo symptom scale (VSS; 0–60) was used to quantify the severity of vertigo (19).

Evaluation of hearing

The four-tone average of thresholds at 0.5, 1, 2, and 3 kHz was adopted to determinate the hearing change as recommended by AAO-HNS (17). The worst hearing level of the affected ear during the previous 6 months was compared with that during the following 18–24 months. A hearing level change ≥10 dB was considered "better" or "worse" and change <10 dB was considered as "no change."

Evaluation of tinnitus

Similar to DHI, the tinnitus handicap inventory (THI, 0–100 scale) (20) was used for self-assessment of tinnitus disorder. The

TABLE 1 Demographics and baseline characteristics.

	TAC ($n = 60$)	ESD ($n = 50$)	ITS ($n = 50$)	Statistic value	*P*-value
Age, Mean ± SD	51.8 ± 12.4	55.2 ± 11.0	52.7 ± 13.2	$F = 1.089$	>0.05
Gender				$\chi^2 = 0.040$	>0.05
Male	27 (45%)	22 (44%)	23 (46%)		
Female	33 (55%)	28 (56%)	27 (54%)		
Duration (months), Mean ± SD	50.2 ± 76.1	57.8 ± 47.1	43.1 ± 59.0	$F = 0.687$	>0.05
Pure-tone average (dB), Mean ± SD	47.2 ± 15.0	48.6 ± 14.1	47.2 ± 21.6	$F = 0.108$	>0.05
Speech discrimination (%), Mean ± SD	62.9 ± 25.2	65.8 ± 20.1	63.3 ± 28.2	$F = 0.200$	>0.05
Abnormal rate of vestibular function tests					
Caloric test	49.1% (27/55)	61.4% (27/44)	39.0% (16/41)	$\chi^2 = 4.267$	>0.05
cVEMP	50.0% (29/58)	48.9% (23/47)	60.9% (28/46)	$\chi^2 = 1.665$	>0.05
oVAMP	60.3% (35/58)	76.6% (36/47)	69.2% (31/46)	$\chi^2 = 3.129$	>0.05
vHIT	35.7% (20/56)	28.3% (13/46)	25.0% (11/44)	$\chi^2 = 1.456$	>0.05

TAC, tympanic antrum catheterization; ESD, endolymphatic sac decompression; ITS, intratympanic steroid; cVEMP, cervical vestibular evoked myogenic potential; oVAMP, ocular vestibular evoked myogenic potential; vHIT, video-head impulse test.

change in THI score ≥20 was considered as "better" or "worse" and change <20 was considered as "no change."

Evaluation of aural fullness

Visual analog scale (VAS, 0–10 scale) was used to quantify the symptoms of aural fullness (21). The change in VAS score ≥2 was defined as "better" or "worse," and a change of <2 was defined as "no change."

Evaluation of functional impairment and disability

A six-point functional level scale (FLS) was used to assess the effects of episodic vertigo on daily activities as per the 1995 AAO-HNS criteria (17). The change of FLS score ≥1 was designated as "better" or "worse" and change <1 was designated as "no change."

Statistics

All statistical analyses were completed using SPSS 27.0 software (SPSS Inc., Chicago, IL, USA). One-way ANOVA and two independent-sample *t*-test were used to compare the mean values among the groups. Comparisons of proportions among groups were performed applying Chi-Squared test. *P*-value (set at correction) < 0.05 was considered statistically significant.

Results

Clinical information

As shown in Table 1, there were no significant differences in demographic and baseline characteristics among the TAC, ESD, and ITS groups ($p > 0.05$).

Vertigo control

Pre-operatively, there were no significant difference among the three groups regarding the frequency of vertigo attacks ($F = 1.193$, $p > 0.05$), DHI score ($F = 0.880$, $p > 0.05$), and VSS score ($F = 1.488$, $p > 0.05$). A decrease in the number of vertigo attacks was noticed in all groups 2 years after the treatment (Figure 2A). The number of vertigo attacks during 6 months in the TAC group decreased from 19.4 ± 15.1 to 2.8 ± 9.4 ($t = 7.074$, $p < 0.001$). However, no significant difference in the number of vertigo attacks in the final 6 months among the three groups was discovered ($F = 0.361$, $p > 0.05$). Notably, the effective vertigo control rate in patients with TAC was 76.7% (46/60) at the 2-year follow-up, with a complete control rate of 58.3% (35/60) and a substantial control rate of 18.3% (11/60). In the ESD and ITS groups, vertigo attacks were effectively controlled in 72.0 and 58.0% of the patients, respectively. The vertigo control rate in the TAC group was significantly higher than that in the ITS group ($\chi^2 = 4.380$, $p < 0.05$; Figure 2B), but there was no significant difference between TAC and ESD ($\chi^2 = 0.313$, $p > 0.05$; Figure 2B). Additionally, all treatments reduced the mean DHI and VSS scores during follow-up (Figure 3). For patients with TAC, mean scores decreased significantly over time for DHI (decreased from 45.6 ± 17.7 to 22.1 ± 18.1; $t = 7.215$, $p < 0.001$)

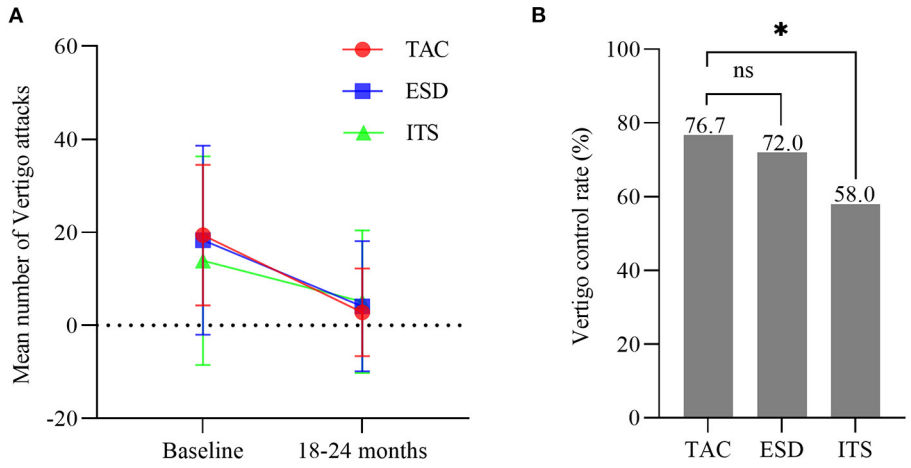

FIGURE 2
(A) Mean number of attacks of vertigo 6 months before treatment and in the final 6 months (bars are SDs). **(B)** The control rate of vertigo in each group (*$p < 0.05$). TAC, tympanic antrum catheterization; ESD, endolymphatic sac decompression; ITS, intratympanic steroid.

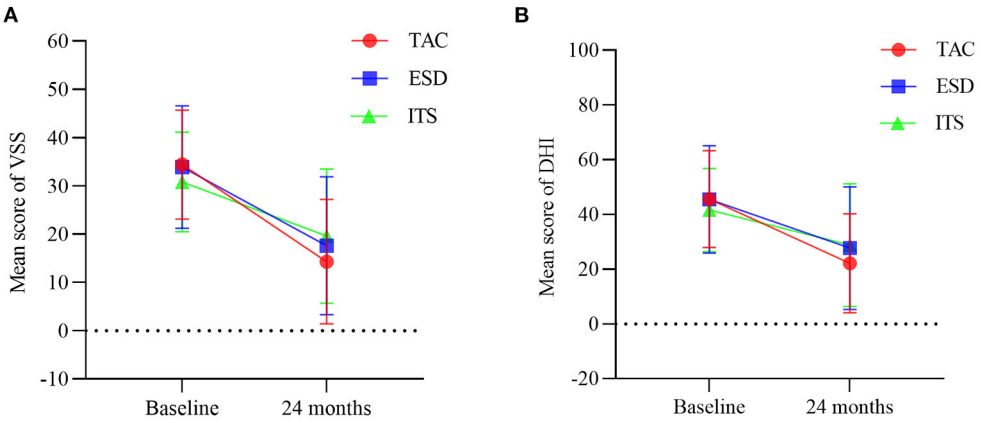

FIGURE 3
Mean scores for **(A)** vertigo symptom scale and **(B)** dizziness handicap inventory at baseline and 24 months (bars are SDs). TAC, tympanic antrum catheterization; ESD, endolymphatic sac decompression; ITS, intratympanic steroid.

and VSS (decreased from 34.4 ± 11.3 ± 17.7 to 14.3 ± 12.9; $t = 9.106$, $p < 0.001$). However, we did not observe significant differences among the three groups for DHI score ($F = 1.674$, $p > 0.05$) and VSS score ($F = 2.167$, $p > 0.05$) at 24 months.

Hearing change

Over the 2 years follow-up, the pure-tone average of patients with TAC improved from 47.2 ± 15.0 to 37.1 ± 18.9 ($t = 2.960$, $p < 0.01$; Figure 4A), but without a significant difference in PTA at 24 months among the three groups ($F = 0.255$, $p > 0.05$). The hearing loss rate in the TAC group was 10.8% (4/37), while hearing loss occurred in 20.7% (6/29) and 25.0% (8/32) of the patients in the ESD and ITS groups, respectively. However, the differences were not statistically significant ($\chi^2 = 2.452$, $p > 0.05$; Figure 4B).

Tinnitus improvement

No significant differences were noted among the three groups for the THI score at baseline ($F = 0.165$, $p > 0.05$). With time, the mean score for THI in patients with TAC decreased from 48.2 ± 19.6 to 34.1 ± 19.8 ($t = 3.927$, $p < 0.001$; Figure 5A), with a significantly lower THI score at 24 months for the TAC group than for the ESD and ITS groups ($t = 3.214$, $p < 0.01$; $t = 2.632$, $p < 0.05$). The tinnitus improvement rate in patients with

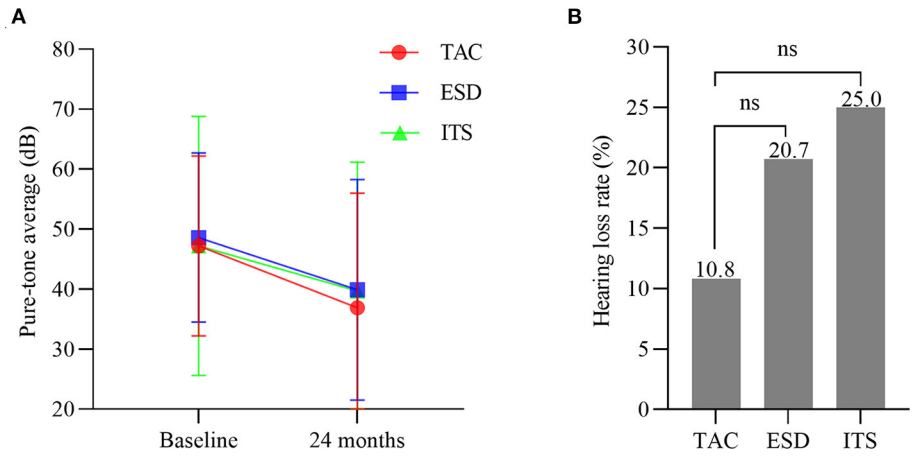

FIGURE 4
(A) Hearing level at baseline and 24 months (bars are SDs). **(B)** The hearing loss rate in each group. TAC, tympanic antrum catheterization; ESD, endolymphatic sac decompression; ITS, intratympanic steroid.

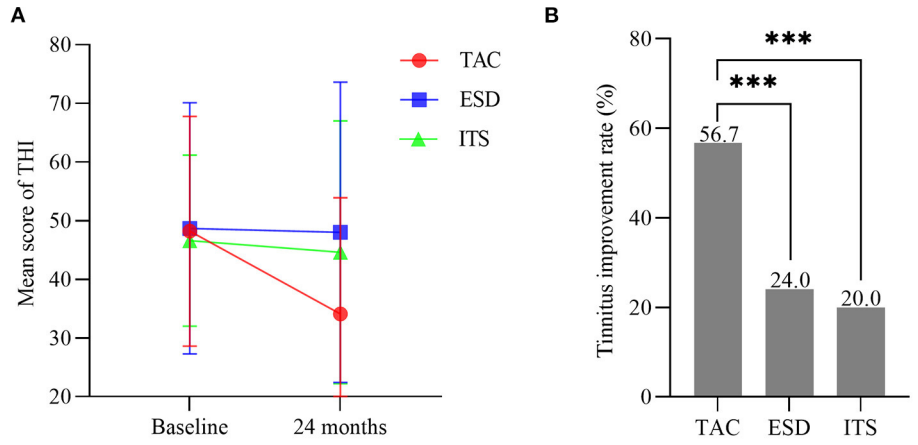

FIGURE 5
(A) Mean scores for tinnitus handicap inventory (bars are SDs). **(B)** The tinnitus improvement rate in each group (***$p < 0.001$). TAC, tympanic antrum catheterization; ESD, endolymphatic sac decompression; ITS, intratympanic steroid.

TAC was 56.7% (34/60). In the ESD and ITS groups, tinnitus improved in 24.0% (12/50) and 20.0% (10/50) of the patients, respectively. The tinnitus improvement rate in the TAC group was significantly higher than that in the ESD and ITS groups ($\chi^2 = 11.962$, $p < 0.001$; $\chi^2 = 15.278$, $p < 0.001$; Figure 5B).

Aural fullness improvement

One-way ANOVA showed no significant difference among groups for the AFVAS score at baseline ($F = 1.299$, $p > 0.05$; Figure 6A). With 2-year follow-up, the mean score for AFVAS in patients with TAC decreased from 5.2 ± 3.2 to 2.0 ± 2.3 ($t = 6.446$, $p < 0.001$), with a significantly lower AFVAS score at 24 months for the TAC group than for the ESD and ITS groups ($t = 7.154$, $p < 0.001$; $t = 4.181$, $p < 0.001$). The aural fullness improvement rate in patients with TAC was 56.7% (34/60). In the ESD and ITS groups, improvement in aural fullness occurred in 24.0% (12/50) and 34.0% (17/50) of the patients, respectively. The aural fullness improvement rate in the TAC group was significantly higher than that in the ESD and ITS groups ($\chi^2 = 11.962$, $p < 0.001$; $\chi^2 = 5.635$, $p < 0.05$; Figure 6B).

Functional level improvement

Baseline FLS score did not differ among the three groups ($F = 0.384$, $p > 0.05$). The mean score for FLS decreased over

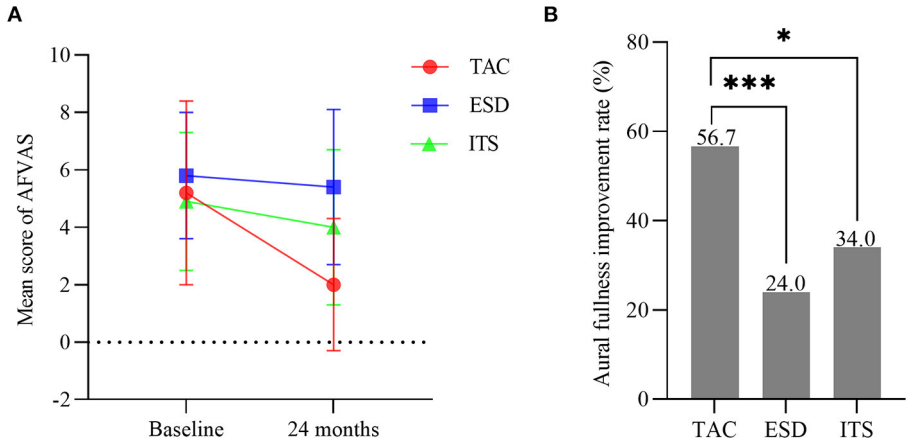

FIGURE 6
(A) Mean scores for aural fullness visual analog scale (bars are SDs). **(B)** The aural fullness improvement rate in each group (*$p < 0.05$, ***$p < 0.001$). TAC, tympanic antrum catheterization; ESD, endolymphatic sac decompression; ITS, intratympanic steroid.

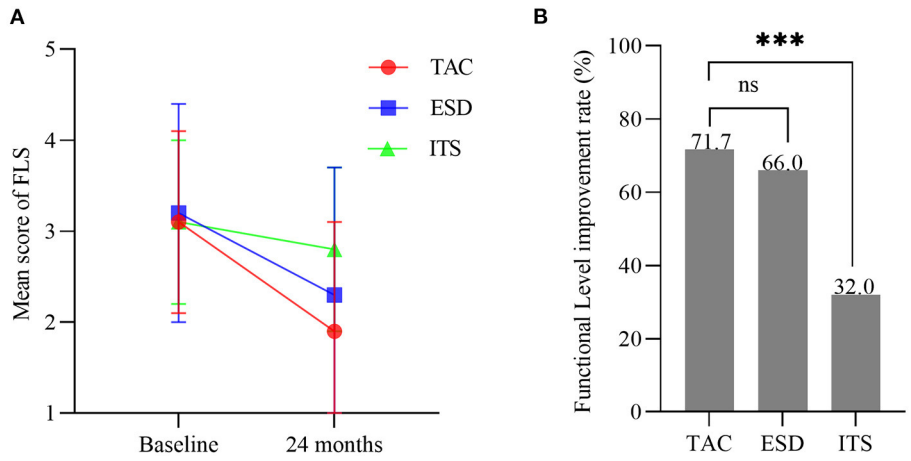

FIGURE 7
(A) Mean scores for functional level scale (bars are SDs). **(B)** The functional level improvement rate in each group (***$p < 0.001$). TAC, tympanic antrum catheterization; ESD, endolymphatic sac decompression; ITS, intratympanic steroid.

the follow-up period in all groups, with significant differences among the groups ($F = 9.912$, $p < 0.001$; Figure 7A). FLS score in patients with TAC decreased from 3.1 ± 1.0 to 1.9 ± 1.2 ($t = 6.419$, $p < 0.001$), which was significantly lower than that in the ITS group ($t = 4.912$, $p < 0.001$), but not statistically different compared to the ESD group ($t = 1.644$, $p > 0.05$). Moreover, the functional level improved in 71.7% (43/60) of patients in the TAC group and 66.0% (33/50) and 32.0% (16/50) of patients in the ESD and ITS groups, respectively. The functional level improvement rate of TAC was much higher than that of ITS ($\chi^2 = 17.256$, $p < 0.001$; Figure 7B), but no significant difference was found between TAC and ESD ($\chi^2 = 0.410$, $p > 0.05$).

Adverse reactions and complications

There was no facial nerve injury, cerebrospinal fluid leakage, encephalic hematoma or infection in patients following TAC or ESD treatment. One case of tympanic membrane perforation occurred in ITS group, with an incidence of 2%.

Discussion

Although there is still no cure for MD, over four-fifths of patients are alleviated from this disorder through lifestyle modification or medications. Surgical interventions such as

ESD, semicircular canal plugging and labyrinthectomy are taken into account for patients with refractory MD who fail to control vertigo conservatively. However, these surgeries are performed under general anesthesia, with high physical condition requirements and poor patient acceptance, and are accompanied by a variety of post-operative complications and the risk of hearing loss.

In addition, there are various topical medication methods, such as tympanic injection, retroauricular injection, and sustained-release pumps. Retroauricular injection has widely used in the clinical management of sudden deafness (22). The dose of administration *via* intratympanic injection is limited due to the volume of the tympanic chamber. Besides, repeated tympanic membrane punctures increase patients' pain and fear, as well as the risk of tympanic membrane perforation, otitis media, and hearing loss (23). Animal studies have demonstrated that the osmotic pump provides a continuous long-term drug delivery to the cochlea (24), but it has not yet been applied on a large scale because of the lack of clinical data support and the high cost.

Therefore, drug administration *via* the tympanic antrum catheter was conceived to make up for aforementioned shortcomings and to allow for topical administration of multiple drugs. First, TAC has the advantage of topical medication, which avoids the blood-labyrinth barrier to maintain a higher drug concentration in the inner ear and avoids the side effects of systemic application. Second, TAC was performed under local anesthesia with less risk. The average operation time of TAC was significantly shorter than that of ESD (TAC, 34.7 ± 6.7 min; ESD, 75.3 ± 19.9 min; $t = 13.808$, $p < 0.001$). Third, TAC had essentially no damage to hearing level, except from a 2.4 ± 10.7 dB transient threshold shift of the affected ear, which was significantly lower than the 10.3 ± 11.2 dB of the ESD group ($t = 3.799$, $p < 0.001$). Notably, the cost of surgery in patients with TAC was significantly lower than that of the ESD group (TAC, 2,161.3 ± 201.4 yuan; ESD, 5,355.2 ± 302.7 yuan; $t = 63.627$, $p < 0.001$), which was more economical and acceptable for patients. Compared with ITS, single placement of TAC greatly reduced the painful experience of repeated punctures. Additionally, TAC is more widely indicated, regardless of age, stage, and unilateral/bilateral MD, for patients in whom conservative treatment is ineffective or who cannot undergo general anesthetic surgery. In particular, it can be re-catheterized for recurrence. The results of this study indicate that 76.7% of 60 intractable MD patients with TAC had effective vertigo control at the 2 years follow-up. Comparable vertigo control rate was observed in the ESD group, which is in line with our previous results (25). The rate of vertigo control with ITS was 58% in our study, which is within the range reported in previous studies (26). Moreover, TAC has significant advantages in improving tinnitus, aural fullness, and patients' functional levels, suggesting that TAC is an effective treatment of intractable MD. The mechanisms of action that we speculate on are as follows.

First, studies have shown that immunity and allergy are closely related to the pathogenesis of MD. There are higher rates of allergy history and immunologic components in patients with MD (27). Published studies have demonstrated the benefits of immunotherapy or dietary restrictions for the improvement of MD symptoms (28). Glucocorticoids are widely used in the clinical treatment of immune-related diseases owing to their anti-inflammatory and immuno-suppressive effects. Froehlich et al. (29) found widespread presence of glucocorticoid receptors in the inner ear, particularly in hair cells, spiral ligaments, and spiral ganglia. Previous studies have shown that local glucocorticoid administration is effective in the treatment of immune-mediated inner ear diseases such as sudden deafness and MD (30, 31). Glucocorticoids specifically bind to receptors to modulate the expression of inflammatory factors, thereby exerting anti-inflammatory and immunosuppressive effects (32). Glucocorticoids maintain endolymphatic fluid homeostasis by regulating aquaporin and Na^+/K^+-ATPase (33), thus reducing endolymphatic hydrops and vertigo attacks. The multiple effects of glucocorticoids, such as inhibition of hair cells senescence and apoptosis, neuroprotection, and antioxidant activity (34), might relieve the symptoms of tinnitus and aural fullness and protect against hearing loss.

There is evidence that MD is associated with middle ear pressure, which influences endolymphatic hydrops (35). Albu et al. (36) reported that, tenotomy of the middle ear muscles tendons blocked the active compression of stapedial footplate on oval window, thereby reducing inner ear hydrops associated with MD. Meniett device, a non-destructive, effective and portable therapy for intractable MD, generates low-pressure alternating pulses and activates the Salt–Rask-Anderson valve in the inner, thereby facilitating the resorbation of excess endolymph (37). Recently, Shojaku et al. (38) reported transtympanic membrane massage device, a new non-invasive treatment for MD, transmitted pressure change to the inner ear *via* the middle ear cavity. Therefore, we suggest that changes in pressure in the middle ear or changes in ossicular chain tension can affect inner ear pressure through the vestibular window or round window. The endolymphatic hydrops could be decompressed by reduction of ossicular chain tension, or could be relieved by the massaging effect of low-pressure pulse, thereby raising the threshold for vertigo attack and attenuating the damage to cochlear hair cells. Similarly, TAC may play a role in the low-pressure pulse effect through tube insertion and repeated drug infusion.

Moreover, Thomsen et al. (39) presented a prospective double-blind study of endolymphatic sac mastoid shunt and mastoidectomy in treatment of MD and demonstrated minor differences. The results of the study call into question the effectiveness of endolymphatic sac surgery, but from another point of view, it also confirms the effectiveness of mastoidectomy in the treatment of MD. Sajjadi and Paparella (40) indicated that mastoidectomy can indirectly decompress the endolymphatic

sac through Trautmann's triangle. We speculate that the vibration of the inner ear triggered by the electric drill during mastoid surgery might also add to the treating effect of mastoidectomy by some means. Therefore, TAC may have a positive effect on MD symptom improvement *via* simple mastoidectomy, although the underlying mechanisms still need to be further explored.

As a preliminary study, a major limitation was the retrospective design of the study and the non-random nature of patient recruitment. And due to certain personal reasons and the COVID-19 epidemic, a limited number of patients came back to the hospital for retests of hearing and vestibular function. However, we obtained enough follow-up data in the form of interviews and questionnaires *via* telephone and E-mail.

Conclusion

In conclusion, TAC has definite long-term effects in the treatment of patients with intractable MD. It had a valid effect on vertigo control and hearing preservation and showed significant advantages in improving tinnitus, aural fullness, and the overall functional level. Further studies are required to optimize the treatment in term of the type, dosage, and course of drug administration. We believe that TAC could be a promising novel modality for treating intractable MD.

Author contributions

DZ, HW, and ZF designed the study. DZ, ZF, and YLy performed surgeries. YLy, JG, XL, HJ, YLi, and JW collected clinical data. JG, YLy, and XL performed data analysis and interpretation. YLy, JG, and DZ completed the manuscript. All authors contributed to the study and approved it for submission.

Funding

This study was funded by the National Natural Science Foundation of China (No. 82171150), the Major Fundamental Research Program of the Natural Science Foundation of Shandong Province, China (No. ZR2021ZD40), Shandong Provincial Natural Science Foundation (No. ZR2020MH179), and Taishan Scholars Program of Shandong Province (No. ts20130913).

Acknowledgments

The authors appreciate the support of all participants in our study and the editing support from Editage (www.editage.jp).

Conflict of interest

The authors declare that the research was conducted in the absence of any commercial or financial relationships that could be construed as a potential conflict of interest.

Publisher's note

All claims expressed in this article are solely those of the authors and do not necessarily represent those of their affiliated organizations, or those of the publisher, the editors and the reviewers. Any product that may be evaluated in this article, or claim that may be made by its manufacturer, is not guaranteed or endorsed by the publisher.

References

1. Alexander TH, Harris JP. Current epidemiology of Meniere's syndrome. *Otolaryngol Clin North Am.* (2010) 43:965–70. doi: 10.1016/j.otc.2010.05.001

2. House JW, Doherty JK, Fisher LM, Derebery MJ, Berliner KI. Meniere's disease: prevalence of contralateral ear involvement. *Otol Neurotol.* (2006) 27:355–61. doi: 10.1097/00129492-200604000-00011

3. Liu Y, Yang J, Duan M. Current status on researches of Meniere's disease: a review. *Acta Otolaryngol.* (2020) 140:808–12. doi: 10.1080/00016489.2020.1776385

4. Zheng G, Liu Y, He J, Li S, Zhang Q, Duan M, et al. A comparison of local endolymphatic sac decompression, endolymphatic mastoid shunt, and wide endolymphatic sac decompression in the treatment of intractable Meniere's disease: a short-term follow-up investigation. *Front Neurol.* (2022) 13:810352. doi: 10.3389/fneur.2022.810352

5. Veleine Y, Brenet E, Labrousse M, Chays A, Bazin A, Kleiber JC, et al. Long-term efficacy of vestibular neurotomy in disabling Meniere's disease and Tumarkin drop attacks. *J Neurosurg.* (2022) 2022:1–7. doi: 10.3171/2021.10.JNS21145

6. Sargent EW, Liao E, Gonda RL Jr. Cochlear patency after transmastoid labyrinthectomy for Meniere's syndrome. *Otol Neurotol.* (2016) 37:937–9. doi: 10.1097/MAO.0000000000001105

7. Zhang D, Lv Y, Han Y, Li Y, Li X, Wang J, et al. Long-term outcomes of triple semicircular canal plugging for the treatment of intractable Meniere's disease: a single center experience of 361 cases. *J Vestib Res.* (2019) 29:315–22. doi: 10.3233/VES-190682

8. Li S, Pyykko I, Zhang Q, Yang J, Duan M. Consensus on intratympanic drug delivery for Meniere's disease. *Eur Arch Otorhinolaryngol.* (2022) 279:3795–9. doi: 10.1007/s00405-022-07374-y

9. Celis-Aguilar E, Castro-Borquez KM, Obeso-Pereda A, Escobar-Aispuro L, Burgos-Paez A, Alarid-Coronel JM, et al. On-demand and low dose intratympanic gentamicin for Meniere's disease: a customized approach. *Otol Neurotol.* (2020) 41:504–10. doi: 10.1097/MAO.0000000000002563

10. Blakley BW. Update on intratympanic gentamicin for Meniere's disease. *Laryngoscope.* (2000) 110:236–40. doi: 10.1097/00005537-200002010-00009

11. Hilton A, McClelland A, McCallum R, Kontorinis G. Duration of symptom control following intratympanic dexamethasone injections in Meniere's disease. *Eur Arch Otorhinolaryngol.* (2022) 279:5191–8. doi: 10.1007/s00405-022-07368-w

12. Alsarhan H, Kadhim S. Treatment of Meniere's disease by multi-session dexamethasone injections. *Int Tinnitus J.* (2022) 26:75–8. doi: 10.5935/0946-5448.20220011

13. Haynes DS, O'Malley M, Cohen S, Watford K, Labadie RF. Intratympanic dexamethasone for sudden sensorineural hearing loss after failure of systemic therapy. *Laryngoscope.* (2007) 117:3–15. doi: 10.1097/01.mlg.0000245058.11866.15

14. Yoshioka M, Naganawa S, Sone M, Nakata S, Teranishi M, Nakashima T. Individual differences in the permeability of the round window: evaluating the movement of intratympanic gadolinium into the inner ear. *Otol Neurotol.* (2009) 30:645–8. doi: 10.1097/MAO.0b013e31819bda66

15. Lopez-Escamez JA, Carey J, Chung WH, Goebel JA, Magnusson M, Mandala M, et al. Diagnostic criteria for Meniere's disease. *J Vestib Res.* (2015) 25:1–7. doi: 10.3233/VES-150549

16. Xie W, Shu T, Liu J, Peng H, Karpeta N, Marques P, et al. The relationship between clinical characteristics and magnetic resonance imaging results of Meniere disease: a prospective study. *Sci Rep.* (2021) 11:7212. doi: 10.1038/s41598-021-86589-1

17. American Academy of Otolaryngology-Head and Neck Foundation, Inc. Committee on Hearing and Equilibrium guidelines for the diagnosis and evaluation of therapy in Meniere's disease. *Otolaryngol Head Neck Surg.* (1995) 113:181–5. doi: 10.1016/S0194-5998(95)70102-8

18. Jacobson GP, Newman CW, Hunter L, Balzer GK. Balance function test correlates of the Dizziness Handicap Inventory. *J Am Acad Audiol.* (1991) 2:253–60. doi: 10.1037/t35080-000

19. Yardley L, Masson E, Verschuur C, Haacke N, Luxon L. Symptoms, anxiety and handicap in dizzy patients: development of the vertigo symptom scale. *J Psychosom Res.* (1992) 36:731–41. doi: 10.1016/0022-3999(92)90131-K

20. Newman CW, Jacobson GP, Spitzer JB. Development of the tinnitus handicap inventory. *Arch Otolaryngol Head Neck Surg.* (1996) 122:143–8. doi: 10.1001/archotol.1996.01890140029007

21. Odkvist LM, Arlinger S, Billermark E, Densert B, Lindholm S, Wallqvist J. Effects of middle ear pressure changes on clinical symptoms in patients with Meniere's disease–a clinical multicentre placebo-controlled study. *Acta Otolaryngol Suppl.* (2000) 543:99–101. doi: 10.1080/000164800454107

22. Zhong Z, Wang X, Xu K, Tao J. Clinical efficacy of retroauricular injection of methylprednisolone sodium succinate in the treatment of sudden deafness with type 2 diabetes. *Comput Math Methods Med.* (2022) 2022:3097436. doi: 10.1155/2022/3097436

23. Barrs DM, Keyser JS, Stallworth C, McElveen JT Jr. Intratympanic steroid injections for intractable Meniere's disease. *Laryngoscope.* (2001) 111:2100–4. doi: 10.1097/00005537-200112000-00003

24. Brown JN, Miller JM, Altschuler RA, Nuttall AL. Osmotic pump implant for chronic infusion of drugs into the inner ear. *Hear Res.* (1993) 70:167–72. doi: 10.1016/0378-5955(93)90155-T

25. Zhang D, Lv Y, Li X, Song Y, Kong L, Fan Z, et al. Efficacy of resection of lateral wall of endolymphatic sac for treatment of Meniere's disease. *Front Neurol.* (2022) 13:827462. doi: 10.3389/fneur.2022.827462

26. Lee SY, Kim YS, Jeong B, Carandang M, Koo JW, Oh SH, et al. Intratympanic steroid versus gentamicin for treatment of refractory Meniere's disease: a meta-analysis. *Am J Otolaryngol.* (2021) 42:103086. doi: 10.1016/j.amjoto.2021.103086

27. Derebery MJ. Allergic and immunologic features of Meniere's disease. *Otolaryngol Clin North Am.* (2011) 44:655–66. doi: 10.1016/j.otc.2011.03.004

28. Di Berardino F, Zanetti D. Delayed immunomodulatory effect of cow milk-free diet in Meniere's disease. *J Am Coll Nutr.* (2018) 37:149–53. doi: 10.1080/07315724.2017.1364181

29. Froehlich MH, Lambert PR. The physiologic role of corticosteroids in Meniere's disease: an update on glucocorticoid-mediated pathophysiology and corticosteroid inner ear distribution. *Otol Neurotol.* (2020) 41:271–6. doi: 10.1097/MAO.0000000000002467

30. Roebuck J, Chang CY. Efficacy of steroid injection on idiopathic sudden sensorineural hearing loss. *Otolaryngol Head Neck Surg.* (2006) 135:276–9. doi: 10.1016/j.otohns.2006.03.035

31. Sajjadi H. Medical management of Meniere's disease. *Otolaryngol Clin North Am.* (2002) 35:581–9. doi: 10.1016/S0030-6665(02)00021-X

32. Rauch SD. Intratympanic steroids for sensorineural hearing loss. *Otolaryngol Clin North Am.* (2004) 37:1061–74. doi: 10.1016/j.otc.2004.04.004

33. Fukushima M, Kitahara T, Fuse Y, Uno Y, Doi K, Kubo T. Changes in aquaporin expression in the inner ear of the rat after ip injection of steroids. *Acta Otolaryngol Suppl.* (2004) 553:13–8. doi: 10.1080/03655230410017599

34. Tabuchi K, Nakamagoe M, Nishimura B, Hayashi K, Nakayama M, Hara A. Protective effects of corticosteroids and neurosteroids on cochlear injury. *Med Chem.* (2011) 7:140–4. doi: 10.2174/157340611794859334

35. Park JJ, Chen YS, Westhofen M. Meniere's disease and middle ear pressure: vestibular function after transtympanic tube placement. *Acta Otolaryngol.* (2009) 129:1408–13. doi: 10.3109/00016480902791678

36. Albu S, Babighian G, Amadori M, Trabalzini F. Endolymphatic sac surgery vs. tenotomy of the stapedius and tensor tympani muscles in the management of patients with unilateral definite Meniere's disease. *Eur Arch Otorhinolaryngol.* (2015) 272:3645–50. doi: 10.1007/s00405-014-3428-1

37. Gates GA. Treatment of Meniere's disease with the low-pressure pulse generator (Meniett device). *Expert Rev Med Devices.* (2005) 2:533–7. doi: 10.1586/17434440.2.5.533

38. Shojaku H, Takakura H, Asai M, Fujisaka M, Ueda N, Do TA, et al. Long-term effect of transtympanic intermittent pressure therapy using a tympanic membrane massage device for intractable meniere's disease and delayed endolymphatic hydrops. *Acta Otolaryngol.* (2021) 141:977–83. doi: 10.1080/00016489.2021.1989485

39. Thomsen J, Bretlau P, Tos M, Johnsen NJ. Placebo effect in surgery for Meniere's disease. A double-blind, placebo-controlled study on endolymphatic sac shunt surgery. *Arch Otolaryngol.* (1981) 107:271–7. doi: 10.1001/archotol.1981.00790410009002

40. Sajjadi H, Paparella MM. Meniere's disease. *Lancet.* (2008) 372:406–14. doi: 10.1016/S0140-6736(08)61161-7

frontiers | Frontiers in Neuroscience

TYPE Original Research
PUBLISHED 13 December 2022
DOI 10.3389/fnins.2022.988733

Check for updates

OPEN ACCESS

EDITED BY
Sulin Zhang,
Huazhong University of Science and Technology, China

REVIEWED BY
Qing Zhang,
Shanghai Jiao Tong University School of Medicine, China
Lorenzo Salerni,
University of Siena, Italy
Dan Bing,
Huazhong University of Science and Technology, China

*CORRESPONDENCE
Wei Wang
wwei1106@hotmail.com
Taisheng Chen
fch_cts@sina.com

SPECIALTY SECTION
This article was submitted to Perception Science, a section of the journal Frontiers in Neuroscience

RECEIVED 07 July 2022
ACCEPTED 22 November 2022
PUBLISHED 13 December 2022

CITATION
Liu Y, Zhang X, Deng Q, Liu Q, Wen C, Wang W and Chen T (2022) The 3D characteristics of nystagmus in posterior semicircular canal benign paroxysmal positional vertigo. *Front. Neurosci.* 16:988733. doi: 10.3389/fnins.2022.988733

COPYRIGHT
© 2022 Liu, Zhang, Deng, Liu, Wen, Wang and Chen. This is an open-access article distributed under the terms of the Creative Commons Attribution License (CC BY). The use, distribution or reproduction in other forums is permitted, provided the original author(s) and the copyright owner(s) are credited and that the original publication in this journal is cited, in accordance with accepted academic practice. No use, distribution or reproduction is permitted which does not comply with these terms.

The 3D characteristics of nystagmus in posterior semicircular canal benign paroxysmal positional vertigo

Yao Liu[1,2,3,4,5], Xueqing Zhang[1,2,3,4,5], Qiaomei Deng[1,2,3,4,5], Qiang Liu[1,2,3,4,5], Chao Wen[1,2,3,4,5], Wei Wang[1,2,3,4,5]* and Taisheng Chen[1,2,3,4,5]*

[1]Department of Otorhinolaryngology Head and Neck Surgery, Tianjin First Central Hospital, Tianjin, China, [2]Institute of Otolaryngology of Tianjin, Tianjin, China, [3]Key Laboratory of Auditory Speech and Balance Medicine, Tianjin, China, [4]Key Medical Discipline of Tianjin (Otolaryngology), Tianjin, China, [5]Quality Control Centre of Otolaryngology, Tianjin, China

Objective: The aim of this study was to observe the 3-dimensional (3D; horizontal, vertical, and torsional) characteristics of nystagmus in patients with posterior semicircular canal canalithiasis (PSC-can)–related benign paroxysmal positional vertigo (BPPV) and investigate its correlation with Ewald's.

Methods: In all, 84 patients with PSC-can were enrolled. The latency, duration, direction, and slow-phase velocity induced by the Dix-Hallpike test in the head-hanging and sitting positions were recorded using 3D video nystagmography (3D-VNG). The characteristics of the horizontal, vertical, and torsional components of nystagmus were quantitatively analyzed.

Results: 3D-VNG showed that the fast phase of the vertical components and torsional components of left and right ear PSC-can as induced by the head-hanging position of the Dix-Hallpike test were upward, clockwise and counterclockwise, and horizontal components were mainly contralateral. The median slow-phase velocity of each of the three components for consecutive 5 s was 26.3°/s (12.3–45.8), 25.0°/s (15.7–38.9), and 9.2°/s (4.9–13.7). When patients were returned to the sitting position, the fast phase of the vertical and torsional components of nystagmus was reversed. Only 54 patients had horizontal components of nystagmus, and 32 of them remained in the same direction. The median slow-phase velocity of the three components for consecutive 5 s was 9.4°/s (6.0–11.7), 6.8°/s (4.5–11.8), and 4.9°/s (2.8–8.0). The ratios of the slow-phase velocity of the horizontal, vertical, and torsional components of the head-hanging position to the sitting position were close to 1.85 (1.0–6.6), 3.7 (1.9–6.6), and 5.1 (2.6–11.3). The ratios of the slow-phase velocity of the vertical to horizontal component, the torsional to horizontal component, and the vertical to torsional component of the head-hanging position were close to

3.3 (1.7–7.6), 3.9 (1.8–7.6), and 1.0 (0.5–1.8). The ratios of the slow-phase velocity of the vertical to horizontal component, the torsional to horizontal component, and the vertical to torsional component of the sitting position were close to 2.1 (1.1–6.8), 1.5 (1.0–3.8), and 1.2 (0.8–2.8).

Conclusion: There were three components of nystagmus induced by the Dix-Hallpike test in patients with PSC-can. The vertical component was the strongest and the horizontal component was the weakest. The 3D characteristics of nystagmus were consistent with those of physiological nystagmus associated with the same PSC with a single-factor stimulus, in accordance with Ewald's law.

KEYWORDS

benign positional paroxysmal vertigo, three-dimensional video nystagmography, canalithiasis, semicircular canal, Ewald's law

Introduction

Benign paroxysmal positional vertigo (BPPV) is the most common peripheral vestibular disorder, accounting for 17–42% of patients with vertigo (Power et al., 2020; Kim et al., 2021; Palmeri and Kumar, 2022). Posterior semicircular canal (PSC) involvement is common (Shigeno and Kitaoka, 2020). BPPV is a common peripheral vestibular disease, whose basic pathologic process is caused by the migration of otoconia from the utricular macula to the semicircular canals (Bhattacharyya et al., 2017). The canalith repositioning procedure has confirmed this pathological theory. In 1824 (Shimizu, 2000) and 1892 (Baloh and Honrubia, 1979), Flourens and Ewald explored the physiological mechanism of the vestibular semicircle from the 2 levels of the phenomenon and mechanism, respectively, through animal physiological models (Yang et al., 2017). Their findings formed the basis of Flouren's law and Ewald's law, Ewald's Law perfected Flourens Law from mechanism and phenomenon, and contributed greatly to the understanding of human vestibular physiology and pathology (Baloh et al., 1977). Whether this law is completely consistent with human semicircular canal physiology has remained difficult to verify in the human body for quite some time. In the horizontal semicircular canal canalithiasis/cupulolithiasis, posterior/anterior semicircular canal canalithiasis/cupulolithiasis, or in the roll test left/right head turning and Dix-Hallpike Test head-hanging/sitting position, otoliths are diagnosed and localized by inducing excitatory or inhibitory effects under the action of a single stimulant, a specific otoconia. Therefore, similar to horizontal semicircular canal BPPV (HSC-BPPV) (Zhang et al., 2021), PSC-BPPV also objectively provides a physiologically effective model for understanding and studying the response effect of single semicircular canal stimulation under the action of a "single factor." BPPV is not so much a disease as a physiological reaction of the vestibular semicircular canal to physiological properties. Through BPPV and positional testing, Flourens and Ewald's laws from animal physiological models were finally interpreted in relation to the human body. Therefore, BPPV is also the best way to understand human semicircular canal physiology and the semicircular canal nystagmus effect, helping to analyze the functional characteristics of the human semicircular canal and its nystagmus effect.

Currently, the diagnosis of PSC canalithiasis (PSC-can) is mainly based on the naked eye observation of the vertical and torsional components of nystagmus induced by the Dix-Hallpike test (Brevern et al., 2017). The application of traditional videonystagmography (VNG) makes the analysis of BPPV nystagmus and the localization of otolith localization from subjective to objective, but the torsion component of PSC could not be observed (Xu et al., 2019; Zhang et al., 2021). Three dimensional (3D)-VNG can accurately quantify the horizontal, vertical, and torsional components of PSC-can nystagmus, but there were few quantitative studies of 3D-VNG for PSC-can (Fetter and Sievering, 1995a,b; Imai et al., 2009; Ichijo, 2013). In this study, 3D-VNG was used to record and quantitatively analyze the horizontal, vertical, and torsional components of nystagmus induced by the Dix-Hallpike test in patients with PSC-can. Furthermore, we explored the correlation between the nystagmus of PSC-can and Ewald's law. We hope the findings can contribute to the study of the physiological characteristics of the posterior semicircular canal and make the diagnosis of PSC-can more objective.

Materials and methods

Participants

This was an observational study involving the assessment of 84 patients with PSC-can who were examined at the Ear, Nose, and Throat (ENT) Department of the Tianjin First Central Hospital between September 2021 and January 2022. All of

the patients had successfully been treated with the canalith repositioning procedure (CRP), and all provided informed consent prior to their inclusion in the study. The study procedures were approved by the Ethics Committee of the Tianjin First Central Hospital (number: 2020N118KY).

The inclusion criteria were the following: a history of positional vertigo as a predominant symptom, accompanied by autonomic symptoms such as nausea and vomiting; and a diagnosis of PSC-can according to the Bárány guidelines (Brevern et al., 2017) with successful repositioning. Meanwhile, the exclusion criteria were the following: horizontal semicircular canal benign paroxysmal positional vertigo (HSC-BPPV), anterior semicircular canal benign paroxysmal positional vertigo (ASC-BPPV), multiple-canal BPPV, or cupulolithiasis; and other types of peripheral and central vertigo, as identified on neurological and imaging examinations. Vestibular migraine was identified and excluded according to the International vestibular Migraine Guidelines.

Methods

The Dix-Hallpike test was performed to diagnose PSC-can by 3D-VNG (VertiGoggles-M, ZEHNIT Medical Technology-VNG-II, Shanghai, China). The directional characteristics of the torsional and vertical components of nystagmus induced in the left and right head-hanging positions and the sitting position were observed by monitor. The latency, duration, direction, and slow-phase velocity of the horizontal, vertical, and torsional components were simultaneously recorded by 3D-VNG. During the Dix-Hallpike test, the patient's eyes should remain directly in front of the face (i.e., the eyes should remain in place at all times). For the Dix-Hallpike test, the patient's eyes should be kept directly in front of the face (i.e., in place at all times).

Based on the Bárány diagnosis and treatment guidelines (Brevern et al., 2015, 2017), from a doctor's perspective, using the apex of the eyeball as a marker and the patient as a reference, the monitor observed vertical upward nystagmus with a torsional component (i.e., the vertical component was marked by upward movement, and the torsional component was marked by the apex of the eyeball turning to the lower ear) when the affected ear at the head-hanging position was turned to the ground in the Dix-Hallpike test. That is, right (R)-PSC-can induced right torsional nystagmus (counterclockwise), and left (L)-PSC-can induced left torsional nystagmus (clockwise). After the patient had returned to the sitting position, the fast phase of nystagmus was reversed. Therefore, on the 3D-VNG diagram, the left/right horizontal nystagmuses were recorded as downward/upward fast phase nystagmus curves, the downward/upward vertical nystagmuses were recorded in the same direction as the real nystagmus, and the clockwise/counterclockwise torsional nystagmuses were recorded as downward/upward fast phase nystagmus curves (**Figures 1**, **2**). Latency time was recorded as the period from the end of a head turn (in the head-hanging or sitting position) to the onset of continuous nystagmus. Duration was recorded as the period of continuous nystagmus, from its onset to the end. Based on the nystagmus duration of <10 s for some patients, the analysis of slow-phase velocity included the average slow-phase velocity of 5 s, 10 s, and the entire duration. The roll test was used to exclude HSC-BPPV and multiple-canal BPPV.

Analysis

The parameters of torsional nystagmus induced by the Dix-Hallpike test were compared within and between the groups. Continuous variables are expressed as the means ± SD or medians (interquartile ranges [IQR], Q1-Q3); categorical variables are expressed as frequencies and percentages. Comparisons of means between the two groups were performed using the independent *t*-test or the Mann-Whitney *U* test as appropriate. The chi-square test was used to compare proportions in demographics. *P*-values < 0.05 were considered statistically significant. SPSS Statistics 25 (IBM Corp., Armonk, NY, USA) was used for the statistical analyses, and GraphPad Prism 5 (GraphPad, San Diego, CA, USA) and R scripts were used to generate the figures.

Results

General demographic characteristics of subjects

In all, 84 patients with PSC-can were enrolled in this study, including 29 males and 55 females (age range 25–80 years; mean age 54.7 years). There were 25 patients with L-PSC-can and 59 patients with R-PSC-can. Demographic data for the BPPV patients are summarized in **Table 1**. The vertigo symptoms of all patients were relieved or disappeared after CRP treatment (Epley, 1992).

The characteristics of nystagmus in patients with PSC-can according to the Dix-Hallpike test

From a doctor's perspective, with the patient used as the reference and the apex of the eyeball as the marker, the directional characteristics of nystagmus induced by the Dix-Hallpike test in the 84 patients with PSC-can were recorded by nystagmus monitoring and 3D-VNG diagram observation. When the affected ear was tilted to the ground in the head-hanging position of the Dix-Hallpike test, the nystagmus monitors could observe torsional vertical jerk nystagmus (the

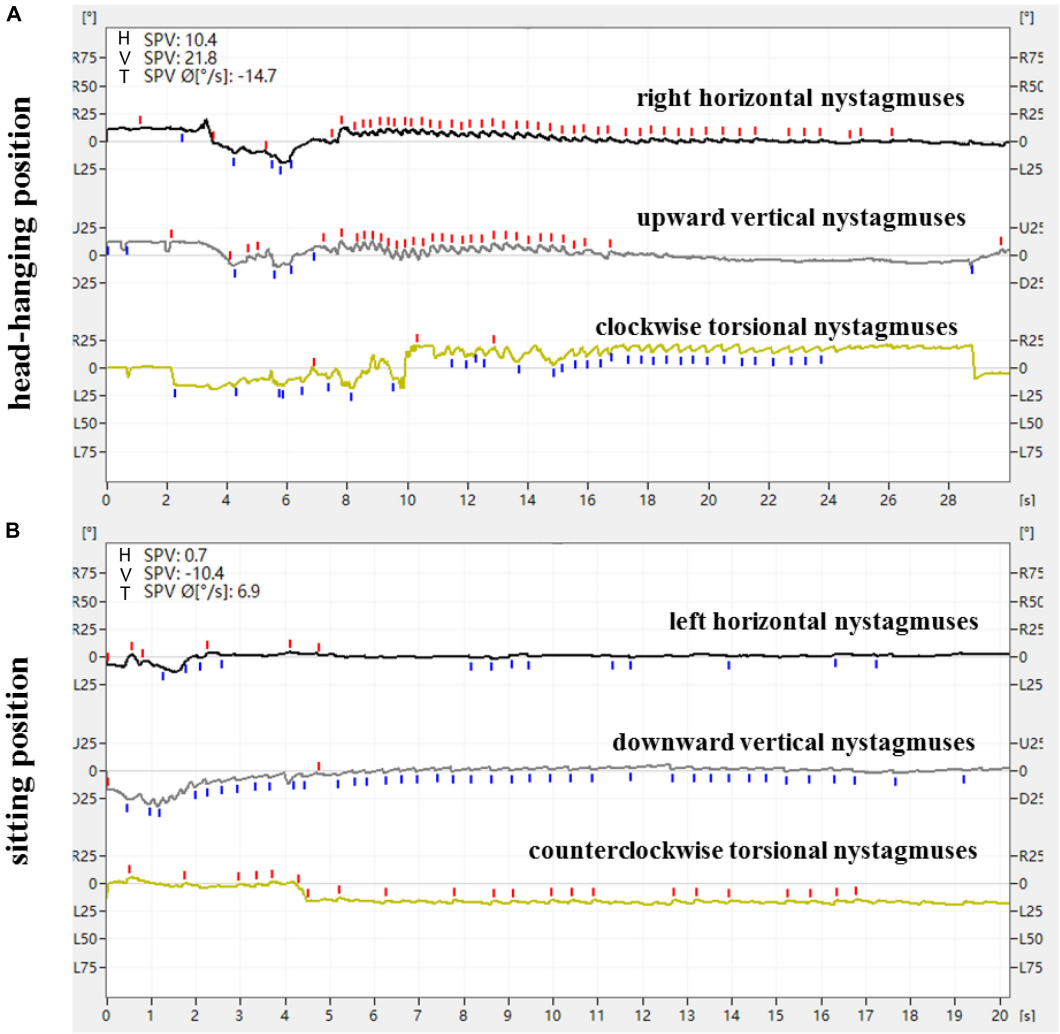

FIGURE 1
Expression of nystagmus on the 3D-VNG by Dix-Hallpike test of a patient with L-PSC-can. **(A)** At the head-hanging position, the right horizontal nystagmuses were recorded as upward fast-phase nystagmus curves, the upward vertical nystagmuses were recorded as upward fast-phase nystagmus curves, and the clockwise torsional nystagmuses were recorded as downward fast-phase nystagmus curves. **(B)** The direction of nystagmus was reversed when the head was recovered from the head-hanging position to the sitting position.

torsional component turned to the downward ear position, and the vertical component turned to the upward-forehead position), with the duration of nystagmus being <1 min. The fast phase of the torsional component of L-PSC-can and R-PSC-can at the head-hanging position was clockwise and counterclockwise, respectively. The fast phase of nystagmus was reversed when the head was recovered from the head-hanging position to the sitting position, but in only one case did the torsional component remain in the same direction. Under 3D-VNG, the vertical component of nystagmus was recorded, and the clockwise/counterclockwise torsional nystagmuses were recorded as downward/upward fast-phase nystagmus curves. In addition, the horizontal component of nystagmus was also recorded by 3D-VNG in 73 patients with PSC-can, with 63 cases in the contralateral and 10 cases in the ipsilateral (Figures 1, 2). The fast phase of nystagmus was reversed when the patients were returned to the sitting position. The vertical component of nystagmus was observed in 74 patients, the torsional component of nystagmus was observed in 62 patients, and the horizontal component of nystagmus was observed in 54 patients (32 cases were contralateral and 22 cases were ipsilateral).

Under 3D-VNG, 84 patients with PSC-can in the head-hanging position of the Dix-Hallpike test were observed. The median latency and duration of the horizontal component of nystagmus induced by the head-hanging position were 2.0 s (1.0–4.0) and 14.0 s (10.0–21.0), those of the vertical component of nystagmus were 2.0 s (1.0–4.0) and 15.0 s (10.0–19.8), and those the torsional component of nystagmus were 2.0 s

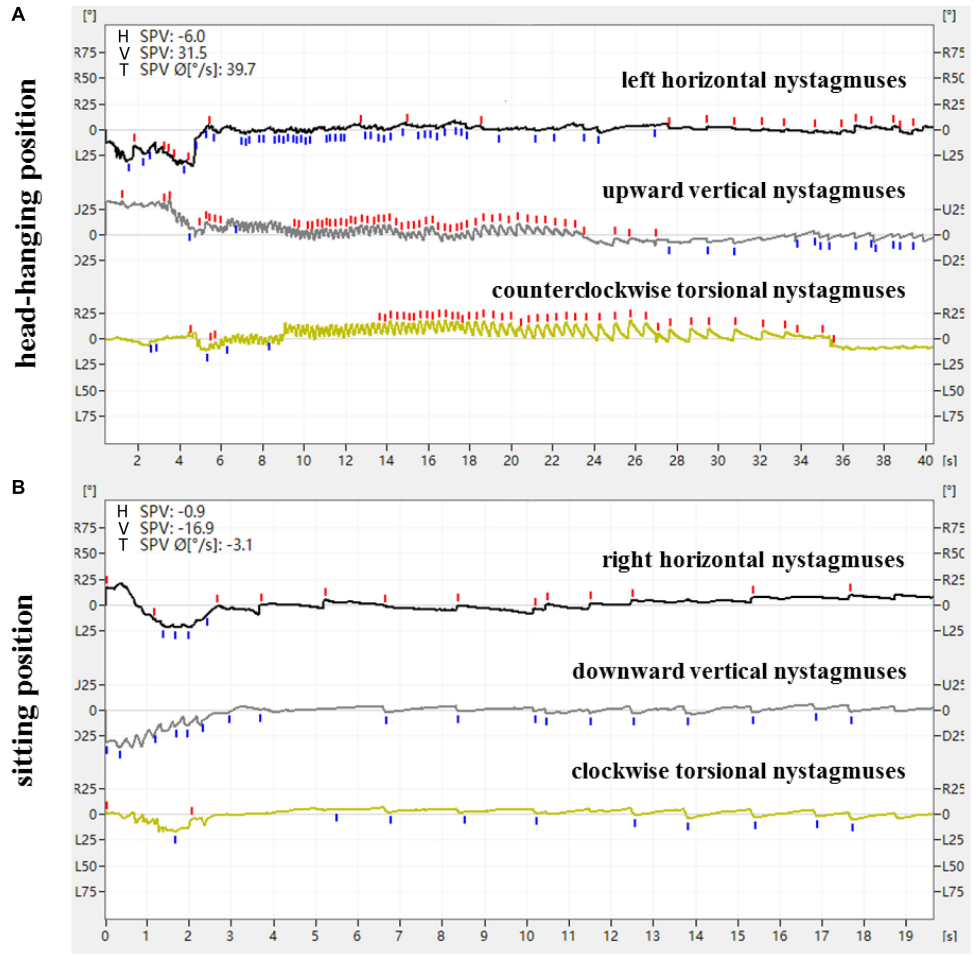

FIGURE 2
Expression of nystagmus on the 3D-VNG by Dix-Hallpike test of a patient with R-PSC-can. **(A)** At the head-hanging position, the left horizontal nystagmuses were recorded as downward fast-phase nystagmus curves, the upward vertical nystagmuses were recorded as upward fast-phase nystagmus curves, and the counterclockwise torsional nystagmuses were recorded as upward fast-phase nystagmus curves. **(B)** The direction of nystagmus was reversed when the head was recovered from the head-hanging position to the sitting position.

(1.0–3.0) and 15.5 s (12.0–21.8), respectively. The median slow-phase velocity of the horizontal component at the entire duration, at the strongest 10 and 5 s were 6.6°/s (3.7–9.4), 7.7°/s (4.0–11), and 9.2°/s (4.9–13.7); those of the vertical component were 19.9°/s (9.8–30.4), 24.5°/s (11.8–36.9), and 26.3°/s (12.3–45.8); and those of the torsion component were 18.3°/s (12.3–26.3), 20.7°/s (13.6–31.6), and 25.0°/s (15.7–38.9), respectively (Table 2). When patients were returned to the sitting position from the head-hanging position, the median latency and duration of the horizontal component of nystagmus were 1.0 s (1.0–2.0) and 15.5 s (12.0–19.3), those of the vertical component of nystagmus were 1.0 s (0.5–2.0) and 16.0 s (11.5–22.3), and those of the torsional component of nystagmus were 1.0 s (0.5–2.0) and 15.0 s (10.0–20.0), respectively. The median slow-phase velocity of the horizontal component at the entire duration, at the strongest 10 and 5 s were 3.5°/s (1.8–4.6), 4.2°/s (2.5–6.6), and 4.9°/s (2.8–8.0); that of the vertical component of nystagmus was 7.2°/s (5.2–9.1), 8.4°/s (6.0–10.5), and 9.4°/s (6.0–11.7); and that of the torsion component of nystagmus was 5.0°/s (3.8–8.9), 5.9°/s (4.0–9.6), and 6.8°/s (4.5–11.8) (Table 3).

TABLE 1 Demographic features of subjects in the patients with PSC-can.

Group feature	Total	PSC-can		*P*-value
		L-PSC-can	R-PSC-can	
Number	84	25	59	
Age (years) ($\overline{X} \pm s$)	54.7 ± 13.2	55.4 ± 12.8	54.4 ± 13.4	0.741
Sex (M:F)	29:55	9:16	20:39	0.853

L-PSC-can, left posterior semicircular canal canalithiasis; R-PSC-can, right posterior semicircular canal canalithiasis; M, male; F, female.

TABLE 2 Nystagmus characteristics of the head-hanging position in 84 patients with PSC-can.

		Median (IQR)		
		Horizontal nystagmus	Vertical nystagmus	Torsional nystagmus
Number		73	84	84
Latency (s)		2.0 (1.0–4.0)	2.0 (1.0–4.0)	2.0 (1.0–3.0)
Duration (s)		14.0 (10.0–21.0)	15.0 (10.0–19.8)	15.5 (12.0–21.8)
Direction	L-PSC-can	Right (18), Left (2)	Upward	Clockwise
	R-PSC-can	Right (8), Left (45)	Upward	Counterclockwise
Slow-phase velocity (∘/s)	Total	6.6 (3.7–9.4) (73)	19.9 (9.8–30.4) (84)	18.3 (12.3–26.3) (84)
	≥10 s	7.7 (4.0–11) (65)	24.5 (11.8–36.9) (77)	20.7 (13.6–31.6) (79)
	≥5 s	9.2 (4.9–13.7) (72)	26.3 (12.3–45.8) (83)	25.0 (15.7–38.9) (84)

TABLE 3 Nystagmus characteristics of the sitting position in 84 patients with PSC-can.

		Median (IQR)		
		Horizontal nystagmus	Vertical nystagmus	Torsional nystagmus
Number		54	74	62
Latency (s)		1.0 (1.0–2.0)	1.0 (0.5–2.0)	1.0 (0.5–2.0)
Duration (s)		15.5 (12.0–19.3)	16.0 (11.5–22.3)	15.0 (10.0–20.0)
Direction	L-PSC-can	Left (4), Right (13)	Downward	Clockwise (1), Counterclockwise (15)
	R-PSC-can	Left (19), Right (18)	Downward	Clockwise (46)
Slow-phase velocity (∘/s)	Total	3.5 (1.8–4.6) (54)	7.2 (5.2–9.1) (74)	5.0 (3.8–8.9) (62)
	≥10 s	4.2 (2.5–6.6) (49)	8.4 (6.0–10.5) (67)	5.9 (4.0–9.6) (54)
	≥5 s	4.9 (2.8–8.0) (54)	9.4 (6.0–11.7) (74)	6.8 (4.5–11.8) (62)

The results showed that the vertical and torsional components of nystagmus induced by the Dix-Hallpike test were dominant in PSC-can patients, with the vertical component being the strongest (Figures 3, 4). The fast phase of the horizontal component was mostly contralateral in the head-hanging position, and the fast phase of the horizontal component after the return to the sitting position varied, being either ipsilateral or contralateral. According to the data, the average slow-phase velocity of the consecutive at 5 s was the strongest, so it is suggested that this slow-phase velocity should be used as a standard for quantitative analysis.

Comparison between the head-hanging position and sitting position nystagmus of patients with PSC-can according to the Dix-Hallpike test

The ratio of latency between the head-hanging position and the sitting position was close to 2 (1.0–6.0) ($p < 0.001$), with the ratio of duration close to 1. The ratios of the slow-phase velocity of the horizontal, vertical, and torsion components of nystagmus for the head-hanging position and the sitting position were close to 1.85 (1.0–6.6), 3.7 (1.9–6.6), and 5.1 (2.6–11.3), respectively (Table 4).

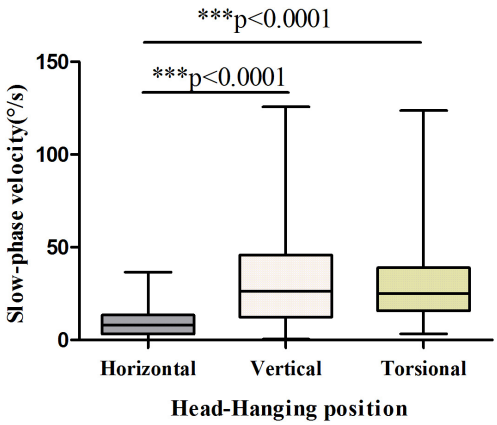

FIGURE 3
Slow-phase velocity of nystagmus in the head-hanging position of patients with PSC-can. The slow-phase velocity of nystagmus differed significantly between the horizontal and vertical components ($p < 0.0001$), horizontal and torsional components ($p < 0.0001$). *$p < 0.05$, **$p < 0.01$, and ***$p < 0.001$, compared with respective control.

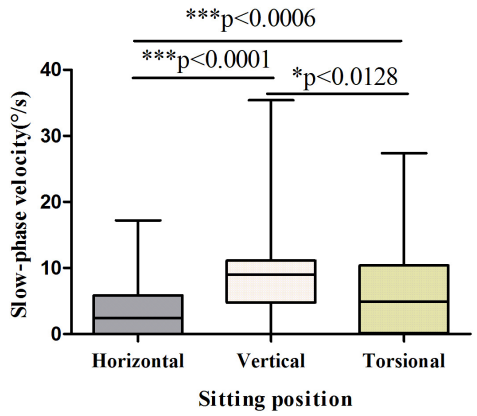

FIGURE 4
Slow-phase velocity of nystagmus in the sitting position of patients with PSC-can. The slow-phase velocity of nystagmus differed significantly between the horizontal and vertical components ($p < 0.0001$), horizontal and torsional components ($p < 0.0006$), vertical and torsional components ($p < 0.0128$). *$p < 0.05$, **$p < 0.01$, and ***$p < 0.001$, compared with respective control.

The ratio of slow-phase velocity in the head-hanging position and sitting position of patients with PSC-can according to the Dix-Hallpike test

The ratios of slow-phase velocity in the head-hanging position of the vertical to horizontal component, the torsional to horizontal component, and the vertical to torsional component were close to 3.3 (1.7–7.6), 3.9 (1.8–7.6), and 1.0 (0.5–1.8), respectively. The ratios of slow-phase velocity in the sitting position of the vertical to horizontal component, the torsional to horizontal component, and the vertical to torsional component were close to 2.1 (1.1–6.8), 1.5 (1.0–3.8), and 1.2 (0.8–2.8), respectively (Table 5).

TABLE 5 The ratio of slow-phase velocity in the head-hanging position and sitting position of 84 patients with PSC-can.

	Vertical/ Horizontal	Torsional/ Horizontal	Vertical/ Torsional
Head-hanging position	3.3 (1.7–7.6)	3.9 (1.8–7.6)	1.0 (0.5–1.8)
Sitting position	2.1 (1.1–6.8)	1.5 (1.0–3.8)	1.2 (0.8–2.8)

Discussion

According to Flourences and Ewald's law, the fast phase of nystagmus induced in this study was in the same plane as that of the stimulated semicircular canal. The endolymph in the posterior semicircular canal flows away from the ampulla with excitatory stimulation (Dix and Hallpike, 1952; Honrubia and House, 2001). The posterior semicircular canal is at an angle of about 45° to the sagittal plane, and the position of the ampulla and the common crus were anteriorly inferior and posteriorly superior, respectively. Therefore, if the right posterior semicircular canal was excited under physiological conditions, it is necessary to turn the head to the left and upward. Then, a VOR synthesis vector is generated in which the slow phase eye movement rotates to the lower right, while the fast phase eye movement rotates to the upper left (the direction of head turning is the same as the direction of the induced nystagmus). In physiological state, the stimulation of the right posterior semicircular canal by turning the head to the left and upward was the same as the stimulation of the R-PSC-can in the right Dix-Hallpike test. In 3D-VNG, the horizontal, vertical and torsional components were to the left, upward and counterclockwise, respectively (Wang et al., 2009).

Compared with HSC-BPPV, PSC-BPPV objectively provides a physiological effect model to understand and study the "single semicircular canal stimulation response effect" under the action of "single factor," but the study of PSC nystagmus mechanism and nystagmus characteristics has been one of the difficulties. In this study, the nystagmus characteristics of 84 patients with PSC-can were analyzed using 3D-VNG. With the patient in the hanging-head position of the Dix-Hallpike test in left ear and right ear PSC-can, the vertical components of nystagmus were upward, the torsional components were clockwise and counterclockwise, respectively, and the horizontal components were mainly contralateral. The median slow-phase velocity of the three components for consecutive 5 s was 26.3°/s (12.3–45.8), 25.0°/s (15.7–38.9) and 9.2°/s (4.9–13.7), respectively. When the patient was returned to the sitting position, the fast phase of the vertical and torsional components of nystagmus was reversed. In only one case the torsional component remained in the same direction. Among 54 patients with

TABLE 4 Comparison between the head-hanging position and sitting position nystagmus of 84 patients with PSC-can.

	Latency (s)			Duration (s)			Slow-phase velocity (o/s)		
	Horizontal	Vertical	Torsional	Horizontal	Vertical	Torsional	Horizontal	Vertical	Torsional
Head-hanging position	2.0 (1.0–3.5)	2.0 (1.0–4.0)	2.0 (1.0–3.5)	13.0 (10.0–19.0)	14.0 (10.0–19.0)	15.0 (12.0–21.0)	8.2 (3.2–12.4)	31.0 (12.8–47.4)	26.8 (16.0–39.3)
Sitting position	1.0 (0.0–1.0)	1.0 (0.5–2.0)	1.0 (0.5–1.0)	12.0 (0.0–19.0)	16.0 (10.0–22.0)	13.0 (5.0–18.0)	3.2 (0.0–6.3)	9.4 (5.6–11.6)	5.6 (2.8–10.7)
Head-hanging position/Sitting position	2 (1.0–6.0)	2 (1.0–5.0)	2 (1.0–5.0)	1.2 (0.8–10.0)	1.0 (0.7–1.4)	1.3 (0.9–5.2)	1.85 (1.0–6.6)	3.7 (1.9–6.6)	5.1 (2.6–11.3)
p-value	$p < 0.001$	$p < 0.001$	$p < 0.001$	$p < 0.165$	$p < 0.966$	$p < 0.001$	$p < 0.001$	$p < 0.001$	$p < 0.001$

horizontal components of nystagmus, 32 patients the fast phase of the nystagmus remained unchanged. The median slow-phase velocity of the three components for consecutive 5 s was 9.4°/s (6.0–11.7), 6.8°/s (4.5–11.8), and 4.9°/s (2.8–8.0), respectively. The fast phase of the vertical and torsional components of nystagmus in patients with PSC-can was basically consistent with that in the BPPV guidelines, but information on the horizontal component of nystagmus was lacking in all of the guidelines. In this study, the horizontal component of nystagmus was not contralateral in 10 patients (13.7%) when the head was at the hanging-head position, and the direction of the horizontal component of nystagmus was not reversed in 32 patients (59.3%) when the head was at the sitting position. The reason leading to this may lies in two aspects: one is the coexistence of other types of vestibular terminal receptor dysfunction; the other is the variation of the anatomy and angle of each individual semicircular canal. For example, the posterior semicircular canal may not be completely perpendicular to the horizontal plane and has a horizontal Angle, resulting in horizontal components in different directions occur at the head-hanging position and sitting position. The 3D-VNG recorded and analyzed the nystagmus of PSC-can patients that was induced by the Dix-Hallpike test, which objectively showed the entirety fast phase of nystagmus, especially, the horizontal component of nystagmus is difficult to see with the naked eye, and more accurately showed the spatial relationship of the posterior semicircular canal plane.

Hiroaki's (Ichijo, 2013) research results showed that Ewald's third law is correct in the PSC, and the slow-phase velocity, the head-hanging position and those in the sitting position showed inversion asymmetry. The results of Zhang et al. (2021) showed the fast phase of nystagmus induced by HSC-can to be the same as the direction of head turning, and the slow-phase velocity ratio of the affected side to the healthy side was about 2:1. It has been reported that horizontal semicircular canal BPPV can be used as a single factor in the physiological effect model of a single horizontal semicircular canal stimulation response (Zhang et al., 2021), but no research report on the three-dimensional nystagmosis characteristics of P-BPPV based on this point of view was found. Xu's (Xu et al., 2019) research results showed that the slow-phase velocity of vertical nystagmus induced by the head-hanging position on the affected side of the PSC-can was significantly greater than that induced by the sitting position, with the ratio of slow-phase velocity being about 2:1. However, the relationship of the slow-phase velocity between each component of PSC-can at two head positions and the relationship of the slow-phase velocity between the three components of each head position have not been reported (Hayashi et al., 2002; Aw et al., 2005; Imai et al., 2009; Eggers et al., 2019). Our results show that the ratios of the slow-phase velocity of the horizontal, vertical, and torsion components between the head-hanging position and sitting position were close to 1.85 (1.0–6.6), 3.7 (1.9–6.6) and 5.1 (2.6–11.3), respectively. The ratios of the slow-phase velocity of the vertical to horizontal component, the torsional to horizontal component, and the vertical to torsional component of the head-hanging position were close to 3.3 (1.7–7.6), 3.9 (1.8–7.6), and 1.0 (0.5–1.8), respectively. The ratios of the slow-phase velocity of the vertical to horizontal component, the torsional to horizontal component, and the vertical to torsional component of the sitting position were close to 2.1 (1.1–6.8), 1.5 (1.0–3.8), and 1.2 (0.8–2.8), respectively. These results suggest that PSC-can is the clinical manifestation of Ewald's law in the human body. This study not only describes the orientation characteristics of the three components of nystagmus, but also further quantitatively analyzes each component. The results of this study further suggest that the three components of horizontal, vertical and torsional nystagmus induced by PSC-can are the result of the joint action of the PSC with the associated eye muscles dominated by ipsilateral superior/inferior oblique and contralateral superior/inferior rectus, but the weight of each group eye muscles and the interaction mechanism need to be further explored.

The limitation of this study is the absence of any control group. Therefore, normal people and PSC-can patients with unilateral and bilateral vestibular dysfunction should be included in subsequent studies for controlled studies. Because the PSC-can patients in this group did not have a comprehensive vestibular function evaluation, such as the ocular/cervical vestibular evoked myogenic potential (o/cVEMP) evaluation of otolithoid function and multifrequency functional testing of the three semicircular canals, the influence of otolithoid and other frequency functions of the three semicircular canals on nystagmus in PSC-can cannot be ruled out. There are other forms of the horizontal component of PSC-can nystagmus, and whether it can be used as an indication of other semicircular canal or otolith organ injury is worth further study in comprehensive vestibular function assessment. The 3D-VNG can only objectively record the characteristics of nystagmus. The diagnostic and differential diagnostic value of positional vertigo should be further verified by accumulating cases and increasing the time of observation and follow-up.

Conclusion

In this study, 3D-VNG technology was applied to objectively record and analyze the direction, slow-phase velocity, and time parameter characteristics of each component of nystagmus in the head-hanging and sitting positions of patients with PSC-can in the Dix-Hallpike test. BPPV also objectively provides a physiological effect model to understand and study the "response effect of single posterior semicircular canal

stimulation" under the action of "single factor on single posterior semicircular canal," suggesting that PSC-Can is also the embodiment of Ewald's law of human body. And can be used as a physiological stimulation model to understand the physiological function of the human posterior semicircular canal. In this study, the diagnosis and treatment of PSC-can was measured from naked eye observation to precise quantification, laying a foundation for future objective diagnosis, big data analysis and intelligent analysis of BPPV. At the same time, 3D-VNG can help to understand the mechanism and characteristics of PSC nystagmus.

Data availability statement

The original contributions presented in this study are included in the article/supplementary material, further inquiries can be directed to the corresponding authors.

Ethics statement

This study was reviewed and approved by the Ethics Committee of the Tianjin First Central Hospital (number: 2020N118KY). Written informed consent was obtained from the individual(s) for the publication of any potentially identifiable images or data included in this article.

Author contributions

YL and TC wrote the main manuscript. XZ and QD collected the literature. QL, CW, and WW revised the manuscript. All authors reviewed the manuscript.

Funding

This work was supported by the Tianjin Key Medical Discipline Construction Project (TJYXZDXK-046A), Tianjin Applied Basic Research Multiple Investment Fund Project (21JCQNJC01670, 21JCQNJC01780, 21JCZDJC01200, and 21JCQNJC01770), and Tianjin Health Research Project (TJWJ2022QN028, TJWJ2022QN027, and ZC20010).

Conflict of interest

The authors declare that the research was conducted in the absence of any commercial or financial relationships that could be construed as a potential conflict of interest.

Publisher's note

All claims expressed in this article are solely those of the authors and do not necessarily represent those of their affiliated organizations, or those of the publisher, the editors and the reviewers. Any product that may be evaluated in this article, or claim that may be made by its manufacturer, is not guaranteed or endorsed by the publisher.

References

Aw, S. T., Todd, M. J., Aw, G. E., McGarvie, L. A., and Halmagyi, G. M. (2005). Benign positional nystagmus: A study of its three-dimensional spatio-temporal characteristics. *Neurology* 64, 1897–1905. doi: 10.1212/01.WNL.0000163545.57134.3D

Baloh, R. W., and Honrubia, V. (1979). Clinical neurophysiology of the vestibular system. *Contemp. Neurol. Ser.* 18, 1–21.

Baloh, R. W., Honrubia, V., and Konrad, H. R. (1977). Ewald's second law re-evaluated. *Acta Otolaryngol.* 83, 475–479. doi: 10.3109/00016487709128874

Bhattacharyya, N., Gubbels, S., and Schwartz, S. (2017). Clinical practice guideline: Benign paroxysmal positional vertigo. *Otolaryngol. Head Neck Surg.* 156 (suppl. 3), S1–S47.

Brevern, M. V., Bertholon, P., Brandt, T., Fife, T., Imai, T., Nuti, D., et al. (2017). Benign paroxysmal positional vertigo: Diagnostic criteria consensus document of the committee for the classification of vestibular disorders of the Barany Society. *Acta Otorrinolaringol. Esp.* 68, 349–360. doi: 10.1016/j.otorri.2017.02.007

Brevern, M. V., Bertholon, P., Brandt, T., Fife, T., Imai, T., Nuti, D., et al. (2015). Benign paroxysmal positional vertigo: Diagnostic criteria. *J. Vestib. Res.* 25, 105–117. doi: 10.3233/VES-150553

Dix, M. R., and Hallpike, C. S. (1952). The pathology, symptomatology and diagnosis of certain common disorders of the vestibular system. *Ann. Otol. Rhinol. Laryngol.* 61, 987–1016.

Eggers, S. D., Bisdorff, A., Brevern, M. V., Zee, D. S., Kim, J., Perez-Fernandez, N., et al. (2019). Classification of vestibular signs and examination techniques: Nystagmus and nystagmus-like movements. *J. Vestib. Res.* 29, 57–87. doi: 10.3233/VES-190658

Epley, J. M. (1992). The canalith repositioning procedure: For treatment of benign paroxysmal positional vertigo. *Otolaryngol. Head Neck Surg.* 107, 399–404. doi: 10.1177/019459989210700310

Fetter, M., and Sievering, F. (1995a). Three-dimensional (3-D) eye movement analysis in patients with positioning nystagmus. *Acta Otolaryngol. Suppl.* 520 Pt 2, 369–371. doi: 10.3109/00016489509125273

Fetter, M., and Sievering, F. (1995b). Three-dimensional eye movement analysis in benign paroxysmal positioning vertigo and nystagmus. *Acta Otolaryngol.* 115, 353–357. doi: 10.3109/00016489509139328

Hayashi, Y., Kanzaki, J., Etoh, N., Higashino, K., Goto, F., Schneider, E., et al. (2002). Three-dimensional analysis of nystagmus in benign paroxysmal positional vertigo. New insights into its pathophysiology. *J. Neurol.* 249, 1683–1688. doi: 10.1007/s00415-002-0905-z

Honrubia, V., and House, M. (2001). Mechanism of posterior semicircular canal stimulation in patients with benign paroxysmal positional vertigo. *Acta Otolaryngol.* 121, 234–240. doi: 10.1080/00016480130004 3640

Ichijo, H. (2013). Asymmetry of positioning nystagmus in posterior canalolithiasis. *Acta Otolaryngol.* 133, 159–164. doi: 10.3109/00016489.2012. 728293

Imai, T., Takeda, N., Ito, M., Sekine, K., Sato, G., Midoh, Y., et al. (2009). 3D analysis of benign positional nystagmus due to cupulolithiasis in posterior semicircular canal. *Acta Otolaryngol.* 129, 1044–1049. doi: 10.1080/ 00016480802566303

Kim, H. J., Park, J., and Kim, J. S. (2021). Update on benign paroxysmal positional vertigo. *J. Neurol.* 268, 1995–2000.

Palmeri, R., and Kumar, A. (2022). *Benign paroxysmal positional vertigo*. Treasure Island, FL: StatPearls Publishing.

Power, L., Murray, K., and Szmulewicz, D. J. (2020). Characteristics of assessment and treatment in benign paroxysmal positional vertigo (BPPV). *J. Vestib. Res.* 30, 55–62.

Shigeno, K., and Kitaoka, K. (2020). A new variant of posterior canal-benign paroxysmal positional vertigo-canalolithiasis. *Auris Nasus Larynx* 47, 924–930.

Shimizu, N. (2000). [Neurology of eye movements]. *Rinsho Shinkeigaku* 40, 1220–1223.

Wang, N., Chen, T., Lin, P., Song, W., and Dong, H. (2009). [Positioning diagnosis of benign positional paroxysmal vertigo by VNG]. *Lin Chung Er Bi Yan Hou Tou Jing Wai Ke Za Zhi* 23, 597–600.

Xu, K. X., Chen, T. S., Wang, W., Liu, Q., Wen, C., Li, S. S., et al. (2019). [Objective characteristics of nystagmus in patients with posterior semicircular canal benign paroxysmal positional vertigo]. *Zhonghua Er Bi Yan Hou Tou Jing Wai Ke Za Zhi* 54, 729–733.

Yang, C. J., Lee, J., Kim, S., Lee, C., and Park, H. J. (2017). Development of a murine model of traumatic benign paroxysmal positional vertigo: A preliminary study. *Acta Otolaryngol.* 137, 29–34. doi: 10.1080/00016489.2016.1217043

Zhang, X., Bai, Y., Chen, T., Wang, W., Han, X., Li, S., et al. (2021). A show of Ewald's law: I horizontal semicircular canal benign paroxysmal positional vertigo. *Front. Neurol.* 12:632489. doi: 10.3389/fneur.2021.632489

frontiers | Frontiers in Neuroscience

TYPE Original Research
PUBLISHED 10 January 2023
DOI 10.3389/fnins.2022.1076109

Check for updates

OPEN ACCESS

EDITED BY
Sulin Zhang,
Huazhong University of Science and Technology, China

REVIEWED BY
Yi Li,
Beijing Tongren Hospital, Capital Medical University, China
Yong Cui,
Guangdong Provincial People's Hospital, China

*CORRESPONDENCE
Xin Ma
✉ 13581709195@163.com

†These authors have contributed equally to this work and share first authorship

SPECIALTY SECTION
This article was submitted to Perception Science, a section of the journal Frontiers in Neuroscience

RECEIVED 21 October 2022
ACCEPTED 16 December 2022
PUBLISHED 10 January 2023

CITATION
Diao T, Chen Y, Jing Y and Ma X (2023) Clinical characteristics and prognosis of acute low-frequency hearing loss and ascending sensorineural sudden sensorineural hearing loss. *Front. Neurosci.* 16:1076109. doi: 10.3389/fnins.2022.1076109

COPYRIGHT
© 2023 Diao, Chen, Jing and Ma. This is an open-access article distributed under the terms of the Creative Commons Attribution License (CC BY). The use, distribution or reproduction in other forums is permitted, provided the original author(s) and the copyright owner(s) are credited and that the original publication in this journal is cited, in accordance with accepted academic practice. No use, distribution or reproduction is permitted which does not comply with these terms.

Clinical characteristics and prognosis of acute low-frequency hearing loss and ascending sensorineural sudden sensorineural hearing loss

Tongxiang Diao†, Yurun Chen†, Yuanyuan Jing and Xin Ma*

Department of Otolaryngology, Head and Neck Surgery, People's Hospital, Peking University, Beijing, China

Objective: The present study aimed to explore the pathogenesis of the ascending sudden sensorineural hearing (SSNHL) loss by comparing the clinical characteristics and prognosis of acute low-frequency hearing loss (ALFHL) and ascending SSNHL.

Methods: A total of 43 patients with ALFHL and 122 patients with ascending SSNHL were enrolled in this study. First, the prognosis of patients with ALFHL and ascending SSNHL were compared, and the prognostic factors of AFHL and ascending SSNHL were analyzed.

Results: Acute low-frequency hearing loss and ascending SSNHL have no remarkable difference in complete recovery rate. Compared to ascending SSNHL, ALFHL has younger onset age, female prevalence, lower hearing threshold, shorter time from onset to recovery, and a lower proportion of combined tinnitus. The PTA at admission and delay from onset to therapy were significantly related to the prognosis of patients with ascending SSNHL, while only delay from onset to therapy was significantly related to the prognosis of patients with ALFHL. The majority of patients with ascending SSNHL and ALFHL recovered completely within 10 days from onset.

Conclusion: Audiogram shape plays a critical role in the prognosis of SSNHL. Ascending SSNHL and ALFHL may share a common pathological mechanism.

KEYWORDS

ALFHL, ascending SSNHL, audiogram shape, prognosis, related factors

Introduction

Acute low-frequency sensorineural hearing loss (ALFHL) has been interpreted as an independent disease entity distinct from idiopathic sudden sensory neural hearing loss (SSNHL) (Imamura et al., 1997), characterized by low-frequency hearing loss, better prognosis, and high recurrence rate (Fuse et al., 2002). The diagnostic criteria for ALFHL

were as follows: (1) acute onset sensorineural hearing loss of >30 dB at two consecutive low frequencies (250 and 500 Hz) within a period of 3 days; (2) 25 dB of normal hearing at hearing thresholds of 1, 2, 3, 4, and 8 kHz on the affected side; (3) 25 dB of normal hearing at hearing thresholds of 250, 500, 1,000, 2,000, 4,000, and 8,000 Hz on the unaffected side; and (4) no history of episodic dizziness or spontaneous nystagmus (Jung et al., 2016). The pathophysiological mechanisms of ALHL are similar to those of sudden hearing loss; this phenotype has been associated with cochlear hydrops (CH) and early stages of Meniere's disease (Yamasoba et al., 1993). Due to the presence of helicotrema, hydrops begin at the apical turn of the cochlea, manifesting as low-frequency deafness, subsequently involving all frequencies with worsening hydrops (Thai-Van et al., 2001).

Sudden sensory neural hearing loss is defined as at least 30 dB sensorineural hearing loss in three sequential frequencies within 3 days with no identifiable cause (Stachler et al., 2012), which has an incidence ranging from 5 to 27/100,000 people in the Western countries and 19/100,000 in mainland China (Xie et al., 2020). The pathogenesis of SSNHL is yet unknown, although several hypotheses have been proposed, including viral infection, vascular compromise, membrane labyrinth hydrops, chronic inflammation, immunological diseases (Rossini et al., 2017), cochlear membrane rupture (Kuhn et al., 2011), inner ear cell stress reaction (Merchant et al., 2005), hemorrhage of the inner ear (Berrettini et al., 2013), and migraine (Hwang et al., 2018). Some studies have proposed that the SSNHL can be divided into four types of audiogram shapes based on the pattern of hearing loss: ascending, flat, profound, and descending. "Ascending or descending" referred to cases in which the average threshold of 0.25–0.5 kHz was 20 dB higher or lower than the average threshold of 4–8 kHz. When the difference in hearing threshold did not exceed 20 dB at any frequency, the audiogram shape was classified as "flat." For patients with a flat audiogram and hearing threshold >90 dB, the audiogram shape was classified as "profound." As shown previously, the ascending type has the best prognosis (Mattox and Simmons, 1977; Qian et al., 2018), with a recovery rate of about 83.33% (Li et al., 2016). The present study aimed to explore the pathogenesis of the ascending SSNHL by comparing the clinical characteristics and prognosis of patients with ALFHL.

Materials and methods

Study design and inclusion and exclusion criteria

This retrospective cohort study included 43 patients in line with the definition of ALFHL and 122 patients with ascending SSNHL hospitalized in our department for treatment from July 2015 to May 2018.

Inclusion criteria

Ascending SSNHL group: (1) 18–70-year-old; (2) no gender requirement; (3) first-onset SSNHL; (4) unilateral hearing loss; (5) time from onset to treatment ≤14 days; (6) the average threshold of 0.25–0.5 kHz was 20 dB higher than the average threshold of 4–8 kHz, and all frequency hearing thresholds were >25 dB; and (7) normal hearing or age-related hearing loss in the contralateral ear.

Acute low-frequency hearing loss group: (1) 18–70-year-old; (2) no gender requirement; (3) first-onset SSNHL; (4) unilateral hearing loss; (5) a time between onset and treatment ≤14 days; (6) hearing loss of >30 dB at two consecutive low frequencies (250 and 500 Hz), but with 25 dB of normal hearing at hearing thresholds of 1, 2, 3, 4, and 8 kHz on the affected side; and (7) normal hearing or age-related hearing loss in the contralateral ear.

Exclusion criteria

(1) Pregnancy or middle ear infections; (2) a definitive cause of deafness identified during treatment; (3) acoustic neuroma and other organic diseases; and (4) anxiety and insomnia.

Treatment

After admission, treatments were applied in accordance with the Editorial Board of Chinese Journal of Otorhinolaryngology Head and Neck Surgery; Society of Otorhinolaryngology Head and Neck Surgery, Chinese Medical Association (2015). The systemic corticosteroids and hemodilution agents were administered as therapeutic measures. All patients received 40 mg of intravenous methylprednisolone for 5 consecutive days and hemodilution agents for 10 days, including 87.5 mg of intravenous EGb-761 (Ginkgo Biloba Extracts) (Dr. Willmar Schwabe GmbH & Co., Germany) daily.

Efficacy evaluation

Pure-tone audiometry was performed at the initial presentation and 1 month after treatment. The pure-tone average of all frequencies (250, 500, 1,000, 2,000, 4,000, and 8,000 Hz) was employed to determine the treatment outcomes according to Siegel's (1975) criteria. Complete recovery (CR) indicated that the "final hearing level was <25 dB." Final hearing at 25–45 dB with a hearing gain of ≥15 dB was "partial recovery." "Slight recovery" meant final hearing >45 dB with hearing gain of ≥15 dB. The final hearing level >75 dB with hearing gain of ≤15 dB represented "no recovery."

Statement of ethics

This cohort research was approved by the Peking University People's Hospital Ethical permission committee (2021PHB149).

Written informed consent for this research was received from each patient.

Statistic

The clinical and epidemiological characteristics of the patients were summarized by descriptive statistics. The datasets were described with median and/or range. Numerical data were compared using *t*-test, and categorical data were compared using the χ^2 test. First, univariate analysis was used to compare the epidemiological and clinical characteristics of ALFHL and ascending SSNHL group, and then binary logistic regression analysis was used to analyze the prognostic factors of ALFHL and ascending SSNHL. The risk ratios were presented with 95% confidence interval (CI). Statistical significance was defined as a two-tailed $P < 0.05$ for all analyses. Statistical analyses were performed using SPSS software version 23.0 and GraphPad Prism 7.0.

Results

Clinical characteristics of ascending SSNHL and ALFHL

A total of 43 ALFHL patients and 122 patients with ascending SSNHL were enrolled in this study. Independent sample *t*-test and c^2-square test were used to compare the clinical characteristics and CR rate between patient groups with ascending SSNHL and ALFHL (Table 1). The statistical results showed statistical differences in age, gender, PTA at admission (the average hearing thresholds of 0.25, 0.5, 1.0, 2.0, 4.0, and 8.0 kHz), 1 kHz pure-tone threshold, 2 kHz pure-tone threshold, tinnitus occurrence, and the delay from onset to CR (onset-CR) between the two groups; however, the CR was not statistically different. Compared to the ascending SSNHL group, patients with ALFHL had a lower age of onset, lower PTA at admission, lower pure-tone threshold at 1 and 2 kHz, female tendency, shorter onset-CR time, and lower tinnitus incidence.

TABLE 1 Clinical characteristics of ascending sudden sensorineural hearing loss (SSNHL) and acute low-frequency hearing loss (ALFHL).

	Ascending SSNHL (*n* = 122)	ALFHL (*n* = 43)	*p*
Age	38.35 ± 12.89	33.33 ± 10.07	0.011*
Sex (female)	62/122 (50.82%)	31/43 (72.09%)	0.020*
Lateral (left)	64/122 (52.46%)	21/43 (48.84%)	0.725
PTA (dB)	44.48 ± 19.07	20.23 ± 4.25	0.000*
Tinnitus	111/122 (90.98%)	33/43 (76.74%)	0.020*
Dizziness	18/122 (14.74%)	12/43 (27.91%)	0.067
Aural fullness	63/122 (51.64%)	25/43 (58.14%)	0.483
Headaches	8/122 (6.56%)	1/43 (2.33%)	0.448
CR rate	84/122 (68.85%)	34/43 (79.07%)	0.241
UR rate	12/122 (9.84%)	4/43 (9.30%)	1.000
Onset-CR			0.004*
3 days	22/122 (18.03%)	20/43 (46.51%)	
3–7 days	38/122 (31.15%)	7/43 (16.28%)	
6–10 days	19/122 (15.57%)	5/43 (11.63%)	
10–14 days	5/122 (4.10%)	1/43 (2.33%)	
14–30 days	0/122 (0.00%)	1/43 (2.33%)	
Un-CR	38/122 (31.15%)	9/43 (20.93%)	
Onset-therapy	3.41 ± 3.12	3.47 ± 2.30	0.920

CR, complete recovery; UR, un-recovery.
*$p < 0.05$.

Factors related to the prognosis of ALFHL

A total of 34/43 patients with ALFHL (79.07%) recovered completely. First, the univariate analysis showed that delay from onset to therapy (onset-therapy) was statistically related to the prognosis of patients with ALFHL. Then, onset-therapy and clinically significant factors, including age, PTA at admission, tinnitus, and dizziness, were included in the binary logistic regression analysis. The results showed that delay from onset-therapy was an independent related factor to the prognosis of ALFHL (Table 2).

Factors related to the prognosis of ascending SSNHL

A total of 118/122 patients with ascending SSNHL (68.85%) completely recovered. First, the univariate analysis showed that delay from onset-therapy was statistically related to the prognosis of patients with ascending SSNHL. Then, onset-therapy and clinically significant factors, including age, PTA at admission, tinnitus, and dizziness, were included in the further binary logistic regression analysis. The results showed that PTA at admission and delay from onset-therapy were independent factors of the prognosis of ascending SSNHL (Table 3).

Distribution of onset-CR of ALFHL and ascending SSNHL

The CR of ALFHL was 79.07% (34/43), of which 94.12% (32/34) were recovered within 10 days after onset. The CR of ascending SSNHL was 68.85% (84/122), which was slightly

TABLE 2 Factors related to prognosis of acute low-frequency hearing loss (ALFHL).

Variable	Un-CR (n = 9)	CR (n = 34)	p
Univariate analysis			
Age	37.67 ± 10.559	32.18 ± 9.778	0.145
Onset-therapy	6.44 ± 4.613	2.68 ± 1.788	0.041*
PTA at admission	21.389 ± 4.167	19.927 ± 4.286	0.365
Gender (female)	6/9 (66.67%)	25/34 (73.53%)	0.692
Lateral (left)	5/9 (55.56%)	16/34 (47.06%)	0.721
Tinnitus	8/9 (88.89%)	25/34 (73.53%)	0.659
Dizziness	5/9 (55.56%)	7/34 (20.59%)	0.088
Aural fullness	6/9 (66.67%)	19/34 (55.88%)	0.712
Headache	1/9 (11.11%)	0/34 (0.00%)	0.209
Multivariate analysis			
	OR (95%CI)		p
Onset-therapy (days)	0.651 (0.463–0.915)		0.013*

*$p < 0.05$.

TABLE 3 Factors related to prognosis of ascending sudden sensorineural hearing loss (SSNHL).

Variable	Un-CR (n = 38)	CR (n = 84)	p
Univariate analysis			
Age	40.08 ± 14.143	37.57 ± 12.283	0.322
Onset-therapy	4.82 ± 4.591	2.77 ± 1.865	0.011*
PTA at admission	46.84 ± 19.723	43.414 ± 18.785	0.360
Gender (female)	19/38 (50%)	43/84 (51.19%)	0.903
Lateral (left)	20/38 (52.63%)	44/84 (52.38%)	0.980
Tinnitus	36/38 (94.74%)	75/84 (89.29%)	0.330
Dizziness	7/38 (18.42%)	11/84 (13.10%)	0.442
Aural fullness	17/38	46/84	0.333
Headache	1/38	7/84	0.433
Multivariate analysis			
	OR (95%CI)		p
PTA at admission	0.981 (0.960–1.003)		0.092
Onset-therapy (days)	0.781 (0.671–0.909)		0.001*

*$p < 0.05$.

lower than that of ALFHL, albeit not significantly. Among them, 64.75% recovered within 10 days after the onset, accounting for 94.05% (79/84) of all recovered patients (**Figure 1**). Therefore, both ALFHL and ascending SSNHL were recovered within 10 days after onset, suggesting that both ALFHL and ascending SSNHL might lie in common pathogenesis. It also suggested that one must have reasonable expectations of patients who have not completely recovered after 10 days from onset (**Table 4**).

Discussion

The present study found that compared to ascending SSNHL, patients with ALFHL had a lower age of onset, lower PTA at admission, lower pure tone threshold at 1 and 2 kHz, female tendency, shorter time from onset to recovery, and a tinnitus incidence; however, the CR was not statistically different.

No difference in the CR between ascending SSNHL and ALFHL

Several studies showed that audiogram shape is a major prognostic factor of SSNHL, divided into four clinical types: ascending, descending, flat, and profound (Chung et al., 2015). These factors guide the prognosis of patients with SSNHL.

Among all the four types, the ascending type has the best prognosis: 63–88% (Watanabe and Suzuki, 2018). Similarly, patients with ALFHL also showed a good prognosis. Typically, ALFHL has a better prognosis than SSNHL and responds well to treatment. Some studies reported that 32–65% of ALFHL patients recover their hearing spontaneously without treatment (Mattox and Simmons, 1977; Conlin and Parnes, 2007). Choo et al. (2017) found that about 70% of ALFHL patients treated with steroid therapy had recovered hearing. Nonetheless, whether ALFHL is an independent disease is yet controversial. Some studies considered ALFHL as a subtype of SSNHL, which has a better prognosis than other types (Shaia and Sheehy, 1976; Mattox and Simmons, 1977). In contrast, because of the good prognosis, high recurrence rate, ease of development into MD, and some other clinical characteristics, some studies classified it as a type of disease independent of SSNHL.

The results of this study did not present any significant difference in the CR between patients with ALFHL and ascending SSNHL. Compared to ascending SSNHL, patients with ALFHL were younger and with less severe hearing loss. In addition, ALFHL might be caused by various causes, among which CH is widely recognized (Noguchi et al., 2004; Junicho et al., 2008). It is illustrated that the apical turn of the cochlea is more sensitive to pressure changes than the basal turn; hence, the inner ear hydrops begins at the apical turn of the cochlea and subsequently extends to the cochlear aqueduct and the vestibular apparatus (7). Thus, ALFHL may be the early stage of ascending SSNHL; with aggravated inner ear hydrops, the degree of hearing loss is also aggravated and combined symptoms, resulting in tinnitus. The pathogenesis of ascending SSNHL is similar to ALFHL and might be related

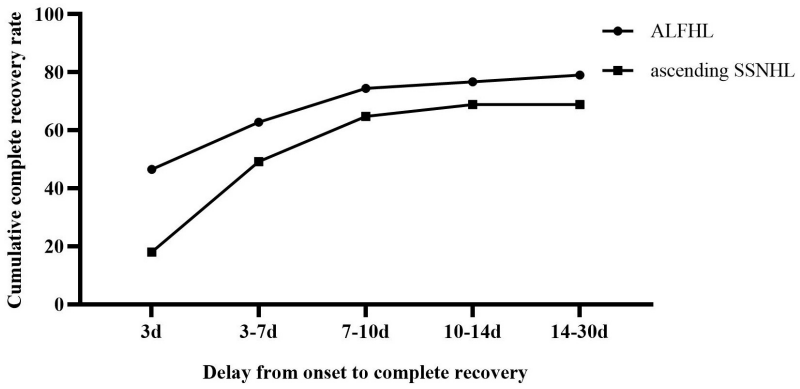

FIGURE 1
Distribution of onset-CR of acute low-frequency hearing loss (ALFHL) and ascending sudden sensorineural hearing loss (SSNHL).

TABLE 4 Distribution of onset-CR of patients with ascending sudden sensorineural hearing loss (SSNHL) and acute low-frequency hearing loss (ALFHL).

		3 days	3–7 days	7–10 days	10–14 days	14–30 days
ALFHL	Cases	20/43	7/43	5/43	1/43	1/43
	CR rate	46.51%	16.28%	11.63%	2.33%	2.33%
	Cumulative frequency	46.51%	62.79%	74.42%	76.74%	79.07%
Ascending SSNHL	Cases	22/122	38/122	19/122	5/122	0/122
	CR rate	18.03%	31.15%	15.57%	4.10%	0.00%
	Cumulative frequency	18.03%	49.18%	64.75%	68.85%	68.85%

to CH (Junicho et al., 2008; Editorial Board of Chinese Journal of Otorhinolaryngology Head and Neck Surgery; Society of Otorhinolaryngology Head and Neck Surgery, Chinese Medical Association, 2015).

Furthermore, in view of the similar prognosis between ascending SSNHL and ALFHL, for patients with ascending SSNHL, partial treatment can be reduced, which is of great significance for optimizing medical resources. Because the etiology is usually unknown, treatments have been empiric (Wei et al., 2013). The lack of one or more uniformly accepted treatment(s) potentially decreases the cost of management.

Factors related to the prognosis of ALFHL and ascending SSNHL

Factors affecting prognosis in patients with SSNHL include delay from onset-therapy, the occurrence of dizziness or tinnitus, type of audiogram, and initial hearing loss (Bespalova et al., 2001). Consistent with these findings, the current study showed that PTA at admission and delay from onset-therapy were independent factors related to the prognosis of ascending SSNHL. Many studies speculated that the earlier the patient receives treatment, the better the prognosis (Shaia and Sheehy, 1976; Byl, 1984). Byl (1984) demonstrated that when patients receive treatment within 7 days from onset, the recovery rate is 56%, while the recovery rate of patients who received treatment for >30 days after onset is only 27%. Shaia and Sheehy (1976) also proposed that the prognosis is improved when patients are treated within 30 days from onset. Moreover, the severity of hearing loss was a major prognostic factor. In the present study, the PTA at admission is an independent prognostic factor for patients with ascending SSNHL. Conversely, in patients with ALFHL, PTA at admission is not related to prognosis, which might be due to mild hearing loss. In the case of delay from onset to complete recovery, Sano et al. (1998) speculated that patients with hearing loss <70 dB at admission are likely to heal within 8 days, which is consistent with the results of this study, i.e., most patients with ascending sudden SSNHL and ALFHL recovered within 10 days (70.3%, 116/165).

Limitations

Nevertheless, the present study also has some limitations. First, this retrospective analysis caused information bias in the statistical analysis. Second, this study collected patients with ascending SSNHL and ALFHL admitted to the hospital; however, several patients with ascending SSNHL, especially with ALFHL, would prefer to receive outpatient treatment because

of mild hearing loss, causing a certain degree of selection bias. Third, the follow-up of this study was short, i.e., followed up to 1 month after treatment, making it impossible to collect data on the long-term prognosis and recurrence of patients with ascending SSNHL and ALFHL; these would be assessed in our follow-up studies.

Conclusion

The PTA at admission and delay from onset-therapy were independent factors related to the prognosis of ascending SSNHL, while only the delay from onset-therapy was remarkably related to the prognosis of ALFHL. Audiogram shape is a prognostic factor of SSNHL; also, no statistical difference was observed in the CR rate between ALFHL and ascending SSNHL, which manifests as a similar audiogram shape, suggesting that ascending SSNHL and ALFHL share some common pathological mechanisms.

Data availability statement

The raw data supporting the conclusions of this article will be made available by the authors, without undue reservation.

Ethics statement

The studies involving human participants were reviewed and approved by the Peking University People's Hospital Ethical Permission Committee. The patients/participants provided their written informed consent to participate in this study.

Author contributions

XM designed and conceptualized this study, interpreted the data, and revised the manuscript. TD, YC, and YJ designed and conceptualized study, collected and analyzed the data, and drafted the manuscript for intellectual content. All authors contributed to the article and approved the submitted version.

Funding

This work was supported by the Peking University People's Hospital Scientific Research Development Funds (RDL2021–14 and RDY2021–25) and National Key Research and Development Program of China (2020YFC2005200).

Conflict of interest

The authors declare that the research was conducted in the absence of any commercial or financial relationships that could be construed as a potential conflict of interest.

Publisher's note

All claims expressed in this article are solely those of the authors and do not necessarily represent those of their affiliated organizations, or those of the publisher, the editors and the reviewers. Any product that may be evaluated in this article, or claim that may be made by its manufacturer, is not guaranteed or endorsed by the publisher.

References

Berrettini, S., Seccia, V., Fortunato, S., Forli, F., Bruschini, L., Piaggi, P., et al. (2013). Analysis of the 3-dimensional fluid-attenuated inversion-recovery (3D-FLAIR) sequence in idiopathic sudden sensorineural hearing loss. *JAMA Otolaryngol. Head Neck Surg.* 139, 456–464. doi: 10.1001/jamaoto.2013.2659

Bespalova, I. N., Van Camp, G., Bom, S. J., Brown, D. J., Cryns, K., DeWan, A. T., et al. (2001). Mutations in the Wolfram syndrome 1 gene (WFS1) are a common cause of low frequency sensorineural hearing loss. *Hum. Mol. Genet.* 10, 2501–2508. doi: 10.1093/hmg/10.22.2501

Byl, F. M. Jr. (1984). Sudden hearing loss: Eight years' experience and suggested prognostic table. *Laryngoscope* 94(5 Pt 1), 647–661.

Choo, O. S., Yang, S. M., Park, H. Y., Lee, J. B., Jang, J. H., Choi, S. J., et al. (2017). Differences in clinical characteristics and prognosis of sudden low- and high-frequency hearing loss. *Laryngoscope* 127, 1878–1884. doi: 10.1002/lary.26382

Chung, J. H., Cho, S. H., Jeong, J. H., Park, C. W., and Lee, S. H. (2015). Multivariate analysis of prognostic factors for idiopathic sudden sensorineural hearing loss in children. *Laryngoscope* 125, 2209–2215. doi: 10.1002/lary.25196

Conlin, A. E., and Parnes, L. S. (2007). Treatment of sudden sensorineural hearing loss: II. A meta-analysis. *Arch. Otolaryngol. Head Neck Surg.* 133, 582–586. doi: 10.1001/archotol.133.6.582

Editorial Board of Chinese Journal of Otorhinolaryngology Head and Neck Surgery; Society of Otorhinolaryngology Head and Neck Surgery, Chinese Medical Association (2015). Guideline of diagnosis and treatment of sudden deafness (2015). *Zhonghua Er Bi Yan Hou Tou Jing Wai Ke Za Zhi* 50, 443–447.

Fuse, T., Aoyagi, M., Funakubo, T., Sakakibara, A., and Yoshida, S. (2002). Short-term outcome and prognosis of acute low-tone sensorineural hearing loss by administration of steroid. *ORL J. Otorhinolaryngol. Relat. Spec.* 64, 6–10. doi: 10.1159/000049079

Hwang, J. H., Tsai, S. J., Liu, T. C., Chen, Y. C., and Lai, J. T. (2018). Association of tinnitus and other cochlear disorders with a history of migraines. *JAMA Otolaryngol. Head Neck Surg.* 144, 712–717. doi: 10.1001/jamaoto.2018.0939

Imamura, S., Nozawa, I., Imamura, M., and Murakami, Y. (1997). Clinical observations on acute low-tone sensorineural hearing loss. Survey and analysis of 137 patients. *Ann. Otol. Rhinol. Laryngol.* 106, 746–750. doi: 10.1177/000348949710600906

Jung, A. R., Kim, M. G., Kim, S. S., Kim, S. H., and Yeo, S. G. (2016). Clinical characteristics and prognosis of low frequency sensorineural hearing loss without vertigo. *Acta Otolaryngol.* 136, 159–163. doi: 10.3109/00016489.2015.1094824

Junicho, M., Aso, S., Fujisaka, M., and Watanabe, Y. (2008). Prognosis of low-tone sudden deafness - does it inevitably progress to Meniere's disease? *Acta Otolaryngol.* 128, 304–308. doi: 10.1080/00016480601002096

Kuhn, M., Heman-Ackah, S. E., Shaikh, J. A., and Roehm, P. C. (2011). Sudden sensorineural hearing loss: A review of diagnosis, treatment, and prognosis. *Trends Amplif.* 15, 91–105. doi: 10.1177/1084713811408349

Li, F. J., Wang, D. Y., Wang, H. Y., Wang, L., Yang, F. B., Lan, L., et al. (2016). Clinical study on 136 children with sudden sensorineural hearing loss. *Chin. Med. J. (Engl.)* 129, 946–952. doi: 10.4103/0366-6999.179791

Mattox, D. E., and Simmons, F. B. (1977). Natural history of sudden sensorineural hearing loss. *Ann. Otol. Rhinol. Laryngol.* 86(4 Pt 1), 463–480. doi: 10.1177/000348947708600406

Merchant, S. N., Adams, J. C., and Nadol, J. B. Jr. (2005). Pathology and pathophysiology of idiopathic sudden sensorineural hearing loss. *Otol. Neurotol.* 26, 151–160. doi: 10.1097/00129492-200503000-00004

Noguchi, Y., Nishida, H., Tokano, H., Kawashima, Y., and Kitamura, K. (2004). Comparison of acute low-tone sensorineural hearing loss versus Meniere's disease by electrocochleography. *Ann. Otol. Rhinol. Laryngol.* 113(3 Pt 1), 194–199. doi: 10.1177/000348940411300304

Qian, Y., Zhong, S., Hu, G., Kang, H., Wang, L., and Lei, Y. (2018). Sudden sensorineural hearing loss in children: A report of 75 cases. *Otol. Neurotol.* 39, 1018–1024. doi: 10.1097/mao.0000000000001891

Rossini, B. A. A., Penido, N. O., Munhoz, M. S. L., Bogaz, E. A., and Curi, R. S. (2017). Sudden sensorioneural hearing loss and autoimmune systemic diseases. *Int. Arch. Otorhinolaryngol.* 21, 213–223. doi: 10.1055/s-0036-1586162

Sano, H., Okamoto, M., Shitara, T., and Hirayama, M. (1998). What kind of patients are suitable for evaluating the therapeutic effect of sudden deafness? *Am. J. Otol.* 19, 579–583.

Shaia, F. T., and Sheehy, J. L. (1976). Sudden sensori-neural hearing impairment: A report of 1,220 cases. *Laryngoscope* 86, 389–398. doi: 10.1288/00005537-197603000-00008

Siegel, L. G. (1975). The treatment of idiopathic sudden sensorineural hearing loss. *Otolaryngol. Clin. North Am.* 8, 467–473.

Stachler, R. J., Chandrasekhar, S. S., Archer, S. M., Rosenfeld, R. M., Schwartz, S. R., Barrs, D. M., et al. (2012). Clinical practice guideline: Sudden hearing loss. *Otolaryngol. Head Neck Surg.* 146(Suppl. 3), S1–S35. doi: 10.1177/0194599812436449

Thai-Van, H., Bounaix, M. J., and Fraysse, B. (2001). Menière's disease: Pathophysiology and treatment. *Drugs* 61, 1089–1102. doi: 10.2165/00003495-200161080-00005

Watanabe, T., and Suzuki, M. (2018). Analysis of the audiogram shape in patients with idiopathic sudden sensorineural hearing loss using a cluster analysis. *Ear Nose Throat J.* 97, E36–E40. doi: 10.1177/014556131809700706

Wei, B. P., Stathopoulos, D., and O'Leary, S. (2013). Steroids for idiopathic sudden sensorineural hearing loss. *Cochrane Database Syst. Rev.* 2013:Cd003998. doi: 10.1002/14651858.CD003998.pub3

Xie, W., Dai, Q., Liu, J., Liu, Y., Hellström, S., and Duan, M. (2020). Analysis of clinical and laboratory findings of idiopathic sudden sensorineural hearing loss. *Sci. Rep.* 10:6057. doi: 10.1038/s41598-020-63046-z

Yamasoba, T., Sugasawa, M., Kikuchi, S., Yagi, M., and Harada, T. (1993). An electrocochleographic study of acute low-tone sensorineural hearing loss. *Eur. Arch. Otorhinolaryngol.* 250, 418–422. doi: 10.1007/bf00180389

frontiers | Frontiers in Neurology

TYPE Original Research
PUBLISHED 16 February 2023
DOI 10.3389/fneur.2022.1054704

Check for updates

OPEN ACCESS

EDITED BY
Sulin Zhang,
Huazhong University of Science and Technology, China

REVIEWED BY
Koji Nishimura,
Teikyo University Mizonokuchi Hospital, Japan
Yuanping Xiong,
First Affiliated Hospital of Nangchang University, China
Ming Xia,
Shandong Provincial Hospital, China

*CORRESPONDENCE
Min Xu
✉ ent551205@163.com
Ying Cheng
✉ smart81110@mail.xjtu.edu.cn

SPECIALTY SECTION
This article was submitted to Neuro-Otology, a section of the journal Frontiers in Neurology

RECEIVED 27 September 2022
ACCEPTED 22 December 2022
PUBLISHED 16 February 2023

CITATION
Ma W, Li H, Hu J, Gao Y, Lv H, Zhang X, Zhang Q, Xu M and Cheng Y (2023) Role of a novel mouse mutant of the *Galnt2*$^{tm1Lat/tm1Lat}$ gene in otitis media. *Front. Neurol.* 13:1054704. doi: 10.3389/fneur.2022.1054704

COPYRIGHT
© 2023 Ma, Li, Hu, Gao, Lv, Zhang, Zhang, Xu and Cheng. This is an open-access article distributed under the terms of the Creative Commons Attribution License (CC BY). The use, distribution or reproduction in other forums is permitted, provided the original author(s) and the copyright owner(s) are credited and that the original publication in this journal is cited, in accordance with accepted academic practice. No use, distribution or reproduction is permitted which does not comply with these terms.

Role of a novel mouse mutant of the *Galnt2*$^{tm1Lat/tm1Lat}$ gene in otitis media

Weijun Ma[1], Heng Li[2], Juan Hu[1], Ying Gao[1], Hui Lv[1], Xiaotong Zhang[1], Qing Zhang[3], Min Xu[1]* and Ying Cheng[1]*

[1]Department of Otolaryngology-Head and Neck Surgery, Second Affiliated Hospital of Xi'an Jiaotong University, Xi'an, Shaanxi, China, [2]Department of Otorhinolaryngology, Shiquan County Hospital, Ankang, Shaanxi, China, [3]Department of Otolaryngology-Head and Neck Surgery, Xinhua Hospital Affiliated to Shanghai Jiao Tong University School of Medicine, Shanghai, China

Genetic susceptibility is one of the most important causes of otitis media (OM). Mutant *Galnt2* homozygote (*Galnt2* $^{tm1Lat/tm1Lat}$) mimics human otitis media in comparable pathology and causes hearing loss. Otitis media is characterized by effusion and dysregulated mucosa proliferation and capillary expansion in the middle ear cavity, which is associated with hearing loss. The mucociliary dysfunction could be seen in the middle ear cavity (MEC) in a patient harboring the disease that develops in severity with age by a scanning electron microscope. Tumor necrosis factor alpha (TNF-α), transforming growth factor-beta 1 (TGF-β1), Muc5ac, and Muc5b upregulate the expression in the middle ear, which correlates with inflammation, craniofacial development, and mucin secretion. The mouse model with a mutation in the *Galnt2* (*Galnt2* $^{tm1Lat/tm1Lat}$) was explored in this study as a novel model of human otitis media.

KEYWORDS

genetic susceptibility, otitis media, mutant *Galnt2* homozygote, hearing loss, mouse model

Introduction

Otitis media (OM) is the main cause of hearing loss among children, which is featured primarily as an inflammation of the middle ear mucosa (1). A marked association of sequelae and complications is observed following OM with hearing loss. The OM-related hearing loss is reported to affect 30.82 per 10,000 patients, with ∼21,000 people dying annually from the complications of OM (2). Human susceptibility to OM is a multifactor process, including the participation of the adaptive and native immune systems, dysfunction of the Eustachian tube, the invasion of a viral load and bacteria, and the participation of genes and environment (3). A growing body of evidence is available to suggest that heredity is an important risk factor for OM (4, 5). The animal models of OM with defined gene defects offer significant value for the study of the disease course and pathogenesis of the OM (6). Tumor necrosis factor alpha (TNF-α) plays a key role in initiating and maintaining inflammatory responses in various diseases. In the OM, the homeostatic imbalance of TNF-α is the main cause of its chronic inflammation. The upregulation of TNF-α is always evident in the OM (7). Genetic defects leading to the upregulation of TNF-α provide insights into the construction of the OM models.

GALNT2 is a gene on chromosome 1q42 within ∼150 kb of the lead single-nucleotide polymorphism (SNP), which is located in an intron of the gene. It belongs to the N-acetyl galactosamine (GalNAc)-transferase family transferring an N-acetyl galactosamine to the hydroxyl group of a serine/threonine residue at the start of O-linked oligosaccharide biosynthesis (8). This glycosylation plays an important role in insulin resistance diabetes and chronic inflammation (9, 10). In addition, polypeptide N-acetylgalactosaminyltransferase 2

(GALNT2) knockout has been demonstrated to significantly upregulate the TNF-α levels through a disintegrin and metalloprotease (ADAM)-mediated ectodomain (10).

Exon 7 deletion in Galnt2 mouse was originally intended to be elaborated in a study on the lungs, but it was unexpectedly discovered that mice have otitis media. This study aimed to analyze the ear to determine whether otitis media was an isolated case or widespread in mutants. The present study hypothesized that if OM were prevalent in Galnt2 mutants, it would probably be due to the upregulation of TNF-α that caused chronic inflammation in the middle ear. It was also found that mice with this mutation develop otitis media from birth and exhibit progressive hearing loss, effusion of the middle ear cavity, and upregulated TNF-α and transforming growth factor beta (TGF-β) in the middle ear. In addition, malformation and dysfunction of the Eustachian tube, dysregulated mucosa proliferation and capillary expansion, and the mucociliary impairment are all found to lead to the incidence of OM in the *Galnt2* homozygous mutant mice.

Materials and methods

Mouse husbandry and genotyping

Galnt2$^{tm1Lat/tm1Lat}$ homozygous mice were obtained from and bred at the Wolstein Animal Research Facility of the Case Western Reserve University. A total of 64 homozygous Galnt2$^{tm1Lat/tm1Lat}$ mutant and 60 wild-type mice were used in the present study. Mice were raised in a ventilated room with a 12-h light/dark cycle and given free access to food at 21°C. Mice of <7 days were genotyped by the polymerase chain reaction (PCR), and the experimental protocol was approved by the Health Sciences Institutional of Animal Care Center and the Ethics Committee of Case Western Reserve University (approval numbers: 2008-0174 and 2008-0156) and the Second Affiliated Hospital of Xi'an Jiaotong University (approval number: 2019-268). The PCR primers used for tail snip genotyping are presented as follows:

P1: GGTCCTGACCTTCCTAGACAGTCACTGC
P2: GCACTCTCCAAGGGCATGACAGAGC
P3: GGGGGAGGATTGGGAAGACAATAGC

A comprehensive evaluation of hearing impairment

Wild-type and mutant mice were anesthetized with avertin (0.5 mg per gram of mice). The procedure was performed at normal temperature in a quiet room. A computer-aided evoking system (Intelligent Hearing Systems, Miami, FL, USA) was used to measure the auditory brainstem response (ABR) and distortion product otoacoustic emission (DPOAE) amplitudes of mice, as reported earlier (11). The present study also utilized a tympanometer from Maico Diagnostics (Maico Co, Ltd., Berlin, Germany) to measure the condition of the tympanic membrane (12). The measurement data were described by normal distribution and recorded by a two-way analysis of variance (ANOVA) with Bonferroni's *post-hoc* test.

Observation of the middle ear and the structure of the adjacent skull base

Both wild-type and Galnt2$^{tm1Lat/tm1Lat}$ mutant mice at the age of 2 months were killed by CO_2 asphyxiation ($n = 6$ in each genotype, including three male and three female mice). The angle from the middle line of the skull base and the bony component of the Eustachian tube were measured for both genotypes. The tympanic membrane and the skull base were examined, and pictures were taken with a microscope (Leica S6D, Leica Microsystems, Wetzlar, Germany). The ImageJ software (Java 1.6.0-20 (32-bit) NIH, USA) was applied for angle measurement. The measurement data were analyzed by Student's *t*-test.

Bacterial culture and identification

Four mice at the age of 3 months in each group were killed by CO_2 asphyxiation. The middle ear of the mice was isolated and washed with sterile saline. After shaking, the water was inoculated onto culture plates and identified by morphological characterization and matrix-assisted laser desorption/ionization-time of flight mass spectrometry (MALDI-TOF MS).

Histological preparation of the middle and inner ears

Both wild-type mice ($n = 4$) and Galnt2$^{tm1Lat/tm1Lat}$ mutant mice ($n = 4$) were killed in a time span ranging from 7 days to 9 months. Bullae were fixed in paraformaldehyde (PFA) with 4% concentration at 4°C for 24 h and then in ethylenediaminetetraacetic acid (EDTA) with 10% concentration for decalcification. After dehydration and cleaning, samples were embedded in a paraffin block and cut into 5-μm sections by a rotary microtome (American Optical, Buffalo, New York, USA) to place on slides (Fisher Scientific Co, Ltd., Pittsburgh, PA, USA). Samples were embedded on Tissue-Tek OCT (Sakura Finetek, Torrance, CA, USA) without dehydration and cut into 10-μm sections with a cryostat microtome (Leica, Nussloch, Germany).

Sample staining

The protocol from Rosen's Lab was used for hematoxylin and eosin (H&E) staining (http://www.bcm.edu/rosenlab), and Mayer's Mucicarmine Staining was used for the identification of goblet cells in accordance with the protocol from Electron Microscopy Sciences. All sample sections were screened under a light microscope (Leica DFC500, Germany).

Scoring for pathology

A 4-point scoring scale was designed to evaluate the pathology of the middle and inner ear samples, as described in an earlier study (13). For recording the absence of pathology in the middle and inner ears, several symbols were assigned: +, scarce pathology; ++, prevalent pathology; and + + +, pathology involving the

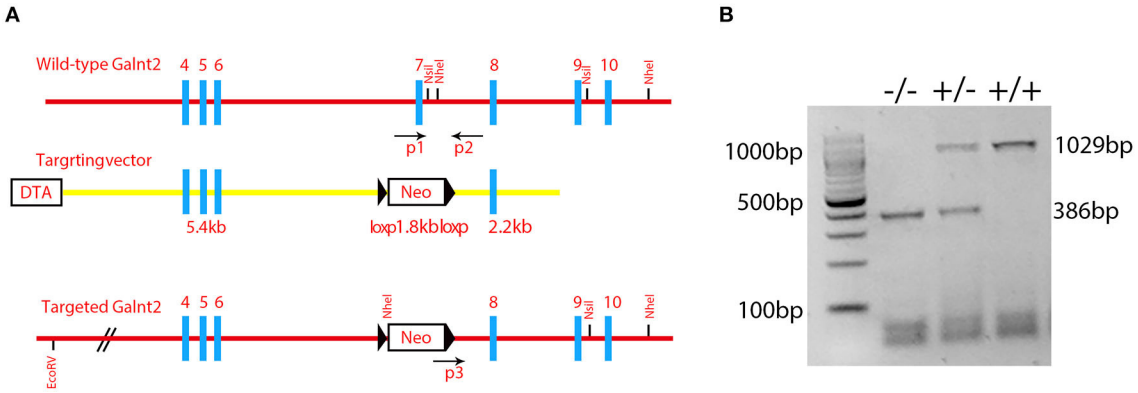

FIGURE 1
Identification of the mutant mice. **(A)** A schematic diagram of the *Galnt2* targeting vector, *Galnt2* genomic sequence, and the targeted allele. Gray rectangles represent exons; bold blue lines represent the region homologous to the *Galnt2* genomic sequence; black triangles represent *lox*P sites. Neo, neomycin positive selection cassette; DTA, diphtheria toxin negative selection cassette. P1, P2, and P3 indicate genotyping primers. A Neo cassette with flanking *lox*P sites and homology mini-arms cloned into the Galnt2 sequence to replace the exon 7 that contains the amino acid residues DSHCEC, crucial for Galnt2 catalytic activity. **(B)** Genotyping of Galnt2 variants. The wild-type mice (+/+) show one band (1029 bp), the mutant mice (-/-) show one band (386 bp), and the heterozygous mice (+/-) show two bands (386 bp and 1029 bp).

entire middle and inner ears. Pathologies scored as aforementioned included middle ear effusion, inner ear effusion, infiltration of inflammatory cells, the proliferation of epithelial cells, and density of goblet cells. Category data were measured by the chi-square test.

Scanning electron microscopy

Wild-type mice ($n = 3$) and Galnt2$^{tm1Lat/tm1Lat}$ mutant mice ($n = 3$) were killed at the ages of 3 months and 6 months. Bullae were dissected and immersed in glutaraldehyde with a 2.5% concentration of cacodylic acid in phosphate-buffered saline (PBS) with 0.1 mol/L (pH = 7.2) at 4°C for one night. Dissection was performed to expose the middle ear cavity. Samples were washed with distilled water 6 times and dehydrated in graded ethanol, after fixing 1% osmium tetroxide in 0.1 M cacodylic acid (pH = 7.2). All samples were dried by the CO_2 critical point, followed by sputter plumbum coating. All samples were screened by a high-resolution electron microscope (Helios NanoLab 650; FEI, Hillsboro, OR, USA).

Reverse transcription-polymerase chain reaction analysis

The mice ($n = 3$ in each group) were killed at 7 months, from which bullae were isolated for RNA analysis, immediately as described in the previous section. The primers used for RT-PCR of these mouse genes were laid out as follows:

GAPDH: AACTTTGGCATTGTGGAAGG and GGAGACAA CCTGGTCCTCAG;

TNF-α: CCACCACGCTCTTCTGTCTAC and CCTTGAAGA GAACCTGGGAGT;

TGF-β1: AGCCCGAAGCGGACTACTAT and TCCACATGTTG CTCCACACT;

Muc5a: TGGAAGGATGCTATCCCAAG and CACCAGCAT TGTGGGTACAG;

Muc5b: GACACCATCTATGGGGTTGG and CAGGACTGTT CACCCAGGTT;

The PCR products were subjected to agarose gel electrophoresis in which the intensity of the gray band was digitalized and calculated using the ImageJ software and referred by GAPDH.

Immunofluorescent staining for TNF-α and TGF-β and proliferating cell nuclear antigen

All sections were washed with PFA at 1.5% concentration for 10 min and then with PBS two times for 5 min. Next, the sections were permeabilized in Triton X-100 with 0.5% concentration for 5 min, then washed with PBS two times for 5 min, and finally blocked in goat serum of 3% concentration + bovine serum albumin (BSA) of 2% concentration for 1 h. All samples were immersed in anti-TNF-α, anti-TGF-β, or anti-PCNA (1:200 dilution) subsequently and incubated at 4°C for one night. All samples were immersed in the antibody Alexa 488 (1:400 dilution) again for 1 h after washing two times with PBS for 5 min. The 4′,6-diamidino-2-phenylindole (DAPI) staining of samples was also performed for 15 min. Finally, Vectashield antifade mounting medium (Vector Laboratories, Burlingame, CA) was used for preserving the fluorescence of the section, and an immunofluorescence microscope (DFC500, Leica Co, Ltd., Germany) was used for further observation.

Results

Characteristics of *Galnt2*

Galnt2 encodes a member of the glycosyltransferase 2 protein family. It is involved in the o-linked glycosylation *via* serine and threonine. The galnt2 genome DNA contains 10 exons. The *Galnt2*(-/-) mutant used in this study was the deletion of exon 7 that contained the amino acid residues DSHCEC crucial for GALNT2 catalytic activity (Figure 1A). The present study designed primers

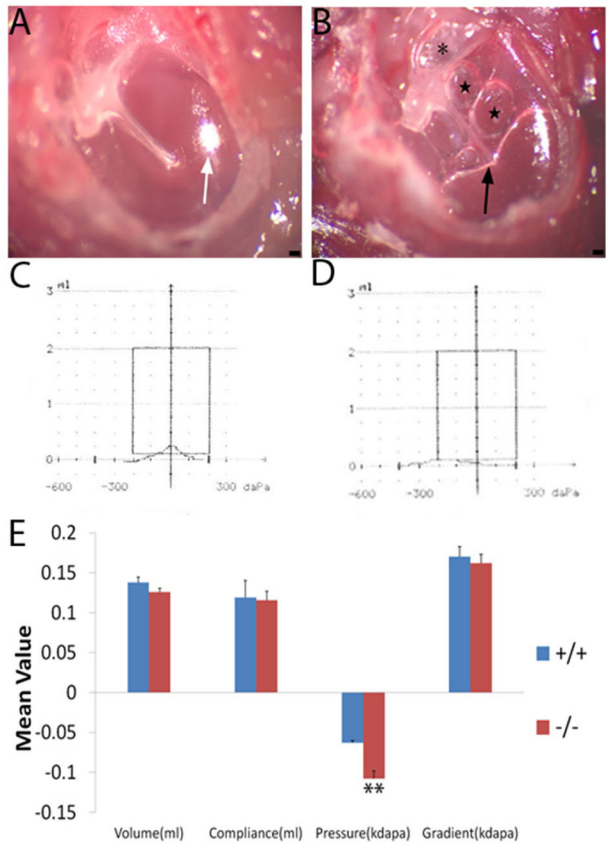

FIGURE 2
Tympanic membrane image and a comparison of the mean value of tympanometry parameters. Nine wild-type mice (+/+) and eight mutant mice (-/-) were used to measure the tympanometry at the age of 2 months. **(A, B)**: Tympanic membrane image ($n = 3$, each group) under an anatomical microscope. The wild-type mouse **(A)** displays a normal tympanic membrane with a subuliform light cone (white arrow) on its anteroinferior quadrant. In the ear of the mutant mouse **(B)**, the retraction and adherence of the tympanal flaccid part (asterisk) were visible, hyperemia around the malleus, effusion (black arrow), and bubbles (star) in the middle ear cavity and an abnormal light cone were detected. **(C, D)**: The wild-type **(C)** mouse shows a normal A-type curve with a peak at 0 pressure. The mutant mouse **(D)** exhibits an abnormal C-type curve with a peak at negative pressure. **(E)** Significant differences in pressure were noticed between the wild type and mutant mice at the age of 2 months. Error bar represents the standard error (SE) of the mean. $^*P < 0.05$, $^{**}P < 0.01$. Scale bar = 50 μm.

near the exon 7 position, identified the wild type galnt2 and mutant galnt2 by PCR, and verified the successful construction of galnt2 mutants (Figure 1B).

Gross observation of the middle ear

The tympanic membrane of the wild-type and the mutant (Figure 1) mouse at 2 months of age was, respectively, observed under an anatomical microscope. The mutant mice exhibited severe effusion of the middle ear cavity, retraction and adherence of the tympanal flaccid part, hyperemia around the melleus, and light-cone deformation and disappearance, when compared with the wildtype ones (Figures 2A, B). The effusion of the middle ear cavity and the retraction and adherence of the tympanal flaccid part were characteristic manifestations of the OM.

The function of the middle ear by the tympanometry assessment

Wild-type ($n = 9$) and mutant mice ($n = 8$) at 2 months of age were measured by tympanometry to assess the function of the middle ear. The tympanogram results were presented for comparison (Figure 2E). There was no difference in volume between wild-type and mutant mice. Similarly, for the compliance and gradient, no difference was found between the wild-type mice and the mutant ones. However, the negative pressure of the middle ear was more significant in the mutant mice when compared with the wild-type ones. Negative pressure was correlated with otitis media and was more likely to cause effusion in the middle ear cavity (14, 15). The tympanogram of a 2-month-old mouse in the wild-type group represented the normal curve (Figure 2C), while that in the mutant group represented the abnormal curve (Figure 2D).

ABR thresholds and DPOAE

The ABR thresholds of mice from 3 weeks to 9 months were consistently measured in both groups. The mean ABR thresholds were 55 (click stimuli), 40 (8 KHz), 35(16 KHz), and 60 (32 KHz) decibel of sound pressure level (dBSPL), respectively, indicating the hearing impairment (16). Along with the growth of age, the ABR thresholds increased in both wild-type and mutant mice groups, especially in the mutant ones. The mean ABR thresholds of mutant mice were significantly higher than those of the wild-type ones at each stimulus frequency and at several time points compared with the wild-type mice (Figures 3A–D). The mean DPOAE amplitudes of mutant mice were markedly lower when compared with those of the wild-type mice at frequencies of 8.8, 13.4, and 15.4 KHz (Figure 3E).

Abnormality in mutant mice by measurement of the Eustachian tube

The craniofacial abnormalities increased the susceptibility to otitis media (17, 18) which were measured between the wild-type and mutant groups matched by age. The 2-month-old wild type (+/+) and the mutant mice (-/-) ($n = 6$ in each genotype, including three male and three female mice) were used to measure the intersection angle between the midline and the Eustachian tube (Figures 4A, B). The intersection angle of the mutant mice was significantly larger than that of the wild-type mice (Figure 4C). The length and the width of the bony component of the Eustachian tube (Figures 4D, E) were also measured. A longer mean length of the Eustachian tube of wild-type mice was observed when compared with the mutant mice, whereas there was an increase in the mean width of the Eustachian tube of mutant mice when compared with the wild type mice. The length/width ratio of the wild type mice was higher than that of the mutant ones (Figure 4F). The Eustachian tube of mutant mice was shorter, wider, and more horizontal, which may increase the predisposition to OM.

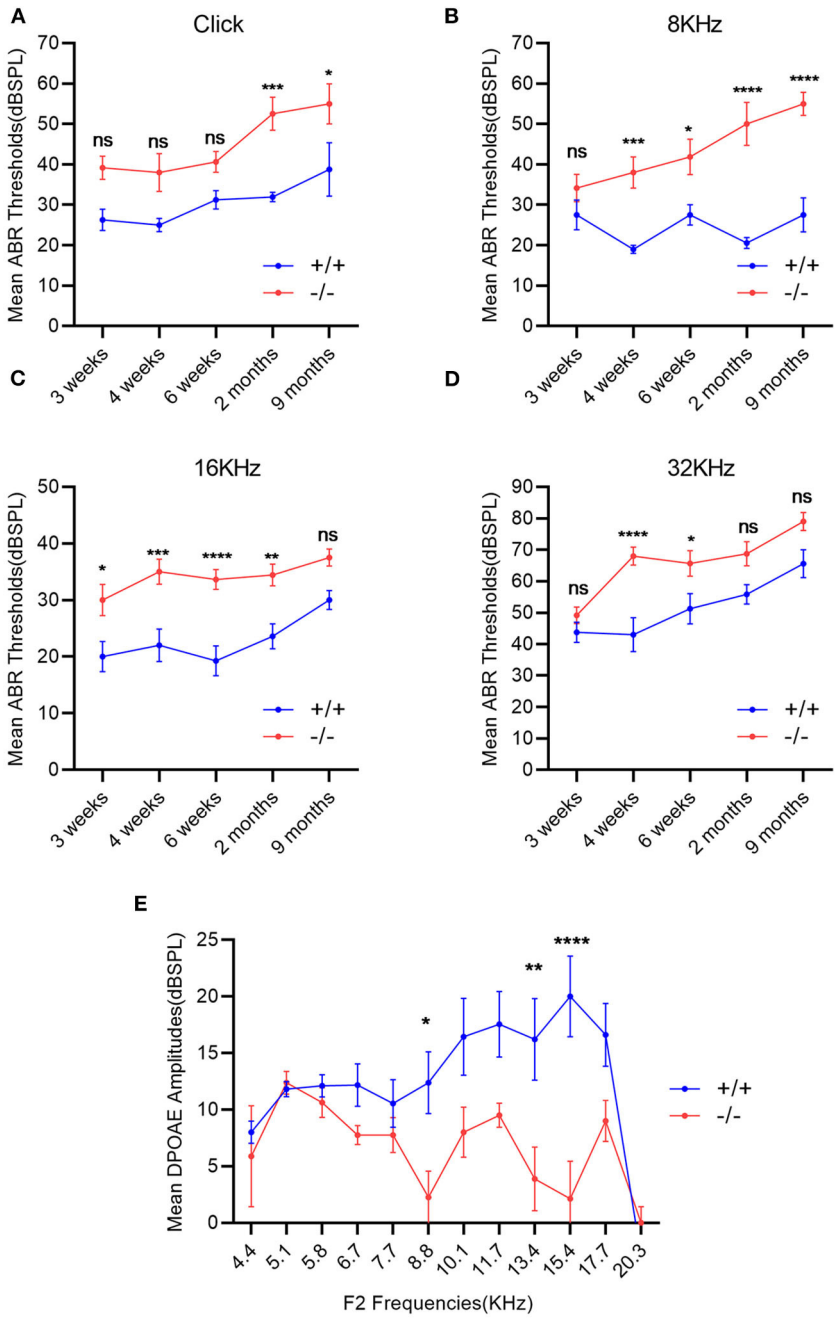

FIGURE 3
Evaluation of hearing impairment through auditory brainstem response (ABR) and distortion product otoacoustic emission (DPOAE). **(A–D)**: Wild-type mice (+/+, $n = 14$) and mutant mice (-/-, $n = 14$) were measured using the ABR thresholds at different stimulus frequencies and different time points. The mutant mice showed significantly higher mean ABR thresholds at each stimulus frequency and at several time points compared with the wild-type mice. **(E)** DPOAE amplitudes were recorded in wild-type mice (+/+, $n = 9$) and mutant mice (-/-, $n = 8$) at the age of 2 months. The mean DPOAE amplitudes of mutant mice were significantly lower than those of the wild-type mice at 8.8 KHz, 13.4 and 15.4 KHz. The error bar represents the standard error (SE) of the mean. *$P < 0.05$, **$P < 0.01$, ***$P < 0.001$, ****$P < 0.0001$.

Isolation of pathogenic bacteria from the middle ears of the mutant mice

Bacteria and their secretion are acknowledged as the most common causes of OM with effusion (19). To investigate the causative agent of OM in mutant mice, lavage of the middle ear from both types of 3-month-old mice was performed. *Bordetella hinzii* was specifically isolated from the middle ears of the mutant mice, whereas nothing was isolated from the middle ears of the wild-type mice. *Bordetella hinzii* belongs to the *Bordetella* genus, which was reported as a Gram-negative and short rod-shaped bacterium with positive oxidase and catalase isolated from both humans and mice suffering from cystic fibrosis (20).

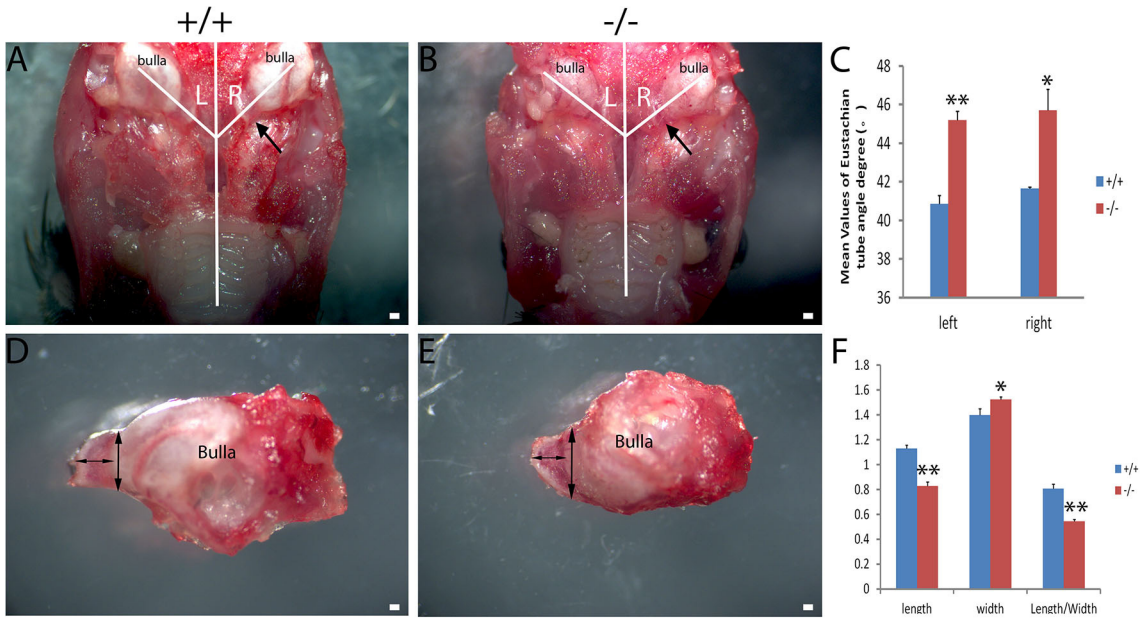

FIGURE 4
Assessment of the Eustachian tube's dysmorphology in Galnt2$^{tm1Lat/tm1Lat}$ mice. Wild-type (+/+) and mutant mice (-/-) at the age of 2 months ($n = 6$ for each genotype, equal numbers of male and female mice were selected) were used to measure the intersection angle between the midline and the Eustachian tube **(A, B)** and the length and width of the bony part of the Eustachian tube **(D, E)**. **(C)** The intersection angle is significantly larger in mutant mice, compared with the wild-type mice. Wild-type and mutant mice were used to measure the length and width of the bony part of the Eustachian tube **(D, E)**. **(F)** The mean length of the Eustachian tube in wild-type mice is longer than that of the mutant mice, whereas the mean width of the Eustachian tube in mutant mice is wider compared with the wild-type mice. The length/width ratio in wild-type mice is greater than that of the mutant mice. The arrow shows the location of the Eustachian tube. The double-ended arrow shows the length and width of the bony part of the Eustachian tube. The error bar represents the standard error (SE) of the mean. *$P < 0.05$, **$P < 0.01$. Scale bar = 200 μm.

Histopathologic evidence of OM in the mutant mice

The histopathology of the middle ear was evaluated to track the OM progression at different ages. In 1-week-old mice, the middle ear cavity was filled with mesenchymal cells in mutant mice, whereas the middle ear cavity was large and clean in wild-type mice (Figures 5A–D). At the age of 2 weeks, the mesenchymal cells disappeared in mutant mice and the middle ear cavity was clean in both groups. The mucosa of the middle ear cavity became thicker in mutant mice than in wild-type mice (Figures 5E–H). In 3-week-old mice, no obvious effusion occurred in mutant mice compared with the wild-type mice. However, the mucosa and submucosa hyperplasia developed further, and capillary proliferation occurred in the mutant mice (Figures 5I–L). At the age of 2 months, in wild-type mice, neither effusion nor inflammation was detected, and the middle ear cavity was covered with monolayer epithelium. In mutant mice, the middle ear cavity was filled with inflammatory infiltration and debris; the mucosa and submucosa hyperplasia progressed to a much greater severity; as regards the capillary proliferation and expansion, the Eustachian tube exhibited general thickening with the proliferation of epithelial cells (Figures 5M–P). Sparsely scattered Goblet cells were found in the mucosa of wild-type mice (Figure 6A). By contrast, goblet cells were presented with high density in the mucosa of mutant mice (Figure 6B). To assess the pathology in OM, a semi-quantitative evaluation was performed (Table 1). It suggested that the mutant mice exhibited an onset of the middle ear pathology at the age of 2 weeks and progressed to typical OM at the age of 2 months.

Cilia impairment in mutant mice by SEM

The present study assessed the cilia impairment of mucosa in mutant mice at two time points through a scanning electron microscope. A thick lawn of morphologically normal and distributed cilia was observed in the mucosa of the middle ear at both of the time points. For mutant mice, the short cilia of mucosa in the middle ear were observed with impairment and disruption. The impairment of the cilia was more serious at 6 months than at 3 months (Figures 7A–D). These results suggest that the mutant mice have difficulty in draining the secretion in the middle ear cavity, which may lead to OM.

Upregulated inflammatory cytokine in mutant mice by RT-PCR and immunofluorescence

The present study assessed the expression of the inflammation-related gene in mutant mice at the age of 7 months. RT-PCR revealed that the messenger RNA (mRNA) of TNF-α, transforming growth factor beta 1 (TGF-β1), Muc5ac, and Muc5b were significantly higher in mutant mice than in wild-type mice (Figure 8). To evaluate the protein levels of TNF-α and TGF-β1, sections of the middle ear of wild-type and mutant mice at the age of 6 months were stained with anti-TNF-α (Figures 9A–H), anti-TGF-β (Figures 9I–P), and anti-PCNA (Figures 9Q–X) antibody. The intensity of TNF-α, TGF-β, and

10.3389/fneur.2022.1054704

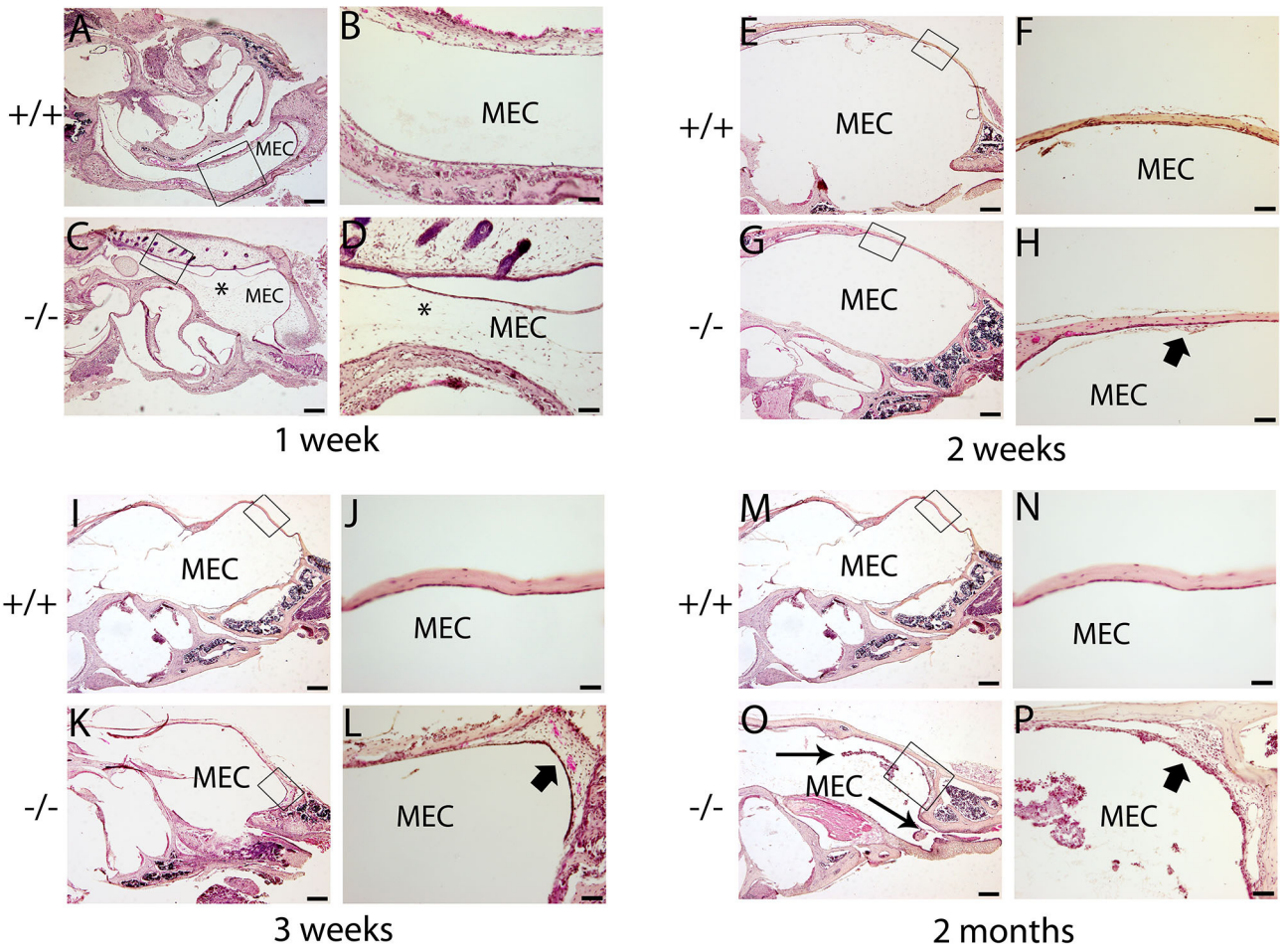

FIGURE 5
Hematoxylin and eosin (H&E) histology shows the development of middle ear structures and pathology. Wild type (+/+) and mutant mice (-/-) were observed for the morphology of the middle ear at each time point ($n = 4$ for each genotype). In each row, the right panel represents the enlarged image corresponding to the rectangular region on the left. **(A–D)** Representative images of mice at the age of 1 week. The middle ear cavity (MEC) was filled with mesenchymal cells [asterisk, **(C, D)**] in mutant mice, whereas the middle ear cavity was large and clean in wild-type mice **(A, B)**. **(E–H)**: Representative images of mice at the age of 2 weeks. The mesenchymal cells disappeared in mutant mice, and the middle ear cavity was clean in both groups **(E, G)**. The mucosa of the middle ear cavity becomes thicker (short arrow) in mutant mice compared with the monolayer epithelium in wild-type mice **(F, H)**. **(I–L)**: Representative images of mice at the age of 3 weeks. There was no obvious effusion in mutant mice, compared with the wild-type mice **(I, K)**. The mucosa and submucosa hyperplasia (short arrow) developed further and capillary proliferation occurred in the mutant mice **(L)**. **(M–P)**: Representative images of mice at the age of 2 months. In wild-type mice, neither effusion nor inflammation was detected, and the middle ear cavity was covered with monolayer epithelium **(M, N)**. In mutant mice, inflammatory infiltration and debris pervaded the middle ear cavity (long arrow), the mucosa and submucosa hyperplasia progressed to a much greater severity (short arrow), and as regards the capillary proliferation and expansion, the Eustachian tube exhibited general thickening with the proliferation of epithelial cells **(O, P)**. Scale bars: 200 μm **(A, C, E, G, I, K, M, O)**; 50 μm **(B, D, F, H, J, L, N, P)**. MEC, middle ear cavity.

PCNA was all higher in the mutant mice than in control (Figures 9F, N, V, H, P, X). The expression of TNF-α in the inflammatory tissue of the middle ear cavity was higher than that in the mucosa of the middle ear cavity (Figures 9F, H). The expression of TGF-β and PCNA was higher in the mucosa of the middle ear cavity compared to the inflammatory tissue of the middle ear cavity (Figures 9N, V, P, X).

Discussion

In this study, we have proven that *Galnt2* mutant mice were prone to OM. The *Galnt2* mutant OM mouse model was similar to the one with the *Hyp-Duk/Y* mutant, which exhibited pus and effusion in the middle ear cavity (5). The OM of mutant mice occurred at the age of 2 weeks. The mutant mice harboring otitis media were characterized by effusion and capillary expansion. Increased goblet cells and PCNA staining indicated mucosa proliferation (21, 22). Effusion originates from the infection and inflammation of the middle ear and is exacerbated by dysfunction of the Eustachian tube and mucociliary impairment (23).

The Eustachian tube is coated with pseudostratified ciliary columnar epithelium and plays an important role in ventilation and secretion clearance (24). Bacteria resident in the upper respiratory tract are able to retrograde infection through the Eustachian tube when its function of ventilation and clearance is poor (16). Eustachian tube with horizontal orientation may impair the function of ventilation and clearance, since the normal position and morphology of Eustachian tube have protective function of the middle ear against

10.3389/fneur.2022.1054704

otitis media (25). As in the setting of the *Galnt2* mutant mice, the Eustachian tube developed to wide and short shape, with an increased intersection angle between the midline and the Eustachian tube, making the Eustachian tube locate to a more horizontal position. Both malformation and dysfunction of the Eustachian tube interfering with ventilation and clearance of middle ear may result in OM.

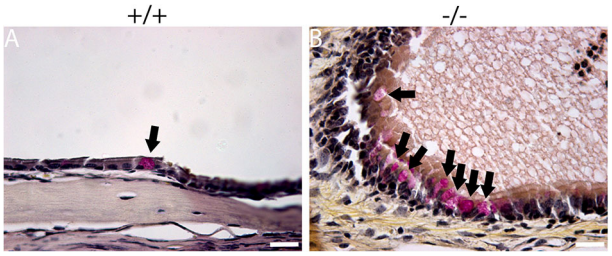

FIGURE 6
Mucin staining reveals goblet cells in mutant mice. Representative sections show the presence of goblet cells (arrow) in the mucosa of the middle ear cavity of wild-type and mutant mice at the age of 2 months. **(A)** Goblet cells were found to be sparsely scattered among other cells in the mucosa of wild-type mice. **(B)** By contrast, goblet cells were present at high density among other cells in the mucosa of mutant mice. Scale bars: 20 μm.

Hearing loss was found in the *Galnt2* mutant mice from 3 weeks old. The tympanograms showed that the negative pressure of the middle ear was more evident in mutant mice, compared to the wild type mice. The ABR thresholds of the mutant mice were significantly higher when compared with those of wild type ones. The DPOAE confirmed lower amplitudes in mutant mice. The mucosa of middle ear cavity was thicker at the age of 2 weeks and gradually developed to cause inflammatory infiltration, mucosa proliferation, and capillary expansion at the age of 2 months. PCNA, an active cell proliferation marker, was highly associated with otitis media (Lim et al., 1971). Our findings depicted that the intensity of PCNA was higher in the mutant mice than in control ones, in accordance with the pathology of the middle ear. Goblet cells in the middle ear mucosa are one of the mucosal secretions responsible for the immune system (26). A high density of goblet cells in the mucosa of mutant mice was seen, which

TABLE 1 Semi-quantitative evaluation of the middle ear pathology in mutant mice.

Mouse ID	Genotype	Age	Effusion	Inflammatory cells	Tissue debris	Tissue hyperplasia	Goblet cells
1	+/+	2W	-	-	-	-	-
2	+/+	2W	-	-	-	-	-
3	+/+	2W	-	-	-	-	-
4	+/+	2W	-	-	-	-	-
5	+/+	3W	-	-	-	-	+
6	+/+	3W	-	-	-	-	-
7	+/+	3W	-	-	-	+	-
8	+/+	3W	-	-	-	-	-
9	+/+	2M	-	-	-	+	+
10	+/+	2M	-	-	-	-	-
11	+/+	2M	-	-	-	-	-
12	+/+	2M	-	-	-	-	+
13	-/-	2W	-	-	-	+	-
14	-/-	2W	-	-	-	+	-
15	-/-	2W	-	-	-	+	+
16	-/-	2W	-	-	-	+	+
17	-/-	3W	-	+	+	++	+
18	-/-	3W	-	-	-	++	++
19	-/-	3W	+	-	-	++	+
20	-/-	3W	-	-	-	++	++
21	-/-	2M	+++	++	++	++	++
22	-/-	2M	+++	+++	+++	+++	+++
23	-/-	2M	+++	+++	+++	+++	+++
24	-/-	2M	+++	+++	+++	+++	+++

To exhibit the degree of pathological alteration in the mutant mice, symbols (-, +, ++, + + +) were used, with (-) indicating no pathology and (+) to (+ + +) indicating a mild-to-severe degree of pathology, respectively. The criteria for pathology included middle ear effusion, inflammatory cells, tissue debris, tissue proliferation, and density of goblet cells. The maximum possible score per mouse was 15 points (1 point for each +). The total score rate (84/180) of the mutant mice was significantly higher than that (4/180) of the wild-type mice ($P < 0.01$, $\chi 2$ test).

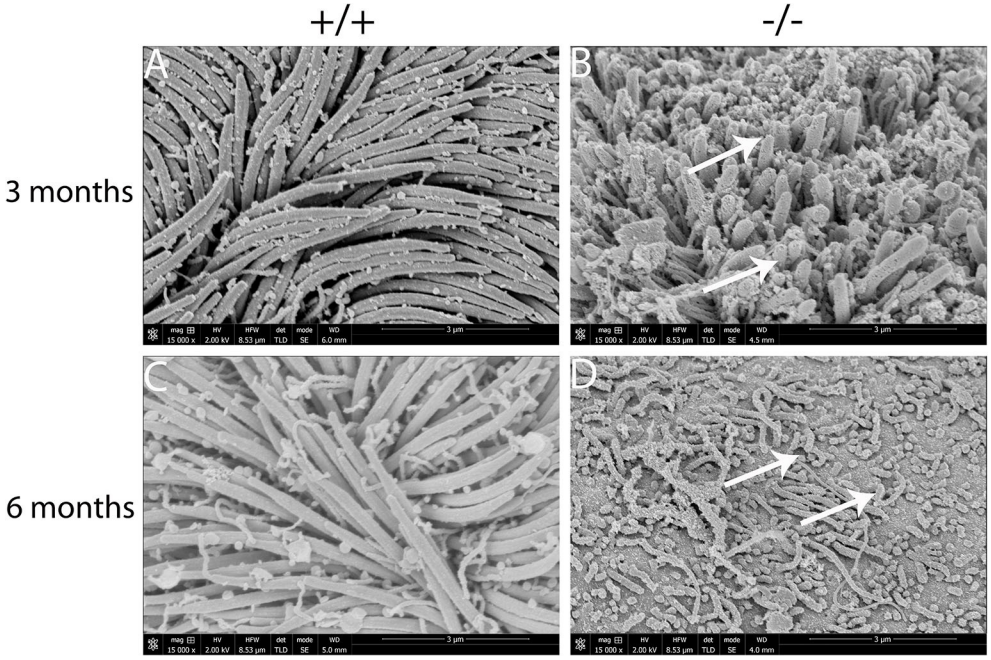

FIGURE 7
Scanning electron microscopy (SEM) observation of the cilia of the middle ear cavity in mutant mice. Wild-type (+/+) and mutant mice (-/-) were observed in the SEM of the middle ear at the ages of 3 and 6 months, respectively ($n = 3$ for each genotype). Wild-type mice exhibited a thick lawn of morphologically normal and distributed cilia in the mucosa of the middle ear at both time points **(A, C)**. The cilia of the mucosa of the middle ear in mutant mice were short, impaired, and disrupted (arrows), and the impairment of the cilia progressed to a much greater severity at 6 months than the cilia at 3 months **(B, D)**. Scale bars: 3 μm.

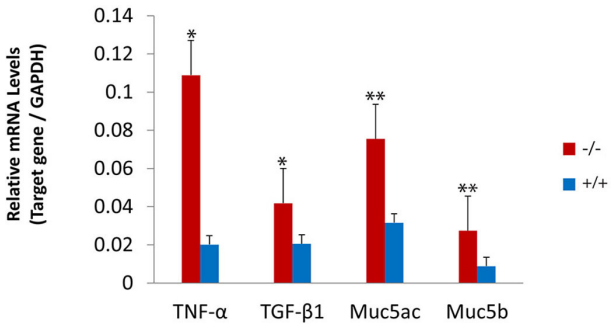

FIGURE 8
Upregulated expression of the inflammatory-related gene in mutant mice. The levels of gene expression were evaluated in wild-type ($n = 3$) and mutant mice ($n = 3$) at the age of 7 months. The messenger RNA (mRNA) accumulation levels of tumor necrosis factor-alpha (TNF-α), transforming growth factor-beta 1 (TGF-β1), Muc5ac, and Muc5b were significantly higher in mutant mice than in wild-type mice. The error bar represents the standard error (SE) of the mean. $^*P < 0.05$, $^{**}P < 0.01$.

might result in an excess effusion in the middle ear cavity. Cilia in the middle ear are critical for the clearance of mucosal secretions, while the abnormal cilia impair normal mucociliary clearance and exacerbate clinical complications (27). Short cilia with impairment and disruption of mucosa in the middle ear were observed and tended to be more serious with the increasing age of mutant mice, revealing that the impairment of cilia elicited significant function in the occurrence of OM.

Inflammation increased with gene levels of TNF-α, TGF-β1, Muc5ac, and muc5b in the middle ear in mutant mice, which were consistent with previous human and animal studies (28). Consistent with our initial hypothesis, the TNF-α levels were significantly upregulated by mutating GALNT2. TNF-α triggers the transcription factor, such as nuclear factor-kappa B (NF-κB), as the basis of various physiological and pathological procedures (29). The *Bordetella hinzii* infection in the middle ear cavity of *Galnt2* mutant mice contributes to inflammation, which upregulates TNF-α and promotes further pathological processes. TGF-β1 controls cellular proliferation and differentiation, and epithelial-mesenchymal transformation, since the TGF-β signaling pathway plays an important role both in tooth and craniofacial development (30). Additionally, the TGF-β1 upregulation in *Galnt2* mutant mice may play a role in the development of the Eustachian tube. Mucins are responsible for the gel-like characteristics of mucoid middle ear fluids. Both Muc5a and Muc5b were found to determine the properties of airway mucus gel (31). The upregulation of Muc5b in the ear may have a role in middle ear effusions (28). These proteins protect the mucosa of the middle ear from pathogen invasion and contribute to the clearance of pathogens. Moreover, upregulation of Muc5ac and Muc5b in *Galnt2* mutant mice resulted in increased middle ear effusion and decreased mucociliary clearance, thereby preventing otitis media.

Admittedly, several limitations should be acknowledged in the present study. First, this is an animal study that includes the uncertainty regarding how truly it is reflected in human studies. Second, future exploration of OM's pathological features induced by Galnt2 mutation is essential to reveal the underlying mechanisms.

10.3389/fneur.2022.1054704

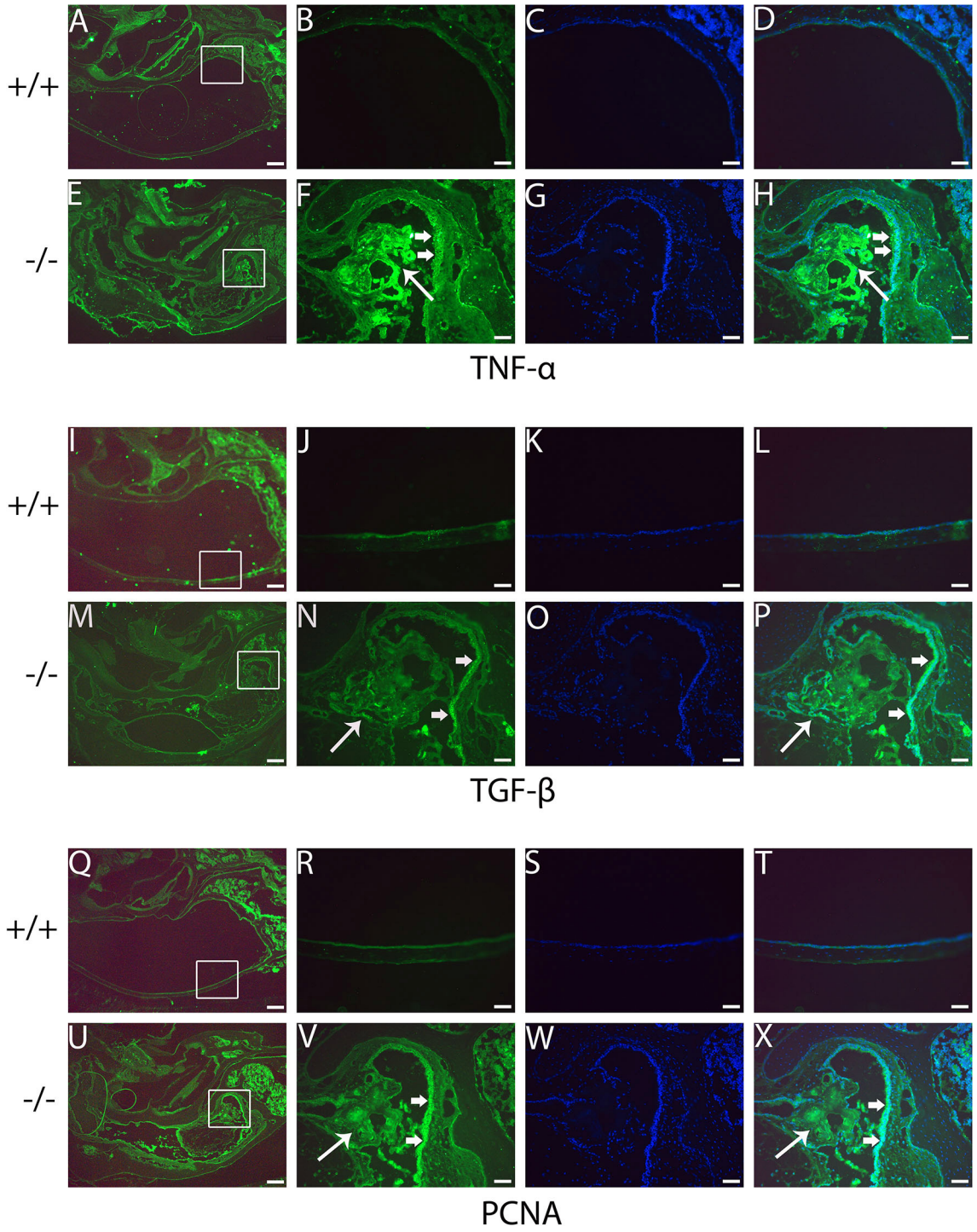

FIGURE 9
Immunofluorescent detection of pro-inflammatory proteins such as tumor necrosis factor-alpha (TNF-α), transforming growth factor-beta (TGF-β), and proliferating cell nuclear antigen (PCNA) in mutant mice. Representative images from 6-month-old wild type (+/+) and mutant (-/-) mice ($n = 3$ for each group) stained with anti-TNF-α, anti-TGF-β, and anti-PCNA antibody and revealed with Alexa Fluor 488 (green). **(A, E, I, M, Q, U)** show gross morphology of the middle ear. **(B, F, J, N, R, V)** represent the enlarged image corresponding to the rectangular region in the left. Images **(C, G, K, O, S, W)** counterstained with 4′,6-diamidino-2-phenylindole (DAPI) reveal the nuclei in these tissues. **(D, H, L, P, T, X)** on the right are merged with the images **(B, F, J, N, R, V)** and the images were counterstained with DAPI. The intensities of TNF-α, TGF-β, and PCNA are all stronger in the mutant mice than in control mice **(F, N, V, H, P, X)**. The expression of TNF-α in the inflammatory tissue of the middle ear cavity (short arrow) is higher than that in the mucosa of the middle ear cavity (long arrow) **(F, H)**. The expression of TGF-β and PCNA is higher in the mucosa of the middle ear cavity (short arrow) compared to the inflammatory tissue of the middle ear cavity (long arrow) **(N, V, P, X)**. Scale bars: 200 μm **(A, E, I, M, Q, U)**; 50 μm **(B–H, J–L, N–P, R–T, V–X)**.

Conclusion

To our knowledge, the current study was the first to report on the occurrence of OM in the Galnt2 $^{tm1Lat/tm1Lat}$ mutant mice. The present study suggests that the mutant *Galnt2* gene may result in the inflammation of the middle ear and mimic human OM. This study suggests the reason that OM in *Galnt2* mutant mice is highly associated with hearing loss, which is mainly presented as a dysfunction of the Eustachian tube, mucosa proliferation, and capillary expansion.

Data availability statement

The original contributions presented in the study are included in the article/supplementary material, further inquiries can be directed to the corresponding authors.

Ethics statement

The animal study was reviewed and approved by Health Sciences Institutional of Animal Care Center and Ethics Committee of Case Western Reserve University.

Author contributions

MX and YC contributed to the conception and design of the study. HLi, JH, and YG contributed to the acquisition of data. HLv and WM performed the experiments. XZ and QZ contributed to the analysis of data. WM wrote the manuscript. MX revised the manuscript. All authors reviewed and approved the final version of the manuscript.

Funding

This study was funded by the National Key R&D Program of Shaanxi Province (No. 2021SF-262) and The Second Affiliated Hospital of Xi'an Jiaotong University Free Exploration Project (No. YJ(ZYTS)2019063).

Conflict of interest

The authors declare that the research was conducted in the absence of any commercial or financial relationships that could be construed as a potential conflict of interest.

Publisher's note

All claims expressed in this article are solely those of the authors and do not necessarily represent those of their affiliated organizations, or those of the publisher, the editors and the reviewers. Any product that may be evaluated in this article, or claim that may be made by its manufacturer, is not guaranteed or endorsed by the publisher.

References

1. Sundgaard JV, Harte J, Bray P, Laugesen S, Kamide Y, Tanaka C, et al. Deep metric learning for otitis media classification. *Med Image Anal.* (2021) 71:102034. doi: 10.1016/j.media.2021.102034

2. Monasta L, Ronfani L, Marchetti F, Montico M, Brumatti LV, Bavcar A, et al. Burden of disease caused by otitis media: systematic review and global estimates. *PLoS ONE.* (2012) 7:e36226. doi: 10.1371/journal.pone.0036226

3. Vanneste P, Page C. Otitis media with effusion in children: pathophysiology, diagnosis, and treatment. A review. *J Otol.* (2019) 14:33–9. doi: 10.1016/j.joto.2019.01.005

4. Darrow DH, Dash N, Derkay SC. Otitis media: concepts and controversies. *Curr Opin Otolaryngol Head Neck Surg.* (2003) 11:416–23. doi: 10.1097/00020840-200312000-00002

5. Han F, Yu H, Li P, Zhang J, Tian C, Li H, et al. Mutation in Phex gene predisposes BALB/c-Phex(Hyp-Duk)/Y mice to otitis media. *PLoS ONE.* (2012) 7:e43010. doi: 10.1371/journal.pone.0043010

6. Davidoss N, Varsak Y, Santa Maria. P. Animal models of acute otitis media–a review with practical implications for laboratory research. *Eur Ann Otorhinolaryngol Head Neck Dis.* (2018) 135:183–90. doi: 10.1016/j.anorl.2017.06.013

7. Willett DN, Rezaee RP, Billy JM, Tighe MB, DeMaria TF. Relationship of endotoxin to tumor necrosis factor–α and interleukin-1β in children with otitis media with effusion. *Ann Otol Rhinol Laryngol.* (1998) 107:28–33. doi: 10.1177/000348949810700106

8. Teslovich TM, Musunuru K, Smith AV, Edmondson AC, Stylianou IM, Koseki M, et al. Biological, clinical and population relevance of 95 loci for blood lipids. *Nature.* (2010) 466:707–13. doi: 10.1038/nature09270

9. Yang X, Ongusaha PP, Miles PD, Havstad JC, Zhang F, So WV, et al. Phosphoinositide signalling links O-GlcNAc transferase to insulin resistance. *Nature.* (2008) 451:964–9. doi: 10.1038/nature06668

10. Goth CK, Halim A, Khetarpal SA, Rader DJ, Clausen H, Schjoldager TBG, et al. A systematic study of modulation of ADAM-mediated ectodomain shedding by site-specific O-glycosylation. *Proc Nat Acad Sci.* (2015) 112:14623–28. doi: 10.1073/pnas.1511175112

11. Qin Z, Wood M, Rosowski JJ. Measurement of conductive hearing loss in mice. *Hear Res.* (2010) 263:93–103. doi: 10.1016/j.heares.2009.10.002

12. Zheng QY, Tong YCI, Alagramam KN, Yu H. Tympanometry assessment of 61 inbred strains of mice. *Hear Res.* (2007) 231:23–31. doi: 10.1016/j.heares.2007.05.011

13. Han F, Yu H, Tian C, Li S, Jacobs MR, Benedict-Alderfer C, et al. Role for toll-like receptor 2 in the immune response to *Streptococcus pneumoniae* infection in mouse otitis media. *Infect Immun.* (2009) 77:3100–8. doi: 10.1128/IAI.00204-09

14. Falk B. Sniff-induced negative middle ear pressure: study of a consecutive series of children with otitis media with effusion. *Am J Otolaryngol.* (1982) 3:155–62. doi: 10.1016/S0196-0709(82)80048-3

15. Kanai R, Kaneko K. Negative middle ear pressure and otitis media with effusion after surgery under general anesthesia. *Acta Otolaryngol.* (2012) 132:1049–53. doi: 10.3109/00016489.2012.687455

16. Trune DR, Zheng QY. Mouse models for human otitis media. *Brain Res.* (2009) 1277:90–103. doi: 10.1016/j.brainres.2009.02.047

17. Yang B, Tian C, Zhang Z, Han F, Azem R, Yu H, et al. Sh3pxd2b mice are a model for craniofacial dysmorphology and otitis media. *PLoS ONE.* (2011) 6:e22622. doi: 10.1371/journal.pone.0022622

18. Tian C, Yu H, Yang B, Han F, Zheng Y, Bartels CF, et al. Otitis media in a new mouse model for CHARGE syndrome with a deletion in the Chd7 gene. *PLoS ONE.* (2012) 7:e34944. doi: 10.1371/journal.pone.0034944

19. Suryani S, Dharma A, Nasir N. Isolation and identification of pathogenic bacteria secretion of chronic suppurative otitis media patients. *Rasayan J Chem.* (2018) 11:1139–43. doi: 10.31788/RJC.2018.1131966

20. Hayashimoto N, Yasuda M, Goto K, Takakura A, Itoh T. Study of a Bordetella hinzii isolate from a laboratory mouse. *Comp Med.* (2008) 58:440–6. doi: 10.1186/1746-6148-4-39

21. Lim DJ, Birck H. Ultrastructural pathology of the middle ear mucosa in serous otitis media. *Ann Otol Rhinol Laryngol.* (1971) 80:838–53.

22. Fons JM, Milmoe NJ, Dack MRG, Joshi L, Thompson H, Tucker AS. The interconnected relationships between middle ear bulla size, cavitation defects, and chronic

otitis media revealed in a syndromic mouse model. *Front Genet.* (2022) 13:933416. doi: 10.3389/fgene.2022.933416

23. Zhang Y, Yu H, Xu M, Han F, Tian C, Kim S, et al. Pathological features in the LmnaDhe/+ mutant mouse provide a novel model of human otitis media and laminopathies. *Am J Pathol.* (2012) 181:761–74. doi: 10.1016/j.ajpath.2012.05.031

24. Cunsolo E, Marchioni D, Leo G, Incorvaia C, Presutti L. Functional anatomy of the Eustachian tube. *Int J Immunopathol Pharmacol.* (2010) 23:4–7.

25. Netto LFS, da Costa SS, Sleifer P, Braga MEL. The impact of chronic suppurative otitis media on children's and teenagers' hearing. *Int J Pediatr Otorhinolaryngol.* (2009) 73:1751–6. doi: 10.1016/j.ijporl.2009.09.033

26. Saunders J, Murray M, Alleman A. Biofilms in chronic suppurative otitis media and cholesteatoma: scanning electron microscopy findings. *Am J Otolaryngol.* (2011) 32:32–7. doi: 10.1016/j.amjoto.2009.09.010

27. Norris CR. Primary Ciliary Dyskinesia[J]. *Am J Respir Crit Care Med.* (2004) 169:459–67.

28. Elsheikh MN, Mahfouz ME. Up-regulation of MUC5AC and MUC5B mucin genes in nasopharyngeal respiratory mucosa and selective up-regulation of MUC5B in middle ear in pediatric otitis media with effusion. *Laryngoscope.* (2006) 116:365–9. doi: 10.1097/01.MLG.0000195290.71090.A1

29. Lei CQ, Wu X, Zhong X, Jiang L, Zhong B, Shu HB. USP19 inhibits TNF-α-and IL-1β-triggered NF-κB activation by deubiquitinating TAK1. *J Immunol.* (2019) 203:259–68. doi: 10.4049/jimmunol.1900083

30. Kouskoura T, Fragou N, Alexiou M, John N, Sommer L, Graf D, et al. The genetic basis of craniofacial and dental abnormalities. *Schweiz Monatsschr Zahnmed.* (2011) 121:636–46. doi: 10.5167/uzh-50358

31. Bonser LR, Erle DJ. Airway mucus and asthma: the role of MUC5AC and MUC5B. *J Clin Med.* (2017) 6:112. doi: 10.3390/jcm6120112

frontiers | Frontiers in Neurology

TYPE Original Research
PUBLISHED 23 February 2023
DOI 10.3389/fneur.2023.1126214

Check for updates

OPEN ACCESS

EDITED BY
Sulin Zhang,
Huazhong University of Science and Technology, China

REVIEWED BY
Haibo Shi,
Shanghai Jiao Tong University, China
Florian Schöberl,
LMU Munich University Hospital, Germany

*CORRESPONDENCE
Guangjian Ni
✉ niguangjian@tju.edu.cn

†These authors have contributed equally to this work

SPECIALTY SECTION
This article was submitted to Neuro-Otology, a section of the journal Frontiers in Neurology

RECEIVED 17 December 2022
ACCEPTED 31 January 2023
PUBLISHED 23 February 2023

CITATION
Han Y, Bai Y, Liu Q, Zhao Y, Chen T, Wang W and Ni G (2023) Assessing vestibular function using electroencephalogram rhythms evoked during the caloric test.
Front. Neurol. 14:1126214.
doi: 10.3389/fneur.2023.1126214

COPYRIGHT
© 2023 Han, Bai, Liu, Zhao, Chen, Wang and Ni. This is an open-access article distributed under the terms of the Creative Commons Attribution License (CC BY). The use, distribution or reproduction in other forums is permitted, provided the original author(s) and the copyright owner(s) are credited and that the original publication in this journal is cited, in accordance with accepted academic practice. No use, distribution or reproduction is permitted which does not comply with these terms.

Assessing vestibular function using electroencephalogram rhythms evoked during the caloric test

Yutong Han[1,2†], Yanru Bai[1,2†], Qiang Liu[3,4,5], Yuncheng Zhao[2,6], Taisheng Chen[3,4,5], Wei Wang[3,4,5] and Guangjian Ni[1,2*]

[1]Academy of Medical Engineering and Translational Medicine, Tianjin University, Tianjin, China, [2]Tianjin Key Laboratory of Brain Science and Neuroengineering, Tianjin, China, [3]Key Laboratory of Auditory Speech and Balance Medicine, Tianjin, China, [4]Institute of Otolaryngology of Tianjin, Tianjin, China, [5]Key Medical Discipline of Tianjin (Otolaryngology), Tianjin, China, [6]Department of Biomedical Engineering, College of Precision Instruments and Optoelectronics Engineering, Tianjin University, Tianjin, China

Introduction: The vestibular system is responsible for motion perception and balance preservation in the body. The vestibular function examination is useful for determining the cause of associated symptoms, diagnosis, and therapy of the patients. The associated cerebral cortex processes and integrates information and is the ultimate perceptual site for vestibular-related symptoms. In recent clinical examinations, less consideration has been given to the cortex associated with the vestibular system. As a result, it is crucial to increase focus on the expression of the cortical level while evaluating vestibular function. From the viewpoint of neuroelectrophysiology, electroencephalograms (EEG) can enhance the assessments of vestibular function at the cortex level.

Methods: This study recorded nystagmus and EEG data throughout the caloric test. Four phases were considered according to the vestibular activation status: before activation, activation, fixation suppression, and recovery. In different phases, the distribution and changes of the relative power of the EEG rhythms (delta, theta, alpha, and beta) were analyzed, and the correlation between EEG characteristics and nystagmus was also investigated.

Results: The results showed that, when the vestibule was activated, the alpha power of the occipital region increased, and the beta power of the central and top regions and the occipital region on the left decreased. The changes in the alpha and beta rhythms significantly correlate with nystagmus values in left warm stimulation.

Discussion: Our findings offer a fresh perspective on cortical electrophysiology for the assessment of vestibular function by demonstrating that the relative power change in EEG rhythms can be used to assess vestibular function.

KEYWORDS

vestibular function, EEG rhythms, caloric test, nystagmus, cortex

1. Introduction

The vestibular system is vital in perceiving spatial position and maintaining balance (1, 2). Damage in the vestibular system would lead to clinical symptoms, such as vertigo (3, 4), and may also affect motor coordination (5, 6) and higher cognitive function (7). A timely and accurate examination of the physiological function of the vestibular system can serve as a crucial guide for determining the cause of associated symptoms in patients as well as for future diagnosis and therapy. The current widely used clinical vestibular

function examinations usually include calibration, spontaneous and gaze-evoked nystagmus, the saccade test, smooth pursuit tracking, positional and positioning nystagmus, and caloric test (8). Notably, existing examinations mainly focus on the nystagmus response of the vestibulo-ocular reflex and the balance function of the vestibulo-spinal reflex system (9). One of the main neural circuits in the vestibular system is the vestibulocortical pathway. The thalamic integration center receives information from the vestibular nerve in the vestibulocortical pathway, which then projects it to the vestibular cortex (10). The final stage in the formation of vestibular-related perception is the vestibular-related brain, which is responsible for processing and integrating information. Therefore, changes in neurological function at the cortex may result from or may be the cause of vestibular hypofunction (11). In current clinical examinations, less attention has been paid to the cortex related to the vestibular system. Even though some examinations concern the vestibulocortical pathway, they are not performed directly from the cortical expression but through evaluating various eye movement functions. Therefore, it is of great interest to add a reference to the expression of the cortex level for assessing vestibular functions.

Electroencephalogram (EEG) and sensory-evoked potentials contain abundant physiological and pathological information, which can reflect the excited or inhibited state of the cortex (12). Moreover, EEG technology has the advantages of non-invasiveness, low cost, and high time resolution (13–15). As EEG has been used to diagnose and treat many neurological-related diseases, such as epilepsy and encephalitis (16, 17), it has the potential to provide a neuro-electrophysiological supplement for vestibular function assessment at the cortex level. Moreover, convenient and fast saline electrodes have evolved recently, avoiding the time-consuming and hair-washing problems of using conductive paste.

Existing EEG studies on the vestibular system are mainly aimed at patients with a specific vestibular-related disease or symptoms to explore changes in EEG characteristics. For example, in patients with chronic balance disturbance, alpha rhythm activity in the posterior cingulate cortex rose significantly, while beta activity in several brain regions decreased (18). The severity of symptoms in patients with motion sickness is related to an increase in the gravitational frequency of the power spectral density of the theta rhythm (19). However, vestibular-related diseases and symptoms are diverse and complex (20–22), and there may be other influencing factors other than vestibular hypofunction. Therefore, there is currently a lack of assessments directly targeting vestibular function at the cortex level.

The following two categories of relevant studies are currently available: resting state and evoked state. The EEG microstates in this study were classified into four categories (A, B, C, and D) as in most resting state studies, and the results showed that patients with recurrent otogenic vertigo have a longer duration of the A state and an increased probability of transitioning from A state to D state compared to healthy people (23). The primary triggers for the evoked state are auditory and visual. For example, in the study of auditory-evoked potential, it was found that latencies of wave I peak, wave III–V inter-peaks, Pa, and P300 in patients with vertigo were prolonged (24–27). Moreover, visual-evoked studies found that patients with vestibular migraine had a higher light actuation (28). However, these stimuli use the intimate connection between the auditory and visual pathways and the vestibular route rather than directly activating the vestibular system (29). The vestibular system cannot be directly activated when a non-vestibular evoked stimulation technique is employed, making the evaluation of vestibular function challenging. The horizontal semicircular canal is excited during the caloric test, which is acknowledged as an assessment technique to stimulate and evaluate the vestibular response (30). The caloric test activates the vestibular system directly and is the gold standard for assessing vestibular hypofunction (9).

In this study, we aimed to explore the characteristics of EEG rhythms in different vestibular activation states in the caloric test and to find the characteristics of EEG rhythms for assessing vestibular function. We examined relative power distribution and changes in each EEG rhythm under various vestibular activation states and searched for a relationship between these changes and the caloric test findings. It was found that the alpha power was enhanced during vestibular activation in channels selected *via* significant changes between phases ($p < 0.05$) dominated by the occipital region, and the beta power was reduced in channels selected by the same criteria mainly in the central, top, and occipital regions on the left. It is interesting to note that both changes significantly correlate with nystagmus values in the left warm condition.

2. Materials and methods

2.1. Subjects

A total of 18 healthy subjects (8 men and 10 women, 23.44 ± 2.33 years) were included in this study. All participants complied with the following requirements: no history of seizures, cardiovascular disease, hypertension, severe head and neck illnesses, ingestion of alcohol within the previous 48 h, ingestion of central excitatory or inhibitory drugs, damage to the external auditory canal or tympanic membrane, or otitis media. The study was approved by the medical ethics review committee at Tianjin University. All subjects gave written informed consent and received payment for participation.

2.2. Stimuli in the caloric test

As illustrated in Figure 1A, volunteers were asked to remain awake with their eyes open during the experiment while lying supine in a dark field with their heads raised by 30° on a firm cushion to place their horizontal semicircular canal in a vertical posture. The caloric test was performed by perfusing each ear with cold (24°C) and warm (50°C) gases. Gas perfusion was performed from the external auditory canal in four conditions: cold gas into the right ear (RC), cold gas into the left ear (LC), warm gas into the right ear (RW), and warm gas into the left ear (LW). The duration of each perfusion was 60 s. It is important to ensure that the nystagmus of the subject due to the previous perfusion has completely subsided before each gas perfusion (no less than 5 min). After reaching the maximum nystagmus, the fixation lamp was turned on to suppress the vestibular activation. For each condition,

we divided the entire experiment into four phases: the phase before stimulation (PBA), the phase of vestibular activation (POVA), the phase of fixation suppression (POFS), and the phase of recovery (POR), as shown in Figure 1B.

2.3. Data recording

During the caloric test, EEG and nystagmus data were concurrently captured.

2.3.1. Nystagmus recording

Before conducting the experiment, calibration was performed. The purpose of calibration is to measure the relationship between the eye movement of a certain angle of view and the corresponding recorded signal (i.e., the displacement of the eye movement curve), which is used to calculate parameters such as amplitude and speed of the eye movement. Then, using video nystagmus (VNG), the maximum slow-phase velocity of spontaneous and caloric test-induced nystagmus from both experiments was captured.

2.3.2. EEG recording

Saline electrode caps (EGI, Geodesic Sensor Net, 64 channels, 1,000 Hz) were used to record EEG data throughout the caloric test, amplified by a Net Amps 400 amplifier. The distribution of electrodes was based on the international 10–20 system, and the impedance was guaranteed to be less than 50 kΩ during the experiment. The volunteers were reminded before the experiment to refrain from unnecessary head and body movements while collecting data to prevent significant data contamination. EEG data for PBA was defined as the data from 50 s before stimulation, for POVA as the data from 20 s centered on the time point of the strongest nystagmus, for POFS as the data from 10 s following the turn-on of the fixation lamp, and for POR as the data from 10 s following the turn-off of the fixation lamp.

2.4. EEG data analysis

2.4.1. Preprocessing

Raw EEG data were preprocessed using EEGLAB, an open-source toolbox of Matlab (R2021a). To lessen the impact of high-frequency noise and low-frequency interference on the data, 30 Hz low-pass filters and 0.5 Hz high-pass filters were first used. We averaged the reference value of data across all electrodes. The spherical approach was used to interpolate the data of electrodes that were detached from the skin during the experiment. To improve the computational efficiency of subsequent processing and analysis, data were down sampled to 200 Hz. Independent component analysis was performed to eliminate artifacts like a heartbeat, muscle tension, and eye movement.

2.4.2. Power spectral density of EEG rhythms

The Welch method was employed to determine the power spectral density of data. The energy of each EEG signal was normalized to reduce the potential difference among subjects. The relative power of EEG rhythms delta (0.5–4 Hz), theta (4–8 Hz), alpha (8–14 Hz), and beta (14–30 Hz) was calculated for each phase. The topographic maps of each phase were created using the relative power findings of all channels to explore the distribution of certain EEG rhythms. Variations in the global brain distribution of each EEG rhythm were observed and examined between phases.

2.5. Statistical analysis

The statistical analysis was carried out using SPSS (26.0). The Wilcoxon signed-rank test was used to examine the relative power findings for each channel for each EEG rhythm across phases shown in Figure 1B, as some of the data did not follow a normal distribution. POVA and PBA, POFS and POVA, POR and POFS, and POR and POVA were contrasted independently to identify the changes caused by caloric vestibular stimulation, fixation suppression, removal of fixation suppression, and following the process of fixation suppression. The channels with significant changes between phases ($p < 0.05$) were selected as the region of interest, and the changing trend of the region of interest was calculated. Additionally, the Pearson correlation test was utilized to determine the discrepancy between the relative power change of the particular EEG rhythm and the result for nystagmus.

3. Results

3.1. Topographic map of EEG rhythms

The whole-brain delta rhythm was observed to have a relative power distribution that was strongest in the forehead in PBA, slightly enhanced in the forehead in POVA, the whole brain enhanced in POFS, and then returned to its previous state between PBA and POVA in POR, leaning more toward POVA. The center frontal region was comparatively strong in PBA, while the forehead and occipital regions were slightly weaker in POVA, according to the observation of the relative power distribution of the whole-brain theta rhythm. The central frontal and occipital regions were considerably enhanced during POFS; even after enhancement, the central frontal region remained the strongest. While the distribution in POR was comparable to that in POVA, the frontal center was weaker. According to an analysis of relative power distribution in the whole-brain alpha rhythm, the energy of the occipital region was more pronounced in PBA and increased in POVA. In POFS, the entire brain was repressed. The relative alpha power in the occipital region in POR was high, and its intensity was midway between PBA and POVA. The relative power of beta rhythm in the temporal region was relatively strong in PBA and suppressed in POVA. The relative beta power in the frontotemporal and occipital regions was enhanced in POFS, and the enhancement of these regions was weakened in POR (as shown in Figure 2).

3.2. Significant differences and trends in EEG rhythm changes among phases

Channels with significant differences ($P < 0.05$) were chosen when theta, alpha, and beta rhythms were evaluated in each

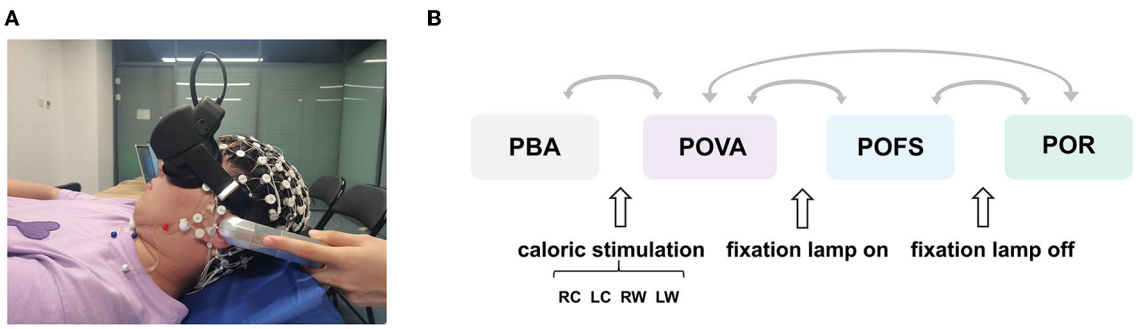

FIGURE 1
Schematic diagram of the experiment. **(A)** Experimental setup. **(B)** Schematic diagram of the overall experimental flow. The two phases connected by each arrow were compared. PBA refers to the phase before activation, POVA refers to the phase of vestibular activation, POFS refers to the phase of fixation suppression, and POR refers to the phase of removing fixation suppression, respectively. RC, LC, RW, and LW are the abbreviations of right cool, left cool, right warm, and left warm, respectively.

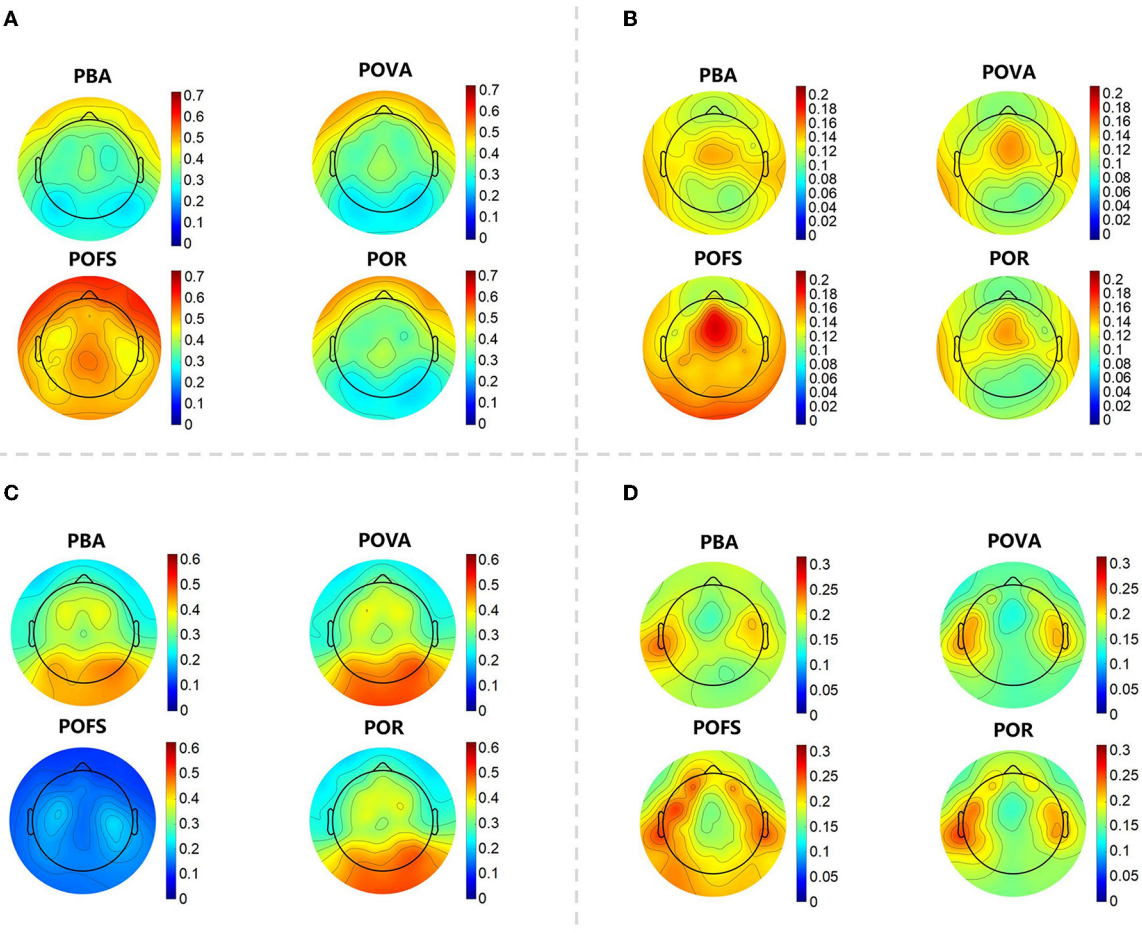

FIGURE 2
The topographic map of each EEG rhythm in each phase. **(A)** The topographic map of the relative power of the delta rhythm in the four phases. **(B)** The topographic map of the relative power of the theta rhythm in the four phases. **(C)** The topographic map of the relative power of the alpha rhythm in the four phases. **(D)** The topographic map of the relative power of the beta rhythm in the four phases.

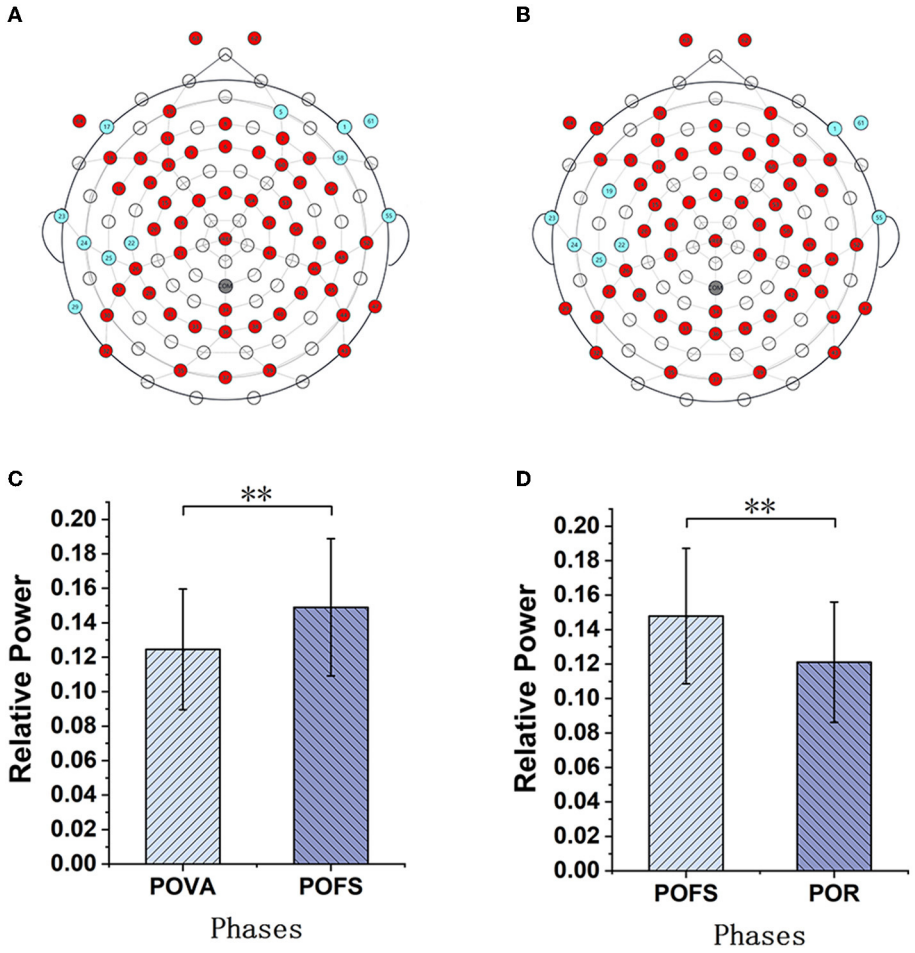

FIGURE 3
The comparison of theta power in different phases. **(A)** and **(B)** are the brain topography distributions of selected channels in the POVA and POFS comparison and POFS and POR comparison, respectively. In the brain topography, the red dots are channels with a significant difference from the comparison of the two phases, the blue dots are channels without significant differences, and the white dots are empty channels. According to the chosen channels shown in red in **(A, B)**, the average relative power changes for POVA and POFS comparison and POFS and POR comparison, respectively, are shown in **(C, D)**. $^{**}p < 0.01$.

phase, as illustrated in Figures 3–5. The changing trend of relative power calculated based on the selected channels was also shown in the lower panels of Figures 3–5. It was discovered that the central frontal, parietal, and occipital areas included most channels exhibiting appreciable variations in theta power. The significantly changed region of the alpha rhythm was occipital and slightly right-lateralized in the comparison of PBA and POVA, and the significantly changed region was the whole brain in POVA and POFS comparison and POFS and POR comparison. Comparing PBA and POVA, significant alterations in beta rhythm were mainly in the central, parietal, and left occipital regions. In the comparison between POVA and POFS, significant changes were evident in the whole brain except for the central region. In comparing POFS, POR, and POVA and POR, significant changes in channels were concentrated in the frontal and parieto-occipital regions. Table 1 summarizes the trends in the relative power of EEG rhythms between phases obtained from the chosen channels.

3.3. Correlation between relative power of EEG rhythms and nystagmus value

The nystagmus value is an index to evaluate the response to vestibular stimulation in the clinic. The nystagmus results were collected synchronously during the EEG recording in the experiment, as listed in Table 2. The relative strength of the alpha and beta rhythms between the POVA and PBA phases demonstrated a substantial difference in the selected brain regions, according to the results of EEG rhythms in various phases. Therefore, under four settings (RC, LC, RW, and LW), a correlation study was done between the change in the relative power of the alpha/beta rhythm and the nystagmus value.

In the four conditions, a significant correlation between the relative power of EEG rhythms and nystagmus values was observed in the LW condition for both alpha and beta rhythms, as shown in Figure 6. It was discovered that the enhancement of alpha power in the region of interest was significantly correlated with the

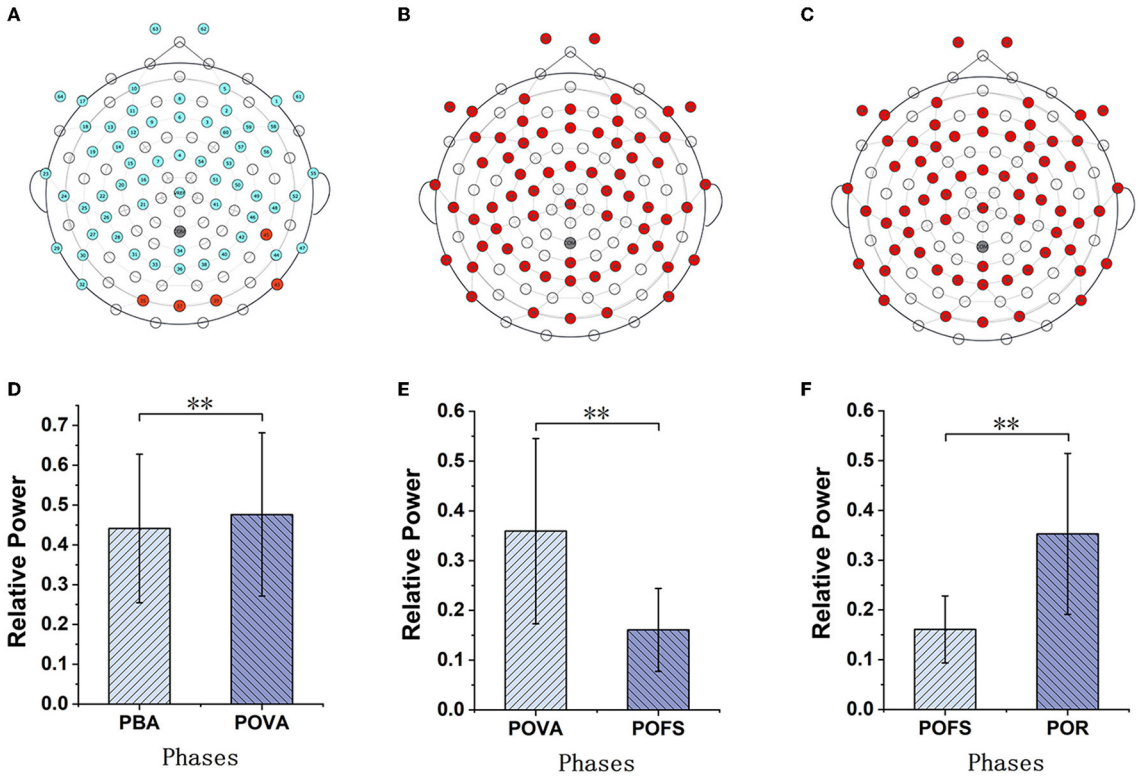

FIGURE 4
The comparison of alpha power in different phases. **(A–C)** are the brain topography distributions of selected channels in the PBA and POVA comparison, POVA and POFS comparison, and POFS and POR comparison, respectively. In the brain topography, the red dots are channels with significant differences between the two comparisons, the blue dots are channels without significant differences, and the white dots are empty channels. Mean relative power changes according to the selected channels are shown in red in **(A–C)** for the PBA and POVA comparison, the POVA and POFS comparison, and the POFS and POR comparison are shown in **(D–F)**, respectively. $^{**}p < 0.01$.

nystagmus value ($r = -0.527$, $p = 0.025$), and the reduction of beta power in the region of interest was also significantly correlated with the nystagmus value ($r = 0.708$, $p = 0.001$).

4. Discussion

This study aimed to examine how the brain reacts to vestibular stimulation and evaluate vestibular function from a cortical electrophysiological standpoint. A caloric test was used to provide direct vestibular stimulation, and brain responses were compared among the following four phases: PBA, POVA, POFS, and POR. The results revealed that the changes in EEG cortex expression under different vestibular activation conditions were significantly different. Notably, in the case of LW stimulation, the enhancement of alpha power and the decrease in beta power in specific brain regions were related to nystagmus values. Therefore, the study offers a novel perspective for assessing vestibular function using characteristic EEG rhythms.

4.1. The basis for the division of phases in the caloric test

The semicircular canals in the peripheral vestibular receptors sense rotational angular acceleration stimulation. Caloric stimulation is an examination that uses caloric vestibular stimulation to stimulate the horizontal semicircular canals to induce and observe vestibular responses (31). When the external ear canal is exposed to cold or warm stimuli, the temperature alteration affects the outer semicircular canal *via* the tympanic membrane, the tympanic chamber, and the bone wall. In the outer semicircular canal, the specific gravity of the endolymph fluid changes due to thermal expansion and contraction, resulting in the convection phenomenon of "warm rises and cool drops" of the endolymph fluid (32). Nystagmus can be seen as a symbol of vestibular stimulation response. The fixation lamp on denotes the start of central inhibition, and the fixation lamp off signals the removal of central inhibition. These critical timings divide the caloric test into different states of vestibular activation. Therefore, although EEG was recorded throughout the entire caloric test, EEG data were divided into four phases for analysis, corresponding to PBA, POVA, POFS, and POR, respectively.

4.2. Beta power has the potential to be used for assessing vestibular function

Regular changes in beta rhythm activity were found in the caloric test, in accordance with the observation made in a study by Brkić about EEG abnormalities in patients with central

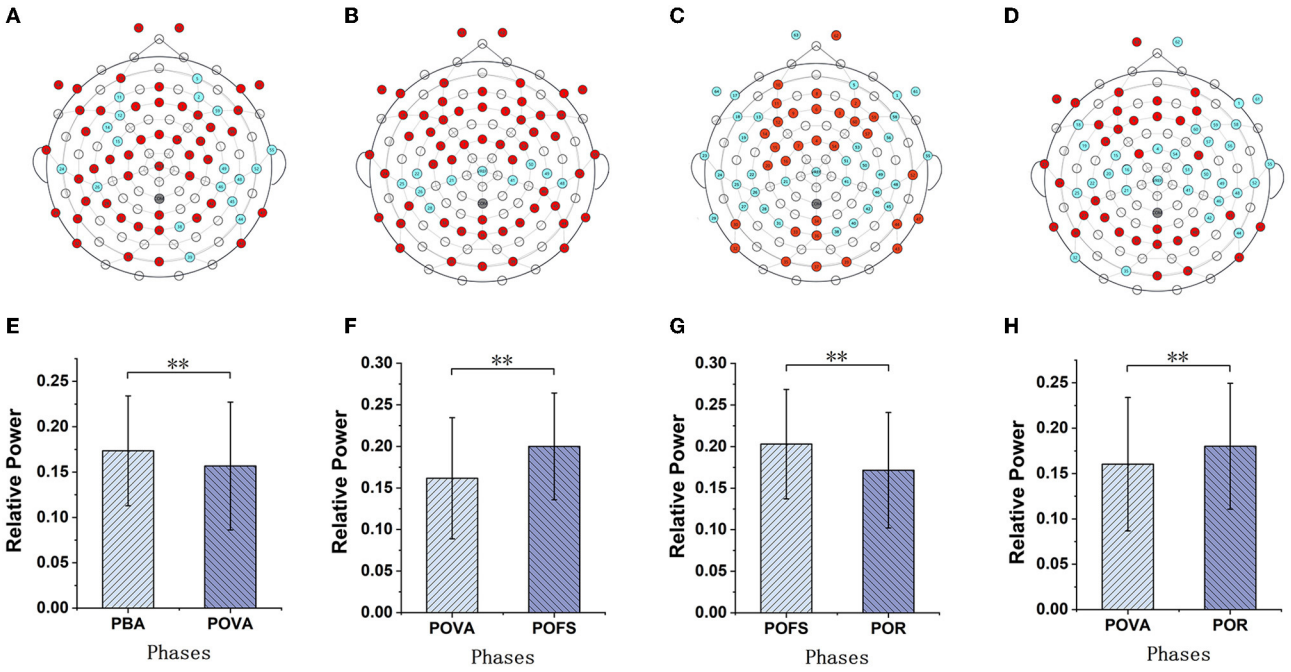

FIGURE 5
The comparison of beta power in different phases. **(A–D)** are the brain topography distributions of selected channels in PBA and POVA comparison, POVA and POFS comparison, POFS and POR comparison, and POVA and POR comparison, respectively. In the brain topography, the red dots are channels with significant differences between the two comparisons, the blue dots are channels without significant differences, and the white dots are empty channels. Mean relative power changes according to the selected channels shown in red in **(A–D)** for the PBA and POVA comparison, POVA and POFS comparison, POFS and POR comparison, and POVA and POR comparison are shown in **(E–H)**, respectively. $^{**}p < 0.01$.

TABLE 1 The trends of the relative power of EEG rhythms in selected channels between phases.

Phase / EEG rhythm	POVA vs. PBA	POFS vs. POVA	POR vs. POFS	POR vs. POVA
Theta	/	Increase	Decrease	/
Alpha	Increase	Decrease	Increase	/
Beta	Decrease	Increase	Decrease	Increase

vertigo utilizing vestibular caloric stimulation. Compared to the control group, more patients showed changes in beta activity during warm stimulation (33). Consistent conclusions indicated that the changes in beta rhythm in this study were induced by caloric vestibular stimulation; in addition, we carried out a quantitative analysis comparing the conclusion of this study with those of the work of Brkić. Brkić did not observe significant changes in healthy subjects and therefore suggested that damage to specific thalamocortical connections was responsible for the EEG changes. In contrast, we found changes in beta rhythm in healthy individuals. We speculate that this may be due to various experimental factors, such as temperature, duration of stimuli, and potential equipment limitations.

We discovered that the relative power of the beta rhythm significantly decreased during the vestibular stimulation response phase. Many classical observations have linked this rhythm to motor function (34). Beta-rhythm activity may have a role in sensorimotor integration. Many authors argue that decreased beta power reflection indicates the activation of the sensorimotor associated with an increase in corticospinal excitability (35), which may correspond to the sensations of dizziness and rotation during the vestibular stimulus response phase, indicating that subjects may be involved in motion perception processes during vestibular stimulus activation. The outcome supports the hypothesis that beta rhythm is strongly related to information processing in the sensory-motor systems. The relative power of the beta rhythm in the central inhibition phase significantly increased and was found to be higher than before, demonstrating that the cerebral cortex response was suppressed. The result was consistent with the observation in the positron emission computed tomography (PET) study of caloric stimulation, in which Naito found that the vestibular response was inactivated during visual fixation (36). After the inhibition was canceled, the beta power decreased again and returned to the same level as the phase before stimulation, indicating that the vestibular stimulation response was no longer suppressed.

The regulation of changes in beta power found in this study corresponds to the activation and inhibition phases in the caloric test. We suggest that beta rhythm is closely related to the state of vestibular activation, and the degree of beta power suppression, especially in LW stimulation, correlates with the intensity of nystagmus. Therefore, it is reasonable to conclude that the relative power of beta rhythm caused by caloric vestibular stimulation reflects the vestibular function condition.

10.3389/fneur.2023.1126214

TABLE 2 Spontaneous and caloric-stimulated nystagmus values.

Subject number	Spontaneous nystagmus	Right warm	Left warm	Left cold	Right cold
1	R1.6	R9.6	L8.7	R5.6	L3.0
2	R0.6	R9.4	L12.8	R10.5	L16.2
3	R2.7	R7.5	L5.3	R4.0	L9.5
4	R1.2	R4.8	L7.3	R8.0	L4.1
5	L0.9	R3.4	L10.3	R4.1	L7.1
6	L1.2	R5.0	L4.5	R3.7	L7.1
7	L0.5	R3.2	L3.2	R6.6	L7.0
8	R1.0	R7.6	L3.8	R18.8	L11.0
9	L0.7	R0.5	L3.1	R2.2	L3.9
10	L0.2	R12.1	L5.4	R4.2	L8.7
11	L0.5	R4.0	L1.3	R4.7	L7.5
12	L1.7	R1.1	L5.0	R1.8	L6.6
13	R0.6	R4.9	L1.4	R5.1	L3.2
14	L0.3	R2.8	L2.0	R1.2	L2.3
15	L1.3	R2.7	L5.5	R9.0	L7.1
16	R1.3	R4.9	L17.1	R7.7	L6.2
17	0	R8.9	L9.7	R11.0	L10.8
18	0	R5.4	L14.7	R8.7	L10.9

L and R refer to the direction of nystagmus as left and right, respectively.

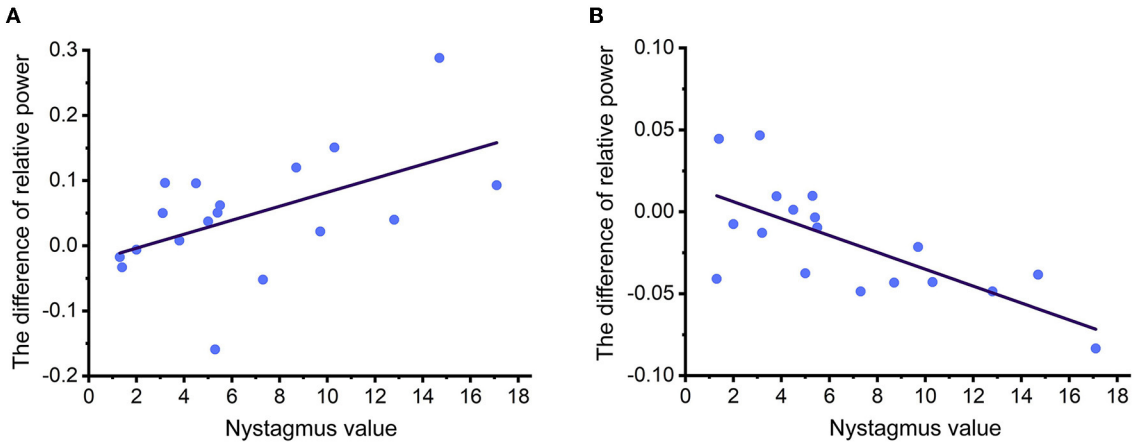

FIGURE 6
(A, B) The fitting curve of correlation coefficients between relative power of EEG rhythms and nystagmus values under LW condition.

4.3. Enhanced alpha power in the occipital region may be associated with vestibular activation

In a PET study, the unilateral caloric test was used to provide vestibular stimulation to healthy subjects, and it was found that the cortical activation pattern of healthy people during vestibular stimulation was identical to that in patients with vestibular neuritis (37–40). According to an EEG study that compared patients with chronic vestibular symptoms to healthy individuals, the occipital region exhibited a difference in alpha activation (18), which was consistent with the change in the region of alpha rhythm that our study found. While these previous studies support the inference that vestibular stimulation does elicit alpha power changes in this study. Considering that alpha waves usually play an important role in regulating cognition and attention (41, 42) and can also inhibit task-irrelevant neural representations (43), it is speculated that this enhanced alpha rhythm caused by vestibular stimulation

may be related to the inhibitory mechanism of attentional disengagement. We found that the enhancement of alpha power was also associated with the degree of nystagmus during vestibular stimulation. Therefore, the degree of alpha power enhancement could be used to evaluate the degree of vestibular activation in clinical practice.

4.4. The necessity of dark field in experimental design

According to some studies, in the closed-eye state, or when the individuals kept their eyes open and were alert in the dark field, alpha power was higher than that in the open field (44–46). We used electronystagmography with an eyecup in the caloric test to create darkroom conditions. In other words, the dark field applied in the caloric test might result in different results for the relative power of EEG rhythms due to the change in the proportion of alpha rhythm. To this end, we performed a comparative experiment by performing the caloric test with an eyecup hood opening. Unfortunately, the results revealed that subjects had neither noticeable nystagmus nor obvious EEG rhythm changes during vestibular stimulation. It is speculated that the condition of open view has a similar effect on central inhibition as turning on the fixation lamp. Therefore, the caloric test can only be carried out in a dark field to achieve vestibular induction. Since all data in our experiments were collected in the dark field, we believe that the change in alpha power is associated with vestibular activation.

4.5. Clinical significance and future directions

Some previous studies have attempted to classify patients and healthy individuals based on resting-state EEG characteristics (18) or auditory-evoked potential characteristics (24–27). Brain responses to vestibular stimulation have been observed (47), but less research has been conducted to explore the possibility of EEG characteristics for assessing vestibular function, as mentioned in this study. The EEG characteristics induced by vestibular stimulation in healthy controls reflect vestibular-evoking conditions similar to those found in patients with vertigo while avoiding the influence of other non-vestibular causes of vertigo. Therefore, this study is of great significance for understanding the mechanisms of vestibular-evoked brain responses and will help to distinguish patients with vertigo from healthy controls more accurately in the next step.

Video nystagmus is widely used in the clinical examination of vestibular dysfunction, but some patients, especially elderly patients, have difficulty keeping their eyes open required by the nystagmus test during the caloric test, resulting in inaccurate results. The EEG responses to vestibular stimulation are not limited by this, increasing its clinical utility. We conclude that EEG characteristics can be used as complementary indicators to evaluate vestibular function in clinical applications in the future.

5. Conclusion

To overcome the lack of specific biomarkers at the cortex level in the current vestibular function assessment, we combined EEG technology and the caloric test to compare the characteristics of EEG rhythms in different phases of the caloric test. We investigated the correlation between changes in EEG rhythm and nystagmus indicators. The results indicate that the inhibition of beta power in the central top and left occipital regions and the enhancement of alpha power in the occipital region in the EEG rhythm can be taken as the cortical electrophysiological characteristics of the response to caloric vestibular stimulation. The changes in the relative power of alpha and beta rhythms in designated brain regions are significantly related to the intensity of nystagmus induced by caloric vestibular stimulation, which verifies the effectiveness of the selected EEG characteristics to be used for assessing vestibular function.

Data availability statement

The raw data supporting the conclusions of this article will be made available by the authors, without undue reservation.

Ethics statement

The studies involving human participants were reviewed and approved by Ethics Review Committee of Tianjin University. The patients/participants provided their written informed consent to participate in this study.

Author contributions

GN, YB, TC, and WW contributed to the conception and design of the work. YH and QL collected data. YH and YZ analyzed data. GN, YB, and YH drafted and revised the manuscript. All authors contributed to the article and approved the submitted version.

Funding

This study was supported by the Key Technologies Research and Development Program of China (No. 2021YFF1200700) and the National Natural Science Foundation of China (82202290).

Conflict of interest

The authors declare that the research was conducted in the absence of any commercial or financial relationships that could be construed as a potential conflict of interest.

Publisher's note

All claims expressed in this article are solely those of the authors and do not necessarily represent those of their affiliated organizations, or those of the publisher, the editors and the reviewers. Any product that may be evaluated in this article, or claim that may be made by its manufacturer, is not guaranteed or endorsed by the publisher.

References

1. Forbes PA, Luu BL, Van der Loos HM, Croft EA, Inglis JT, Blouin JS. Transformation of vestibular signals for the control of standing in humans. *J Neurosci.* (2016) 36:11510–20. doi: 10.1523/JNEUROSCI.1902-16.2016

2. Cohen HS, Mulavara AP, Peters BT, Sangi-Haghpeykar H, Bloomberg JJ. Tests of walking balance for screening vestibular disorders. *J Vestibul Res-Equil.* (2012) 22:95–104. doi: 10.3233/VES-2012-0443

3. Brandt T, Dieterich M. The dizzy patient: don't forget disorders of the central vestibular system. *Nat Rev Neurol.* (2017) 13:352–62. doi: 10.1038/nrneurol.2017.58

4. Neuhauser HK. The epidemiology of dizziness and vertigo. *Handb Clin Neurol.* (2016) 137:67–82. doi: 10.1016/B978-0-444-63437-5.00005-4

5. Cullen KE. The vestibular system: multimodal integration and encoding of self-motion for motor control. *Trends Neurosci.* (2012) 35:185–96. doi: 10.1016/j.tins.2011.12.001

6. Cullen KE. Vestibular processing during natural self-motion: implications for perception and action. *Nat Rev Neurosci.* (2019) 20:346–63. doi: 10.1038/s41583-019-0153-1

7. Wang Y, Huang X, Feng Y, Luo Q, He Y, Guo Q, et al. Resting-state electroencephalography and P300 evidence: age-related vestibular loss as a risk factor contributes to cognitive decline. *J Alzheimers Dis.* (2022) 86:1107. doi: 10.3233/JAD-215467

8. Jia H, Wu Z, Liu B, Wang Q, Han J, Jiang Z, et al. Expert consensus on vestibular function examination(one). *Chinese J Otol.* (2019) 17:117–23. doi: 10.3969/j.issn.1672-2922.2019.01.020

9. Wu ZM, Ren LL, Zhang SZ. Necessity and urgency of vestibular function screening. *Chinese J Otol.* (2022) 20:1–3. doi: 10.3969/j.issn.1672-2922.2013.03.014

10. Brandt T, Dieterich M. The vestibular cortex - Its locations, functions, and disorders. *Ann NY Acad Sci.* (1999) 871:293–312. doi: 10.1111/j.1749-6632.1999.tb09193.x

11. Li Y, Wang H, Yu D, Feng Y, Zhang S, Shi H, et al. Exploration of brain function assessment technique in otogenic vertigo. *J Otorhinol Head N.* (2021) 56:517–21. doi: 10.3760/cma.j.cn115330-20200412-00291

12. Michel CM, Murray MM. Towards the utilization of EEG as a brain imaging tool. *Neuroimage.* (2012) 61:371–85. doi: 10.1016/j.neuroimage.2011.12.039

13. Craik A, He Y, Contreras-Vidal JL. Deep learning for electroencephalogram (EEG) classification tasks: a review. *J Neural Eng.* (2019) 16:031001. doi: 10.1088/1741-2552/ab0ab5

14. Lashgari E, Liang D, Maoz U. Data augmentation for deep-learning-based electroencephalography. *J Neurosci Meth.* (2020) 346:108885. doi: 10.1016/j.jneumeth.2020.108885

15. Yildirim O, Baloglu UB, Acharya UR. A deep convolutional neural network model for automated identification of abnormal EEG signals. *Neural Comput Appl.* (2020) 32:15857–68. doi: 10.1007/s00521-018-3889-z

16. Acharya UR, Fujita H, Sudarshan VK, Bhat S, Koh JEW. Application of entropies for automated diagnosis of epilepsy using EEG signals: A review. *Knowl-Based Syst.* (2015) 88:85–96. doi: 10.1016/j.knosys.2015.08.004

17. Faust O, Acharya UR, Adeli H, Adeli A. Wavelet-based EEG processing for computer-aided seizure detection and epilepsy diagnosis. *Seizure-Eur J Epilep.* (2015) 26:56–64. doi: 10.1016/j.seizure.2015.01.012

18. Alsalman O, Ost J, Vanspauwen R, Blaivie C, De Ridder D, Vanneste S. The neural correlates of chronic symptoms of vertigo proneness in humans. *PLoS ONE.* (2016) 11:e0152309. doi: 10.1371/journal.pone.0152309

19. Zhao L, Li C, Ji L, Yang T. EEG characteristics of motion sickness subjects in automatic driving mode based on virtual reality tests. *J Tsinghua Univ Sci Technol.* (2020) 60:993–8. doi: 10.16511/j.cnki.qhdxxb.2020.25.001

20. Bisdorff A, Von Brevern M, Lempert T, Newman-Toker DE. Classification of vestibular symptoms: Towards an international classification of vestibular disorders. *J Vestib Res-Equilib Orientat.* (2009) 19:1–13. doi: 10.3233/VES-2009-0343

21. Bisdorff AR, Staab JP, Newman-Toker DE. Overview of the international classification of vestibular disorders. *Neurol Clin.* (2015) 33:541. doi: 10.1016/j.ncl.2015.04.010

22. Ludman H. ABC of Ear, Nose and throat, 6th edition vertigo and imbalance. *Brit Med J.* (2014) 348:g283. doi: 10.1136/bmj.g283

23. Li Y, Lu W, Li J, Li M, Fang J, Xu T, et al. Electroencephalography microstate alterations in otogenic vertigo: a potential disease marker. *Front Aging Neurosci.* (2022) 14:914920. doi: 10.3389/fnagi.2022.914920

24. Matas CG, Silva SM, Wen DDM, da Silva Nunes C, Sanches SGG. Auditory evoked potentials in peripheral vestibular disorder individuals Potenciais evocados auditivos em indivíduos com síndrome vestibular periférica. *Int Arch Otorhinolar.* (2011) 15:308–13. doi: 10.1590/S1809-48722011000300007

25. He JW, Gong Q, Wang XF, Xiao Z. High stimulus rate brainstem auditory evoked potential in benign paroxysmal positional vertigo. *Eur Arch Oto-Rhino-L.* (2015) 272:2095100. doi: 10.1007/s00405-014-3172-6

26. Santos Filha VA, Bruckmann M, Garcia MV. Short- and long-latency auditory evoked potentials in individuals with vestibular dysfunction. *Codas.* (2018) 30:e2016260. doi: 10.1590/2317-1782/20182016260

27. Ahmed I. Brainstem auditory evoked potentials in dizziness. *Clin Electroencephalogr.* (1984) 15:110–5. doi: 10.1177/155005948401500208

28. Goto F, Oishi N, Tsutsumi T, Ito T, Arai M, Ogawa K. Characteristic electroencephalographic findings by photic driving in patients with migraine-associated vertigo. *Acta Otolaryngol.* (2013) 133:253–6. doi: 10.3109/00016489.2012.728718

29. Curthoys IS. The new vestibular stimuli: sound and vibration-anatomical, physiological and clinical evidence. *Exp Brain Res.* (2016) 235:957–72. doi: 10.1007/s00221-017-4874-y

30. Perez-Vazquez P, Franco-Gutierrez V. The caloric test. *Revista Orl.* (2018) 9:193–213. doi: 10.14201/orl.17699

31. Goncalves DU, Felipe L, Lima TMA. Interpretation and use of caloric testing. *Braz J Otorhinolar.* (2008) 74:440–6. doi: 10.1016/S1808-8694(15)30580-2

32. Kassemi M, Oas JG, Deserranno D. Fluid-structural dynamics of ground-based and microgravity caloric tests. *J Vestibul Res.-Equil.* (2005) 15:93–107. doi: 10.3233/VES-2005-15205

33. Brkic F, Gortan D, Kapidzic A, Sinanovic O, Brkic S. The effects of caloric vestibular stimulation on EEGs in patients with central vertigo. *Eur Arch Oto-Rhino-L.* (2002) 259:334–8. doi: 10.1007/s00405-002-0464-z

34. Engel AK, Fries P. Beta-band oscillations - signalling the status quo? *Curr Opin Neurobiol.* (2010) 20:156–65. doi: 10.1016/j.conb.2010.02.015

35. Kilavik BE, Zaepffel M, Brovelli A, MacKay WA, Riehle A. The ups and downs of beta oscillations in sensorimotor cortex. *Exp Neurol.* (2013) 245:15–26. doi: 10.1016/j.expneurol.2012.09.014

36. Naito Y, Tateya I, Hirano S, Inoue M, Funabiki K, Toyoda H, et al. Cortical correlates of vestibulo-ocular reflex modulation: a PET study. *Brain.* (2003) 126:1562–78. doi: 10.1093/brain/awg165

37. Bense S, Bartenstein P, Lochmann M, Schlindwein P, Brandt T, Dieterich M. Metabolic changes in vestibular and visual cortices in acute vestibular neuritis. *Ann Neurol.* (2004) 56:624–30. doi: 10.1002/ana.20244

38. Fasold O, von Brevern M, Kuhberg M, Ploner CJ, Villringer A, Lempert T, et al. Human vestibular cortex as identified with caloric stimulation in functional magnetic resonance imaging. *Neuroimage.* (2002) 17:1384–93. doi: 10.1006/nimg.2002.1241

39. Suzuki M, Kitano H, Ito R, Kitanishi T, Yazawa Y, Ogawa T, et al. Cortical and subcortical vestibular response to caloric stimulation detected by functional magnetic resonance imaging. *Cogn Brain Res.* (2001) 12:441–9. doi: 10.1016/S0926-6410(01)00080-5

40. Wang X, Long M, Yin J, Chen T. Progress in functional brain imaging of vestibular function. *Medical Recapitulate.* (2015) 21:1663–6. doi: 10.3969/j.issn.1006-2084.2015.09.048

41. Van Diepen RM, Foxe JJ, Mazaheri A.The functional role of alpha-band activity in attentional processing: the current zeitgeist and future outlook. *Curr Opin Psychol.* (2019) 29:229–38. doi: 10.1016/j.copsyc.2019.03.015

42. Yamagishi N, Anderson SJ. The relationship between self-awareness of attentional status, behavioral performance and oscillatory brain rhythms. *PLoS ONE.* (2013) 8:e74962. doi: 10.1371/journal.pone.0074962

43. Wang C, Rajagovindan R, Han SM, Ding M. Top-down control of visual alpha oscillations: sources of control signals and their mechanisms of action. *Front Human Neurosci.* (2016) 10:15. doi: 10.3389/fnhum.2016.00015

44. Barry RJ, Clarke AR, Johnstone SJ, Brown CR. EEG differences in children between eyes-closed and eyes-open resting conditions. *Clin Neurophysiol.* (2009) 120:1806–11. doi: 10.1016/j.clinph.2009.08.006

45. Li L, Zhang J. Study of the Alpha Wave Differences Between Eyes-Closed and Eyes-Open Resting States. *J Univ Electr Sci Technol China.* (2010) 39:450–3. doi: 10.1109/WICOM.2010.5600726

46. Benedetto A, Lozano-Soldevilla D, VanRullen R. Different responses of spontaneous and stimulus-related alpha activity to ambient luminance changes. *Eur J Neurosci.* (2018) 48:2599–608. doi: 10.1111/ejn.13791

47. Ertl M, Moser M, Boegle R, Conrad J, Zu Eulenburg P, Dieterich M. The cortical spatiotemporal correlate of otolith stimulation: Vestibular evoked potentials by body translations. *Neuroimage.* (2017) 155:50–9. doi: 10.1016/j.neuroimage.2017.02.044

frontiers | Frontiers in Neuroscience

TYPE Original Research
PUBLISHED 16 March 2023
DOI 10.3389/fnins.2023.1087488

Check for updates

OPEN ACCESS

EDITED BY
Fushun Wang,
Nanjing University of Chinese Medicine, China

REVIEWED BY
Paolo Papale,
Netherlands Institute for Neuroscience (KNAW), Netherlands
Daniel Leeds,
Fordham University, United States

*CORRESPONDENCE
Qingguo Ding
✉ qingguo_d2015@163.com
Pei Liang
✉ liangpei0108@126.com

†These authors share first authorship

SPECIALTY SECTION
This article was submitted to Perception Science, a section of the journal Frontiers in Neuroscience

RECEIVED 03 November 2022
ACCEPTED 28 February 2023
PUBLISHED 16 March 2023

CITATION
Wei L, Li X, Huang L, Liu Y, Hu L, Shen W, Ding Q and Liang P (2023) An fMRI study of visual geometric shapes processing. *Front. Neurosci.* 17:1087488. doi: 10.3389/fnins.2023.1087488

COPYRIGHT
© 2023 Wei, Li, Huang, Liu, Hu, Shen, Ding and Liang. This is an open-access article distributed under the terms of the Creative Commons Attribution License (CC BY). The use, distribution or reproduction in other forums is permitted, provided the original author(s) and the copyright owner(s) are credited and that the original publication in this journal is cited, in accordance with accepted academic practice. No use, distribution or reproduction is permitted which does not comply with these terms.

An fMRI study of visual geometric shapes processing

Liuqing Wei[1,2†], Xueying Li[1†], Lina Huang[3†], Yuansheng Liu[1], Luming Hu[4], Wenbin Shen[3], Qingguo Ding[3*] and Pei Liang[1,2,3*]

[1]Department of Psychology, Faculty of Education, Hubei University, Wuhan, China, [2]Brain and Cognition Research Center, Faculty of Education, Hubei University, Wuhan, China, [3]Imaging Department, Changshu No. 2 People's Hospital, The Clinical Medical College Affiliated to Xuzhou Medical University, Changshu, China, [4]Department of Psychology, School of Arts and Sciences, Beijing Normal University, Zhuhai, China

Cross-modal correspondence has been consistently evidenced between shapes and other sensory attributes. Especially, the curvature of shapes may arouse the affective account, which may contribute to understanding the mechanism of cross-modal integration. Hence, the current study used the functional magnetic resonance imaging (fMRI) technique to examine brain activity's specificity when people view circular and angular shapes. The circular shapes consisted of a circle and an ellipse, while the angular shapes consisted of a triangle and a star. Results show that the brain areas activated by circular shapes mainly involved the sub-occipital lobe, fusiform gyrus, sub and middle occipital gyrus, and cerebellar VI. The brain areas activated by angular shapes mainly involve the cuneus, middle occipital gyrus, lingual gyrus, and calcarine gyrus. The brain activation patterns of circular shapes did not differ significantly from those of angular shapes. Such a null finding was unexpected when previous cross-modal correspondence of shape curvature was considered. The different brain regions detected by circular and angular shapes and the potential explanations were discussed in the paper.

KEYWORDS

vision, circular and angular shapes, emotion, fMRI, cross-modal correspondence

Introduction

Plenty of literature has provided evidence that shapes' curvilinearity (roundedness and angularity) may have consistent cross-modal correspondences with other sensory attributes (Spence, 2011; Spence and Ngo, 2012; Ghoshal et al., 2016; Lee and Spence, 2022). For instance, people associate curved shapes with a sweet taste, quiet or calm sound, vanilla smell, green color, smooth texture, relieved emotion, female gender, and wide-vowel names; while they associate angular shapes with sour taste, loud or dynamic sound, spicy or citrus smell, red color, rough texture, excited or surprise emotion, male gender, and narrow-vowel names (Blazhenkova and Kumar, 2017). Different hypotheses have been proposed for the cross-modal correspondence effect (Lee and Spence, 2022). One is the statistical account, which means the internalization of the multisensory statistics of the environment. The other is the affective account, and cross-modal correspondences are mediated by emotion (Wang et al., 2016). Thus, an intriguing question arises: how does the brain process geometric shapes, particularly circular and angular shapes?

People generally prefer circular stimuli over angular ones (Wang and Zhang, 2016; Cotter et al., 2017). The geometric stimuli may convey different emotions. For example, diagonal and angular shapes tend to be associated with threat, while rounded features and curved lines are associated with pleasure and happiness (Bar and Neta, 2007, 2016; Larson et al., 2012). At the behavioral level, Bar and Neta (2016) found that people disliked sharp-angled neutral objects more than curved neutral objects. They proposed that people may perceive the sharp contour as threatening, thus influencing their attitudes toward sharp-angled objects to be negative (Bar and Neta, 2016). Bar and Neta (2007) found that compared to objects with curving contours, neutral objects (abstract figures, everyday objects) containing sharp contours elicited greater activation of the amygdala, a brain structure that involves in fear processing and is proportional to arousal in genera. Larson et al. (2016) also validated the greater activation of the amygdala by the presentation of downward-pointing V-shapes, compared to the identical V-shape pointing upward. Moreover, recent electrophysiological evidence has shown that ellipse and triangle shapes were found to arouse similar ERP responses (N1, N2, P1, and P2 recorded from parietal lobes) to line-drawn happy and angry faces (Li et al., 2018). These findings suggest that simple shapes can induce threat and negative affection at the low-level perceptual stage.

Recently, the brain areas involved in geometric shape processing have been proposed in a distributed network (Freud et al., 2017; Freud and Behrmann, 2020) or *via* a skeletal structure located in V3 and lateral occipital cortex for perceptual organization and object recognition (Ayzenberg et al., 2019a,b; Ayzenberg and Lourenco, 2019). Bracci and de Beeck (2016) found that shape and category information interacts throughout the ventral and dorsal visual pathways for successful object recognition. Ayzenberg et al. (2022) used models that approximate early-, mid- and high-level visual processing. Indeed, V3 has been consistently implicated in creating shape percepts (Montaser-Kouhsari et al., 2007; Caplovitz et al., 2008; McMains and Kastner, 2010). Perceptual organization is accomplished by border ownership cells in V2 and the subsequent visual region V3, to specify the contours of a figure (Zhou et al., 2000; von der Heydt, 2015). Temporal dynamics analysis has shown that low-level properties like contrast and spatial frequencies, medial-axis like shape and category have an independent process at the early time window (100–150 ms) (Papale et al., 2019). Hence, the object shape is encoded along different dimensions and each representing orthogonal features (Papale et al., 2020).

Based on the above research results, geometric information is not only processed according to the statistical account throughout the visual cortex. The affective account of the geometric shapes is also involved in different stages of visual pathways. In particular, shapes' curvilinearity (roundedness and angularity) can lead to different preferences and affective effects with cross-modal experiments (Velasco et al., 2015). What brain areas are involved in the processing of circular and angular shapes? Is shape curvature processed differently by different regions? This study aimed to answer these questions. Using the fMRI technique, the current study adopted a simple geometric shape viewing task and explored the brain activation of simple circular and angular shapes processing. It was expected to find different activation of brain areas for circular and angular shapes. If yes, which brain regions are involved and the possible explanation will be discussed later.

Materials and methods

Participants

In our experiment, a total of 12 subjects volunteered to participate in the experiment, including three males and nine females. The average age of the participants is 21.75 ± 0.62 (from 21 to 23) years old. All participants had normal or corrected to normal vision and reported no history of neurological or psychiatric disorder. All participants were well informed about the study's procedures and provided informed written consent. The study was approved by the Ethics Committee of the No. 2 People's Hospital of Changshu (license number 2018–68). All participants received payments for their time.

Stimuli

The basic geometric shapes with different curvatures were applied. Circular shapes included a circle and an ellipse. Angular shapes contain triangles and stars. The two types of shapes are comparable in contrast, color, and size when presented on display (**Figure 1**).

Tasks

The experiment contained four blocks, and each block included six trials. In each trial, participants watched one geometric shape for 6 s, then rested for 14 s. Each block repeated, displaying the same shape six times and lasted 120 s. The whole experiment lasted around 8 min. The order of the blocks was balanced among the participants.

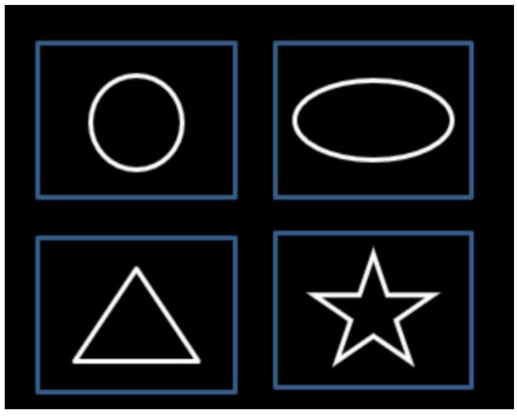

FIGURE 1
Four shapes, circle and ellipse as circular type, and triangle and star as angular type. Each of the shapes was displayed randomly as visual stimuli in the experiment.

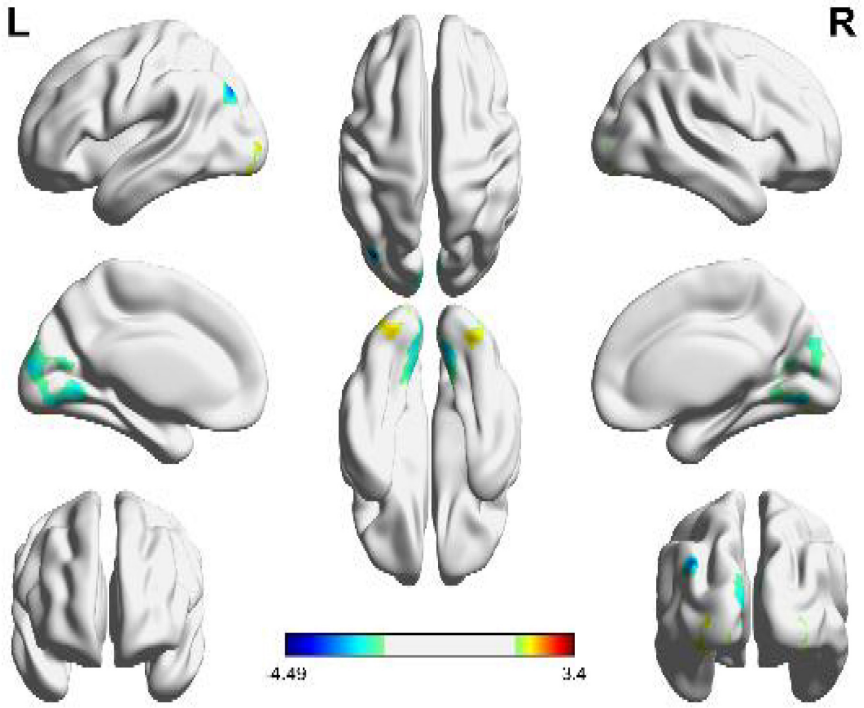

FIGURE 2
Brain activation regions of geometric shapes (circular and angular shapes). The color bar indicates the size of the activation intensity. The values indicate positive or negative activation.

MRI data acquisition

Structural and functional MRI data were collected using the GE Discovery MR750W 3.0T scanning system. The scanner is with an 8-channel head coil. During the scanning process, the participants quietly lay on the back of the magnetic resonance examination bed, fixing the head inside the head coil with foam padding, and wearing earplugs to reduce machine noise. The participants watched the visual stimuli through a reflector mirror mounted on the head coil. Through the mirror, the visual stimuli were reflected from the projector screen, placed outside the gate of the MRI. For structural imaging, high-resolution T1 weighted scans were acquired. The 3D T1 BRAVO_SPM volume sequence was applied with TR = 8.5 ms, TE = 3.2 ms, flip angle = 12°, FOV = 24 cm, 256 × 256 matrix size, and 1 mm slice thickness. The MR sequence for T2-weighted functional imaging was acquired using TR = 2000 ms, TE = 30 ms, flip angle = 90°, scan resolution of 64 × 64, 33 slices, intervals of 2 mm with slice thickness = 3.6 mm, FOV = 24 cm, voxel size = 3.75 × 3.75 × 3.75 mm^3.

fMRI data analysis

Shape fMRI data analysis

The preprocessing and statistical analysis of NMR data mainly used the SPM12 toolbox (Wellcome Department of Imaging Neuroscience, University College London, UK)[1] and DPAIBI toolbox (a toolbox for Data Processing and Analysis for Brain Imaging, China)[2] based on Matlab 2012b (Mathworks, MA)[3] platform.

The preprocessing of functional image data includes head movement correction, tissue segmentation, spatial registration and spatial Standardization (mapped to MNI (Montreal Neurological Institute)) standard space established by Montreal Institute of Neurology [bounding box: – 126 – 72; 90 108; – 90 90 90], with a resolution of 3 × 3 × 3 mm^3, and spatial smoothing (using a three-dimensional Gaussian kernel with a half height and width of 6 mm). Among them, the sequences in which the translation amount of the head movement range exceeds 2 mm or the rotation amount exceeds 2° are eliminated (around 6% of sequences are eliminated).

After the pretreatment, in the first-order analysis, the design parameters of the three conditions are combined with Hemodynamic Response Function (HRF) to construct the parameter model of a unified general linear model (GLM), and the head movement parameters are included in the model as covariates. At the first-order individual level, four groups of comparative analysis were carried out, namely geometric shapes (circular + angular) > resting condition, circular condition > resting condition, angular condition > resting condition, and circular condition > angular condition.

At the second-order group level, the four groups for each participant were grouped and combined by DPABI software, and then the group single sample *t*-test was performed. In the group

1 http://www.fil.ion.ucl.ac.uk/spm

2 http://rfmri.org/dpabi

3 http://www.mathworks.com

TABLE 1 Clusters of brain activation areas for geometric shapes.

Labels	Brain side	Voxels	*t*	MNI		
				x	*y*	*z*
Inferior occipital gyrus	L	190	3.395	−24	−90	−3
Middle occipital gyrus	L	102	−4.487	−39	−78	36
Fusiform gyrus	R	152	2.704	30	−84	−6
Cerebellum (VI)	R	1151	−2.962	12	−72	−9
Cerebellum (VI)	L	1151	−2.669	−15	−72	−15
Cerebellum (VII)	L	11	−1.995	−21	−75	−42
Cuneus	L	1151	−2.822	3	−87	27
Precuneus	L	17	−2.675	−3	−54	69
Precuneus	L	17	−1.972	0	−72	51
Caudate nucleus	R	11	−2.138	21	−9	27

Tables 1–3, L, left brain; R, right brain. *t*-value shows the mean difference of activation.

single sample *t*-test, the non-parametric permutation test method is used for treatment, the number of permutations is 5000, and the cluster-forming threshold is set to $P < 0.001$. Finally, voxels with $P < 0.05$ are presented. All the above comparisons were performed on a custom gray matter removal template. The whole brain activation map was rendered by BrainNet view software.

Results

We compared circular shapes vs angular shapes first. However, no significant brain activation was detected (we presented the details of the null results in the **Supplementary material**). The results would be insignificant if the voxels of the detected brain regions were below 10. Hence, we looked at the common brain regions stimulated by geometric shapes and the regions by circular and angular shapes separately.

Analysis of common brain regions stimulated by geometric shapes

Through the whole brain fMRI analysis, we analyzed the activated brain regions by viewing geometric shapes (circular shapes and angular shapes). We obtained the three-dimensional brain map, as shown in **Figure 2**. The details of the active voxel group in the figure are shown in **Table 1**.

As can be seen from **Figure 2**, the brain activation functional areas of the geometric shapes are mainly located in the cuneus, cerebellum VI, fusiform gyrus, middle occipital gyrus and suboccipital gyrus, followed by pre-cuneus lobe and cerebellum VII.

According to the details of the activated voxel group in **Table 1**, it can be seen that the maximum range includes 1151 voxels, including the cuneus and cerebellar VI. This is because the cuneus is related to basic visual processing; Cerebellar VI is related to motor planning and coordination. Secondly, the fusiform, suboccipital, and middle occipital gyrus were activated. This is because the function of the fusiform gyrus is related to object and face recognition (Keshav and Hof, 2013). The middle occipital gyrus is the brain region of early visual processing, mainly responsible for extracting shapes and external visual features of words and objects (Beharelle and Small, 2016).

Analysis of independent brain regions stimulated by different shapes

In order to further examine the brain regions excited by circular and angular shapes, the brain activation maps of the two shapes were obtained, respectively. As shown in **Figure 3**, it is the activation of circular shapes in the brain region. The details of activated voxel groups are shown in **Table 2**.

It can be seen from **Figure 3** and **Table 2** that the positive activation areas of brain functional regions with circular shapes mainly involve the suboccipital lobe, fusiform gyrus, suboccipital gyrus and cerebellar VI, followed by the anterior central gyrus, posterior medial frontal lobe and superior frontal gyrus; The negative activation areas mainly involve the middle occipital gyrus and cerebellar VI. Both the left and right brains have positive and negative activation reactions, but the primary activation reaction is positive. As shown in **Table 2**, the voxel group information activated by circular shapes includes 454 voxels when the activation range is the largest, which are concentrated in the suboccipital lobe and fusiform gyrus of the left brain, followed by 346 voxels, which are concentrated in the suboccipital lobe, cerebellar VI and fusiform gyrus of the right brain. The negative activation was mainly in the middle occipital gyrus of the left brain, containing 17 voxels; Cerebellum VI of the right brain contains 15 voxels.

As shown in **Figure 4**, the independent brain regions are activated by angular patterns, and the details of activated voxel groups are shown in **Table 3**.

It can be seen from **Figure 4** and **Table 3** that the positive activation of functional brain areas by angular shapes mainly involve the fusiform gyrus and cerebellum, the negative activation mainly involves the middle occipital gyrus, cuneus and lingual gyrus, followed by the superior medial gyrus, middle frontal gyrus, middle temporal gyrus and angular gyrus. The left and right brains have positive and negative activation, mainly negative activation. As shown in **Table 3**, voxel group information is activated by angular shapes. The largest range is concentrated in the middle occipital gyrus, cuneus and lingual gyrus, including 9551 voxels, which are all negatively activated. Positive activation is mainly in the fusiform gyrus of the left brain, containing 44 voxels, and the cerebellar region of the right brain, containing 28 voxels.

To sum up, the brain activation of circular shapes is mainly positive, while the activation of angular shapes is mainly negative. Viewing circular shapes and angular shapes may involve different neural computations.

Discussion

Circular shapes tend to be perceived as positive, while angular shapes tend to be perceived as negative (Aronoff et al., 1988, 1992; Bar and Neta, 2016). Previous studies have indicated the non-arbitrary correspondence between circular and angular shapes and

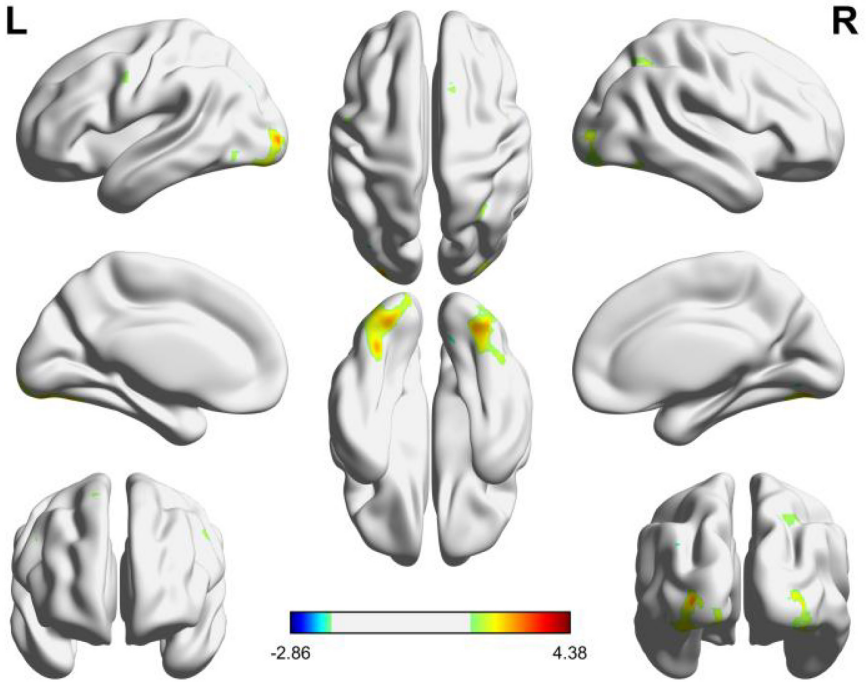

FIGURE 3
Brain functional areas activated by circular shapes. The color bar indicates the size of the activation intensity. The values indicate positive or negative activation.

various attributes (Spence et al., 2010; Spence, 2011; Hanson-Vaux et al., 2013; Fryer et al., 2014). However, there are few studies on the specific brain regions involving different geometric shapes in brain processing. The brain regions involved in the processing of circular shapes and angular shapes and their differences are unclear. Thus, this study used a simple shape-viewing task to study the activation responses of brain regions when viewing these two different types of shapes through fMRI.

The results showed that the brain regions activated by geometric shapes were mainly in the cuneus and cerebellar VI region. Cuneus is involved in basic visual processing, and Cerebellar VI is related to motor planning and coordination (Guell et al., 2018). The cerebellum involvement might be explained by the reasons for motor affordances of shapes (Lewis et al., 2003). It should be noted that the different stages of visual processing involve the activity coming from the pre-cuneus, lateral occipital and posterior inferotemporal cortex (Coppen et al., 2018). Moreover, the activation of brain regions involved the fusiform, suboccipital, and middle occipital gyrus. This is because the function of the fusiform gyrus is related to object and face recognition (Keshav and Hof, 2013). The middle occipital gyrus is the brain region of early visual processing, mainly responsible for extracting shapes and external visual features of words and objects (Beharelle and Small, 2016).

TABLE 2 Clusters of brain areas activated by circular shapes.

Labels	Brain side	Voxels	*t*	MNI		
				x	*y*	*z*
Inferior occipital	L	454	4.381	−21	−93	0
Inferior occipital gyrus	R	346	3.174	30	−93	0
Middle occipital gyrus	L	17	−2.864	−33	−81	39
Fusiform gyrus	L	454	3.218	−33	−69	−12
Fusiform gyrus	R	346	2.256	42	−63	−15
Cerebellum (VI)	R	346	3.053	27	−78	−15
Cerebellum (VII)	R	15	−2.236	12	−72	−9
Precentral gyrus	L	34	2.454	−48	−3	36
Precentral gyrus	R	21	2.033	48	3	36
Posterior-medial frontal	L	11	2.266	−9	12	63
Posterior-medial frontal	R	18	2.112	9	3	63
Superior-medial gyrus	R	15	2.252	15	18	60

For the brain activation of circular and angular shapes, circular shapes are mainly positive, while angular shapes are mainly negative. These observations suggest that the brain's basis of circular and angular shapes processing involves different computations. The different, often neighboring, brain regions are more active for round versus for sharp surface, which also supports the different computation theroy, or a gradient-of-representation theories (Freiwald, 2020; Hesse and Tsao, 2020). However, no significant brain area was detected comparing circular and angular shapes. This result was different from our expectations. One reason could be that the experiment design was not sensitive enough. In future, we should record the rating of the different shapes during fMRI scanning so that the valence ratings of the circular and angular shapes should be confirmed to be different.

We also hypothesized that geometry is processed in the primary visual cortex and brain areas such as higher emotion. The current study emphasizes the role of emotion processing in angular and

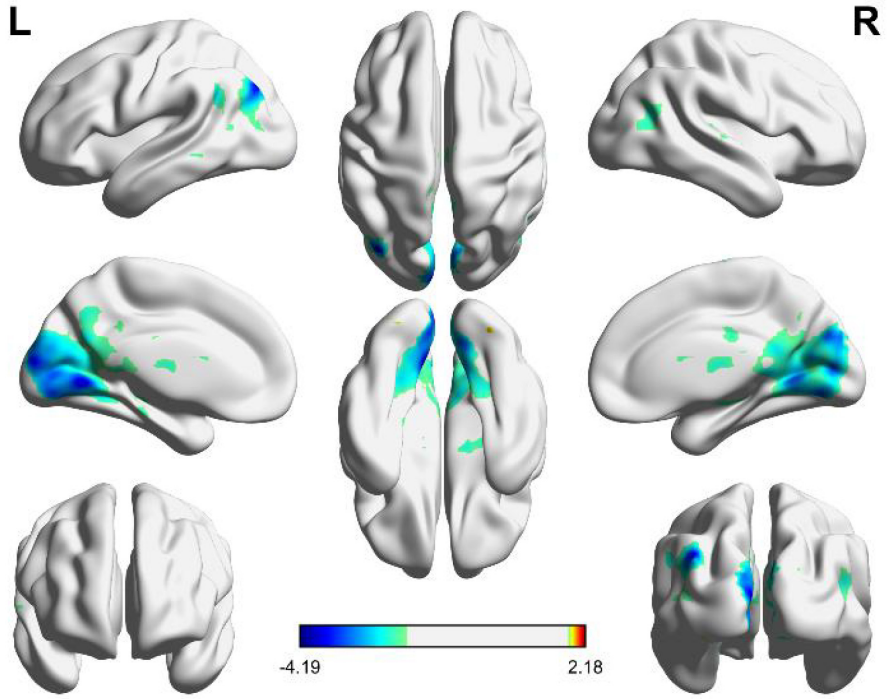

FIGURE 4
Brain functional areas activated by angular shapes. The color bar indicates the size of the activation intensity. The values indicate positive or negative activation.

curved correspondence, which is also supported by neuroscience evidence, which emphasizes the role of emotion in multisensory perception and shape perception (Drevets et al., 1998; Vuilleumier, 2005; Bar and Neta, 2007; Palmer et al., 2013). However, the current study did not find amygdala activation in the angular-shape or circular-shape conditions. One explanation is that simple geometric shapes are more abstract and have weaker emotional cues than facial expressions or scenes with emotional meanings. Therefore, in future studies, we can consider a more active task and choosing more specific or more emotional geometric figures, which may lead to more different results.

One limitation of this study is that it adopts a simple shape-viewing task. Moreover, in the geometric sense, only two types of figures are simple and have the same topological properties. Other than the curvature of the shape, the spatial frequencies, inked size and local contrast should be considered in future experiment design. In further studies, we may consider adopting a more sensitive experimental paradigm to identify the brain activation of circular and angular shapes, and localize the ROI at amygdala and cuneus. Moreover, the number of subjects in this study is relatively small. More samples in the future study will guarantee better reliability and validity.

TABLE 3 Clusters of brain areas activated by angular shapes.

Labels	Brain side	Voxels	*t*	MNI		
				x	*y*	*z*
Middle occipital gyrus	L	9551	−4.190	−39	−78	36
Fusiform gyrus	L	44	2.184	−30	−87	−12
Cerebellum (VI)	R	28	2.177	27	−81	−18
Cerebellum (crus 1)	L	13	−2.184	−42	−60	−27
Calcarine gyrus	R	9551	−2.027	12	−75	21
Cuneus	L	9551	−4.171	3	−75	30
Lingual gyrus	L	9551	−3.993	−9	−63	0
Superior medial gyrus	L	31	−3.244	3	36	54
Angular gyrus	L	16	−2.499	−42	−63	51
Angular gyrus	R	14	−2.043	57	−57	36
Middle frontal gyrus	L	17	−2.238	−30	36	42
Superior frontal gyrus	L	13	−1.953	−21	51	30
Middle temporal gyrus	R	24	−1.993	60	−6	−18

Data availability statement

The original contributions presented in this study are included in the article/**Supplementary material**, further inquiries can be directed to the corresponding authors.

Ethics statement

The studies involving human participants were reviewed and approved by the Ethics Committee of the No. 2 People's Hospital of Changshu. The patients/participants provided their written informed consent to participate in this study.

Author contributions

LW, XL, LiH, QD, and PL conceived and designed the experiments and contributed to the writing of the manuscript. YL, LuH, and WS performed the experiments and analyzed the data. All authors contributed to the article and approved the submitted version.

Funding

This work has been supported by the National Natural Science Foundation of China (61703058).

Conflict of interest

The authors declare that the research was conducted in the absence of any commercial or financial relationships that could be construed as a potential conflict of interest.

Publisher's note

All claims expressed in this article are solely those of the authors and do not necessarily represent those of their affiliated organizations, or those of the publisher, the editors and the reviewers. Any product that may be evaluated in this article, or claim that may be made by its manufacturer, is not guaranteed or endorsed by the publisher.

Supplementary material

The Supplementary Material for this article can be found online at: https://www.frontiersin.org/articles/10.3389/fnins.2023.1087488/full#supplementary-material

References

Aronoff, J., Barclay, A., and Stevenson, L. (1988). The recognition of threatening facial stimuli. *J. Pers. Soc. Psychol.* 54, 647–655. doi: 10.1037/0022-3514.54.4.647

Aronoff, J., Woike, B., and Hyman, L. (1992). Which are the stimuli in facial displays of anger and happiness? configurational bases of emotion recognition. *J. Pers. Soc. Psychol.* 62, 1050–1066. doi: 10.1037/0022-3514.62.6.1050

Ayzenberg, V., Chen, Y., Yousif, S. R., and Lourenco, S. F. (2019a). Skeletal representations of shape in human vision: Evidence for a pruned medial axis model. *J. Vis.* 19:6. doi: 10.1167/19.6.6

Ayzenberg, V., Kamps, F. S., Dilks, D. D., and Lourenco, S. F. (2019b). A dual role for shape skel- etons in human vision: Perceptual organization and object recognition. *Biorxiv* [Preprint]. doi: 10.1101/799650

Ayzenberg, V., Kamps, F. S., Dilks, D. D., and Lourenco, S. F. (2022). Skeletal representations of shape in the human visual cortex. *Neuropsychologia* 164:108092. doi: 10.1016/j.neuropsychologia.2021.108092

Ayzenberg, V., and Lourenco, S. F. (2019). Skeletal descriptions of shape provide unique perceptual information for object recognition. *Sci. Rep.* 9:9359. doi: 10.1038/s41598-019-45268-y

Bar, M., and Neta, M. (2007). Visual elements of subjective preference modulate amygdala activation. *Neuropsychologia* 45, 2191–2200. doi: 10.1016/j.neuropsychologia.2007.03.008

Bar, M., and Neta, M. (2016). Humans prefer curved visual objects. *Psychol. Sci.* 17, 645–648. doi: 10.1111/j.1467-9280.2006.01759.x

Beharelle, A. R., and Small, S. L. (2016). "Imaging Brain Networks for Language," in *Neurobiology of language*, eds G. Hickok and S. L. Small (Amsterdam: Elsevier), 805–814.

Blazhenkova, O., and Kumar, M. M. (2017). Angular versus curved shapes: Correspondences and emotional processing. *Perception* 47, 67–89. doi: 10.1177/0301006617731048

Bracci, S., and de Beeck, H. (2016). Dissociations and associations between shape and category representations in the two visual pathways. *J. Neurosci.* 36, 432–444. doi: 10.1523/JNEUROSCI.2314-15.2016

Caplovitz, G. P., Barroso, D. J., Hsieh, P. J., and Tse, P. U. (2008). fMRI reveals that non-local processing in ventral retinotopic cortex underlies perceptual grouping by temporal synchrony. *Hum. Brain Mapp.* 29, 651–661. doi: 10.1002/hbm.20429

Coppen, E. M., Grond, J. V., Hafkemeijer, A., Barkey Wolf, J. J. H., and Roos, R. A. C. (2018). Structural and functional changes of the visual cortex in early Huntington's disease. *Hum. Brain Mapp.* 39, 4776–4786. doi: 10.1002/hbm.24322

Cotter, K. N., Silvia, P. J., Bertamini, M., Palumbo, L., and Vartanian, O. (2017). Curve appeal: Exploring individual differences in preference for curved versus angular objects. *Iperception* 8:2041669517693023. doi: 10.1177/2041669517693023

Drevets, W., Price, J., Simpson, J., Todd, R., Reich, T., Vannier, M., et al. (1998). Subgenual prefrontal cortex abnormalities in mood disorders. *Nature* 386, 824–827. doi: 10.1038/386824a0

Freiwald, W. A. (2020). The neural mechanisms of face processing: Cells, areas, networks, and models. *Curr. Opin. Neurobiol.* 60, 184–191. doi: 10.1016/j.conb.2019.12.007

Freud, E., and Behrmann, M. (2020). Altered large-scale organization of shape processing in visual agnosia. *Cortex* 129, 423–435. doi: 10.1016/j.cortex.2020.05.009

Freud, E., Culham, J. C., Plaut, D. C., and Behrmann, M. (2017). The large-scale organization of shape processing in the ventral and dorsal pathways. *Elife* 6:e27576. doi: 10.7554/eLife.27576

Fryer, L., Freeman, J., and Pring, L. (2014). Touching words is not enough: How visual experience influences haptic-auditory associations in the "Bouba-Kiki" effect. *Cognition* 132, 164–173. doi: 10.1016/j.cognition.2014.03.015

Ghoshal, T., Boatwright, P., and Malika, M. (2016). "Curvature from all angles: An integrative review and implications for product design," in *The psychology of design: Creating consumer appeal*, eds R. Batra, C. Seifert, and D. Brei (Abingdon, UK: Routledge/Taylor & Francis Group), 91–106.

Guell, X., Schmahmann, J. D., Gabrieli, J., and Ghosh, S. S. (2018). Functional gradients of the cerebellum. *Elife* 7:e36652. doi: 10.7554/eLife.36652

Hanson-Vaux, G., Crisinel, A. S., and Spence, C. (2013). Smelling shapes: Crossmodal correspondences between odors and shapes. *Chem. Senses* 38, 161–166. doi: 10.1093/chemse/bjs087

Hesse, J. K., and Tsao, D. Y. (2020). The macaque face patch system: A turtle's underbelly for the brain. *Nat. Rev. Neurosci.* 21, 695–716. doi: 10.1038/s41583-020-00393-w

Keshav, N., and Hof, P. (2013). "Discrete Cortical Neuropathology in Autism Spectrum Disorders," in *The neuroscience of autism spectrum disorders*, eds J. Buxbaum and P. R. Hof (Oxford: Elsevier), 313–325. doi: 10.1016/B978-0-12-391924-3.00022-3

Larson, C. L., Aronoff, J., Sarinopoulos, I. C., and Zhu, D. C. (2016). Recognizing threat: A simple geometric shape activates neural circuitry for threat detection. *J. Cogn. Neurosci.* 21, 1523–1535. doi: 10.1162/jocn.2009.21111

Larson, C. L., Aronoff, J., and Steuer, E. L. (2012). Simple geometric shapes are implicitly associated with affective value. *Motiv. Emot.* 36, 404–413. doi: 10.1007/s11031-011-9249-2

Lee, B. P., and Spence, C. (2022). Crossmodal correspondences between basic tastes and visual design features: A narrative historical review. *Iperception* 13:20416695221127325. doi: 10.1177/20416695221127325

Lewis, S., Tzagarakis, C., and Georgopoulos, A. P. (2003). Cerebellar activation during copying geometrical shapes. *J. Neurophysiol.* 90, 3874–3887. doi: 10.1152/jn.00009.2003

Li, Y., Ding, Q., Zhao, Y., Bu, Y., Tang, X., Wang, P., et al. (2018). Direct electrophysiological mapping of shape-induced affective perception. *Neural Plast.* 2018:9795013. doi: 10.1155/2018/9795013

McMains, S. A., and Kastner, S. (2010). Defining the units of competition: Influences of perceptual organization on competitive interactions in human visual cortex. *J. Cogn. Neurosci.* 22, 2417–2426. doi: 10.1162/jocn.2009.21391

Montaser-Kouhsari, L., Landy, M. S., Heeger, D. J., and Larsson, J. (2007). Orientation-selective adaptation to illusory contours in human visual cortex. *J. Neurosci.* 27, 2186–2195. doi: 10.1523/JNEUROSCI.4173-06.2007

Palmer, S. E., Schloss, K. B., Xu, Z., and Prado-Leon, L. R. (2013). Music-color associations are mediated by emotion. *Proc. Natl. Acad. Sci. U. S. A.* 110, 8836–8841. doi: 10.1073/pnas.1212562110

Papale, P., Betta, M., Handjaras, G., Malfatti, G., Cecchetti, L., Rampinini, A., et al. (2019). Common spatiotemporal processing of visual features shapes object representation. *Sci. Rep.* 9:7601. doi: 10.1038/s41598-019-43956-3

Papale, P., Leo, A., Handjaras, G., Cecchetti, L., Pietrini, P., and Ricciardi, E. (2020). Shape coding in occipito-temporal cortex relies on object silhouette, curvature, and medial axis. *J. Neurophysiol.* 124, 1560–1570. doi: 10.1152/jn.00212.2020

Spence, C. (2011). Managing sensory expectations concerning products and brands: Capitalizing on the potential of sound and shape symbolism. *J. Consum. Psychol.* 22, 37–54. doi: 10.1016/j.jcps.2011.09.004

Spence, C., Levitan, C. A., Shankar, M. U., and Zampini, M. (2010). Does food color influence taste and flavor perception in humans? *Chem. Percept.* 3, 68–84. doi: 10.1007/s12078-010-9067-z

Spence, C., and Ngo, M. (2012). Assessing the shape symbolism of the taste, flavour, and texture of foods and beverages. *Flavour* 1:12. doi: 10.1186/2044-7248-1-12

Velasco, C., Woods, A. T., Deroy, O., and Spence, C. (2015). Hedonic mediation of the crossmodal correspondence between taste and shape. *Food Qual. Prefer.* 41, 151–158. doi: 10.1016/j.foodqual.2014.11.010

von der Heydt, R. (2015). Figure-ground organization and the emergence of proto-objects in the visual cortex. *Front. Psychol.* 6:1695. doi: 10.3389/fpsyg.2015.01695

Vuilleumier, P. (2005). How brains beware: Neural mechanisms of emotional attention. *Trends Cogn. Sci.* 9, 585–594. doi: 10.1016/j.tics.2005.10.011

Wang, Q. J., Wang, S., and Spence, C. (2016). "Turn Up the Taste": Assessing the role of taste intensity and emotion in mediating crossmodal correspondences between basic tastes and pitch. *Chem. Senses* 41, 345–356. doi: 10.1093/chemse/bjw007

Wang, Y., and Zhang, Q. (2016). Affective priming by simple geometric shapes: Evidence from event-related brain potentials. *Front. Psychol.* 7:917. doi: 10.3389/fpsyg.2016.00917

Zhou, H., Friedman, H., and von der Heydt , R. (2000). Coding of border ownership in monkey visual cortex. *J. Neurosci.* 20, 6594–6611. doi: 10.1523/jneurosci.20-17-06594.2000

frontiers | Frontiers in Neurology

TYPE Review
PUBLISHED 23 June 2023
DOI 10.3389/fneur.2022.1047876

Check for updates

OPEN ACCESS

EDITED BY
Jian-hua Zhuang,
Shanghai Changzheng Hospital, China

REVIEWED BY
Xin Ma,
Peking University People's Hospital, China
Binbin Xiong,
Zhuhai Hospital of Integrated of Traditional Chinese Medicine and Western Medicine, China

*CORRESPONDENCE
Ganggang Chen
chenganggang@vip.163.com

†These authors have contributed equally to this work

SPECIALTY SECTION
This article was submitted to Neuro-Otology, a section of the journal Frontiers in Neurology

RECEIVED 19 September 2022
ACCEPTED 17 October 2022
PUBLISHED 23 June 2023

CITATION
Chen G, Zhang J, Qiao Q, Zhou L, Li Y, Yang J, Wu J and Huangfu H (2023) Advances in dynamic visual acuity test research. *Front. Neurol.* 13:1047876. doi: 10.3389/fneur.2022.1047876

COPYRIGHT
© 2023 Chen, Zhang, Qiao, Zhou, Li, Yang, Wu and Huangfu. This is an open-access article distributed under the terms of the Creative Commons Attribution License (CC BY). The use, distribution or reproduction in other forums is permitted, provided the original author(s) and the copyright owner(s) are credited and that the original publication in this journal is cited, in accordance with accepted academic practice. No use, distribution or reproduction is permitted which does not comply with these terms.

Advances in dynamic visual acuity test research

Ganggang Chen[1*†], Jin Zhang[2†], Qi Qiao[3], Liyuan Zhou[1], Ying Li[1], Jie Yang[1], Jiaxin Wu[1] and Hui Huangfu[1]

[1]Department of Otorhinolaryngology-Head and Neck Surgery, First Hospital of Shanxi Medical University, Taiyuan, China, [2]Department of Otorhinolaryngology-Head and Neck Surgery, Shaanxi Provincial People's Hospital, Xi'an, China, [3]Department of Otorhinolaryngology-Head and Neck Surgery, Xijing Hospital of Air Force Military Medical University, Xi'an, China

The dynamic visual acuity test (DVAT) is a functional evaluation tool for the impairment and compensation of the vestibular system, which could reflect the Vestibulo-ocular reflex (VOR) function. We present an overview of DVAT research, displaying recent advances in test methods, application, and influencing factors; and discussing the clinical value of DVAT to provide a reference for clinical application. There are two primary types of DVAT: dynamic-object DVAT and static-object DVAT. For the latter, in addition to the traditional bedside DVAT, there are numerous other approaches, including Computerized DVAT (cDVAT), DVAT on a treadmill, DVAT on a rotary, head thrust DVA (htDVA) and functional head impulse testing (fHIT), gaze shift dynamic visual acuity with walking (gsDVA), translational dynamic visual acuity test (tDVAT), pediatric DVAT. The results of DAVT are affected by subject [occupation, static visual acuity (SVA), age, eyeglass lenses], testing methods, caffeine, and alcohol. DVAT has numerous clinical applications, such as screening for vestibular impairment, assessing vestibular rehabilitation, predicting fall risk, and evaluating ophthalmology-related disorders, vestibular disorders, and central system disorders.

KEYWORDS

dynamic visual acuity test (DVAT), Vestibulo-ocular reflex (VOR), vestibular disorders, dynamic visual acuity (DVA), static visual acuity (SVA)

Introduction

Dynamic visual acuity is the ability to discriminate fine details of dynamic objects during head fixation or in static objects during head or body rotation (1). DVAT is a functional evaluation tool for the impairment and compensation of the vestibular system. DVAT mainly consists of two types: dynamic-object DVAT, in which the observer identifies dynamic objects with a stationary head, and static-object DVAT, in which the observer identifies static objects with a moving head (1). When the head movement frequency is $\geq$2 Hz, the VOR system is activated (2), which generates compensatory eye movements in the opposite direction of the head movement to maintain stable vision. When the patient has severe vestibular dysfunction or inadequate vestibular compensatory capacity, the visual image slips on the retina, resulting in a loss in dynamic

visual acuity, leading to oscillopsia, dizziness, and nausea. This is the fundamental idea underlying the evaluation of vestibular function by DVAT, which can be viewed as a quantitative test of this phenomenon.

Static visual acuity (SVA)

Visual acuity is the capacity of the eye to distinguish fine details. SVA is defined as the capacity to detect the details of stationary objects whose image is formed on the retina when the subject being evaluated is also stationary. SVA is one of the most frequently used clinical tests for visual acuity. The levels of visual acuity on a visual acuity chart are typically expressed as the Log of the Minimum Angle Resolvable (LogMAR). LogMAR units describe the size of an image based on a ratio of its absolute size to its distance from the eye. Using only SVA to evaluate visual system is inadequate for two primary reasons (3): Many of the visual stimuli to which we must respond in daily life and many sports are frequently in motion; the SVA tests refer to letters or symbols that are commonly exhibited under conditions of maximum contrast (black on white), which is rarely encountered in the various scenarios of everyday life. Therefore, DVA is an essential component of a comprehensive clinical assessment in addition to SVA.

DVAT methods

Currently, there are various methods of DVAT, but the basic principle remains the same: to access the VOR function by comparing the difference between DVA and SVA. The dynamic visual acuity loss (DVA loss) is calculated as the difference between DVA and SVA.

Static-object DVAT

Bedside DVAT (or non-instrumented DVAT)

Bedside DVAT is a traditional test method, with detailed descriptions reported previously. In brief, the SVA test was performed under static head movement first, using the Snellen visual acuity chart, Landolt C visual acuity chart, or standard logarithmic visual acuity chart. Then the DVA test was performed with the subject rotating his head either actively or by the examiner. The subject's visual acuity was determined to be readable for 50% and above the line of the visual acuity chart, i.e., they could see the lowest line of the visual acuity chart. The DVA loss was calculated by subtracting SVA from DAV. Generally, DVA decreased by no more than three lines on the visual acuity chart compared to SVA or by no more than 0.2 ± 0.08 log MAR; exceeding these ranges often indicates impaired VOR function.

Another method was to ask the subject to identify the optotypes that appear 1 in 1 second when the head is turned.

FIGURE 1
Optotype keypad. Dynamic visual acuity instrument developed by Shanghai ZEHNIT Medical Technology Co., Ltd., Shanghai, China.

The visual acuity was calculated by the number of correct read optotypes. This method was more sensitive in assessing small changes in visual acuity. However, the traditional DVA test did not specify head movements' amplitude, speed, and frequency. When testing DVA, subjects involuntarily slowed down their head movements to see the optotypes clearly (4, 5), resulting in smooth pursuit rather than eliciting VOR (5). The reliability of the examiner and intra-examiner was also poor for assessing subjects with vestibular hypofunction (6).

Computerized DVAT (cDVA)

A computerized DVAT with a rate sensor to control the head velocity and software to control when the optotype is presented, thus increasing its validity (7).

When performing cDVA, the subject wore a velocity sensor on his head and held a keypad to select the visual optotype's direction (Figure 1). The optotypes letters "E"/"C" appeared on the computer monitor with different opening directions when the subject performed a sinusoidal movement of his head in the horizontal or vertical direction (Figures 2, 3) with a velocity between 120 and 180°/s for more than 40 ms (8, 9). The optotypes decreased by 0.1 LogMAR per line (5).

The velocity of head movement of the cDVAT test was tolerable for most subjects and avoided the problem of subjects remembering the paper version of the visual acuity chart, which

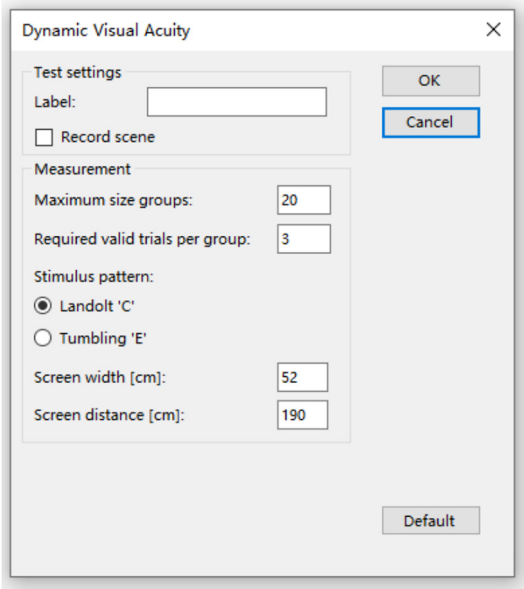

FIGURE 2
Select the optotype and set the parameters. Dynamic visual acuity instrument developed by Shanghai ZEHNIT Medical Technology Co., Ltd., Shanghai, China.

FIGURE 3
The patient rotated her head to the left/upward passively. Dynamic visual acuity instrument developed by Shanghai ZEHNIT Medical Technology Co., Ltd., Shanghai, China.

avoided the disadvantages of traditional DVAT and improved the accuracy of the test (10). DVA could be significantly improved by patients' vestibular function rehabilitation (7). So cDVAT can be used to assess the degree of vestibular dysfunction and also to determine rehabilitation treatment goals (5) and has been widely used to evaluate the recovery of gaze stability in patients with unilateral and bilateral vestibular disorders (11).

In a healthy population, the intra-group correlation coefficient (ICC) for cDVAT was 0.87 (>0.75 means better confidence), while in the vestibular dysfunction group, the intra-group correlation coefficient was 0.83 with a sensitivity of 94.5% and specificity of 95.2% (7); the sensitivity of the head during vertical movements was only 37.5% with a specificity of 90% (5).

DVAT on a treadmill

Subjects were first tested for SVA while standing on the treadmill and then for DVA while walking at 2, 4, and 6 km/h, respectively. A safety rope attached to the emergency brake of the treadmill was tied around the subject's waist to ensure safety. A chart of Sloan letters (CDHKNORSVZ, ten in total), which consisted of lines of 5 randomly chosen letters, was displayed on a monitor 2.8 m away from the subject. Five randomly selected letters by the computer for each line of sight (the five letters appeared in sequence) if the subject could read two letters accurately and proceeds to the following line (the size of the optotypes is decreased by 0.1 LogMAR).

Subjects were first tested for DVA at a walking speed of 2 km/h, after which they continued to measure DVA at 4 km/h. The test ended when subjects were unable to walk at higher speeds; subjects were excluded if they were unable to walk at 2 km/h on a treadmill (12). It was found that the sensitivity of the DVAT to discriminate patients with bilateral vestibular hypofunction (BVH) was 76% when testing the DVA at a walking speed of 2 km/h only and increased to 97% when measured in combination with speeds of 2, 4, and 6 km/h (13). The DVAT on a treadmill could better reflect the visual acuity change during vertical head movement in daily life. However, the test is challenging for those with BVH and the elderly (12).

DVAT on a rotary chair

The DVAT on the rotary chair (10) can be used to detect the effect of the horizontal semicircular on the VOR, which includes a steady-state sinusoidal test and a transient test. The test was performed with the subject's head and torso fixed in the rotary chair at a distance of 6 m. Measurements were made using the letter "E" optotype. A dark red laser dot was used to project the position of the optotype to control gaze when the optotype was not present.

During steady-state testing, the rotary chair was rotated at a frequency of 2Hz sinusoidally at a peak velocity of 10, 20, 40, 70, 100, and 130°/s. The optotype "E" was presented only when the velocity reached 80% of the peak. In transient rotation testing, the subject was rotated at 1,000, 1,600, and 2,800°/s^2 peak accelerations of the rotary chair. The optotype "E" was presented when the head started to rotate for 50 ms and lasted for 300 ms. The transient rotation test consists of both predictable and unpredictable conditions. For predictable transients, each peak acceleration transmits 40 transients to the right or left in a period of 100 s. For unpredictable transients, there are 60 unpredictable sudden rotations in each direction for each head peak acceleration within a total interval of 150 s, half in each direction. The rotary chair test is not commonly used in clinical practice due to cost and space requirements (14), and the search coil technique and local anesthetic used may cause vision damage during testing (15).

Head thrust DVA (htDVA) and functional head impulse testing (fHIT)

Schubert et al. (16) invented a novel method known as htDVA to assess the function of individual semicircular canals. DVA was tested using transient, unpredictable, SCC-plane head thrusts rather than the active head rotation paradigm traditionally used. Some researchers (9, 15, 17–19) used the head impulse testing device-functional test (HITD-FT), also called functional head impulse testing (fHIT), to evaluate the DVA of patients during passive head movements in the horizontal direction (e.g., Figure 3).

Subjects wearing a head-mounted acceleration detector were first tested for SVA. 0.8 LogMAR was then added to the SVA, and subjects were requested to observe the line of the visual acuity chart that was eight lines larger than the SVA, with 10 to 20 effective pulses in both the left and right directions. The subject's head motion amplitude ranged from 10 to 20°, and the pulse direction and timing were randomized to avoid the expected catch-up saccade. When the acceleration reaches 3,000 to 6,000°/s^2 of effective pulses, the display will show the Landolt C optotypes (the letter "C" has eight directions), which has a duration of 33 ms each time. The fHIT calculates the correct answers (CA%) of the optotypes, which can exceed 98% in normal subjects (9). The test may also be used to plot the curve of head movement and eye movement velocity over time to understand the effect of VOR gain and covert saccade on DVA results. Consequently, its positive detection rate is greater than that of other tests (18, 19).

Gaze shift dynamic visual acuity with walking (gsDVA)

The gsDVA test, modified based on the traditional cDVA, now includes a gaze shift component. Chen et al. (11) measured SVA, gsDVA in stance (gsDVAs), and gsDVA with walking (gsDVAw) in healthy subjects and patients with unilateral vestibulopathy (UVH), respectively. The gsDVAw has some significant advantages over the conventional measure of cDVA. The gsDVAs and gsDVAw were measured using three monitors, with the middle monitor appearing randomly as an arrow to the left or right, and the subject turning his head 60° in the direction of the arrow as fast as possible to look at the optotype "E" on the second monitor. The subject then read the direction of the letter as rapidly as possible. The letter's direction remained on the screen until the investigator recorded the response. Once the response was recorded, the letter disappeared from the side screen, signaling the subject to return the gaze to the central display and wait for 2 s before the arrow randomly guided the next head rotation. The gsDVAw was performed by the subject on a treadmill at an appropriate speed, and the rest was similar to the gsDVAs. The gsDVAw tests the patient's visual acuity while walking with head rotation, which is closer to daily life. GsDVAw can distinguish patients with UVH from healthy controls and is regarded as a more realistic measure of gaze stability than the cDVA test.

Translational dynamic visual acuity test (tDVAT)

The methods mentioned above are rotational dynamic visual acuity (rDVAT), which assesses the effect of the semicircular canal on the VOR; another test is the translational dynamic visual acuity test (tDVAT), which evaluates the effect of the otolithic organ on the VOR. The tDVAT includes horizontal and vertical forms of movements (20, 21). The patient's body and head are fixed to the examination device, and the test distance is generally within 30 cm, with a horizontal or vertical displacement. Before the optotype on the monitor appears, a "cross" shaped target appears in this location to ensure that the patient is always fixed at the position of the optotype during the movement. A study of healthy subjects showed that tDVA values were worse than rDVA values, and tDVA in the vertical direction was worse than tDVA in the horizontal direction (21).

Pediatric DVAT

The pediatric DVAT has been developed and used for years (22–24), showing both reliability and validity. But it has not been studied as wildly as that in adults. Unlike tests for adults, pediatric DVAT typically uses a limited set of letters (H, O, T and V) or common shapes (i.e., Lea vision chart: house, apple, window, ring, circle, square), posted on a 15-line version optotype chart. The positive and negative predictive values, sensitivity, and specificity of pediatric DVAT for detecting children with vestibular hypofunction range from 63 to 100% (22, 25).

The vestibular system may not be developing adequately in children under 6 years of age, which could account for the false-positive results at 2 Hz. But it appears that this interaction is mature enough to be exploited in a walking task by the age of five. Vervecque et al. (26) found DVAT on a treadmill useful for preschoolers of age 5. Rine et al. (23) showed that hDVA is reliable for children as young as 3 years, with excellent screening for vestibular hypofunction. In addition, it is interesting to note that DVA in children with sensorineural hearing, and children with cochlear implants were also decreased (27, 28).

Dynamic-object DVAT

Redondo et al. (29) examined subjects with heads stationary to look at a monitor 4 m away and measured the DVA for two conditions: the horizontal left-to-right sliding of the optotype "E" at 5, 10, 20, 30°/s, and random appearance (random Brownian motion). Each optotype was displayed for a maximum of 20 s during the test. Optotypes of the same size were measured five times, beginning with letters of 0.8 LogMAR in size. When the subject had three correct identifications, the optotypes decreased by 0.1 LogMAR; when <3, the visual acuity corresponding to that optotype was the subject's final visual acuity.

Another study (30) designed a novel DVA system capable of measuring DVA in the presence of predictable, random, and jittering target motion. When measuring DVA, the optotypes on the monitor were presented for a maximum of 16 s with horizontal, vertical, oblique, or random movement. This DVA system was shown to closely agree with the early treatment diabetic retinopathy study (ETDRS)visual acuity chart (ICC = 0.726), and the retest reliability was good.

The Dynamic-object DVAT mainly reflects a smooth pursuit ability and is commonly used for visual acuity evaluation of some athletes tracking balls.

Clinical applications

Vestibular disorders assessment

DVAT can be used to assess vestibular disease by stimulating the peripheral vestibular organs and the corresponding signaling pathways, where impairment of these can lead to a decrease in DVA. The DVAT evaluation of UVH, Benign Paroxysmal Positional Vertigo (BPPV), and vestibular neuritis (VN) is based on this principle.

Vestibular hypofunction

In some related studies (5, 11), for UVH patients (n = 168), the affected side DVA was worse than the healthy side ($p < 0.001$), while the asymmetry was not found in most BVH patients; secondly, both UVH and BVH patients had worse DVA than normal subjects. As a result, this asymmetry may help to distinguish between UVH and BVH patients, as well as the healthy/affected side of UVH patients.

BPPV

A study (31) evaluating DVA in horizontal and vertical directions in patients with horizontal and posterior semicircular BPPV found that BPPV patients had worse DVA than healthy subjects ($p < 0.01$). However, it is unclear whether this was due to vertigo symptoms or abnormal vestibular function. Neither horizontal nor vertical DVAT could distinguish between the affected and healthy sides of the patients.

VN

The study by Viciana et al. (32), which included patients with unilateral vestibular neuritis and healthy subjects, evaluated the three semicircular canal functions using htDVA in the horizontal and vertical directions, respectively. The results indicate that htDVA has low sensitivity (22%) and high specificity (85%), making it potentially helpful in monitoring vestibular rehabilitation and DVA in patients with VN.

Ophthalmic diseases assessment

Currently, DVATs are used to evaluate patients with ophthalmic diseases such as cataracts, optic neuritis, and glaucoma (33).

Cataract

Cataract is a prevalent ocular disorder with a cloudy area in the lens of the eye that leads to vision loss. Several studies (34, 35) have shown that dynamic visual motion significantly impacts age-related cataract patients, and DVA can be remarkably improved after phacoemulsification combined with Intraocular lens (IOL) implantation surgery. It has more significant advantages over traditional SVAT in evaluating the visual function during driving and exercising.

Optic neuritis

Optic neuritis is one of the most prevalent clinical features in multiple sclerosis that results in acute visual acuity decrease. The demyelination of optic nerves causing reduced projection rate along the visual pathways might be detected by DVAT (36). As compared with SVAT, DVAT may be more appropriate to quantify projection latencies caused by demyelination because the generation of DVA requires a sufficient amount and velocity

of visual input projection, while SVA only depends on the amount (36, 37).

Glaucoma

Glaucoma is characterized by progressive degeneration and death of retinal ganglion cells. The moving-optotypes DVAT using high temporal frequency optotypes has potential clinical value in the earlier detection of functional defects in glaucoma (38, 39).

Finally, it is essential to note that the current study showed that htDVA does not help diagnose superior canal dehiscence syndrome (SCDS) (8). Janky et al. (8) showed that SVA and active DVA are not significantly affected in SCDS patients after surgical canal plugging. However, postoperative htDVA was reduced considerably in the SC plane on the affected side, and this reduction persisted beyond 6 weeks. This may be a permanent effect of surgical occlusion.

Evaluation of central system disorders

DVAT can assess central system disorders such as cerebral concussion, multiple sclerosis (MS), and cerebellar ataxia (CA).

Cerebral concussion

Gottshall et al. (40) determined that patients with acute traumatic brain injury (TBI) scored higher on DVAT compared to healthy controls. They recommended the DVA test as an outcome measurement tool in assessing TBI patients.

Athletes are often prone to concussions from intense exercise and should undergo DVAT early to help initiate vestibular rehabilitation exercises for patients as soon as possible to avoid delayed recovery (41). Pediatric patients with concussions require longer recovery times compared to adults. Zhou and Brodsky (42) found DVA abnormalities in 57% of children with sports-related concussions with dizziness and balance disturbances, which suggests that high-frequency VOR injury may be the primary cause of dizziness in children.

MS

About 70% of MS patients may have brainstem injury, and 87% have abnormal brainstem reflexes (43), leading to abnormalities in their VOR mediated by brainstem pathways and thus abnormal DVA. Compared to healthy controls of the same age, dDVAT levels in MS patients were 2.5 times worse (44). Mañago et al. (43) evaluated MS patients using GST with cDVAT. It was found that both tests could distinguish MS patients from the healthy population, but the cDVAT was unable to distinguish the degree of functional impairment in MS patients.

CA

One study (45) found a decrease in DVA of up to 84% in CA patients, mainly associated with impaired VOR, and only marginally to the degree of ataxia. CA patients with concomitant vestibular impairment showed a similar decrease in DVA as BVH patients. However, DVA impairment was also seen in patients with CA who lacked a severe vestibular lesion (45), indicating the involvement of central mechanisms such as the impairment of central adaption of VOR. The evaluation of DVA in patients with progressive CA could offer information to target vestibular and oculomotor rehabilitation.

Migraine

A recent study (46) found that migraine patients had significant DVA loss as compared with control subjects in four positions (left DVA, right DVA, up DVA, and down DVA, respectively. These abnormal DVA findings may be due to impaired VOR reflex and visuo-vestibular cortical interactions, which could explain the pathophysiology of head movement hypersensitivity and visual motion sensitivity encountered by migraine patients. Given this finding, oculomotor and gaze stability exercises that improve VOR gain may be a promising therapeutic option that could decrease head movement hypersensitivity and visual motion sensitivity and reduce the frequency of migraine attacks.

Evaluation of the effects of vestibular rehabilitation

The DVAT is frequently used to evaluate the effectiveness of vestibular rehabilitation in patients during active head movements (17, 47). UVH patients who underwent vestibular rehabilitation exercises showed a significant improvement in DVA during active head movements ($P < 0.01$), whereas patients who underwent placebo exercises showed no improvement ($P = 0.07$) (48). Vestibular rehabilitation exercises also improved DVA in patients with BVH (5). Additionally, fHIT was also used to assess compensations of the acute phase and 3 months after the onset of VN (19). Several studies have also used cDVAT to evaluate the effect of gaze stabilization exercises (49).

In addition, DVAT can also assess the effect of the vestibular implant (VI) on gaze stabilization in BVH patients. According to one study (50), when the vestibular implant system was open, the difference between SVA and DVA in BVH patients was 0-0.16 LogMAR. This implies that DVA can approach normal values in patients with VI and indicates that VI has good prospects for application (50). Because of the close relationship between DVA and ball sports (e.g., basketball, soccer, volleyball, table tennis, etc.), DVA is also commonly used to evaluate the effect of physical activity on improving visual acuity (1).

Prediction of fall risk

The coordination of visual, proprioceptive, and vestibular senses is essential for maintaining body balance. When the VOR pathway is impaired, patients especially those with BVH, may experience oscillopsia and be at risk of falling if they rely only on proprioception (51). Age-related decline in balance function is accompanied by vestibular impairment, seen in three-quarters of seniors who needed fall risk assessments. This suggests that vestibular impairment may contribute to the risk of falling in the elderly (52).

Hall et al. (51) combined the dynamic gait index (DGI) and DVA scores to construct a model that could predict the risk of falls in patients with UVH. The patient's DGI and DVA scores were brought into the formula to derive the patient's fall risk, and the sensitivity and specificity of the model were 77 and 90%, respectively. Honaker and Shepard (53) used the DGI score (DGI $\leq$ 19 as susceptible to falls) as the gold standard in a screening study of 16 patients with a history of falls. When the DVAT value was >0.25 LogMAR, it suggested the need to assess patients for fall risk with a sensitivity and specificity of 92 and 61%, respectively. Bayan et al. (47, 54) also suggested the DVAT as an additional means of assessing the risk of falls in patients with mild cognitive impairment.

Influencing factors

Subjects

Age

The relationship between age and DVA is unclear. It has been suggested that age has a negative effect on DVA in both healthy people and patients with vestibular dysfunction, i.e., the DVA will get worse as one gets older (5, 7, 8, 32, 55–57) and that DVA is more degenerated than SVA (58). It has also been suggested that DVA remains stable until the age of 50 and begins to decline after that (24, 59). The possible reason for this is the physiological degeneration of neuronal function in the vestibular nuclear complex (59). However, other studies did not find a correlation between age and DVA in patients with UVH/BVH (11, 55). Therefore, the relationship between age and DVA in patients with vestibular dysfunction needs further investigation.

Occupations

In one study, the DVA of water polo players (58) and soccer players (60) was compared to the DVA of the general population and showed that the DVA of athletes was better than that of the general population. Additionally, the DVA varies between occupations and even within the same occupation. For instance, water polo players have a DVA of about 0.5 (61), while among soccer players, goalkeepers have the best DVA (0.82) and strikers have the worst DVA (0.62).

SVA

Some studies suggested that DVA is possibly dependent on SVA. This might be related to the difference in focusing with different SVA. Poorer SVA can cause the defocus of the retinal image, which affects DVA (62). SVA is mainly related to the power of ocular resolution, while DVA is also closely related to the functionality of the oculomotor system. Nakatsuka et al. (62) examined 42 subjects with normal visual acuity and demonstrated a strong correlation between SVA and DVA ($r = 0.87$, $P < 0.001$).

However, the correlation between DVA and SVA was not significant, according to a different study (63), probably because SVA is related to the discriminative ability of the eye, whereas DVA is related to VOR function. It is common to find significant individual differences in DVA in subjects with similar SVA (64).

Weissman and Freeburne (65) examined the relationship between DVA and SVA in 30 female college students with Landolt C scopes at six speeds (20, 60, 90, 120, 150, and 180°/s). The results showed a significant linear relationship between DVA and SVA at the first four speeds ($P < 0.01$). However, the distribution range of SVA was different, and the linear relationship between the two was different; the linear relationship between the two disappeared at the latter two speeds ($P > 0.09$). The correlation between DVA and SVA is usually low and inversely proportional to the speed of stimulation. Therefore, the different conclusions reached by the various studies may be due to the different speeds of the movement.

Subjects' eyeglass lenses

Eyeglass correction may have an impact on DVA because of peripheral defocus and prism effects, which result in unclear and skewed images in the peripheral region. The subjects' DVA declined with increasing diopter (66, 67). Multifocal contact lenses reduced these effects, resulting in better DVA in subjects compared to regular glasses, but the difference was not statistically significant ($p = 0.4$) (67).

Testing methods

Several studies (5, 17, 48, 68) have indicated that patients with active htDVAT have higher DVA values than those with passive htDVAT. This might be due to the activation of the cervico-ocular reflex when patients actively perform head movements (15) and a shorter latency for the appearance of covert saccades, which reduces the slipping time of the optotype on the retina (17, 68, 69). As a result, some researchers have suggested that measurements performing passive head rotation

are closer to the true DVA values (13, 16, 21), while others have suggested that active head rotation in patients is more consistent with daily life (17). Therefore, some researchers believe that measurements during passive head rotation of patients are closer to the true DVA values (13, 16, 21). In contrast, others believe that measures during active head rotation of patients are more comparable to daily life (17). In addition, because of saccade suppression, the shorter the appearance time of the optotype on the monitor, and the faster it moves, the worse the DVA results. The linear relationship between visual acuity and angular velocity of the optotype is $Y = a + bX$ (30, 58). The time of optotype appearance has a more significant effect on DVA compared to the movement velocity (63). Regarding movement track, horizontal movement of the optotype gets better DVA results compared to tilted movement (58).

Roberts and Gans (70) showed that the sensitivity and specificity of the vertical DVAT (vDVAT) were 42.4 and 93.8%, respectively, and the horizontal DVAT (hDVAT) were 66.7 and 86.2%, respectively. However, the accuracy of these two DVAs did not have a significant difference, 76.5 and 79.6%, respectively (70). Another study revealed that vDVAT was <55% accurate in identifying patients with abnormal vestibular function vs. those with dizziness but normal vestibular function (with 23.1% accuracy for UVH and 54.5% accuracy for BVH), whereas hDVAT was more than 90% accurate in identifying both (with 93.1% accuracy for UVH and 96.1% accuracy for BVH) (59). The difference between vDVA and hDVA may relate to the detection of the acceleration signal. Both studies suggest that hDVAT is more sensitive and accurate compared to vDVAT. The reason for this may be that the bilateral vertical semicircular canals are able to complement each other during vDVA testing, making it easier to maintain visual field stability and thus less likely to detect dysfunction. In contrast, only the unilateral horizontal semicircular canals perceive head motion acceleration during hDVA testing, which is not conducive to maintaining visual field stability, thus making it simpler to detect dysfunction on the affected side (59).

Caffeine and alcohol

Caffeine also influences vision, as it increases eye movement speed and contrast sensitivity (71). A randomized controlled study analyzed the effects of caffeine on DVA (29). The study was conducted on a population with low levels of coffee intake (2 cups of espresso per day). The test and control groups consumed 4 mg/kg of caffeine and placebo, respectively, and were then measured for DVA after 60 min of consumption, i.e., the acute effects of caffeine on DVA. The study measured the visual acuity and reaction time of the subjects and found that caffeine consumption increased the DVA values in horizontal and random directions and shortened the reaction time of the subjects to horizontal motion optotypes in a short period of time. However, the effect of high levels of caffeine intake on DVA has not been studied.

Alcohol affects the nervous system and cognitive function. The degree of DVA loss in subjects after alcohol intake increases, although SVA remains unchanged (72). This is associated with reduced responsiveness of the oculomotor and vestibular systems after alcohol intake, especially the reduction of VOR function.

Discussion

DVAT is a safe and effective screening method for VOR function. Studies have demonstrated that the DVAT can be used to screen for vestibular impairment, assess vestibular rehabilitation, assess ophthalmology-related disorders, evaluate central system disorders, and screen athletes and pilots. DVAT can also be complemented with other vestibular function tests for a comprehensive evaluation. As a diagnostic tool, the DVA test should be used with caution since the test score reflects central compensation for vestibular dysfunction and, therefore, is not a pure measure of peripheral vestibular function.

Nowadays, clinicians increasingly realize the significance of the DVAT, which was recommended as a standard diagnostic evaluation tool for vestibular diseases in some worldwide clinical guidelines and consensus (73, 74), and was chosen by the NIH Toolbox as an assessment of the vestibular system's contribution to gaze stability (23).

However, there is still a lack of studies with large samples to define DVAT's criteria, application indications, abnormal values, and specific applications in different diseases. The prospective clinical applications of DVAT are expansive.

Future studies on the role of DVAT in the diagnosis and treatment of various diseases are needed to explore more effective testing methods and better clinical applications.

Author contributions

GC: study concept and design, study supervision, and manuscript writing. JZ: study concept and design, collection and analysis of relevant literature, and manuscript writing and revision. QQ: collection and analysis of relevant literature and manuscript writing. LZ: manuscript reviewing and manuscript revision. YL: study concept and design and collection and analysis of relevant literature. JY and JW: collection and analysis of relevant literature and create figures. HH: critical revision of

the manuscript for important intellectual content. All authors contributed to the article and approved the submitted version.

Funding

This work was supported by Shanxi Province Medical Key Scientific Research Project (2020XM13) from Shanxi Provincial Health Commission.

Conflict of interest

The authors declare that the research was conducted in the absence of any commercial or financial relationships that could be construed as a potential conflict of interest.

Publisher's note

All claims expressed in this article are solely those of the authors and do not necessarily represent those of their affiliated organizations, or those of the publisher, the editors and the reviewers. Any product that may be evaluated in this article, or claim that may be made by its manufacturer, is not guaranteed or endorsed by the publisher.

References

1. Palidis DJ, Wyder-Hodge PA, Fooken J, Spering M. Distinct Eye Movement Patterns Enhance Dynamic Visual Acuity. *PLoS One.* (2017) 12:e0172061. doi: 10.1371/journal.pone.0172061

2. Verbecque E, Van Criekinge T, Vanloot D, Coeckelbergh T, Van de Heyning P, Hallemans A, et al. Dynamic visual acuity test while walking or running on treadmill: reliability and normative data. *Gait Posture.* (2018) 65:137–42. doi: 10.1016/j.gaitpost.2018.07.166

3. Quevedo L, Aznar-Casanova JA, Silva J. Dynamic visual acuity. *Trends in Psychol.* (2018) 26:1267–81. doi: 10.9788/TP2018.3-06Es

4. Bhansali SA, Stockwell CW, Bojrab DI. Oscillopsia in patients with loss of vestibular function. *Otolaryngol Head Neck Surg J Am Aca.* (1993) 109:120–5. doi: 10.1177/019459989310900122

5. Herdman SJ. Computerized dynamic visual acuity test in the assessment of vestibular deficits. *Handbook Clin Neurophysiol.* (2010) 9:181–90. doi: 10.1016/S1567-4231(10)09014-3

6. Cochrane GD, Christy JB, Kicker ET, Kailey RP, England BK. Inter-rater and test-retest reliability of computerized clinical vestibular tools. *J Vestibul Res Equilib Orient.* (2021) 31:365–73. doi: 10.3233/VES-201522

7. Herdman SJ, Tusa RJ, Blatt P, Suzuki A, Venuto PJ, Roberts D. Computerized dynamic visual acuity test in the assessment of vestibular deficits. *Am J Otol.* (1998) 19:790–6.

8. Janky KL, Zuniga MG, Ward B, Carey JP, Schubert MC. Canal plane dynamic visual acuity in superior canal dehiscence. *J Am Otol Soc Am Neurotol Soc Eu Aca Otol Neurotol.* (2014) 35:844–9. doi: 10.1097/MAO.0000000000000336

9. Ramat S, Colnaghi S, Boehler A, Astore S, Falco P, Mandalà M, et al. A Device for the functional evaluation of the vor in clinical settings. *Front Neurol.* (2012) 3:39. doi: 10.3389/fneur.2012.00039

10. Tian JR, Shubayev I, Demer JL. Dynamic visual acuity during transient and sinusoidal yaw rotation in normal and unilaterally vestibulopathic humans. *Experimental Brain Res.* (2001) 137:12–25. doi: 10.1007/s002210000640

11. Chen PY, Jheng YC, Huang SE, Po-Hung Li L, Wei SH, Schubert MC, et al. Gaze shift dynamic visual acuity: a functional test of gaze stability that distinguishes unilateral vestibular hypofunction. *J Vesti Res Equilib Orient.* (2021) 31:23–32. doi: 10.3233/VES-201506

12. Starkov D, Snelders M, Lucieer F, Janssen AML, Pleshkov M, Kingma H, et al. Bilateral vestibulopathy and age: experimental considerations for testing dynamic visual acuity on a treadmill. *J Neurol.* (2020) 267:265–72. doi: 10.1007/s00415-020-10249-z

13. Guinand N, Pijnenburg M, Janssen M, Kingma H. Visual acuity while walking and oscillopsia severity in healthy subjects and patients with unilateral and bilateral vestibular function loss. *Arch Otolaryngol Head Neck Surg.* (2012) 138:301–6. doi: 10.1001/archoto.2012.4

14. Gimmon Y, Schubert MC. Vestibular testing-rotary chair and dynamic visual acuity tests. *Adv Otorhinolaryngol.* (2019) 82:39–46. doi: 10.1159/000490270

15. Colagiorgio P, Colnaghi S, Versino M, Ramat S. A new tool for investigating the functional testing of the vor. *Front Neurol.* (2013) 4:165. doi: 10.3389/fneur.2013.00165

16. Schubert MC, Migliaccio AA, Della Santina CC. Dynamic visual acuity during passive head thrusts in canal planes. *J Assoc Res Otolaryngol JARO.* (2006) 7:329–38. doi: 10.1007/s10162-006-0047-6

17. Sjögren J, Fransson PA, Karlberg M, Magnusson M, Tjernström F. Functional head impulse testing might be useful for assessing vestibular compensation after unilateral vestibular loss. *Front Neurol.* (2018) 9:979. doi: 10.3389/fneur.2018.00979

18. Ramaioli C, Colagiorgio P, Saglam M, Heuser F, Schneider E, Ramat S, et al. The effect of vestibulo-ocular reflex deficits and covert saccades on dynamic vision in opioid-induced vestibular dysfunction. *PLoS ONE.* (2014) 9:e110322. doi: 10.1371/journal.pone.0110322

19. Corallo G, Versino M, Mandalà M, Colnaghi S, Ramat S. The functional head impulse test: preliminary data. *J Neurol.* (2018) 265:35–9. doi: 10.1007/s00415-018-8910-z

20. Cheng RC, Walker MF. Vertical head translation impairs dynamic visual acuity during near viewing. *J Vestib Res Equilib Orient.* (2016) 26:417–23. doi: 10.3233/VES-160596

21. Ramaioli C, Cuturi LF, Ramat S, Lehnen N, MacNeilage PR. Vestibulo-ocular responses and dynamic visual acuity during horizontal rotation and translation. *Front Neurol.* (2019) 10:321. doi: 10.3389/fneur.2019.00321

22. Rine RM, Braswell J. A clinical test of dynamic visual acuity for children. *Int J Pediatr Otorhinolaryngol.* (2003) 67:1195–201. doi: 10.1016/j.ijporl.2003.07.004

23. Rine RM, Schubert MC, Whitney SL, Roberts D, Redfern MS, Musolino MC, et al. Vestibular function assessment using the Nih toolbox. *Neurology.* (2013) 80(11 Supplement 3):S25–31. doi: 10.1212/WNL.0b013e3182872c6a

24. Li C, Beaumont JL, Rine RM, Slotkin J, Schubert MC. Normative scores for the Nih toolbox dynamic visual acuity test from 3 to 85 years. *Front Neurol.* (2014) 5:223. doi: 10.3389/fneur.2014.00223

25. Christy JB, Payne J, Azuero A, Formby C. Reliability and diagnostic accuracy of clinical tests of vestibular function for children. *Pediatr Phys Ther.* (2014) 26:180–9. doi: 10.1097/PEP.0000000000000039

26. Verbecque E, De Belder N, Marijnissen T, Vereeck L, Van de Heyning P, Hallemans A. Feasibility of the clinical dynamic visual acuity test in typically developing preschoolers. *Eur Arch Otorhinolaryngol.* (2018) 275:1343–8. doi: 10.1007/s00405-018-4919-2

27. Martin W, Jelsma J, Rogers C. Motor proficiency and dynamic visual acuity in children with bilateral sensorineural hearing loss. *Int J Pediatr Otorhinolaryngol.* (2012) 76:1520–5. doi: 10.1016/j.ijporl.2012.07.007

28. Janky KL, Givens D. Vestibular, visual acuity, and balance outcomes in children with cochlear implants: a preliminary report. *Ear Hear.* (2015) 36:e364–72. doi: 10.1097/AUD.0000000000000194

29. Redondo B, Jiménez R, Molina R, Dalton K, Vera J. Effects of caffeine ingestion on dynamic visual acuity: a placebo-controlled, double-blind, balanced-crossover study in low caffeine consumers. *Psychopharmacology.* (2021) 238:3391–8. doi: 10.1007/s00213-021-05953-1

30. Hirano M, Hutchings N, Simpson T, Dalton K. Validity and repeatability of a novel dynamic visual acuity system. *Optometry Vision Science J Am Academy Optometry.* (2017) 94:616–25. doi: 10.1097/OPX.0000000000001065

31. Yetiser S, Ince D. Dynamic visual acuity in benign paroxysmal positional vertigo. *Acta Otolaryngol.* (2018) 138:987–92. doi: 10.1080/00016489.2018.1498595

32. Viciana D, Ferrer J, Palma MJ, Zapata C, Lopez-Escamez JA. Dynamic visual acuity during head-thrust test in canal planes in healthy subjects and patients with vestibular neuritis. *Acta Otolaryngol.* (2010) 130:1260–6. doi: 10.3109/00016481003785994

33. Wu TY, Wang YX Li XM. Applications of dynamic visual acuity test in clinical ophthalmology. *Int J Ophthalmol.* (2021) 14:1771–8. doi: 10.18240/ijo.2021.11.18

34. Ao M, Li X, Huang C, Hou Z, Qiu W, Wang W. Significant improvement in dynamic visual acuity after cataract surgery: a promising potential parameter for functional vision. *PLoS ONE.* (2014) 9:e115812. doi: 10.1371/journal.pone.0115812

35. Wang MF, Xiu-Xiang JI, Wang RF, Liu Y, Xia LI, Ophthalmology DO, et al. *The Changes of Dynamic Visual Acuity after Ultrasonic Emulsification Cataract Combined with Intraocular Lens Implantation in Patients with Age-Related Cataract*. Beijing: Medical Recapitulate (2015). doi: 10.3969/j.issn.1006-2084.2015.20.055

36. Raz N, Hallak M, Ben-Hur T, Levin N. Dynamic visual tests to identify and quantify visual damage and repair following demyelination in optic neuritis patients. *J Visual Exp JoVE.* (2014) 86:51107. doi: 10.3791/51107

37. Raz N, Dotan S, Chokron S, Ben-Hur T, Levin N. Demyelination affects temporal aspects of perception: an optic neuritis study. *Ann Neurol.* (2012) 71:531–8. doi: 10.1002/ana.22692

38. Gupta N, Ang LC, Noel de. Tilly L, Bidaisee L, Yucel YH. Human glaucoma and neural degeneration in intracranial optic nerve, lateral geniculate nucleus, and visual cortex. *Br J Ophthalmol.* (2006) 90:674–8. doi: 10.1136/bjo.2005.086769

39. Wen W, Zhang P, Liu T, Zhang T, Gao J, Sun X, et al. A novel motion-on-color paradigm for isolating magnocellular pathway function in preperimetric glaucoma. *Invest Ophthalmol Vis Sci.* (2015) 56:4439–46. doi: 10.1167/iovs.15-16394

40. Gottshall K, Drake A, Gray N, McDonald E, Hoffer ME. Objective vestibular tests as outcome measures in head injury patients. *Laryngoscope.* (2003) 113:1746–50. doi: 10.1097/00005537-200310000-00016

41. Marquez C, Lininger M, Raab S. Establishing normative change values in visual acuity loss during the dynamic visual acuity test. *Int J Sports Phys Ther.* (2017) 12:227–32.

42. Zhou G, Brodsky JR. Objective vestibular testing of children with dizziness and balance complaints following sports-related concussions. *Otolaryngol Head Neck Surg J Am Aca Otolaryngol Head Neck Surg.* (2015) 152:1133–9. doi: 10.1177/0194599815576720

43. Mañago MM, Schenkman M, Berliner J, Hebert JR. Gaze stabilization and dynamic visual acuity in people with multiple sclerosis. *J Vestib Res Equilib Orient.* (2016) 26:469–77. doi: 10.3233/VES-160593

44. Loyd BJ, Agnew L, Fangman A, Thackeray A, Peterson DS, Schubert MC, et al. Characterizing gaze and postural stability deficits in people with multiple sclerosis. *Mult Scler Relat Disord.* (2021) 55:103205. doi: 10.1016/j.msard.2021.103205

45. Dankova M, Jerabek J, Jester DJ, Zumrova A, Paulasova Schwabova J, Cerny R, et al. Clinical dynamic visual acuity in patients with cerebellar ataxia and vestibulopathy. *PLoS ONE.* (2021) 16:e0255299. doi: 10.1371/journal.pone.0255299

46. Atilla MH, Kesici GG. Dynamic visual acuity test findings of migraine patients: observational case-control study. *Am J Otolaryngol.* (2022) 43:103559. doi: 10.1016/j.amjoto.2022.103559

47. Schubert MC, Migliaccio AA, Clendaniel RA, Allak A, Carey JP. Mechanism of dynamic visual acuity recovery with vestibular rehabilitation. *Arch Phys Med Rehabil.* (2008) 89:500–7. doi: 10.1016/j.apmr.2007.11.010

48. Herdman SJ, Schubert MC, Das VE, Tusa RJ. Recovery of dynamic visual acuity in unilateral vestibular hypofunction. *Arch Otolaryngol Head Neck Surg.* (2003) 129:819–24. doi: 10.1001/archotol.129.8.819

49. Michel L, Laurent T, Alain T. Rehabilitation of dynamic visual acuity in patients with unilateral vestibular hypofunction: earlier is better. *Eur Arch Otorhinolaryngol.* (2020) 277:103–13. doi: 10.1007/s00405-019-05690-4

50. Guinand N, Van de Berg R, Cavuscens S, Stokroos R, Ranieri M, Pelizzone M, et al. Restoring visual acuity in dynamic conditions with a vestibular implant. *Front Neurosci.* (2016) 10:577. doi: 10.3389/fnins.2016.00577

51. Hall CD, Schubert MC, Herdman SJ. Prediction of fall risk reduction as measured by dynamic gait index in individuals with unilateral vestibular hypofunction. *Eur Arch Otorhinolaryngol.* (2004) 25:746–51. doi: 10.1097/00129492-200409000-00017

52. Jacobson GP, McCaslin DL, Grantham SL, Piker EG. Significant vestibular system impairment is common in a cohort of elderly patients referred for assessment of falls risk. *J Am Acad Audiol.* (2008) 19:799–807. doi: 10.3766/jaaa.19.10.7

53. Honaker JA, Shepard NT. Use of the dynamic visual acuity test as a screener for community-dwelling older adults who fall. *J Vestib Research Equilib Orient.* (2011) 21:267–76. doi: 10.3233/VES-2011-0427

54. Baydan M, Caliskan H, Balam-Yavuz B, Aksoy S, Böke B. The interaction between mild cognitive impairment with vestibulo-ocular reflex, dynamic visual acuity and postural balance in older adults. *Exp Gerontol.* (2020) 130:110785. doi: 10.1016/j.exger.2019.110785

55. Herdman SJ, Schubert MC, Tusa RJ. Role of central preprogramming in dynamic visual acuity with vestibular loss. *Arch Otolaryngol Head Neck Surg.* (2001) 127:1205–10. doi: 10.1001/archotol.127.10.1205

56. Pelisson D, Prablanc C, Urquizar C. Vestibuloocular reflex inhibition and gaze saccade control characteristics during eye-head orientation in humans. *J Neurophysiol.* (1988) 59:997–1013. doi: 10.1152/jn.1988.59.3.997

57. Vital D, Hegemann SC, Straumann D, Bergamin O, Bockisch CJ, Angehrn D, et al. A new dynamic visual acuity test to assess peripheral vestibular function. *Arch Otolaryngol Head Neck Surg.* (2010) 136:686–91. doi: 10.1001/archoto.2010.99

58. Quevedo-Junyent L, Aznar-Casanova JA, Merindano-Encina D, Cardona G, Solé-Fortó J. Comparison of dynamic visual acuity between water polo players and sedentary students. *Res Q Exerc Sport.* (2011) 82:644–51. doi: 10.1080/02701367.2011.10599801

59. Schubert MC, Herdman SJ, Tusa RJ. Vertical dynamic visual acuity in normal subjects and patients with vestibular hypofunction. *Eur Arch Otorhinolaryngol.* (2002) 23:372–7. doi: 10.1097/00129492-200205000-00025

60. Roberts JW, Strudwick AJ, Bennett SJ. Visual function of english premier league soccer players. *Science and Medicine in Football.* (2017) 1:178–82. doi: 10.1080/24733938.2017.1330552

61. Jorge J, Fernandes P. Static and dynamic visual acuity and refractive errors in elite football players. *Clin Exp Optometry.* (2019) 102:51–6. doi: 10.1111/cxo.12812

62. Nakatsuka M, Ueda T, Nawa Y, Yukawa E, Hara T, Hara Y. Effect of static visual acuity on dynamic visual acuity: a pilot study. *Percept Mot Skills.* (2006) 103:160–4. doi: 10.2466/pms.103.1.160-164

63. Fergenson PE, Suzansky JW. An investigation of dynamic and static visual acuity. *Perception.* (1973) 2:343–56. doi: 10.1068/p020343

64. Long GM, Penn DL. Dynamic visual acuity: normative functions and practical implications. *Bull Psychon Soc.* (1987) 25:253–6. doi: 10.3758/BF03330347

65. Weissman S, Freeburne CM. Relationship between static and dynamic visual activity. *J Exp Psychol.* (1965) 70:141–6. doi: 10.1037/h0022214

66. Wang Y, Guo Y, Wei S, Yuan Y, Wu T, Zhang Y, et al. Binocular dynamic visual acuity in eyeglass-corrected myopic patients. *J Visualiz Exp JoVE.* (2022) 181:3864. doi: 10.3791/63864

67. Fogt JS, Weisenberger K, Fogt N. Visual performance with multifocal contact lenses and progressive addition spectacles. *J Br Contact Lens Assoc.* (2021) 3:101472. doi: 10.1016/j.clae.2021.101472

68. Riska KM, Bellucci J, Garrison D, Hall C. Relationship between corrective saccades and measures of physical function in unilateral and bilateral vestibular loss. *Ear Hear.* (2020) 41:1568–74. doi: 10.1097/AUD.0000000000000885

69. Starkov D, Strupp M, Pleshkov M, Kingma H, van de Berg R. Diagnosing vestibular hypofunction: an update. *J Neurol.* (2021) 268:377–85. doi: 10.1007/s00415-020-10139-4

70. Roberts RA, Gans RE. Comparison of horizontal and vertical dynamic visual acuity in patients with vestibular dysfunction and non-vestibular dizziness. *J Am Acad Audiol.* (2007) 18:236–44. doi: 10.3766/jaaa.18.3.5

71. Connell CJW, Thompson B, Turuwhenua J, Hess RF, Gant N. Caffeine Increases the velocity of rapid eye movements in unfatigued humans. *Psychopharmacology.* (2017) 234:2311–23. doi: 10.1007/s00213-017-4638-1

72. Roth TN, Weber KP, Wettstein VG, Marks GB, Rosengren SM, Hegemann SC. Ethanol consumption impairs vestibulo-ocular reflex function measured by the video head impulse test and dynamic visual acuity. *J Vestib Res Equilib Orient.* (2014) 24:289–95. doi: 10.3233/VES-140520

73. Hall CD, Herdman SJ, Whitney SL, Cass SP, Clendaniel RA, Fife TD, et al. Vestibular rehabilitation for peripheral vestibular hypofunction: an evidence-based clinical practice guideline: from the American physical therapy association neurology section. *J Neurol Phys Ther.* (2016) 40:124–55. doi: 10.1097/NPT.0000000000000120

74. Strupp M, Kim JS, Murofushi T, Straumann D, Jen JC, Rosengren SM, et al. Bilateral vestibulopathy: diagnostic criteria consensus document of the classification committee of the barany society. *J Vestib Res Equilib Orient.* (2017) 27:177–89. doi: 10.3233/VES-170619

Frontiers in Neurology

Explores neurological illness to improve patient care

The third most-cited clinical neurology journal explores the diagnosis, causes, treatment, and public health aspects of neurological illnesses. Its ultimate aim is to inform improvements in patient care.

Discover the latest Research Topics

See more →

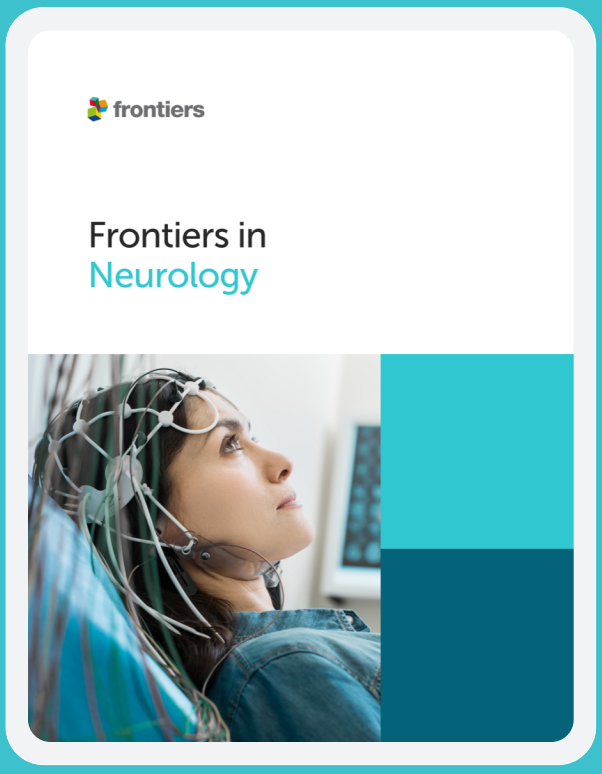

Frontiers

Avenue du Tribunal-Fédéral 34
1005 Lausanne, Switzerland
frontiersin.org

Contact us

+41 (0)21 510 17 00
frontiersin.org/about/contact